frontiers
RESEARCH TOPICS

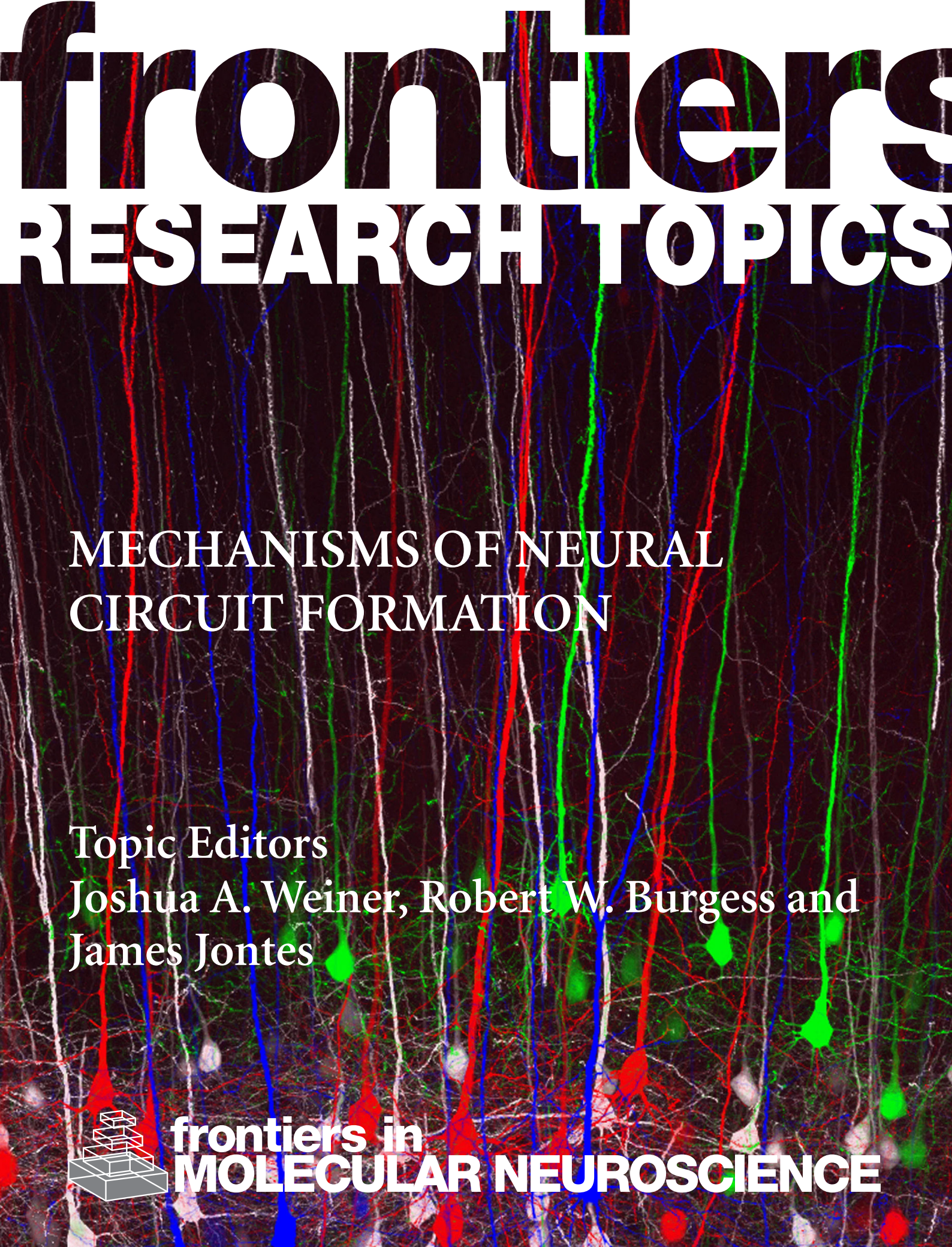

MECHANISMS OF NEURAL CIRCUIT FORMATION

Topic Editors
Joshua A. Weiner, Robert W. Burgess and James Jontes

frontiers in
MOLECULAR NEUROSCIENCE

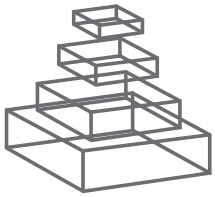

frontiers

ISSN 1664-8714
ISBN 978-2-88919-403-2
DOI 10.3389/978-2-88919-403-2

ABOUT FRONTIERS

Frontiers is more than just an open-access publisher of scholarly articles: it is a pioneering approach to the world of academia, radically improving the way scholarly research is managed. The grand vision of Frontiers is a world where all people have an equal opportunity to seek, share and generate knowledge. Frontiers provides immediate and permanent online open access to all its publications, but this alone is not enough to realize our grand goals.

FRONTIERS JOURNAL SERIES

The Frontiers Journal Series is a multi-tier and interdisciplinary set of open-access, online journals, promising a paradigm shift from the current review, selection and dissemination processes in academic publishing.
All Frontiers journals are driven by researchers for researchers; therefore, they constitute a service to the scholarly community. At the same time, the Frontiers Journal Series operates on a revolutionary invention, the tiered publishing system, initially addressing specific communities of scholars, and gradually climbing up to broader public understanding, thus serving the interests of the lay society, too.

DEDICATION TO QUALITY

Each Frontiers article is a landmark of the highest quality, thanks to genuinely collaborative interactions between authors and review editors, who include some of the world's best academicians. Research must be certified by peers before entering a stream of knowledge that may eventually reach the public - and shape society; therefore, Frontiers only applies the most rigorous and unbiased reviews.
Frontiers revolutionizes research publishing by freely delivering the most outstanding research, evaluated with no bias from both the academic and social point of view.
By applying the most advanced information technologies, Frontiers is catapulting scholarly publishing into a new generation.

WHAT ARE FRONTIERS RESEARCH TOPICS?

Frontiers Research Topics are very popular trademarks of the Frontiers Journals Series: they are collections of at least ten articles, all centered on a particular subject. With their unique mix of varied contributions from Original Research to Review Articles, Frontiers Research Topics unify the most influential researchers, the latest key findings and historical advances in a hot research area!
Find out more on how to host your own Frontiers Research Topic or contribute to one as an author by contacting the Frontiers Editorial Office: researchtopics@frontiersin.org

MECHANISMS OF NEURAL CIRCUIT FORMATION

Topic Editors:
Joshua A. Weiner, The University of Iowa, USA
Robert W. Burgess, The Jackson Laboratory, USA
James Jontes, Ohio State University, USA

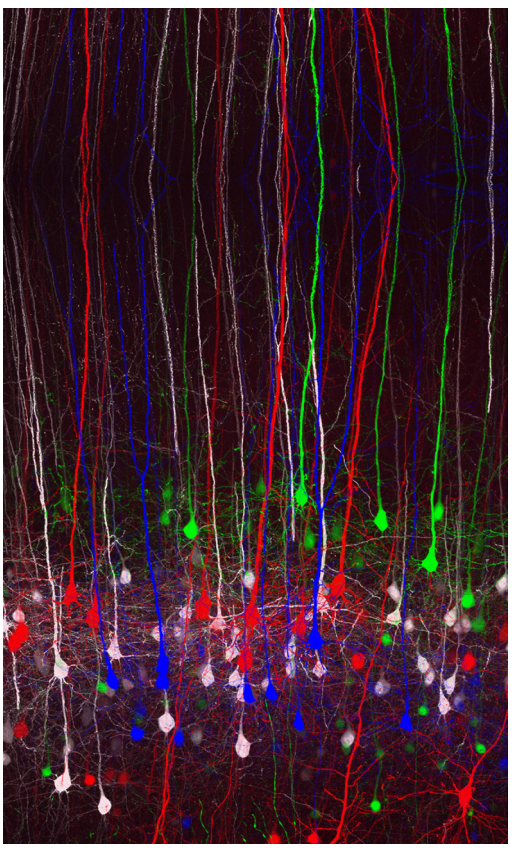

False-colored montage of fluorescently-labeled pyramidal neurons in the cortex of a Thy1-YFPH transgenic mouse. Image provided by Drs. Andrew Garrett and Joshua Weiner, taken from work reviewed in Weiner and Jontes (2013), part of this e-book.

Table of Contents

05 ***Introduction to Mechanisms of Neural Circuit Formation***
Joshua A. Weiner, James D. Jontes and Robert W. Burgess

07 ***Wired for Behaviors: From Development to Function of Innate Limbic System Circuitry***
Katie Sokolowski and Joshua G. Corbin

22 ***Protocadherins, not Prototypical: A Complex Tale of their Interactions, Expression and Functions***
Joshua A. Weiner and James D. Jontes

32 ***Molecular Codes for Neuronal Individuality and Cell Assembly in the Brain***
Takeshi Yagi

43 ***Direct and Indirect Regulation of Spinal Cord Ia Afferent Terminal Formation by the γ-Protocadherins***
Tuhina Prasad and Joshua A. Weiner

55 ***DSCAMs: Restoring Balance to Developmental Forces***
Andrew M. Garrett, Abigail L. D. Tadenev and Robert W. Burgess

62 ***Neural Cell Adhesion Molecule, NCAM, Regulates Thalamocortical Axon Pathfinding and the Organization of the Cortical Somatosensory Representation in Mouse***
Lilian Enriquez-Barreto, Cecilia Palazzetti, Leann H. Brennaman, Patricia F. Maness and Alfonso Fairén

75 ***Guidance of Longitudinally Projecting Axons in the Developing Central Nervous System***
Nozomi Sakai and Zaven Kaprielian

89 ***RhoA is Dispensable for Axon Guidance of Sensory Neurons in the Mouse Dorsal Root Ganglia***
Jennifer R. Leslie, Fumiyasu Imai, Xuan Zhou, Richard A. Lang, Yi Zheng and Yutaka Yoshida

98 ***Semaphorin Signaling in Vertebrate Neural Circuit Assembly***
Yutaka Yoshida

114 ***Fibroblast Growth Factor 22 Contributes to the Development of Retinal Nerve Terminals in the Dorsal Lateral Geniculate Nucleus***
Rishabh Singh, Jianmin Su, Justin Brooks, Akiko Terauchi, Hisashi Umemori and Michael A. Fox

127 ***Presynaptic Active Zone Density During Development and Synaptic Plasticity***
Gwenaëlle L. Clarke, Jie Chen and Hiroshi Nishimune

139 ***Synaptic Clustering During Development and Learning: The why, when, and how***
Johan Winnubst and Christian Lohmann

148 ***Cortical Development of AMPA Receptor Trafficking Proteins***
Kathryn M. Murphy, Lilia Tcharnaia, Simon P. Beshara and David G. Jones

160 ***Generation of Neuromuscular Specificity in Drosophila: Novel Mechanisms Revealed by New Technologies***
Akinao Nose

171 ***Transgenic Strategy for Identifying Synaptic Connections in Mice by Fluorescence Complementation (GRASP)***
Masahito Yamagata and Joshua R. Sanes

frontiers in
MOLECULAR NEUROSCIENCE

EDITORIAL
published: 13 May 2013
doi: 10.3389/fnmol.2013.00012

Introduction to mechanisms of neural circuit formation

Joshua A. Weiner[1], James D. Jontes[2] and Robert W. Burgess[3]*

[1] *Department of Biology, University of Iowa, Iowa City, IA, USA*
[2] *Department of Neuroscience, The Ohio State University, Columbus, OH, USA*
[3] *The Jackson Laboratory, Bar Harbor, ME, USA*
**Correspondence: robert.burgess@jax.org*

Edited by:
Robert J. Harvey, UCL School of Pharmacy, UK

Reviewed by:
Robert J. Harvey, UCL School of Pharmacy, UK

Much progress has been made in recent years toward understanding the underlying causes of neurodevelopmental disorders. Whereas catastrophic failures in early events such as cell fate specification or cell migration give rise to profound developmental defects including microcephaly and lissencephaly, more subtle conditions such as autism, intellectual disability or neuropsychiatric disorders increasingly appear to result from comparatively minor changes in neural circuit formation and function. The formation of proper neuronal circuitry relies on later developmental processes such as axon guidance, the arborization both of axons and their target dendrites, the recognition of appropriate synaptic partners, the establishment and maturation of synaptic connections, and the subsequent elimination of improper connections. The research topic presented here, "Mechanisms of Neural Circuit Formation," addresses recent advances in our understanding of the cellular and molecular bases of these processes.

The papers in this volume generally fall into three broad areas of developmental neurobiology, including new techniques for the study of these processes: (1) cell adhesion molecules (CAMs) and their downstream roles in cell identity, recognition, and synaptic specificity; (2) axon guidance, formation of terminals, and dendritic arborization; and (3) formation of synaptic structures themselves, the essential final step in circuit formation which, nevertheless, remains subject to remodeling and plasticity throughout development and even in adult animals.

The volume opens with a review by Sokolowski and Corbin (2012), highlighting the importance of neuronal circuit formation for behavior through an examination of the development of the limbic circuitry. This is followed by a series of papers on CAMs: a review from Weiner and Jontes (2013), and a hypothesis paper from Yagi (2012) that describe the roles of protocadherins. These are followed by the new results of Prasad and Weiner (2011) on a requirement for γ-protocadherins in Ia afferent terminal formation in the spinal cord. Next is a review from Garrett et al. (2012) on the immunoglobulin (Ig) superfamily proteins Down Syndrome Cell Adhesion Molecule and related proteins (DSCAMs), addressing issues of molecular diversity, cell identity and cell adhesion as they contribute to synapse and circuit formation. Finally, Enriquez-Barreto et al. (2012) present original research on the function of the Ig superfamily member Neural Cell Adhesion Molecule (NCAM) in axon pathfinding and organization in the thalamocortical system.

This last paper transitions into a section focused on axon guidance, including both signaling and cytoskeletal mechanisms. Sakai and Kaprielian (2012) review the literature on the guidance of longitudinally projecting axons, a prominent focus of study in both vertebrates and invertebrates. An original paper by Leslie et al. (2012), examines the requirement of RhoA in sensory axon guidance. The relationship of axon guidance mechanisms to other processes involved in synaptic specificity is highlighted in a review of semaphorin signaling by Yoshida (2012). Finally, the importance of FGF22 in axon termination and synaptogenesis in the lateral geniculate is demonstrated by Singh et al.'s original research (2012).

The penultimate group of papers concerns mechanisms regulating the formation of pre-and post-synaptic structures. The assembly and plasticity of the presynaptic active zone is reviewed in Clarke et al. (2012). A review from Winnubst and Lohmann (2012) discusses the mechanisms and implications for synaptic clustering on target neurons. An original research paper from Murphy et al. (2012) investigates the developmental regulation of AMPA receptor trafficking proteins.

The E-book closes with two papers describing powerful new techniques for studying neural circuit formation that are revealing novel biology both in Drosophila, as described by Nose (2012), and in mice, as described in Yamagata and Sanes (2012).

Together, these papers provide a broad reflection of the state of our knowledge concerning the molecular cues that direct axon and dendrite development, promote the formation of synaptic connections, and allow the refinement of connectivity and plasticity during development. An interesting observation that comes from these studies is that few, if any, of the key molecules are single-purpose; each pathway is used at distinct stages of neural development and serves multiple functions. The extent to which these functions relate varies. For example, semaphorins broadly influence both axonal and dendritic development, perhaps not surprisingly given the large number of different ligands and receptors involved. Fibroblast Growth Factor family members (FGFs), critical players in a wide variety of developmental events in the early embryo, are much later re-purposed to regulate the formation of synaptic circuitry. CAMs like the γ-protocadherins and DSCAMs, regulate several key processes, including neuronal survival, dendrite arborization, and axonal targeting; here, it remains unclear whether these functions are achieved through common signaling pathways, or whether they represent distinct roles for these CAMs. Thus, despite the daunting complexity of the task, the cast of key players is not increasing as rapidly as the number of roles assigned to each cast member. This could facilitate future progress by focusing efforts on a

smaller number of molecules. Conversely, efforts could be complicated by the need to dissect primary and secondary effects for each pathway. This highlights the need to be particularly rigorous in defining where, when and how the functions of these proteins are analyzed. As the methods and specificity of these analyses improve, so will our understanding of neural circuit formation.

Considering the finely-tuned complexity of the mature nervous system, the robustness of neurodevelopment is amazing; despite genetic and environmental variability during development, and the stochastic variation inherent in biological systems, most brains end up working pretty well. The experimental investigation of small circuits and defined aspects of neural circuit formation is facilitating progress in this area, as the papers in this volume demonstrate. However, a key challenge for the future is to integrate the information we are gaining on individual molecular pathways into a larger model in order to understand how the neural circuitry of the mature nervous system is assembled during development.

REFERENCES

Clarke, G. L., Chen, J., and Nishimune, H. (2012). Presynaptic active zone density during development and synaptic plasticity. *Front. Mol. Neurosci.* 5:12. doi: 10.3389/fnmol.2012.00012

Enriquez-Barreto, L., Palazzetti, C., Brennaman, L. H., Maness, P. F., and Fairén, A. (2012). Neural cell adhesion molecule, NCAM, regulates thalamocortical axon pathfinding and the organization of the cortical somatosensory representation in mouse. *Front. Mol. Neurosci.* 5:76. doi: 10.3389/fnmol.2012.00076

Garrett, A. M., Tadenev, A. L. D., and Burgess, R. W. (2012). DSCAMs: restoring balance to developmental forces. *Front. Mol. Neurosci.* 5:86. doi: 10.3389/fnmol.2012.00086

Leslie, J. R., Imai, F., Zhou, X., Lang, R. A., Zheng, Y., and Yoshida, Y. (2012). RhoA is dispensable for axon guidance of sensory neurons in the mouse dorsal root ganglia. *Front. Mol. Neurosci.* 5:67. doi: 10.3389/fnmol.2012.00067

Murphy, K. M., Tcharnaia, L., Beshara, S. P., and Jones, D. G. (2012). Cortical development of AMPA receptor trafficking proteins. *Front. Mol. Neurosci.* 5:65. doi: 10.3389/fnmol.2012.00065

Nose, A. (2012). Generation of neuromuscular specificity in Drosophila: novel mechanisms revealed by new technologies. *Front. Mol. Neurosci.* 5:62. doi: 10.3389/fnmol.2012.00062

Prasad, T., and Weiner, J. A. (2011). Direct and indirect regulation of spinal cord ia afferent terminal formation by the γ-protocadherins. *Front. Mol. Neurosci.* 4:54. doi: 10.3389/fnmol.2011.00054

Sakai, N. and Kaprielian, Z. (2012). Guidance of longitudinally projecting axons in the developing central nervous system. *Front. Mol. Neurosci.* 5:59. doi: 10.3389/fnmol.2012.00059

Singh, R., Su, J., Brooks, J., Terauchi, A., Umemori, H., and, Fox, M. A. (2012). Fibroblast growth factor 22 contributes to the development of retinal nerve terminals in the dorsal lateral geniculate nucleus. *Front. Mol. Neurosci.* 4:61. doi: 10.3389/fnmol.2011.00061

Sokolowski, K., and Corbin, J. G. (2012). Wired for behaviors: from development to function of innate limbic system circuitry. *Front. Mol. Neurosci.* 5:55. doi: 10.3389/fnmol.2012.00055

Weiner, J. A., and Jontes, J. D. (2013). Protocadherins, not prototypical: a complex tale of their interactions, expression, and functions. *Front. Mol. Neurosci.* 6:4. doi: 10.3389/fnmol.2013.00004

Winnubst, J., and Lohmann, C. (2012). Synaptic clustering during development and learning: the why, when, and how. *Front. Mol. Neurosci.* 5:70. doi: 10.3389/fnmol.2012.00070

Yagi, T. (2012). Molecular codes for neuronal individuality and cell assembly in the brain. *Front. Mol. Neurosci.* 5:45. doi: 10.3389/fnmol.2012.00045

Yamagata, M., and Sanes, J. R. (2012). Transgenic strategy for identifying synaptic connections in mice by fluorescence complementation (GRASP). *Front. Mol. Neurosci.* 5:18. doi: 10.3389/fnmol.2012.00018

Yoshida, Y. (2012). Semaphorin signaling in vertebrate neural circuit assembly. *Front. Mol. Neurosci.* 5:71. doi: 10.3389/fnmol.2012.00071

Received: 11 April 2013; accepted: 26 April 2013; published online: 13 May 2013.

Citation: Weiner JA, Jontes JD and Burgess RW (2013) Introduction to mechanisms of neural circuit formation. Front. Mol. Neurosci. ***6****:12. doi: 10.3389/fnmol.2013.00012*

frontiers in
MOLECULAR NEUROSCIENCE

REVIEW ARTICLE
published: 26 April 2012
doi: 10.3389/fnmol.2012.00055

Wired for behaviors: from development to function of innate limbic system circuitry

Katie Sokolowski and Joshua G. Corbin*

Children's National Medical Center, Center for Neuroscience Research, Children's Research Institute, Washington, DC, USA

Edited by:
Robert W. Burgess, The Jackson Laboratory, USA

Reviewed by:
Erik Maronde, University of Frankfurt, Germany
Hansen Wang, University of Toronto, Canada

****Correspondence:***
Joshua G. Corbin, Children's National Medical Center, Center for Neuroscience Research (CNR), Children's Research Institute, 111 Michigan Avenue, NW, Washington, DC 20010-2970, USA.
e-mail: jcorbin@cnmcresearch.org

The limbic system of the brain regulates a number of behaviors that are essential for the survival of all vertebrate species including humans. The limbic system predominantly controls appropriate responses to stimuli with social, emotional, or motivational salience, which includes innate behaviors such as mating, aggression, and defense. Activation of circuits regulating these innate behaviors begins in the periphery with sensory stimulation (primarily via the olfactory system in rodents), and is then processed in the brain by a set of delineated structures that primarily includes the amygdala and hypothalamus. While the basic neuroanatomy of these connections is well-established, much remains unknown about how information is processed within innate circuits and how genetic hierarchies regulate development and function of these circuits. Utilizing innovative technologies including channel rhodopsin-based circuit manipulation and genetic manipulation in rodents, recent studies have begun to answer these central questions. In this article we review the current understanding of how limbic circuits regulate sexually dimorphic behaviors and how these circuits are established and shaped during pre- and post-natal development. We also discuss how understanding developmental processes of innate circuit formation may inform behavioral alterations observed in neurodevelopmental disorders, such as autism spectrum disorders, which are characterized by limbic system dysfunction.

Keywords: innate, limbic system, development, olfaction, amygdala, hypothalamus, behaviors

INTRODUCTION

The limbic system links external cues possessing emotional, social, or motivational relevance to a specified set of contextual and species-specific appropriate behavioral outputs. While a fair amount of these behaviors are enhanced through experiential learning and reinforcement, a number of these behaviors are innate or inborn, meaning that they manifest without prior learning. These innate behaviors include courtship, maternal care, defense (both to conspecific and predator cues) and establishment of social hierarchy, all of which ensure survival of the individual or offspring and propagation of the species. These behaviors are regulated and influenced by sensory stimuli such as touch, sound, and, most importantly in rodents, smell. An animal's inability to correctly detect or process social or environmental cues results in abnormal social behaviors and increases risk of attack and/or predation. In humans, abnormal development of aspects of innate behavior, most prominently circuits that regulate social behavior, appear to underlie disorders such as autism spectrum disorders and schizophrenia that are characterized by inappropriate or altered social interactions.

Until relatively recently, humans were the only species thought to possess emotion. Initially documented by Papez (1937) and elaborated by MacLean (1949), social cognition occurs through a complex neural network of interconnected structures, which includes areas in the ventromedial aspect of the temporal and frontal lobes, and their connections with the hypothalamus and brainstem. This neural network, dubbed the "limbic system" is centered around the amygdala, a small almond shaped structure located deep within the temporal lobe. Emotional salience, produced in the amygdala, is generally thought of as a prime driving force behind innate human behaviors, typically social in nature (Brothers, 1989; Barbas, 1995; Aggleton, 2000; LeDoux, 2012). As the scientific community accepted emotions such as fear, anxiety, reward, and attraction as a result of neural wiring in humans, other species including rodents were gradually accepted as possessing similar circuits and, therefore, similar emotions (see **Figure 1** for comparison of human and rodent limbic system structures). Since the realization that emotions are not exclusively human, understanding the neural circuits involved in processing emotions and other social cues has advanced rapidly through the use of experimental rodent models. In rodent models, emotional states (e.g., fear, anxiety, and social receptivity) are generally quantified by their behaviors. When translating from rodent models to humans, it is important to understand that the sensory inputs of rodents are primarily olfactory, auditory, and somatosensory, with minimal visual inputs. Therefore, in this review we focus primarily on chemosensation in the rodent and how it relates to innate limbic responses to social conspecific cues such as mating, maternal care, and territorial behaviors as well as non-social defensive responses to predator cues.

NEUROANATOMY OF INNATE BEHAVIORS

Most of our knowledge of the circuitry that regulates innate behaviors has come from structural or cellular loss-of-function lesion and cytotoxic injury approaches. However, as the collection of brain regions within the innate circuitry contains a number of

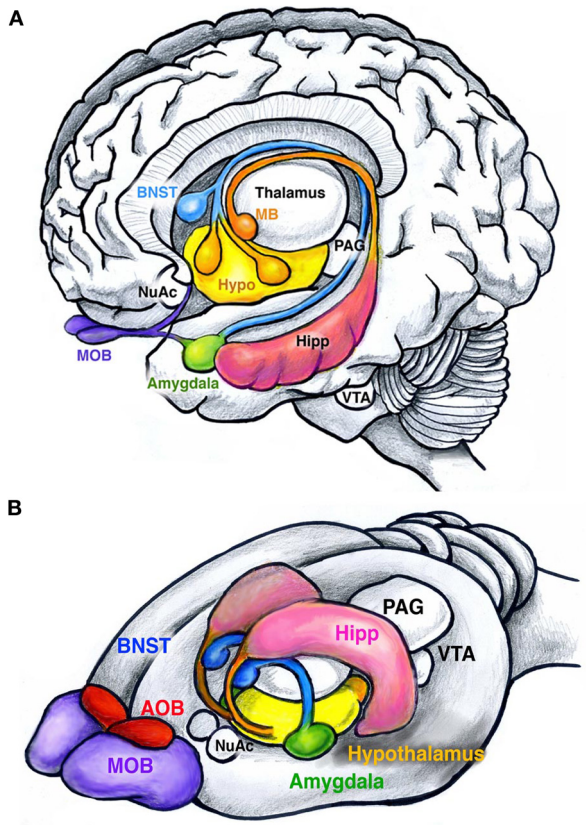

FIGURE 1 | Main structures of the human and rodent limbic system. **(A)** Human brain showing the amygdala (green), bed nucleus of stria terminalis (BNST, blue), hypothalamus (yellow), and hippocampus (pink). The hippocampus (pink) attaches to the mamillary bodies (orange) through the fimbria-fornix. Olfactory inputs are received by the olfactory bulbs (MOB, purple). Other structures include the nucleus accumbens (NuAc), ventral tegmental area (VTA), and the periaqueductal gray (PAG). **(B)** Similar structures are found in rodents. Note the enlarged olfactory bulbs compared to humans, and the presence of the accessory olfactory bulbs (AOB, red). Together these structures facilitate the execution and reinforcement of innate behaviors.

intertwined fibers of passage, lesion studies by their very nature are limited in their ability to discern the function of discrete nuclei from other connected brain regions. Despite this drawback, these types of classical studies have painted a relatively consistent picture of the major structures that comprise innate circuitry. These structures include the main and accessory olfactory system, olfactory/piriform cortex, amygdala, bed nucleus of stria terminalis (BNST) and hypothalamus (Swanson, 2000; Dulac and Wagner, 2006) (see **Table 1** for abbreviations).

Many behaviors such as fear/aversion to predator odors and reward/attraction to odors of the opposite sex are considered to be innate, meaning no prior learning is needed for their manifestation. For example, a naïve female rodent shows preference to male urine odors over female or no odors (Drickamer, 1992; Sawrey and Dewsbury, 1994). Similarly, a laboratory rat or mouse that has never encountered a predator of any kind will display stereotypical signs of fear and avoidance in response to predator odors (Apfelbach et al., 2005). Specific fear responses are also initiated by the detection of alarm pheromones thought to be emitted from dead or stressed conspecifics. These alarm pheromones are detected in the Grueneberg Ganglion, located in the tip of the rodent nose (Brechbühl et al., 2008). With the exception of alarm pheromones, innate responses have been tied to specific chemicals (Papes et al., 2010; Ferrero et al., 2011; Isogai et al., 2011) that are detected by two organs in the nose: the vomeronasal organ (VNO) and to a lesser extent the main olfactory epithelium (MOE). The VNO, located in the palate, primarily detects non-volatile chemicals such as pheromones with high specificity, while the MOE located on turbinates deep in the nasal cavity, detects volatile chemicals. Sensory input from the VNO and MOE are received by and processed in the accessory olfactory bulb (AOB) and main olfactory bulb (MOB), respectively. Projections from the AOB and MOB directly or indirectly synapse on a number of higher order structures including the olfactory/piriform cortex and amygdala. The amygdala is generally believed to be a central processing station where the level of salience is imparted to a given stimulus (or stimuli) (LeDoux, 1993). The amygdala then sends projections to the hypothalamus for further integration and coordination with the brain stem to initiate the body's "fight or flight" responses (e.g., increase in blood pressure, respiratory rate, etc.) (Swanson and Petrovich, 1998). Although we will focus our attention on the VNO-AOB-amygdalar-BNST-hypothalamic circuit (see **Figure 2**), the main components of the innate circuit, we would like to emphasize that these brain hubs and their many feedback loops are not the sole components of a highly complex neural network important for the regulation of sociability and innate emotions. We begin by summarizing what is currently known regarding the neuroanatomy of circuits for olfactory-based reproductive, maternal care, predator defense and conspecific defense (aggression) rodent innate behaviors and the individual functions of these nuclei in information processing.

MATING BEHAVIORS

Mating behaviors in males and females consist of two phases: the initial appetitive phase followed by the consummatory phase. In males the appetitive phase includes angiogenital chemoinvestigation, or sniffing, of the female. Pheromonal stimulation of the VNO-AOB olfactory system is relayed to the medial amygdala (MeA), usually via direct connections (Meurisse et al., 2009; Kang et al., 2011). The MeA acts as a hub, dispersing the signal to the BNST, and to anatomically segregated subsets of nuclei of the hypothalamus including the medial preoptic nucleus (mPN), ventrolateral portion of the ventromedial hypothalamus (VMHvl) and ventral premammillary nucleus (PMNv) (Emery and Sachs, 1976). Lesion studies have found the mPN of the hypothalamus to be intimately tied to female preference and pursuit (Kondo and Arai, 1995; Been and Petrulis, 2010). The mPN integrates inputs from the MeA either directly or via the BNST to increase dopamine levels (Newman, 1999; Hull and Dominguez, 2006; Balthazart and Ball, 2007). The mPN then signals to the ventral tegmental area (VTA) and nucleus accumbens (NuAc) to initiate appetitive phase responses such as sniffing. The same circuit (VNO-AOB-MeA-BNST-mPN) also controls consummatory phase behaviors such as mounting, intromission and

Table 1 | Abbreviations of limbic structures and summary of their role in innate behaviors.

Summary of abbreviated anatomical regions		
AH	Anterior hypothalamus	Involved in predator defense/fear and pup aversion; afferents and efferents from/to VMHdm in predator defense circuit
AOB	Accessory olfactory bulb	Receives afferents from VNO and projects to limbic structures including amygdala; main relay for innate behaviors
BNST	Bed nucleus of stria terminalis	Limbic structure with afferents from amygdala and projects to hypothalamus; associated with mating and maternal behavior
MeA	Medial amygdala	Receives afferents from the olfactory bulbs and provides emotional tag to information; projects to BNST and hypothalamus
MeApd	Posterior dorsal MeA	*Lhx6*+, *Lmo3*+ cells; mating/conspecific defense; projects to mPOA/VMHvl
MeApv	Posterior ventral MeA	Involved in predator defense; projects to VMHdm
MeAvl	Ventral lateral MeA	*Lhx9*+ cells; predator defense; projects to VMHdm; may inhibit VMHvl
MOB	Main olfactory bulb	Receives afferents from MOE and projects to limbic structures
MOE	Main olfactory epithelium	Detects volatile chemical cues; olfactory receptor neurons in the MOE project to MOB
NuAc	Nucleus accumbens	Part of the appetitive phase of mating and maternal care; receives afferents from the mPOA
PAG	Periaqueductal gray	Part of the consummative phase of innate behaviors (mating, maternal, and defense)
PMN	Premammillary nucleus	A posterior hypothalamic nuclei involved in innate behaviors
PMNd	Dorsal PMN	Conspecific defense, afferents from VMHvl/MeA, efferents to PAG
PMNv	Ventral PMN	Mating, afferents from MeA; and predator defense, afferents from VMHdm; projects to PAG
mPN	Medial preoptic nucleus	Conspecific defense, afferents from MeA; maternal care and mating, afferents from MeA/BNST; maternal care, efferent to VTA/PAG; mating, efferents to VTA/NuAc and VMHvl
POA	Embryonic preoptic area	Ventral telencephalic domain just below the MGE, major source of projection neurons destined for the MeA
PVN	Paraventricular nucleus	Alar domain of the hypothalamus. Embryonic PVN progenitors express *Sim1*
VMH	Ventral medial hypothalamus	Involved in mating and defensive behaviors; stimulated by projections from MeA directly or via mPN
VMHdm	Dorsal medial VMH	Involved in predator defense, afferents from MeApv, efferents to PMNv
VMHvl	Ventral lateral VMH	Mating, afferents from mPN; conspecific defense, afferents from MeA
VNO	Vomeronasal organ	Detects nonvolatile pheromones via V1R and V2R receptors. Olfactory receptor neurons in the VNO project to AOB
VTA	Ventral tegmental area	Part of the appetitive phase of mating and maternal care receives afferents from the mPN

ejaculation via afferents to VMHvl and then areas of the midbrain and spinal cord: periaqueductal gray (PAG), nucleus paragiganta and finally the lumbosacral spinal cord (see **Figure 3A**) (Marson, 2004; Normandin and Murphy, 2011a,b).

Female innate reproductive behaviors can be initiated through the same olfactory-amygdala circuit as males. Both the appetitive phase and consummatory phase of female mating begins with pheromonal cues picked up by the VNO and MOE (Baum and Kelliher, 2009). Signals are then passed to MeA via the olfactory bulb (Kang et al., 2011). Afferents from the MeA connect to the mPN of the hypothalamus directly or via the BNST and PMNv in a similar fashion as in the male circuit. While the mPN controls both the appetitive and consummatory phase in males, the female mPN primarily influences appetitive responses such as approaching a male to mate or proceptive behaviors (ear twitching, running short distances away—"teasing"). However the mPN is upstream of female consummatory behaviors, explicitly lordosis, which is initiated in the VMHvl. Lesioning of the VMH results in a decrease in lordosis while electrical stimulation of this region produces lordosis in primed females out of context (no male present) (Pfaff and Sakuma, 1979). These brain regions, particularly the VMH, are highly influenced by the female's natural cycle of hormones (estrodiol and progesterone) (Blaustein et al., 1988; Petitti et al., 1992; Mani et al., 1994; Kow et al., 1995; Flanagan-Cato et al., 2001). Further supporting these lesioning studies, many of these regions also show increased expression of the activity-dependent intermediate early gene, cFos, after sexual behavior (Coolen et al., 1996). Female consummatory behaviors such as lordosis, similar to males, are also relayed to the PAG, nucleus paragiganta and the lumbosacral spinal cord (Lonstein and Stern, 1998).

Quite interestingly, disruption of particular portions of the above-mentioned reproductive circuit results in male behaviors in females or otherwise altered sexual behaviors. Specifically, surgical removal of the VNO or genetic deletion of *TRPC2*, a channel involved in translating pheromone reception into an electrical signal in olfactory receptor neurons, has been shown to increase male mounting behaviors toward other males (Leypold et al., 2002). Conversely, female mice without a functioning VNO ($TRPC2^{-/-}$ females) mount males (Leypold et al., 2002; Stowers et al., 2002). Moreover, in V1R receptor knockout (V1R receptors in the VNO identify physiological state of the animal) male mice display a decrease in mounts with females, and females display decreased maternal aggression (Del Punta et al., 2002). Despite these interesting findings, results to the contrary have been observed in studies directly probing the role of VNO in sex discrimination in mice and other rodents using either volatile (detected in MOE) or non-volatile (detected in the VNO) urinary

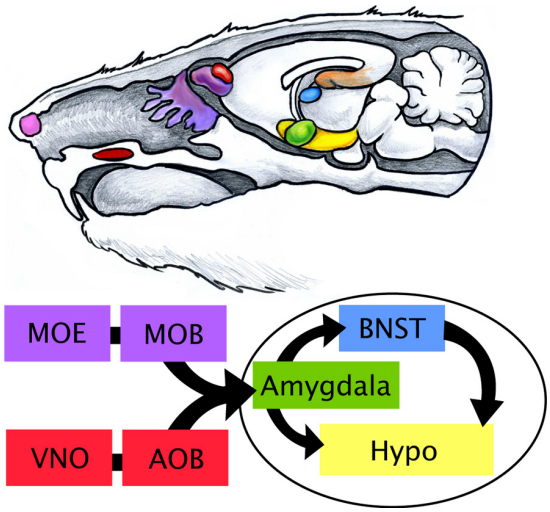

FIGURE 2 | Limbic processing of olfactory information in the rodent. The rodent limbic system is highly influenced by olfactory cues received by the main olfactory epithelium (MOE, purple) and vomeronasal organ (VNO, red). The Grueneberg ganglion (pink), which senses stress in conspecifics, is depicted in the tip of the rodent nose. The VNO, located on the palate, of the mouth detects non-volatile or lipophilic chemicals that are channeled by the tongue through a pore in the roof of the mouth. Volatile chemical scents are more readily aerosolized and travel further back into the nasal cavity to reach the MOE on the turbinates. Projections from sensory neurons in the VNO and MOE are received in the accessory olfactory bulb (AOB) and main olfactory bulb (MOB), respectively, located in the brain. Signal is then passed to other structures of the limbic system including the amygdala (green), bed nucleus of stria terminalis (BNST, blue), and hypothalamus (Hypo, yellow).

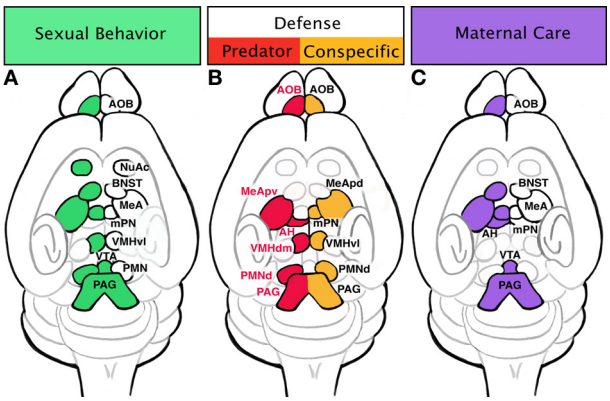

FIGURE 3 | Specific innate behaviors are controlled by distinct regions of the limbic system. (A) Sexual behaviors include activation of the vomeronasal organ (VNO), accessory olfactory bulb (AOB), and medial amygdala (MeA). Signal transduction from sensation to physical motivation is not always linear; once signal has reached the MeA, it is dispersed to a few areas: bed nucleus of stria terminalis (BNST), medial preoptic nucleus (mPN), and premammillary nucleus (PMN). The BNST will shunt signal from the MeA to the mPN. The mPN can activate appetitive behaviors (sniffing and pursuit) through innervation of the nucleus accumbens (NuAc) and ventral tegmental area (VTA). Additionally, the mPN passes information to the ventrolateral portion of the ventral medial hypothalamus (VMHvl), which in turn can initiate consummative behaviors through the periaqueductal gray (PAG) and spinal cord. Consummative behaviors such as mounting, intromission, and ejaculation can also be influenced by PMN inputs on the PAG and spinal cord. **(B)** Defensive behaviors trigger slightly different areas of the amygdala and hypothalamus depending if the stimulus is a predator or an animal of the same species (conspecific). Defense in response to a predator initiated in the AOB sends signals to the posterioventral MeA (MeApv), then to the dorsomedial portion of the ventral medial hypothalamus (VMHdm). The VMHdm will then cross-talks with the anterior hypothalamus (AH), an instance of bidirectional communication. The VMHdm, then signals to the ventrolateral portion of the dorsal PMN (PMNd), which then signals to the dorsolateral and dorsomedial PAG. Defense responses to a conspecific are initiated in the AOB which sends afferents directly to the anterior dorsal and posterior dorsal MeA (MeApd). The MeApd acts as a hub dispersing signal to three areas: mPN, VMHvl, and dorsomedial portion of the PMNd. The VMHvl will engage in cross-talk with the PMNd, which ultimately communicates with the dorsomedial and lateral PAG. **(C)** Maternal behavior circuit may begin in the AOB, which sends signal to the MeA. The MeA will send information to the mPN either directly or through the BNST. Pup avoidance is suppressed in the MeA and AH to initiate pup approach. Appetitive behaviors such as pup retrieval occur through activation of the VTA by the mPN. Consummative behaviors such as nursing are executed via activation of the PAG and spinal cord by the mPN.

odors as a stimulus (Beauchamp et al., 1982; Petrulis et al., 1999; Pankevich et al., 2004). When exposed to whole urine, mice with their VNO removed compensated by using their MOE to detect volatile discriminatory odors. Yet, mice lacking a VNO lose their discriminatory abilities when exposed exclusively to non-volatile odor elements of urine undetectable by the MOE (Keller et al., 2006). While these results reveal a partially redundant role for the MOE in sex discrimination, it appears clear that the VNO is central to the expression of appropriate sex-specific mating behaviors. Interestingly, other accounts of unusual feminization also occur by lesioning deeper portions of the male innate reproductive circuit. Lordosis, a female consummatory behavior, has been observed in males after lesioning the preoptic nucleus of the hypothalamus (Hennessey et al., 1986). Thus, appropriate sexual behavior appears to be controlled at multiple levels of the circuit, from pheromone detection in the VNO down to the hypothalamus and spinal cord.

DEFENSE/FEAR

Innate fear and the resulting defensive/aversive behaviors can be evoked by odors from predators, dominant conspecifics, or the "scent" of fear from a conspecific. Fear responses can be conditioned (learned) or unconditioned (innate). Rodents will innately respond with stereotypical fear behaviors when presented with the scent of stressed or dead mice. Detection of these conspecific alarm pheromones evokes freezing after stimulation of the Grueneberg ganglion cells (Brechbühl et al., 2008). Rodents also have an innate fear of cat and fox odors even in lab settings without prior exposure. Additionally for mice, there is an innate fear of rats, a natural predator of mice in the wild. Exposure to rat odors may induce flight, hiding, freezing, or risk assessment behaviors in mice as part of the unconditioned fear response (Blanchard et al., 2001). These unconditioned responses suggest an evolutionary "hardwiring" of circuits for such behaviors. Upregulation of cFos expression after introduction to predator odors has been documented in the posterior ventral medial amygdala (MeApv) and VMH (Canteras

et al., 1997). Similar to reproductive olfactory cues, predator odors appear to be processed more readily in the AOB as opposed to the MOB (McGregor et al., 2004). This also indicates the existence of "kairomones," a chemical emitted by one species that conveys information to another. Recent comprehensive mapping of receptor expression in conjunction with neuronal activation in the VNO has uncovered the receptor-based molecular code by which rodents identify cues associated with defense (predator and conspecific) and mating (Isogai et al., 2011). Perhaps the most striking finding of this study was the revelation that subsets of these receptors are solely dedicated to predator cues from individual species. Thus, in rodents the VNO appears to have evolved specifically to respond to cues that depend on the animal's survival in the wild, consistent with the notion that these circuits are largely hardwired. Downstream of the VNO, predator cues are processed in the AOB, and then conducted to the MeA (primarily the ventral aspect) and in turn feed directly to the dorsomedial portion of the VMH (VMHdm). However, as part of a conditioned fear response when context is dependent, cues are relayed from the hippocampus to the anterior nucleus of the hypothalamus (AH). Both the conditioned and innate fear response circuits converge on the dorsal premammillary nuclei (PMNd) of the hypothalamus which acts as an "amplifier" by triggering the pituitary and adrenal hormone release (Canteras et al., 1997; Dielenberg et al., 2001; Cezario et al., 2008) (see **Figure 3B**). Although a specific role in defense has not been found in the BNST, there are suggestions that it may modulate defensive rage and startle reflex (Dong and Swanson, 2004).

Similar endpoints, namely the PMNd, are involved in defense responses to dominant conspecifics. A common behavior test replicating a dominant conspecific scenario involves placing an "intruder" male in a "resident" male's cage. The resident male assumes a dominant role, threatening the intruder with posturing, biting, and attack. Interestingly, the medial hypothalamic circuitry of reproductive behaviors (VMH) is activated in the intruder, evidenced by increased cFos expression (Kollack-Walker and Newman, 1995; Kollack-Walker et al., 1999; Veening et al., 2005). However, in contrast to reproductive circuits, the defense response circuits converge on the "amplifier" of the predator aversion, the PMNd (Cezario et al., 2008; Motta et al., 2009). Intruders may react with passive (freezing) or active defense (rearing, boxing, or dashing away) in response to the approach of the resident. Lesioning of the PMNd results in decreases in passive defense while active defenses are maintained, suggesting the possibility that the intruder has a reduced fear of the dominant conspecific (Motta et al., 2009) (see **Figure 3B**).

MATERNAL CARE

Similar to reproductive behaviors, maternal care can be parsed into appetitive and consummatory phases, with appetitive behaviors including nesting and pup retrieval while consummatory behaviors consist of pup grooming and nursing. It has been suggested that there are two mechanisms at play during maternal behaviors: activation of pup attraction and repression of pup avoidance. Pup avoidance has been observed in unprimed virgin female mice. However, the natural avoidance response in these virgins can be damaged with lesions of the MeA, thus stimulating maternal care of pups (Numan et al., 1993). Likewise, lesioning the AH results in the same behavior (Sheehan et al., 2001), suggesting that pup olfactory cues are processed in both the MeA and AH (regions associated with predator fear response) to stimulate avoidance behaviors in young virgin rodents. The opposing circuit regulating pup attraction, is seeded within the mPN of the hypothalamus. The mPN expresses receptors for estrogen, prolactin, and oxytocin, suggesting it may be a major target of hormone activity (Rosenblatt et al., 1994; Consiglio and Bridges, 2009; Ruthschilling et al., 2012). Lesions of this area decrease pup retrieval and nest building in postpartum females, and cFos has been noted to increase in this region after maternal behaviors (Numan and Smith, 1984; Champagne et al., 2003). It is very likely that activation of the mPN by hormones causes an inactivation of the anterior hypothalamic avoidance behaviors in addition to activating the VTA and NuAc to initiate the appetitive phase and the PAG-lumbosacral spinal cord to advance consummatory behaviors (see **Figure 3C**) (Lonstein and Stern, 1998).

CIRCUIT CONTROL AND REGULATION

Through classical neuroanatomical approaches, we have now reached a stage at which the basic circuitry regulating reproductive, defensive and maternal care behaviors are generally established. More recent studies utilizing a combination of techniques at the vanguard of science are revealing the molecular underpinnings of circuit formation and function. For example, novel optogenetic techniques allow for the subtype-specific and temporal control of neuronal activity in order to elucidate the circuitry driving innate behaviors. In addition, we are also gaining a significantly greater understanding of not only the genes that are required for normal circuit formation and function, but also how non-cell autonomous stimuli such as hormones shape neuronal populations comprising innate circuits.

One of the first studies to correlate gene expression patterns to subsets of innate behaviors made use of reporter gene knock-in methodologies to trace projections of genetically marked neuronal subpopulations (Choi et al., 2005). By gene expression analysis it was revealed that anatomically distinct subsets of MeA populations differentially express combinations of the LIM-homeodomain containing genes (*Lhx5*, *Lhx6,* and *Lhx9*), genes which are known to endow neuronal identity across the neuraxis (Shirasaki and Pfaff, 2002). Interestingly, these marked populations seperately respond to different innate behavioral cues (reproductive or defensive). Specifically, *Lhx6+* neurons in the posterior dorsal MeA (MeApd) are almost exclusively activated by reproductive olfactory cues and project to an area of the hypothalamus involved in initiating mating behaviors, the ventral lateral portion of the ventral medial hypothalamus (VMHvl). Complimentary, *Lhx6−* cells in the posterior ventral MeA (MeApv) respond to predator odors and project to an area of the hypothalamus regulating defense, the dorsal medial portion of the ventral medial hypothalamus (VMHdm). Most surprisingly, molecular mapping also revealed that predator cue-responsive *Lhx6−* cells in the MeAvl also project to areas of the hypothalamus regulating reproductive behaviors, the VMHvl, an apparent contradiction. To reconcile this discrepency a model was put forth in which predator odor-activated *Lhx6−* cells can inhibit

the VMHvl, thereby suppressing reproductive behaviors, while simultaneously activating the VMHdm and initiating defensive behaviors (Choi et al., 2005).

Following this study, the same group more recently used optogenetic activation combined with pharmacological silencing of hypothalamic neurons to determine how mating and defensive behaviors are coordinated in the hypothalamus (Lin et al., 2011). Direct light stimulation of the neurons in the VMHvl expressing channel rhodopsin evokes mice to not only display the appropriate defensive behaviors to other males, but also inappropriately to females and inanimate objects (Lin et al., 2011). However, light-activation of this circuit during consummative mating behavior will not evoke aggression. Thus, utilizing state of the art approaches; both genetic and optogenetic, these studies revealed that the VMH collectively integrates information for apparently non-compatable behaviors (e.g., mating and defense/aggression). However, at what level these context-appropriate behavioral outputs are controlled by cross-talk between VMH subdivisions remains to be elucidated. This analysis also resolves previous apparently contradictory studies, which showed that the VMH is activated by both mating and aggression (Kollack-Walker and Newman, 1995; Kollack-Walker et al., 1999; Veening et al., 2005). These tools will also most likely prove invaluable for understanding how information is gated at the synaptic level as well as which genetic networks are involved in specification and function of these subcircuits.

The neural circuitry that regulates innate behaviors, perhaps more so than other brain circuits, are dramatically shaped by endocrine factors, primarily sex hormones such as testosterone and estrogen (Simerly, 2005). Both circulating and local brain levels of testosterone and estrogen are expressed in a sex-dependent manner act to refine the neural circuits involved in sexually dimorphic behaviors (Reviewed in Hill and Boon, 2009; Wu and Shah, 2011). Major structures of the limbic circuit (e.g., amygdala, BNST, mPN) express estrogen receptors in both females and males. In females, estrogen is the primary hormone in the induction of maternal care. Specifically, virgin female rats will inhibit their aversion and stimulate attraction to pups after supplementation with estrodiol, thereby behaving more like nursing females (Fleming, 1986). The role of estrogen is especially interesting in the context of development of the male brain. Recent work has revealed that estrogen is required for the development of sexual dimorphism in the amygdala and even male-specific defensive behaviors (Wu et al., 2009). In male brains, testosterone is converted to estrogen by the enzyme aromatase, which is found in select neurons of the MeA, BNST, and hypothalamus (Ogawa et al., 1998). Circulating levels of testosterone can be controlled experimentally through gonadalectomy; however, even castrated males generate estrogen from testosterone produced in the adrenals. Therefore, only genetic deletion of aromatase in male mice eliminates estrogen action, resulting in a complete loss of aggressive behaviors against intruder males. Supplementation with estradiol in aromatase-null males soon after birth restores intermale aggression, albeit mild compared to wild type males. However, estradiol replacement one week after birth does not restore male-typical aggression in aromatase-null males (Toda et al., 2001), suggesting a developmental time window in construction of the male neural circuit. These hormones also appear to regulate neuronal plasticity in the adult (Cooke et al., 2003; Cooke, 2006; Dugger et al., 2008; Morris et al., 2008). For example, estrogen affects alterations of dendritic morphology in the MeA (Gomez and Newman, 1991), which can alter the perception of external cues (Mohedano-Moriano et al., 2007). As mentioned before, the circuit controlling reproduction and defense occupy similar limbic nuclei, and influence conflicting behaviors (sexually receptivity or aggression) to a single stimulus (male approach) in females depending on her maternal/hormonal status. Thus, an alternative hypothesis is that the hormonal state of an animal influences the connectivity, thereby affecting behaviors.

While estrogens shape the programming of sexually dimorphic circuits, testosterone acting directly via the androgen receptor is required for the activation and modulation of components of male-typical displays such as mating, territorial aggression, and urine marking. In addition to dramatic anatomical changes such as decrease in angio-genital distance and visibility of a nipple line, genetic deletion of the androgen receptor in male mice causes reduced male-typical behaviors (Juntti et al., 2010). This is in contrast to estrogen receptor-null males, which never or rarely display aggressive behaviors. Therefore, while testosterone or the androgen receptor is not necessary for establishing the circuitry required for innate behaviors, it is necessary to modulate the degree of innate sex-specific behaviors. Thus, in both sexes neuroendocrines, such as estrogen and testosterone have important, but genetically separable functions, in shaping sexually dimorphic brain circuits and related innate behavior.

While much focus has been given to the role that sex hormones play in modulating behavior and associated circuits, a number of studies have also revealed important roles for non-sex hormones. The most prominent of the neuropeptides are oxytocin and vasopressin, which are expressed within the diencephalon and function throughout numerous telencephalic structures including the amygdala and BNST (Hammock and Young, 2006). As supported by a number of experimental lines of evidence, oxytocin, and vasopressin play key roles in promoting mating and bonding (both pair and maternal) behaviors. Indeed, oxytocin administration via nasal spray is currently under clinical trials in attempt to alleviate the social withdrawal associated with autism (Guastella and Macleod, 2012). However, aside from these well-characterized pathways, much still remains unknown regarding how genetic pathways work in concert with hormones to regulate the full repertoire of innate behaviors. Toward bridging this gap in understanding, a recent study by Xu et al. (2012) stands out. Using unbiased microarray transcriptome screening, validated with *in situ* hybridization expression analyses, they identified a novel cohort of genes expressed in a sexually dimorphic manner in the amygdala, BNST, and hypothalamus. While many of these genes were not previously implicated in sexually dimorphic behavior, expression of many were found to be modulated directly by hormone levels. Moreover, a battery of innate behavior tasks in mice mutant for one of four genes (*Brs3*, *Cckar*, *Irs4,* or *Sytl4*) revealed specific non-overlapping defects in aspects of male sexual behavior, intermale aggression, maternal behavior or female sexual behavior (Xu et al., 2012). Thus, it appears that

while hormonal influences modulate sexually dimorphic gene expression, distinct genetic modules control the complete pattern of sexually dimorphic innate behaviors. The results of this study also suggest that more sensitive screening methodologies such as RNAseq, will also be fruitful in identifying other components of genetic networks regulating the full cohort of innate behaviors.

EMBRYONIC PATTERNING OF THE INNATE LIMBIC SYSTEM AND POTENTIAL LINK TO BEHAVIOR

Since innate behaviors are established without prior experience, the regulatory circuitry must be established during embryonic or early post-natal stages of neurodevelopment, likely through a series of hierarchical stages of genetic programming. Below we review our current knowledge of innate limbic system development, and present a novel model in which innate behaviors are generated by a coordination of genetic expression events and environmental (hormonal) cues.

Birth dating studies in labeled neurons reveal that the vast majority of neurons that comprise the innate limbic system are generated during early embryonic neurogenesis, embryonic day 11–15 (E11–15) in mice (McConnell and Angevine, 1983). By late gestation, E18, most neurons dedicated for the limbic system (with the notable exception of subsets of olfactory bulb interneurons and hippocampal granule cells of the dentate gyrus which are generated throughout the lifetime of the animal) have migrated to their final locations in the brain and, in some cases, begun to make connections (Marín and Rubenstein, 2003; Batista-Brito and Fishell, 2009; Corbin and Butt, 2011). The early post-natal period is then primarily characterized by the elaboration of both short- and long-range connections and shaping of circuits via experience and, as described above, sex-specific hormonal levels. The embryonic events of neuronal patterning and specification of neurons throughout the entire neuraxis is accomplished via the actions of delineated sets of transcription factors, typically of the homeodomain and bHLH classes (Campbell, 2003; Wonders and Anderson, 2006; Corbin et al., 2008). These genes have been conserved through evolution and act in multiple species from fly and worm to mammals, underscoring their importance in neuronal development. As described below in more detail, embryonic developmental studies over the past decade have elucidated the "how" and "where" neurons of the limbic system are generated. Similar to what has been found in the spinal cord and forebrain, neuronal subtype identity in the limbic system appears to be established during the proliferative phase of embryogenesis before migration, suggesting this is a common mechanism used in the nervous system. This early endowment of identity implies that the remainder of development may largely be dedicated to carrying out a genetically predetermined program of migration, differentiation, synaptogenesis and maturation. Therefore, understanding development, especially the genetic mechanisms by which diverse types of neurons are specified, will likely have broad implications for understanding behaviors.

DEVELOPMENT OF THE MOE AND VNO

Neurons that comprise the structures of the innate limbic system are generated within the first two weeks of gestation. The innate circuit begins with the peripheral olfactory sensory neurons, also called receptor neurons, that reside in two areas of the rostrum: MOE and VNO. In rodents, the MOE covers the surface of the convoluted ethmoid turbinates formed during the first two weeks of gestation when the nasal cavity begins to develop from the olfactory placodes, which indent forming the olfactory pits. The olfactory pits deepen and eventually fuse to form the primitive nasal cavity and ventral margins of the embryonic nasal septum between E12–13 (Herbert and Leininger, 1999). The VNO develops from bilateral invaginations of the olfactory epithelium in the ventral anterior portion of the developing nasal septum. By E15 the VNO is completely formed, however studies have suggested that it is not fully functional until after post-natal development (Coppola et al., 1993), and thus may be highly influenced by early olfactory cues.

Olfactory epithelial neurons arise from the olfactory placode and have recently been shown to be in part neural crest-derived (Katoh et al., 2011). Studies investigating lineage determination and differentiation of olfactory sensory neurons have implicated the bHLH transcription factors *Mammalian Achaete Scute Homology 1* (*Mash1*) and *Neurogenin1* (*Ngn1*) as important factors for epithelial neuronal specification. *Mash1* appears to be required for the generation of the deeper layer of the olfactory epithelial neurons, while *Ngn1* regulates genes that fine-tune the neuronal lineage to a more differentiated fate (Cau et al., 2002). *Ngn1*+ progenitors will terminally differentiate into olfactory sensory neuron precursors, which then express other factors such as Neuronal cell adhesion molecules (NCAMs) that may play a role in the final stages of synapse formation (Calof et al., 2002). As a single olfactory sensory neuron matures, it will express a single olfactory receptor type, which detects a specific chemical cue (Malnic et al., 1999). During fetal development, olfactory receptor genes are turned on synchronously in a spatially restricted manner, establishing zones (Strotmann et al., 1995; Sullivan et al., 1995). The MOE is broken into four zones (I–IV), each of which connect to respective domains in the (MOB) and have distinct transcriptional expression. For example, the transcription factor *Osp94* is expressed solely in zone 1 and 2, while *PAPS-S2* is only expressed in zones 3 and 4 of the dorsal olfactory epithelium (Tietjen et al., 2005). Similarly, the VNO is segregated into two zones or domains, apical and basal, which correlate with receptor type. Receptor neurons residing in the apical layer of the VNO express V1 receptors that primarily detect physiological state of conspecifics and predators (e.g., pregnant, stressed), while sensory neurons in the basal layer express V2R that detect sex and species signatures (male, female, fox, cat) (Dulac and Torello, 2003; Papes et al., 2010).

Axons of olfactory receptor neurons project a long distance into the brain to reach their target, the olfactory bulbs. In contrast to the peripherial olfactory epithelium, the olfactory bulbs are considered a forebrain structure and represent the most rostral aspect of the telencephalon. The olfactory bulbs arise from the rostral pallium (cortical region) of the telecephalon and can be distinguished as early as E13.5 in the mouse. The zonal specification in the MOE may act as a guide map for axons to their target glomeruli. Glomerulization or glomerulogenesis is estimated to occur over several days (E12–P7) (Royal and Key, 1999)

through a hierarchical process (Miller et al., 2010), establishing a discrete topography (Luo and Flanagan, 2007). That is, olfactory sensory epithelial neurons expressing the same receptor type innervate common glomeruli in the olfactory bulb. The mechanisms by which these axons find their glomerular targets in the olfactory bulb has been suggested to be broken into two stages: general and specific targeting. General or pre-targeting from zone in MOE to appropriate domain in MOB has been shown to be influenced by zonal expression of the olfactory cell adhesion molecules (OCAMs) (Yoshihara et al., 1997; Reviewed in Yoshihara and Mori, 1997; Alenius and Bohm, 2003). The specific targeting mechanism of axons into a glomerulus has been suggested to be driven by the olfactory receptor itself where a mechanism downstream of the actual olfactory receptors enables fasciculation of axons that express similar receptors (Reviewed in Mombaerts, 2001, 2006; Imai et al., 2009; see also Yoshihara et al., 1997; Imai and Sakano, 2007, 2009). Specifically, olfactory receptors provide the means for axon-axon interaction by acting through G-coupled receptors to generate a unique level of cAMP, which subsequently regulates the expression of guidance factors: Nrp1 and Sema3A (Reviewed in Imai and Sakano, 2009; see also Imai et al., 2009). More recently the Slit and Roundabout (Robo) families of axon guidance molecules, have been demonstrated to control pathfinding and targeting of olfactory axons to glomeruli in olfactory bulb. Indeed, refined targeting of olfactory receptor axons to appropriate glomeruli is pertubed in Slit1/2- or Robo1/2-null mice (Nguyen-Ba-Charvet et al., 2008). However, how this system interacts with the fine-tuning of connectivity via the olfactory receptors themselves remains unclear (Cho et al., 2007; Nguyen-Ba-Charvet et al., 2008).

DEVELOPMENT OF THE MOB AND AOB

The main output neurons of the MOB and AOB are the mitral cell. These neurons project to deeper brain structures through the lateral olfactory tract (LOT). Growth of axonal projections from the olfactory bulb to deeper brain regions occurs at embryonic stages: between E13 and birth. This process is concurrent with olfactory epithelial targeting of the bulb, suggesting that these guidance events are independent of each other and sensory inputs (López-Mascaraque et al., 1996). Axonal pathfinding of mitral axons to the olfactory cortex along the LOT is influenced by the function of cell adhesion molecules such as cartilage acidic protein-1B, later renamed lateral olfactory tract ushering substance (LOTUS). This occurs through the ability of LOTUS to suppress the natural repulsive activities of Nogo. LOTUS antagonistically binds Nogo receptor a1 (NRa1), thus blocking Nogo binding and allowing the LOT to fasiculate and find its target in the olfactory cortex. Deletion of LOTUS causes the defasiculation of LOT axons, an effect that is rescued by co-deletion of NRa1 (Sato et al., 2011). Many other factors including *Pax6* and ephrins also cooperate to form the olfactory circuit to the cortex (Nomura et al., 2006). In contrast, less is known about the development of olfactory projections that directly synapse in the amygdala, primarily due to insufficient markers of functionally distinct olfactory-limbic pathways. Effectors of axonal guidance from the MOB and AOB to other regions of the limbic system provide a challenging area of active research.

DEVELOPMENT OF THE AMYGDALA

The development of the downstream targets of the olfactory system (amygdala and hypothalamus) has been the subject of recent intense investigation. Initial concepts into the development of these structures came primarily from comparative embryonic and post-natal anatomical studies. Although much of the amygdala and hypothalamus has been anatomically catalogued (Risold et al., 1994; Swanson and Petrovich, 1998; Swanson, 2000; Petrovich et al., 2001; LeDoux, 2007), relationships between embryonic primordia based on morphology only goes so far when attempting to correlate embryonic development to post-natal structures. This is due to the fact that many neuronal cell types within the brain are in fact generated far from the mature structures that they will eventually populate. Thus, initial hypotheses regarding simplified models of amygdala and hypothalamic development (Puelles and Rubenstein, 1993; Swanson and Petrovich, 1998) have recently been superseded by a more complex picture in which distinct embryonic progenitor zones (or niches) are dedicated for the generation of individual neuronal subtypes that subsequently migrate to these emerging structures (Marín and Rubenstein, 2003; Corbin and Butt, 2011).

With regard to the amygdala, extensive work has revealed that neuronal cell diversity is generated from two sets of progenitor pools: those that contribute neurons to multiple telencephalic structures (e.g., cerebral cortex, hippocampus) and those that are unique to the amygdala. The shared sources include aspects of the cerebral cortex, the ventrally located telencephalic ganglionic eminences [medial (MGE), lateral (LGE) and caudal (CGE)], as well as diencephalic sources (Nery et al., 2002; Remedios et al., 2007; García-Moreno et al., 2010; Bupesh et al., 2011; Cocas et al., 2011) (see **Figure 4**). Progenitor pools located within each of these domains express combinations of the homedomain and bHLH containing genes, *Lhx6*, *Nkx2.1*, *Gsx2*, *Mash1,* and *Ngn2*, just to name a few. As mentioned previously, differential expression of the LIM-homeodomain containing gene family marks anatomically segregated amygdalar efferent projections that separately regulate reproductive and defensive behaviors (Zirlinger et al., 2001; Choi et al., 2005). Interestingly, each amygdaloid nucleus expresses distinct patterns of LIM-homeodomain containing genes transiently during development. For example, the posterior dorsal medial amygdala (MeApd, associated primarily with reproductive behaviors) expresses *Lhx6* and *Lmo3*, the posterior ventral medial amygdala (MeApv, associated primarily with defensive behaviors) expresses *Lhx9*, and the dorsal anterior amygdala expresses *Lhx6*, *Lhx7,* and *Lmo3* (Remedios et al., 2004; Choi et al., 2005). Thus, the combinatorial expression patterns of LIM genes may provide a comprehensive mechanism for patterning the amygdala, reflecting a similarity with the LIM-code in the spinal cord.

In addition to these shared progenitor pools, there also exist embryonic progenitor pools that appear to be dedicated primarily for the amygdala. These include populations present at the pallial-subpallial border (PSB), the junction of apposition between the dorsal (pallial) and ventral (subpallial) telencephalon. These

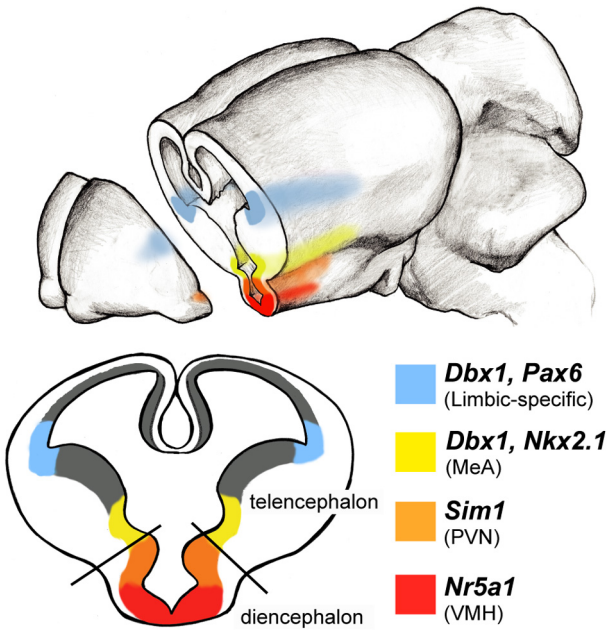

FIGURE 4 | Limbic system progenitor pools in the rodent embryonic brain. Schematic of a coronal view of an embryonic brain at midneurogenesis (~E14) reveals expression patterns of select transcription factors along the ventricular zones of the telencephalon and diencephalon. Combinatorial codes of transcription factor expression during embryogenesis determine the identity of neurons destined for various brain regions. A large portion of amygdala neuronal populations arise from two regions of the developing brain: the pallial-subpallial boundary (blue) and preoptic area (yellow) each of which express unique combinations of transcription factors. Areas of the hypothalamus also express regionally specific transcription factors: for example *Sim1* (orange) is expressed more dorsally to specify cells in the paraventricular nucleus (PVN), while *Nra51* (red) is expressed ventrally and specifies neurons in the ventral medial hypothalamus (VMH).

populations express combinations of the homeodomain genes *Pax6*, *Emx1*, *Gsx2,* and *Dbx1*, which collectively supply the entire population of excitatory neurons to the amygdala as well as the specialized intercalated interneuronal populations which gate fear conditioning and extinction. (Puelles et al., 2000; García-López et al., 2008; Xu et al., 2008; Hirata et al., 2009; Soma et al., 2009; Carney et al., 2010; Kaoru et al., 2010; Cocas et al., 2011).

Of the above-mentioned genes, the function of *Pax6* in amygdalar development has been the most explored. *Pax6* is required for *Gsx2*+ cells to form correct excitatory and inhibitory neuron populations in the amygdala and olfactory bulb (populations also likely derived from the PSB) (Cocas et al., 2011). Moreover, *Pax6* cooperates with the nuclear receptor *Tailess* (*Tlx*) to form the PSB (Stenman et al., 2003). *Tlx* mutants display reductions in region-specific gene expression in the ventral-most pallial regions and corresponding malformations in lateral and basolateral amygdala. Interestingly, *Tlx* mutants also display aggressive behavior, a phenotype that is consistent with amygdala dysfunction (Monaghan et al., 1997). Moreover, haplosufficient *Pax6* mutants that express only one functional copy display autistic-like social deficits (Umeda et al., 2010), supporting an important role of these genes in amygdalar development. In addition to the PSB, the *Dbx1*+ progenitor pool located in the embryonic preoptic area (POA), a ventral telencephalic domain just below the MGE, is a major source of projection neurons destined specifically for the MeA (Hirata et al., 2009). Interestingly, these neurons are homogeneous by electrophysiological and molecular criteria, and electrophysiologically and molecularly distinct from *FoxP2*+ neighboring MeA neurons (Hirata et al., 2009; Carney et al., 2010). This genetic parcellation of MeA neuronal cell types suggest that, consistent with the amygdala LIM-code (Choi et al., 2005), other genetically tagged populations may have separable functions in the processing of different innate behaviors.

DEVELOPMENT OF THE HYPOTHALAMUS

A major termination area of projections from the MeA is the hypothalamus. Similar to the amygdala, the hypothalamus is a nuclear structure comprised of separate nuclei with varying connections, neuronal compositions and separable functions in processing innate information. The hypothalamus is located in and arises from the ventral diencephalon, is visible as early as E9 and is clearly distinguished from the telencephalon at E12.5 both anatomically and molecularly. Similar to other regions of the central nervous system, a number of genes encoding transcription factors and secreted protein morphogens help to pattern and determine the regional specificity of the hypothalamus (Blackshaw et al., 2010). This molecular scaffolding that delineates progenitor domains of the hypothalamus can be categorized into two alar (paraventricular and subparaventricular areas) and three basal domains (tuberal hypothalamus, premammillary area and mamillary area). These domains lie along the longitudinal axis and are influenced by secreted factors such as Shh, Wnts, BMPs, and Fgf. In response to these secreted factors, cells in different developmental zones express a temporal and spatial fingerprint of transcription factors that pattern development of the subnuclei of the hypothalamus (Shimogori et al., 2010). For example, the bHLH-containing transcription factors *Sim1* and *Neurog2* and homeodomain-containing transcription factor *Otp*, delineate the embryonic paraventriclular area, which is the primordial of the supraopto-paraventricular nuclear complex in the dorsal hypothalamus (Fan et al., 1996; Puelles and Rubenstein, 2003; Shimogori et al., 2010). Loss-of-function studies have revealed that *Sim1* is required for the correct positioning of paraventricular neurons (Caqueret et al., 2006), while *Otp*-null mice fail to produce somatostatin, vasopressin, oxytocin, corticotropin-releasing hormone, thyrotropin-releasing hormone in the primordial periventricular, paraventricular, and supraoptic nuclei. These mice are not only devoid of these three hypothalamic nuclei but are non-viable after birth (Wang and Lufkin, 2000).

PROPOSED MODEL FOR CIRCUIT PATTERNING

Despite the above-described circuitry and the growing understanding of developmental mechanisms governing specification and migration of neurons, the link between developmental mechanisms, circuit formation and ultimately behavior remains to be clarified. There appears to be a common strategy to generate

neuronal diversity across the central nervous system, wherein the combinatorial expression of different transcription factors specifies regional- and subtype-specific neuronal identity. However, an open question is whether this process also encodes the molecular identity responsible for connectivity. Indeed, although experimental evidence is scarce, such a link has already been proposed in the spinal cord, in which a transcriptional matching code acts to instruct connections between specific sensory and motor neurons (Lin et al., 1998). Although the evidence for this within the brain is also highly circumstantial, it presents an attractive and simplified mechanism whereby developmental gene expression is utilized not only to direct cell fate, but also to pre-pattern circuit connectivity. In this model, in addition to patterning neuronal identity, key transcription factors encode subsets of genes, most likely cell adhesion molecules that would be required for limbic circuit specific connectivity (**Figure 5**). In support of this model in the innate limbic circuit are two provocative sets of observations. First, fate mapping and gene expression analyses have revealed that progenitor pools that generate neurons within known connected structures of the innate limbic system (e.g., olfactory system, amygdala, hypothalamus) express common sets of transcription factors whose general function in other parts of the brain and nervous system is to control neuronal identity. These genes include, for example, *FoxP2* and *Dbx1* (Hirata et al., 2009; Carney et al., 2010; Allen Brain atlas).

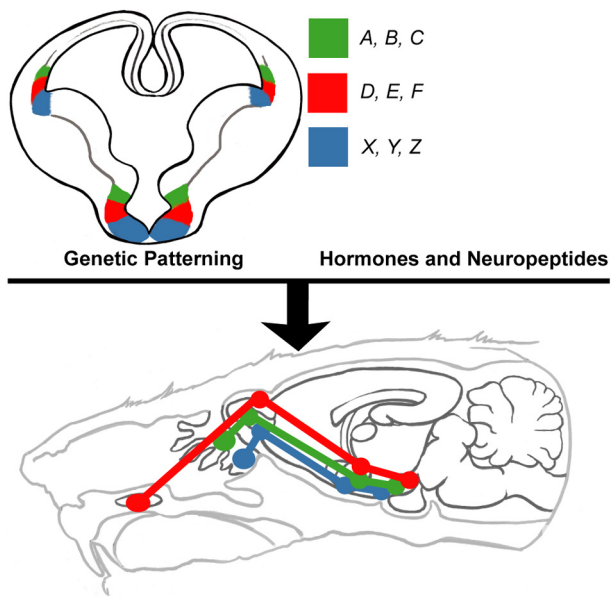

FIGURE 5 | Proposed model of innate limbic circuit development. In this model, combinations of select subsets of transcription factors (e.g., A, B, C) that endow neuronal identity also encode genes required for formation of connections (e.g., cadherins) with neurons located in other parts of the brain. Neurons destined to connect are derived from progenitors that express the same sets of transcription factors. Thus, developmentally regulated transcription factors are the driving force behind setting up complex circuits. This pre-patterned circuitry is then extensively shaped and modified by the actions of select hormones (e.g., testosterone and estrogen) and neuropeptides (e.g., oxytocin and vasopressin).

Second, there are multiple classes of cell adhesion molecules that specifically mark the interconnected limbic system. These include Limbic system associated membrane protein (Lsamp) as well as sets of cadherins (Redies and Takeichi, 1993; Mann et al., 1998; Pimenta and Levitt, 2004). A cadherin matching code for limbic connectivity is especially attractive as it has recently been shown that expression of the same subclasses of cadherin cell adhesion molecules are required for establishment of axon-target matching in other systems such as retinal to midbrain projections and intra-hippocampal connections (Hirano et al., 2002; Osterhout et al., 2011; Williams et al., 2011). In conjunction, other studies have found cadherin expression patterns to be regulated by *Pax6* (Stoykova et al., 1997). Thus, perhaps cadherin (or other cell adhesion molecules) codes, initially established by restricted expression of key "selector" transcription factors in the embryonic brain, produce a layout for limbic system connectivity.

LIMBIC CIRCUITS AND NEURODEVELOPMENTAL DISORDERS

In humans, the limbic system is intimately tied to emotion and social behaviors, and disruption of the genetic programming of limbic circuitry may be a prime mechanism underlying a variety of social disorders, such as autism spectrum disorders (Rodrigues et al., 2004; Amaral et al., 2008; Herry et al., 2008; Markram et al., 2008; Monk, 2008) including Fragile X and Rett syndrome (Hessl et al., 2007; Adachi et al., 2009). Therefore, using the mouse olfactory-limbic system to understand how an intricate circuit forms may greatly inform human disorders. Innate behaviors such as reproduction, aggression and fear all require assimilation of social cues to produce behaviors that ensure survival. Research in rodents and primates indicate the amygdala and surrounding anatomy play a critical role in innate behaviors and social cognition. Defects in amygdala growth, cellularity and function are consistently found in individuals on the autistic spectrum disorder (Baron-Cohen et al., 2000). Consistent with this, it will be highly informative to study the potential role of the hypothalamus in autism, a very understudied area of investigation.

In support of limbic-specific defects in autism, genes known to be involved in specific aspects of development of the limbic system have already been identified and validated as high-ranking autism susceptibility genes (see https://gene.sfari.org/autdb/Welcome.do. for autism linked gene annotation). One such well-studied gene is the receptor tyrosine kinase *Met* (Campbell et al., 2006, 2007). *In vitro* studies suggest that *Met* is required for GnRH migration from the nasal placode to the hypothalamus (Giacobini et al., 2007) and *Met* expression has been detected in key limbic areas: cortex, amygdala, hypothalamus, and septum. Expression temporally peaks at P14 in rodent, a period of extensive outgrowth and synaptogenesis (Judson et al., 2009). Curiously, *Met* can decrease arbor complexity (Gutierrez et al., 2004), increase growth and excitatory synapse formation (Tyndall and Walikonis, 2006), or increase motility of interneurons (Powell et al., 2003; Martins et al., 2011) all depending on the identity of the cultured cells (cortical, hippocampal or basal forebrain). This suggests that *Met* may integrate intrinsic programs and external cues that cooperate to form functional neural networks. Moreover, massive information obtained from human

genome wide association studies (GWAS) also implicates a number of cell adhesion molecules in autism, including multiple members of the cadherin family (Walsh et al., 2008). Although some of these genes may broadly regulate synapse formation and function across multiple domains of the nervous system (e.g., Neuroligin), quite interestingly others such as cadherin-10 (CDH10) appear to be limbic system specific (Bekirov et al., 2002; Wang et al., 2009). Therefore, unraveling the mechanisms of limbic system development will likely provide significant insight into the etiology of autism and related disorders of social cognition and create avenues of therapy for individuals afflicted by these disorders.

ACKNOWLEDGMENTS

We would like to thank Jason Triplett, Ph.D., and Sarah Ferrante for their valuble comments on the draft of this review. Additionally we thank Brandon Martin for his guidance in creating the anatomical figures. Work in the Corbin lab is funded by Autism Speaks and the NIH (RO1 DA020140 and ARRA supplement).

REFERENCES

Adachi, M., Autry, A. E., Covington, H. E. 3rd., and Monteggia, L. M. (2009). MeCP2-mediated transcription repression in the basolateral amygdala may underlie heightened anxiety in a mouse model of Rett syndrome. *J. Neurosci.* 29, 4218–4227.

Aggleton, J. (2000). *The Amygdala: A Functional Analysis,* 2nd Edn. New York, NY: Oxford University Press Inc.

Alenius, M., and Bohm, S. (2003). Differential function of RNCAM isoforms in precise target selection of olfactory sensory neurons. *Development* 130, 917–927.

Amaral, D. G., Schumann, C. M., and Nordahl, C. W. (2008). Neuroanatomy of autism. *Trends Neurosci.* 31, 137–145.

Apfelbach, R., Blanchard, C. D., Blanchard, R. J., Hayes, R. A., and McGregor, I. S. (2005). The effects of predator odors in mammalian prey species: a review of field and laboratory studies. *Neurosci. Biobehav. Rev.* 29, 1123–1144.

Balthazart, J., and Ball, G. F. (2007). Topography in the preoptic region: differential regulation of appetitive and consummatory male sexual behaviors. *Front. Neuroendocrinol.* 28, 161–178.

Barbas, H. (1995). Anatomic basis of cognitive-emotional interactions in the primate prefrontal cortex. *Neurosci. Biobehav. Rev.* 19, 499–510.

Baron-Cohen, S., Ring, H. A., Bullmore, E. T., Wheelwright, S., Ashwin, C., and Williams, S. C. (2000). The amygdala theory of autism. *Neurosci. Biobehav. Rev.* 24, 355–364.

Batista-Brito, R., and Fishell, G. (2009). The developmental integration of cortical interneurons into a functional network. *Curr. Top. Dev. Biol.* 87, 81–118.

Baum, M. J., and Kelliher, K. R. (2009). Complementary roles of the main and accessory olfactory systems in mammalian mate recognition. *Annu. Rev. Physiol.* 71, 141–160.

Beauchamp, G. K., Martin, I. G., Wysocki, C. J., and Wellington, J. L. (1982). Chemoinvestigatory and sexual behavior of male guinea pigs following vomeronasal organ removal. *Physiol. Behav.* 29, 329–336.

Been, L. E., and Petrulis, A. (2010). The role of the medial preoptic area in appetitive and consummatory reproductive behaviors depends on sexual experience and odor volatility in male Syrian hamsters. *Neuroscience* 170, 1120–1132.

Bekirov, I. H., Needleman, L. A., Zhang, W., and Benson, D. L. (2002). Identification and localization of multiple classic cadherins in developing rat limbic system. *Neuroscience* 115, 213–227.

Blackshaw, S., Scholpp, S., Placzek, M., Ingraham, H., Simerly, R., and Shimogori, T. (2010). Molecular pathways controlling development of thalamus and hypothalamus: from neural specification to circuit formation. *J. Neurosci.* 30, 14925–14930.

Blanchard, R. J., Yang, M., Li, C. I., Gervacio, A., and Blanchard, D. C. (2001). Cue and context conditioning of defensive behaviors to cat odor stimuli. *Neurosci. Biobehav. Rev.* 25, 587–595.

Blaustein, J. D., King, J. C., Toft, D. O., and Turcotte, J. (1988). Immunocytochemical localization of estrogen-induced progestin receptors in guinea pig brain. *Brain Res.* 474, 1–15.

Brechbühl, J., Klaey, M., and Broillet, M. C. (2008). Grueneberg ganglion cells mediate alarm pheromone detection in mice. *Science* 321, 1092–1095.

Brothers, L. (1989). A biological perspective on empathy. *Am. J. Psychiatry* 146, 10–19.

Bupesh, M., Legaz, I., Abellán, A., and Medina, L. (2011). Multiple telencephalic and extratelencephalic embryonic domains contribute neurons to the medial extended amygdala. *J. Comp. Neurol.* 519, 1505–1525.

Calof, A. L., Bonnin, A., Crocker, C., Kawauchi, S., Murray, R. C., Shou, J., and Wu, H. H. (2002). Progenitor cells of the olfactory receptor neuron lineage. *Microsc. Res. Tech.* 58, 176–188.

Campbell, K. (2003). Dorsal-ventral patterning in the mammalian telencephalon. *Curr. Opin. Neurobiol.* 13, 50–56.

Campbell, D. B., D'Oronzio, R., Garbett, K., Ebert, P. J., Mirnics, K., Levitt, P., and Persico, A. M. (2007). Disruption of cerebral cortex MET signaling in autism spectrum disorder. *Ann. Neurol.* 62, 243–250.

Campbell, D. B., Sutcliffe, J. S., Ebert, P. J., Militerni, R., Bravaccio, C., Trillo, S., Elia, M., Schneider, C., Melmed, R., Sacco, R., Persico, A. M., and Levitt, P. (2006). A genetic variant that disrupts MET transcription is associated with autism. *Proc. Natl. Acad. Sci. U.S.A.* 103, 16834–16839.

Canteras, N. S., Chiavegatto, S., Ribeiro do Valle, L. E., and Swanson, L. W. (1997). Severe reduction of rat defensive behavior to a predator by discrete hypothalamic chemical lesions. *Brain Res. Bull.* 44, 297–305.

Carney, R. S., Mangin, J. M., Hayes, L., Mansfield, K., Sousa, V. H., Fishell, G., Machold, R. P., Ahn, S., Gallo, V., and Corbin, J. G. (2010). Sonic hedgehog expressing and responding cells generate neuronal diversity in the medial amygdala. *Neural. Dev.* 5, 14.

Caqueret, A., Boucher, F., and Michaud, J. L. (2006). Laminar organization of the early developing anterior hypothalamus. *Dev. Biol.* 298, 95–106.

Cau, E., Casarosa, S., and Guillemot, F. (2002). Mash1 and Ngn1 control distinct steps of determination and differentiation in the olfactory sensory neuron lineage. *Development* 129, 1871–1880.

Cezario, A. F., Ribeiro-Barbosa, E. R., Baldo, M. V., and Canteras, N. S. (2008). Hypothalamic sites responding to predator threats–the role of the dorsal premammillary nucleus in unconditioned and conditioned antipredatory defensive behavior. *Eur. J. Neurosci.* 28, 1003–1015.

Champagne, F. A., Weaver, I. C., Diorio, J., Sharma, S., and Meaney, M. J. (2003). Natural variations in maternal care are associated with estrogen receptor alpha expression and estrogen sensitivity in the medial preoptic area. *Endocrinology* 144, 4720–4724.

Cho, J. H., Lépine, M., Andrews, W., Parnavelas, J., and Cloutier, J. F. (2007). Requirement for Slit-1 and Robo-2 in zonal segregation of olfactory sensory neuron axons in the main olfactory bulb. *J. Neurosci.* 27, 9094–9104.

Choi, G. B., Dong, H. W., Murphy, A. J., Valenzuela, D. M., Yancopoulos, G. D., Swanson, L. W., and Anderson, D. J. (2005). Lhx6 delineates a pathway mediating innate reproductive behaviors from the amygdala to the hypothalamus. *Neuron* 46, 647–660.

Cocas, L. A., Georgala, P. A., Mangin, J. M., Clegg, J. M., Kessaris, N., Haydar, T. F., Gallo, V., Price, D. J., and Corbin, J. G. (2011). Pax6 is required at the telencephalic pallial-subpallial boundary for the generation of neuronal diversity in the postnatal limbic system. *J. Neurosci.* 31, 5313–5324.

Consiglio, A. R., and Bridges, R. S. (2009). Circulating prolactin, MPOA prolactin receptor expression and maternal aggression in lactating rats. *Behav. Brain Res.* 197, 97–102.

Cooke, B. M. (2006). Steroid-dependent plasticity in the medial amygdala. *Neuroscience* 138, 997–1005.

Cooke, B. M., Breedlove, S. M., and Jordan, C. L. (2003). Both estrogen receptors and androgen receptors contribute to testosterone-induced changes in the morphology of the

medial amygdala and sexual arousal in male rats. *Horm. Behav.* 43, 336–346.

Coolen, L. M., Peters, H. J., and Veening, J. G. (1996). Fos immunoreactivity in the rat brain following consummatory elements of sexual behavior: a sex comparison. *Brain Res.* 738, 67–82.

Coppola, D. M., Budde, J., and Millar, L. (1993). The vomeronasal duct has a protracted postnatal development in the mouse. *J. Morphol.* 218, 59–64.

Corbin, J. G., and Butt, S. J. (2011). Developmental mechanisms for the generation of telencephalic interneurons. *Dev. Neurobiol.* 71, 710–732.

Corbin, J. G., Gaiano, N., Juliano, S. L., Poluch, S., Stancik, E., and Haydar, T. F. (2008). Regulation of neural progenitor cell development in the nervous system. *J. Neurochem.* 106, 2272–2287.

Del Punta, K., Leinders-Zufall, T., Rodriguez, I., Jukam, D., Wysocki, C. J., Ogawa, S., Zufall, F., and Mombaerts, P. (2002). Deficient pheromone responses in mice lacking a cluster of vomeronasal receptor genes. *Nature* 419, 70–74.

Dielenberg, R. A., Hunt, G. E., and McGregor, I. S. (2001). "When a rat smells a cat": the distribution of Fos immunoreactivity in rat brain following exposure to a predatory odor. *Neuroscience* 104, 1085–1097.

Dong, H. W., and Swanson, L. W. (2004). Projections from bed nuclei of the stria terminalis, posterior division: implications for cerebral hemisphere regulation of defensive and reproductive behaviors. *J. Comp. Neurol.* 471, 396–433.

Drickamer, L. C. (1992). Behavioral selection of odor cues by young female mice affects age of puberty. *Dev. Psychobiol.* 25, 461–470.

Dugger, B. N., Morris, J. A., Jordan, C. L., and Breedlove, S. M. (2008). Gonadal steroids regulate neural plasticity in the sexually dimorphic nucleus of the preoptic area of adult male and female rats. *Neuroendocrinology* 88, 17–24.

Dulac, C., and Torello, A. T. (2003). Molecular detection of pheromone signals in mammals: from genes to behaviour. *Nat. Rev. Neurosci.* 4, 551–562.

Dulac, C., and Wagner, S. (2006). Genetic analysis of brain circuits underlying pheromone signaling. *Annu. Rev. Genet.* 40, 449–467.

Emery, D. E., and Sachs, B. D. (1976). Copulatory behavior in male rats with lesions in the bed nucleus of the stria terminalis. *Physiol. Behav.* 17, 803–806.

Fan, C. M., Kuwana, E., Bulfone, A., Fletcher, C. F., Copeland, N. G., Jenkins, N. A., Crews, S., Martinez, S., Puelles, L., Rubenstein, J. L., and Tessier-Lavigne, M. (1996). Expression patterns of two murine homologs of Drosophila single-minded suggest possible roles in embryonic patterning and in the pathogenesis of Down syndrome. *Mol. Cell. Neurosci.* 7, 1–16.

Ferrero, D. M., Lemon, J. K., Fluegge, D., Pashkovski, S. L., Korzan, W. J., Datta, S. R., Spehr, M., Fendt, M., and Liberles, S. D. (2011). Detection and avoidance of a carnivore odor by prey. *Proc. Natl. Acad. Sci. U.S.A.* 108, 11235–11240.

Flanagan-Cato, L. M., Calizo, L. H., and Daniels, D. (2001). The synaptic organization of VMH neurons that mediate the effects of estrogen on sexual behavior. *Horm. Behav.* 40, 178–182.

Fleming, A. (1986). Psychobiology of rat maternal behavior: how and where hormones act to promote maternal behavior at parturition. *Ann. N.Y. Acad. Sci.* 474, 234–251.

García-López, M., Abellán, A., Legaz, I., Rubenstein, J. L., Puelles, L., and Medina, L. (2008). Histogenetic compartments of the mouse centromedial and extended amygdala based on gene expression patterns during development. *J. Comp. Neurol.* 506, 46–74.

García-Moreno, F., Pedraza, M., Di Giovannantonio, L. G., Di Salvio, M., López-Mascaraque, L., Simeone, A., and De Carlos, J. A. (2010). A neuronal migratory pathway crossing from diencephalon to telencephalon populates amygdala nuclei. *Nat. Neurosci.* 13, 680–689.

Giacobini, P., Messina, A., Wray, S., Giampietro, C., Crepaldi, T., Carmeliet, P., and Fasolo, A. (2007). Hepatocyte growth factor acts as a motogen and guidance signal for gonadotropin hormone-releasing hormone-1 neuronal migration. *J. Neurosci.* 27, 431–445.

Gomez, D. M., and Newman, S. W. (1991). Medial nucleus of the amygdala in the adult Syrian hamster: a quantitative Golgi analysis of gonadal hormonal regulation of neuronal morphology. *Anat. Rec.* 231, 498–509.

Guastella, A. J., and Macleod, C. (2012). A critical review of the influence of oxytocin nasal spray on social cognition in humans: evidence and future directions. *Horm. Behav.* 61, 410–418.

Gutierrez, H., Dolcet, X., Tolcos, M., and Davies, A. (2004). HGF regulates the development of cortical pyramidal dendrites. *Development* 131, 3717–3726.

Hammock, E. A., and Young, L. J. (2006). Oxytocin, vasopressin and pair bonding: implications for autism. *Philos. Trans. R. Soc. Lond. B Biol. Sci.* 361, 2187–2198.

Hennessey, A. C., Wallen, K., and Edwards, D. A. (1986). Preoptic lesions increase the display of lordosis by male rats. *Brain Res.* 370, 21–28.

Herbert, R. A., and Leininger, J. R. (1999). "Nose, larynx, and trachea," in *Pathology of the Mouse,* ed R. R. Maronpot (St. Louis: Cache River Press), 259–262.

Herry, C., Ciocchi, S., Senn, V., Demmou, L., Müller, C., and Lüthi, A. (2008). Switching on and off fear by distinct neuronal circuits. *Nature* 454, 600–606.

Hessl, D., Rivera, S., Koldewyn, K., Cordeiro, L., Adams, J., Tassone, F., Hagerman, P. J., and Hagerman, R. J. (2007). Amygdala dysfunction in men with the fragile X premutation. *Brain* 130, 404–416.

Hill, R. A., and Boon, W. C. (2009). Estrogens, brain, and behavior: lessons from knockout mouse models. *Semin. Reprod. Med.* 27, 218–228.

Hirano, S., Wang, X., and Suzuki, S. T. (2002). Restricted expression of protocadherin 2A in the developing mouse brain. *Brain Res. Mol. Brain Res.* 98, 119–123.

Hirata, T., Li, P., Lanuza, G. M., Cocas, L. A., Huntsman, M. M., and Corbin, J. G. (2009). Identification of distinct telencephalic progenitor pools for neuronal diversity in the amygdala. *Nat. Neurosci.* 12, 141–149.

Hull, E. M., and Dominguez, J. M. (2006). Getting his act together: roles of glutamate, nitric oxide, and dopamine in the medial preoptic area. *Brain Res.* 1126, 66–75.

Imai, T., and Sakano, H. (2007). Roles of odorant receptors in projecting axons in the mouse olfactory system. *Curr. Opin. Neurobiol.* 17, 507–515.

Imai, T., and Sakano, H. (2009). Odorant receptor gene choice and axonal projection in the mouse olfactory system. *Results Probl. Cell Differ.* 47, 57–75.

Imai, T., Yamazaki, T., Kobayakawa, R., Kobayakawa, K., Abe, T., Suzuki, M., and Sakano, H. (2009). Pre-target axon sorting establishes the neural map topography. *Science* 325, 585–590.

Isogai, Y., Si, S., Pont-Lezica, L., Tan, T., Kapoor, V., Murthy, V. N., and Dulac, C. (2011). Molecular organization of vomeronasal chemoreception. *Nature* 478, 241–245.

Judson, M. C., Bergman, M. Y., Campbell, D. B., Eagleson, K. L., and Levitt, P. (2009). Dynamic gene and protein expression patterns of the autism-associated met receptor tyrosine kinase in the developing mouse forebrain. *J. Comp. Neurol.* 513, 511–531.

Juntti, S. A., Tollkuhn, J., Wu, M. V., Fraser, E. J., Soderborg, T., Tan, S., Honda, S., Harada, N., and Shah, N. M. (2010). The androgen receptor governs the execution, but not programming, of male sexual and territorial behaviors. *Neuron* 66, 260–272.

Kaoru, T., Liu, F. C., Ishida, M., Oishi, T., Hayashi, M., Kitagawa, M., Shimoda, K., and Takahashi, H. (2010). Molecular characterization of the intercalated cell masses of the amygdala: implications for the relationship with the striatum. *Neuroscience* 166, 220–230.

Kang, N., McCarthy, E. A., Cherry, J. A., and Baum, M. J. (2011). A sex comparison of the anatomy and function of the main olfactory bulb-medial amygdala projection in mice. *Neuroscience* 172, 196–204.

Katoh, H., Shibata, S., Fukuda, K., Sato, M., Satoh, E., Nagoshi, N., Minematsu, T., Matsuzaki, Y., Akazawa, C., Toyama, Y., Nakamura, M., and Okano, H. (2011). The dual origin of the peripheral olfactory system: placode and neural crest. *Mol. Brain* 4, 34.

Keller, M., Pierman, S., Douhard, Q., Baum, M. J., and Bakker, J. (2006). The vomeronasal organ is required for the expression of lordosis behaviour, but not sex discrimination in female mice. *Eur. J. Neurosci.* 23, 521–530.

Kollack-Walker, S., Don, C., Watson, S. J., and Akil, H. (1999). Differential expression of c-Fos mRNA within neurocircuits of male hamsters exposed to acute or chronic defeat. *J. Neuroendocrinol.* 11, 547–559.

Kollack-Walker, S., and Newman, S. W. (1995). Mating and agonistic behavior produce different patterns of Fos immunolabeling in the male Syrian hamster brain. *Neuroscience* 66, 721–736.

Kondo, Y., and Arai, Y. (1995). Functional association between the medial amygdala and the medial

preoptic area in regulation of mating behavior in the male rat. *Physiol. Behav.* 57, 69–73.

Kow, L. M., Tsai, Y. F., Weiland, N. G., McEwen, B. S., and Pfaff, D. W. (1995). *In vitro* electro-pharmacological and autoradiographic analyses of muscarinic receptor subtypes in rat hypothalamic ventromedial nucleus: implications for cholinergic regulation of lordosis. *Brain Res.* 694, 29–39.

LeDoux, J. (2007). The amygdala. *Curr. Biol.* 17, R868–R874.

LeDoux, J. E. (1993). Emotional memory systems in the brain. *Behav. Brain Res.* 58, 69–79.

LeDoux, J. E. (2012). Evolution of human emotion: a view through fear. *Prog. Brain Res.* 195, 431–442.

Leypold, B. G., Yu, C. R., Leinders-Zufall, T., Kim, M. M., Zufall, F., and Axel, R. (2002). Altered sexual and social behaviors in trp2 mutant mice. *Proc. Natl. Acad. Sci. U.S.A.* 99, 6376–6381.

Lin, D., Boyle, M. P., Dollar, P., Lee, H., Lein, E. S., Perona, P., and Anderson, D. J. (2011). Functional identification of an aggression locus in the mouse hypothalamus. *Nature* 470, 221–226.

Lin, J. H., Saito, T., Anderson, D. J., Lance-Jones, C., Jessell, T. M., and Arber, S. (1998). Functionally related motor neuron pool and muscle sensory afferent subtypes defined by coordinate ETS gene expression. *Cell* 95, 393–407.

Lonstein, J. S., and Stern, J. M. (1998). Site and behavioral specificity of periaqueductal gray lesions on postpartum sexual, maternal, and aggressive behaviors in rats. *Brain Res.* 804, 21–35.

López-Mascaraque, L., De Carlos, J. A., and Valverde, F. (1996). Early onset of the rat olfactory bulb projections. *Neuroscience* 70, 255–266.

Luo, L., and Flanagan, J. G. (2007). Development of continuous and discrete neural maps. *Neuron* 56, 284–300.

MacLean, P. D. (1949). Psychosomatic disease and the visceral brain; recent developments bearing on the Papez theory of emotion. *Psychosom. Med.* 11, 338–353.

Malnic, B., Hirono, J., Sato, T., and Buck, L. B. (1999). Combinatorial receptor codes for odors. *Cell* 96, 713–723.

Mani, S. K., Blaustein, J. D., Allen, J. M., Law, S. W., O'Malley, B. W., and Clark, J. H. (1994). Inhibition of rat sexual behavior by antisense oligonucleotides to the progesterone receptor. *Endocrinology* 135, 1409–1414.

Mann, F., Zhukareva, V., Pimenta, A., Levitt, P., and Bolz, J. (1998). Membrane-associated molecules guide limbic and nonlimbic thalamocortical projections. *J. Neurosci.* 18, 9409–9419.

Marín, O., and Rubenstein, J. L. (2003). Cell migration in the forebrain. *Annu. Rev. Neurosci.* 26, 441–483.

Markram, K., Rinaldi, T., La Mendola, D., Sandi, C., and Markram, H. (2008). Abnormal fear conditioning and amygdala processing in an animal model of autism. *Neuropsychopharmacology* 33, 901–912.

Martins, G. J., Shahrokh, M., and Powell, E. M. (2011). Genetic disruption of Met signaling impairs GABAergic striatal development and cognition. *Neuroscience* 176, 199–209.

Marson, L. (2004). Lesions of the periaqueductal gray block the medial preoptic area-induced activation of the urethrogenital reflex in male rats. *Neurosci. Lett.* 367, 278–282.

McConnell, J., and Angevine, J. B. Jr. (1983). Time of neuron origin in the amygdaloid complex of the mouse. *Brain Res.* 272, 150–156.

McGregor, I. S., Hargreaves, G. A., Apfelbach, R., and Hunt, G. E. (2004). Neural correlates of cat odor-induced anxiety in rats: region-specific effects of the benzodiazepine midazolam. *J. Neurosci.* 24, 4134–4144.

Meurisse, M., Chaillou, E., and Lévy, F. (2009). Afferent and efferent connections of the cortical and medial nuclei of the amygdala in sheep. *J. Chem. Neuroanat.* 37, 87–97.

Miller, A. M., Maurer, L. R., Zou, D. J., Firestein, S., and Greer, C. A. (2010). Axon fasciculation in the developing olfactory nerve. *Neural. Dev.* 5, 20.

Mohedano-Moriano, A., Pro-Sistiaga, P., Ubeda-Bañón, I., Crespo, C., Insausti, R., and Martinez-Marcos, A. (2007). Segregated pathways to the vomeronasal amygdala: differential projections from the anterior and posterior divisions of the accessory olfactory bulb. *Eur. J. Neurosci.* 25, 2065–2080.

Mombaerts, P. (2001). How smell develops. *Nat. Neurosci.* 4, 1192–1198.

Mombaerts, P. (2006). Axonal wiring in the mouse olfactory system. *Annu. Rev. Cell Dev. Biol.* 22, 713–737.

Monaghan, A. P., Bock, D., Gass, P., Schwäger, A., Wolfer, D. P., Lipp, H. P., and Schütz, G. (1997). Defective limbic system in mice lacking the tailless gene. *Nature* 390, 515–517.

Monk, C. S. (2008). The development of emotion-related neural circuitry in health and psychopathology. *Dev. Psychopathol.* 20, 1231–1250.

Morris, J. A., Jordan, C. L., King, Z. A., Northcutt, K. V., and Breedlove, S. M. (2008). Sexual dimorphism and steroid responsiveness of the posterodorsal medial amygdala in adult mice. *Brain Res.* 1190, 115–121.

Motta, S. C., Goto, M., Gouveia, F. V., Baldo, M. V., Canteras, N. S., and Swanson, L. W. (2009). Dissecting the brain's fear system reveals the hypothalamus is critical for responding in subordinate conspecific intruders. *Proc. Natl. Acad. Sci. U.S.A.* 106, 4870–4875.

Nery, S., Fishell, G., and Corbin, J. G. (2002). The caudal ganglionic eminence is a source of distinct cortical and subcortical cell populations. *Nat. Neurosci.* 5, 1279–1287.

Newman, S. W. (1999). The medial extended amygdala in male reproductive behavior. A node in the mammalian social behavior network. *Ann. N.Y. Acad. Sci.* 877, 242–257.

Nguyen-Ba-Charvet, K. T., Di Meglio, T., Fouquet, C., and Chédotal, A. (2008). Robos and slits control the pathfinding and targeting of mouse olfactory sensory axons. *J. Neurosci.* 28, 4244–4249.

Nomura, T., Holmberg, J., Frisen, J., and Osumi, N. (2006). Pax6-dependent boundary defines alignment of migrating olfactory cortex neurons via the repulsive activity of ephrin A5. *Development* 133, 1335–1345.

Normandin, J. J., and Murphy, A. Z. (2011a). Serotonergic lesions of the periaqueductal gray, a primary source of serotonin to the nucleus paragigantocellularis, facilitate sexual behavior in male rats. *Pharmacol. Biochem. Behav.* 98, 369–375.

Normandin, J. J., and Murphy, A. Z. (2011b). Somatic genital reflexes in rats with a nod to humans: anatomy, physiology, and the role of the social neuropeptides. *Horm. Behav.* 59, 656–665.

Numan, M., Numan, M. J., and English, J. B. (1993). Excitotoxic amino acid injections into the medial amygdala facilitate maternal behavior in virgin female rats. *Horm. Behav.* 27, 56–81.

Numan, M., and Smith, H. G. (1984). Maternal behavior in rats: evidence for the involvement of preoptic projections to the ventral tegmental area. *Behav. Neurosci.* 98, 712–727.

Ogawa, S., Washburn, T. F., Taylor, J., Lubahn, D. B., Korach, K. S., and Pfaff, D. W. (1998). Modifications of testosterone-dependent behaviors by estrogen receptor-alpha gene disruption in male mice. *Endocrinology* 139, 5058–5069.

Osterhout, J. A., Josten, N., Yamada, J., Pan, F., Wu, S. W., Nguyen, P. L., Panagiotakos, G., Inoue, Y. U., Egusa, S. F., Volgyi, B., Inoue, T., Bloomfield, S. A., Barres, B. A., Berson, D. M., Feldheim, D. A., and Huberman, A. D. (2011). Cadherin-6 mediates axon-target matching in a non-image-forming visual circuit. *Neuron* 71, 632–639.

Pankevich, D. E., Baum, M. J., and Cherry, J. A. (2004). Olfactory sex discrimination persists, whereas the preference for urinary odorants from estrous females disappears in male mice after vomeronasal organ removal. *J. Neurosci.* 24, 9451–9457.

Papes, F., Logan, D. W., and Stowers, L. (2010). The vomeronasal organ mediates interspecies defensive behaviors through detection of protein pheromone homologs. *Cell* 141, 692–703.

Papez, J. W. (1937). A proposed mechanism of emotion. *J. Neuropsychiatry Clin. Neurosci.* 7, 103–112.

Petitti, N., Karkanias, G. B., and Etgen, A. M. (1992). Estradiol selectively regulates alpha 1B-noradrenergic receptors in the hypothalamus and preoptic area. *J. Neurosci.* 12, 3869–3876.

Petrovich, G. D., Canteras, N. S., and Swanson, L. W. (2001). Combinatorial amygdalar inputs to hippocampal domains and hypothalamic behavior systems. *Brain Res. Brain Res. Rev.* 38, 247–289.

Petrulis, A., Peng, M., and Johnston, R. E. (1999). Effects of vomeronasal organ removal on individual odor discrimination, sex-odor preference, and scent marking by female hamsters. *Physiol. Behav.* 66, 73–83.

Pfaff, D. W., and Sakuma, Y. (1979). Deficit in the lordosis reflex of female rats caused by lesions in the ventromedial nucleus of the hypothalamus. *J. Physiol.* 288, 203–210.

Pimenta, A. F., and Levitt, P. (2004). Characterization of the genomic structure of the mouse limbic system-associated membrane protein (Lsamp) gene. *Genomics* 83, 790–801.

Powell, E. M., Mühlfriedel, S., Bolz, J., and Levitt, P. (2003). Differential regulation of thalamic and cortical axonal growth by hepatocyte growth factor/scatter factor. *Dev. Neurosci.* 25, 197–206.

Puelles, L., Kuwana, E., Puelles, E., Bulfone, A., Shimamura, K., Keleher, J., Smiga, S., and Rubenstein, J. L. (2000). Pallial and subpallial derivatives in the embryonic chick and mouse telencephalon, traced by the expression of the genes Dlx-2, Emx-1, Nkx-2.1, Pax-6, and Tbr-1. *J. Comp. Neurol.* 424, 409–438.

Puelles, L., and Rubenstein, J. L. (1993). Expression patterns of homeobox and other putative regulatory genes in the embryonic mouse forebrain suggest a neuromeric organization. *Trends Neurosci.* 16, 472–479.

Puelles, L., and Rubenstein, J. L. (2003). Forebrain gene expression domains and the evolving prosomeric model. *Trends Neurosci.* 26, 469–476.

Redies, C., and Takeichi, M. (1993). Expression of N-cadherin mRNA during development of the mouse brain. *Dev. Dyn.* 197, 26–39.

Remedios, R., Huilgol, D., Saha, B., Hari, P., Bhatnagar, L., Kowalczyk, T., Hevner, R. F., Suda, Y., Aizawa, S., Ohshima, T., Stoykova, A., and Tole, S. (2007). A stream of cells migrating from the caudal telencephalon reveals a link between the amygdala and neocortex. *Nat. Neurosci.* 10, 1141–1150.

Remedios, R., Subramanian, L., and Tole, S. (2004). LIM genes parcellate the embryonic amygdala and regulate its development. *J. Neurosci.* 24, 6986–6990.

Risold, P. Y., Canteras, N. S., and Swanson, L. W. (1994). Organization of projections from the anterior hypothalamic nucleus: a Phaseolus vulgaris-leucoagglutinin study in the rat. *J. Comp. Neurol.* 348, 1–40.

Rodrigues, S. M., Schafe, G. E., and LeDoux, J. E. (2004). Molecular mechanisms underlying emotional learning and memory in the lateral amygdala. *Neuron* 44, 75–91.

Rosenblatt, J. S., Wagner, C. K., and Morrell, J. I. (1994). Hormonal priming and triggering of maternal behavior in the rat with special reference to the relations between estrogen receptor binding and ER mRNA in specific brain regions. *Psychoneuroendocrinology* 19, 543–552.

Royal, S. J., and Key, B. (1999). Development of P2 olfactory glomeruli in P2-internal ribosome entry site-tau-LacZ transgenic mice. *J. Neurosci.* 19, 9856–9864.

Ruthschilling, C. A., Albiero, G., Lazzari, V. M., Becker, R. O., de Moura, A. C., Lucion, A. B., Almeida, S., Veiga, A. B., and Giovenardi, M. (2012). Analysis of transcriptional levels of the oxytocin receptor in different areas of the central nervous system and behaviors in high and low licking rats. *Behav. Brain Res.* 228, 176–184.

Sato, Y., Iketani, M., Kurihara, Y., Yamaguchi, M., Yamashita, N., Nakamura, F., Arie, Y., Kawasaki, T., Hirata, T., Abe, T., Kiyonari, H., Strittmatter, S. M., Goshima, Y., and Takei, K. (2011). Cartilage acidic protein-1B (LOTUS), an endogenous Nogo receptor antagonist for axon tract formation. *Science* 333, 769–773.

Sawrey, D. K., and Dewsbury, D. A. (1994). Conspecific odor preferences in Montane voles (Microtus montanus): effects of sexual experience. *Physiol. Behav.* 56, 339–344.

Sheehan, T., Paul, M., Amaral, E., Numan, M. J., and Numan, M. (2001). Evidence that the medial amygdala projects to the anterior/ventromedial hypothalamic nuclei to inhibit maternal behavior in rats. *Neuroscience* 106, 341–356.

Shimogori, T., Lee, D. A., Miranda-Angulo, A., Yang, Y., Wang, H., Jiang, L., Yoshida, A. C., Kataoka, A., Mashiko, H., Avetisyan, M., Qi, L., Qian, J., and Blackshaw, S. (2010). A genomic atlas of mouse hypothalamic development. *Nat. Neurosci.* 13, 767–775.

Shirasaki, R., and Pfaff, S. L. (2002). Transcriptional codes and the control of neuronal identity. *Annu. Rev. Neurosci.* 25, 251–281.

Simerly, R. B. (2005). Wired on hormones: endocrine regulation of hypothalamic development. *Curr. Opin. Neurobiol.* 15, 81–85.

Soma, M., Aizawa, H., Ito, Y., Maekawa, M., Osumi, N., Nakahira, E., Okamoto, H., Tanaka, K., and Yuasa, S. (2009). Development of the mouse amygdala as revealed by enhanced green fluorescent protein gene transfer by means of in utero electroporation. *J. Comp. Neurol.* 513, 113–128.

Stenman, J., Yu, R. T., Evans, R. M., and Campbell, K. (2003). Tlx and Pax6 co-operate genetically to establish the pallio-subpallial boundary in the embryonic mouse telencephalon. *Development* 130, 1113–1122.

Stowers, L., Holy, T. E., Meister, M., Dulac, C., and Koentges, G. (2002). Loss of sex discrimination and male-male aggression in mice deficient for TRP2. *Science* 22, 1493–1500.

Stoykova, A., Götz, M., Gruss, P., and Price, J. (1997). Pax6-dependent regulation of adhesive patterning, R-cadherin expression and boundary formation in developing forebrain. *Development* 124, 3765–3777.

Strotmann, J., Wanner, I., Helfrich, T., and Breer, H. (1995). Receptor expression in olfactory neurons during rat development: *in situ* hybridization studies. *Eur. J. Neurosci.* 1, 492–500.

Sullivan, S. L., Bohm, S., Ressler, K. J., Horowitz, L. F., and Buck, L. B. (1995). Target-independent pattern specification in the olfactory epithelium. *Neuron* 15, 779–789.

Swanson, L. W. (2000). Cerebral hemisphere regulation of motivated behavior. *Brain Res.* 15, 113–164.

Swanson, L. W., and Petrovich, G. D. (1998). What is the amygdala? *Trends Neurosci.* 21, 323–331.

Tietjen, I., Rihel, J., and Dulac, C. G. (2005). Single-cell transcriptional profiles and spatial patterning of the mammalian olfactory epithelium. *Int. J. Dev. Biol.* 49, 201–207.

Toda, K., Saibara, T., Okada, T., Onishi, S., and Shizuta, Y. (2001). A loss of aggressive behaviour and its reinstatement by oestrogen in mice lacking the aromatase gene (Cyp19). *J. Endocrinol.* 168, 217–220.

Tyndall, S. J., and Walikonis, R. S. (2006). The receptor tyrosine kinase Met and its ligand hepatocyte growth factor are clustered at excitatory synapses and can enhance clustering of synaptic proteins. *Cell Cycle* 5, 1560–1568.

Umeda, T., Takashima, N., Nakagawa, R., Maekawa, M., Ikegami, S., Yoshikawa, T., Kobayashi, K., Okanoya, K., Inokuchi, K., and Osumi, N. (2010). Evaluation of Pax6 mutant rat as a model for autism. *PLoS One* 5:e15500. doi: 10.1371/journal.pone.0015500

Veening, J. G., Coolen, L. M., de Jong, T. R., Joosten, H. W., de Boer, S. F., Koolhaas, J. M., and Olivier, B. (2005). Do similar neural systems subserve aggressive and sexual behaviour in male rats? Insights from c-Fos and pharmacological studies. *Eur. J. Pharmacol.* 5, 226–239.

Walsh, C. A., Morrow, E. M., and Rubenstein, J. L. (2008). Autism and brain development. *Cell* 135, 396–400.

Wang, K., Zhang, H., Ma, D., Bucan, M., Glessner, J. T., Abrahams, B. S., Salyakina, D., Imielinski, M., Bradfield, J. P., Sleiman, P. M., Kim, C. E., Hou, C., Frackelton, E., Chiavacci, R., Takahashi, N., Sakurai, T., Rappaport, E., Lajonchere, C. M., Munson, J., Estes, A., Korvatska, O., Piven, J., Sonnenblick, L. I., Alvarez Retuerto, A. I., Herman, E. I., Dong, H., Hutman, T., Sigman, M., Ozonoff, S., Klin, A., Owley, T., Sweeney, J. A., Brune, C. W., Cantor, R. M., Bernier, R., Gilbert, J. R., Cuccaro, M. L., McMahon, W. M., Miller, J., State, M. W., Wassink, T. H., Coon, H., Levy, S. E., Schultz, R. T., Nurnberger, J. I., Haines, J. L., Sutcliffe, J. S., Cook, E. H., Minshew, N. J., Buxbaum, J. D., Dawson, G., Grant, S. F., Geschwind, D. H., Pericak-Vance, M. A., Schellenberg, G. D., and Hakonarson, H. (2009). Common genetic variants on 5p14.1 associate with autism spectrum disorders. *Nature* 28, 528–533.

Wang, W., and Lufkin, T. (2000). The murine Otp homeobox gene plays an essential role in the specification of neuronal cell lineages in the developing hypothalamus. *Dev. Biol.* 5, 432–449.

Williams, M. E., Wilke, S. A., Daggett, A., Davis, E., Otto, S., Ravi, D., Ripley, B., Bushong, E. A., Ellisman, M. H., Klein, G., and Ghosh, A. (2011). Cadherin-9 regulates synapse-specific differentiation in the developing hippocampus. *Neuron* 71, 640–655.

Wonders, C. P., and Anderson, S. A. (2006). The origin and specification of cortical interneurons. *Nat. Rev. Neurosci.* 7, 687–696.

Wu, M. V., Manoli, D. S., Fraser, E. J., Coats, J. K., Tollkuhn, J., Honda, S., Harada, N., and Shah, N. M. (2009). Estrogen masculinizes neural pathways and sex-specific behaviors. *Cell* 139, 61–72.

Wu, M. V., and Shah, N. M. (2011). Control of masculinization of the brain and behavior. *Curr. Opin. Neurobiol.* 21, 116–123.

Xu, Q., Tam, M., and Anderson, S. A. (2008). Fate mapping Nkx2.1-lineage cells in the mouse telencephalon. *J. Comp. Neurol.* 506, 16–29.

Xu, X., Coats, J. K., Yang, C. F., Wang, A., Ahmed, O. M., Alvarado, M., Izumi, T., and Shah, N. M. (2012). Modular genetic control of sexually dimorphic behaviors. *Cell* 148, 596–607.

Yoshihara, Y., Kawasaki, M., Tamada, A., Fujita, H., Hayashi, H., Kagamiyama, H., and Mori, K. (1997). OCAM: a new member of the neural cell adhesion molecule family related to zone-to-zone

projection of olfactory and vomeronasal axons. *J. Neurosci.* 17, 5830–5842.

Yoshihara, Y., and Mori, K. (1997). Basic principles and molecular mechanisms of olfactory axon pathfinding. *Cell Tissue Res.* 290, 457–463.

Zirlinger, M., Kreiman, G., and Anderson, D. J. (2001). Amygdala-enriched genes identified by microarray technology are restricted to specific amygdaloid subnuclei. *Proc. Natl. Acad. Sci. U.S.A.* 98, 5270–5275.

Conflict of Interest Statement: The authors declare that the research was conducted in the absence of any commercial or financial relationships that could be construed as a potential conflict of interest.

Received: 01 March 2012; accepted: 04 April 2012; published online: 26 April 2012.

*Citation: Sokolowski K and Corbin JG (2012) Wired for behaviors: from development to function of innate limbic system circuitry. Front. Mol. Neurosci. **5**:55. doi: 10.3389/fnmol.2012.00055*

frontiers in
MOLECULAR NEUROSCIENCE

REVIEW ARTICLE
published: 19 March 2013
doi: 10.3389/fnmol.2013.00004

Protocadherins, not prototypical: a complex tale of their interactions, expression, and functions

Joshua A. Weiner[1]* and James D. Jontes[2]*

[1] *Department of Biology, The University of Iowa, Iowa City, IA, USA*
[2] *Department of Neuroscience, The Ohio State University, Columbus, OH, USA*

Edited by:
Robert W. Burgess, The Jackson Laboratory, USA

Reviewed by:
Deanna L. Benson, Mount Sinai School of Medicine, USA
George W. Huntley, Mount Sinai School of Medicine, USA
Zhong-Wei Zhang, The Jackson Laboratory, USA

****Correspondence:***
Joshua A. Weiner, Department of Biology, The University of Iowa, 143 Biology Building, Iowa City, IA 52242, USA.
e-mail: joshua-weiner@uiowa.edu;
James D. Jontes, Department of Neuroscience, The Ohio State University, 119 Rightmire Hall, Columbus, OH 43210, USA.
e-mail: jontes.1@osu.edu

The organization of functional neural circuits requires the precise and coordinated control of cell–cell interactions at nearly all stages of development, including neuronal differentiation, neuronal migration, axon outgrowth, dendrite arborization, and synapse formation and stabilization. This coordination is brought about by the concerted action of a large number of cell surface receptors, whose dynamic regulation enables neurons (and astrocytes) to adopt their proper roles within developing neural circuits. The protocadherins (Pcdhs) comprise a major family of cell surface receptors expressed in the developing vertebrate nervous system whose cellular and developmental roles are only beginning to be elucidated. In this review, we highlight selected recent results in several key areas of Pcdh biology and discuss their implications for our understanding of neural circuit formation and function.

Keywords: protocadherins, cadherin superfamily, adhesion, neural circuits, Pcdh

INTRODUCTION

The organization of functional neural circuits requires the precise and coordinated control of cell–cell interactions at nearly all stages of development, including neuronal differentiation, neuronal migration, axon outgrowth, dendrite arborization, and synapse formation and stabilization. This coordination is brought about by the concerted action of a large number of cell surface receptors, whose dynamic regulation enables neurons (and astrocytes) to adopt their proper roles within developing neural circuits. While a large number of protein families have been identified that may play roles in neural circuit formation, detailed cellular functions and, especially, molecular mechanisms have been elucidated for only a handful.

The protocadherins (Pcdhs) comprise a major family of >80 cadherin superfamily molecules expressed primarily in the developing vertebrate nervous system, with lower expression seen in other organs such as lung and kidney. The cadherin superfamily is a diverse collection of cell-surface molecules defined by the presence of several ∼110 amino acid extracellular cadherin (EC) motifs (Nollet et al., 2000; Hulpiau and Van Roy, 2009, 2011). The canonical members of this superfamily, the classical cadherins, are type I transmembrane proteins containing 5 EC repeats and a conserved cytoplasmic domain that interacts with the armadillo repeat proteins, β-catenin and p120ctn (Gumbiner, 2005; Takeichi, 2007; Nelson, 2008; Niessen et al., 2011). The classical cadherins mediate calcium-dependent, primarily homophilic, adhesion through interactions between their EC1 domains (N-terminal, most distal from the cell membrane). In a search for additional classical cadherins using degenerate PCR, Suzuki and colleagues discovered a related family of molecules, which they named "Pcdhs" (Sano et al., 1993). The Pcdhs are structurally similar to classical cadherins in that they are also type I transmembrane proteins containing 6 or 7 EC repeats, but their cytoplasmic domains are distinct and lack catenin-binding sites (Sano et al., 1993; Wu and Maniatis, 1999; Nollet et al., 2000; Vanhalst et al., 2005). Subsequently, Pcdhs have been shown to comprise a large and diverse collection of molecules, which are expressed broadly in the developing and mature vertebrate nervous system.

Pcdhs can be divided into two broad classes: the clustered Pcdhs (encoded by the *Pcdh-α*, *-β*, and *-γ* gene clusters, encompassing ∼60 genes in mammals) and the non-clustered Pcdhs (so-called δ-Pcdhs) (Hulpiau and Van Roy, 2009, 2011). In mammals, the clustered Pcdh genes lie in three tandem arrays encompassing ∼1 MB at human chromosome 5q31 and on mouse chromosome 18 (Wu and Maniatis, 1999; Sugino et al., 2000; Wu et al., 2001). Within the *Pcdh-α* and *-γ* clusters, multiple large "variable" exons encoding 6 EC domains, a transmembrane domain, and a variable cytoplasmic domain are each expressed from their own promoters and spliced to three small "constant" exons that encode a shared C-terminal domain (the *Pcdh-β* locus contains no such "constant" exons) (Tasic et al., 2002; Wang et al., 2002a; see **Figure 2B**). The largest group of non-clustered Pcdhs consists of the δ1 (7 EC domains) and δ2 (6 EC domains) sub-families, which are distantly related, yet exhibit short, conserved sequence motifs in their

cytoplasmic domains (Wolverton and Lalande, 2001; Vanhalst et al., 2005).

The involvement of Pcdhs in neural circuit formation has been inferred on the basis of their structural homology to the classical cadherins, their molecular diversity and their differential and combinatorial expression by neurons and glia (Shapiro and Colman, 1999; Yagi and Takeichi, 2000; Takeichi, 2007). Genetic analysis of the *Pcdh-α* and *Pcdh-γ* clusters in mice has uncovered phenotypes that are consistent with such roles, including disrupted dendrite arborization (Garrett et al., 2012; Lefebvre et al., 2012; Suo et al., 2012), impaired synaptic development (Weiner et al., 2005; Garrett and Weiner, 2009), mistargeting of axons (Hasegawa et al., 2008, 2012; Katori et al., 2009; Prasad and Weiner, 2011), and neuronal cell death (Wang et al., 2002b; Emond and Jontes, 2008; Lefebvre et al., 2008; Prasad et al., 2008; Chen et al., 2012). Similarly, recent work has implicated several Pcdh genes in a variety of human neurodevelopmental disorders (Redies et al., 2012). However, clear cellular functions, molecular mechanisms of protein interaction, and signaling partners have yet to be determined for several Pcdh subfamilies, and definitive evidence for Pcdh roles in synaptic recognition and adhesion does not yet exist. While much remains obscure about these fascinating cell-surface molecules, their demonstrated critical importance to neural development and their potential links to human disease suggest that further elucidation of the mechanisms regulating their expression, trafficking, interaction, and signaling will generate important new neurobiological insights.

In this review, we highlight selected recent results in several key areas of Pcdh biology and discuss their implications for our understanding of neural circuit formation and function. For comprehensive reviews of the Pcdh families see the following publications Yagi and Takeichi (2000), Redies et al. (2005, 2012), Morishita and Yagi (2007), and Kim et al. (2011).

CLUSTERED PROTOCADHERINS: ROLES IN NEURAL CIRCUIT FORMATION

Thus far, the best evidence in favor of a role for the clustered Pcdhs in neural circuit formation has been obtained for the *Pcdh-γ* family (Wang et al., 2002b; Weiner et al., 2005; Prasad et al., 2008; Garrett and Weiner, 2009; Prasad and Weiner, 2011; Chen et al., 2012; Garrett et al., 2012; Lefebvre et al., 2012; Suo et al., 2012). *Pcdh-γ* genes are expressed widely in the CNS, and γ-Pcdh proteins are found immunohistochemically at some, though far from all, synapses (Wang et al., 2002b; Phillips et al., 2003), as well as in dendrites, axons, and perisynaptic astrocytic processes (Garrett and Weiner, 2009). Mice in which all 22 *Pcdh-γ* genes (Wang et al., 2002b), or just the 3′-most variable exons (C-type exons; Chen et al., 2012) have been deleted lack voluntary movements and reflexes, and die shortly after birth. This phenotype is likely due to severe apoptosis and neurodegeneration of spinal interneurons and concomitant loss of synapses in the late embryonic period (Wang et al., 2002b; Prasad et al., 2008; Chen et al., 2012). A reduction in synaptic density is apparently a primary function of the γ-Pcdhs in the spinal cord, and not merely secondary to the observed neurodegeneration: When apoptosis is blocked in *Pcdh-γ* null mice by the additional loss of the pro-apoptotic gene *Bax* (Deckwerth et al., 1996), neuronal survival is rescued, but both excitatory and inhibitory synaptic puncta remain reduced by 40–50% and the double-mutant mice die at birth (Weiner et al., 2005). Further, when loss of the γ-Pcdhs is restricted to astrocytes, spinal cord synaptogenesis is delayed, but with no concomitant effect on apoptosis (Garrett and Weiner, 2009). Interestingly, mice lacking only the three C-type *Pcdh-γ* exons, in a $Bax^{-/-}$ background, can survive past weaning, although they exhibit neurological impairments (Chen et al., 2012). This indicates that the loss of the C-type exons alone does not produce an exact phenocopy of the whole-cluster null.

In the retina, loss of all γ-Pcdhs also leads to apoptosis and synapse loss; however, in contrast to the spinal cord data, in this case blocking cell death by deletion of *Bax* does rescue synaptic density (Lefebvre et al., 2008). Conversely, when *Pcdh-γ* loss is restricted to the cerebral cortex, no excessive apoptosis is observed, but rather a major reduction in the dendritic arborization of cortical pyramidal neurons (Garrett et al., 2012). Together, these results from multiple regions of the CNS indicate that distinct neuronal types respond in different ways to the loss of the γ-Pcdhs. This is borne out by recent evidence that the γ-Pcdhs can mediate dendritic self-avoidance, in a manner very similar to that of the immunoglobulin superfamily molecule DSCAM (Fuerst et al., 2008, 2009), in both retinal starburst amacrine cells and cerebellar Purkinje neurons (Lefebvre et al., 2012). The dendritic phenotype (reduced arborization) observed in *Pcdh-γ* knockout cortical neurons (Garrett et al., 2012) and hippocampal neurons in which γ-Pcdh expression has been knocked down via RNAi (Suo et al., 2012) are not obviously consistent with such a self-avoidance role. Thus, it appears that the role of γ-Pcdhs in dendrite arborization may differ depending on the neuronal type, presumably due to a different repertoire of *cis*-interacting proteins and/or downstream signaling pathways.

The α-Pcdhs (originally termed Cadherin-related Neuronal Receptors, or CNRs) were the first of the clustered Pcdhs to be identified as synaptic molecules (Kohmura et al., 1998). The α-Pcdhs localize to developing axons (Blank et al., 2004; Morishita et al., 2004), consistent with the phenotypes subsequently observed in *Pcdh-α* mutant mice, which unlike the *Pcdh-γ* mutants are viable and fertile and do not exhibit increased neuronal apoptosis. Mice in which the *Pcdh-α* constant exons have been deleted exhibit an axonal targeting defect in the olfactory system, with axons expressing a given odorant receptor failing to coalesce on a single glomerulus in the olfactory bulb, as occurs in wildtype mice (Hasegawa et al., 2008, 2012). These disorganized axons appear to be able to form terminals and synapses at the glomeruli they contact; thus, the α-Pcdhs may be more important for axon guidance than they are for synaptogenesis (Hasegawa et al., 2008). Consistent with this, serotonergic axonal projections are also disorganized in mice lacking the α-Pcdhs, in some cases failing to penetrate the proper target area (Katori et al., 2009). Interestingly, morpholino knockdown of the *Pcdh-α* genes in zebrafish results in neuronal apoptosis, suggesting some distinct roles for the α-Pcdhs in different vertebrate systems (Emond and Jontes, 2008).

The *Pcdh-β* cluster remains the least studied of the three, perhaps because the lack of a shared constant domain among its members makes it more difficult to study. Using antibodies

specific for two β-Pcdh proteins, β16 and β22, Junghans et al. (2008) found that both are present in the synaptic zones of the retina, the inner and outer plexiform layers, though only β16 was tightly localized to synapses, primarily the postsynaptic compartment. To date, no functional analysis of the *Pcdh-β* cluster has been published. However, Wu et al. (2007) have reported the generation of mice harboring large deletions within the clustered Pcdh loci, including loss of the *Pcdh-β* cluster, and presumably forthcoming analyses of such mice will yield functional data on the role of the β-Pcdhs in the nervous system.

CLUSTERED PROTOCADHERINS: COMBINATORIAL COMPLEXITY

The assumption that Pcdhs are *bona fide* cell adhesion molecules, acting in a manner analogous to that of the classical cadherins, is central to most views of Pcdh function (Shapiro and Colman, 1999; Redies et al., 2005; Takeichi, 2007). Though not essential for Pcdhs to play a role in neural circuit formation, differential homophilic cell adhesion is conceptually the most straightforward hypothesis, and there is some support for this. Multiple studies have shown that γ-Pcdhs can mediate homophilic interactions in a variety of cell types; the strength of adhesion, however, is modest in comparison to that of the classical cadherins (Frank et al., 2005; Fernandez-Monreal et al., 2009; Schreiner and Weiner, 2010). However, γ-Pcdhs overexpressed in heterologous cells do not efficiently reach the cell surface unless their cytoplasmic domains are truncated (Frank et al., 2005; Fernandez-Monreal et al., 2009; Schreiner and Weiner, 2010), suggesting that in some experiments "weak" adhesion may be due to low surface delivery of the molecules, which is typically not assessed. The α-Pcdhs have not yet been found to exhibit significant adhesive activity, suggesting that they do not act as homophilic cell adhesion molecules (Morishita et al., 2006), though some may exhibit heterophilic interactions with β1 integrins (Mutoh et al., 2004). However, only one (Pcdh-α4) of the 8 α-Pcdhs that contain an integrin-binding RGD site within EC1 has been tested for binding to integrins. Furthermore, the ubiquitously-expressed Pcdh-αC1 and -αC2 do not contain such an RGD site, making it unlikely that they interact with integrins. Therefore, the role of α-Pcdhs in cell adhesion remains uncertain.

Schreiner and Weiner (2010) recently provided the strongest evidence to date that any of the clustered Pcdhs can mediate homophilic interactions, while at the same time demonstrating that the rules governing these interactions are likely to be much more complex than had been assumed. Using a quantitative, colorimetric assay for cell adhesion, these authors confirm that γ-Pcdhs mediate homophilic interactions, but go on to show that these homophilic *trans*-interactions occur between heteromeric *cis* complexes that are most likely tetramers based on their size (**Figure 1**; Schreiner and Weiner, 2010). These tetramers are formed by the 22 γ-Pcdhs promiscuously, with no apparent isoform restriction. Thus, the maximal number of *cis*-tetramers

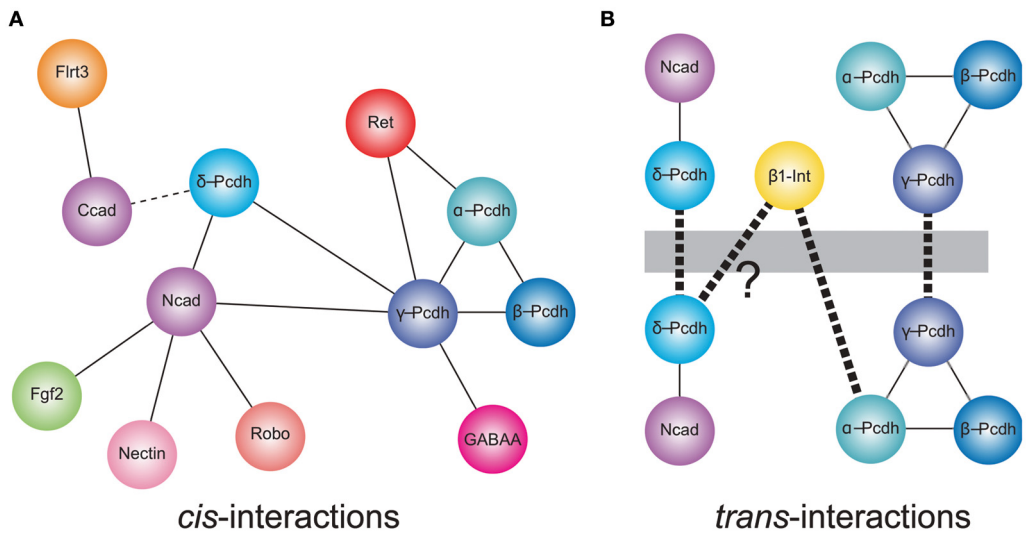

FIGURE 1 | *Cis*- and *trans*-interactions of the protocadherins. (A) Shown are cis-interactions at the membrane that have been identified for each of the protocadherin sub-families. Proteins containing cadherin repeats in their ectodomains (Ncad, α-, β-, γ- and δ-Pcdhs, and Ret) may mediate a core set of protein–protein interactions. These may be augmented by an expanded set of cis-interacting partners. In addition, δ-Pcdhs and γ-Pcdh isoforms can exist as homo- or hetero-oligomers, respectively. Lines represent direct interactions reported in the literature. The dashed line indicates that a direct interaction between C-cadherin and PAPC has not yet been demonstrated. **(B)** Members of each of δ-protocadherin and γ-protocadherin sub-families have been shown to mediate trans-homophilic interactions *in vitro*. These interactions occur in the context of larger macromolecular complexes. In the case of the δ2-protocadherin, Pcdh19, a Pcdh19-Ncad complex mediates *trans*-interactions. For γ-Pcdhs, heteromeric complexes of γ-Pcdh isoforms mediate trans-association *in vitro*. Proteomics studies also suggest that the clustered protocadherins exist in complexes that include α-Pcdh, β-Pcdh, and γ-Pcdh. Thus, the α-Pcdhs and β-Pcdhs could act as co-factors to modulate the γ-Pcdhs or could contribute to expanding the combinatorial complexity of cell interactions. In addition, mammalian α-Pcdhs contain an RGD sequence and exhibit trans-heterophilic interactions with β1-integrin. Similar RGD sequences are present in the δ2-Pcdhs, Pcdh17, and Pcdh19 suggesting that these proteins may also mediate heterophilic binding [indicated by (?)]. Heavy dashed line indicates *trans*-interactions.

that can form is 234,256 (22^4), though assuming a degree of functional equivalence among tetramers with the same composition (that is, assuming topological organization within the membrane is not critical) the number is more likely to be on the order of 10^4 (Zipursky and Sanes, 2010; Yagi, 2012).

In addition to cis-heteromers of γ-Pcdh isoforms, evidence suggests that α-Pcdh, β-Pcdh, and γ-Pcdh proteins also associate in complexes. A potential functional relationship between the α-Pcdhs and γ-Pcdhs was initially shown by Murata et al. (2004), who found that the γ-Pcdhs could facilitate trafficking of α-Pcdhs to the cell surface in transfected HEK293 cells, in which the latter rarely make it to the plasma membrane alone (Murata et al., 2004). In the absence of γ-Pcdhs, α-Pcdhs are retained in the endoplasmic reticulum and Golgi apparatus, with only low levels delivered to the cell surface (Murata et al., 2004). More recently, biochemical studies have demonstrated that α-, β-, and γ-Pcdhs can all be co-isolated by immunoprecipitation, both *in vitro* and *in vivo* (Chen et al., 2009a; Han et al., 2010; Biswas et al., 2012). The functional significance of such pan-cluster complexes remains unclear, but it is tempting to suggest that the α- and β-Pcdhs could modify the homophilic specificity exhibited by γ-Pcdh multimers. If so, the resulting combinatorial explosion in adhesive interfaces would mean, in theory, that the clustered Pcdhs have the ability to endow essentially every neuron with a unique molecular identity (Yagi, 2012).

PROTOCADHERIN–CADHERIN INTERACTIONS

There is increasing evidence for a relationship between the non-clustered δ-Pcdhs and classical cadherins (**Figure 1**). The Pcdh8-like molecule, PAPC (paraxial Pcdh), mediates cell sorting in Xenopus animal cap assays, which was initially taken as evidence for homophilic cell adhesion (Kim et al., 1998). More recently, Gumbiner and colleagues showed that PAPC does not itself mediate cell adhesion. Stable lines expressing PAPC failed to exhibit adhesion either in laminar flow assays or in cell aggregation assays (Chen and Gumbiner, 2006). Moreover, fusions of the PAPC ectodomain to the Fc region of IgG failed to mediate adhesion in bead aggregation assays (Chen and Gumbiner, 2006). Thus, despite the ability to effect cell sorting, PAPC does not function as a cell adhesion molecule. Chen and Gumbiner (2006) went on to resolve this apparent conflict by demonstrating that PAPC actually antagonizes adhesion by C-cadherin, although they did not demonstrate a physical interaction between the two proteins (Chen and Gumbiner, 2006). A similar antagonistic relationship was found between Pcdh8/Arcadlin and N-cadherin in cultured hippocampal neurons (Yasuda et al., 2007). Induction of Pcdh8 expression by electroconvulsive shock treatment in rats results in internalization of Ncad and removal from synaptic junctions. In this instance, there is a physical interaction of Pcdh8 with N-cadherin, as the proteins can be co-immunoprecipitated. Upon expression, Pcdh8 associates with Ncad, and *trans*-interactions mediated by Pcdh8 induce internalization through a pathway that involves the TAO2β kinase and p38 MAPK (Yasuda et al., 2007). Thus, there appears to be a close functional relationship between δ2-Pcdhs and classical cadherins.

More recently, Biswas et al. (2010) found that the δ2-Pcdh, Pcdh19, interacts with Ncad, both physically and functionally in the developing zebrafish. Knockdown of Pcdh19 in zebrafish embryos impairs neural plate convergence, resulting in malformation of the anterior neural tube. This phenotype is very similar to that of Ncad mutant embryos (Lele et al., 2002; Hong and Brewster, 2006; Biswas et al., 2010), suggesting that these molecules participate in a common pathway. Partial loss of both Pcdh19 and Ncad was shown to be synergistic, indicating that these two proteins cooperate during neural plate convergence. In addition to this functional interaction, Pcdh19 and Ncad associated physically to form a *cis*-complex (Biswas et al., 2010). In a follow up study, Emond et al. (2011) showed that secreted, epitope-tagged ectodomains of Pcdh19 and Ncad associate and can be purified from culture medium as a complex (Emond et al., 2011). When used in bead aggregation studies, this Pcdh19-Ncad complex mediates robust homophilic adhesion, although Pcdh19 on its own is not adhesive. Importantly, three lines of evidence support the idea that, within the complex, Pcdh19, rather than Ncad, is responsible for the adhesive interaction: (1) Pcdh19-Ncad complexes formed using adhesion-deficient Ncad mutants still mediate adhesion; (2) Mutations in Pcdh19 abolish adhesion by the complex; and (3) the Pcdh19-Ncad complex does not interact in *trans* with Ncad alone. Thus, Ncad appears to act as a cofactor to facilitate adhesive interactions of Pcdh19. Moreover, these results also indicate that Ncad is unavailable to mediate homophilic interactions when in complex with Pcdh19. These data suggest a model in which Ncad exists in one of two adhesive states: (1) Ncad directly mediates homophilic adhesion on its own; or (2) Ncad acts as a co-factor in *cis* to facilitate adhesion by Pcdh19 in *trans*. As another δ2-Pcdh, Pcdh17, exhibited similar behavior, Ncad may participate in multiple adhesive complexes with mutually incompatible specificities. Collectively, the data on PAPC, Pcdh8, Pcdh17, and Pcdh19 suggest that δ2-Pcdhs, at least, may affect cell adhesion (both positively and negatively) by forming complexes with classical cadherins.

There are hints that the participation of Pcdhs in homophilic interactions could be further complicated by the formation of larger macromolecular assemblies (**Figure 1**). In addition to a *cis*-interaction with δ-Pcdhs, Ncad also associates with other cell surface proteins, including Fgf receptor 2 (Williams et al., 2001), Nectin-2 (Morita et al., 2010), Cdo (Kang et al., 2003), and Robo (Rhee et al., 2002, 2007), and interacts functionally with β1-integrin (Arregui et al., 2000; Li et al., 2000). Moreover, C-cadherin, which interacts with PAPC, can also associate with the leucine-rich repeat protein, Flrt3 (Chen et al., 2009b). In addition, there is evidence that individual clustered Pcdhs or heteromeric complexes of α-, β-, and γ-Pcdhs can interact with classical cadherins (Ncad and Rcad) and δ-Pcdhs (Pcdh17) (Han et al., 2010), as well as Ret (Schalm et al., 2010) and GABA-A receptors (Li et al., 2012). Thus, the distinct cellular roles of clustered (α-Pcdh, β-Pcdh, and γ-Pcdh), non-clustered (δ-Pcdh), and classical cadherins may be difficult to define, due to the possibility of both crosstalk between and cooperation among the distinct family members. The association of Pcdhs with other gene families also suggests that a shifting protein composition within these complexes could influence the specificity of *trans*-interactions and the resulting downstream signaling pathways.

REGULATION OF PROTOCADHERIN TRAFFICKING

A key element in the regulation of many cell surface proteins is the control of their trafficking, and recent data suggest this especially to be true for Pcdhs. Initial work with γ-Pcdhs found that they are present largely in intracellular organelles, with a surprisingly low proportion present on the plasma membrane (Phillips et al., 2003; Murata et al., 2004). The control of γ-Pcdh trafficking appears to be largely dependent on elements within the cytoplasmic domain: deletion of either the constant domain, or the entire cytoplasmic domain, significantly increases surface delivery of the γ-Pcdhs (Fernandez-Monreal et al., 2009; Schreiner and Weiner, 2010). In addition, the receptor tyrosine kinase, Ret, may regulate the trafficking and stability of α-Pcdh/γ-Pcdh complexes through phosphorylation (Schalm et al., 2010). Ret was shown to associate with α- and γ-Pcdhs in a neural tumor cell line and to control their protein levels: knockdown of Ret resulted in a corresponding reduction in the levels of Pcdhs (Schalm et al., 2010). Interestingly, the ectodomain of Ret contains cadherin repeats, reinforcing the notion that cadherin EC repeats may be protein–protein modules that act as scaffolds to assemble *cis*-macromolecular assemblies. These results are reminiscent of the observations of Yasuda et al. (2007), which showed that the δ2-Pcdh Pcdh8/Arcadlin associates with Ncad to induce endocytosis and removal from synaptic junctions. Thus, complex formation may be a fundamental mechanism for regulating Pcdh localization, adhesion, trafficking, and stability.

While surface delivery of the γ-Pcdhs is regulated by their cytoplasmic domains (Fernandez-Monreal et al., 2009; Schreiner and Weiner, 2010), there is also evidence that the γ-Pcdhs themselves may regulate vesicular traffic in the cell. Using correlative light and electron microscopy (CLEM), Hanson et al. (2010) showed that overexpression of γ-Pcdhs, but not Ncad, in HEK293 cells leads to the formation of elaborate membrane tubules that appear to emanate from lysosomes. Intriguingly, tubules did not form when γ-Pcdh isoforms lacking a variable cytoplasmic domain were expressed (O'Leary et al., 2011), and the width of the tubules produced was reduced when half of the ectodomain was deleted (Hanson et al., 2010). While this last result provocatively suggests that homophilic γ-Pcdh ectodomain interactions could occur within intracellular organelles, the functional significance of the tubules formed by overexpression of γ-Pcdh cDNAs in heterologous cell lines remains unclear.

REGULATION OF CLUSTERED PROTOCADHERIN EXPRESSION

One of the most fascinating aspects of the clustered Pcdh families is their differential and combinatorial expression in cells of the nervous system. A decade ago, Tasic et al. (2002) and Wang et al. (2002a) concurrently identified the mechanism of *Pcdh-α* and *-γ* transcription. The sequence upstream of each variable (V) exon contains its own promoter region including a ∼20 base pair conserved sequence element (CSE) that is required for expression. Through mechanisms that are still not entirely clear, a given V exon promoter is "chosen" and transcription through the remaining portion of the *Pcdh-α* or *-γ* cluster proceeds; intervening V exons are then removed when the 5′ V exon is *cis*-spliced to the three downstream constant (C) exons (Tasic et al., 2002; Wang et al., 2002a) (**Figure 2**). Although the *Pcdh-β* cluster does not contain its own C exons, each *Pcdh-β* V exon harbors a consensus 5′ splice site near its end (Wu and Maniatis, 1999) suggesting the possibility of splicing to the C exons of other clusters. Such intercluster spliced transcripts, while rare, are apparently present in neurons, as are low levels of αV/γC and γV/αC hybrid transcripts produced by *trans*-splicing between separate pre-mRNA intermediates (Tasic et al., 2002; Wang et al., 2002a). Most of the *Pcdh-α, -β,* and *-γ* V exons are expressed monoallelically; though both cluster alleles are transcriptionally active in a given cell, an individual V exon promoter is only "chosen" from one of the two alleles (Esumi et al., 2005; Kaneko et al., 2006). The exception to this rule are the nearly ubiquitously-expressed *Pcdh-αC1* and *αC2* V exons, and the related *Pcdh-γ C3*, *C4*, and *C5* V exons, all of which can be biallelically expressed (Esumi et al., 2005; Kaneko et al., 2006). Single-cell RT-PCR analysis of cerebellar Purkinje cell neurons suggests that each cell expresses ∼4 *Pcdh-α* isoforms (2 of the monoallelically expressed genes plus the 2 ubiquitous 3′ genes), ∼2 *Pcdh-β* isoforms and ∼7 *Pcdh-γ* isoforms (∼4 of the monoallelically expressed genes plus the 3 ubiquitous 3′ genes) (Hirano et al., 2012; Yagi, 2012).

A key insight into the control of clustered *Pcdh* expression came with the discovery by Ribich et al. (2006) of two long-range regulatory elements located near the 3′ end of the *Pcdh-α* cluster. These sites were identified based on sequence conservation and hypersensitivity to DNase I degradation; hypersensitive sites (HS) 5-1 lie 3′ of the third α constant exon, and HS7 lies between α constant exon 2 and 3 (**Figure 2**). Addition of HS5-1 (or to a much lesser extent, HS7) downstream of a minimal promoter-*LacZ* cassette resulted in reporter expression throughout the CNS, demonstrating that this site can independently promote gene expression in regions known to express the *Pcdh-α* genes (Ribich et al., 2006). Deletion of the HS5-1 site in mice led to significantly reduced expression of most *Pcdh-α* genes: Expression of the 5′ V exons, *Pcdh-α1-5*, was moderately reduced, while that of the more 3′ *Pcdh-α6-12* and *-αC1* were greatly reduced (Kehayova et al., 2011; Yokota et al., 2011). The *Pcdh-αC2* gene was unaffected by HS5-1 deletion, consistent with prior *in vitro* results (Ribich et al., 2006). Deletion of the HS7 enhancer site resulted in a more moderate, but more uniform, negative effect on *Pcdh-α* gene expression, with expression of all V exons significantly reduced in the cerebellum (Kehayova et al., 2011). Further HS sites downstream of the *Pcdh-γ* cluster were identified and termed HS16-20 by Yokota et al. (2011), who showed that deletion of these sites in mice led to a nearly complete loss of expression across the *Pcdh-β* cluster. Surprisingly, deletion of HS16-20 had a much less drastic effect on the more closely adjacent *Pcdh-γ* cluster; no effect was found on genes of the *Pcdh-α* cluster in these mice (Yokota et al., 2011).

The identification of these long-range regulatory sites provides a likely explanation for the results of Noguchi et al. (2009), who generated several lines of mice harboring deletions or duplications within the *Pcdh-α* cluster using targeted meiotic recombination. Across 4 lines of mice (deletion of α11-C2; deletion of α2-11; duplication of α2-10; duplication of α12-C2), the total *Pcdh-α* transcript levels, as measured by assaying the shared constant exons, remained fairly consistent (Noguchi et al., 2009).

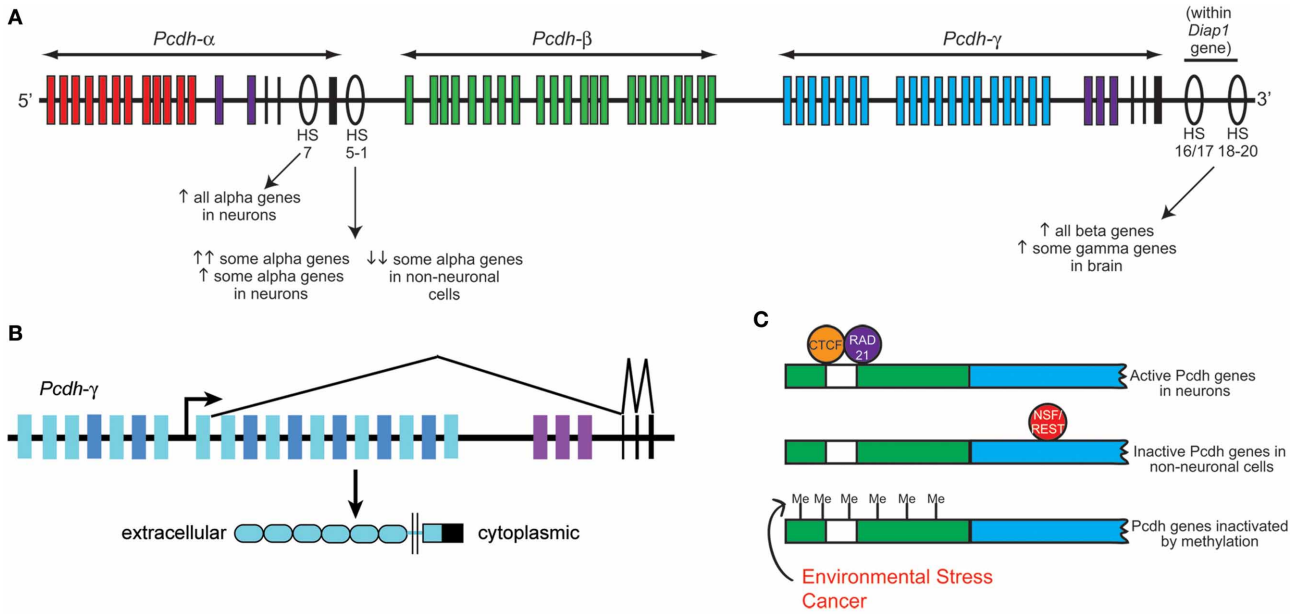

FIGURE 2 | Clustered protocadherin gene regulation. (A) Schematic of the *Pcdh-α*, *-β*, and *-γ* clusters found in the mammalian genome. *Pcdh-α 1-12* variable exons are shown in red, *Pcdh-β* genes in green, *Pcdh-γ* A and B subfamily variable exons in blue, and the homologous *Pcdh-α* and *-γ* C family variable exons in purple. *Pcdh-α* and *-γ* constant exons are shown in black. Several DNase I hypersensitive sites (HS) that have been identified as enhancers are shown as ovals, with their reported effects on clustered Pcdh gene expression noted below. Schematic shows approximate locations along the chromosome but is not to strictly to scale. **(B)** Schematic of the mouse *Pcdh-γ* cluster showing an example pattern of gene transcription and splicing. Each variable exon has its own upstream promoter from which transcription is initiated. A long transcript through the rest of the cluster is subsequently spliced such that each transcript contains only the 5′-most variable exon (which encodes the entire extracellular domain, the transmembrane domain, and a proximal cytoplasmic domain) and the three constant exons (which encode a further ∼125 amino acid C-terminal cytoplasmic domain). *Pcdh-α* transcription and splicing occurs similarly. **(C)** Schematics of a typical clustered Pcdh promoter region (green) containing the conserved sequence element (CSE; white) and an adjacent variable exon (blue). In neurons, CTCF and Rad21 bind near the CSE and promote expression in concert with the HS5-1 enhancer element. In non-neuronal cells, NSF/REST may suppress gene expression by binding to canonical and non-canonical NRSE sites either in the promoters (*Fugu*) or within the coding sequences (mammals). Hypermethylation of clustered Pcdh promoters may also inactivate gene expression; increased methylation has been reported in various cancerous cell types and in brain following environmental stressors such as poor maternal care.

In the deletion lines, the remaining exons were upregulated, while in the duplication lines, individual exons were downregulated, to maintain expression levels. Consistently, the 3′-most V exon in each line took on the ubiquitous expression pattern normally found only for *Pcdh-αC1* and *-αC2* (Noguchi et al., 2009). This suggests that proximity to the HS5-1 and/or HS7 sites, in part, regulates expression levels of individual exons and may account for the varying expression levels across the *Pcdh-α* cluster.

Two zinc finger transcription factors recently have been identified to regulate the clustered *Pcdh* genes: neuron-restrictive silencer factor/RE-1 silencing transcription factor (NRSF/REST), and CTCF (CCCTC-binding factor). NRSF/REST binds to neuron-restrictive silencer elements (NRSEs) to repress neuronal gene expression in non-neuronal cells (Chong et al., 1995; Schoenherr and Anderson, 1995). There are multiple canonical and non-canonical NRSF-binding sites (NRSEs) within the fugu (pufferfish), mouse, and human *Pcdh* clusters (Tan et al., 2010), and deletion of NRSEs from *Pcdh* constructs causes their expression in transgenic *Xenopus* tadpoles to shift from neural-specific to ubiquitous. Kehayova et al. (2011) confirm that the HS5-1 element contains a non-canonical NRSE site, and that this site is required for the suppression of mouse *Pcdh-α* promoter activity in a kidney cell line.

CTCF binding sites are found within the promoters of *Pcdh-α* V exons, as well as within HS5-1 (Kehayova et al., 2011; Golan-Mashiach et al., 2012). This is particularly interesting, as CTCF is known to mediate enhancer/promoter interactions through DNA looping (Gillen and Harris, 2011). Several experimental observations are consistent with such a role at the *Pcdh-α* locus: (1) Knockdown of CTCF with siRNAs reduces the expression of 2 assayed *Pcdh-α* genes in the HEC1-B cell line (Golan-Mashiach et al., 2012); (2) As assayed by chromatin immunoprecipitation (ChIP) from brain samples, deletion of HS5-1 leads to reduced CTCF binding at those *Pcdh-α* promoters that are strongly affected by HS5-1 deletion, but not at those that are only weakly affected (Kehayova et al., 2011); and (3) Transcriptionally active *Pcdh-α* promoters bind both CTCF and the nuclear phosphoprotein Rad21, a subunit of the cohesin complex involved in sister chromatid cohesion during mitosis. The HS5-1 enhancer also binds CTCF and Rad21, and knockdown of either CTCF or Rad21 reduces the expression of several alternatively-expressed *Pcdh-α* isoforms (Monahan et al., 2012). It will be important in the future to determine whether similar roles for NRSF/REST, CTCF, and

cohesin exist at the *Pcdh-γ* cluster, and to uncover the mechanisms by which these factors collaborate to render a "promoter choice" within individual neurons.

A spate of recent papers has revealed that the clustered Pcdh genes can be epigenetically silenced by methylation, and that dysregulation of this process may underlie multiple types of cancer as well as the deleterious effects of environmental stress. Using two mouse cell lines, Kawaguchi et al. (2008) showed that methylation of each *Pcdh-α* promoter, as well as the 5′ region of each V exon, correlates negatively with its expression level; experimentally inducing demethylation increased *Pcdh-α* transcription, while inducing hyper methylation decreased it. Consistent with their ubiquitous expression in neurons, the promoters of *Pcdh-αC1* and *-αC2* are hypomethylated *in vivo* (Kawaguchi et al., 2008). Studies have found that hypermethylation of CpG islands (CGIs) within *Pcdh-α* and *-β* variable exons was highly predictive of poor prognosis across a large group of neuroblastoma samples (Abe et al., 2005). However, this increased methylation does *not* result in the decreased expression of *Pcdh-β* genes in tumor samples, indicating that while *Pcdh* hypermethylation is statistically predictive of cancer outcomes, the underlying mechanism does not involve *Pcdh* expression levels *per se* (Abe et al., 2005).

A more direct link between the clustered *Pcdhs* and cancer progression has been forged by studies from Karim Malik and colleagues (Dallosso et al., 2009, 2012). Genome-wide analysis of promoter hypermethylation in Wilms' tumor (WT), a pediatric cancer of the kidney, identified the three *Pcdh* clusters in patient samples. Multiple *Pcdh-α*, *-β*, and *-γ* genes were found to be hypermethylated in WT samples; while *Pcdh-α* gene expression is not normally detectable in fetal kidney, *Pcdh-β* and *-γ* expression is, and the latter is consistently downregulated in WT, with some genes ∼90% silenced (Dallosso et al., 2009). Importantly, siRNA knockdown of *Pcdh-γ* genes in kidney cell lines leads to increased β-catenin/TCF reporter gene activity and increased expression of known target genes of the canonical Wnt pathway, which is known to be constitutively active in WT. Conversely, overexpression of *Pcdh-γ* cDNAs in WT and HEK293 cell lines leads to growth inhibition in soft agar assays (Dallosso et al., 2009). More recently, a tumor suppressor function was confirmed specifically for *Pcdh-γC3* in colorectal adenoma and carcinoma cells: overexpression of constructs encoding γ-Pcdh-C3 suppresses Wnt and mTOR signaling and reduces colony formation in the colon carcinoma cell line HCT116 (Dallosso et al., 2012).

Together, these exciting results suggest that Pcdhs may be an important new therapeutic target in multiple types of cancer. Importantly, several of the classical cadherins have been implicated in cancer progression; for example, loss of E-cad is a common event in a variety of epithelial cancers (Cavallaro and Christofori, 2004). The demonstrated interaction between classical cadherins and members of the Pcdh family, therefore, suggests that modulation of Pcdh expression or localization could have follow-on effects on the classical cadherins that could regulate tumor progression. It will be important in future studies to reassess the vast literature on classical cadherins in cancer in light of their demonstrated regulation by Pcdhs, as well as to determine whether Pcdh expression is disrupted in various tumor cell types.

The clustered Pcdhs may also play a role in the brain's response to environmental stress, based on studies showing that poor maternal care [assessed by the frequency of maternal licking and grooming (LG) behaviors] correlates with changes in the methylation of their genes. McGowan et al. (2011) analyzed methylation, histone H3-lysine-9 (H3K9) acetylation, and gene expression patterns across 7 MB surrounding the gene encoding the glucocorticoid receptor NR3C1, a prominent target for mediating response to stress, in hippocampal samples from offspring of rat mothers who exhibited high or low LG (McGowan et al., 2011). The three Pcdh gene clusters are located within this region on rat chromosome 18, and hypermethylation of multiple Pcdh genes was observed in offspring of low LG mothers. Conversely, many of the genes across the three Pcdh clusters show significantly higher expression in offspring of high LG mothers (McGowan et al., 2011). A follow-up study showed that this pattern is conserved in humans: hippocampal samples from suicide completers with a history of severe child abuse exhibited hypermethylation across the *Pcdh* gene clusters (Suderman et al., 2012). These epigenetic studies are particularly compelling given the dependence of proper serotonergic axon targeting on the α-Pcdhs (Katori et al., 2009), and of cortical dendrite arborization on the γ-Pcdhs (Garrett et al., 2012), and indicate that the clustered Pcdhs may be critical mediators of neural circuit changes in response to environmental stress during brain development.

CONCLUSIONS

The standard, *a priori* view of Pcdhs was that they simply represented an expanded complement of classical cadherin-like cell adhesion molecules. Accumulating evidence suggests that this model is incomplete. From the recent literature, several insights into Pcdhs can be gleaned. First, Pcdhs appear to function as part of larger macromolecular assemblies. The clustered Pcdhs form heteromeric *cis*-complexes that include α-, β-, and γ-Pcdhs, as well as Ret kinase, and, potentially, many other proteins (Chen et al., 2009a; Han et al., 2010; Schalm et al., 2010; Schreiner and Weiner, 2010). In addition, δ2-Pcdhs can physically associate with classical cadherins, and the Pcdh-Cad complexes appear to be important *in vivo* (Yasuda et al., 2007; Biswas et al., 2010; Emond et al., 2011). As Ret also contains cadherin repeats in its ectodomain, these results could suggest that the cadherin motif functions as a mediator of protein–protein interactions to assemble multiprotein *cis*-complexes, in addition to their known role in homophilic *trans*-interactions. Second, the role of Pcdhs in cell adhesion can be complex and indirect. Some Pcdhs may be able to act as adhesion molecules on their own, others appear to mediate adhesion only by associating with one or more cofactors or coreceptors, while still others clearly inhibit cell adhesion by antagonizing classical cadherin interactions.

When considered broadly, the recent data suggest two significant concerns: (1) Adhesion studies in reduced *in vitro* systems (including those based in heterologous cells and those utilizing purified proteins on beads or substrates) may not recapitulate the nature of adhesive interactions as they would occur in endogenously-expressing cell types *in vivo*. Thus, the individual ectodomains used in bead-based assays or the expression of molecules in heterologous cells likely will not reflect the

adhesive interactions of multimolecular protein assemblies occurring *in vivo*. In the future, this should be addressed by better defining the complexes that exist *in vivo*, which would then allow for a more realistic reconstitution of complexes for *in vitro* studies. (2) Interpreting functional experiments, such as knockouts, as demonstrating a specific role for a molecule *per se* should be seen as provisional, as further work is needed to show whether the observed phenotype is due specifically and directly to the loss of the targeted molecule, or to shifts in the composition and function of multi-protein assemblies that may vary with cell-type and developmental time. It will, thus, be important to consider carefully the results of biochemical and proteomic experiments in reduced systems when interpreting functional studies, and to develop new strategies for dissecting this biological complexity (e.g., looking for genetic interactions in animals heterozygous for both a Pcdh and a known interactor). The recent biochemical experiments (e.g., Schreiner and Weiner, 2010; Emond et al., 2011) that have elucidated molecular mechanisms of Pcdh interactions have actually shown that it may be more difficult than initially believed to understand the cellular and developmental processes in which these molecules participate. With this in mind, we can likely look forward to many surprises as further studies of these far-from-prototypical adhesion molecules emerge.

REFERENCES

Abe, M., Ohira, M., Kaneda, A., Yagi, Y., Yamamoto, S., Kitano, Y., et al. (2005). CpG island methylator phenotype is a strong determinant of poor prognosis in neuroblastomas. *Cancer Res.* 65, 828–834.

Arregui, C., Pathre, P., Lilien, J., and Balsamo, J. (2000). The nonreceptor tyrosine kinase fer mediates cross-talk between N-cadherin and beta1-integrins. *J. Cell Biol.* 149, 1263–1274.

Biswas, S., Emond, M. R., and Jontes, J. D. (2010). Protocadherin-19 and N-cadherin interact to control cell movements during anterior neurulation. *J. Cell Biol.* 191, 1029–1041.

Biswas, S., Emond, M. R., and Jontes, J. D. (2012). The clustered protocadherins Pcdhalpha and Pcdhgamma form a heteromeric complex in zebrafish. *Neuroscience* 219, 280–289.

Blank, M., Triana-Baltzer, G. B., Richards, C. S., and Berg, D. K. (2004). Alpha-protocadherins are presynaptic and axonal in nicotinic pathways. *Mol. Cell. Neurosci.* 26, 530–543.

Cavallaro, U., and Christofori, G. (2004). Cell adhesion and signalling by cadherins and Ig-CAMs in cancer. *Nat. Rev. Cancer* 4, 118–132.

Chen, J., Lu, Y., Meng, S., Han, M. H., Lin, C., and Wang, X. (2009a). alpha- and gamma-Protocadherins negatively regulate PYK2. *J. Biol. Chem.* 284, 2880–2890.

Chen, X., Koh, E., Yoder, M., and Gumbiner, B. M. (2009b). A protocadherin-cadherin-FLRT3 complex controls cell adhesion and morphogenesis. *PLoS ONE* 4:e8411. doi: 10.1371/journal.pone.0008411

Chen, X., and Gumbiner, B. M. (2006). Paraxial protocadherin mediates cell sorting and tissue morphogenesis by regulating C-cadherin adhesion activity. *J. Cell Biol.* 174, 301–313.

Chen, W., Alvarez, F. J., Lefebvre, J. L., Friedman, B., Nwakeze, C., Geiman, E., et al. (2012). Functional significance of isoform diversification in the protocadherin gamma gene cluster. *Neuron* 75, 402–409.

Chong, J. A., Tapia-Ramirez, J., Kim, S., Toledo-Aral, J. J., Zheng, Y., Boutros, M. C., et al. (1995). REST: a mammalian silencer protein that restricts sodium channel gene expression to neurons. *Cell* 80, 949–957.

Dallosso, A. R., Hancock, A. L., Szemes, M., Moorwood, K., Chilukamarri, L., Tsai, H. H., et al. (2009). Frequent long-range epigenetic silencing of protocadherin gene clusters on chromosome 5q31 in Wilms' tumor. *PLoS Genet.* 5:e1000745. doi: 10.1371/journal.pgen.1000745

Dallosso, A. R., Oster, B., Greenhough, A., Thorsen, K., Curry, T. J., Owen, C., et al. (2012). Long-range epigenetic silencing of chromosome 5q31 protocadherins is involved in early and late stages of colorectal tumorigenesis through modulation of oncogenic pathways. *Oncogene* 31, 4409–4419.

Deckwerth, T. L., Elliott, J. L., Knudson, C. M., Johnson, E. M. Jr., Snider, W. D., and Korsmeyer, S. J. (1996). BAX is required for neuronal death after trophic factor deprivation and during development. *Neuron* 17, 401–411.

Emond, M. R., Biswas, S., Blevins, C. J., and Jontes, J. D. (2011). A complex of Protocadherin-19 and N-cadherin mediates a novel mechanism of cell adhesion. *J. Cell Biol.* 195, 1115–1121.

Emond, M. R., and Jontes, J. D. (2008). Inhibition of protocadherin-alpha function results in neuronal death in the developing zebrafish. *Dev. Biol.* 321, 175–187.

Esumi, S., Kakazu, N., Taguchi, Y., Hirayama, T., Sasaki, A., Hirabayashi, T., et al. (2005). Monoallelic yet combinatorial expression of variable exons of the protocadherin-alpha gene cluster in single neurons. *Nat. Genet.* 37, 171–176.

Fernandez-Monreal, M., Kang, S., and Phillips, G. R. (2009). Gamma-protocadherin homophilic interaction and intracellular trafficking is controlled by the cytoplasmic domain in neurons. *Mol. Cell. Neurosci.* 40, 344–353.

Fuerst, P. G., Koizumi, A., Masland, R. H., and Burgess, R. W. (2008). Neurite arborization and mosaic spacing in the mouse retina require DSCAM. *Nature* 451, 470.

Fuerst, P. G., Bruce, F., Tian, M., Wei, W., Elstrott, J., Feller, M. B., et al. (2009). DSCAM and DSCAML1 function in self-avoidance in multiple cell types in the developing mouse retina. *Neuron* 64, 484–497.

Frank, M., Ebert, M., Shan, W., Phillips, G. R., Arndt, K., Colman, D. R., et al. (2005). Differential expression of individual gamma-protocadherins during mouse brain development. *Mol. Cell. Neurosci.* 29, 603–616.

Garrett, A. M., and Weiner, J. A. (2009). Control of CNS synapse development by γ-protocadherin-mediated astrocyte-neuron contact. *J. Neurosci.* 29, 11723–11731.

Garrett, A. M., Schreiner, D., Lobas, M. A., and Weiner, J. A. (2012). gamma-protocadherins control cortical dendrite arborization by regulating the activity of a FAK/PKC/MARCKS signaling pathway. *Neuron* 74, 269–276.

Gillen, A. E., and Harris, A. (2011). The role of CTCF in coordinating the expression of single gene loci. *Biochem. Cell Biol.* 89, 489–494.

Golan-Mashiach, M., Grunspan, M., Emmanuel, R., Gibbs-Bar, L., Dikstein, R., and Shapiro, E. (2012). Identification of CTCF as a master regulator of the clustered protocadherin genes. *Nucleic Acids Res.* 40, 3378–3391.

Gumbiner, B. M. (2005). Regulation of cadherin-mediated adhesion in morphogenesis. *Nat. Rev. Mol. Cell Biol.* 6, 622–634.

Han, M. H., Lin, C., Meng, S., and Wang, X. (2010). Proteomics analysis reveals overlapping functions of clustered protocadherins. *Mol. Cell. Proteomics* 9, 71–83.

Hanson, H. H., Kang, S., Fernandez-Monreal, M., Oung, T., Yildirim, M., Lee, R., et al. (2010). LC3-dependent intracellular membrane tubules induced by gamma-protocadherins A3 and B2: a role for intraluminal interactions. *J. Biol. Chem.* 285, 20982–20992.

Hasegawa, S., Hamada, S., Kumode, Y., Esumi, S., Katori, S., Fukuda, E., et al. (2008). The protocadherin-alpha family is involved in axonal coalescence of olfactory sensory neurons into glomeruli of the olfactory bulb in mouse. *Mol. Cell. Neurosci.* 38, 66–79.

Hasegawa, S., Hirabayashi, T., Kondo, T., Inoue, K., Esumi, S., Okayama, A., et al. (2012). Constitutively expressed Protocadherin-alpha regulates the coalescence and elimination of homotypic olfactory axons through its cytoplasmic region. *Front. Mol. Neurosci.* 5:97. doi: 10.3389/fnmol.2012.00097

Hirano, K., Kaneko, R., Izawa, T., Kawaguchi, M., Kitsukawa, T., and Yagi, T. (2012). Single-neuron diversity generated by Protocadherin-beta cluster in mouse central and peripheral nervous systems. *Front. Mol. Neurosci.* 5:90. doi: 10.3389/fnmol.2012.00090

Hong, E., and Brewster, R. (2006). N-cadherin is required for the polarized cell behaviors that drive neurulation in the zebrafish. *Development* 133, 3895–3905.

Hulpiau, P., and Van Roy, F. (2009). Molecular evolution of the cadherin superfamily. *Int. J. Biochem. Cell Biol.* 41, 349–369.

Hulpiau, P., and Van Roy, F. (2011). New insights into the evolution of metazoan cadherins. *Mol. Biol. Evol.* 28, 647–657.

Junghans, D., Heidenreich, M., Hack, I., Taylor, V., Frotscher, M., and Kemler, R. (2008). Postsynaptic and differential localization to neuronal subtypes of protocadherin beta16 in the mammalian central nervous system. *Eur. J. Neurosci.* 27, 559–571.

Kaneko, R., Kato, H., Kawamura, Y., Esumi, S., Hirayama, T., Hirabayashi, T., et al. (2006). Allelic gene regulation of Pcdh-alpha and Pcdh-gamma clusters involving both monoallelic and biallelic expression in single Purkinje cells. *J. Biol. Chem.* 281, 30551–30560.

Kang, J. S., Feinleib, J. L., Knox, S., Ketteringham, M. A., and Krauss, R. S. (2003). Promyogenic members of the Ig and cadherin families associate to positively regulate differentiation. *Proc. Natl. Acad. Sci. U.S.A.* 100, 3989–3994.

Katori, S., Hamada, S., Noguchi, Y., Fukuda, E., Yamamoto, T., Yamamoto, H., et al. (2009). Protocadherin-alpha family is required for serotonergic projections to appropriately innervate target brain areas. *J. Neurosci.* 29, 9137–9147.

Kawaguchi, M., Toyama, T., Kaneko, R., Hirayama, T., Kawamura, Y., and Yagi, T. (2008). Relationship between DNA methylation states and transcription of individual isoforms encoded by the protocadherin-alpha gene cluster. *J. Biol. Chem.* 283, 12064–12075.

Kehayova, P., Monahan, K., Chen, W., and Maniatis, T. (2011). Regulatory elements required for the activation and repression of the protocadherin-alpha gene cluster. *Proc. Natl. Acad. Sci. U.S.A.* 108, 17195–17200.

Kim, S. H., Yamamoto, A., Bouwmeester, T., Agius, E., and Robertis, E. M. (1998). The role of paraxial protocadherin in selective adhesion and cell movements of the mesoderm during Xenopus gastrulation. *Development* 125, 4681–4690.

Kim, S. Y., Yasuda, S., Tanaka, H., Yamagata, K., and Kim, H. (2011). Non-clustered protocadherin. *Cell Adh. Migr.* 5, 97–105.

Kohmura, N., Senzaki, K., Hamada, S., Kai, N., Yasuda, R., Watanabe, M., et al. (1998). Diversity revealed by a novel family of cadherins expressed in neurons at a synaptic complex. *Neuron* 20, 1137–1151.

Lefebvre, J. L., Zhang, Y., Meister, M., Wang, X., and Sanes, J. R. (2008). gamma-Protocadherins regulate neuronal survival but are dispensable for circuit formation in retina. *Development* 135, 4141–4151.

Lefebvre, J. L., Kostadinov, D., Chen, W. V., Maniatis, T., and Sanes, J. R. (2012). Protocadherins mediate dendritic self-avoidance in the mammalian nervous system. *Nature* 488, 517–521.

Lele, Z., Folchert, A., Concha, M., Rauch, G.-J., Geisler, R., Rosa, F., et al. (2002). parachute/n-cadherin is required for morphogenesis and maintained integrity of the zebrafish neural tube. *Development* 129, 3281–3294.

Li, H., Leung, T. C., Hoffman, S., Balsamo, J., and Lilien, J. (2000). Coordinate regulation of cadherin and integrin function by the chondroitin sulfate proteoglycan neurocan. *J. Cell Biol.* 149, 1275–1288.

Li, Y., Xiao, H., Chiou, T. T., Jin, H., Bonhomme, B., Miralles, C. P., et al. (2012). Molecular and functional interaction between protocadherin-gammaC5 and GABAA receptors. *J. Neurosci.* 32, 11780–11797.

McGowan, P. O., Suderman, M., Sasaki, A., Huang, T. C., Hallett, M., Meaney, M. J., et al. (2011). Broad epigenetic signature of maternal care in the brain of adult rats. *PLoS ONE* 6:e14739. doi: 10.1371/journal.pone.0014739

Monahan, K., Rudnick, N. D., Kehayova, P. D., Pauli, F., Newberry, K. M., Myers, R. M., et al. (2012). Role of CCCTC binding factor (CTCF) and cohesin in the generation of single-cell diversity of protocadherin-alpha gene expression. *Proc. Natl. Acad. Sci. U.S.A.* 109, 9125–9130.

Morishita, H., Kawaguchi, M., Murata, Y., Seiwa, C., Hamada, S., Asou, H., et al. (2004). Myelination triggers local loss of axonal CNR/protocadherin alpha family protein expression. *Eur. J. Neurosci.* 20, 2843–2847.

Morishita, H., Umitsu, M., Murata, Y., Shibata, N., Udaka, K., Higuchi, Y., et al. (2006). Structure of the cadherin-related neuronal receptor/protocadherin-alpha first extracellular cadherin domain reveals diversity across cadherin families. *J. Biol. Chem.* 281, 33650–33663.

Morishita, H., and Yagi, T. (2007). Protocadherin family: diversity, structure, and function. *Curr. Opin. Cell Biol.* 19, 584–592.

Morita, H., Nandadasa, S., Yamamoto, T. S., Terasaka-Iioka, C., Wylie, C., and Ueno, N. (2010). Nectin-2 and N-cadherin interact through extracellular domains and induce apical accumulation of F-actin in apical constriction of Xenopus neural tube morphogenesis. *Development* 137, 1315–1325.

Murata, Y., Hamada, S., Morishita, H., Mutoh, T., and Yagi, T. (2004). Interaction with protocadherin-gamma regulates the cell surface expression of protocadherin-alpha. *J. Biol. Chem.* 279, 49508–49516.

Mutoh, T., Hamada, S., Senzaki, K., Murata, Y., and Yagi, T. (2004). Cadherin-related neuronal receptor 1 (CNR1) has cell adhesion activity with beta1 integrin mediated through the RGD site of CNR1. *Exp. Cell Res.* 294, 494–508.

Nelson, W. J. (2008). Regulation of cell-cell adhesion by the cadherin-catenin complex. *Biochem. Soc. Trans.* 36, 149–155.

Niessen, C. M., Leckband, D., and Yap, A. S. (2011). Tissue organization by cadherin adhesion molecules: dynamic molecular and cellular mechanisms of morphogenetic regulation. *Physiol. Rev.* 91, 691–731.

Noguchi, Y., Hirabayashi, T., Katori, S., Kawamura, Y., Sanbo, M., Hirabayashi, M., et al. (2009). Total expression and dual gene-regulatory mechanisms maintained in deletions and duplications of the Pcdha cluster. *J. Biol. Chem.* 284, 32002–32014.

Nollet, F., Kools, P., and Van Roy, F. (2000). Phylogenetic analysis of the cadherin superfamily allows identification of six major subfamilies besides several solitary members. *J. Mol. Biol.* 299, 551–572.

O'Leary, R., Reilly, J. E., Hanson, H. H., Kang, S., Lou, N., and Phillips, G. R. (2011). A variable cytoplasmic domain segment is necessary for gamma-protocadherin trafficking and tubulation in the endosome/lysosome pathway. *Mol. Biol. Cell* 22, 4362–4372.

Phillips, G. R., Tanaka, H., Frank, M., Elste, A., Fidler, L., Benson, D. L., et al. (2003). Gamma-protocadherins are targeted to subsets of synapses and intracellular organelles in neurons. *J. Neurosci.* 23, 5096–5104.

Prasad, T., Wang, X., Gray, P. A., and Weiner, J. A. (2008). A differential developmental pattern of spinal interneuron apoptosis during synaptogenesis: insights from genetic analyses of the protocadherin-gamma gene cluster. *Development* 135, 4153–4164.

Prasad, T., and Weiner, J. A. (2011). Direct and indirect regulation of spinal cord Ia afferent terminal formation by the γ-Protocadherins. *Front. Mol. Neurosci.* 4:54. doi: 10.3389/fnmol.2011.00054

Redies, C., Hertel, N., and Hubner, C. A. (2012). Cadherins and neuropsychiatric disorders. *Brain Res.* 1470, 130–144.

Redies, C., Vanhalst, K., and Roy, F. (2005). delta-Protocadherins: unique structures and functions. *Cell. Mol. Life Sci.* 62, 2840–2852.

Rhee, J., Buchan, T., Zukerberg, L., Lilien, J., and Balsamo, J. (2007). Cables links Robo-bound Abl kinase to N-cadherin-bound beta-catenin to mediate Slit-induced modulation of adhesion and transcription. *Nat. Cell Biol.* 9, 883–892.

Rhee, J., Mahfooz, N. S., Arregui, C., Lilien, J., Balsamo, J., and Vanberkum, M. F. (2002). Activation of the repulsive receptor Roundabout inhibits N-cadherin-mediated cell adhesion. *Nat. Cell Biol.* 4, 798–805.

Ribich, S., Tasic, B., and Maniatis, T. (2006). Identification of long-range regulatory elements in the protocadherin-alpha gene cluster. *Proc. Natl. Acad. Sci. U.S.A.* 103, 19719–19724.

Sano, K., Tanihara, H., Heimark, R. L., Obata, S., Davidson, M., St. John, T., et al. (1993). Protocadherins: a large family of cadherin-related molecules in central nervous system. *EMBO J.* 12, 2249–2256.

Schalm, S. S., Ballif, B. A., Buchanan, S. M., Phillips, G. R., and Maniatis, T. (2010). Phosphorylation of protocadherin proteins by the receptor tyrosine kinase Ret. *Proc. Natl. Acad. Sci. U.S.A.* 107, 13894–13899.

Schoenherr, C. J., and Anderson, D. J. (1995). Silencing is golden: negative regulation in the control of neuronal gene transcription. *Curr. Opin. Neurobiol.* 5, 566–571.

Schreiner, D., and Weiner, J. A. (2010). Combinatorial homophilic interaction between gamma-protocadherin multimers greatly expands the molecular diversity of cell adhesion. *Proc. Natl. Acad. Sci. U.S.A.* 107, 14893–14898.

Shapiro, L., and Colman, D. R. (1999). The diversity of cadherins and implications for a synaptic adhesive code in the CNS. *Neuron* 23, 427–430.

Suderman, M., McGowan, P. O., Sasaki, A., Huang, T. C., Hallett, M. T., Meaney, M. J., et al. (2012). Conserved epigenetic sensitivity to early life experience in the rat and human hippocampus. *Proc. Natl.*

Acad. Sci. U.S.A. 109(Suppl. 2), 17266–17272.

Sugino, H., Hamada, S., Yasuda, R., Tuji, A., Matsuda, Y., Fujita, M., et al. (2000). Genomic organization of the family of CNR cadherin genes in mice and humans. *Genomics* 63, 75–87.

Suo, L., Lu, H., Ying, G., Capecchi, M. R., and Wu, Q. (2012). Protocadherin clusters and cell adhesion kinase regulate dendrite complexity through Rho GTPase. *J. Mol. Cell Biol.* 4, 362–376.

Takeichi, M. (2007). The cadherin superfamily in neuronal connections and interactions. *Nat. Rev. Neurosci.* 8, 11–20.

Tan, Y. P., Li, S., Jiang, X. J., Loh, W., Foo, Y. K., Loh, C. B., et al. (2010). Regulation of protocadherin gene expression by multiple neuron-restrictive silencer elements scattered in the gene cluster. *Nucleic Acids Res.* 38, 4985–4997.

Tasic, B., Nabholz, C. E., Baldwin, K. K., Kim, Y., Rueckert, E. H., Ribich, S. A., et al. (2002). Promoter choice determines splice site selection in protocadherin alpha and gamma pre-mRNA splicing. *Mol. Cell* 10, 21–33.

Vanhalst, K., Kools, P., Staes, K., Van Roy, F., and Redies, C. (2005). delta-Protocadherins: a gene family expressed differentially in the mouse brain. *Cell. Mol. Life Sci.* 62, 1247–1259.

Wang, X., Su, H., and Bradley, A. (2002a). Molecular mechanisms governing Pcdh-gamma gene expression: evidence for a multiple promoter and cis-alternative splicing model. *Genes Dev.* 16, 1890–1905.

Wang, X., Weiner, J. A., Levi, S., Craig, A. M., Bradley, A., and Sanes, J. R. (2002b). Gamma protocadherins are required for survival of spinal interneurons. *Neuron* 36, 843–854.

Weiner, J. A., Wang, X., Tapia, J. C., and Sanes, J. R. (2005). Gamma protocadherins are required for synaptic development in the spinal cord. *Proc. Natl. Acad. Sci. U.S.A.* 102, 8–14.

Williams, E. J., Williams, G., Howell, F. V., Skaper, S. D., Walsh, F. S., and Doherty, P. (2001). Identification of an N-cadherin motif that can interact with the fibroblast growth factor receptor and is required for axonal growth. *J. Biol. Chem.* 276, 43879–43886.

Wolverton, T., and Lalande, M. (2001). Identification and characterization of three members of a novel subclass of protocadherins. *Genomics* 76, 66–72.

Wu, Q., and Maniatis, T. (1999). A striking organization of a large family of human neural cadherin-like cell adhesion genes. *Cell* 97, 779–790.

Wu, S., Ying, G., Wu, Q., and Capecchi, M. R. (2007). Toward simpler and faster genome-wide mutagenesis in mice. *Nat. Genet.* 39, 922–930.

Wu, Q., Zhang, T., Cheng, J. F., Kim, Y., Grimwood, J., Schmutz, J., et al. (2001). Comparative DNA sequence analysis of mouse and human protocadherin gene clusters. *Genome Res.* 11, 389–404.

Yagi, T. (2012). Molecular codes for neuronal individuality and cell assembly in the brain. *Front. Mol. Neurosci.* 5:45. doi: 10.3389/fnmol.2012.00045

Yagi, T., and Takeichi, M. (2000). Cadherin superfamily genes: functions, genomic organization, and neurologic diversity. *Genes Dev.* 14, 1169–1180.

Yasuda, S., Tanaka, H., Sugiura, H., Okamura, K., Sakaguchi, T., Tran, U., et al. (2007). Activity-induced protocadherin arcadlin regulates dendritic spine number by triggering N-cadherin endocytosis via TAO2beta and p38 MAP kinases. *Neuron* 56, 456–471.

Yokota, S., Hirayama, T., Hirano, K., Kaneko, R., Toyoda, S., Kawamura, Y., et al. (2011). Identification of the cluster control region for the protocadherin-beta genes located beyond the protocadherin-gamma cluster. *J. Biol. Chem.* 286, 31885–31895.

Zipursky, S. L., and Sanes, J. R. (2010). Chemoaffinity revisited: dscams, protocadherins, and neural circuit assembly. *Cell* 143, 343–353.

Conflict of Interest Statement: The authors declare that the research was conducted in the absence of any commercial or financial relationships that could be construed as a potential conflict of interest.

Received: 20 December 2012; accepted: 01 March 2013; published online: 19 March 2013.

*Citation: Weiner JA and Jontes JD (2013) Protocadherins, not prototypical: a complex tale of their interactions, expression, and functions. Front. Mol. Neurosci. **6**:4. doi: 10.3389/fnmol.2013.00004*

frontiers in
MOLECULAR NEUROSCIENCE

HYPOTHESIS AND THEORY ARTICLE
published: 12 April 2012
doi: 10.3389/fnmol.2012.00045

Molecular codes for neuronal individuality and cell assembly in the brain

Takeshi Yagi [1,2]*

[1] KOKORO-Biology Group, Graduate School of Frontier Biosciences, Laboratories for Integrated Biology, Osaka University, Yamadaoka, Suita, Osaka, Japan
[2] CREST, Osaka University, Suita, Japan

Edited by:
Joshua A. Weiner, The University of Iowa, USA

Reviewed by:
Joshua A. Weiner, The University of Iowa, USA
Woj M. Wojtowicz, University of California, Berkeley, USA

***Correspondence:**
Takeshi Yagi, Graduate School of Frontier Biosciences, Osaka University, 1–3 Yamadaoka, Suita, Osaka 565–0871, Japan.
e-mail: yagi@fbs.oska-u.ac.jp

The brain contains an enormous, but finite, number of neurons. The ability of this limited number of neurons to produce nearly limitless neural information over a lifetime is typically explained by combinatorial explosion; that is, by the exponential amplification of each neuron's contribution through its incorporation into "cell assemblies" and neural networks. In development, each neuron expresses diverse cellular recognition molecules that permit the formation of the appropriate neural cell assemblies to elicit various brain functions. The mechanism for generating neuronal assemblies and networks must involve molecular codes that give neurons individuality and allow them to recognize one another and join appropriate networks. The extensive molecular diversity of cell-surface proteins on neurons is likely to contribute to their individual identities. The clustered protocadherins (Pcdh) is a large subfamily within the diverse cadherin superfamily. The clustered *Pcdh* genes are encoded in tandem by three gene clusters, and are present in all known vertebrate genomes. The set of clustered *Pcdh* genes is expressed in a random and combinatorial manner in each neuron. In addition, *cis*-tetramers composed of heteromultimeric clustered Pcdh isoforms represent selective binding units for cell-cell interactions. Here I present the mathematical probabilities for neuronal individuality based on the random and combinatorial expression of clustered Pcdh isoforms and their formation of *cis*-tetramers in each neuron. Notably, clustered *Pcdh* gene products are known to play crucial roles in correct axonal projections, synaptic formation, and neuronal survival. Their molecular and biological features induce a hypothesis that the diverse clustered Pcdh molecules provide the molecular code by which neuronal individuality and cell assembly permit the combinatorial explosion of networks that supports enormous processing capability and plasticity of the brain.

Keywords: protocadherin, Pcdh, CNR, neuron, neural circuits, complex networks, combinatorics, complexity

INTRODUCTION

The mammalian brain is a complex multi-cellular system composed of an enormous number of cells, including neurons and glia. In the brain, the individual neurons are highly differentiated and well organized into neural networks that generate various brain functions, and the activity of each neuron reflects the encoded information.

Recent progress in neuroscience has revealed mechanisms by which many brain functions are controlled, but essential questions remain concerning the precise nature of information processing in the brain (reviewed by Buzsaki, 2010). How can nearly limitless number of information be processed by a finite number of neurons? How can such information be integrated with other information in the brain? How are different sets of information processed in parallel? The answers to these "how" questions require the existence of a basic neuronal code for information processing in the brain (reviewed by Sakurai, 1999). An individual neuron, the basic functional unit of the brain, has a specific firing activity, and is uniquely coordinated in a circuit with many other neurons in response to specific stimuli. A single neuron can have several to 10,000 synaptic contacts on it, and therefore receive several to ten thousand inputs.

Donald Hebb hypothesized that a discrete interconnected group of active neurons, a "cell assembly," represents a distinct cognitive entity (Hebb, 1949). Although the experimental identification of these hypothesized cell assemblies proved difficult for decades, recent rapid progress in the large-scale recording from individual neurons has experimentally defined putative cell assemblies (reviewed by Buzsaki, 2010). Under Hebb's cell assembly hypothesis, a nearly limitless number of combinatorial neuronal groups can be theoretically produced from the limited number of neurons by combinatorial explosion. Thus, the "how" questions posed above can be solved, at least theoretically, by the cell assembly hypothesis. Furthermore, recent reports show that predictive neuronal activity by spontaneous firing is observed even before an event or experience happens (Kenet et al., 2003; Dragoi and Tonegawa, 2011). These findings might mean that each "cell assembly" is intrinsically predetermined before experiences are processed in the brain.

The immune system is a genetically predetermined system for recognizing external antigens (Tonegawa, 1983; Lieber, 1992). Enormous numbers of diverse immune cells are produced developmentally by the nearly random DNA rearrangement of immunoglobulin and T-cell receptor genes; these cells include the proper immune cells for responding to certain antigens (refer **Figure 7**). This system can learn and memorize a nearly limitless number of antigens, against which it produces antibodies when an animal is attacked again by the same antigen. The molecular mechanism for the predetermined immune memory system was solved decades ago, when only limited genomic information was available with random combinations. The identification of similar molecular mechanisms may explain the "how" questions of the enormous information processing capability of the brain. In particular, the molecular codes for neuronal individuality and interconnectivity are likely to be important; for example, the discovery of thousands of odorant receptors opened new avenues of investigation in the field of odorant sensory system biology (Buck and Axel, 1991).

By analyzing nerve regeneration, Langley and Sperry similarly hypothesized that there was some type of special chemical relationship between each class of nerve fiber and each class of nerve target cell (Sperry, 1963; Langley, 1895). Sperry's chemoaffinity hypothesis proposed the existence of individual identification tags that linked each axon to only specific target cells. Recent efforts to find "molecular tags" have led to the identification of "gradient molecules." Complementary gradients of Eph kinases and their ligands, ephrins, play significant roles in establishing topographically organized maps, i.e., the retinotectal map (Cheng et al., 1995; Drescher et al., 1995; McLaughlin and O'Leary, 2005). In addition, axonal guidance molecules and receptors, which guide each axon to its target cells by contact-mediated and diffusible mechanisms, have been identified, and include ephrins, semaphorins, netrins, plexins, robos, slits, and others. The guidance cues act as both attractants and repellents (Dickson, 2002). In addition, specific adhesion and adhesion-inducing proteins are expressed differentially in specific neuronal populations. These include the cadherins and non-clustered Pcdh (∼20 genes, Takeichi, 2007), the neurexins and neuroligins, which have a large number of alternative splicing forms (Sudhof, 2008), and the olfactory receptors (∼1000 genes, Buck and Axel, 1991), which have all been proposed as supporting evidence for (and likely contributors to) the "area code hypothesis" (Dreyer, 1998).

Recent studies reported that two large protein families, Dscam1 in insects and clustered protocadherin (Pcdh) in vertebrates, are promising candidates for the molecular code that stamps individuality and specific interconnectivity on a given neuron (reviewed by Zipursky and Sanes, 2010). In both cases, a large diversity of proteins encoded in a complex genome structure is expressed in combinatorial and random patterns by individual neurons. These proteins mediate homophilic binding and play critical roles in neural development. In particular, the clustered Pcdh family is proposed to provide the molecular basis for neuronal individuality through their combinatorial and random expression, which is conserved in vertebrates, including humans (Yagi, 2008). In this paper, I summarize recent findings about the clustered Pcdh molecules and suggest a hypothesis of candidates for the molecular code for neuronal individuality and cell assembly in the brain.

CLUSTERED Pcdh MOLECULES

In 1998, the identification of a group of eight homologous transmembrane proteins, called cadherin-related neuronal receptors (CNRs) has been reported (Kohmura et al., 1998). In 1999, Wu and Maniatis found a large gene cluster in the human genome project data by performing a BLAST search for CNRs (Wu and Maniatis, 1999). A total of 52 genes, called clustered Pcdh, are encoded in the human genome at 5q31. Exons encoding extracellular, transmembrane, and short intracellular domains are arranged in three groups called Pcdh-α, Pcdh-β, and Pcdh-γ, which have 15, 15, and 22 members, respectively. The *Pcdh-α* genes include the 8 *CNR* genes discovered in mice. The Pcdh-α and Pcdh-γ genes have very large first exons that encode almost an entire molecule, and that the 3 constant exons (exons 2–4) are very small and encode only the last 125–150 amino acids, which are shared by all Pcdh-α and Pcdh-γ genes. Their large exons have multipule promoters and are *cis*-spliced to the constant exons (Wang et al., 2002a). In addition, there are alternative splicing (A and B) forms in the constant exons of *Pcdh-α* genes (Sugino et al., 2000). The Pcdh-β cluster has no constant exons. Their cytoplasmic tails are distinct sequences, but highly conserved. In mice, a total of 58 genes are arranged in Pcdh-α, -β, and -γ, which have 14, 22, and 22 members, respectively, (Wu et al., 2001).

The Pcdhs are fascinating for several reasons (**Figure 1**). First, their ectodomains have cadherin motifs. They belong to the cadherin superfamily, many other members of which play critical roles in developmental processes including synapse formation (Yagi and Takeichi, 2000). Mice lacking Pcdh-α are viable and fertile but have axon projection defects (Hasegawa et al., 2008; Katori et al., 2009). The loss of Pcdh-γ leads to neonatal death with neurological defects, including cell death and decreased numbers of synapses (Wang et al., 2002b). Thus, the Pcdhs are important for building proper neural networks in the brain. Second, they have a remarkable genomic organization, similar to that of immunoglobulin and T-cell receptor gene clusters. The N-terminal extracellular, transmembrane, and short cytoplasmic domains are encoded by a distinct and large exon, while the C-terminal cytoplasmic domain of each protein is identical among the α or γ members (Wu and Maniatis, 1999). Third, Pcdhs are expressed predominantly in the nervous system. Almost all of their isoforms are expressed in a scattered pattern over wide regions of the brain (Esumi et al., 2005; Kaneko et al., 2006; Noguchi et al., 2009; Yokota et al., 2011). In addition, at the single-cell level, individual family members are randomly expressed in combinatorial patterns (Esumi et al., 2005; Kaneko et al., 2006). Fourth, the gene regulation of Pcdhs is epigenetically controlled independently and monoallelically (Tasic et al., 2002; Kawaguchi et al., 2008). Their random expression in each neuron depends on the structure of the gene cluster (**Figure 2**) (Noguchi et al., 2009), and is controlled by *cis*-regulatory elements that independently influence the α and β gene clusters (**Figure 3**) (Ribich et al., 2006; Yokota et al.,

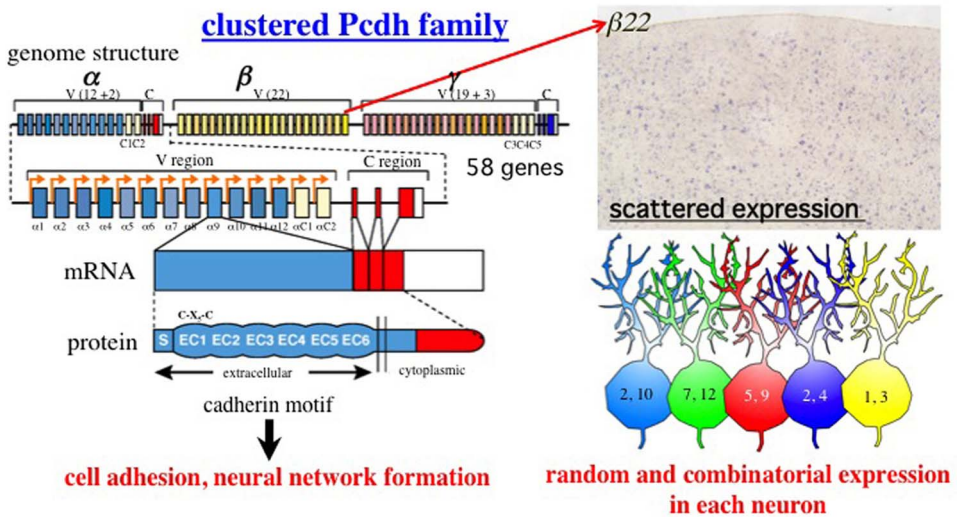

FIGURE 1 | Summary of the clustered Pcdh family. Genomic organization of the *Pcdh-α*, *Pcdh-β*, and *Pcdh-γ* gene clusters in mouse chromosome 18. A total of 58 isoforms are encoded in these gene clusters. The mouse *Pcdh-α* gene consists of 14 exons (12 randomly and two constitutively expressed) in the variable (V) region and a set of three constant (C) region exons (A-type alterative splicing), Not shown here, B-type is derived from four constant region exons (Kohmura et al., 1998). Similar to Pcdh-α, the Pcdh-γ cluster consists of 22 variable exons (19 randomly and three constitutively expressed) and a set of three constant region exons. Mature mRNAs of the *Pcdh-α* and *Pcdh-γ* isoforms are produced from one of these variable exons and either the α or γ constant exons. The αC1, αC2, γC3, γC4, and γC5 exons are closely related in homology and gene regulation. The Pcdh-β cluster does not have constant exons; instead, 22 mature isoforms are produced from large single exons. All the Pcdh-α, Pcdh-β, and Pcdh-γ isoforms consist of a signal peptide (S) with six extracellular cadherin (EC) domains in the extracellular region, followed by a single transmembrane (TM) domain and cytoplasmic region. Interestingly, a Cys-$(X)_5$-Cys (C-X_5-C) motif in the EC1 domain is completely conserved in the vertebrate clustered Pcdh family (Morishita and Yagi, 2007). Loss-of-function analyzes have revealed that the Pcdh family has homologous cell adhesion activity, and critical roles in building neural networks, including axonal targeting, synapse formation, cell death, and dendritic arborization. Each of the 12 α, 22 β, and 19 γ isoforms exhibits random and combinatorial expression in individual neurons at the allelic level. Thus, they exhibit a scattered expression pattern in wide regions of the brain. The photograph shows the expression pattern of the β22 isoform in the cerebral cortex (provided by K. Hirano). The figures in the neurons are the a isoforms, illustrating the random and combinatorial expression in each individual neuron. Different colors represent different combinations.

2011). Fifth, the Pcdh proteins form heteromultimeric protein oligomers. The heterotetramer formed by the Pcdh-γ proteins is a homophilic binding unit that induces cell-cell adhesion and interaction (**Figure 4**) (Schreiner and Weiner, 2010). Finally, Pcdh orthologs are present in vertebrates but not in invertebrates (Hill et al., 2001; Noonan et al., 2004b; Hirayama and Yagi, 2006).

Interestingly, there are many nucleotide polymorphisms among the clustered *Pcdh* genes of mouse subspecies (Taguchi et al., 2005) and individual humans (Noonan et al., 2003; Miki et al., 2005). Evolutionarily, the clustered *Pcdh* gene clusters are conserved and homogenized (appeared similar sequences specified in species) within each vertebrate species (Noonan et al., 2004a; Ishii et al., 2004; Schmutz et al., 2004; Yagi, 2008). Together, these molecular features suggest the clustered Pcdhs as possible candidates for producing complex neural networks at the individual neuron level in vertebrates.

GENE REGULATION OF CLUSTERED Pcdhs AT THE INDIVIDUAL NEURON LEVEL

The clustered Pcdhs are candidates for the molecular code for neuronal individuality. Single-cell RT-PCR analysis of Purkinje cells, which contain a large amount of mRNA, revealed strong evidence for the stochastic, combinatorial expression of clustered Pcdhs in individual neurons (Esumi et al., 2005; Kaneko et al., 2006). Each Purkinje cell expresses ∼2 of the 5′ members of the 12 Pcdh-α isoforms and ∼4 of the 5′ members of the 19 Pcdh-γ isoforms. In addition, ∼4 of the 22 Pcdh-β isoforms are expressed (Hirano et al, unpublished data; their scattered expression referring in Yokota et al., 2011). These expressions are stochastically regulated monoallelically. Interestingly, their random expressions depend on the number of variable exons in the cluster. When a deletion allele of exons Pcdh-α2 to α11, which spares only exons α1 and α12, was used to make a transgenic knock-in mouse, the expression frequencies of the α1 and α12 isoforms differed from those of the wild-type allele (**Figure 2**) (Noguchi et al., 2009). Namely, each individual neuron always expressed α1, α12, or both isoforms from the deletion allele, whereas the α1 and α12 isoforms are only sometimes expressed from among the 12 variable exons of the wild-type allele. Thus, the expressions of the variable exons are random or stochastic, like the results of throwing dice.

The random and scattered expression of variable exons is found in Purkinje neurons (Esumi et al., 2005; Kaneko et al., 2006), suggesting almost all the neurons in the brain have random and scattered expression pattern of variable exons of clustered Pcdh (Noguchi et al., 2009; Yokota et al., 2011). In contrast, the 3′ members ("C" isoforms) of each cluster, αC1 and αC2 in

Pcdh-α and γC3, γC4, and γC5 in Pcdh-γ, are expressed constitutively and biallelically by Purkinje neurons (Kaneko et al., 2006). Their biallelic expressions also depend on the position of the C exon in the gene cluster; when a deletion construct that removes Pcdh-α11–the αC2 exon is knocked-in, the nearest exon from the constant region, α10, is expressed constitutively and biallelically (Noguchi et al., 2009). Thus, the monoallelic and biallelic expressions of the Pcdh isoforms are regulated by the structure of the gene cluster.

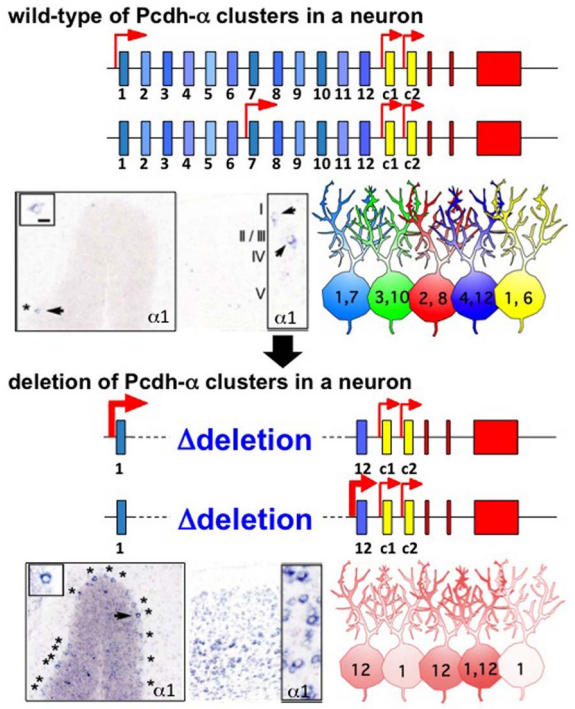

FIGURE 2 | Random regulation of the Pcdh-α1 to α12 isoforms from the gene cluster in individual neurons. In wild-type, one (or two) is randomly chosen from 12 variable exons in a monoallelic manner. As a result, a random and a combinatorial expression of a isoforms are established in each individual neuron. The photographs show the representative, scattered expression patterns of the α1 isoform in Purkinje neurons and the cerebral cortex, by in situ hybridization. The numbers in the illustrated neurons give the number of a isoforms expressed in individual neurons. In a gene cluster in which variable exons α2–α11 are deleted, one (or two) is randomly chosen from the remaining two exons α1 and α12 in the monoallelic. As a result, either α1 or α12 is always expressed in individual neurons. The expression frequencies of α1 and α12 are therefore increased in the deletion mutants. The photographs show the expression patterns of the α1 isoform in the Purkinje cells and cortex of this mutant.

From each allele in individual neurons, 1, 2, and 2 isoforms, respectively, are randomly expressed from among the total 12 in the α, 22 in the β, and 19 in the γ cluster (**Figure 4**). The calculation of the number of possible combinations in each allele is represented as $\binom{n}{k}$, where n is the number of total isoforms, and k is the number expressed in a cell, calculated by a formula of $n!/(n-k)!k!$.

$$\alpha\binom{12}{1} = 12$$

$$\beta\binom{22}{2} = 231$$

$$\gamma\binom{19}{2} = 171$$

Thus, the number of combinations with repetition from both alleles, is $\binom{m+2-1}{2}$, where m is the number of permutations from each monoallelice, and 2 is the number of alleles.

$$\alpha\binom{12+2-1}{2} = \binom{13}{2} = 78$$

$$\beta\binom{231+2-1}{2} = \binom{232}{2} = 26,796$$

$$\gamma\binom{171+2-1}{2} = \binom{172}{2} = 14,706$$

Therefore, a total of $78 \times 26{,}796 \times 14{,}706 = 30{,}736{,}834{,}128$ (approximate 3×10^{10}) variations are possible for each neuron. In addition, the five "C" isoforms αC1, αC2, γC3, γC4, and γC5, which are constitutively expressed in neurons, increase the total number of isoforms expressed per neuron but does not contribute to variation. It is estimated that the cerebral cortex of the human brain contains 10^{10} neurons. Therefore, these calculations

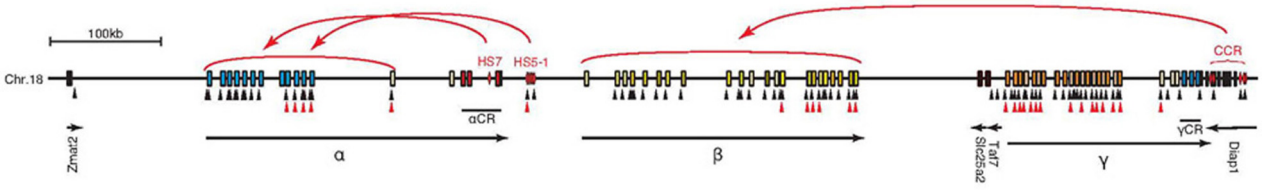

FIGURE 3 | Schematic diagram of the independent regulation of the *Pcdh-α*, *β*, and *γ* gene clusters by *cis*-regulatory elements. The HS5–1 element controls the expression of α3–αC1 depending on the distance. The HS-7 element controls the whole Pcdh-α cluster. The *cis*-regulatory elements, called the cluster control region (CCR), control Pcdh-β and are located downstream from the Pcdh-γ cluster. The control elements for the Pcdh-γ cluster have not been identified yet. Several CTCF-binding and cohesin-SA1-binding sites exist in the large clustered *Pcdh* gene cluster locus. Black and red triangles indicate CTCF-binding and cohesin-SA1-binding sites, respectively.

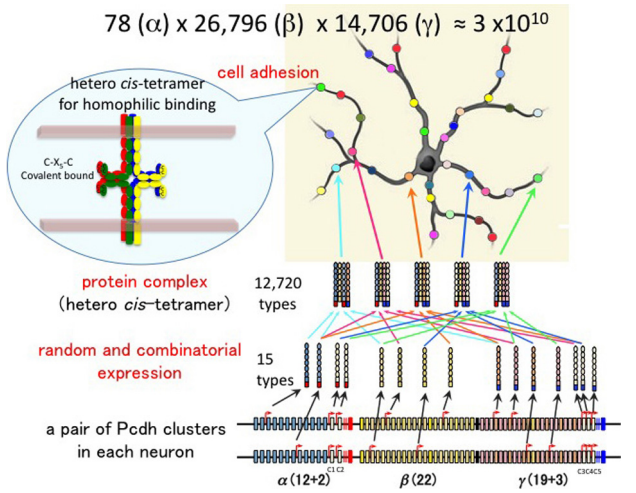

FIGURE 4 | Individuality of neurons determined by the random expression of clustered Pcdh isoforms and the random production of heteromultimeric *cis*-tetramers. From each clustered Pcdh cluster allele, 1 of the α, 2 of the β, and 2 of the γ isoforms are randomly expressed in combination. From the two alleles in each neuron, 2 of the α, 4 of the β, and 4 of the γ isoforms are randomly expressed in combination and with repetition, e.g., sometimes the same isoform is chosen from both alleles. Thus, the 78 possible combinations from 12 (α), 26,796 from 22 (β), and 14,706 from 19 (β) yield approximately 3×10^{10} variations that could be expressed by individual neurons. The five C-type isoforms are constitutively expressed from both alleles in each neuron. Therefore, a total of 15 isoforms is expressed in each neuron, 10 ($2\alpha + 4\beta + 4\gamma$) random and five constitutive isoforms. From 15 isoforms, 12,720 types of *cis*-tetramers are possible by combination with repetition and considering the topological variations (see **Figure 5**). The protein structure of the heteromultimeric *cis*-tetramers has not been revealed yet. The C-X_5-C motif is conserved among all clustered Pcdh isoforms and is important for forming the *cis*-tetramers Schreiner and Weiner (2010). Actually the clustered Pcdh proteins are localized as their protein dots in neuritis Phillips et al. (2003); Murata et al. (2004), and also shown that over expression of intact and truncated Pcdh-γ isoform can inhibit synaptogenesis Femandez-Monreal et al. (2009).

suggest that the variations caused by the random expression of clustered Pcdh isoforms could account for the individuality of all the neurons in the brain.

All the variable exons of clustered Pcdh have promoters that contain a conserved sequence element (CGCT) (**Figure 3**). Therefore, their isoform expressions are regulated by a mechanism of promoter choice in individual neurons (Tasic et al., 2002). The expression of clustered Pcdh isoforms is epigenetically controlled. Cell lines expressing specific clustered Pcdh isoforms have differential DNA-methylation patterns in their promoter regions: the active promoters are hypomethylated, and silent ones are methylated (Kawaguchi et al., 2008). *In vivo*, Purkinje neurons have distinct and variable DNA-methylation patterns in the clustered Pcdh promoter regions. In addition, the *cis*-regulatory elements HS7 and HS5–1 control Pcdh-α (Ribich et al., 2006; Kehayova et al., 2011) and CCR controls Pcdh-β (Yokota et al., 2011), respectively, (**Figure 3**). Interestingly, the zinc finger DNA-binding protein CTCF binds to almost all the variable exons and *cis*-elements (Handoko et al., 2011), and regulates the expression of clustered Pcdh isoforms (Golan-Mashiach et al., 2011; Kehayova et al., 2011). The regulator of chromatin conformation, cohesin-SA1, also binds to several variable exons and regulates the expression of clustered Pcdh isoforms (Remeserio et al., 2012) (**Figure 3**). The Pcdh cluster is also modified by histone methylation and acetylation (Mikkelsen et al., 2007), and is enriched in binding sites for the demethylation factor Tet1 (Xu et al., 2011). Thus, the stochastic expression of clustered Pcdh isoforms in individual neurons appears to be regulated by epigenetic factors and by interactions between each promoter and *cis*-elements within the gene clusters.

HETEROMULTIMERIC PROTEIN COMPLEX

The clustered Pcdh proteins have a punctate localization (Phillips et al., 2003; Murata et al., 2004; Femandez-Monreal et al., 2009), and may function in complexes: Pcdh-α and Pcdh-γ may form heteromultimers (**Figure 4**). The Pcdh-γ proteins induce the membrane surface expression of Pcdh-α proteins (Murata et al., 2004). In addition, Pcdh-β proteins associate with Pcdh-α and Pcdh-γ proteins (Han et al., 2010), and locate in synapses (Junghans et al., 2008). Schreiner and Weiner (2010) showed that 7 Pcdh-γ members exhibit isoform-specific homophilic binding, and that heteromultimeric *cis*-tetramers function as a homophilic binding unit (Schreiner and Weiner, 2010). The binding behavior of the *cis*-tetramers is very different from that of classical cadherins, which do not form multimers, and mediate cell-cell interactions by binding an identical cadherin on a different cell (**Figure 5A**). The clustered Pcdh *cis*-tetramers are formed before they engage in cell-cell interactions. As shown in **Figure 5A**, if two cells express two Pcdh isoforms, and only one of them is expressed in common, only one type of *cis*-tetramer on each cell is capable of cell-cell homophilic binding. In fact, cells that express only 1 or 2 of the four isoforms in common bind very poorly, whereas those expressing three or four of the four isoforms in common bind well, which supports the proposed *cis*-tetramer binding activity (Schreiner and Weiner, 2010).

Combinations with repetition are calculated as $\binom{4+i-1}{i}$, where 4 is the number of protein isoforms for a *cis*-tetramer, and i is the number of different protein isoforms expressed in an individual neuron. When 4 different isoforms are expressed in cells, the number of distinct *cis*-tetramers is $\binom{4+4-1}{4} = \binom{7}{4} = 35$. One, two and three isoforms expressing cells have $\binom{4+1-1}{4} = \binom{4}{4} = 1$, $\binom{4+2-1}{4} = \binom{5}{4} = 5$ and $\binom{4+3-1}{4} = \binom{6}{4} = 15$ distinct *cis*-tetramers, respectively. Therefore, in cells that express four isoforms with 1, 2, and 3 isoforms in common, 1/35 (2.8%), 4/35 (11.4%), and 15/35 (42.9%) *cis*-tetramers will match, respectively.

However, the *cis*-tetramers also have possible topological variations. **Figure 5B** shows the topological variations of *cis*-tetramers. Therefore, considering the topological variations of *cis*-tetramers, one, two, three, and four kinds of isoforms produce 1, 4, 9, and 6 distinct *cis*-tetramers, respectively. If there are

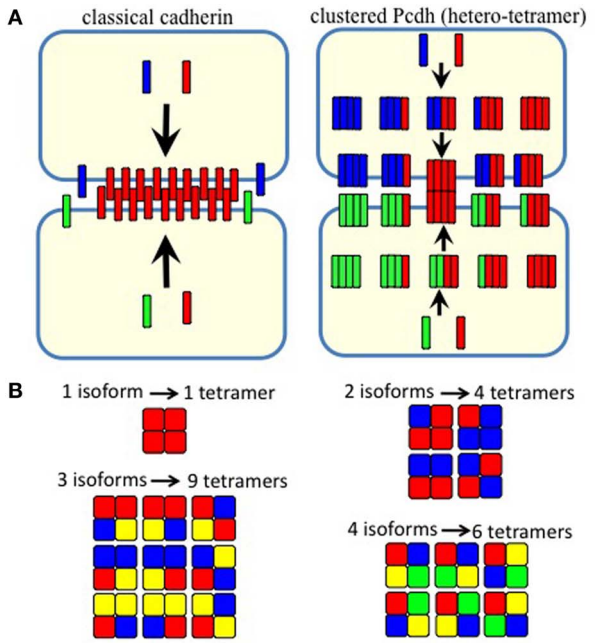

C

No of isoforms	1	2	3	4
combinations with repetition	1	5	15	35
combinations with topology	1	6	24	70
permutations with repetition	1	16	81	264

FIGURE 5 | (A) Homophilic cell adhesion as achieved by classical cadherins versus the *cis*-tetramers of clustered Pcdh isoforms. Red bars represent the common type of cadherin or clustered isoform molecules expressed on and binding between two interacting cells. Blue and green bars show additional cadherins or clustered Pcdh isoforms that are differentially expressed in the interacting cells. From two clustered Pcdh isoforms, five types of *cis*-tetramers can be produced in combination with repetition. In this example, only the red *cis*-tetramers can bind homophilically. **(B)** Variations of heteromultimeric *cis*-tetramers from each combination. One, two, three, and four isoforms can form 1, 4, 9, and 6 possible combinations, respectively, with repetition and topological variation. **(C)** Table shows the number of possible *cis*-tetramers from *i* isoforms calculated by combinations with repetition $\binom{4+i-1}{i}$, combinations with topological variations ($i = 1$, $\binom{1}{1}X1 = 1$; $i = 2$, $\binom{2}{1}X1 + \binom{2}{2}X4 = 6$; $i = 3$, $\binom{3}{1}X1 + \binom{3}{2}X4 + \binom{3}{3}X9 = 24$; $i = 4$, $\binom{4}{1}X1 + \binom{4}{2}X4 + \binom{4}{3}X9 + \binom{4}{4}X6 = 70$) and permutations with repetition i^4.

4 different isoforms expressed in cells, the total number of distinctive topological *cis*-tetramers is 70 ($70 = 4 + 24 + 36 + 6$; 1 choice from $4\binom{4}{1} = 4$, $4 \times 1 = 4$; 2 choices from $4\binom{4}{2} = 6$, $6 \times 4 = 24$; 3 choices from $4\binom{4}{3} = 4$, $4 \times 9 = 36$; 4 choices from $4\binom{4}{4} = 1$, $1 \times 6 = 6$). Calculating the topological variation, cells expressing 1, 2, and 3 isoforms have 1, 6, and 24 distinct topological *cis*-tetramers, respectively. Therefore, in cells sharing one, two, or three isoforms versus cells expressing four types of isoforms, 1/70 (1.4%), 6/70 (8.6%), or 24/70 (34.3%) *cis*-tetramers are matched.

On the other hand, this calculation does not consider the molecular amounts of each type of *cis*-tetramer. If *i* types of isoforms are expressed in equal amounts in cells, the total amount of *cis*-tetramers can be represented by a permutation with a repetition of i^4. Therefore, although repetitions of the same type of *cis*-tetramer exist, cells sharing one, two, and three isoforms versus cells expressing four types of isoforms are calculated as $1^4/4^4 = 1/264$ (0.4%), $2^4/4^4 = 16/264$ (6.1%), and $3^4/4^4 = 81/264$ (30.1%), respectively. These calculations contain several simplifications and assumptions for equal transcription and translation of each isoform (summarized in **Figure 5C**). In any cases, these calculations support the above-described experimental results of poor cell adhesion in cells expressing different isoform combinations, and together these findings suggest that the heteromultimeric *cis*-tetramer of clustered Pcdh protein isoforms could serve as the specific binding unit for cell adhesion and neuronal interconnections (Schreiner and Weiner, 2010).

In addition to Pcdh-γ isoforms, the heteromultimeric *cis*-tetramers may contain a combination of Pcdh-α, Pcdh-β, and Pcdh-γ isoforms. The evidence is as follows. First, α and γ isoforms are immunoprecipitated with each other's specific antibody (Murata et al., 2004), and β proteins associate with Pcdh-α and Pcdh-γ proteins (Han et al., 2010). Second, various Pcdh-α isoforms translocate to the cell- surface upon the expression of various Pcdh-γ isoforms, and various combinations of Pcdh-α and Pcdh-γ isoforms have been confirmed (Murata et al., 2004). In addition, the Cys-$(X)_5$-Cys (C-X_5-C) motif was found to be important for the formation and cell-surface expression of covalently bound *cis*-tetramers (Schreiner and Weiner, 2010) (**Figure 4**), and the C-X_5-C motif in the first cadherin domain (EC1) is completely conserved among all clustered Pcdh proteins in vertebrates. Furthermore, analysis of the protein structure of the EC1 domain of Pcdh-α4 indicated that the motif is located at the protein's surface (Morishita et al., 2006), and the C-X_5-C motif of the EC1 domain is also conserved in the solitary Pcdh-δ2 proteins (Morishita and Yagi, 2007).

In the isoform-specific binding activity, both the EC2 and EC3 domains are important for homophilic binding specificity (Schreiner and Weiner, 2010). Notably, among all the clustered Pcdh isoforms, the EC2 and EC3 domains are the most divergent (Kohmura et al., 1998; Wu and Maniatis, 1999).

If 15 isoforms of clustered Pcdhs are expressed in an individual neuron, this number of isoforms could generate $\binom{15+4-1}{4} = \binom{18}{4} = 3{,}060$ possible combinations with repetition and $\binom{15}{1}X1 + \binom{15}{2}X4 + \binom{15}{3}X9 + \binom{15}{4}X6 = 12{,}720$ types of *cis*-tetramers in an individual neuron (**Figure 4**). However, in these cells, 5 "C" isoforms are constitutively expressed, and the remaining 10 isoforms are randomly chosen and expressed. The expression of 15 isoforms in

an individual neuron contains assumptions of randomly chosen 4 Pcdh-β isoforms by our unpublished data (Hirano et al. in preparation). An individual neuron is estimated to form several to tens of thousands of synapses, suggesting that the variation created by *cis*-tetramers of cluster Pcdh isoforms could cover the number of synapses in a neuron.

Next, I calculated the number of kinds of *cis*-tetramers that could be generated from the number of distinct isoforms (**Figure 6A**), and the probability of matching *cis*-tetramers (the matching probability) occurring between a pair of neurons, each of which expresses 15 clustered Pcdh isoforms, when the number of different isoforms between them changes (**Figure 6B**). The matching probabilities (P) of the isoforms decrease exponentially with as the number of different (d) isoforms increases.

$$P = \binom{15-d}{1} X1 + \binom{15-d}{2} X4 + \binom{15-d}{3} X9 + \binom{15-d}{4} X6/12,\ 720,\ \text{if } d \leq 11$$

$$P = 0\ (d = 15),\ P = 7.8 \times x10^{-5}\ (d = 14),\ P = 0.00047\ (d = 13),\ P = 0.0018\ (d = 12)$$

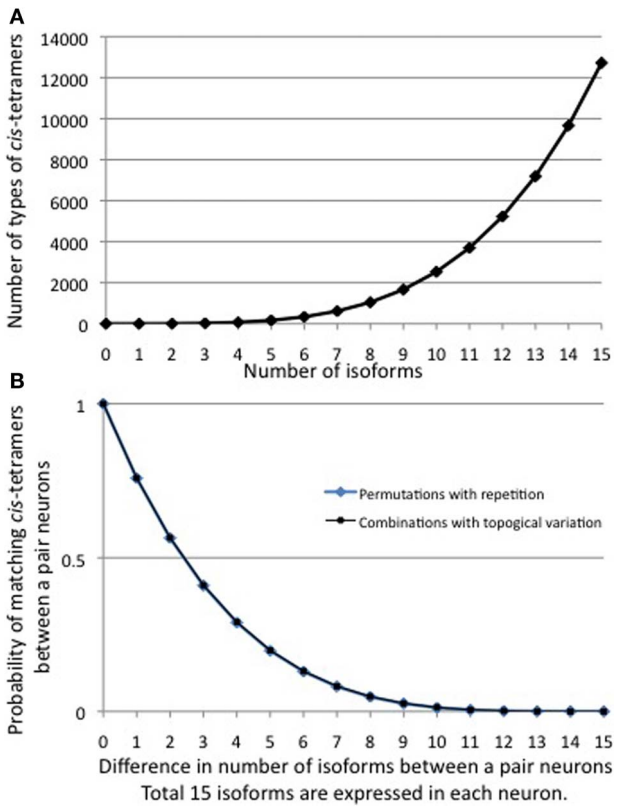

FIGURE 6 | (A) The number of combinations of heteromultimeric *cis*-tetramers increases as the number of isoforms increases, as a combination function. If 15 isoforms are expressed in individual neurons, the number of possible *cis*-tetramer combinations is 12,720. **(B)** The probability that matching *cis*-tetramers will be expressed on a pair of neurons, as a function of the number of isomers that are different between the two neurons, if each neuron expresses 15 isoforms. Calculations are done by two methods: combinations with topological variations (black thin line), and permutations with repetitions (blue bold line). A small number of different isoforms expressed between a pair of neurons will sharply decrease the matching probability of *cis*-tetramers, e.g., a difference of only 3 of a total of 15 isoforms leads to 0.41 (41%) *cis*-tetramers matching between a pair neurons. However, 10 differences in a total of 15 isoforms (5 isoforms in common between a pair of neurons) yields a score of 0.013, meaning that only 1.3% of the *cis*-tetramers match between the pair of neurons.

Surprisingly, the matching probability of the types of *cis*-tetramers decreases rapidly with small differences in the number of different isoforms between the two cells; for example, a difference of only 3 isoforms yields a matching probability of 41.1% (below 50%). On the other hand, these calculations do not consider the molecular amount of each type of *cis*-tetramer. If i types of isoforms are expressed at equal amounts in each cell, the total number of possible *cis*-tetramers is represented by i^4 of permutation with repetition though including the same type of *cis*-tetramers. Considering the total amount of *cis*-tetramers, the amounts of different *cis*-tetramers can be shown as i^4-$(i\text{-}d)^4$. Then, i^4-$(i\text{-}d)^4/i^4$ represents the probability of the total difference in the amounts of *cis*-tetramers between a pair of neurons expressing different numbers of isoforms. In our analysis with Purkinje neurons, we estimated that $i = 15$ in individual neurons. Here I hypothesize that the total number of possible *cis*-tetramers is 15^4, when every isoform has the same propensity for producing *cis*-tetramers. If 1 of the 15 isoforms is different (14 isoforms shared) between a pair of neurons, 14^4 (38,416) of the total 15^4 (50,625) are the same types of *cis*-tetramers, and thus 15^4—$14^4 = 12{,}209$ are different *cis*-tetramers. The function curve of the permutation with repetition is similar to the calculation curve of the differences of *cis*-tetramers considering the variations of their combinations with repetition and topology (**Figure 6B**).

In any case, these calculations demonstrate that a few distinctly expressed clustered Pcdh isoforms can lead to distinct neuronal individuality by virtue of their heteromultimeric *cis*-tetramers. In addition, interestingly, the common expression of several clustered Pcdh isoforms has little effect on the amount of variation between a pair of neurons. For example, a difference of 10 isoforms among a total of 15 (5 isoforms expressed in common) is calculated as generating only 1.3% matching *cis*-tetramers. Thus, even if the five "C" type clustered Pcdh isoforms are constitutively expressed in each neuron, the individuality of the neurons can be robustly maintained with 98% different *cis*-tetramers by the random expression of clustered Pcdh isoforms in each neuron. Thus, the stochastic expression of clustered Pcdh isoforms may provide a molecular code capable of stamping a high degree of individuality on every neuron in the brain. To examine this possibility, we need to study the function of the homophilic activity of the heteromultimeric *cis*-tetramers of clustered Pcdh isoforms in the brain.

Similar stochastic expressions have been reported for Dscam1 isoforms in insect neurons, and these molecules might serve as molecular codes for neuronal individuality in the insect brain. In *Drosophila*, alternative splicing of the single

gene *Dscam1* can generate 19,008 isoforms. The homophilic binding of the isoforms results in the repulsion of self-neurites. Individual neurons randomly express multiple isoforms; the number of Dscam isoforms expressed by each neuron is estimated to be 10 to 50 (Hattori et al., 2009). The Dscam1 protein isoforms have homophilic activity at the single isoform level. Calculation using a Monte Carlo simulation (Hattori et al., 2009) and combinatorics by closed-form solutions (Forbes et al., 2011) indicated a 4.4% chance that a pair of neurons shares at least one isoform, from 30 random expressions of 20,000 isoforms. Similar probabilities are estimated for Dscam1 in insects and clustered Pcdhs in vertebrates, even though the mechanism for randomness is different; that is, alternative splicing of Dscam1 or promoter choice and *cis*-tetramers for clustered Pcdh. Thus, neuronal individuality could be important in both vertebrates and invertebrates for developing complex neural networks.

CELL ASSEMBLY AND CLUSTERED Pcdhs

The functions of the clustered Pcdhs have been examined by producing loss-of-function mice. Mice lacking Pcdh-α are viable and fertile, but they have defects in contextual learning and special working memory (Fukuda et al., 2008). The olfactory sensory neurons and serotonergic neurons of these mutants have projection errors (Hasegawa et al., 2008; Katori et al., 2009). In wild-type mice, the axons of olfactory neurons that express the same olfactory receptor converge to innervate the proper glomeruli of the olfactory bulb. However, in the mutants, abnormal ectopic convergence is observed, even in adults (Hasegawa et al., 2008). Similarly, serotonergic fibers are abnormally distributed and condensed in several brain areas of serotonergic targeting (Katori et al., 2009). These axonal targeting phenotypes are also detected in the cytoplasmic deletion mutants, suggesting that the constant cytoplasmic tail of the Pcdh-α proteins is important for correct axonal targeting. In addition, loss of Pcdh-α in mice has functional impairments of cortico-cortical pathways between both hemispheres of primary somatosensory cortex by different mechanism on NMDA receptor (Yamashita et al., 2012).

The loss of Pcdh-γ in mice leads to neonatal lethality with neurological defects involving apoptosis and decreased synapses (Wang et al., 2002b). The increased apoptosis occurs during the

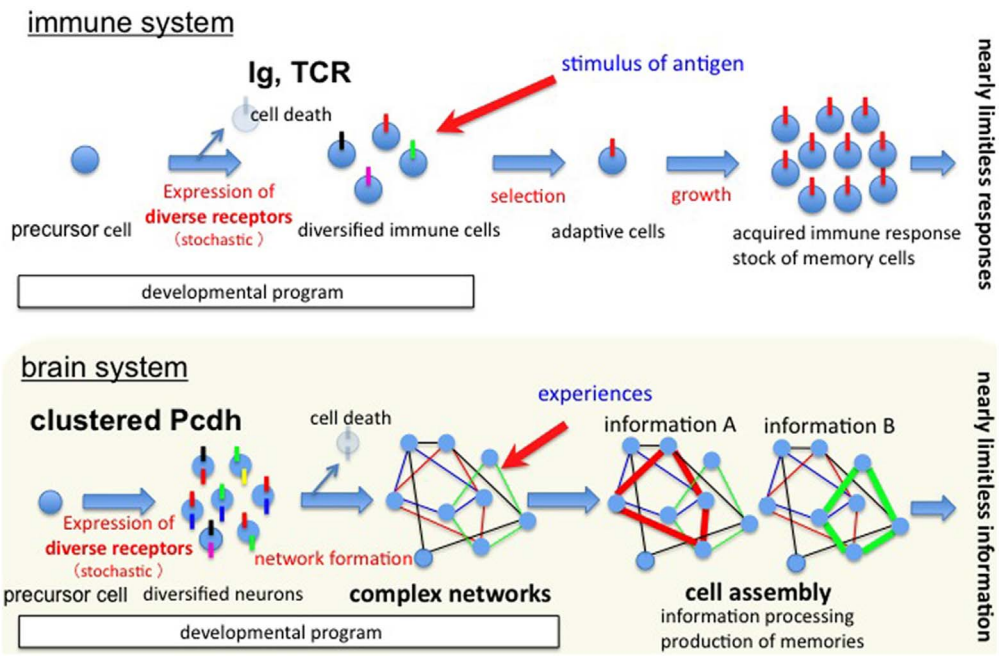

FIGURE 7 | Diagrams of memory systems for both the immune system and the brain. (A) In the immune system, an enormous number of diverse immune cells are developmentally produced; thus a set of pre-functional immune cells prepared early in life. The mechanism for diversity is the stochastic DNA rearrangement of the immunoglobulin (*Ig*) and T-cell receptor (*TCR*) genes. After infection with external antigens, the appropriate immune cells for responding to the antigen are selected, expanded, and stored in memory in the form of memory cells. In this way, numerous and nearly limitless adaptive immune responses and antigen memories are generated. Thus, the functional immune cells are predetermined by developmental programming, including a stochastic mechanism. **(B)** In the brain system, clustered Pcdh isoforms from the α, β, and γ gene clusters are stochastically expressed in neurons to produce individual neuronal identities. The expressed clustered Pcdh isoforms produce functional *cis*-tetramers. At the individual neuron level, each neuron is incorporated into neural networks via the affinity of its cellular interactions. The randomly expressed clustered Pcdh isoforms in an individual neuron form *cis*-tetramers that specifically bind the matching *cis*-tetramers on other neurons, generating a complex neural network that is determined by randomness and by high cluster coefficients during development. Thus, the process network formation during development results in numerous cell assemblies. As a result of experiences, the cell assemblies that respond to a specific experience are selected, strengthened, and the experience is memorized in the form of the strengthened cell assembly. In this way, nearly limitless neural information processing and memories can be generated. Thus, functional cell assemblies might be predetermined by developmental programs that involve stochastic expression and specific cellular interactions to form neural networks in the brain.

period of naturally occurring neuronal cell death (Lefebvre et al., 2008; Prasad et al., 2008). Even when the apoptosis defects are eliminated using Bax mutants, the Pcdh-γ mutants still show decreased synapses in the spinal cord (Weiner et al., 2005). In the retina, the Pcdh-γs are also indispensable for neuronal survival, and decreased synapses are seen in the Pcdh-γ mutants, although these are not rescued by Bax deletion, unlike in the spinal cord. Therefore it is not yet clear that in the retina there is a clear circuit formation role for the Pcdh-γs (Lefebvre et al., 2008).

There are no data to date that demonstrate the clustered Pcdh diversity is required *in vivo*. Genetic studies of the clustered Pcdhs, however, have gradually revealed their functions for building the correct neural networks. Also diversity of Pcdh-γ proteins has crucial roles for their selective homophilic adhesion activity in cultured K562 cells. The clustered Pcdhs are randomly expressed in every individual neuron and form an enormous number of variable *cis*-tetramers, speculating their function for building neural networks at an individual neuron level in the brain.

Recent physiological approaches have revealed that local neural networks form complex networks with neuronal ensembles at an individual neuron level (Song et al., 2005; Yoshimura et al., 2005). In addition, specific local connectivity develops preferentially among sister excitatory cortical neurons (Yu et al., 2009). Theoretical analyzes analyzes of neural networks suggest that complex networks exist in the brain (Sporns, 2011). Interestingly, Watts and Strogatz showed that "small-world" networks [by analogy with the small-world phenomenon known as six degrees of separation (Guare, 1990)] with high clustering coefficients and short characteristic path lengths emerge as a consequence of both random interactions and highly regulated ones (Watts and Strogatz, 1998).

To understand how complex brain networks form and function, we must first understand the mechanisms for creating randomness and regularity in the brain. In addition, considering the recent physiological results on spontaneous neural assembly and predetermined neural activity (Buzsaki, 2010), we need to examine the intrinsic and individual mechanisms for generating neural networks with randomness and regularity during brain development. In this line, the random expression of the clustered Pcdh family molecules in individual neurons during development and their specific cell adhesion activities for neural network formation make them intriguing candidates for molecules that enable intrinsic neural network formation; they could provide both the "small-world" cell assembly feature and account for the nearly limitless neural information processed within the limited brain mass. As shown in **Figure 7**, both the immune system and the brain might be similarly predetermined systems involving diverse individual cells created randomly before being exposed to external experiences for acquiring nearly limitless memories. In the immune system, antigens serve as the "external experiences." In the brain system, the mechanisms that serve as the "external experiences" that assemble the predetermined neural circuits in the context of developmental programs and that generate functional networks by means of synaptic plasticity have not been fully elucidated, but the continued examination of the clustered Pcdh family may uncover some of the answers.

ACKNOWLEDGMENTS

I thank T. Kitsukawa, A. Uchimura, and S. Hasegawa for discussion and calculation of the combinations of *cis*-tetramers. I also thank members of our laboratories, especially K. Hirano, R. Kaneko, T. Hirayama, and T. Hirabayashi for the expression analysis for Pcdh-β and discussion. I thank K. Shibuki, E. Tarusawa, and Y. Yoshimura for discussion and colaboration of the cell assembly hypothesis in the brain. This work was supported in part by Grant-in-Aid for Scientific Research (S), a Grant-in-Aid for Scientific Research on Innovative Area "Mesoscopic Neurocircuitry" from the Ministry of Education, Science, Sports, and Culture of Japan (MEXT), and CREST from Japan Science and Technology Agency (JST) (Takeshi Yagi)

REFERENCES

Buck, L., and Axel, R. (1991). A novel multigene family may encode odorant receptors: a molecular basis for odor recognition. *Cell* 65, 175–187.

Buzsaki, G. (2010). Neural syntax: cell assemblies, synapsembles, and readers. *Neuron* 68, 362–385.

Cheng, H. J., Nakamoto, M., Bergemann, A. D., and Flanagan, J. G. (1995). Complementary gradients in expression and binding of ELF-1 and Mek4 in development of the topographic retinotectal projection map. *Cell* 82, 371–381.

Dickson, B. J. (2002). Molecular mechanisms of axon guidance. *Science* 298, 1959–1964.

Dragoi, G., and Tonegawa, S. (2011). Preplay of future place cell sequences by hippocampal cellular assemblies. *Nature* 469, 397–401.

Drescher, U., Kremoser, C., Handwerker, C., Loschinger, J., Noda, M., and Bonhoeffer, F. (1995). *In vitro* guidance of retinal ganglion cell axons by RAGS, a 25 kDa tectal protein related to ligands for Eph receptor tyrosine kinases. *Cell* 82, 359–370.

Dreyer, W. J. (1998). The area code hypothesis revisited: olfactory receptors and other related transmembrane receptors may function as the last digits in a cell surface code for assembling embryos. *Proc. Natl. Acad. Sci. U.S.A.* 95, 9072–9077.

Esumi, S., Kakazu, N., Taguchi, Y., Hirayama, T., Sasaki, A., Hirabayashi, T., Koide, T., Kitsukawa, T., Hamada, S., and Yagi, T. (2005). Monoallelic yet combinatorial expression of variable exons of the protocadherin-alpha gene cluster in single neurons. *Nat. Genet.* 37, 171–176.

Femandez-Monreal, M., Kang, S., and Phillips, G. R. (2009). Gamma-protocadherin homophilic interaction and intracellular trafficking is controlled by the cytoplasmic domain in neurons. *Mol. Cell. Neurosci.* 40, 344–353.

Forbes, E. M., Hunt, J. J., and Goodhill, G. J. (2011). The combinatorics of neurite self-avoidance. *Neural Comput.* 23, 2746–2769.

Fukuda, E., Hamada, S., Hasegawa, S., Katori, S., Sanbo, M., Miyakawa, T., Yamamoto, T., Yamamoto, H., Hirabayashi, T., and Yagi, T. (2008). Down-regulation of protocadherin-alpha A isoforms in mice changes contextual fear conditioning and spatial working memory. *Eur. J. Neurosci.* 28, 1362–1376.

Golan-Mashiach, M., Grunspan, M., Emmanuel, R., Gibbs-Bar, L., Dikstein, R., and Shapiro, E. (2011). Identification of CTCF as a master regulator of the clustered protocadherin genes. *Nucleic Acids Res.*

Guare, J. (1990). *Six Degrees of Separation: A Play*. New York, :NY: Vintage Books.

Han, M. H., Lin, C., Meng, S., and Wang, X. (2010). Proteomics analysis reveals overlapping functions of clustered protocadherins. *Mol. Cell Proteomics* 9, 71–83.

Handoko, L., Xu, H., Li, G., Ngan, C. Y., Chew, E., Schnapp, M., Lee, C. W., Ye, C., Ping, J. L., Mulawadi, F., Wong, E., Sheng, J., Zhang, Y., Poh, T., Chan, C. S., Kunarso, G., Shahab, A., Bourque, G., Cacheux-Rataboul, V., Sung, W. K., Ruan, Y., and Wei, C. L. (2011). CTCF-mediated

functional chromatin interactome in pluripotent cells. *Nat. Genet.* 43, 630–638.

Hasegawa, S., Hamada, S., Kumode, Y., Esumi, S., Katori, S., Fukuda, E., Uchiyama, Y., Hirabayashi, T., Mombaerts, P., and Yagi, T. (2008). The protocadherin-alpha family is involved in axonal coalescence of olfactory sensory neurons into glomeruli of the olfactory bulb in mouse. *Mol. Cell. Neurosci.* 38, 66–79.

Hattori, D., Chen, Y., Matthews, B. J., Salwinski, L., Sabatti, C., Grueber, W. B., and Zipursky, S. L. (2009). Robust discrimination between self and non-self neurites requires thousands of Dscam1 isoforms. *Nature* 461, 644–648.

Hebb, D. O. (1949). *The Organization of Behavior*. New York, NY: JohnWiley and Sons.

Hill, E., Broadbent, I. D., Chothia, C., and Pettitt, J. (2001). Cadherin superfamily proteins in Caenorhabditis elegans and Drosophila melanogaster. *J. Mol. Biol.* 305, 1011–1024.

Hirayama, T., and Yagi, T. (2006). The role and expression of the protocadherin-alpha clusters in the CNS. *Curr. Opin. Neurobiol.* 16, 336–342.

Ishii, Y., Asakawa, S., Taguchi, Y., Ishibashi, S., Yagi, T., and Shimizu, N. (2004). Construction of BAC library for the amphibian Xenopus tropicalis. *Genes Genet. Syst.* 79, 49–51.

Junghans, D., Heidenreich, M., Hack, I., Taylor, V., Frotscher, M., and Kemler, R. (2008). Postsynaptic and differential localization to neuronal subtypes of protocadherin beta16 in the mammalian central nervous system. *Eur. J. Neurosci.* 27, 559–571.

Kaneko, R., Kato, H., Kawamura, Y., Esumi, S., Hirayama, T., Hirabayashi, T., and Yagi, T. (2006). Allelic gene regulation of Pcdh-αlpha and Pcdh-gamma clusters involving both monoallelic and biallelic expression in single Purkinje cells. *J. Biol. Chem.* 281, 30551–30560.

Katori, S., Hamada, S., Noguchi, Y., Fukuda, E., Yamamoto, T., Yamamoto, H., Hasegawa, S., and Yagi, T. (2009). Protocadherin-alpha family is required for serotonergic projections to appropriately innervate target brain areas. *J. Neurosci.* 29, 9137–9147.

Kawaguchi, M., Toyama, T., Kaneko, R., Hirayama, T., Kawamura, Y., and Yagi, T. (2008). Relationship between DNA methylation states and transcription of individual isoforms encoded by the protocadherin-alpha gene cluster. *J. Biol. Chem.* 283, 12064–12075.

Kehayova, P., Monahan, K., Chen, W., and Maniatis, T. (2011). Regulatory elements required for the activation and repression of the protocadherin-alpha gene cluster. *Proc. Natl. Acad. Sci. U.S.A.* 108, 17195–17200.

Kenet, T., Bibitchkov, D., Tsodyks, M., Grinvald, A., and Arieli, A. (2003). Spontaneously emerging cortical representations of visual attributes. *Nature* 425, 954–956.

Kohmura, N., Senzaki, K., Hamada, S., Kai, N., Yasuda, R., Watanabe, M., Ishii, H., Yasuda, M., Mishina, M., and Yagi, T. (1998). Diversity revealed by a novel family of cadherins expressed in neurons at a synaptic complex. *Neuron* 20, 1137–1151.

Langley, J. N. (1895). Note on regeneration of prae-ganglionic fibres of the sympathetic. *J. Physiol.* 18, 280–284.

Lefebvre, J. L., Zhang, Y., Meister, M., Wang, X., and Sanes, J. R. (2008). gamma-Protocadherins regulate neuronal survival but are dispensable for circuit formation in retina. *Development* 135, 4141–4151.

Lieber, M. R. (1992). The mechanism of V(D)J recombination: a balance of diversity, specificity, and stability. *Cell* 70, 873–876.

McLaughlin, T., and O'Leary, D. D. (2005). Molecular gradients and development of retinotopic maps. *Annu. Rev. Neurosci.* 28, 327–355.

Miki, R., Hattori, K., Taguchi, Y., Tada, M. N., Isosaka, T., Hidaka, Y., Hirabayashi, T., Hashimoto, R., Fukuzako, H., and Yagi, T. (2005). Identification and characterization of coding single-nucleotide polymorphisms within human protocadherin-alpha and -beta gene clusters. *Gene* 349, 1–14.

Mikkelsen, T. S., Ku, M., Jaffe, D. B., Issac, B., Lieberman, E., Giannoukos, G., Alvarez, P., Brockman, W., Kim, T. K., Koche, R. P., Lee, W., Mendenhall, E., O'Donovan, A., Presser, A., Russ, C., Xie, X., Meissner, A., Wernig, M., Jaenisch, R., Nusbaum, C., Lander, E. S., and Bernstein, B. E. (2007). Genome-wide maps of chromatin state in pluripotent and lineage-committed cells. *Nature* 448, 553–560.

Morishita, H., Umitsu, M., Murata, Y., Shibata, N., Udaka, K., Higuchi, Y., Akutsu, H., Yamaguchi, T., Yagi, T., and Ikegami, T. (2006). Structure of the cadherin-related neuronal receptor/protocadherin-alpha first extracellular cadherin domain reveals diversity across cadherin families. *J. Biol. Chem.* 281, 33650–33663.

Morishita, H., and Yagi, T. (2007). Protocadherin family: diversity, structure, and function. *Curr. Opin. Cell Biol.* 19, 584–592.

Murata, Y., Hamada, S., Morishita, H., Mutoh, T., and Yagi, T. (2004). Interaction with protocadherin-gamma regulates the cell surface expression of protocadherin-alpha. *J. Biol. Chem.* 279, 49508–49516.

Noguchi, Y., Hirabayashi, T., Katori, S., Kawamura, Y., Sanbo, M., Hirabayashi, M., Kiyonari, H., Nakao, K., Uchimura, A., and Yagi, T. (2009). Total expression and dual gene-regulatory mechanisms maintained in deletions and duplications of the Pcdha cluster. *J. Biol. Chem.* 284, 32002–32014.

Noonan, J. P., Grimwood, J., Danke, J., Schmutz, J., Dickson, M., Amemiya, C. T., and Myers, R. M. (2004a). Coelacanth genome sequence reveals the evolutionary history of vertebrate genes. *Genome Res.* 14, 2397–2405.

Noonan, J. P., Grimwood, J., Schmutz, J., Dickson, M., and Myers, R. M. (2004b). Gene conversion and the evolution of protocadherin gene cluster diversity. *Genome Res.* 14, 354–366.

Noonan, J. P., Li, J., Nguyen, L., Caoile, C., Dickson, M., Grimwood, J., Schmutz, J., Feldman, M. W., and Myers, R. M. (2003). Extensive linkage disequilibrium, a common 16.7-kilobase deletion, and evidence of balancing selection in the human protocadherin alpha cluster. *Am. J. Hum. Genet.* 72, 621–635.

Phillips, G. R., Tanaka, H., Frank, M., Elste, A., Fidler, L., Benson, D. L., and Colman, D. R. (2003). Gamma-protocadherins are targeted to subsets of synapses and intracellular organelles in neurons. *J. Neurosci.* 23, 5096–5104.

Prasad, T., Wang, X., Gray, P. A., and Weiner, J. A. (2008). A differential developmental pattern of spinal interneuron apoptosis during synaptogenesis: insights from genetic analyses of the protocadherin-gamma gene cluster. *Development* 135, 4153–4164.

Remeserio, S., Cuadrado, A., Gomez-Lopez, G., Pisano, D. G., and Losada, A. (2012). A unique role of cohesin-SA1 in gene regulation and development. *EMBO J.*

Ribich, S., Tasic, B., and Maniatis, T. (2006). Identification of long-range regulatory elements in the protocadherin-alpha gene cluster. *Proc. Natl. Acad. Sci. U.S.A.* 103, 19719–19724.

Sakurai, Y. (1999). How do cell assemblies encode information in the brain? *Neurosci. Biobehav. Rev.* 23, 785–796.

Schmutz, J., Martin, J., Terry, A., Couronne, O., Grimwood, J., Lowry, S., Gordon, L. A., Scott, D., Xie, G., Huang, W., Hellston, U., Tran-Gyamfi, M., She, X., Prabhakar, S., Aerts, A., Altherr, M., Bajorek, E., Black, S., Branscomb, E., Caoile, C., Challacombe, J. F., Chan, Y. m., Denys, M., Detter, J. C., Escobar, J., Flowers, D., Fotopulos, D., Glavina, T., Gomez, M., Gonzales, E., Goodstein, D., Grigoriev, I., Groza, M., Hammon, N., Hawkins, T., Haydu, L., Israni, S., Jett, J., Kadner, K., Kimball, H., Kobabyashi, A., Lopez, G., Lou, Y., Martinez, D., Medina, C., Morgan, J., Nandkeshwar, R., Noonan, J. P., Pitluck, S., Pollard, M., Predki, P., Priest, J., Ramirez, L., Retterer, J., Rodriguez, A., Rogers, S., Salamov, A., Salazar, A., Thayer, N., Tice, H., Tsai, M., Ustaszewska, A., Vo, N., Wheeler, J., Wu, K., Yang, J., Dickson, M., Cheng, J. F., Eichler, E. E., Olsen, A., Pennacchio, L. A., Rokhsar, D. S., Richardon, P., Lucas, S. M., Myers, R. M., and Rubin, E. M. (2004). The DNA sequence and comparative analysis of human chromosome 5. *Nature* 431, 268–274.

Schreiner, D., and Weiner, J. A. (2010). Combinatorial homophilic interaction between gamma-protocadherin multimers greatly expands the molecular diversity of cell adhesion. *Proc. Natl. Acad. Sci. U.S.A.* 107, 14893–14898.

Song, S., Sjostrom, P. J., Reigl, M., Nelson, S., and Chklovskii, D. B. (2005). Highly nonrandom features of synaptic connectivity in local cortical circuits. *PLoS Biol.* 3:e68. doi: 10.1371/journal.pbio.0030068

Sperry, R. W. (1963). Chemoaffinity in the orderly growth of nerve fiber patterns and connections. *Proc. Natl. Acad. Sci. U.S.A.* 50, 703–710.

Sporns, O. (2011). *Networks of the Brain*. Cambridge, MA: The MIT Press.

Sudhof, T. C. (2008). Neuroligins and neurexins link synaptic function to cognitive disease. *Nature* 455, 903–911.

Sugino, H., Hamada, S., Yasuda, R., Tuji, A., Matsuda, Y., Fujita, M., and Yagi, T. (2000). Genomic

organization of the family of CNR cadherin genes in mice and humans. *Genomics* 63, 75–87.

Taguchi, Y., Koide, T., Shiroishi, T., and Yagi, T. (2005). Molecular evolution of cadherin-related neuronal receptor/protocadherin(alpha) [CNR/Pcdh(alpha)] gene cluster in Mus musculus subspecies. *Mol. Biol. Evol.* 22, 1433–1443.

Takeichi, M. (2007). The cadherin superfamily in neuronal connections and interactions. *Nat. Rev. Neurosci.* 8, 11–20.

Tasic, B., Nabholz, C. E., Baldwin, K. K., Kim, Y., Rueckert, E. H., Ribich, S. A., Cramer, P., Wu, Q., Axel, R., and Maniatis, T. (2002). Promoter choice determines splice site selection in protocadherin alpha and gamma pre-mRNA splicing. *Mol. Cell* 10, 21–33.

Tonegawa, S. (1983). Somatic generation of antibody diversity. *Nature* 302, 575–581.

Wang, X., Su, H., and Bradley, A. (2002a). Molecular mechanisms governing Pcdh-gamma gene expression: evidence for a multiple promoter and cis-alternative splicing model. *Genes Dev.* 16, 1890–1905.

Wang, X., Weiner, J. A., Levi, S., Craig, A. M., Bradley, A., and Sanes, J. R. (2002b). Gamma protocadherins are required for survival of spinal interneurons. *Neuron* 36, 843–854.

Watts, D. J., and Strogatz, S. H. (1998). Collective dynamics of "small-world" networks. *Nature* 393, 440–442.

Weiner, J. A., Wang, X., Tapia, J. C., and Sanes, J. R. (2005). Gamma protocadherins are required for synaptic development in the spinal cord. *Proc. Natl. Acad. Sci. U.S.A.* 102, 8–14.

Wu, Q., and Maniatis, T. (1999). A striking organization of a large family of human neural cadherin-like cell adhesion genes. *Cell* 97, 779–790.

Wu, Q., Zhang, T., Cheng, J. F., Kim, Y., Grimwood, J., Schmutz, J., Dickson, M., Noonan, J. P., Zhang, M. Q., Myers, R. M., and Maniatis, T. (2001). Comparative DNA sequence analysis of mouse and human protocadherin gene clusters. *Genome Res.* 11, 389–404.

Xu, Y., Wu, F., Tan, L., Kong, L., Xiong, L., Deng, J., Barbera, A. J., Zheng, L., Zhang, H., Huang, S., Min, J., Nicholson, T., Chen, T., Xu, G., Shi, Y., Zhang, K., and Shi, Y. G. (2011). Genome-wide regulation of 5hmC, 5mC, and gene expression by Tet1 hydroxylase in mouse embryonic stem cells. *Mol. Cell* 42, 451–464.

Yagi, T. (2008). Clustered protocadherin family. *Dev. Growth Differ.* 50 (Suppl. 1), S131–S140.

Yagi, T., and Takeichi, M. (2000). Cadherin superfamily genes: functions, genomic organization, and neurologic diversity. *Genes Dev.* 14, 1169–1180.

Yamashita, H., Shanlin, C., Komagata, S., Hishida, R., Iwasato, T., Itohara, S., Yagi, T., Endo, N., Shibata, M., and Shibuki, K. (2012). Restoration of contralateral representation in the mouse somatosensory cortex after crossing nerve transfer. *Plos One.* (in press).

Yokota, S., Hirayama, T., Hirano, K., Kaneko, R., Toyoda, S., Kawamura, Y., Hirabayashi, M., Hirabayashi, T., and Yagi, T. (2011). Identification of the cluster control region for the protocadherin-beta genes located beyond the protocadherin-gamma cluster. *J. Biol. Chem.* 286, 31885–31895.

Yoshimura, Y., Dantzker, J. L., and Callaway, E. M. (2005). Excitatory cortical neurons form fine-scale functional networks. *Nature* 433, 868–873.

Yu, Y.-C., Bultje, R. S., Wang, X., and Shi, S.-H. (2009). Specific synapses develop preferentially among sister excitatory neurons in the neocortex. *Nature* 458, 501–505.

Zipursky, S. L., and Sanes, J. R. (2010). Chemoaffinity revisited: dscams, protocadherins, and neural circuit assembly. *Cell* 143, 343–353.

Conflict of Interest Statement: The author declares that the research was conducted in the absence of any commercial or financial relationships that could be construed as a potential conflict of interest.

Received: 26 February 2012; accepted: 22 March 2012; published online: 12 April 2012.

Citation: Yagi T (2012) Molecular codes for neuronal individuality and cell assembly in the brain. Front. Mol. Neurosci. 5:45. doi: 10.3389/fnmol.2012.00045

frontiers in
MOLECULAR NEUROSCIENCE

ORIGINAL RESEARCH ARTICLE
published: 23 December 2011
doi: 10.3389/fnmol.2011.00054

Direct and indirect regulation of spinal cord Ia afferent terminal formation by the γ-Protocadherins

Tuhina Prasad [†] ***and Joshua A. Weiner*** [*]

Department of Biology, The University of Iowa, Iowa City, IA, USA

Edited by:
Alistair N. Garratt, Max Delbrück Center for Molecular Medicine, Germany

Reviewed by:
John Oberdick, The Ohio State University, USA
Zaven Kaprielian, Albert Einstein College of Medicine of Yeshiva University, USA

[*]Correspondence:
Joshua A. Weiner, Department of Biology, The University of Iowa, 143 Biology Building, Iowa City, IA 52242, USA.
e-mail: joshua-weiner@uiowa.edu

[†]Present address:
Tuhina Prasad, Brain Research Centre, Department of Psychiatry, University of British Columbia, Vancouver, BC, Canada V6T 2B5.
e-mail: tuhina.prasad@ubc.ca

The *Pcdh-γ* gene cluster encodes 22 protocadherin adhesion molecules that interact as homophilic multimers and critically regulate synaptogenesis and apoptosis of interneurons in the developing spinal cord. Unlike interneurons, the two primary components of the monosynaptic stretch reflex circuit, dorsal root ganglion sensory neurons and ventral motor neurons (MNs), do not undergo excessive apoptosis in *Pcdh-γ*$^{del/del}$ null mutants, which die shortly after birth. However, as we show here, mutants exhibit severely disorganized Ia proprioceptive afferent terminals in the ventral horn. In contrast to the fine net-like pattern observed in wild-type mice, central Ia terminals in *Pcdh-γ* mutants appear clumped, and fill the space between individual MNs; quantitative analysis shows a ∼2.5-fold increase in the area of terminals. Concomitant with this, there is a 70% loss of the collaterals that Ia afferents extend to ventral interneurons (vINs), many of which undergo apoptosis in the mutants. The Ia afferent phenotype is ameliorated, though not entirely rescued, when apoptosis is blocked in *Pcdh-γ* null mice by introduction of a *Bax* null allele. This indicates that loss of vINs, which act as collateral Ia afferent targets, contributes to the disorganization of terminals on motor pools. Restricted mutation of the *Pcdh-γ* cluster using conditional mutants and multiple Cre transgenic lines (*Wnt1-Cre* for sensory neurons; *Pax2-Cre* for vINs; *Hb9-Cre* for MNs) also revealed a direct requirement for the γ-Pcdhs in Ia neurons and vINs, but not in MNs themselves. Together, these genetic manipulations indicate that the γ-Pcdhs are required for the formation of the Ia afferent circuit in two ways: First, they control the survival of vINs that act as collateral Ia targets; and second, they provide a homophilic molecular cue between Ia afferents and target vINs.

Keywords: proprioception, axons, synaptogenesis, spinal cord, cell adhesion molecule, motor neuron, interneuron, apoptosis

INTRODUCTION

The formation of complex neuronal circuits essential for normal behavior depends on a series of sequential events that include neuron subtype differentiation, axon guidance, terminal formation, target selection and synapse formation. Studies have shown that expression of specific transcription factors (reviewed by Dalla Torre di Sanguinetto et al., 2008), trophic factors (reviewed by da Silva and Wang, 2011) and semaphorin/Plexin signaling (Messersmith et al., 1995; Fu et al., 2000; Cheng et al., 2001; Cohen et al., 2005; Yoshida et al., 2006; Pecho-Vrieseling et al., 2009) all play important roles in this process. Cell adhesion molecules, particularly those of the large and diverse immunoglobulin and cadherin superfamilies, have been shown to regulate multiple steps in the process of circuit assembly, including axon fasciculation, axon pathfinding, terminal arborization, and synaptic specificity (reviewed by Takeichi, 2007; Arikkath and Reichardt, 2008; Margeta et al., 2008; Giagtzoglou et al., 2009). A major goal of developmental neurobiology today is to identify the molecular cues that guide the formation of distinct neuronal circuits.

One of the most basic of CNS circuits is the monosynaptic spinal stretch reflex circuit, which is made up of two distinct functional units: a sensory unit and an effector unit. The sensory unit is composed of muscle spindles, which are mechanoreceptors embedded in skeletal muscles, and a specific subpopulation of dorsal root ganglion (DRG) sensory neurons (termed "Ia afferents") that peripherally innervate these muscle spindles and relay proprioceptive information into the CNS. The central Ia axons interact with components of the effector unit, which is made up of α-motor neurons (MNs) along with particular interneurons located in the ventral horn of the spinal cord. The proprioceptive Ia afferents make precise excitatory monosynaptic connections with the MNs, which project axons to the same target muscle from which they receive sensory feedback. In addition, the Ia afferents send collateral branches to a group of ventral interneurons (vINs), which then inhibit MNs that project to antagonistic muscles; the addition of this collateral projection allows for coordinated muscle movement in response to proprioceptive input (Chen et al., 2003). Proprioceptive afferents thus make very selective monosynaptic connections with MNs supplying the same muscles, and avoid making connections with MNs supplying antagonistic muscles. The formation of their collateral branches onto vINs is also restricted to particular groups, including a population of V1-derived interneurons (Sapir et al., 2004; Alvarez et al., 2005).

In addition to proprioceptive Ia afferents, the DRG neurons extend axons conveying three other sensory modalities into the spinal cord: touch, pain (nociception), and temperature (Brown, 1981). The central projections of all DRG neurons extend dorsally to enter the spinal cord through the dorsal root with their branches terminating in specific target regions of the dorsal or ventral spinal cord. The Ia afferents extend from large DRG neurons that express parvalbumin, vesicular glutamate transporter 1 (VGLUT1), and the TrkC neurotrophin receptor (which selectively binds NT3). Smaller DRG neurons express TrkA (which selectively binds NGF) and project small diameter unmyelinated axons that convey pain, touch, and temperature information into distinct laminae of the dorsal horn (Brown, 1981; Koerber and Mendell, 1992; Mu et al., 1993).While genetic studies to define factors that regulate the differentiation of sensory neurons and the targeting of their axons have revealed roles for several transcription factors such as Ngn-1, Runx, Erg1, Pea3, and others (Dalla Torre di Sanguinetto et al., 2008), there is perhaps less information on cell surface receptors with more direct roles in controlling sensory axonal projection pattern as well as in forming specific synaptic connections with their target neurons. In chick embryos, the immunoglobulin superfamily members F11 and axonin-1 are required for the correct spinal cord pathfinding of, respectively, proprioceptive Ia afferents and nociceptive axons (Perrin et al., 2001). Elegant genetic studies have shown that expression of Sema3e by specific MNs and its high affinity receptor PlexinD1 by Ia afferents is a critical mediator of sensory-motor synaptic connectivity in mice. Genetic manipulation of either Sema3e or PlexinD1 expression results in an aberrant pattern of sensory-motor monosynaptic connections but has no effect on the segregation of MNs into specific pools (Pecho-Vrieseling et al., 2009). PlexinA1 is also specifically expressed in the proprioceptive sensory axons and is a receptor for Sema6c and Sema6d repulsive cues, which are dynamically expressed in the dorsal horn. Loss of plexinA1 signaling resulted in proprioceptive axons following an aberrant pathway through the medial region of the dorsal horn, thereby disrupting the organization of cutaneous sensory afferents (Yoshida et al., 2006). Despite this aberrant pathway followed by the central projection of Ia afferent axons, they still reach their ventral horn target areas and form connections in the spinal cord, however (Yoshida et al., 2006). It has also been found that type II classical cadherins are expressed by distinct subpopulations of DRG sensory neurons and for at least two of them, T-cad and MN-cad, this expression pattern is correlated in subsets of MNs supplying the same muscle (Price et al., 2002).

Over 50 cadherin superfamily genes are present in three clusters, termed *Protocadherin- (Pcdh-)*α, β, and γ, that together encompass ∼900 kb on human chromosome 5q31 and mouse chromosome 18 (Wu and Maniatis, 1999; Wu et al., 2001). We have previously shown that the 22-gene *Pcdh-γ* cluster is critically required for the development of the CNS. Each γ-Pcdh isoform is encoded by a unique large "variable" exon encoding six extracellular cadherin repeats, a transmembrane domain, and a ∼90 amino acid cytoplasmic domain; each variable exon is spliced to three small "constant" exons that encode a further 125 amino acid shared C-terminal domain (Wu and Maniatis, 1999; Tasic et al., 2002; Wang et al., 2002a; a schematic of the locus is shown in **Figure 7A**). The 22 γ-Pcdh isoforms form *cis*-homo- or hetero-tetramers that interact in a strictly homophilic manner in *trans*, indicating that the *Pcdh-γ* locus could specify at least 10^4 distinct adhesive interfaces (Schreiner and Weiner, 2010). The γ-Pcdhs are expressed throughout the embryonic and postnatal CNS with individual neurons expressing different subsets of the γ-Pcdh isoforms (Wang et al., 2002b; Kaneko et al., 2006; Zou et al., 2007). The γ-Pcdh proteins are preferentially localized to synaptic and perisynaptic sites, and are expressed by astrocytes as well as by neurons (Wang et al., 2002b; Phillips et al., 2003; Garrett and Weiner, 2009). Mice in which the entire *Pcdh-γ* gene cluster has been deleted (*Pcdh-*$\gamma^{del/del}$) lack voluntary movements and spinal reflexes and die within a few hours of birth (Wang et al., 2002b). Null mutants exhibit extensive interneuron cell death and reduced synaptic density in the spinal cord during late embryonic development (Wang et al., 2002b; Weiner, 2006; Prasad et al., 2008). We previously showed that loss of the γ-Pcdhs exacerbates an underlying, normal developmental pattern of spinal interneuron apoptosis, the extent of which differs among the many molecularly defined interneuron subsets (Prasad et al., 2008). Intriguingly, neither DRG sensory neurons nor MNs undergo increased apoptosis in *Pcdh-γ* null mice (Wang et al., 2002b; Prasad et al., 2008; see **Figure 2** below), leaving open the question of whether these molecules might regulate the formation of the monosynaptic stretch reflex circuit.

Here, we have uncovered a role for the γ-Pcdhs in the formation of Ia afferent terminals onto their target cells. We conducted a genetic analysis including *Pcdh-*$\gamma^{del/del}$ null mutants, *Pcdh-*$\gamma^{del/del}$; *Bax*$^{-/-}$ double mutants, and a conditional *Pcdh-γ* mutant allele (*Pcdh-*γ^{fcon3}) along with four Cre transgenic lines to bring about selective loss of the γ-Pcdhs in discrete neuronal populations. We show that γ-Pcdhs are required in a cell autonomous manner in sensory neurons to bring about a normal arborization pattern of Ia afferent terminals onto MNs. Our manipulations further suggest that loss of the γ-Pcdhs from vINs affects the Ia afferent terminal field both directly, by disrupting contacts made by sensory axons, and indirectly, by increasing apoptosis and removing potential target neurons. Interestingly, the loss of γ-Pcdhs in the MNs, which are the primary targets, does not significantly affect the arborization pattern of Ia afferent neurons. Our data suggest that the *Pcdh-γ* family plays essential roles in specifying the connectivity between Ia afferent collaterals and vINs, which in turn regulates the formation of the primary terminal field on MNs.

MATERIALS AND METHODS

MOUSE STRAINS

The *Pcdh-*γ^{del}, *Pcdh-*γ^{fus} (Wang et al., 2002b), and *Pcdh-*γ^{fcon3} alleles (Prasad et al., 2008) and *Bax*$^{-/-}$ mutants (Knudson et al., 1995; Deckwerth et al., 1996; White et al., 1998) were described previously. *Actin-Cre* (Lewandoski et al., 1997), *Wnt1-Cre* (Danielian et al., 1998), and *Hb9-Cre* (Arber et al., 1999) mouse lines were obtained from The Jackson Laboratory (Bar Harbor, ME). *Pax2-Cre* mice (Ohyama and Groves, 2004) were the kind gift of Dr. Andy Groves (House Ear Institute, Los Angeles, CA). All lines utilized were congenic or nearly congenic with C57BL/6; all were backcrossed onto this strain for at least 6–10 generations. All animal procedures were performed in accordance with the University of Iowa's Institutional Animal Care and Use Committee and NIH guidelines.

ANTIBODIES

The following antibodies were utilized: rabbit anti-cleaved caspase-3 (Cell Signaling Technologies); rabbit anti-GFP (Invitrogen); mouse anti-NeuN (Chemicon); rabbit anti-parvalbumin (Swant); mouse anti-parvalbumin (Sigma); mouse anti-PSD-95 (Affinity BioReagents); guinea pig anti-VGLUT1 (Chemicon). Anti-TrkA antibody was the kind gift of Dr. Louis Reichardt (UCSF). The mouse anti-γ-Pcdh constant domain (N159/5) and mouse anti-γ-Pcdh-B2 (N148/30) were generated by the UC Davis/NIH NeuroMab Facility using antigens produced in our laboratory, and are characterized in detail in Lobas et al. (2011). They are available commercially through Antibodies, Inc.

IMMUNOFLUORESCENCE

Embryonic and neonatal mice were killed by decapitation, and vertebral columns were exposed and removed. Spinal columns were prepared for immunofluorescence using one of two methods: (1) Fixation for 2 h in 4% paraformaldehyde in phosphate buffered saline (PBS) at 4˚C, followed by washes with cold PBS, cryoprotection in 30% sucrose in PBS at 4˚C, and freezing on dry ice in OCT compound (Tissue Tek/Sakura); or (2) Snap freezing in OCT using dry ice/ethanol-cooled isopentane. In either case, transverse cryostat sections were cut at 12 μm. Slides containing fresh-frozen sections were fixed in 100% methanol for 10 min at −20˚C. Sections were blocked in 2.5% BSA, 0.1% Triton X100 in PBS for 1 h followed by overnight incubation at 4˚C with primary antibodies diluted in the same blocking solution. Sections were washed in PBS and incubated for 1 h at room temperature with the appropriate secondary antibodies conjugated to Alexa 488, 568, or 647 (Molecular Probes/Invitrogen). Sections were washed in PBS containing the nuclear counterstain DAPI (4′,6-diamidino-2-phenylindole), and mounted in Gel/Mount (Biomeda) aqueous mounting media. Some sections were counterstained with NeuroTrace 435 fluorescent Nissl stain (Invitrogen).

IN SITU HYBRIDIZATION

In situ hybridization using an antisense riboprobe corresponding to the *Pcdh-γ* constant exons was performed as described (Wang et al., 2002b). Vertebral columns collected from neonatal mice were snap frozen in OCT using dry ice/ethanol-cooled isopentane. Twenty micron cryostat sections were cut and post-fixed for 5 min at room temperature. Sections were rinsed and then immersed in acetylation solution (295 ml of H_2O, 4 ml of triethanolamine, 0.525 ml of concentrated HCl, 0.75 ml of acetic anhydride) for 10 min at room temperature. The sections were then rinsed and incubated with hybridization solution (50% formamide, 5× SSC, 5× Denhardt's solution, 250 mg/ml yeast tRNA, 500 mg/ml salmon sperm DNA, 50 mg/ml heparin) at room temperature for 1 h followed by overnight hybridization at 65˚C with fluorescein–UTP labeled riboprobe diluted in hybridization solution. The next day, the sections were washed for several hours at 65˚C in 0.2× SSC, rinsed at room temperature in TBS, and blocked for 1 h with 0.2% Blocking Reagent (Roche) in TBS. Probes were detected by overnight incubation at 4˚C with anti-fluorescein antibodies (1:1000) conjugated to peroxidase (Roche), followed by amplification using the TSA Plus system (Perkin-Elmer Life sciences) according to manufacturer's protocol.

IMAGE ACQUISITION AND ANALYSIS

For interneuron counts, synapse and terminal density quantification 12 μm thick sections were cut from mouse spinal cords. Each quantification was performed on six to eight sections from at least three animals (i.e., at least 18 sections each per genotype per time point). Images were taken of control and mutant spinal cord sections at equivalent thoracolumbar locations and camera exposures using 10× (for cell counts), 20×, or 63× (for synapse and terminal density quantification) PlanApo objectives on a Leica DM5000B digital epifluorescence microscope or on a Leica SP2 AOBS laser scanning confocal microscope. Digital images were captured in Adobe Photoshop and similarly adjusted for brightness and contrast. Cell counts were performed manually. For synaptic puncta and terminal density quantifications images were thresholded in NIH Image/J and the number of puncta and/or total area occupied by terminals was quantified by using the Analyze Particles function. Statistical significance was determined by two-way ANOVA followed by Bonferroni-corrected *post hoc* tests using Prism software.

RT-PCR

Control and mutant neonatal mice were killed by decapitation, vertebral columns were exposed and removed and the dorsal root ganglia were dissected out and collected in RNAlater (Ambion). Total RNA was extracted by using the RNAqueous-4PCR kit (Ambion) from thoracic (T2–T6) DRGs that were pooled together to get a sufficient amount of RNA. RNA concentration was quantified spectrophotometrically and cDNA was synthesized from 2 μg of RNA using random hexamer primers and Superscript III reverse transcriptase (Invitrogen). An array of PCR reactions was performed to amplify various *Pcdh-γ* variable exon-constant exon spliced transcripts. The forward and reverse primer sequences utilized were the same as those reported in Prasad et al. (2008). Cycling parameters were: 94˚C, 1 min; 55˚C, 1 min; 72˚C 3 min, for 30 cycles.

RESULTS

EXPRESSION OF *Pcdh-γ* ISOFORMS BY DRG SENSORY NEURONS

Earlier studies have shown that the *Pcdh-γ* gene cluster is expressed throughout the developing and adult CNS, and that individual neurons express varying subsets of *Pcdh-γ* isoforms (Wang et al., 2002a,b; Phillips et al., 2003; Frank et al., 2005; Kaneko et al., 2006; Zou et al., 2007). To confirm that sensory neurons in the DRG express the γ-Pcdhs, we examined tissues from *Pcdh-γ^{fusg}* mice, in which the third constant exon is fused to GFP (Wang et al., 2002b), and performed *in situ* hybridization using a probe against the shared constant exons, which detects expression of all 22 possible *Pcdh-γ* transcripts (see schematic of the cluster in **Figure 7A**). Both methods showed that all cells within the DRG expressed the γ-Pcdhs between E12 and P0 (**Figures 1A,B**, and data not shown). To investigate further if all 22 distinct *Pcdh-γ* RNA transcripts are expressed by DRG neurons we performed RT-PCR using a reverse primer in the shared constant exons and 22 forward primers specific to each variable exon (Prasad et al., 2008; Garrett and Weiner, 2009). At least 20 of the 22 possible transcripts were readily detectable in RNA from P0 thoracic DRG (**Figure 1C**). Double immunostaining with antibodies against the

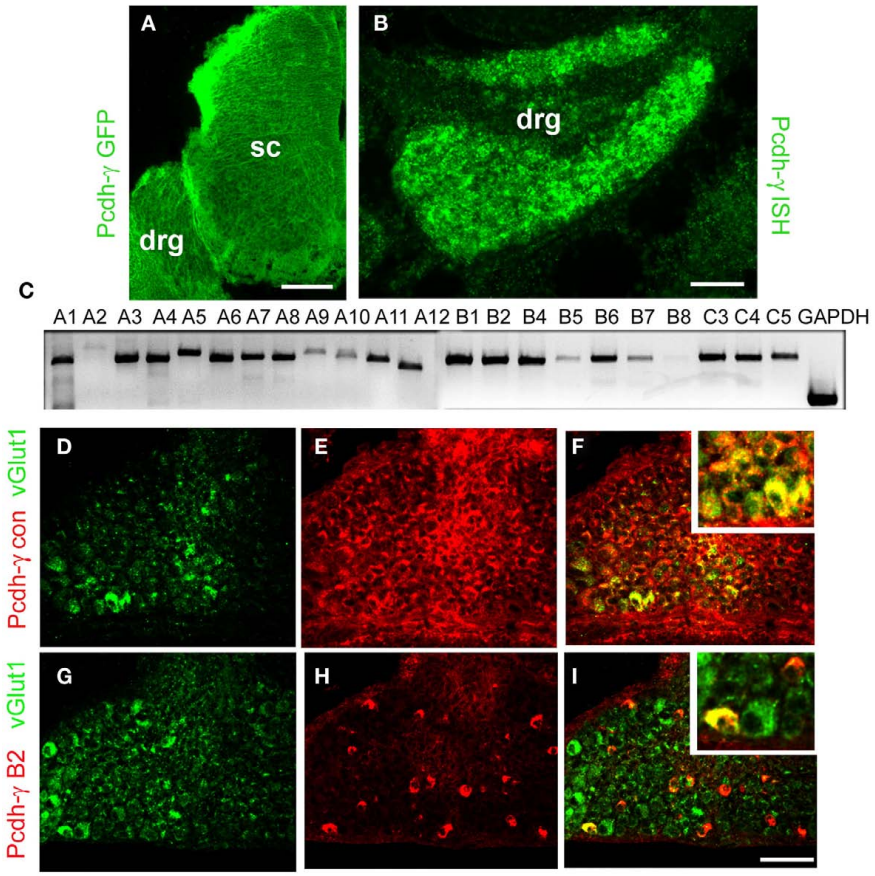

FIGURE 1 | Expression of γ-Pcdhs by DRG sensory neurons. (A) Anti-GFP staining of E12 *Pcdh-γ*^{fus} spinal cord demonstrates uniform expression of γ-Pcdh-GFP fusion proteins throughout the DRG and spinal cord (sc). **(B)** *In situ* hybridization using a riboprobe against the *Pcdh-γ* constant exon also yields uniform labeling in P0 DRG. Sense control riboprobes gave no signal (data not shown). **(C)** RT-PCR analysis of P0 thoracic (T2–T6) DRG using a constant exon reverse primer and forward primers in each of the indicated variable exons demonstrates that all, or nearly all, of the 22 possible *Pcdh-γ* transcripts are expressed. **(D–F)** Immunostaining of P0 control DRG's with antibodies against the γ-Pcdh constant region (red) and the Ia afferent neuron marker VGLUT1 (green) shows that all Ia neurons express some γ-Pcdh isoforms. **(G–I)** Immunostaining with antibodies specific for a single γ-Pcdh isoform (B2, red) and VGLUT1 (green) demonstrates that only a subset of sensory neurons, including a small number of Ia afferent neurons, expresses a given γ-Pcdh isoform. Insets, higher magnification view of a region in the main panel. Scale bar: 100 μm in **(A)**, 50 μm in **(B)** and **(D–I)**.

γ-Pcdh constant domain (shared by all 22 isoforms) and VGLUT1 indicated that all Ia afferent neurons (as well as all other DRG neurons) express γ-Pcdh proteins (**Figures 1D–F**). Previous analyses have suggested that individual neurons express a subset of the 22 *Pcdh-γ* genes (Wang et al., 2002b; Frank et al., 2005; Kaneko et al., 2006). Using a novel γ-Pcdh-B2-specific antibody (Lobas et al., 2011), we found that, indeed, a small percentage of DRG neurons express this γ-Pcdh isoform (**Figures 1G–I**). Double-labeling for VGLUT1 identified a small number of γ-Pcdh-B2+, and many more γ-Pcdh-B2−, Ia afferent neurons, consistent with the overall occurrence of B2+ cells. Though limited to a single isoform, these data are consistent with the expression of distinct γ-Pcdh isoform subsets in individual sensory neurons.

NORMAL DRG NEURON SURVIVAL IN *Pcdh-γ* NULL MICE

Our previous study had shown that in *Pcdh-γ* null mutant spinal cord there is an accentuation of apoptotic cell death in discrete spinal interneuron populations with a corresponding reduction in excitatory and inhibitory synaptic density (Prasad et al., 2008). However, loss of γ-Pcdhs did not have any effect on the survival of MNs (Wang et al., 2002b; Prasad et al., 2008). To investigate if the γ-Pcdhs are required for survival of sensory neurons, we stained DRG sections taken from postnatal day 0 (P0) control and null mutant mice with antibodies against cleaved caspase-3, a marker for apoptotic cell death, and either NeuN, to label all neurons, or parvalbumin, a marker specific for Ia afferent neurons in the DRG (Honda, 1995; Arber et al., 2000). There was no increase in the number of cleaved caspase-3 stained cells in DRG from *Pcdh-γ*$^{del/del}$ mice compared to control mice (**Figures 2A,B**); at this age, which is after the main period of developmental apoptosis in the DRG (Coggeshall et al., 1994; White et al., 1998) few if any cells were labeled at all. In addition, there was no change in the number of parvalbumin+ (**Figures 2A–D**; control = 13.9 per section, mutant = 14.1 per section, $N = 18$ sections per genotype taken from three sets of animals) or VGLUT1+ (data not shown) neurons, and a similar overall density of NeuN+ cells

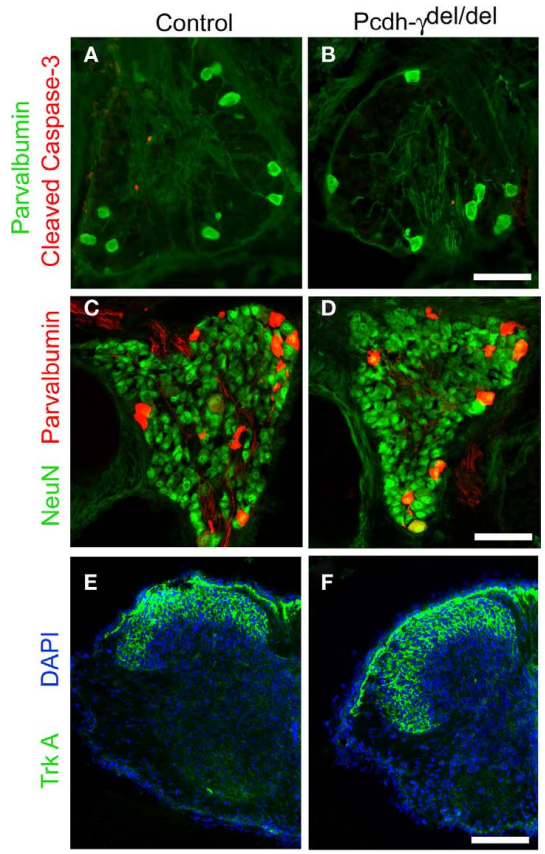

FIGURE 2 | Normal survival and differentiation of DRG sensory neurons in *Pcdh-γ* null mutants. DRGs from P0 control and *Pcdh-γ*$^{del/del}$ mice were immunostained with antibodies against cleaved caspase-3 [red; **(A,B)**] or against the neuronal marker NeuN [green **(C,D)**], along with those against the Ia neuron marker parvalbumin [green, **(A,B)**; red, **(C,D)**]. No excessive apoptosis of mutant sensory neurons was observed and the neuronal density, Ia neuron number, and overall size of mutant DRGs are all similar to controls. **(E)** P0 Control and **(F)** *Pcdh-γ* null mutant spinal cords stained with antibodies against TrkA+ cutaneous sensory axons indicate that these terminate normally in the superficial part of the dorsal horn in the absence of the γ-Pcdhs. Scale bar: 50 μm in **(A–D)**; 100 μm in **(E,F)**.

(**Figures 2C,D**). These data confirm our earlier preliminary finding (Wang et al., 2002b) that loss of the γ-Pcdhs does not affect the survival of DRG sensory neurons.

Pcdh-γ NULL MUTATION DISRUPTS THE FORMATION OF Ia AFFERENT TERMINALS IN THE VENTRAL HORN

We next asked if the ingrowth and trajectory of sensory axons is affected by loss of the γ-Pcdhs. To assess this, we stained sensory axons with antibodies that detect cutaneous axons projecting to the dorsal horn (TrkA) or Ia afferents projecting to the ventral horn (parvalbumin, VGLUT1) in control and *Pcdh-γ*$^{del/del}$ spinal cord between embryonic day 14 (E14) and P0, when the mutant mice die. Our earlier preliminary analysis had suggested that loss of the γ-Pcdhs did not have any obvious effect on the dorsal horn projection of substance P+ cutaneous sensory neurons (Wang et al., 2002b). Here, we similarly found that mutant TrkA+ axons projected to the upper dorsal horn as in controls, and appeared normal in their density and spatial restriction at all ages (**Figures 2E,F** and data not shown). The neonatal lethality of *Pcdh-γ* null mice (and more restricted mutants as described below), however, prevented us from analyzing any potential role for the γ-Pcdhs in the maturation and formation of specific synapses by cutaneous sensory axons, which takes place during the early postnatal period (Fitzgerald, 1987; Mirnics and Koerber, 1995).

In contrast to cutaneous axons, Ia afferents project to the ventral horn and form synaptic connections with MNs and vINs during the late embryonic period (Mears and Frank, 1997; Chen et al., 2003). By E14 in *Pcdh-γ* null mutant embryos, the Ia afferent axons had entered the spinal cord through the dorsal root entry zone and were localized medially, just as in controls (**Figures 3A,B**). The Ia afferent axons enter the ventral horn by E15 in both the *Pcdh-γ* mutants and controls, and begin to extend collateral branches toward vINs (**Figures 3C,D**). At no age were any aberrant collateral branches into the dorsal horn observed in mutants, indicating that the γ-Pcdhs are not required for normal Ia afferent axon segregation and guidance into the ventral horn. By E17, a disruption in the pattern of Ia afferent terminals is apparent in the *Pcdh-γ* mutants: While control terminals have attained a fine net-like pattern of parvalbumin+ puncta around the MN and vIN regions, mutant presynaptic terminals appear clumped together in the MN region (**Figures 3E,F**). By P0, this phenotype has become more severe, and the lack of laterally positioned collateral branches off of the main MN-contacting axons is clear (**Figures 3G,H** and **4A–D**).

To quantify the disruption of Ia afferent terminal formation on MN pools, we examined high magnification images of P0 sections stained for parvalbumin, VGLUT1, and PSD-95 (a postsynaptic marker of glutamatergic synapses). We counterstained sections with NeuroTrace 435, a fluorescent Nissl stain that easily distinguishes MNs, with their large soma size and prominent nucleoli, from the much smaller surrounding vINs and glia (confirmed in a set of experiments utilizing the Nissl stain and a specific marker of MNs, ChAT; **Figure 4E**). We measured the area taken up by parvalbumin and VGLUT1 staining in small microscope fields containing several MNs, and divided this by the number of MNs to obtain a terminal area/MN measure. We found an increase of ∼2.5-fold in the area of both parvalbumin- and VGLUT1+ terminals per MN in *Pcdh-γ* mutants (**Figures 4E–J**; **Table 1**). We next asked if there was a corresponding increase in postsynaptic sites by measuring the density of PSD-95+ puncta in the same fields in which VGLUT1 staining was analyzed. Surprisingly, we found that the area of PSD-95 staining per MN was unaffected in *Pcdh-γ* null mutants (**Figures 4G,H,K**), suggesting that many of the mutant Ia terminals do not properly contact a postsynaptic site. This would be consistent with the overt phenotype of the neonatal mutants in the hours prior to death, which includes a lack of voluntary movement and of reflexes (Wang et al., 2002b).

LOSS OF Ia AFFERENT COLLATERALS TO VENTRAL INTERNEURONS IN *Pcdh-γ* NULL MUTANTS

Ia afferent axons not only make specific connections with MNs; they also send collaterals to discrete vIN populations including V1-derived En1+ "Ia interneurons," V1-derived calbindin+ Renshaw cells, and several V0-derived interneurons, many of which express

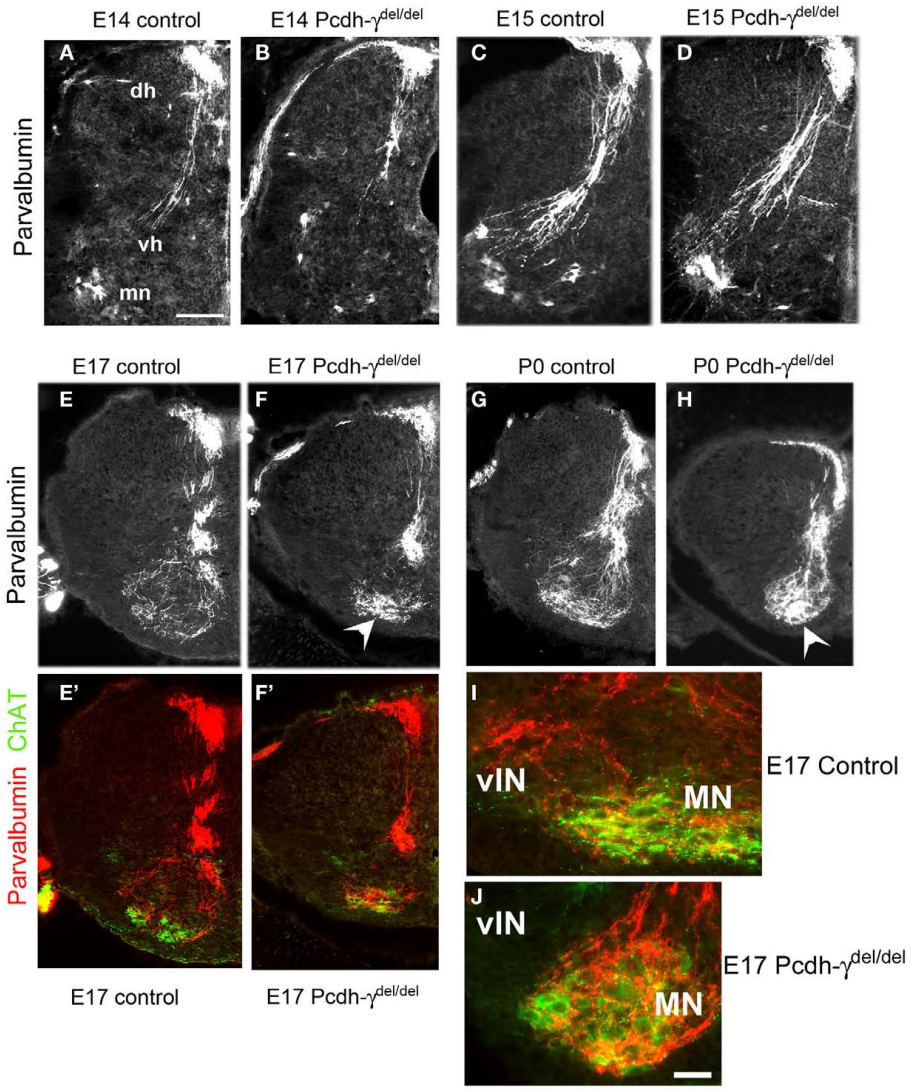

FIGURE 3 | The pattern of Ia afferent terminal arbors in the ventral horn is disrupted in *Pcdh-γ* null mutant mice. (A–H) Hemi-spinal cords from control **(A,C,E,G)** and *Pcdh-γ*$^{del/del}$ **(B,D,F,H)** mice were immunostained with antibodies against parvalbumin at the indicated time points during embryonic development. Mutant parvalbumin+ Ia axons grow into the spinal cord at the correct time and penetrate as normal into the ventral horn, with no pathfinding errors. By E17, however, as the pattern of Ia afferent terminals emerges as a fine net-like pattern in controls, the mutant terminals appear clumped around motor neurons (arrowheads), with a loss of collateral projections to ventral interneurons. This phenotype has worsened by P0. **(E′,F′)** show the same fields as **(E,F)**, but with ChAT staining added to indicate where the motor neuron pools are located. Higher magnification views of parvalbumin/ChAT-double stained ventral horn shows that while control Ia axons send collaterals laterally to the ventral interneuron region [vIN, **(I)**], these collaterals are absent in mutants **(J)** (dh, dorsal horn; vh, ventral horn; mn, motor neurons). Scale bar: 100 μm in **(A–H)**, 50 in **(I,J)**.

Pax2 at some time during development (Burrill et al., 1997; Sapir et al., 2004; Lewis, 2006). These interneurons are a part of the central pattern generator and are, for the most part, inhibitory GABAergic neurons that mediate presynaptic and postsynaptic inhibition, thereby playing a critical role in controlling the amount of excitatory input that passes from sensory neurons onto MNs (reviewed by Goulding, 2009). Very little is known about the molecular mechanisms involved in the formation of specific connections between Ia afferents and vINs, which act as collateral targets. We quantified the apparent loss of Ia collaterals (**Figure 3**) in *Pcdh-γ* null mutant spinal cords in two ways. First, because many of the vINs receiving Ia collaterals lie lateral to the MN pools in the thoracolumbar sections we examined, we determined the extent of the spread of parvalbumin+ Ia afferent terminals in the ventral horn, normalized to the total width of the spinal cord (which is smaller in the *Pcdh-γ* mutants due to excessive vIN apoptosis; Prasad et al., 2008; see schematic, **Figure 5A**). Second, we quantified the area per neuron of parvalbumin+ Ia terminals in microscope fields containing either MN pools or vINs (see schematic, **Figure 5B**). Both measures indicated that between E17 and P0, there is a significant reduction in Ia collaterals projecting to vINs in the mutants (**Figure 5A**) accompanying the corresponding

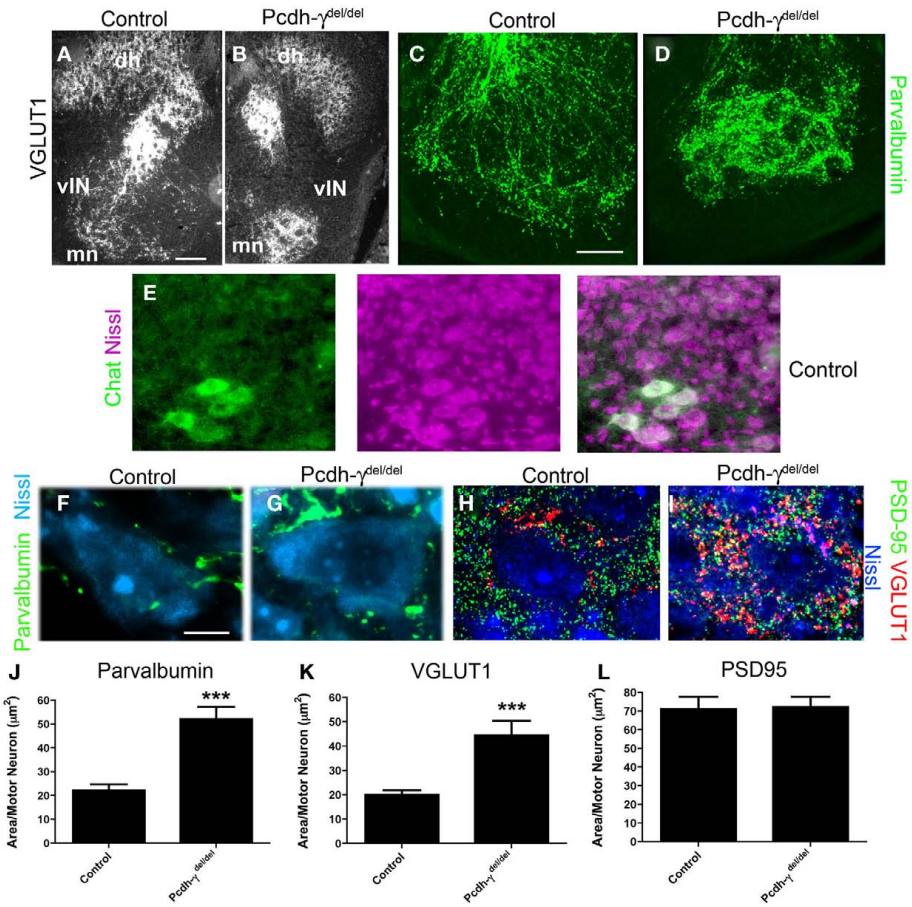

FIGURE 4 | Ia afferent terminals on motor neurons are significantly increased in area in *Pcdh-γ* null mutants. (A,B) P0 control and *Pcdh-γ*$^{del/del}$ spinal cord immunostained with antibodies against VGLUT1 shows clumping of terminals around motor neurons (mn) with a corresponding reduction of collateral terminals (lateral to motor neurons) on ventral interneurons (vIN), similar to the parvalbumin staining in **Figure 3**, and at higher magnification in **(C,D)**. **(E)** Motor neurons can be reliably identified by their distinctive Nissl staining profile, as confirmed by double staining with antibodies against ChAT. **(F–H)** High magnification views of P0 control and *Pcdh-γ*$^{del/del}$ spinal cord in the ventral motor neuron pools, stained with the indicated antibodies (parvalbumin and VGLUT1 for Ia terminals; PSD-95 for glutamatergic postsynaptic sites on motor neurons, which are Nissl stained), show expansion of Ia terminals on individual motor neurons but no change in the density of PSD-95 puncta. **(I–K)** Quantification of the density of Parvalbumin or VGLUT1-stained Ia terminals per motor neuron indicates a significant increase in *Pcdh-γ* null mutant when compared to control, while quantification of PSD-95 density is identical. ***$p < 0.001$. Scale bar: 100 μm in **(A,B)**; 40 μm in **(C,D)**; 10 μm in **(E–H)**.

increase in the density of terminals surrounding MNs (**Figures 4** and **5B**). In our previous work (Prasad et al., 2008), we showed that between E17 and P0, there is massive aberrant apoptosis of vIN populations in *Pcdh-γ* null mutants. The fact that the reduction in Ia terminals in fields occupied by vINs is observed even when normalized to the density of these cells (**Figure 5B**), suggests that apoptosis is not the only cause of the lost collateral branches (see below).

BLOCKING VENTRAL INTERNEURON APOPTOSIS ONLY PARTIALLY RESCUES Ia AFFERENT TERMINALS

The loss of γ-Pcdhs affects vIN subsets differentially during late embryogenesis: while 80% of V1-derived En1+ neurons are lost, calbindin+ Renshaw cells, which are also V1-derived, are not affected at all. About 52% of all Pax2+ vINs, which derive from both V0 and V1 and include an En1+ population, are lost in *Pcdh-γ* null embryos (Prasad et al., 2008). To examine if the excessive loss of vINs is solely responsible for the aberrant pattern of Ia afferent terminals in *Pcdh-γ* null mutants, we crossed these mice with *Bax*$^{-/-}$ mice. Loss of Bax, a proapoptotic Bcl-2 family member protein, prevents neurons from undergoing apoptotic cell death (Deckwerth et al., 1996) and rescues vIN numbers on a *Pcdh-γ* null background (Prasad et al., 2008). Quantification of Ia afferent terminals showed that blocking apoptosis does partially rescue the phenotype: in *Pcdh-γ*$^{del/del}$; *Bax*$^{-/-}$ double mutants, parvalbumin- or VGLUT1+ terminal area per MN was increased by only 40% (compared to ∼2.5-fold in *Pcdh-γ* single mutants). This increase was, however, still significant compared to controls (note that the double mutants were compared to *Bax*$^{-/-}$ mice, to control for increased neuronal numbers when apoptosis is blocked; **Figure 6**). These results suggest that γ-Pcdhs can affect the formation of Ia terminals indirectly, due to their effect

Table 1 | Summary of phenotypes in the various *Pcdh-γ* mouse strains examined.

Mouse strain	Sensory neuron genotype	Ventral interneuron genotype	Motor neuron genotype	Parvalbumin+ terminal area per MN (% control)	VGLUT1+ terminal area per MN (% control)	PAX2+ vIN survival (% control)
Pcdh-$\gamma^{+/+}$ and Pcdh-$\gamma^{del/+}$	WT	WT	WT	100	100	100
Pcdh-$\gamma^{del/del}$ ^	KO	KO	KO	220**	236**	48**
Pcdh-$\gamma^{del/del}$; $Bax^{-/-}$ #	KO	KO	KO	146*	167*	100
Actin-Cre; Pcdh-$\gamma^{fcon3/fcon3}$ †	KO	KO	KO	242**	190**	60**
Wnt1-Cre; Pcdh-$\gamma^{fcon3/fcon3}$ †	KO	WT	WT	143*	144*	105
Pax2-Cre; Pcdh-$\gamma^{fcon3/fcon3}$ †	WT	KO	WT	143*	151*	72*
HB9-Cre; Pcdh-$\gamma^{fcon3/fcon3}$ †	WT	WT	KO	110	117	104

^ *Compared to Pcdh-$\gamma^{+/+}$ and Pcdh-$\gamma^{del/+}$ as control.*

Compared to $Bax^{-/-}$ as control.

† *Compared to Pcdh-$\gamma^{fcon3/fcon3}$ as control.*

**$p < 0.05$ vs. control.*

***$p < 0.01$ vs. control.*

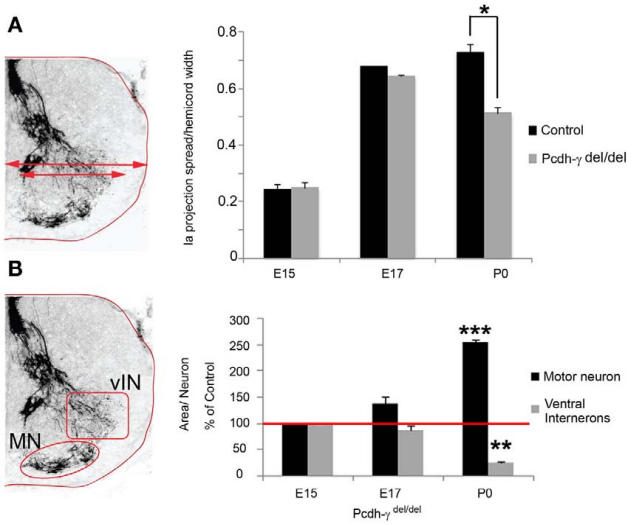

FIGURE 5 | Loss of Ia axon collateral projections to ventral interneurons in *Pcdh-γ* null mutants. (A) The extent of the spread in parvalbumin+ Ia terminal arbors, normalized to hemi-cord width, was quantified as one measure of collateral formation (schematized at left). A significant reduction in the extent of Ia afferent terminal spread becomes apparent at P0. **(B)** Quantification of the area covered by parvalbumin+ Ia terminals in the motor neuron (MN) and ventral interneuron (vIN) fields was normalized to neuron number (schematized at left). As mutant terminal density increases around MNs, it decreases around vINs, becoming significant at P0 (data are graphed as percent of E15 control levels). Red line indicates 100%. *$p < 0.05$; **$p < 0.01$; ***$p < 0.001$.

on interneuron survival, but that this indirect effect cannot fully account for the defects observed in *Pcdh-γ* null mutants.

Ia AFFERENT SENSORY NEURONS REQUIRE γ-Pcdhs IN A CELL AUTONOMOUS MANNER FOR NORMAL CENTRAL TERMINAL FORMATION

To ask whether γ-Pcdhs have a direct role in the formation of Ia afferent terminals, we mutated the *Pcdh-γ* cluster in a cell type-specific fashion, using the conditional *Pcdh-γ^{fcon3}* allele (Lefebvre et al., 2008; Prasad et al., 2008). In this allele, the third constant exon is fused to GFP and flanked by loxP sites (**Figure 7A**). Cre-mediated excision of the *Pcdh-γ^{fcon3}* allele results in a null or near-null: Ubiquitous deletion using *Actin-Cre* transgenics essentially phenocopies *Pcdh-$\gamma^{del/del}$* spinal cord phenotypes (**Table 1**; **Figure 7D**), and no truncated γ-Pcdh proteins can be detected, presumably because deletion of constant exon 3, including the polyadenylation site and 3′UTR for all *Pcdh-γ* mRNAs, leads to reduced transcript stability (Prasad et al., 2008). We crossed *Pcdh-γ^{fcon3}* mice to three previously characterized Cre transgenic lines: 1) *Wnt1-Cre* (Danielian et al., 1998), to target all DRG neurons; 2) *Pax2-Cre* (Ohyama and Groves, 2004), to target Pax2+ spinal interneurons including Ia-contacted vINs; and 3) *Hb9-Cre* (Arber et al., 1999), to target MNs (see schematic, **Figure 7B**). We also crossed all of these Cre lines to *Z/EG* reporter mice to confirm that the pattern of Cre activity was as expected from the published literature [Prasad et al., 2008, and data not shown; note that in our prior work we utilized a different *Hb9-Cre* line (Umemori et al., 2004) that is not as cleanly restricted to MNs as the superior line utilized here]. We first assessed the survival of Pax2+ vINs, and found no difference from control in *Wnt1-Cre*; *Pcdh-$\gamma^{fcon3/fcon3}$* and *Hb9-Cre*; *Pcdh-$\gamma^{fcon3/fcon3}$* mice (**Table 1**). As we reported previously (Prasad et al., 2008), survival of V0/V1-derived Pax2+ vINs in *Pax2-Cre*; *Pcdh-$\gamma^{fcon3/fcon3}$* neonates is intermediate between wild-type and *Pcdh-$\gamma^{del/del}$* null mutant levels (**Table 1**).

Wnt1-Cre-mediated mutation of *Pcdh-γ* in DRG neurons resulted in an approximately 40% increase in the density of Ia afferent terminals on MNs (**Figures 7C,E–H**; **Table 1**) and a corresponding ∼40% reduction in the density of the terminals on vINs (**Figures 7I,J**). Because in *Wnt1-Cre*; *Pcdh-$\gamma^{fcon3/fcon3}$* mice Ia afferent neurons lack the γ-Pcdhs while the two target neuronal populations (vINs and MNs) do not, this effect can be ascribed to a cell autonomous requirement for the γ-Pcdhs in the afferents. In *Pax2-Cre*; *Pcdh-$\gamma^{fcon3/fcon3}$* mice, Ia afferent terminals exhibit a phenotype nearly identical to that seen in the *Wnt1-Cre*-restricted mutants: a ∼40% increase in area per MN (**Table 1**). This could be due either to the partial loss of V0/V1-derived vINs in

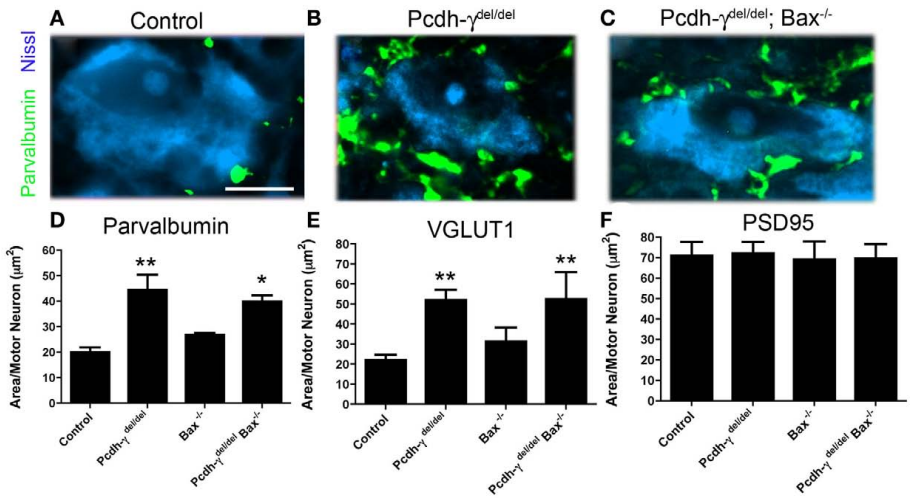

FIGURE 6 | Genetic block of apoptosis ameliorates, but does not completely rescue, the Ia afferent phenotype observed in *Pcdh-γ* null mutants. (A–C) Spinal cords from P0 control, *Pcdh-γ*$^{del/del}$ and *Pcdh-γ*$^{del/del}$; *Bax*$^{-/-}$ mice were immunostained with antibodies against parvalbumin and imaged at high magnification to show Ia terminals around motor neurons, which were Nissl stained. **(D–F)** The aberrant expansion of parvalbumin- or VGLUT1+ terminals in the absence of the γ-Pcdhs is ameliorated when apoptosis is blocked by the additional mutation of *Bax*. Double mutant terminals are, however, still significantly affected compared to *Bax*$^{-/-}$ single mutant controls. No effect on the area covered by PSD-95+ puncta is observed. Scale bar: 20 μm. $*p < 0.05$ and $**p < 0.01$, compared to appropriate control mice.

Pax2-restricted mutants (**Table 1**), or to a cell autonomous requirement for the γ-Pcdhs in Pax2+ vINs, which due to the homophilic nature of γ-Pcdh interactions (Schreiner and Weiner, 2010) would be expected given their requirement in Ia neurons themselves. The fact that the ubiquitous loss of the γ-Pcdhs in the absence of apoptosis in *Pcdh-γ*$^{del/del}$; *Bax*$^{-/-}$ double mutants yields a phenotype quantitatively similar to both Wnt1- and Pax2-restricted mutants (**Table 1**) supports the latter conclusion. Finally, we analyzed *Hb9-Cre*; *Pcdh-γ*$^{fcon3/fcon3}$ mice, and, surprisingly, found no significant change in the density of Ia afferent terminals on MNs (**Table 1**). This suggests that the γ-Pcdhs act primarily to facilitate interactions between Ia afferents and vINs, and that disruptions in these interactions indirectly affect the formation of the primary Ia terminals on MNs.

DISCUSSION

The clustered protocadherins have been suggested to play an important role in providing molecular identity to neuronal subpopulations, which in turn could control the specificity of neuronal connectivity as well as neuronal survival (Morishita and Yagi, 2007; Schreiner and Weiner, 2010; Zipursky and Sanes, 2010). Consistent with this, in mice lacking the α-Pcdhs there is a failure of olfactory axons bearing a single type of odorant receptor to coalesce properly into glomeruli in olfactory bulbs (Hasegawa et al., 2008). *Pcdh-α* mutant mice also exhibit disruptions in the arborization pattern of serotonergic terminals in the brain (Katori et al., 2009). We earlier showed that deletion of the *Pcdh-γ* cluster results in widespread interneuron apoptosis in the embryonic spinal cord that reflects an exacerbation of a normal developmental pattern of cell death (Wang et al., 2002b; Prasad et al., 2008). The affected vIN populations include those involved in stereotyped motor circuits (the central pattern generator), which receive inputs from DRG sensory neurons as well as from higher brain centers and play a critical role in controlling motor output (Goulding, 2009). Intriguingly, the survival of DRG sensory neurons and ventral horn MNs is *not* affected by the loss of the γ-Pcdhs (Wang et al., 2002b; Prasad et al., 2008, the present study). This, along with the observation that *Pcdh-γ* null mutant neonates lack spinal reflexes, suggested that the γ-Pcdhs might regulate the formation of spinal proprioceptive circuits.

Here, we took advantage of genetic techniques to disrupt γ-Pcdh function in the neurons comprising the proprioceptive stretch reflex circuit in the developing spinal cord. Our data show that loss of γ-Pcdhs results in the expansion and disorganization of Ia afferent terminals on MNs, but does not affect axon pathfinding, as shown by the developmentally appropriate growth of Ia axons into the ventral horn and the lack of aberrant branching into dorsal horn. Because Ia terminal area per MN is increased without any corresponding increase in the area occupied by PSD-95+ puncta, the clumped terminals do not appear to represent functional synaptic connections, consistent with mutant neonates' outward phenotype. Along with expansion of terminals onto MNs there is a simultaneous loss of terminals formed onto vINs. As the disruption in the pattern of Ia afferent terminals occurs during the same time period when vINs are undergoing aberrant apoptotic cell death in *Pcdh-γ* null mutants (Prasad et al., 2008), we asked whether the disrupted Ia terminals were due to an extensive loss of vIN targets. Our data from the *Pcdh-γ*$^{del/del}$; *Bax*$^{-/-}$ double mutants show that blocking apoptosis ameliorates, but does not completely rescue, the Ia phenotype. Further analyses of mice in which *Pcdh-γ* mutation is restricted to sensory neurons, interneurons, or MNs showed that the γ-Pcdhs are required in sensory and interneuron populations, but not in MNs, for the normal pattern of Ia terminal arborization. Taking these data

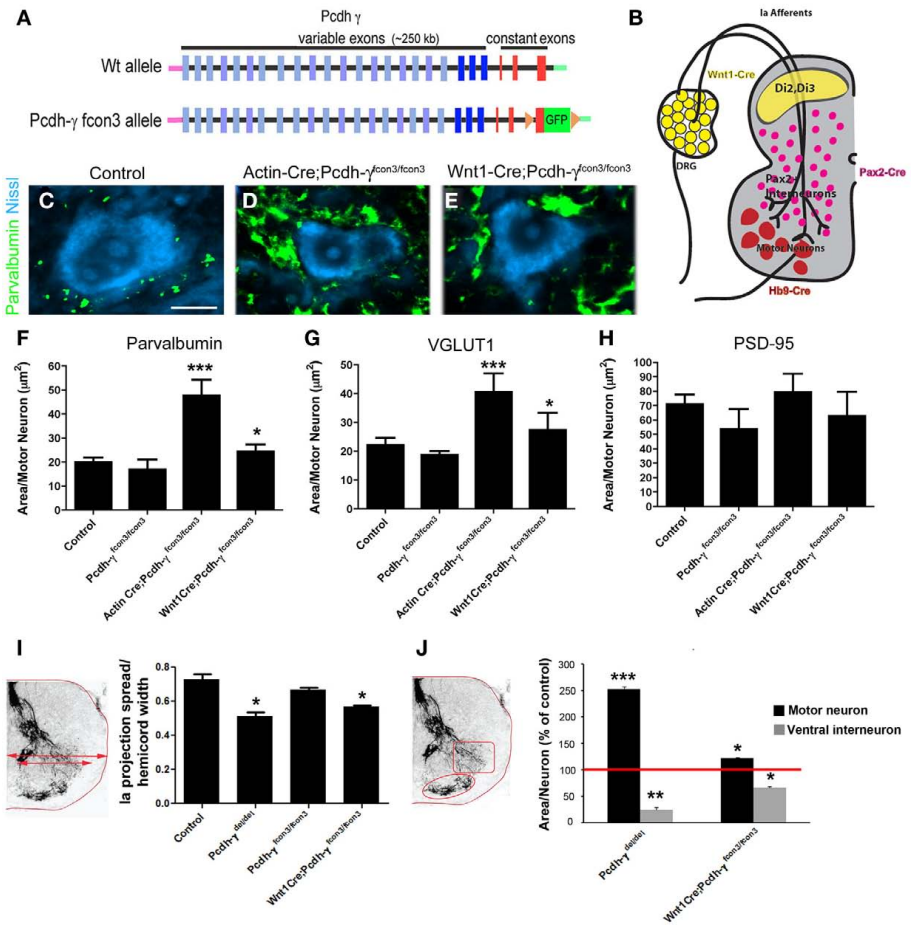

FIGURE 7 | Restricted mutation of the *Pcdh-γ* gene cluster in DRG sensory neurons reveals a cell autonomous requirement for the γ-Pcdhs in Ia afferent terminal arborization. (A) Schematic diagram showing the wild-type (wt) and conditional mutant *Pcdh-γ* alleles (*Pcdh-γ*^{fcon3}). The fcon3 alleles harbors loxP sites on either side of the third constant exon to which GFP is fused. **(B)** Schematic diagram of a P0 spinal hemi-cord showing the neuronal subsets in which the *Pcdh-γ* gene cluster is disrupted when crossed with the indicated Cre transgenic lines. **(C–E)** Individual motor neurons from control, *Actin-cre*; *Pcdh-γ* $^{fcon3/fcon3}$ (ubiquitous excision) and *Wnt1-Cre*; *Pcdh-γ*$^{fcon3/fcon3}$ (DRG and dorsal horn-specific excision) spinal cords stained for parvalbumin and Nissl counterstain. Ubiquitous excision of the conditional allele phenocopies *Pcdh-γ*$^{del/del}$ null mutants (compare to **Figure 4F**), while *Wnt1-Cre*-restricted mice show an intermediate Ia phenotype. **(F–H)** Quantification of the area occupied by parvalbumin- or VGLUT1+ Ia terminals and PSD-95+ postsynaptic puncta per motor neuron. **(I,J)** Measures of Ia terminal spread and area of terminals per neuron in both the MN and vIN fields, quantified as in **Figure 5**. Scale bar: 20 μm in **(C–E)**. $*p < 0.05$ and $**p < 0.01$; $***p < 0.001$.

together with our recent demonstration of homophilic γ-Pcdh interactions (Schreiner and Weiner, 2010), we thus suggest that the γ-Pcdhs regulate the formation of spinal proprioceptive circuits both directly and indirectly: Directly via homophilic interactions between incoming Ia axons and vINs, and indirectly by controlling the survival of these vIN target neurons.

Our results raise the possibility that collateral vIN targets somehow regulate the formation of monosynaptic Ia terminals on MNs. As some vINs are located at slightly more dorsal positions than MNs, it may be that collateral branches of the Ia afferents make contact with them first. If so, Ia afferent-vIN contacts mediated by the γ-Pcdhs could provide an instructive signal that regulates the arborization of the main axonal branches onto MNs. Alternatively, it may simply be that Ia axons need to make a particular number of terminals, or to establish a particular area of terminal arborization, and if vIN targets are missing or non-receptive due to γ-Pcdh loss, the MN terminal field is increased in area accordingly to make up for this deficit. Intriguingly, though MNs do express the γ-Pcdhs, this expression is not required for the formation of the Ia circuit, and the number of postsynaptic PSD-95+ puncta does not change even in null mutants. The question of whether the γ-Pcdhs regulate the *specificity* of proprioceptive synapse formation, as Sema3e-PlexinD1 signaling has been shown to do (Pecho-Vrieseling et al., 2009), remains unclear. The neonatal lethality of *Pcdh-γ*$^{del/del}$, *Wnt1-Cre*; *Pcdh-γ*$^{fcon3/fcon3}$, and *Pax2-Cre*; *Pcdh-γ*$^{fcon3/fcon3}$ mutants unfortunately precludes the kind of electrophysiological studies that can address this issue directly. Although limited to the DRG and the superficial dorsal horn in the spinal sensorimotor system, *Wnt1-Cre* activity is also found in other brain regions (Rico et al., 2002), including

brainstem and basal forebrain nuclei in which loss of the γ-Pcdhs results in increased apoptosis (Wang et al., 2002b), a likely cause of the observed lethality. Future studies utilizing more restricted Cre lines may allow us to circumvent this neonatal lethality and allow for electrophysiological studies of sensorimotor circuit specificity to be performed.

The cell signaling mechanisms by which the γ-Pcdhs might regulate the elaboration of Ia afferent terminals is unknown. One intriguing possibility is that they negatively regulate Wnt signaling. Wnt-3, expressed by MNs, can promote branching and increase the growth cone size of growing NT3-responsive (i.e., Ia afferent), but not NGF-responsive (i.e., cutaneous), DRG neurons *in vitro* (Krylova et al., 2002). Recently, in studies of kidney tumor cell lines, it was shown that the γ-Pcdhs act to repress Wnt signaling-induced gene transcription by β-catenin/TCF (Dallosso et al., 2009). Although the mechanisms by which the γ-Pcdhs might do so remain unclear, it is an intriguing possibility that Wnts, released by MNs and/or by vINs, promote the elaboration of Ia terminal arbors, while the γ-Pcdhs serve to limit this signal. If so, we might expect just the results that we describe here: loss of the γ-Pcdhs on sensory neurons leads to expansion of terminals and arbors on MNs. The fact that the γ-Pcdhs are not required in MNs themselves raises the possibility that, in addition to their role as homophilic adhesion molecules (Schreiner and Weiner, 2010), this diverse family can cell autonomously regulate signaling pathways during neural development. Future studies aimed at testing this hypothesis may uncover unexpected new roles for the γ-Pcdh family.

ACKNOWLEDGMENTS

We thank Leah Fuller and Claire Vernon for expert assistance with animal breeding and genotyping, and Dr. Louis Reichardt (UCSF) for the anti-TrkA antibody. This work was funded by a grant from the NIH to Joshua A. Weiner (R01 NS055272).

REFERENCES

Alvarez, F. J., Jonas, P. C., Sapir, T., Hartley, R., Berrocal, M. C., Geiman, E. J., Todd, A. J., and Goulding, M. (2005). Postnatal phenotype and localization of spinal cord V1 derived interneurons. *J. Comp. Neurol.* 493, 177–192.

Arber, S., Han, B., Mendelsohn, M., Smith, M., Jessell, T. M., and Sockanathan, S. (1999). Requirement for the homeobox gene Hb9 in the consolidation of motor neuron identity. *Neuron* 23, 659–674.

Arber, S., Ladle, D. R., Lin, J. H., Frank, E., and Jessell, T. M. (2000). ETS gene Er81 controls the formation of functional connections between group Ia sensory afferents and motor neurons. *Cell* 101, 485–498.

Arikkath, J., and Reichardt, L. F. (2008). Cadherins and catenins at synapses: roles in synaptogenesis and synaptic plasticity. *Trends Neurosci.* 31, 487–494.

Brown, A. G. (1981). *Organization in the Spinal Cord.* New York: Springer.

Burrill, J. D., Moran, L., Goulding, M. D., and Saueressig, H. (1997). PAX2 is expressed in multiple spinal cord interneurons, including a population of EN1+ interneurons that require PAX6 for their development. *Development* 124, 4493–4503.

Chen, H. H., Hippenmeyer, S., Arber, S., and Frank, E. (2003). Development of the monosynaptic stretch reflex circuit. *Curr. Opin. Neurobiol.* 13, 96–102.

Cheng, H. J., Bagri, A., Yaron, A., Stein, E., Pleasure, S. J., and Tessier-Lavigne, M. (2001). Plexin-A3 mediates semaphorin signaling and regulates the development of hippocampal axonal projections. *Neuron* 32, 249–263.

Coggeshall, R. E., Pover, C. M., and Fitzgerald, M. (1994). Dorsal root ganglion cell death and surviving cell numbers in relation to the development of sensory innervation in the rat hindlimb. *Brain Res. Dev. Brain Res.* 82, 193–212.

Cohen, S., Funkelstein, L., Livet, J., Rougon, G., Henderson, C. E., Castellani, V., and Mann, F. (2005). A semaphorin code defines subpopulations of spinal motor neurons during mouse development. *Eur. J. Neurosci.* 21, 1767–1776.

da Silva, S., and Wang, F. (2011). Retrograde neural circuit specification by target-derived neurotrophins and growth factors. *Curr. Opin. Neurobiol.* 21, 61–67.

Dalla Torre di Sanguinetto, S. A., Dasen, J. S., and Arber, S. (2008). Transcriptional mechanisms controlling motor neuron diversity and connectivity. *Curr. Opin. Neurobiol.* 18, 36–43.

Dallosso, A. R., Hancock, A. L., Szemes, M., Moorwood, K., Chilukamarri, L., Tsai, H. H., Sarkar, A., Barasch, J., Vuononvirta, R., Jones, C., Pritchard-Jones, K., Royer-Pokora, B., Lee, S. B., Owen, C., Malik, S., Feng, Y., Frank, M., Ward, A., Brown, K. W., and Malik, K. (2009). Frequent long-range epigenetic silencing of protocadherin gene clusters on chromosome 5q31 in Wilms' tumor. *PLoS Genet.* 5, e1000745. doi: 10.1371/journal.pgen.1000745

Danielian, P. S., Muccino, D., Rowitch, D. H., Michael, S. K., and McMahon, A. P. (1998). Modification of gene activity in mouse embryos in utero by a tamoxifen-inducible form of cre recombinase. *Curr. Biol.* 8, 1323–1326.

Deckwerth, T. L., Elliott, J. L., Knudson, C. M., Johnson, E. M. Jr., Snider, W. D., and Korsmeyer, S. J. (1996). BAX is required for neuronal death after trophic factor deprivation and during development. *Neuron* 17, 401–411.

Fitzgerald, M. (1987). Cutaneous primary afferent properties in the hind limb of the neonatal rat. *J. Physiol. (Lond.)* 383, 79–92.

Frank, M., Ebert, M., Shan, W., Phillips, G. R., Arndt, K., Colman, D. R., and Kemler, R. (2005). Differential expression of individual gamma-protocadherins during mouse brain development. *Mol. Cell. Neurosci.* 29, 603–616.

Fu, S. Y., Sharma, K., Luo, Y., Raper, J. A., and Frank, E. (2000). SEMA3A regulates developing sensory projections in the chicken spinal cord. *J. Neurobiol.* 45, 227–236.

Garrett, A. M., and Weiner, J. A. (2009). Control of CNS synapse development by γ-protocadherin-mediated astrocyte-neuron contact. *J. Neurosci.* 29, 11723–11731.

Giagtzoglou, N., Ly, C. V., and Bellen, H. J. (2009). Cell adhesion, the backbone of the synapse: "vertebrate" and "invertebrate" perspectives. *Cold Spring Harb Perspect. Biol.* 4, a003079.

Goulding, M. (2009). Circuits controlling vertebrate locomotion: moving in a new direction. *Nat. Rev. Neurosci.* 10, 507–518.

Hasegawa, S., Hamada, S., Kumode, Y., Esumi, S., Katori, S., Fukuda, E., Uchiyama, Y., Hirabayashi, T., Mombaerts, P., and Yagi, T. (2008). The protocadherin-alpha family is involved in axonal coalescence of olfactory sensory neurons into glomeruli of the olfactory bulb in mouse. *Mol. Cell. Neurosci.* 38, 66–79.

Honda, C. N. (1995). Differential distribution of calbindin-D28k and parvalbumin in somatic and visceral sensory neurons. *Neuroscience* 68, 883–892.

Kaneko, R., Kato, H., Kawamura, Y., Esumi, S., Hirayama, T., Hirabayashi, T., and Yagi, T. (2006). Allelic gene regulation of Pcdh-alpha and Pcdh-gamma clusters involving both monoallelic and biallelic expression in single Purkinje cells. *J. Biol. Chem.* 41, 30551–30560.

Katori, S., Hamada, S., Noguchi, Y., Fukuda, E., Yamamoto, T., Yamamoto, H., Hasegawa, S., and Yagi, T. (2009). Protocadherin-alpha family is required for serotonergic projections to appropriately innervate target brain areas. *J. Neurosci.* 29, 9137–9147.

Knudson, C. M., Tung, K. S., Tourtellotte, W. G., Brown, G. A., and Korsmeyer, S. J. (1995). Bax-deficient mice with lymphoid hyperplasia and male germ cell death. *Science* 270, 96–99.

Koerber, H. R., and Mendell, L. M. (1992). "Functional heterogeneity of dorsal root ganglion cells," in *Sensory Neurons: Diversity, Development and Plasticity*, ed. S. A. Scott (New York: Oxford University Press), 77–96.

Krylova, O., Herreros, J., Cleverley, K. E., Ehler, E., Henriquez, J. P., Hughes, S. M., and Salinas, P. C. (2002). WNT-3, expressed by motoneurons, regulates terminal arborization of neurotrophin-3-responsive spinal sensory neurons. *Neuron* 12, 1043–1056.

Lefebvre, J. L., Zhang, Y., Meister, M., Wang, X., and Sanes, J. R. (2008). gamma-Protocadherins regulate neuronal survival but are dispensable for circuit formation in retina. *Development* 135, 4141–4151.

Lewandoski, M., Meyers, E. N., and Martin, G. R. (1997). Analysis of Fgf8 gene function in vertebrate development. *Cold Spring Harb. Symp. Quant. Biol.* 62, 159–168.

Lewis, K. E. (2006). How do genes regulate simple behaviours? Understanding how different neurons in the vertebrate spinal cord are genetically specified. *Philos. Trans. R. Soc. Lond. B Biol. Sci.* 361, 45–66.

Lobas, M. A., Helsper, L., Vernon, C. G., Schreiner, D., Zhang, Y., Holtzman, M. J., Thedens, D. R., and Weiner, J. A. (2011). Molecular heterogeneity in the choroid plexus epithelium: the 22-member g-protocadherin family is differentially expressed, apically localized, and implicated in CSF regulation. *J. Neurochem.* (in press).

Margeta, M. A., Shen, K., and Grill, B. (2008). Building a synapse: lessons on synaptic specificity and presynaptic assembly from the nematode *C. elegans*. *Curr. Opin. Neurobiol.* 18, 69–76.

Mears, S. C., and Frank, E. (1997). Formation of specific monosynaptic connections between muscle spindle afferents and motoneurons in the mouse. *J. Neurosci.* 17, 3128–3135.

Messersmith, E. K., Leonardo, E. D., Shatz, C. J., Tessier-Lavigne, M., Goodman, C. S., and Kolodkin, A. L. (1995). Semaphorin III can function as a selective chemorepellent to pattern sensory projections in the spinal cord. *Neuron* 14, 949–959.

Mirnics, K., and Koerber, H. R. (1995). Prenatal development of rat primary afferent fibers: II. Central projections. *J. Comp. Neurol.* 355, 601–614.

Morishita, H., and Yagi, T. (2007). Protocadherin family: diversity, structure, and function. *Curr. Opin. Cell Biol.* 19, 584–592.

Mu, X., Silos-Santiago, I., Carroll, S. L., and Snider, W. D. (1993). Neurotrophin receptor genes are expressed in distinct patterns in developing dorsal root ganglia. *J. Neurosci.* 13, 4029–4041.

Ohyama, T., and Groves, A. K. (2004). Generation of Pax2-Cre mice by modification of a Pax2 bacterial artificial chromosome. *Genesis* 38, 195–199.

Pecho-Vrieseling, E., Sigrist, M., Yoshida, Y., Jessell, T. M., and Arber, S. (2009). Specificity of sensory-motor connections encoded by Sema3e-Plxnd1 recognition. *Nature* 459, 842–846.

Perrin, F. E., Rathjen, F. G., and Stoeckli, E. T. (2001). Distinct subpopulations of sensory afferents require F11 or axonin-1 for growth to their target layers within the spinal cord of the chick. *Neuron* 30, 707–723.

Phillips, G. R., Tanaka, H., Frank, M., Elste, A., Fidler, L., Benson, D. L., and Colman, D. R. (2003). Gamma-protocadherins are targeted to subsets of synapses and intracellular organelles in neurons. *J. Neurosci.* 23, 5096–5104.

Prasad, T., Wang, X., Gray, P. A., and Weiner, J. A. (2008). A differential developmental pattern of spinal interneuron apoptosis during synaptogenesis: insights from genetic analyses of the protocadherin-gamma gene cluster. *Development* 135, 4153–4164.

Price, S. R., De Marco Garcia, N. V., Ranscht, B., and Jessell, T. M. (2002). Regulation of motor neuron pool sorting by differential expression of type II cadherins. *Cell* 109, 205–216.

Rico, B., Xu, B., and Reichardt, L. F. (2002). TrkB receptor signaling is required for establishment of GABAergic synapses in the cerebellum. *Nat. Neurosci.* 5, 225–233.

Sapir, T., Geiman, E. J., Wang, Z., Velasquez, T., Mitsui, S., Yoshihara, Y., Frank, E., Alvarez, F. J., and Goulding, M. (2004). Pax6 and engrailed 1 regulate two distinct aspects of renshaw cell development. *J. Neurosci.* 24, 1255–1264.

Schreiner, D., and Weiner, J. A. (2010). Combinatorial homophilic interaction between gamma-protocadherin multimers greatly expands the molecular diversity of cell adhesion. *Proc. Natl. Acad. Sci. U.S.A.* 107, 14893–14898.

Takeichi, M. (2007). The cadherin superfamily in neuronal connections and interactions. *Nat. Rev. Neurosci.* 8, 11–20.

Tasic, B., Nabholz, C. E., Baldwin, K. K., Kim, Y., Rueckert, E. H., Ribich, S. A., Cramer, P., Wu, Q., Axel, R., and Maniatis, T. (2002). Promoter choice determines splice site selection in protocadherin alpha and gamma pre-mRNA splicing. *Mol. Cell* 10, 21–33.

Umemori, H., Linhoff, M. W., Ornitz, D. M., and Sanes, J. R. (2004). FGF22 and its close relatives are presynaptic organizing molecules in the mammalian brain. *Cell* 118, 257–270.

Wang, X., Su, H., and Bradley, A. (2002a). Molecular mechanisms governing Pcdh-gamma gene expression: evidence for a multiple promoter and cis-alternative splicing model. *Genes Dev.* 16, 1890–1905.

Wang, X., Weiner, J. A., Levi, S., Craig, A. M., Bradley, A., and Sanes, J. R. (2002b). Gamma protocadherins are required for survival of spinal interneurons. *Neuron* 36, 843–854.

Weiner, J. A. (2006). "Protocadherins and synapse development," in *Molecular Mechanisms of Synaptogenesis*, eds A. Dityatev, and A. El-Husseini (New York: Springer), 137–162.

White, F. A., Keller-Peck, C. R., Knudson, C. M., Korsmeyer, S. J., and Snider, W. D. (1998). Widespread elimination of naturally occurring neuronal death in bax-deficient mice. *J. Neurosci.* 18, 1428–1439.

Wu, Q., and Maniatis, T. (1999). A striking organization of a large family of human neural cadherin-like cell adhesion genes. *Cell* 97, 779–790.

Wu, Q., Zhang, T., Cheng, J. F., Kim, Y., Grimwood, J., Schmutz, J., Dickson, M., Noonan, J. P., Zhang, M. Q., Myers, R. M., and Maniatis, T. (2001). Comparative DNA sequence analysis of mouse and human protocadherin gene clusters. *Genome Res.* 11, 389–404.

Yoshida, Y., Han, B., Mendelsohn, M., and Jessell, T. M. (2006). PlexinA1 signaling directs the segregation of proprioceptive sensory axons in the developing spinal cord. *Neuron* 52, 775–788.

Zipursky, S. L., and Sanes, J. R. (2010). Chemoaffinity revisited: dscams, protocadherins, and neural circuit assembly. *Cell* 143, 343–353.

Zou, C., Huang, W., Ying, G., and Wu, Q. (2007). Sequence analysis and expression mapping of the rat clustered protocadherin gene repertoires. *Neuroscience* 144, 579–603.

Conflict of Interest Statement: The authors declare that the research was conducted in the absence of any commercial or financial relationships that could be construed as a potential conflict of interest.

Received: 16 September 2011; paper pending published: 02 November 2011; accepted: 03 December 2011; published online: 23 December 2011.

Citation: Prasad T and Weiner JA (2011) Direct and indirect regulation of spinal cord Ia afferent terminal formation by the γ-Protocadherins. Front. Mol. Neurosci. ***4****:54. doi: 10.3389/fnmol.2011.00054*

frontiers in
MOLECULAR NEUROSCIENCE

REVIEW ARTICLE
published: 17 August 2012
doi: 10.3389/fnmol.2012.00086

DSCAMs: restoring balance to developmental forces

Andrew M. Garrett , Abigail L. D. Tadenev and Robert W. Burgess*

The Jackson Laboratory, Bar Harbor, ME, USA

Edited by:
Joshua A. Weiner, The University of Iowa, USA

Reviewed by:
Florentina Soto, Washington University in St. Louis, USA
Wesley Grueber, Columbia University, USA

****Correspondence:***
Robert W. Burgess, The Jackson Laboratory, 600 Main St., Bar Harbor, ME 04609, USA.
e-mail: robert.burgess@jax.org

Many of the models of neurodevelopmental processes such as cell migration, axon outgrowth, and dendrite arborization involve cell adhesion and chemoattraction as critical physical or mechanical aspects of the mechanism. However, the prevention of adhesion or attraction is under-appreciated as a necessary, active process that balances these forces, insuring that the correct cells are present and adhering in the correct place at the correct time. The phenomenon of not adhering is often viewed as the passive alternative to adhesion, and in some cases this may be true. However, it is becoming increasingly clear that active signaling pathways are involved in preventing adhesion. These provide a balancing force during development that prevents overly exuberant adhesion, which would otherwise disrupt normal cellular and tissue morphogenesis. The strength of chemoattractive signals may be similarly modulated. Recent studies, described here, suggest that Down Syndrome Cell Adhesion Molecule (DSCAM), and closely related proteins such as DSCAML1, may play an important developmental role as such balancers in multiple systems.

Keywords: DSCAM, Dscaml1, cell adhesion, chemoattraction, retina, self-avoidance, chemorepulsion

INTRODUCTION

Despite its molecular classification as a cell adhesion molecule, Down Syndrome Cell Adhesion Molecule (DSCAM) is recognized for its physiological role in "self-avoidance" in Drosophila and mammals. Self-avoidance involves the repulsion of processes from the same cell during dendrite arborization or axon branching, and the prevention of fasciculation and clumping of cells of the same subtype during the development of structures with well-defined anatomies such as the mammalian retina. In this way, self-avoidance counteracts cell adhesion, which knits cells together. DSCAM is the best molecular entry point into the process of self-avoidance, which has been described, but little studied, for almost 30 years (Kramer and Stent, 1985; Kramer et al., 1985). Interestingly, recent work indicates that Drosophila Dscam1 may also be counteracting netrin-dependent chemoattraction, another well-characterized developmental process. Thus, Dscam is emerging as an active antagonist of cellular and molecular mechanisms that were previously viewed as acting largely unopposed. This view is unique because modulation was thought to be achieved simply by adjusting the strength of the positive signal and not by a distinct counteracting cue. In this review, we describe how this view has evolved as our understanding of Dscam's *in vivo* roles has grown.

THERE ARE TWO SIDES TO THE FORCE

Cell adhesion in many forms plays a critical role in development in general and in neurodevelopment in particular (Rutishauser and Jessell, 1988). Cells adhere to other cells and to the extracellular matrix during development through a variety of mechanisms including integrins, Ca^{2+}-dependent cadherins, and Ca^{2+}-independent cell adhesion molecules (Milner and Campbell, 2002; Gibson, 2011; Hirano and Takeichi, 2012). These adhesive interactions have been repeatedly shown to underlie many key aspects of development, including differentiation, cell migration, cell morphogenesis, and cell survival. An extreme view of cell adhesion as a motive force during development is put forward in the differential adhesion hypothesis (DAH). This idea proposes that the sorting of cells into different strata and tissues during development is similar to fluids separating based on differing miscibilities and surface tensions (Steinberg, 2007). Those cells that bind most tightly to each other form a dense core, and those that bind least tightly form the outermost layer, just as liquids separate based on surface tension. The forces in play are the attractive forces between cells and the tensions at the interfaces between two strata of differing adhesiveness. This model does a very good job of describing some developmental events such as epiboly, the expansion of cells over the yolk in some species during early development, but is probably not adequate to explain more complex cellular and tissue morphologies. Also, cells are active players in morphogenesis and are willing and able to expend energy to establish conformations that would not arise from passive processes. The elaborate dendritic and axonal arbors of neurons certainly challenge a simple model of morphogenesis.

A more nuanced view of adhesion is put forward in an excellent review of retinal development (Galli-Resta et al., 2008). This review proposes that both the vertical, laminar structure of the retina, and the non-random, mosaic spacing of neuronal cell types in circumferential space of the retina can be explained by mechanical forces acting during development. To oversimplify the arguments made, the vertical organization arises because retinal ganglion cells adhere tightly to the extracellular matrix of the inner limiting membrane, whereas the adherens junctions of the

outer limiting membrane knit the outermost cells of the retina together (**Figure 1A**). As cells proliferate in the space between, they occupy different strata based on their relative adhesiveness, much as one might predict from the DAH. These intermediate cells have also "let go" of both the innermost and outermost cells. The laminar and horizontal structures are further refined by adhesion between the processes of cells of a given type. In an analogy to a net, where the cell bodies are knotted nodes and the processes are the mesh, if the cells start in a heap, but are pulled as the eye grows, the result is a network of cells in a single layer that are evenly spaced from one another. This is a very attractive model that relies largely on adhesion between cells of a given type and mechanical forces of an expanding retina to achieve a final, highly organized anatomy. One interesting question that arises from this model is whether adhesion must be balanced by other forces. For example, do the cells of the inner nuclear layer (INL), the middle stratum of the retina, passively let go of the inner limiting membrane and ganglion cells, or are they kicked off? Similarly, as the heaped net of neurons is pulled outward, the cells of the heap have to be able to separate from one another, or the final anatomy looks like poorly cooked pasta. Thus, the adhesive forces between these cells allowing the network of processes to form must be counter balanced to prevent over-exuberant adhesion. This may occur with cell type specificity, since the pattern of each neuronal subpopulation in the retina arises largely independently, or even with subcellular specificity, allowing adhesion of distal processes, but preventing adhesion more proximally.

Work on the arborization of dendrites and patterning of neuronal territories in Drosophila and invertebrates such as the leech suggests that some neuronal subtypes "tile" through active repulsion, an opponent mechanism to adhesion. The processes of such cells occupy discrete, non-overlapping territories (hence the term tiling), and appear to actively repel neighbors from their space. When an axonal branch is ablated, for example, the vacated space is filled by the neighboring branch until they again abut without overlapping (Kramer and Stent, 1985). In Drosophila, some instances of tiling may reflect cell processes responding to a physical demarcation such as a segment boundary or the midline, which may have a specialized matrix or extracellular environment. However, neurons can be made to cross such boundaries by mutating genes such as the atypical cadherin Flamingo (Gao et al., 2000; Grueber et al., 2002). Therefore, the territories occupied by the processes of these cells are not necessarily constrained in their inherent physical size, but are limited by repellent interactions with their neighbors or their extracellular environment.

It is currently unclear if repulsion represents an extreme form of preventing adhesion, or if those mechanisms that counter balance adhesion are distinct from those that actually promote repulsion, although the possibility that adhesive mechanisms can be coopted for such purposes has been discussed (Cavallaro and Dejana, 2011). However, the relationship between repulsion and self-avoidance remains unanswered largely because neither mechanism is well understood.

Perhaps processes analogous to dendrite arborization are axon guidance and cell migration. It is clear that in these processes, both attractive and repellent signals are integrated to achieve complex effects such as attraction to and crossing of the midline, and doing so only a single time without turning back (Stein and Tessier-Lavigne, 2001). Interestingly, the same signal can be both attractive and repellent, depending on the receptors present on the receiving cell (Hong et al., 1999). In another example, the guidance of migrating inhibitory neurons from the ganglionic eminence during cortical development, SLIT proteins appear to direct migration through repulsion. However, some of this activity may be more accurately described as funneling migrating neurons to their destinations by creating a non-permissive environment for their migration (Zhu et al., 1999; Wichterle et al., 2003). Such differences border on semantics, but demonstrate mechanistic distinctions. Is an extrinsic guidance signal actively attractive or repellent, or is it simply more or less attractive to growth? With cell adhesion, the question could become whether cells not sticking is a passive failure to adhere, an active repulsion, or an active prevention of adhesion that simply renders cells indifferent to one another.

Interestingly, DSCAM may be a key player in both of these analogous developmental processes of cell adhesion and chemoattraction. DSCAM is a cell adhesion molecule in the immunoglobulin superfamily with one additional closely related vertebrate gene family member, Dscam-like1 (*Dscaml1*), and four Drosophila homologs, DSCAMs 1–4 (Yamakawa et al., 1998; Agarwala et al., 2001; Millard et al., 2007). DSCAMs (used here to refer collectively to all gene family members) bind specifically and homophilically in cell aggregation assays (Agarwala et al., 2000, 2001; Yamagata and Sanes, 2008). However, only some of their proposed functions in neurodevelopment are consistent with adhesion, and in other instances they appear to balance both chemoattraction and cell adhesion, and can even serve as a repellent, as described below.

Much of our knowledge of DSCAMs comes from Drosophila, in which *Dscam1* has the distinction of extensive molecular diversity that arises through alternative exon usage (Schmucker et al., 2000). In total, the Drosophila *Dscam1* gene can encode 19008 extracellular domains, and these bind homophilically with isoform specificity (Wojtowicz et al., 2004). Individual neurons express a stochastic handful of *Dscam1* isoforms on their cell surfaces and in this way can be uniquely identified, able to recognize "self"—other processes of the same cell—but remaining blind to the processes of neighboring cells (Neves et al., 2004). This self-recognition leads to self-avoidance, and two processes of a given cell end up repelling, promoting functions like dendrite arborization or axon branching within a single cell (isoneuronally) (Wang et al., 2002; Zhan et al., 2004; Hughes et al., 2007; Matthews et al., 2007; Soba et al., 2007). Thus, Dscam1-mediated self-avoidance prevents self-crossings within dendritic arbors, but allows overlap with neighboring neurons through its molecular diversity and the isoform specificity of the interactions.

The self-avoidance mechanism described above is contact dependent; two Dscam1-laden processes of the same cell must encounter one another to signal self-avoidance and repulsion through homophilic recognition. This process is much more efficient when the processes are constrained to a two-dimensional space and therefore more likely to encounter one another. In this function, Dscam1 function intersects with integrin-mediated adhesion to the extracellular matrix (Han et al., 2012; Kim

et al., 2012). The developing dendrites of Drosophila dendrite arborization neurons (da neurons) exhibit Dscam1-dependent self-avoidance and grow largely in contact with the laminin rich ECM on the basal surface of the body wall epithelium through integrin-dependent adhesion to laminin. In the absence of integrins, these dendrites become "enclosed," where segments of the dendrites become engulfed or surrounded by the epithelial cell. Under these conditions, the incidence of self-crossings within the dendritic arbor of an individual da neuron increases, but these are "non-contacting" self-crossings, where an enclosed dendrite segment crosses another dendrite, but the intervening epithelial cell prevents contact, and therefore, Dscam1-mediated self-avoidance. These studies clearly demonstrate that Dscam1's function is integrated with, and to some extent dependent upon, other cell adhesion systems such as integrins, but is Dscam1's repellent self-avoidance function balancing adhesion? Results from studies of the mammalian DSCAMs would suggest that they are indeed counteracting adhesion.

SELF-ADHESION: YOU MUST LEARN TO CONTROL YOUR FEELINGS

The function of DSCAMs has been studied in the mouse retina in both wild type mice and mice mutant for either *Dscam* or *Dscaml1* (Fuerst et al., 2008, 2009). In the mouse, *Dscam* is expressed in a subset of amacrine interneurons (dopaminergic amacrine cells (DA) and b-NOS-positive amacrine cells) and most retinal ganglion cells (**Figure 1A**). *Dscaml1* has a different, non-overlapping expression pattern, with expression in the rod circuit: rod photoreceptors, rod bipolar cells (RBCs), and AII amacrine cells. In the absence of *Dscam* or *Dscaml1*, the cells that would normally express the gene adhere abnormally and in a cell-type-specific manner (**Figures 1B,C**). Cells of a given type, DA cells for example, have fasciculated dendrites and the cell bodies are clumped together. Notably, while bNOS-positive amacrines exhibit a similar phenotype, these two cells types do not co-clump or co-fasciculate, despite the physical proximity of the DA and bNOS-positive cells. DSCAML1 mediates a similar self-avoidance function in RBC dendrites and AII amacrine cells. The defects in the *Dscam* mutant retina are consistent with homophilic cell-to-cell interactions based on studies of chimeric eyes (Fuerst et al., 2012).

Is this cell-type-specific fasciculation and clumping truly a failure of self-avoidance analogous to Drosophila Dscam1 function? It appears to be. Individual DA neurons examined in isolation before their dendrites overlap extensively with those of neighboring sister cells showed significantly more isoneuronal self-crossing in the *Dscam* mutant mice than in wild type controls (Fuerst et al., 2008). However, the *Dscam* mutant retina is also

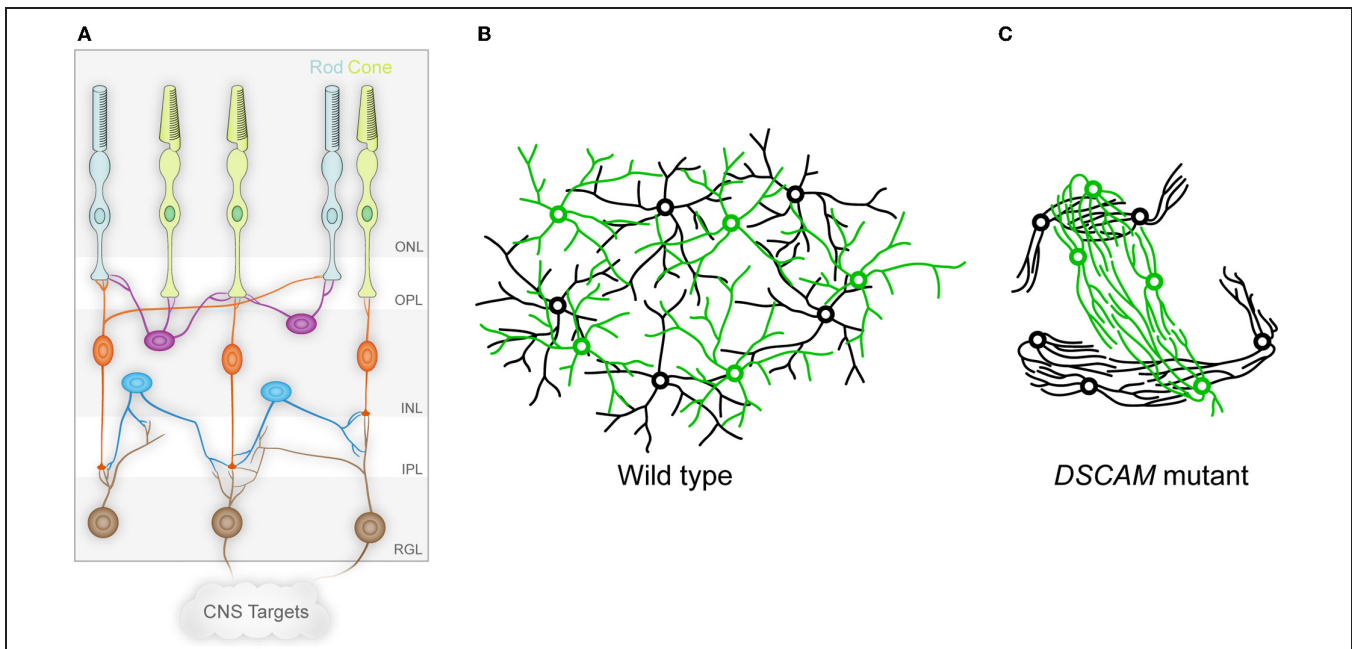

FIGURE 1 | The vertebrate retina and DSCAM in self-avoidance. (A) The vertebrate retina is organized in columnar microcircuits connecting rod and cone photoreceptors in the outer nuclear layer (ONL) to horizontal (purple), bipolar (orange), and amacrine (blue) interneurons in the inner nuclear layer (INL) by synapses formed in the outer plexiform layer (OPL). The interneurons in turn form synapses in the inner plexiform layer (IPL) onto the dendrites of ganglion cells in the retinal ganglion cell layer (RGL), which project axons to the brain through the optic nerve. Establishing this anatomy involves both vertical organization into the different layers, and horizontal organization in which cells of a given type are non-randomly spaced and their dendritic arbors process information uniformly in circumferential space. **(B)** The circumferential spacing in a wild type retina is depicted for two cell types, in which the cell bodies of each cell type are non-randomly spaced from other cells of the same type, but are randomly distributed in relation to the cell bodies of other cell types. In addition, the dendritic arbors of these cells overlap, even within single cell types. This spacing is referred to as a mosaic. **(C)** In the absence of DSCAM, the dendrites and cell bodies of the neurons fasciculate and clump in a cell-type-specific manner, representing a loss of self-avoidance at the level of both individual cells and between cells of a given subtype. (A adapted from Garrett and Burgess, 2011.)

"vertically" disorganized: dendrites from particular cell types are no longer strictly confined to laminar strata within the plexiform layers. Perhaps the fasciculation observed in the *Dscam* mutant retina represents non-contacting crossings, such as one sees in Drosophila when the normal two-dimensional stratification of processes is disrupted even with intact Dscam1 function? One way to answer this question would be to investigate DSCAM function in a two-dimensional system, such as cultured neurons. If mutant neurons exhibit increased self-crossings when adherent to a culture dish, this would establish that DSCAM has a legitimate isoneuronal self-avoidance function, which may also extend to self-avoidance between cells of a given subtype.

An exciting implication of this cell-type-specific clumping and adhesion is that there is a cell-type-specific adhesion code that is unmasked by the loss of DSCAM, leading to the overly exuberant adhesion seen in the mutant retina (Fuerst and Burgess, 2009; Garrett and Burgess, 2011). The identities of the molecules that underlie this adhesion code remain unknown, but in this scenario, DSCAM-mediated self-avoidance is once again balancing adhesion. Whether this self-avoidance function truly involves repulsion or simply makes cells indifferent to one another remains to be determined in a vertebrate system. In support of the indifference model, *Dscam*-expressing cell types have heavily overlapping dendritic arbors, creating many self-type crossings, although as described above, careful examination in the *Z*-axis may show these to be non-contacting crossings. Similarly, developing processes of DA neurons do not show an interaction consistent with an actively repellent response (Keeley and Reese, 2010). Finally, the *Dscam* and *Dscaml1* genes are expressed in some abundant and closely packed cell types, including *Dscam* expression in most retinal ganglion cell types from a very early age, and *Dscaml1* expression in rod bipolar cells (Fuerst et al., 2009). It is hard to imagine how a cell in such a population could be actively repellent to all other cells in the population. Furthermore, such a repulsion mechanism could force some cells to leave the lamina in which they belong. In favor of a repellent mechanism are the results from Drosophila showing active repulsion (Montague and Friedlander, 1991; Matthews et al., 2007). Nonetheless, whether actively repellent or simply indifferent, mouse DSCAMs do seem to mediate self-avoidance both isoneuronally and between cells of a specific type. One interpretation of the clumping and fasciculation phenotype that is seen in the absence of the DSCAMs is that these proteins are serving to balance self-adhesion that otherwise runs unopposed.

In opposing self-adhesion, DSCAMs may allow mosaic spacing of cell bodies to occur without actively promoting it. Indeed, the non-random spacing of cells and the establishment of exclusion zones may depend on cells finding a homogeneous position in a gradient of a secreted signal. The MEGF10 and 11 proteins appear to be serving such a role in the retina, and alterations in their expression levels lead to alterations in the cell body spacing pattern at the interface between high and low expressing regions (Kay et al., 2012). The DSCAMs are not the only molecules that balance self-adhesion in the retina; there are several cell types that do not appear to express either *Dscam* or *DscamL1*. Indeed, horizontal cells mutant for *PlexinA4* exhibit increased dendritic self-crossings, although their arbors are not as severely disrupted as the affected cell types in *Dscam* mutants and the cell body spacing is maintained (Matsuoka et al., 2012).

DSCAM IN GUIDANCE: THIS IS NOT THE NETRIN YOU ARE LOOKING FOR

Interestingly, DSCAMs serving such a balancing role may also be true in the analogous process of axon guidance. DSCAMs are proposed to function as netrin receptors (Ly et al., 2008; Li et al., 2009). This is based on a similar domain structure to DCC and Neogenin (Unc41-family netrin receptors), as well as physical interactions with both DCC and netrin. In addition, knockdown of *Dscam* in filleted spinal cord preparations resulted in a defect in commissural axon guidance consistent with impaired netrin function. Furthermore, Drosophila *Dscam1* acts semi-redundantly with *Dscam3* to affect axon guidance in both netrin-dependent and –independent ways (Andrews et al., 2008). However, an examination of *Dscam* knockout mice failed to show netrin-like defects in axon guidance, suggesting DSCAM's interaction with netrin signaling might have more subtle effects (Palmesino et al., 2012).

A study of Drosophila dendrite arborization suggests that Dscam1's impact on netrin signaling may indeed be more complex, with Dscam1-mediated self-avoidance effectively balancing netrin-dependent attraction (Matthews and Grueber, 2011). In the absence of Dscam1, some of the dendrite arborization defects observed could be accounted for by dendrite attraction to sources of netrin. Ectopic expression of netrin could redirect the poorly arborized *Dscam1* mutant dendrites in an attractive manner. Finally, neurons mutant for both *Dscam1* and the netrin receptor Frazzled/DCC had disorganized dendritic arbors that were not attracted to the netrin source. Thus, Dscam-mediated self-avoidance of developing dendrites seems to promote the formation of a normal arbor by balancing the attractive cues provided by netrins. In other contexts, the loss of such a balancing factor could indeed cause an axon guidance phenotype that would have to be carefully interpreted to be sure it was not the result of overly exuberant attraction or repulsion.

It is also interesting to consider that DSCAM is proposed to function as a netrin receptor in axon guidance, and Dscam1 and -2 are involved in axonal branching and tiling in Drosophila, but axonal phenotypes are poorly studied in vertebrates (Wang et al., 2002; Millard et al., 2007). Some defects in targeting and ipsilateral/contralateral segregation of retinal ganglion cell axons within the lateral geniculate nucleus have been observed, but it remains to be determined if these effects are the result of DSCAM loss in the retina, the target, or both (Blank et al., 2011). Thus, Drosophila DSCAMs appear to impact netrin signaling for both axon and dendrite guidance, with the latter being a function of Dscam1-dependent self-avoidance balancing netrin-dependent attraction.

Do vertebrate DSCAMs function exclusively to balance adhesion or attraction in self-avoidance? Perhaps not, based on results from the chick retina (Yamagata and Sanes, 2008). In this system, Dscam and related adhesion molecules Dscam-like, Sidekick1, and Sidekick2 define distinct sublaminae in the synaptic inner plexiform layer (IPL). The knockdown of each of these proteins causes cells that normally stratify in that sublamina to mislocalize,

and driving the ectopic expression of one of these proteins in a cell that does not normally express it redirects the dendrites to the lamina of the overexpressed protein. The most straightforward explanation of these data is that the adhesion molecules define the lamina in which neurons will arborize their processes and thus promote synaptic connectivity. As the IPL contains the presynaptic processes of amacrine and bipolar cells and the postsynaptic dendrites of retinal ganglion cells, this interaction is presumably a homophilic adhesion that promotes their co-stratification. Such a mechanism essentially fits the DAH, where the segregation of cell types, or in this case their processes, is determined by a selective or differential adhesiveness.

The extent to which the DSCAMs drive laminar specificity in the IPL of the mouse retina remains unclear. Studies of the first reported *Dscam* allele (*Dscam*^{del17}) and the *Dscaml1* mutant mice suggest that laminar specificity is intact (Fuerst et al., 2008, 2009). Other studies in a second, spontaneous allele of *Dscam* did show a disruption of laminar specificity, but whether these differences are due to allele-specific effects or the differences in the genetic background of the mutant mouse strains also remains to be determined (Fuerst et al., 2010). Furthermore, the Semaphorin/Plexin signaling pathway mediates laminar specificity for at least some retinal cell types in the mouse (Matsuoka et al., 2011a,b).

DSCAM INTRACELLULAR SIGNALING: I THOUGHT THESE THINGS WERE COMPLICATED ON THE OUTSIDE

How do DSCAMs mediate self-avoidance, and could the same molecules really be responsible for effects ranging from balancing netrin-dependent attraction and cell-type-specific adhesion to promoting laminar specificity through homophilic binding? It seems possible, although the molecular mechanisms are only just being explored.

Human DSCAM binds to P21 Activated Kinase1 (PAK1) through its juxtamembrane intracellular domain (Liu and Guan, 2004). This same interaction is preserved in Drosophila, although in flies it is indirect and mediated by Dock, an SH2-SH3 adapter protein (Schmucker et al., 2000). PAK1 has many developmental roles, most notably being downstream of small GTPases and mediating actin cytoskeletal rearrangements. The role of PAK1 in DSCAM-mediated neurodevelopmental processes is unknown. Furthermore, it is unknown if PAK1 interacts with related molecules such as DSCAML1, which is divergent in sequence in the proximal intracellular domain. It is attractive to postulate that those functions that are shared between mammalian DSCAM and Drosophila Dscaml1 will use the same intracellular pathways, but this remains to be tested.

An interaction that does appear to be shared between DSCAM and DSCAML1, and also with more divergent family members such as Sidekick1 and Sidekick2, is an interaction of the C-termini of these proteins with multi-PDZ domain containing proteins such as MAGIs, PSD95, and Chapsyn110 (Yamagata and Sanes, 2010). This interaction was identified in a yeast-2-hybrid assay, and knockdown of MAGI2 in the chick retina perturbs Sidekick2 function in laminar specificity.

Interestingly, since these interacting proteins are multi-PDZ containing scaffolding molecules, the composition of these DSCAM-containing complexes may contribute to DSCAM's numerous possible functions. For example, in a complex with proteins specifying the cell-type-specific adhesion code, DSCAMs could serve to mask their function to balance adhesion. This could be through a physical inhibition of their extracellular adhesion properties, or through an inactivation of their intracellular signaling pathways. A similar interaction with components of the netrin signaling apparatus could also underlie DSCAM's role in balancing attraction; however, since DSCAM also directly interacts with DCC through an extracellular domain, complexing with other proteins scaffolded by multi-PDZ domain proteins may not be necessary. Furthermore, a change in the composition of the complex could easily allow DSCAMs to mediate self-avoidance early in development and to serve an adhesive function later in development, directing laminar specificity, such as in the chick retina, or synapse maturation, as suggested by DSCAML1 in the rod circuit in the mouse retina. Finally, it is a hypothetical possibility that DSCAMs could serve multiple roles simultaneously in a single cell if the complexes have different composition in different subcellular compartments.

A caveat to the idea that the composition of complexes scaffolded by multi-PDZ domain proteins confers specialized function to DSCAMs is the fact that Drosophila DSCAMs do not have an obvious PDZ-interacting C-terminus. Again, it is tempting to assume that conserved functions such as self-avoidance will happen through conserved intracellular signaling pathways, but this does not have to be the case, and as PAK1 demonstrates, the same pathways may be activated through direct or indirect interactions in one species or another. These ideas concerning signaling/adhesion complexes remain highly speculative, but are an active line of investigation.

SUMMARY

DSCAMs are important neurodevelopmental proteins conserved from flies to mammals. Much of their function appears to be to provide balance to better understood processes such as cell adhesion or chemoattraction. In their absence, there is overly exuberant adhesion and fasciculation between cells of specific subtypes in the mouse retina, and overly exuberant outgrowth of sensory dendrites toward sources of netrin in the fly body wall. These phenotypes demonstrate the importance of balancing these developmental mechanisms, and that this is sometimes an active process; not adhering is more than simply failing to adhere. DSCAMs serve additional roles, including potentially adhesive functions in examples such as the chick IPL. This diversity of activities may be dependent on interactions with other proteins in an adhesion/signaling complex, as suggested by DSCAMs' binding to multi-PDZ domain scaffolding proteins. Thus, while the diversity of DSCAM activities may rival its molecular diversity in Drosophila, the emerging commonality is that DSCAM balances competing forces.

ACKNOWLEDGMENTS

The authors wish to thank Drs. Phuong Hoang and Greg Cox for comments on the manuscript and the National Eye Institute for funding (RO1 EY018605, F32 EY021942).

REFERENCES

Agarwala, K. L., Ganesh, S., Tsutsumi, Y., Suzuki, T., Amano, K., and Yamakawa, K. (2001). Cloning and functional characterization of DSCAML1, a novel DSCAM-like cell adhesion molecule that mediates homophilic intercellular adhesion. *Biochem. Biophys. Res. Commun.* 285, 760–772.

Agarwala, K. L., Nakamura, S., Tsutsumi, Y., and Yamakawa, K. (2000). Down syndrome cell adhesion molecule DSCAM mediates homophilic intercellular adhesion. *Brain Res. Mol. Brain Res.* 79, 118–126.

Andrews, G. L., Tanglao, S., Farmer, W. T., Morin, S., Brotman, S., Berberoglu, M. A., Price, H., Fernandez, G. C., Mastick, G. S., Charron, F., and Kidd, T. (2008). Dscam guides embryonic axons by Netrin-dependent and -independent functions. *Development* 135, 3839–3848.

Blank, M., Fuerst, P. G., Stevens, B., Nouri, N., Kirkby, L., Warrier, D., Barres, B. A., Feller, M. B., Huberman, A. D., Burgess, R. W., and Garner, C. C. (2011). The down syndrome critical region regulates retinogeniculate refinement. *J. Neurosci.* 31, 5764–5776.

Cavallaro, U., and Dejana, E. (2011). Adhesion molecule signalling: not always a sticky business. *Nat. Rev. Mol. Cell Biol.* 12, 189–197.

Fuerst, P. G., Bruce, F., Rounds, R. P., Erskine, L., and Burgess, R. W. (2012). Cell autonomy of DSCAM function in retinal development. *Dev. Biol.* 361, 326–337.

Fuerst, P. G., Bruce, F., Tian, M., Wei, W., Elstrott, J., Feller, M. B., Erskine, L., Singer, J. H., and Burgess, R. W. (2009). DSCAM and DSCAML1 function in self-avoidance in multiple cell types in the developing mouse retina. *Neuron* 64, 484–497.

Fuerst, P. G., and Burgess, R. W. (2009). Adhesion molecules in establishing retinal circuitry. *Curr. Opin. Neurobiol.* 19, 389–394.

Fuerst, P. G., Harris, B. S., Johnson, K. R., and Burgess, R. W. (2010). A novel null allele of mouse DSCAM survives to adulthood on an inbred C3H background with reduced phenotypic variability. *Genesis* 48, 578–584.

Fuerst, P. G., Koizumi, A., Masland, R. H., and Burgess, R. W. (2008). Neurite arborization and mosaic spacing in the mouse retina require DSCAM. *Nature* 451, 470–474.

Galli-Resta, L., Leone, P., Bottari, D., Ensini, M., Rigosi, E., and Novelli, E. (2008). The genesis of retinal architecture: an emerging role for mechanical interactions? *Prog. Retin. Eye Res.* 27, 260–283.

Gao, F. B., Kohwi, M., Brenman, J. E., Jan, L. Y., and Jan, Y. N. (2000). Control of dendritic field formation in *Drosophila*: the roles of flamingo and competition between homologous neurons. *Neuron* 28, 91–101.

Garrett, A. M., and Burgess, R. W. (2011). Candidate molecular mechanisms for establishing cell identity in the developing retina. *Dev. Neurobiol.* 71, 1258–1272.

Gibson, N. J. (2011). Cell adhesion molecules in context: CAM function depends on the neighborhood. *Cell Adh. Migr.* 5, 48–51.

Grueber, W. B., Jan, L. Y., and Jan, Y. N. (2002). Tiling of the *Drosophila* epidermis by multidendritic sensory neurons. *Development* 129, 2867–2878.

Han, C., Wang, D., Soba, P., Zhu, S., Lin, X., Jan, L. Y., and Jan, Y. N. (2012). Integrins regulate repulsion-mediated dendritic patterning of *Drosophila* sensory neurons by restricting dendrites in a 2D space. *Neuron* 73, 64–78.

Hirano, S., and Takeichi, M. (2012). Cadherins in brain morphogenesis and wiring. *Physiol. Rev.* 92, 597–634.

Hong, K., Hinck, L., Nishiyama, M., Poo, M. M., Tessier-Lavigne, M., and Stein, E. (1999). A ligand-gated association between cytoplasmic domains of UNC5 and DCC family receptors converts netrin-induced growth cone attraction to repulsion. *Cell* 97, 927–941.

Hughes, M. E., Bortnick, R., Tsubouchi, A., Baumer, P., Kondo, M., Uemura, T., and Schmucker, D. (2007). Homophilic Dscam interactions control complex dendrite morphogenesis. *Neuron* 54, 417–427.

Kay, J. N., Chu, M. W., and Sanes, J. R. (2012). MEGF10 and MEGF11 mediate homotypic interactions required for mosaic spacing of retinal neurons. *Nature* 483, 465–469.

Keeley, P. W., and Reese, B. E. (2010). Morphology of dopaminergic amacrine cells in the mouse retina: independence from homotypic interactions. *J. Comp. Neurol.* 518, 1220–1231.

Kim, M. E., Shrestha, B. R., Blazeski, R., Mason, C. A., and Grueber, W. B. (2012). Integrins establish dendrite-substrate relationships that promote dendritic self-avoidance and patterning in *Drosophila* sensory neurons. *Neuron* 73, 79–91.

Kramer, A. P., Goldman, J. R., and Stent, G. S. (1985). Developmental arborization of sensory neurons in the leech *Haementeria ghilianii*. I. Origin of natural variations in the branching pattern. *J. Neurosci.* 5, 759–767.

Kramer, A. P., and Stent, G. S. (1985). Developmental arborization of sensory neurons in the leech *Haementeria ghilianii*. II. Experimentally induced variations in the branching pattern. *J. Neurosci.* 5, 768–775.

Li, W., and Guan, K. L. (2004). The Down syndrome cell adhesion molecule (DSCAM) interacts with and activates Pak. *J. Biol. Chem.* 279, 32824–32831.

Liu, G., Li, W., Wang, L., Kar, A., Guan, K. L., Rao, Y., and Wu, J. Y. (2009). DSCAM functions as a netrin receptor in commissural axon pathfinding. *Proc. Natl. Acad. Sci. U.S.A.* 106, 2951–2956.

Ly, A., Nikolaev, A., Suresh, G., Zheng, Y., Tessier-Lavigne, M., and Stein, E. (2008). DSCAM is a netrin receptor that collaborates with DCC in mediating turning responses to netrin-1. *Cell* 133, 1241–1254.

Matsuoka, R. L., Chivatakarn, O., Badea, T. C., Samuels, I. S., Cahill, H., Katayama, K., Kumar, S. R., Suto, F., Chedotal, A., Peachey, N. S., Nathans, J., Yoshida, Y., Giger, R. J., and Kolodkin, A. L. (2011a). Class 5 transmembrane semaphorins control selective mammalian retinal lamination and function. *Neuron* 71, 460–473.

Matsuoka, R. L., Nguyen-Ba-Charvet, K. T., Parray, A., Badea, T. C., Chedotal, A., and Kolodkin, A. L. (2011b). Transmembrane semaphorin signalling controls laminar stratification in the mammalian retina. *Nature* 470, 259–263.

Matsuoka, R. L., Jiang, Z., Samuels, I. S., Nguyen-Ba-Charvet, K. T., Sun, L. O., Peachey, N. S., Chedotal, A., Yau, K. W., and Kolodkin, A. L. (2012). Guidance-cue control of horizontal cell morphology, lamination, and synapse formation in the mammalian outer retina. *J. Neurosci.* 32, 6859–6868.

Matthews, B. J., and Grueber, W. B. (2011). Dscam1-mediated self-avoidance counters netrin-dependent targeting of dendrites in *Drosophila*. *Curr. Biol.* 21, 1480–1487.

Matthews, B. J., Kim, M. E., Flanagan, J. J., Hattori, D., Clemens, J. C., Zipursky, S. L., and Grueber, W. B. (2007). Dendrite self-avoidance is controlled by Dscam. *Cell* 129, 593–604.

Millard, S. S., Flanagan, J. J., Pappu, K. S., Wu, W., and Zipursky, S. L. (2007). Dscam2 mediates axonal tiling in the *Drosophila* visual system. *Nature* 447, 720–724.

Milner, R., and Campbell, I. L. (2002). The integrin family of cell adhesion molecules has multiple functions within the CNS. *J. Neurosci. Res.* 69, 286–291.

Montague, P. R., and Friedlander, M. J. (1991). Morphogenesis and territorial coverage by isolated mammalian retinal ganglion cells. *J. Neurosci.* 11, 1440–1457.

Neves, G., Zucker, J., Daly, M., and Chess, A. (2004). Stochastic yet biased expression of multiple Dscam splice variants by individual cells. *Nat. Genet.* 36, 240–246.

Palmesino, E., Haddick, P. C., Tessier-Lavigne, M., and Kania, A. (2012). Genetic analysis of DSCAM's role as a netrin-1 receptor in vertebrates. *J. Neurosci.* 32, 411–416.

Rutishauser, U., and Jessell, T. M. (1988). Cell adhesion molecules in vertebrate neural development. *Physiol. Rev.* 68, 819–857.

Schmucker, D., Clemens, J. C., Shu, H., Worby, C. A., Xiao, J., Muda, M., Dixon, J. E., and Zipursky, S. L. (2000). *Drosophila* Dscam is an axon guidance receptor exhibiting extraordinary molecular diversity. *Cell* 101, 671–684.

Soba, P., Zhu, S., Emoto, K., Younger, S., Yang, S. J., Yu, H. H., Lee, T., Jan, L. Y., and Jan, Y. N. (2007). *Drosophila* sensory neurons require Dscam for dendritic self-avoidance and proper dendritic field organization. *Neuron* 54, 403–416.

Stein, E., and Tessier-Lavigne, M. (2001). Hierarchical organization of guidance receptors: silencing of netrin attraction by slit through a Robo/DCC receptor complex. *Science* 291, 1928–1938.

Steinberg, M. S. (2007). Differential adhesion in morphogenesis: a modern view. *Curr. Opin. Genet. Dev.* 17, 281–286.

Wang, J., Zugates, C. T., Liang, I. H., Lee, C. H., and Lee, T. (2002).

Drosophila Dscam is required for divergent segregation of sister branches and suppresses ectopic bifurcation of axons. *Neuron* 33, 559–571.

Wichterle, H., Alvarez-Dolado, M., Erskine, L., and Alvarez-Buylla, A. (2003). Permissive corridor and diffusible gradients direct medial ganglionic eminence cell migration to the neocortex. *Proc. Natl. Acad. Sci. U.S.A.* 100, 727–732.

Wojtowicz, W. M., Flanagan, J. J., Millard, S. S., Zipursky, S. L., and Clemens, J. C. (2004). Alternative splicing of *Drosophila* Dscam generates axon guidance receptors that exhibit isoform-specific homophilic binding. *Cell* 118, 619–633.

Yamagata, M., and Sanes, J. R. (2008). Dscam and Sidekick proteins direct lamina-specific synaptic connections in vertebrate retina. *Nature* 451, 465–469.

Yamagata, M., and Sanes, J. R. (2010). Synaptic localization and function of Sidekick recognition molecules require MAGI scaffolding proteins. *J. Neurosci.* 30, 3579–3588.

Yamakawa, K., Huot, Y. K., Haendelt, M. A., Hubert, R., Chen, X. N., Lyons, G. E., and Korenberg, J. R. (1998). DSCAM: a novel member of the immunoglobulin superfamily maps in a Down syndrome region and is involved in the development of the nervous system. *Hum. Mol. Genet.* 7, 227–237.

Zhan, X. L., Clemens, J. C., Neves, G., Hattori, D., Flanagan, J. J., Hummel, T., Vasconcelos, M. L., Chess, A., and Zipursky, S. L. (2004). Analysis of Dscam diversity in regulating axon guidance in *Drosophila* mushroom bodies. *Neuron* 43, 673–686.

Zhu, Y., Li, H., Zhou, L., Wu, J. Y., and Rao, Y. (1999). Cellular and molecular guidance of GABAergic neuronal migration from an extracortical origin to the neocortex. *Neuron* 23, 473–485.

Conflict of Interest Statement: The authors declare that the research was conducted in the absence of any commercial or financial relationships that could be construed as a potential conflict of interest.

Received: 14 June 2012; paper pending published: 10 July 2012; accepted: 30 July 2012; published online: 17 August 2012.
Citation: Garrett AM, Tadenev ALD and Burgess RW (2012) DSCAMs: restoring balance to developmental forces. Front. Mol. Neurosci. 5:86. doi: 10.3389/fnmol.2012.00086

frontiers in
MOLECULAR NEUROSCIENCE

ORIGINAL RESEARCH ARTICLE
published: 20 June 2012
doi: 10.3389/fnmol.2012.00076

Neural cell adhesion molecule, NCAM, regulates thalamocortical axon pathfinding and the organization of the cortical somatosensory representation in mouse

Lilian Enriquez-Barreto[1,2†], Cecilia Palazzetti[1], Leann H. Brennaman[2], Patricia F. Maness[2*‡] and Alfonso Fairén[1*‡]

[1] *Instituto de Neurociencias, Consejo Superior de Investigaciones Científicas—Universidad Miguel Hernández, San Juan de Alicante, Spain*
[2] *Department of Biochemistry and Biophysics, University of North Carolina School of Medicine, Chapel Hill, NC, USA*

Edited by:
Joshua A. Weiner, The University of Iowa, USA

Reviewed by:
Hansjürgen Volkmer, Universität Tübingen, Germany
Joshua A. Weiner, The University of Iowa, USA

****Correspondence:***
Patricia F. Maness, Department of Biochemistry and Biophysics, University of North Carolina School of Medicine, Genetic Medicine Building, 120 Mason Farm Road, Suite 3010, Campus Box #7260, Chapel Hill, NC 27599-7260, USA. e-mail: patricia_maness@med.unc.edu

Alfonso Fairén, Instituto de Neurociencias, Consejo Superior de Investigaciones Científicas and Universidad Miguel Hernández, Campus de San Juan, Avenida Ramón y Cajal, s/n, 03550 San Juan de Alicante, Spain. e-mail: fairen@umh.es

† Present address:
Centro de Investigación Biomédica de La Rioja, 26006 Logroño, Spain.
‡ Senior co-authors.

To study the potential role of neural cell adhesion molecule (NCAM) in the development of thalamocortical (TC) axon topography, wild type, and NCAM null mutant mice were analyzed for NCAM expression, projection, and targeting of TC afferents within the somatosensory area of the neocortex. Here we report that NCAM and its α-2,8-linked polysialic acid (PSA) are expressed in developing TC axons during projection to the neocortex. Pathfinding of TC axons in wild type and null mutant mice was mapped using anterograde DiI labeling. At embryonic day E16.5, null mutant mice displayed misguided TC axons in the dorsal telencephalon, but not in the ventral telencephalon, an intermediate target that initially sorts TC axons toward correct neocortical areas. During the early postnatal period, rostrolateral TC axons within the internal capsule along the ventral telencephalon adopted distorted trajectories in the ventral telencephalon and failed to reach the neocortex in NCAM null mutant animals. NCAM null mutants showed abnormal segregation of layer IV barrels in a restricted portion of the somatosensory cortex. As shown by Nissl and cytochrome oxidase staining, barrels of the anterolateral barrel subfield (ALBSF) and the most distal barrels of the posteromedial barrel subfield (PMBSF) did not segregate properly in null mutant mice. These results indicate a novel role for NCAM in axonal pathfinding and topographic sorting of TC axons, which may be important for the function of specific territories of sensory representation in the somatosensory cortex.

Keywords: thalamocortical axons, axonal pathfinding, axonal tract tracing, barrel cortex, adhesion and signaling molecules, NCAM

INTRODUCTION

Establishment of topographic connectivity between thalamic nuclei and neocortical areas is fundamental to sensory function, yet the molecular signals that govern thalamocortical (TC) axon guidance and synaptic targeting are incompletely understood. In the developing TC pathway, axons from motor, somatosensory, and visual thalamic nuclei project topographically to primary motor and sensory cortical areas along strict rostro-caudal and medio-lateral axes. Once arriving in the neocortex, TC axons are guided to area- and laminar-specific synaptic targets by poorly defined cortical cues, and then synapses are formed and further refined by activity (reviewed in López-Bendito and Molnár, 2003; Molnár et al., 2012). One emerging concept is that cell adhesion molecules guide proper TC axon guidance. The L1 family cell adhesion molecules, L1, CHL1, and NrCAM, are key determinants of guidance for specific subpopulations of TC axons at the ventral telencephalon and in the cortex (Ohyama et al., 2004; Wiencken-Barger et al., 2004; Wright et al., 2007; Demyanenko et al., 2011a,b). L1 family cell adhesion molecules are structurally related to the neural cell adhesion molecule (NCAM). However, a role for NCAM has not been established in TC axon guidance.

NCAM is a pivotal regulator of axon growth, cell adhesion, and migration. NCAM polymorphisms and altered expression have been associated with schizophrenia, bipolar disorder, and Alzheimer's disease. In addition, the entire extracellular region of NCAM is excessively released by proteolysis as a soluble fragment in affected brain regions in schizophrenia. NCAM null mutant mice lacking the three principal NCAM isoforms (NCAM180, 140, and 120) exhibit impaired learning, working memory, and hippocampal long-term potentiation (LTP). Mice expressing the soluble NCAM extracellular domain demonstrate impaired sensory gating (Pillai-Nair et al., 2005), working memory, and prefrontal cortical LTP (Brennaman et al., 2011). NCAM is also highly glycosylated, and is the principal carrier of α-2,8 polysialic acid (PSA). PSA is highly expressed during embryonic

and early postnatal development and persists at low levels in the adult for plasticity (Bonfanti, 2006; Gascon et al., 2007; Rutishauser, 2008). PSA decreases NCAM–NCAM homophilic and heterophilic adhesion (Johnson et al., 2005). Mice lacking the polysialyltransferases that attach PSA to NCAM, ST8SiaII or ST8SiaIV, have decreased social interaction and motivation, impaired fear conditioning, increased exploration and aggression and impaired hippocampal LTP (Angata et al., 2004; Calandreau et al., 2010). Similar to NCAM, changes in PSA expression or polymorphisms in ST8SiaII have been observed in schizophrenia (Barbeau et al., 1995; Arai et al., 2006; Tao et al., 2007; Isomura et al., 2011), bipolar disorder (Lee et al., 2011), and autism (Anney et al., 2010). Interestingly, mice lacking PSA but not NCAM exhibit TC pathfinding defects, such that TC axons defasciculate and fail to enter the ventral telencephalon or cortex (Schiff et al., 2011). Additional deletion of NCAM partially restored TC axon guidance, suggesting that NCAM may have distinct roles from PSA in this trajectory.

Here, we report that NCAM null mutant mice exhibited aberrant TC axon guidance and an altered somatosensory map. However, projection through the ventral telencephalon was normal prenatally and demonstrates selective roles for NCAM vs. PSA in TC axon guidance.

MATERIALS AND METHODS

MICE

All procedures were conducted in accordance with the National Institutes of Health and European Union guidelines and with the approval of the institutional animal care and use committees of University of North Carolina and the Instituto de Neurociencias. Homozygous-null NCAM mutant mice (C57Bl/6 background) were provided by Dr. H. Cremer (Developmental Biology Institute of Marseille Luminy, Marseille, France). NCAM deficient (KO) mice and wild type (WT) littermates were generated by crossing heterozygotes. Midday of the vaginal plug was considered as E0.5, and postnatal day 0 (P0) as day of birth.

IMMUNOHISTOCHEMISTRY

Timed-pregnant dams were anaesthetized by intraperitoneal injection of ketamine (110 mg/kg) and xylazine (10 mg/kg) and the embryos were extracted by caesarean section. Embryos (E13.5, E14.5, E16.5, and E18.5) were fixed in 4% paraformaldehyde in PBS. Postnatal (P0, P2, P4, and P6) and adult (P30) mice were anaesthetized similarly and were fixed by intracardiac perfusion. Vibratome sections, 100 μm-thick, were blocked in 4% bovine serum albumin (BSA), 3% NHS, 0.2% Triton X-100 in PBS at room temperature for 1 h and incubated with primary antibodies diluted in blocking solution at room temperature overnight. Primary antibodies were: rat monoclonal antibody P61 to an intracellular epitope of the 140/180 isoforms of NCAM (gift of Drs. C. Goridis and H. Cremer, 1:50), mouse monoclonal antibodies 12E3 to α2-8 linked neuraminic acid $(\text{NeuAc-}\alpha2\text{-}8)_n$ with $n = 5$ (oligo/polysialic acid; gift from Dr. T. Seki; 1:1000); rabbit polyclonal antibodies to L1 (gift from Dr. F. G. Rathjen, 1:1000) and serotonin (DiaSorin, Stillwater, IL, USA; 1:2000). The specificity of these antibodies in mouse forebrain from E13.5 through adulthood has been demonstrated (Gennarini et al., 1984; Rathjen and Schachner, 1984; Seki and Arai, 1991; Nadanaka et al., 2001). Secondary antibodies were as follows: ImmunoPure biotinylated goat anti mouse IgM (Pierce, Rockford, IL, USA; 1:100); Cy3 conjugated streptavidin (Jackson ImmunoResearch, West Grove, PA, USA; 1:500); AlexaFluor 488 anti-mouse IgM, AlexaFluor 555 goat anti rat IgG, AlexaFluor 546 anti-rabbit IgG (Molecular Probes–Invitrogen; 1:500). Sections were mounted on microscope slides and covered with AF2 (Citifluor Ltd., London, UK) or Vectashield (Vector Labs) mounting media.

DiI INJECTIONS AND ANALYSIS

Fixed brains of E14.5, E16.5, E18.5, P0, P2, and P4 wild type and NCAM-deficient mice were vibratome sectioned from the caudal end of the cerebrum. Once the dorsal thalamus was reached, the brains were removed from the vibratome and a crystal of DiI (Molecular Probes–Invitrogen) was inserted at mid rostrocaudal levels of the dorsal thalamus, comprising the primordium of the ventrobasal complex, to anterogradely label TC axons that project to the somatosensory cortex.

Mice remained in 0.05 % azide in PBS for 3–4 weeks. Brains were then sectioned at 100 μm in a vertical plane oriented 45° with respect to the coronal plane, in order to recover the maximum number of TC axons in each single section (Agmon and Connors, 1991; see schematics in **Figure 4**). For combined DiI—immunofluorescence staining, selected sections from DiI injected brains were processed without detergents. Sections were mounted onto glass slides with Citifluor.

The geometry of individual TC axons in the early postnatal cortex was studied in P2 and P4 wild type and null-mutant brains implanted with small DiI crystals in the dorsal thalamus. DiI labeled axons in obliquely oriented sections were imaged in a confocal microscope traced using Neurolucida 7.0 and analyzed using NeuroExplorer software (MicroBrightField, Inc.). For the analysis we considered the following parameters: number of nodes, branch order, and planar angle of bifurcations. We used the unpaired Student's t-test with statistical significance set at $p < 0.05$.

NISSL STAINING AND CYTOCHROME OXIDASE HISTOCHEMISTRY

For Nissl staining, vibratome sections from adult mouse brains were mounted on gelatin-coated slides and dried overnight. Sections were defatted in an ascending series of ethanol and xylene, rehydrated again and stained in 1% aqueous cresyl violet.

For cytochrome oxidase histochemistry, adult wild type and null-mutant mice were perfusion fixed with 4% paraformaldehyde, 0.2 glutaraldehyde and 4% glucose in 0.1 phosphate buffer, stored in fixative overnight and sectioned at 100 μm in the coronal plane or in a plane parallel to the pial surface in flattened tissue blocks. Sections were processed to reveal cytochrome oxidase activity as described (Kageyama and Wong-Riley, 1982).

Sections were analyzed in a Leica DM5000 epifluorescence microscope and in confocal microscopes Leica TCS-SL and Olympus FV500.

RESULTS

EXPRESSION OF PSA-NCAM AND NCAM IN THALAMOCORTICAL AXONS

We assessed the presence of PSA and NCAM in thalamocortical (TC) axons during prenatal development using axonal tract-tracing and immunohistochemistry. As a first step to verify that TCAs expressed NCAM and its polysialilated form PSA-NCAM, small crystals of DiI were inserted in the dorsal thalamus of E14.5 wild type mice. DiI is a lipophilic tracer that diffuses within the lipid bilayer of the plasma membrane and accurately labels axonal projections in brain tissues fixed with aldehydes (Godement et al., 1987). DiI-labeled TC axons were immunofluorescently labeled with antibodies to the cytoplasmic domain of transmembrane NCAM isoforms (140 and 180 kDa) and PSA. DiI labeled TC axons displayed both NCAM and PSA (**Figures 1A,B**). DiI was excited with a HeNe 543 nm laser, while an Ar/Kr 488 nm laser excited AlexaFluor 488 used to detect NCAM and PSA immunoreactivities. Comparison of **Figures 1A',A",B',B"** shows that no bleeding occurred between the two detection channels in the confocal microscope, thus confirming the localization of NCAM or PSA detection signals in DiI-labeled TC axons.

Next, wild type and NCAM null mutant E13.5 and E15.5 mice (Cremer et al., 1994) were immunolabeled with antibodies to NCAM or PSA along with L1, which labels TC axons (Chung et al., 1991; Fukuda et al., 1997; Demyanenko et al., 2011b). L1-immunoreactive axons expressed transmembrane NCAM isoforms, as detected with a monoclonal antibody (mAb P61) that recognizes the cytoplasmic domain of both NCAM140 and NCAM180 (**Figures 2A–A"** and **3A–A"**; Gennarini et al., 1984), but not NCAM120. NCAM immunoreactivity was absent in NCAM null mutant mice (**Figures 2B–B"** and **3B–B"**), demonstrating the specificity of this antibody. Using monoclonal antibody 12E3 that reacts with small chains of PSA (Seki and Arai, 1991; Nadanaka et al., 2001), we found that L1-expressing TC axons displayed immunoreactivity for PSA of low sialic acid content in wild type mice (**Figures 2C–C"**

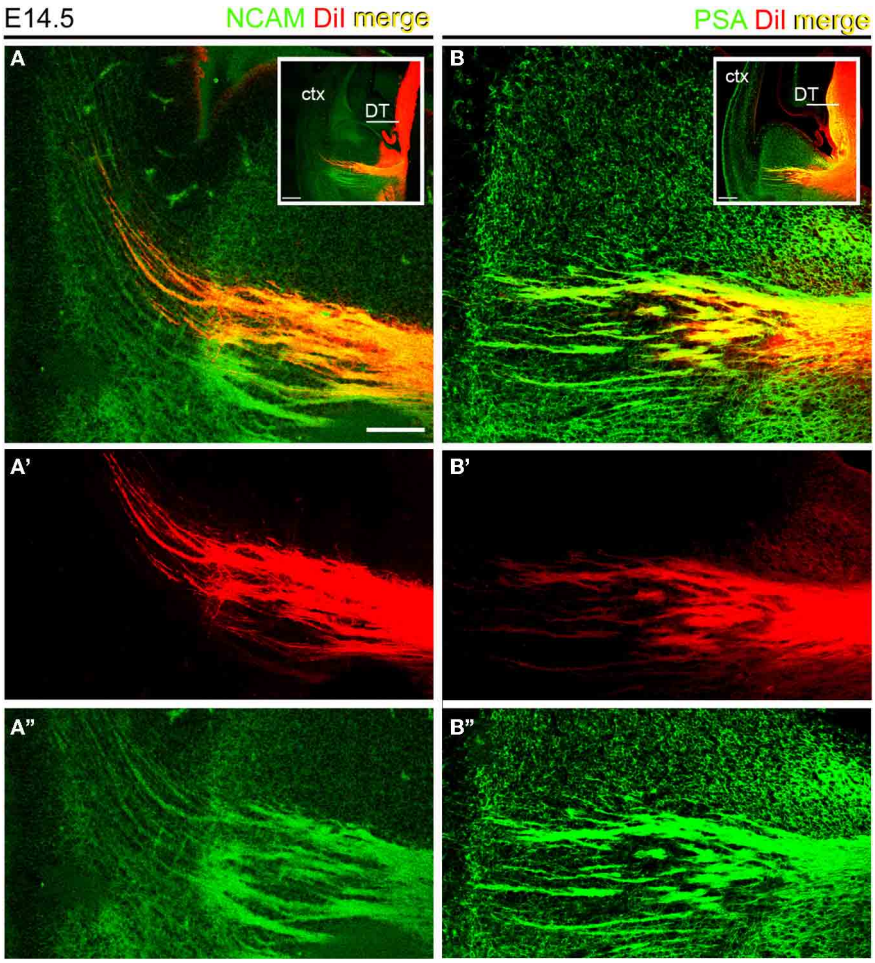

FIGURE 1 | Thalamocortical axons expressed NCAM and PSA at E14.5. Sections containing DiI-labeled TC axons were labeled with antibodies to the intracellular domains of large NCAM isoforms **(A)** and PSA **(B)**. Insets show the regions analyzed. **A'**, **A"** and **B** and **B"** show the detection channels separately. Note that the red signal of DiI labeled axons in the ventral telencephalon coincided in all cases with the green signal corresponding to NCAM **(A–A")** or PSA **(B–B")** immunoreactivities. Maximum projections of confocal microscope stacks. DT, dorsal thalamus; ctx, cortex. Bars in **A**, **B**, 200 μm; insets, 100 μm.

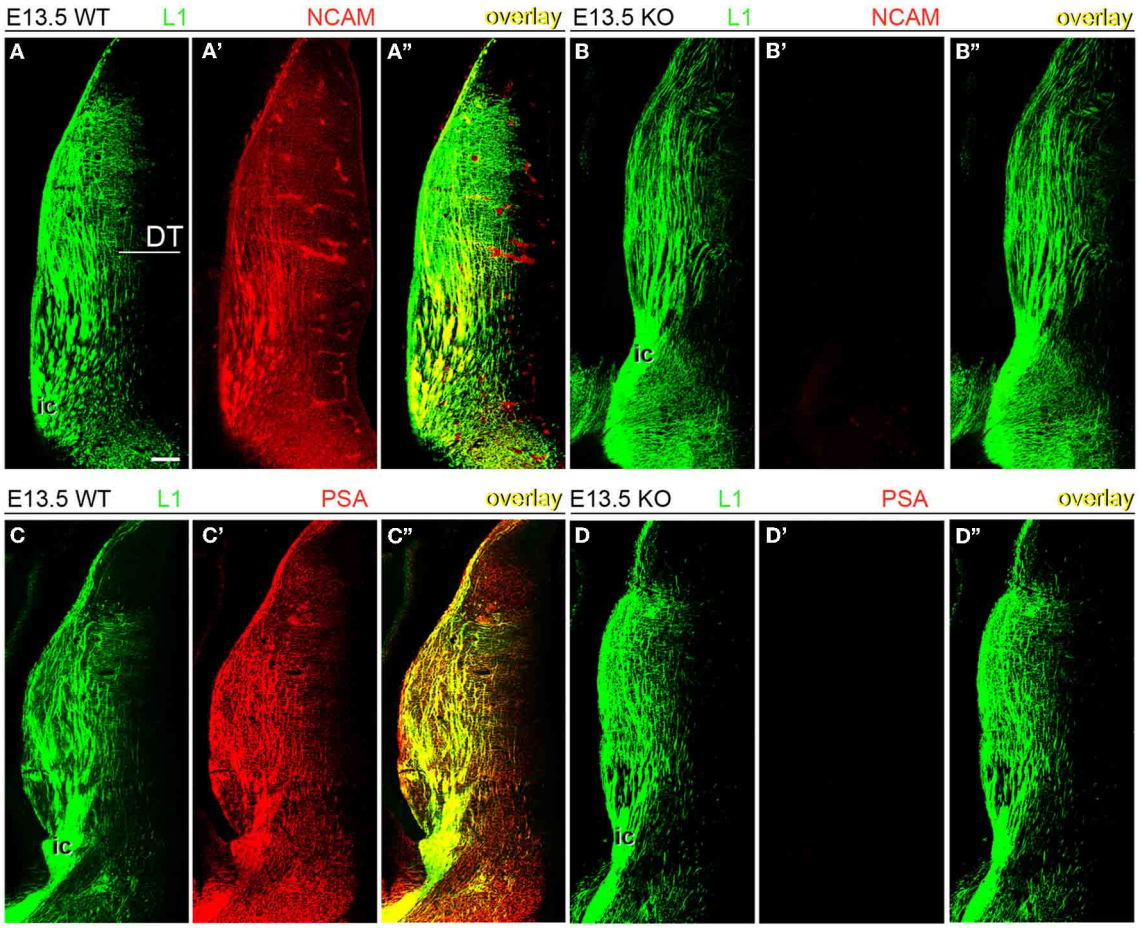

FIGURE 2 | Expression of NCAM and oligopolysialylated NCAM in thalamocortical axons in the dorsal thalamus at E13.5. (A–A") TC axons co-labeled by L1 and NCAM antibodies in wild type mice. **(B–B")** In NCAM null mutant mice, NCAM immunostaining was absent, confirming the specificity of monoclonal antibody P61 in our material. **(C–C",D–D")** PSA immunoreactivity was present in L1-immunoreactive axons in the dorsal thalamus of wild type mice **(C)** but absent in NCAM null mice **(D)**, suggesting that PSA is linked to NCAM in these axons. L1-immunoreactive TC axons formed descending fascicles that converged into the caudal limb of the internal capsule (ic) leading through the ventral telencephalon to the developing cortex. Single confocal optical sections. DT, dorsal thalamus; ic, internal capsule. Bar (in **A**): 100 μm.

and **3C–C"**). In NCAM null mutant mice, 12E3 immunoreactivity was abolished (**Figures 2D–D"** and **3D–D"**), suggesting that NCAM was the only carrier of PSA in TC axons at this stage (Seki and Arai, 1993; Cremer et al., 1997; Dityatev et al., 2004). NCAM and PSA exhibited similar patterns of immunoreactivity. PSA showed more extensive labeling than NCAM, which may be due to antibody sensitivity or PSA linkage to NCAM120, secreted NCAM, or other splice variants not recognized by our NCAM antibody. However, very little NCAM120 is present at this stage (Edelman and Chuong, 1982; Brennaman and Maness, 2008).

THE GENETIC DELETION OF ALL THREE PRINCIPAL NCAM ISOFORMS CAUSES TOPOGRAPHICALLY LOCALIZED DEFECTS IN THALAMOCORTICAL AXONAL GUIDANCE

In the mouse, the TC axonal projection courses through the ventral telencephalon within a narrow vertical parallelepiped oriented at 45° from the midsagittal plane (Agmon and Connors, 1991). Thus, to further study possible defects in axonal fasciculation and pathfinding in the TC axonal pathway of NCAM null mutant mice, we examined the anatomical distributions of DiI labeled TC axons in tissue sections oriented to include the maximum rostrolateral-to-caudomedial extent of this axonal projection. The sections analyzed were controlled for similar injection size and location to minimize artifacts. In these sections (**Figures 4A,B**, see inset), the laterally located axons were rostral and medial axons were caudal in comparative terms.

The analysis of wild type and null mutant mouse embryos during the prenatal period revealed no major changes in the anatomical trajectory of TC fibers along their subpallial course through the ventral telencephalon. At E16.5 (**Figure 4**), the TC axonal projection along the subpallium was sparser in null mutant mice as compared to wild type mice (**Figures 4A,B**), and fewer TC axons were detected in the cortical subplate impinging into the lower levels of the cortical plate (**Figures 4C,D**).

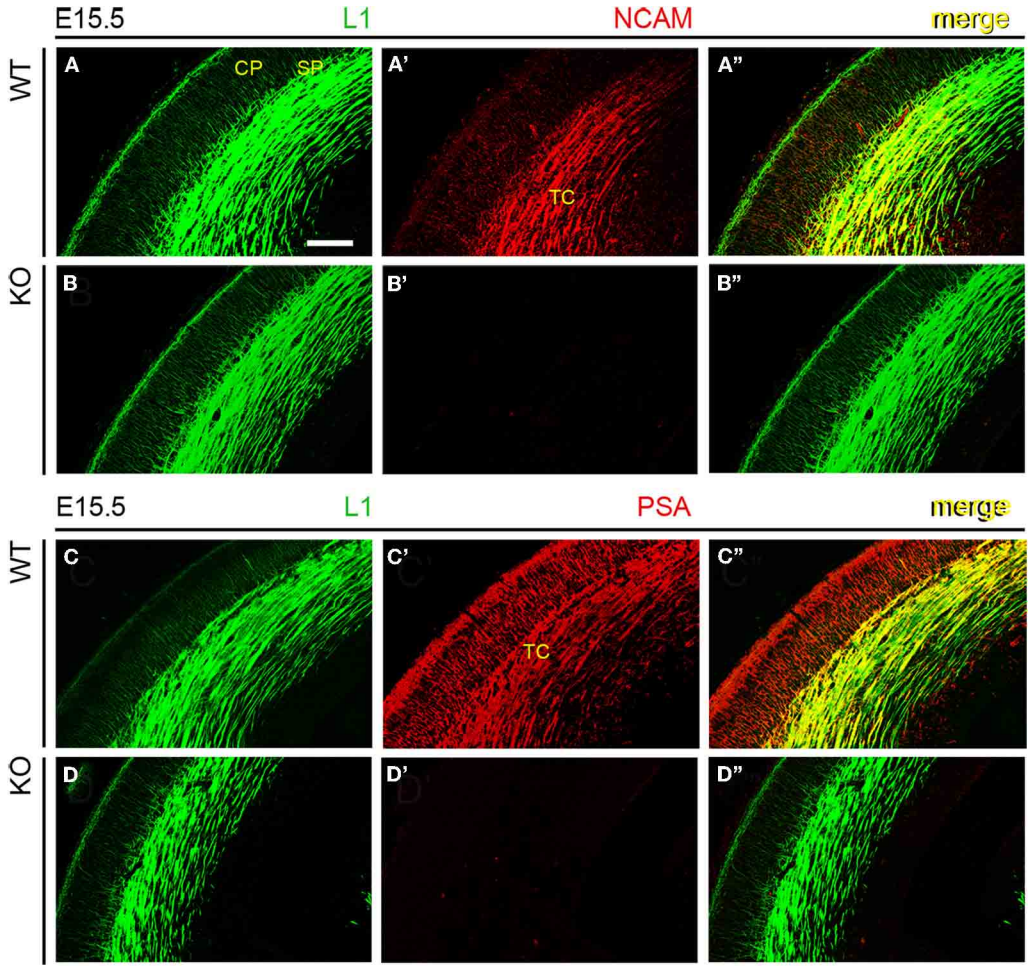

FIGURE 3 | NCAM and PSA expression in thalamocortical axons. An antibody to adhesion molecule L1 labeled TC axons approaching the subplate in E15.5 mouse embryos, irrespective of phenotype. **(A–A")** Monoclonal antibody P61, directed against an intracellular epitope of NCAM, showed the co-expression of L1 and NCAM in TC axons. **(B–B")** Absence of NCAM immunoreactivity in NCAM null mutant mice. **(C–C")** Monoclonal antibody 12E3 recognized oligopolysialylated chains of PSA in L1-immunoreactive TC axons. **(D–D")** Absence of PSA-NCAM immunoreactivity in NCAM null mutant mice. The absence of NCAM **(B")** and PSA **(D")** immunoreactivities in null mutant mice suggested that, under our experimental conditions, NCAM is the sole carrier of polysialic acid in the developing cortex. Single confocal optical sections. CP, cortical plate; SP, subplate; TC, thalamocortical axons. Bar: 200 μm.

DEFECTS IN TC AXONAL GUIDANCE THROUGH THE VENTRAL TELENCEPHALON IN EARLY POSTNATAL NULL MUTANT MICE

NCAM removal caused a more visible phenotype of altered guidance of TC axons during early postnatal development. As TC axons course through the ventral telencephalon, their characteristic fan-like distribution as seen in the obliquely oriented vertical sections (**Figure 5A**) was altered in early postnatal NCAM null mice with respect to wild type animals. In null mutant P0 mice, TC axons navigated in a disorderly manner and, unlike in wild type mice, gave rise to local axon collaterals in the ventral telencephalon (**Figures 5A,B**). In addition, NCAM null TC axons in the rostrolateral tier of the internal capsule became disoriented within the ventral telencephalon, bent abruptly at right angles (**Figure 5B**, arrows), and failed to reach the cortex unlike wild type mice (**Figure 5A**). The packing density of TC axons in the cortex in null mutant mice (P0) was also visibly decreased, consistent with the observed disorientation (**Figures 5C,D**).

The localized anatomical changes in the subpallial course of TC axons persisted by P2 (**Figures 5E,F**), at the time TC axons start to achieve their final distribution within the cerebral cortex, and cortical layers start their cytoarchitectonic differentiation (Agmon et al., 1993; López-Bendito and Molnár, 2003). Thus, in P2 null mutant mice, the most medially located axons seemed unchanged. On the contrary, TC axons located in the rostrolateral sector of the internal capsule dispersed laterally at difference to wild type axons (**Figures 5C,D**).

DiI crystals were inserted into the middle third of the dorsal thalamus where the ventrobasal complex of the thalamus that projects to the somatosensory cortex will develop, and

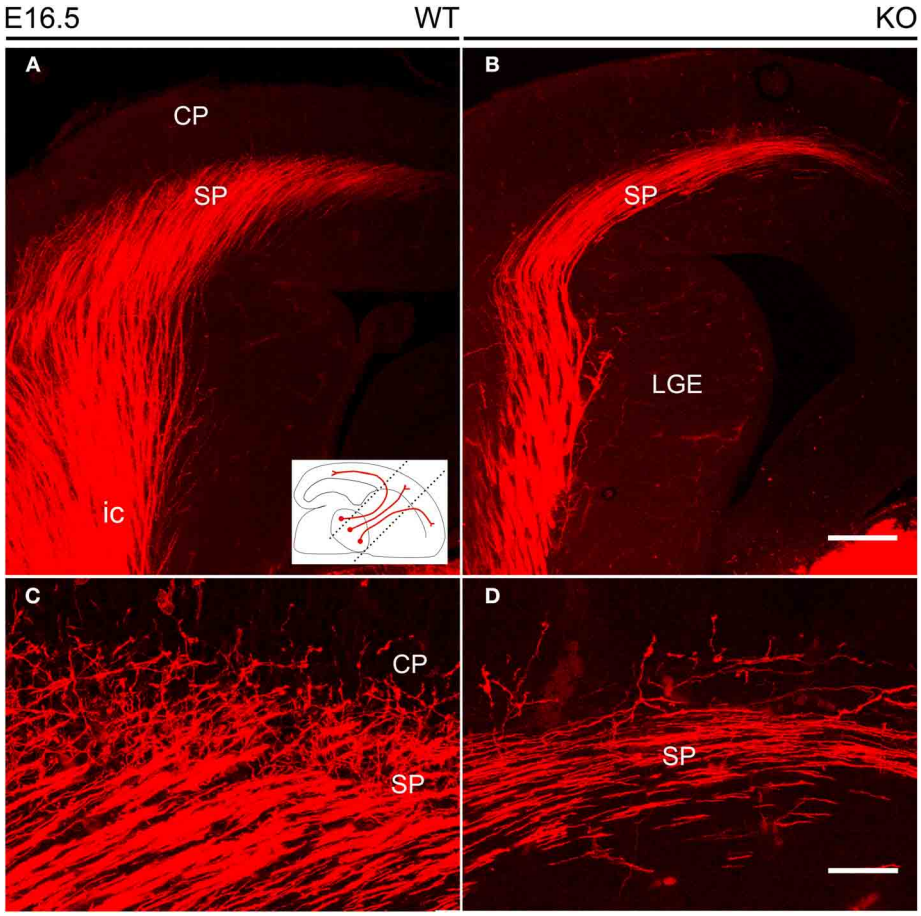

FIGURE 4 | Thalamocortical axons labeled by DiI inserted into the dorsal thalamus at E16.5. (A,B) DiI-labeled TC axons followed the internal capsule in the ventral forebrain to reach the subplate. The inset shows the orientation of the vertical slices at 45° from the midsagittal plane used to image DiI labeling. In these sections, TC axons in the lateral part of the internal capsule are more anterior than those located medially. **(C,D)** TC axons started their entry into the cortical plate, but these axonal arborizations were visibly more profuse in wild type **(C)** than in NCAM null mice **(D)**. Images are maximum projections of confocal optical sections, covering total thicknesses of 29 μm **(A,B)** or 11 μm **(C,D)**. CP, cortical plate; ic, internal capsule; LGE, lateral ganglionic eminence; SP, subplate. Bars: 200 μm **(A,B)**; 50 μm **(C,D)**.

avoided the lateral geniculate primordium located more caudally. Thus, the somatosensory cortex was the probable cortical area of destination of the DiI labeled TC axons. This prompted the question as to whether localized changes in the TC axons as they course through the ventral telencephalon during the early postnatal period might result in alterations in the distribution of TC axons within the cerebral cortex and localized alterations in the cytoarchitectonic organization of this target cortical area.

INTRACORTICAL ARBORIZATIONS OF THALAMOCORTICAL AXONS IN NCAM NULL MUTANT MICE

NCAM null mutant mice consistently showed reduced packing density of DiI labeled TC axons in the developing cortex (**Figures 6A,B**) in spite of the variability of DiI labeling. However, it was unclear whether this was accompanied by changes in the TC axon arborizations within the postnatal cerebral cortex. Prompted by the finding by Yamamoto et al. (2000) that PSA removal alters the orientation and layer targeting of TC axons in slice culture experiments, we analyzed whether NCAM deletion likewise causes alterations in the branching patterns of preterminal TC axons labeled anterogradely with DiI. We studied two different ages corresponding to the first week after birth when segregation into barrels occurs, at P2 (WT, $n = 6$ hemispheres; KO, $n = 6$ hemispheres) and at P4 (WT, $n = 7$ hemispheres; KO, $n = 10$ hemispheres).

For the analysis of the geometry of individual TC axons in the cortex, we considered the following parameters: number of nodes, branch order, and planar angle of preterminal TC axons. The number of nodes and the branch order give idea of the complexity of the axonal trees. The Student's *t*-test detected no differences between wild type and null mutant mice. At P2 (**Figure 6C**), the values for number of nodes were 3.21 ± 0.22 per axon for wild type mice vs. 2.79 ± 0.21 for null mutant mice (mean ± s.e.m.), $p = 0.09$. At P4 (**Figure 6D**), values were 3.04 ± 0.25 for WT mice vs. 3.15 ± 0.24 for null mutant mice, $p = 0.38$ (**Figure 6D**). Branch order was also unchanged: at P2—WT, 3.96 ± 0.19 vs. null mutant, 3.54 ± 0.18 (**Figure 6C**),

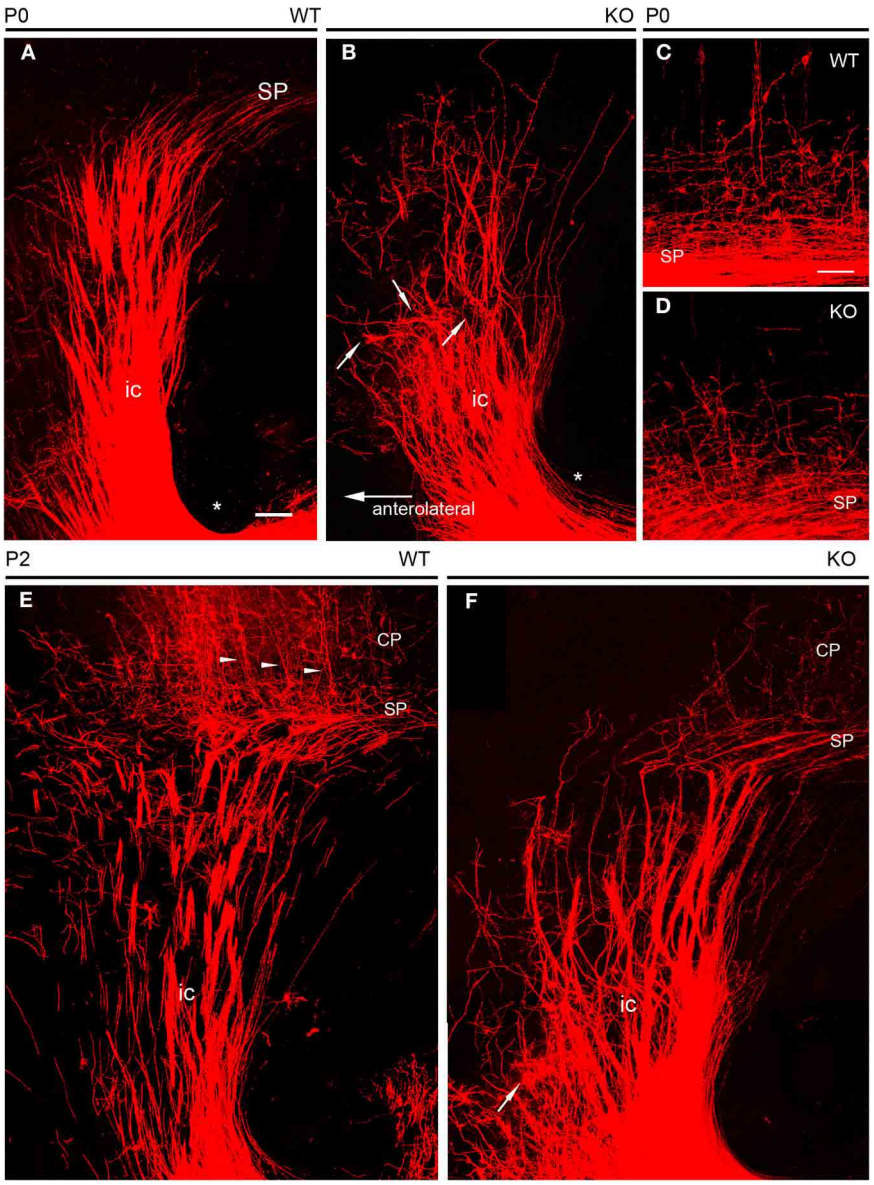

FIGURE 5 | DiI tracing of thalamocortical fibers at early postnatal ages. **(A,B)** At P0, thick fascicles of DiI-labeled TC axons traversed the ventral telencephalon in their way to the developing cortex. The course of TC axons along the internal capsule was straight in wild type embryos **(A)**, where few axon collaterals dispersed laterally. In null mutant mice **(B)**, TC axon fascicles in the lateral parts of the pathway bent abruptly, failing to reach the cortex; arrows point at selected examples of dispersed axon fascicles. Axons at more medial locations, although less dispersed, navigated in a disorderly manner, giving rise to abundant axon collaterals in the ventral telencephalon. Asterisks in **A** and **B** mark the inferior level of the internal capsule in the ventral telencephalon. **(C,D)** TC axons entering the lower tier of the cortical plate in wild type and knockout mice at P0. Null mutant mice showed less densely packed axonal arborizations than wild type mice. **(E,F)** At P2, compared to wild type mice **(C)**, TC axons in the ventral telencephalon of null mutant mice **(D)** dispersed laterally; one extreme example is marked with an arrow. Null mutant mice showed sparser TC axons in the cortex than wild type mice. Arrowheads in **E** point to retrogradely DiI labeled neurons in the cortical plate. The subplate was identified as the level TC axons bend medially to adopt trajectories parallel to the palial surface. Maximum confocal projections. Bar: 100 μm.

$p = 0.06$; at P4—WT, 3.74 ± 0.21 vs. null mutant, 3.83 ± 0.18, $p = 0.38$ (**Figure 6D**) The *planar angle* is that formed in the section plane by the two segments uniting an n order node with the next order (n +1) node in an arborization, and measures a characteristic of the branching pattern of the axons disregarding the axonal trajectory. Planar angles were also unchanged at P2 and P4: P2—WT, 40.97° ± 1.17 vs. null mutant, 40.69° ± 1.45, $p = 0.44$ (**Figure 6C**); P4—WT, 41.22° ± 1.55 vs. null mutant, 41.48° ± 1.31, $p = 0.45$ (**Figure 6D**). Together, these results indicated that, contrary to PSA removal, NCAM removal does not alter the branching patterns of TC axons in the cortex.

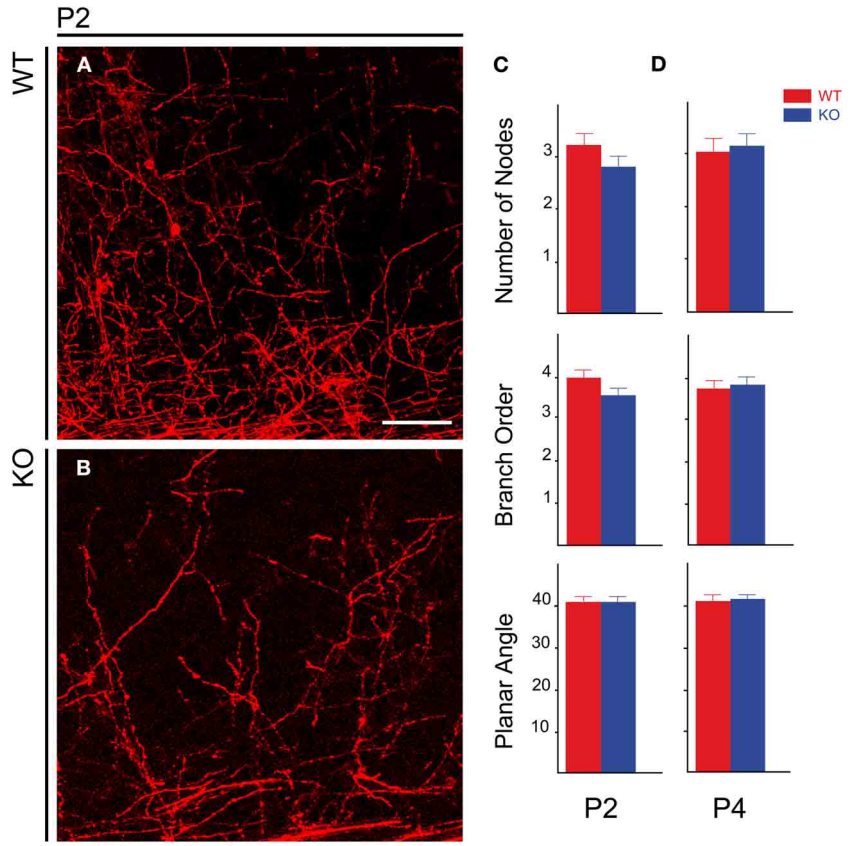

FIGURE 6 | Distribution of TC axons in the lower layers of the developing cerebral cortex in postnatal animals. (A,B) Distribution of TC preterminal axons in the cortical plate of P2 wild type **(A)** and mutant **(B)** mice. **(C,D)** Bar graphs showing the absence of modifications in the geometry of TC axons within the cortex in null mutant mice at P2 **(C)** and P4 **(D)**. Bar: 50 μm.

THE GENETIC DELETION OF NCAM ALTERS THE SOMATOSENSORY MAP IN THE CEREBRAL CORTEX

Layer IV of the rodent somatosensory cortex contains multicellular units called barrels so arranged as to form a visible map of the sensory periphery (Woolsey and Van der Loos, 1970; Van der Loos and Woolsey, 1973). This distinctive feature makes the somatosensory system a remarkable model to study molecular mechanisms implicated in the topographic sorting of TC axons to neocortical areas. We focused on the anatomical representation of the sensory map in the somatosensory cortex, whose refinement along development requires the correct targeting of TC axons.

We first analyzed in early postnatal mice the distribution of TC axons within layer IV of the somatosensory cortex (**Figure 7**). During the first postnatal week, thalamic fibers navigate through layers V and VI and invade layer IV, which is incompletely differentiated. TC axons assume their characteristic periphery-related pattern and impose a barrel arrangement onto layer IV (Agmon et al., 1993; López-Bendito and Molnár, 2003). Developing TC axons ascend to layer IV where they form spatially periodic clusters of terminations of gradually increasing complexity that correspond to the barrels, rather than branching profusely within lower cortical layers with subsequent retraction (Agmon et al., 1993, 1995). To see how TC axons segregate in NCAM null mice, we analyzed the pattern of distribution of thalamic terminals by means of serotonin (5-HT) immunohistochemistry. Thalamic relay neurons transiently express the plasma 5-HT transporter (5-HTT) and the vesicular monoamine transporter type 2 (VMAT2), allowing 5-HT to concentrate in the TC axons and axon terminals during early postnatal life (Lebrand et al., 1996). 5-HT immunostaining was continuous in the forming layer IV of P2 mice, but at P6 it suggested a discrete pattern in wild type mice, but not NCAM null mice (**Figure 7**).

Nissl staining of coronal sections of adult brains revealed mild disruptions of the somatosensory map in NCAM null mutant mice (**Figures 8A–D**). As compared to the well-defined barrels of wild type animals ($n = 5$) due to the presence of distinct barrel septa, null mutant mice ($n = 5$) showed indistinct barrels with no discernible septa between them (**Figures 8A,C**) and the Nissl stain revealed a microlaminar deposition of cells within layer IV (**Figures 8C,D**). These changes occurred through all antero-posterior levels of the somatosensory area of the cortex. Layer IV of the somatosensory cortex in null mutant mice remained prominent, suggesting reorganization of TC axons (**Figures 8A–B**). Cytochrome oxidase histochemistry (Wong-Riley and Welt, 1980) in coronal sections highlighted individual barrels in null mutant mice ($n = 3$), though the staining was

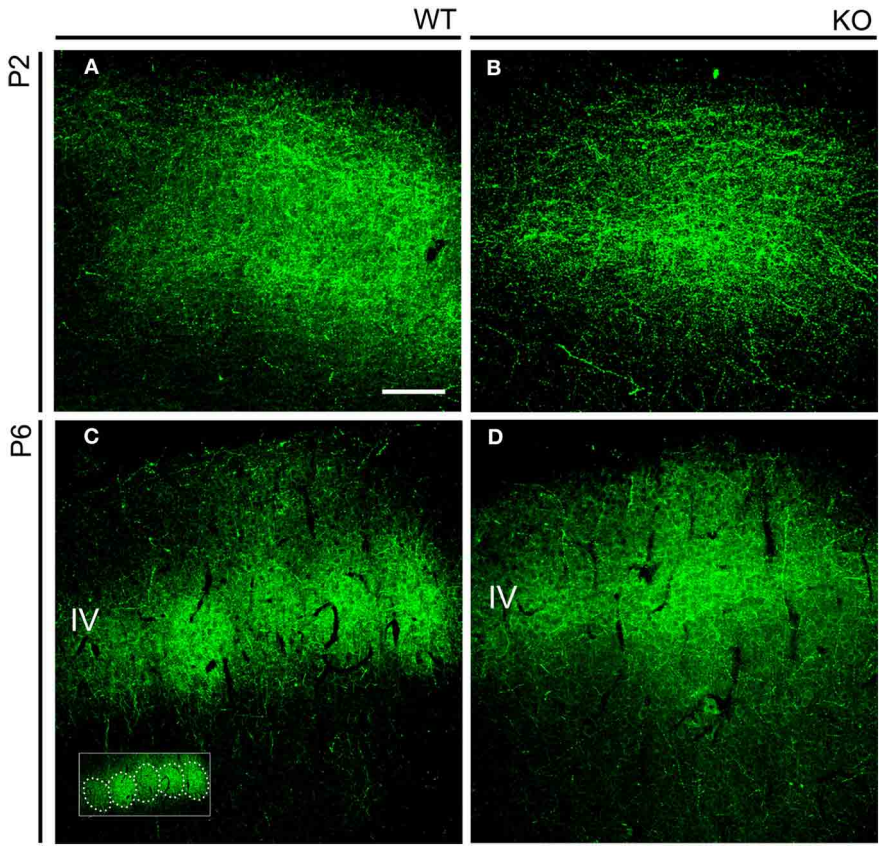

FIGURE 7 | Serotonin immunohistochemistry in the early postnatal somatosensory cortex. (A,B). Serotonin immunostaining highlighted the distribution of TC axons in the developing cortex. At P2, at a time barrel units are not yet formed, immunostaining revealed a uniform distribution of axons in both wild type and mutant mice. **(C,D)**. At P6, serotonin immunoreactivity clustered in layer IV in a manner reminiscent of barrels (highlighted in the inset) in wild type animals **(C)**. In P6 NCAM null mutant mice, TC axons also localized to layer IV but showed a continuous distribution **(D)**. Confocal optical sections. IV, cortical layer IV. Bar: 100 μm.

fainter in null mice as compared to their wild type ($n = 3$) littermates, as shown for rostral barrels (**Figures 8E,F**). This was taken as an indication that the overall organization of the somatosensory cortex was preserved in null mutant mice, although the refined cytoarchitectonic organization of the barrels was somewhat altered, indicating that layer IV neurons could be abnormally deployed in the barrels and septa.

Then, we analyzed the somatosensory map in tangential sections of the cortex for the occurrence of topographic changes in adult NCAM null mutants. The posteromedial barrel subfield (PMBSF) contains a group of large, ovoid barrels whose topographic distribution is homeomorphic to that of the largest vibrissa follicles of the animal's snout. The anterolateral barrel subfield (ALBSF) contains similar yet smaller barrels, which correspond to the smallest and less prominent whiskers of the animal's face. As shown in tangential reconstructions of Nissl staining (**Figures 9A,B**), the barrel septa were less prominent in null mutant mice ($n = 4$) than in wild type mice ($n = 4$) and were indiscernible at rostral positions within the PMBSF of null mutant mice (**Figure 9B**). Cytochrome oxidase staining delineated distinct barrels in both genotypes (wild type, $n = 4$; null mutant, $n = 6$). However, in null mutant mice, only the most caudomedial part of the PMBSF that contains the straddler barrels (α–δ) and the first large barrels of rows A–E, showed such a clear delineation and their overall topography seemed unchanged (**Figures 9C,D**). The other barrels in the PMBSF and in the entire ALBSF were profoundly altered in null mutant mice, and were virtually indistinct. Both Nissl staining and cytochrome oxidase histochemistry unveiled a prominent phenotype trait, the disruption of barrels in the ALBSF and of the most rostral barrels in the PMBSF. These alterations in the barrel field of the somatosensory cortex suggested that the regional alteration of NCAM null TC axons might contribute to disrupted topographic mapping, and that NCAM may be required for the topographical anatomical distribution of TC axons in the somatosensory cortex.

DISCUSSION

We have shown here that NCAM participates in the guidance of TC axons to the somatosensory cortex, and provide the first evidence for a role for NCAM in TC topography. PSA and NCAM were expressed on developing TC axons from E13.5 to E15.5. In embryonic stages, NCAM null TC axons traversed the ventral telencephalon normally, but a contingent of axons appeared to ectopically branch in the ventral telencephalon and misproject

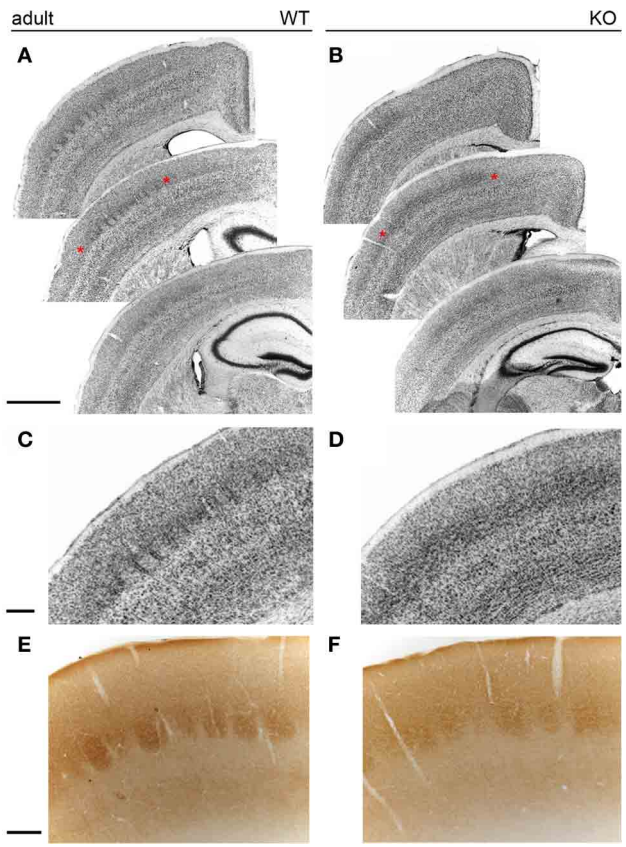

FIGURE 8 | The barrelfield in the adult somatosensory cortex. In wild type animals **(A)**, Nissl staining revealed individual cytoarchitectonic units (barrels) in layer IV of the somatosensory cortex. In contrast, Nissl staining of NCAM mutant mice **(B)** showed less distinct barrels. **(C,D)** Enlarged views of the areas marked with asterisks in **(A,B)**. While septa were evident in wild type animals **(C)**, null mutant mice **(D)** lacked well-delineated septa and layer IV cells formed horizontally placed microlaminae in knockout mice. **(E,F)** Cytochrome oxidase histochemistry of coronal sections revealed no obvious changes between wild type and null mutant mice. Bars: **A**, **B**, 1 mm (in **A**); **C**, **D**, 200 μm (in **C**); **E**, **F**, 200 μm (in **E**).

into the dorsal telencephalon in early postnatal stages. In anterograde DiI labeling at E16.5, NCAM null mutant mice appeared to have fewer axons projecting from the middle third of the dorsal thalamus which forms the ventrobasal complex and sends axons to the somatosensory cortex. The rostral third of the thalamus will give rise to ventroanterior and ventrolateral nuclei which project to the motor cortex, while the caudal third of the thalamus will give rise to the dorsal lateral geniculate nucleus that projects to the visual cortex. Accordingly, rostral TC axons in the internal capsule failed to appropriately target the dorsal telencephalon. Together, these results suggest that TC axon guidance to the motor and somatosensory cortices may be altered in NCAM null mice. In accordance with these findings, NCAM null mutant mice displayed aberrant barrel architecture at P6 and in adult somatosensory cortex.

Our findings are distinct from those observed with PSA-deficient mice. TC axons from mice lacking both polysialyltransferases (ST8SiaII and ST8SiaIV) failed to enter the ventral telencephalon at E15.5, and instead terminated in the reticular thalamic nucleus (Weinhold et al., 2005; Schiff et al., 2011). The consequence of PSA removal is increased and precocious NCAM-dependent adhesion (Hildebrandt et al., 2007). The prominent role of PSA elimination as the origin of this phenotype contrasted with the absence of major phenotype differences in the TC axonal projection in triple knockout animals for ST8SiaII, ST8SiaIV, and NCAM (Schiff et al., 2011), suggesting that additional NCAM removal can restore normal TC axon trajectory in the ventral telencephalon. NCAM null TC axons enter the ventral telencephalon and sort normally at embryonic stages. However, our study also shows that NCAM null TC axons showed pathfinding defects in the ventral telencephalon during the early postnatal life, at the time TC axons establish their connections in the cerebral cortex, and also regional defects in the establishment of the somatosensory map in the cerebral cortex that are described here for the first time. Thus, our new results on a postnatal role for NCAM in TC axon projections complement the role of PSA, by identifying specific roles for NCAM in this trajectory.

The role of other members of the immunoglobulin superfamily of neural cell adhesion molecules in TC axonal pathfinding has been studied intensively in the last few years. L1 family cell adhesion molecules also show shifts of contingents of rostral thalamic axons to caudal regions in the developing and final topographic map. Close homolog of L1, CHL1, directs TC axons to the somatosensory cortex (Wright et al., 2007), and cooperates with L1 to guide axons to the motor cortex (Demyanenko et al., 2011b). Additionally, NrCAM also participates in topographic mapping of TC axons to the motor and somatosensory cortices (Demyanenko et al., 2011a). Together these results suggest that Ig superfamily cell adhesion molecules are critical for proper TC axon guidance to motor and somatosensory cortices. However, this also raises the question as to whether the adhesion molecules cooperate on the same axon or guide subpopulations of axons from the thalamus. Of particular interest in this regard is that L1, CHL1, and NrCAM respond to different guidance cues to promote proper targeting of TC axons. Repellant guidance cues such as ephrins (Dufour et al., 2003) and semaphorins (Wright et al., 2007; Demyanenko et al., 2011a) are expressed in gradients within the ventral telencephalon and allow for preliminary sorting of thalamic axons based on their expression of Eph and Neuropilin receptors. CHL1 interacts with Neuropilin 1 to respond to Sema3A, which is required for proper topographic mapping to the somatosensory cortex (Wright et al., 2007). In mapping motor axons, CHL1, and L1 differentially interact with EphA7 and EphA3, 4 or 7, respectively, to mediate repellant axon guidance in response to ephrinA5 (Demyanenko et al., 2011b). NrCAM associates with Neuropilin 2 and Sema3F to promote proper mapping of motor and somatosensory axons (Demyanenko et al., 2011a). While we did not identify which repellent guidance cue cooperates with NCAM, a recent study has shown that NCAM can associate with EphA3 to promote proper inhibitory synaptic targeting in response to ephrinA5 (Brennaman et al., 2012). The differential responses of these adhesion molecules to repellent guidance cues, suggest that while some axons may express L1, CHL1, and NCAM to respond to ephrinA5, others may only express NrCAM or CHL1.

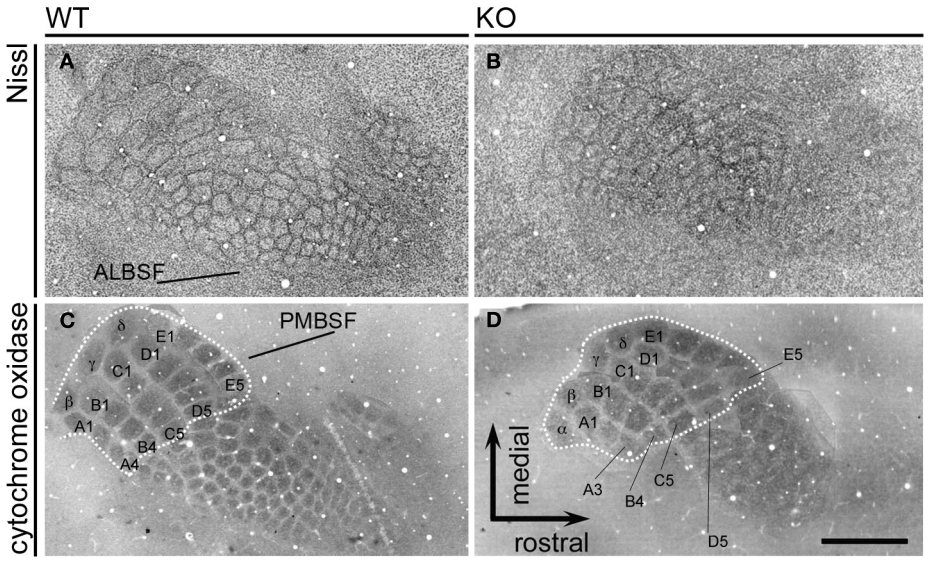

FIGURE 9 | The adult barrelfield in tangential sections. Nissl staining **(A,B)** of tangential sections show the PosteroMedial Barrel SubField (PMBSF) and the AnteroLateral Barrel SubField (ALBSF) subdivisions of the primary somatosensory area. The PMBSF barrels displayed blurred septa in null mutant mice, and ALBSF barrels were less distinct in mutant than in wild type mice. Cytochrome oxidase histochemistry **(C,D)** was used to assess possible changes in null mutant mice. The dotted lines delineate the part of the PMBSF containing the straddler barrels (α–δ) and the first posteromedial barrels of each row A to E (A1–A3, B1–B4, C1–C5, D1–D5, E1–E5); these barrels seemed unmodified in mutant animals. On the contrary, the rostrolateral barrels in the PMBSF and the barrels in the ALBSF were blurred and indistinct in mutant mice, suggesting that the genetic deletion of NCAM causes selective topographical changes in the somatosensory map. Images are reconstructions of serial sections. Bar: 1 mm.

This combinatorial effect would allow all axons from individual thalamic nuclei to project to their correct targets.

A limitation of this study is that retrograde TC labeling analysis was not performed in P5 mice once the final map is established. While our results suggest that motor and somatosensory axons misproject at early time points, only the somatosensory barrel field was examined in adult animals. TC axons shape the barrel field into the pattern of the whiskers (Erzurumlu and Jhaveri, 1990; Agmon et al., 1993; Schlaggar and O'Leary, 1994; Agmon et al., 1995; Wu et al., 2011), followed by the organization of layer IV neurons into discrete barrel units 1–2 days later (Rice and Van der Loos, 1977; Jhaveri et al., 1991). Therefore, our findings that the formation of barrels in layer IV at P6 were altered and the disorganization of the ALBSF and of the rostrolateral tier of the PMBSF in NCAM null mutant mice is likely a result of TC axon misguidance. However, we cannot determine whether these observations are a result of misprojection of axons to the visual cortex or if the axons degenerated.

The results presented here provide insight into a novel role for NCAM in TC topographic mapping. This may have profound implications in neuropsychiatric disorders where mutations in NCAM or changes in expression are observed, suggesting that TC mapping may be disturbed resulting in impaired sensory function.

ACKNOWLEDGMENTS

Supported by grants from National Institutes of Health Grants NS049109 (Patricia F. Maness) and MH064056 (Silvio Conte Center for Neuroscience of Mental Disorders) (Patricia F. Maness) and the Spanish Ministerio de Ciencia e Innovación/Fondo Europeo para el Desarrollo Regional (FEDER), BFU2004-04660, BFU2007-60263, and BFU2010-17305 (Alfonso Fairén). Thanks to H. Cremer, C. Goridis, F. J. Rathjen, and T. Seki for antibodies, Galina P. Demyanenko and Cristina Gil-Sanz for advice and Belén Andrés for excellent technical help.

REFERENCES

Agmon, A., and Connors, B. W. (1991). Thalamocortical responses of mouse somatosensory (barrel) cortex *in vitro*. *Neuroscience* 41, 365–379.

Agmon, A., Yang, L. T., Jones, E. G., and O'Dowd, D. K. (1995). Topological precision in the thalamic projection to neonatal mouse barrel cortex. *J. Neurosci.* 15, 549–561.

Agmon, A., Yang, L. T., O'Dowd, D. K., and Jones, E. G. (1993). Organized growth of thalamocortical axons from the deep tier of terminations into layer IV of developing mouse barrel cortex. *J. Neurosci.* 13, 5365–5382.

Angata, K., Long, J. M., Bukalo, O., Lee, W., Dityatev, A., Wynshaw-Boris, A., Schachner, M., Fukuda, M., and Marth, J. D. (2004). Sialyltransferase ST8Sia-II assembles a subset of polysialic acid that directs hippocampal axonal targeting and promotes fear behavior. *J. Biol. Chem.* 279, 32603–32613.

Anney, R., Klei, L., Pinto, D., Regan, R., Conroy, J., Magalhaes, T. R., Correia, C., Abrahams, B. S., Sykes, N., Pagnamenta, A. T., Almeida, J., Bacchelli., E., Bailey, A. J., Baird, G., Battaglia, A., Berney, T., Bolshakova, N., Bölte, S., Bolton, P. F., Bourgeron, T., Brennan, S., Brian, J., Carson, A. R., Casallo, G., Casey, J., Chu, S. H., Cochrane, L., Corsello, C., Crawford, E. L., Crossett, A., Dawson, G., de Jonge, M., Delorme, R., Drmic, I., Duketis, E., Duque, F., Estes, A., Farrar, P., Fernandez, B. A., Folstein, S. E., Fombonne, E., Freitag, C. M., Gilbert, J., Gillberg, C., Glessner,

J. T., Goldberg, J., Green, J., Guter, S. J., Hakonarson, H., Heron, E. A., Hill, M., Holt, R., Howe, J. L., Hughes, G., Hus, V., Igliozzi, R., Kim, C., Klauck, S. M., Kolevzon, A., Korvatska, O., Kustanovich, V., Lajonchere, C. M., Lamb, J. A., Laskawiec, M., Leboyer, M., Le Couteur, A., Leventhal, B. L., Lionel, A. C., Liu, X. Q., Lord, C., Lotspeich, L., Lund, S. C., Maestrini, E., Mahoney, W., Mantoulan, C., Marshall, C. R., McConachie, H., McDougle, C. J., McGrath, J., McMahon, W. M., Melhem, N. M., Merikangas, A., Migita, O., Minshew, N. J., Mirza, G. K., Munson, J., Nelson, S. F., Noakes, C., Noor, A., Nygren, G., Oliveira, G., Papanikolaou, K., Parr, J. R., Parrini, B., Paton, T., Pickles, A., Piven, J., Posey, D. J., Poustka, A., Poustka, F., Prasad, A., Ragoussis, J., Renshaw, K., Rickaby, J., Roberts, W., Roeder, K., Roge, B., Rutter, M. L., Bierut, L. J., Rice, J. P., Salt, J., Sansom, K., Sato, D., Segurado, R., Senman, L., Shah, N., Sheffield, V. C., Soorya, L., Sousa, I., Stoppioni, V., Strawbridge, C., Tancredi, R., Tansey, K., Thiruvahindrapduram, B., Thompson, A. P., Thomson, S., Tryfon, A., Tsiantis, J., Van Engeland, H., Vincent, J. B., Volkmar, F., Wallace, S., Wang, K., Wang, Z., Wassink, T. H., Wing, K., Wittemeyer, K., Wood, S., Yaspan, B. L., Zurawiecki, D., Zwaigenbaum, L., Betancur, C., Buxbaum, J. D., Cantor, R. M., Cook, E. H., Coon, H., Cuccaro, M. L., Gallagher, L., Geschwind, D. H., Gill, M., Haines, J. L., Miller, J., Monaco, A. P., Nurnberger, J. I. Jr., Paterson, A. D., Pericak-Vance, M. A., Schellenberg, G. D., Scherer, S. W., Sutcliffe, J. S., Szatmari, P., Vicente, A. M., Vieland, V. J., Wijsman, E. M., Devlin, B., Ennis, S., and Hallmayer, J. (2010). A genome-wide scan for common alleles affecting risk for autism. *Hum. Mol. Genet.* 19, 4072–4082.

Arai, M., Yamada, K., Toyota, T., Obata, N., Haga, S., Yoshida, Y., Nakamura, K., Minabe, Y., Ujike, H., Sora, I., Ikeda, K., Mori, N., Yoshikawa, T., and Itokawa, M. (2006). Association between polymorphisms in the promoter region of the sialyltransferase 8B (SIAT8B) gene and schizophrenia. *Biol. Psychiatry* 59, 652–659.

Barbeau, D., Liang, J. J., Robitalille, Y., Quirion, R., and Srivastava, L. K. (1995). Decreased expression of the embryonic form of the neural cell adhesion molecule in schizophrenic brains. *Proc. Natl. Acad. Sci. U.S.A.* 92, 2785–2789.

Bonfanti, L. (2006). PSA-NCAM in mammalian structural plasticity and neurogenesis. *Prog. Neurobiol.* 80, 129–164.

Brennaman, L. H., Kochlamazashvili, G., Stoenica, L., Nonneman, R. J., Moy, S. S., Schachner, M., Dityatev, A., and Maness, P. F. (2011). Transgenic mice overexpressing the extracellular domain of NCAM are impaired in working memory and cortical plasticity. *Neurobiol. Dis.* 43, 372–378.

Brennaman, L. H., and Maness, P. F. (2008). Developmental regulation of GABAergic interneuron branching and synaptic development in the prefrontal cortex by soluble neural cell adhesion molecule. *Mol. Cell. Neurosci.* 37, 781–793.

Brennaman, L. H., Zhang, X., Guan, H., Triplett, J. W., Brown, A., Demyanenko, G. P., Manis, P. B., Landmesser, L., and Maness, P. F. (2012). Polysialylated NCAM and ephrinA/EphA regulate synaptic development of GABAergic interneurons in prefrontal cortex. *Cereb. Cortex.* doi: 10.1093/cercor/bhr392. [Epub ahead of print].

Calandreau, L., Márquez, C., Bisaz, R., Fantin, M., and Sandi, C. (2010). Differential impact of polysialyltransferase ST8SiaII and ST8SiaIV knockout on social interaction and aggression. *Genes Brain Behav.* 9, 958–967.

Chung, W. W., Lagenaur, C. F., Yan, Y. M., and Lund, J. S. (1991). Developmental expression of neural cell adhesion molecules in the mouse neocortex and olfactory bulb. *J. Comp. Neurol.* 314, 290–305.

Cremer, H., Chazal, G., Goridis, C., and Represa, A. (1997). NCAM is essential for axonal growth and fasciculation in the hippocampus. *Mol. Cell. Neurosci.* 8, 323–335.

Cremer, H., Lange, R., Christoph, A., Plomann, M., Vopper, G., Roes, J., Brown, R., Baldwin, S., Kraemer, P., Scheff, S., Barthels, D., Rajewsky, K., and Wille, W. (1994). Inactivation of the N-CAM gene in mice results in size reduction of the olfactory bulb and deficits in spatial learning. *Nature* 367, 455–459.

Demyanenko, G. P., Riday, T. T., Tran, T. S., Dalal, J., Darnell, E. P., Brennaman, L. H., Sakurai, T., Grumet, M., Philpot, B. D., and Maness, P. F. (2011a). NrCAM deletion causes topographic mistargeting of thalamocortical axons to the visual cortex and disrupts visual acuity. *J. Neurosci.* 31, 1545–1558.

Demyanenko, G. P., Siesser, P. F., Wright, A. G., Brennaman, L. H., Bartsch, U., Schachner, M., and Maness, P. F. (2011b). L1 and CHL1 cooperate in thalamocortical axon targeting. *Cereb. Cortex* 21, 401–412.

Dityatev, A., Dityateva, G., Sytnyk, V., Delling, M., Toni, N., Nikonenko, I., Muller, D., and Schachner, M. (2004). Polysialylated neural cell adhesion molecule promotes remodeling and formation of hippocampal synapses. *J. Neurosci.* 24, 9372–9382.

Dufour, A., Seibt, J., Passante, L., Depaepe, V., Ciossek, T., Frisen, J., Kullander, K., Flanagan, J. G., Polleux, F., and Vanderhaeghen, P. (2003). Area specificity and topography of thalamocortical projections are controlled by ephrin/Eph genes. *Neuron* 39, 453–465.

Edelman, G. M., and Chuong, C. M. (1982). Embryonic to adult conversion of neural cell adhesion molecules in normal and staggerer mice. *Proc. Natl. Acad. Sci. U.S.A.* 79, 7036–7040.

Erzurumlu, R. S., and Jhaveri, S. (1990). Thalamic axons confer a blueprint of the sensory periphery onto the developing rat somatosensory cortex. *Dev. Brain Res.* 56, 229–234.

Fukuda, T., Kawano, H., Ohyama, K., Li, H. P., Takeda, Y., Oohira, A., and Kawamura, K. (1997). Immunohistochemical localization of neurocan and L1 in the formation of thalamocortical pathway of developing rats. *J. Comp. Neurol.* 382, 141–152.

Gascon, E., Vutskits, L., and Kiss, J. Z. (2007). Polysialic acid-neural cell adhesion molecule in brain plasticity: from synapses to integration of new neurons. *Brain Res. Rev.* 56, 101–118.

Gennarini, G., Rougon, G., Deagostini-Bazin, H., Hirn, M., and Goridis, C. (1984). Studies on the transmembrane disposition of the neural cell adhesion molecule N-CAM. A monoclonal antibody recognizing a cytoplasmic domain and evidence for the presence of phosphoserine residues. *Eur. J. Biochem.* 142, 57–64.

Godement, P., Vanselow, J., Thanos, S., and Bonhoeffer, F. (1987). A study in developing visual systems with a new method of staining neurones and their processes in fixed tissue. *Development* 101, 697–713.

Hildebrandt, H., Mühlenhoff, M., Weinhold, B., and Gerardy-Schahn, R. (2007). Dissecting polysialic acid and NCAM functions in brain development. *J. Neurochem.* 103(Suppl. 1), 56–64.

Isomura, R., Kitajima, K., and Sato, C. (2011). Structural and functional impairments of polysialic acid by a mutated polysialyltransferase found in schizophrenia. *J. Biol. Chem.* 286, 21535–21545.

Jhaveri, S., Erzurumlu, R. S., and Crossin, K. (1991). Barrel construction in rodent neocortex: role of thalamic afferents versus extracellular matrix molecules. *Proc. Natl. Acad. Sci. U.S.A.* 88, 4489–4493.

Johnson, C. P., Fujimoto, I., Rutishauser, U., and Leckband, D. E. (2005). Direct evidence that neural cell adhesion molecule (NCAM) polysialylation increases intermembrane repulsion and abrogates adhesion. *J. Biol. Chem.* 280, 137–145. Erratum in *J. Biol. Chem*. 280, 23424.

Kageyama, G. H., and Wong-Riley, M. T. (1982). Histochemical localization of cytochrome oxidase in the hippocampus: correlation with specific neuronal types and afferent pathways. *Neuroscience* 7, 2337–2361.

Lebrand, C., Cases, O., Adelbrecht, C., Doye, A., Alvarez, C., El Mestikawy, S., Seif, I., and Gaspar, P. (1996). Transient uptake and storage of serotonin in developing thalamic neurons. *Neuron* 17, 823–835.

Lee, M. T., Chen, C. H., Lee, C. S., Chen, C. C., Chong, M. Y., Ouyang, W. C., Chiu, N. Y., Chuo, L. J., Chen, C. Y., Tan, H. K., Lane, H. Y., Chang, T. J., Lin, C. H., Jou, S. H., Hou, Y. M., Feng, J., Lai, T. J., Tung, C. L., Chen, T. J., Chang, C. J., Lung, F. W., Chen, C. K., Shiah, I. S., Liu, C. Y., Teng, P. R., Chen, K. H., Shen, L. J., Cheng, C. S., Chang, T. P., Li, C. F., Chou, C. H., Chen, C. Y., Wang, K. H., Fann, C. S., Wu, J. Y., Chen, Y. T., and Cheng, A. T. (2011). Genome-wide association study of bipolar I disorder in the Han Chinese population. *Mol. Psychiatry* 16, 548–556.

López-Bendito, G., and Molnár, Z. (2003). Thalamocortical development: how are we going to get there? *Nat. Rev. Neurosci.* 4, 276–289.

Molnár, Z., Garel, S., López-Bendito, G., Maness, P., and Price, D. J. (2012). Mechanisms controlling the guidance of thalamocortical axons through the embryonic forebrain. *Eur. J. Neurosci.* 35, 1573–1585.

Nadanaka, S., Sato, C., Kitajima, K., Katagiri, K., Irie, S., and Yamagata, T. (2001). Occurrence of oligosialic acids on integrin alpha 5 subunit and their involvement in cell adhesion to fibronectin. *J. Biol. Chem.* 276, 33657–33664.

Ohyama, K., Tan-Takeuchi, K., Kutsche, M., Schachner, M., Uyemura, K.,

and Kawamura, K. (2004). Neural cell adhesion molecule L1 is required for fasciculation and routing of thalamocortical fibres and corticothalamic fibres. *Neurosci. Res.* 48, 471–475.

Pillai-Nair, N., Panicker, A. K., Rodriguiz, R. M., Gilmore, K. L., Demyanenko, G. P., Huang, J. Z., Wetsel, W. C., and Maness, P. F. (2005). Neural cell adhesion molecule-secreting transgenic mice display abnormalities in GABAergic interneurons and alterations in behavior. *J. Neurosci.* 25, 4659–4671.

Rathjen, F. G., and Schachner, M. (1984). Immunocytological and biochemical characterization of a new neuronal cell surface component (L1 antigen) which is involved in cell adhesion. *EMBO J.* 3, 1–10.

Rice, F. L., and Van der Loos, H. (1977). Development of the barrels and barrel field in the somatosensory cortex of the mouse. *J. Comp. Neurol.* 171, 545–460.

Rutishauser, U. (2008). Polysialic acid in the plasticity of the developing and adult vertebrate nervous system. *Nat. Rev. Neurosci.* 9, 26–35.

Schiff, M., Röckle, I., Burkhardt, H., Weinhold, B., and Hildebrandt, H. (2011). Thalamocortical pathfinding defects precede degeneration of the reticular thalamic nucleus in polysialic acid-deficient mice. *J. Neurosci.* 31, 1302–1312.

Schlaggar, B. L., and O'Leary, D. D. (1994). Early development of the somatotopic map and barrel patterning in rat somatosensory cortex. *J. Comp. Neurol.* 346, 80–96.

Seki, T., and Arai, Y. (1991). Expression of highly polysialylated NCAM in the neocortex and piriform cortex of the developing and the adult rat. *Anat. Embryol. (Berl.)* 184, 395–401.

Seki, T., and Arai, Y. (1993). Distribution and possible roles of the highly polysialylated neural cell adhesion molecule (NCAM-H) in the developing and adult central nervous system. *Neurosci. Res.* 17, 265–290.

Tao, R., Li, C., Zheng, Y., Qin, W., Zhang, J., Li, X., Xu, Y., Shi, Y. Y., Feng, G., and He, L. (2007). Positive association between SIAT8B and schizophrenia in the Chinese Han population. *Schizophr. Res.* 90, 108–114.

Van der Loos, H., and Woolsey, T. A. (1973). Somatosensory cortex: structural alterations following early injury to sense organs. *Science* 179, 395–398.

Weinhold, B., Seidenfaden, R., Röckle, I., Mühlenhoff, M., Schertzinger, F., Conzelmann, S., Marth, J. D., Gerardy-Schahn, R., and Hildebrandt, H. (2005). Genetic ablation of polysialic acid causes severe neurodevelopmental defects rescued by deletion of the neural cell adhesion molecule. *J. Biol. Chem.* 280, 42971–42977.

Wiencken-Barger, A. E., Mavity-Hudson, J., Bartsch, U., Schachner, M., and Casagrande, V. A. (2004). The role of L1 in axon pathfinding and fasciculation. *Cereb. Cortex* 14, 121–131.

Wong-Riley, M. T., and Welt, C. (1980). Histochemical changes in cytochrome oxidase of cortical barrels after vibrissal removal in neonatal and adult mice. *Proc. Natl. Acad. Sci. U.S.A.* 70, 2333–2337.

Woolsey, T. A., and Van der Loos, H. (1970). The structural organization of layer IV in the somatosensory region (SI) of mouse cerebral cortex. The description of a cortical field composed of discrete cytoarchitectonic units. *Brain Res.* 17, 205–242.

Wu, C. S., Ballester Rosado, C. J., and Lu, H. C. (2011). What can we get from 'barrels': the rodent barrel cortex as a model for studying the establishment of neural circuits. *Eur. J. Neurosci.* 34, 1663–1676.

Wright, A. G., Demyanenko, G. P., Powell, A., Schachner, M., Enriquez-Barreto, L., Tran, T. S., Polleux, F., and Maness, P. F. (2007). Close homolog of L1 (CHL1) and neuropilin1 mediate guidance of thalamocortical axons at the ventral telencephalon. *J. Neurosci.* 27, 13667–13679.

Yamamoto, N., Inui, K., Matsuyama, Y., Harada, A., Hanamura, K., Murakami, F., Ruthazer, E. S., Rutishauser, U., and Seki, T. (2000). Inhibitory mechanism by polysialic acid forlamina-specific branch formation of thalamocortical axons. *J. Neurosci.* 20, 9145–9151.

Conflict of Interest Statement: The authors declare that the research was conducted in the absence of any commercial or financial relationships that could be construed as a potential conflict of interest.

Received: 01 March 2012; accepted: 05 June 2012; published online: 20 June 2012.

Citation: Enriquez-Barreto L, Palazzetti C, Brennaman LH, Maness PF and Fairén A (2012) Neural cell adhesion molecule, NCAM, regulates thalamocortical axon pathfinding and the organization of the cortical somatosensory representation in mouse. Front. Mol. Neurosci. 5:76. doi: 10.3389/fnmol.2012.00076

frontiers in
MOLECULAR NEUROSCIENCE

REVIEW ARTICLE
published: 04 May 2012
doi: 10.3389/fnmol.2012.00059

Guidance of longitudinally projecting axons in the developing central nervous system

Nozomi Sakai [1] ***and Zaven Kaprielian*** [1,2] ***

[1] *Dominick P. Purpura Department of Neuroscience, Albert Einstein College of Medicine, Bronx, NY, USA*
[2] *Department of Pathology, Albert Einstein College of Medicine, Bronx, NY, USA*

Edited by:
Joshua A. Weiner, The University of Iowa, USA

Reviewed by:
Patricia Maness, University of North Carolina, USA
Esther Stoeckli, University of Zurich, Switzerland

***Correspondence:**
Zaven Kaprielian, Dominick P. Purpura Department of Neuroscience and Department of Pathology, Albert Einstein College of Medicine, 1410 Pelham Parkway South, Bronx, NY 10461, USA.
e-mail: zaven.kaprielian@einstein.yu.edu

The directed and stereotypical growth of axons to their synaptic targets is a crucial phase of neural circuit formation. Many axons in the developing vertebrate and invertebrate central nervous systems (CNSs), including those that remain on their own (ipsilateral), and those that cross over to the opposite (commissural), side of the midline project over long distances along the anterior-posterior (A-P) body axis within precisely positioned longitudinally oriented tracts to facilitate the transmission of information between CNS regions. Despite the widespread distribution and functional importance of these longitudinal tracts, the mechanisms that regulate their formation and projection to poorly characterized synaptic targets remain largely unknown. Nevertheless, recent studies carried out in a variety of invertebrate and vertebrate model systems have begun to elucidate the molecular logic that controls longitudinal axon guidance.

Keywords: longitudinal axon guidance/targeting, Robo, CAMs, Sema, Wnt

INTRODUCTION

Longitudinally projecting axons connect different regions of the central nervous system (CNS) by extending over long distances along the anterior-posterior (A-P) body axis. Here, we review recent evidence supporting *in vivo* roles for long- and short-range guidance systems in regulating the pathfinding of longitudinally projecting ipsilateral and commissural axons. We first examine dye tracing and reporter gene expression data that reveal a previously unanticipated diversity and complexity of commissural and ipsilateral projections, which originate from neurons in the spinal cord and project longitudinally in the marginal zone; the outermost layer of the spinal cord proper that surrounds the gray matter. We then consider the reported roles of the morphogens, Sonic hedgehog (Shh) and Wnts, and potential interplay between these factors, in regulating the rostrally directed turn executed by post-crossing spinal commissural axons immediately after they cross the midline. Next, we address how Robo-Slit signaling, operating on its own or, potentially, in conjunction with particular cell adhesion molecules (CAMs), directs decussated commissural and ipsilateral axons into longitudinal tracts in the vertebrate CNS. We also evaluate the likely possibility that invertebrate model systems use a conserved set of, as well as unique, guidance cues and their receptors to ensure that commissural and ipsilateral axons are properly organized into stereotypically arranged longitudinal-oriented fascicles. In addition, we consider the mechanisms that appear to control the pathfinding of longitudinally projecting commissural and ipsilateral axons, which emanate from neurons located in various brain regions and descend into the spinal cord. Finally, we briefly discuss the few studies aimed at identifying the synaptic targets of genetically distinct populations of neurons/axons in the vertebrate CNS.

PATHFINDING OF LONGITUDINALLY PROJECTING AXONS IN VERTEBRATES: ASCENDING SPINAL PROJECTION AND DESCENDING MIDBRAIN NEURONS

SPATIAL ORGANIZATION OF LONGITUDINAL AXON TRACTS WITHIN THE SPINAL CORD MARGINAL ZONE

By extending over long distances along the antero-posterior (A-P) axis of the CNS, ascending and descending spinal projection neurons transmit information to the brain and spinal cord, respectively. In vertebrates, projection neuron axons are contained within the spinal cord marginal zone (**Figure 1**). These axons assemble into longitudinal tracts or fascicles that are spatially organized in register with the positions of their brain targets (ascending axons) or brain origins (descending axons) in the spinal cord marginal zone (Burt, 1993; Brodal, 1998). Numerous anatomical and physiological studies have characterized the relative positioning of particular ascending and descending tracts within the spinal cord marginal zone (Burt, 1993; Brodal, 1998). For example, with specific regard to ascending projections, the spinothalamic tract is a major component of anterolateral system, which is housed within the ventral funiculus (VF) and ventrolateral funiculus (vLF) (Kerr, 1975; Giesler et al., 1981; Björkeland and Boivie, 1984; Willis, 2007). On the other hand, the spinocerebellar tract represents the predominant ascending pathway and is formed by axons located within both the dorsolateral funiculus (dLF) and the vLF (Xu and Grant, 1994, 2005; Willis, 2007). In addition, the dorsal funiculus (DF) contains the fasciculus gracilis

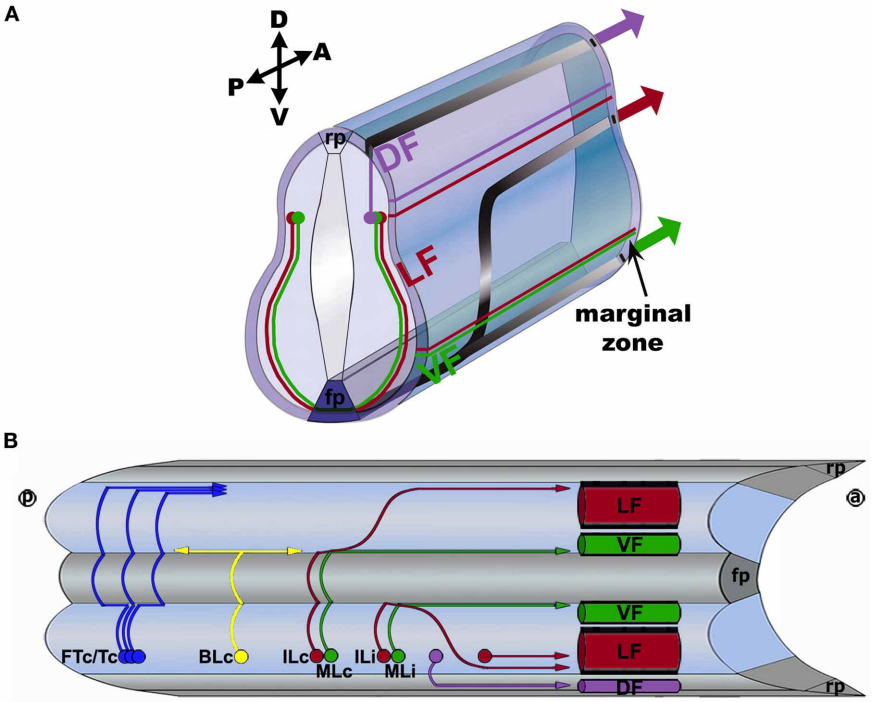

FIGURE 1 | Spinal axon trajectories within the vertebrate spinal cord. **(A)** Transverse view of the spinal cord shows ipsilaterally and contralaterally projecting axons growing within the spinal gray matter and, subsequently, the right side of the marginal zone. The axons of red neurons grow alongside the floor plate (fp), and project into the lateral funiculus (LF) of the spinal cord marginal zone, along either Intermediate Longitudinal commissural (ILc) or Intermediate Longitudinal ipsilateral (ILi) trajectories. The axons of green neurons extend adjacent to the fp along either Medial Longitudinal commissural (MLc) or Medial Longitudinal ipsilateral (MLi) trajectories to form the ventral funiculus (VF). The axons of purple neurons project ipsilaterally and dorsally to form the dorsal funiculus (DF) together with a subset of DRG axons (not shown). The cell body locations do not necessarily represent their settling positions. A, anterior; P, posterior; D, dorsal; V, ventral; rp, roof plate. **(B)** Open book view of the spinal cord shows the trajectories of unilaterally labeled axons. Commissural axons cross the floor plate (fp) and elaborate Forked Transverse commissural (FTc), Transverse commissural (Tc), Bifurcating Longitudinal commissural (BLc), ILc, and MLc projections. Ipsilaterally projecting axons remain on the same side of the CNS as their cell bodies and elaborate ILi and MLi projections. Ipsilaterally projecting axons can also directly project to the LF or to the dorsal funiculus (DF). Each of the depicted trajectories are present from thoracic to lumber levels of the spinal cord, and the locations of neuronal cell bodies do not necessarily represent their settling positions. ⓐ, anterior; ⓟ, posterior; rp, roof plate.

and the fasciculus cuneatus, which terminate in the medulla oblongata (Giesler et al., 1984).

DIVERSITY OF CONTRALATERAL COMMISSURAL AND IPSILATERAL PROJECTIONS IN THE VERTEBRATE SPINAL CORD

Although the spatial arrangement of longitudinally projecting tracts within the spinal cord marginal zone has long been appreciated, the trajectories that the component axons adopt in the spinal cord proper, and which presumably prefigure this organization, have only recently been characterized. Since most ascending and descending tracts are comprised of both ipsilateral and commissural projections, and given the bilateral symmetry of the spinal cord, "one-sided/unilateral" labeling strategies are required to visualize the individual axons or sets of axons contained within a particular tract and to clearly delineate its ipsilateral and commissural components. Utilizing the lipophilic axon-tracer, 1,1′-dioctadecyl-3,3,3′,3′ tetramethylindocarbocyanine perchlorate (DiI), unilateral labeling of open book spinal cord preparations derived from various age chick and mouse embryos was previously carried out to selectively characterize the projections elaborated by post-crossing commissural axons. Importantly, this unilateral labeling strategy provided unobstructed views of post-crossing commissural axons and revealed a previously unappreciated complexity and diversity in their projections within the spinal cord marginal zone (Imondi and Kaprielian, 2001; Kadison and Kaprielian, 2004).

All spinal commissural axons initially project to their common intermediate target, the floor plate located at the ventral midline, along a simple linear pre-crossing trajectory (Bovolenta and Dodd, 1990; Imondi and Kaprielian, 2001) (**Figure 1A**). After crossing the floor plate, the contralateral segments of decussated commissural axons adopt at least five distinct trajectories (**Figure 1B**). The most commonly observed contralateral projections are elaborated by medial longitudinal commissural (MLc) axons, which extend in the longitudinal plane alongside the floor plate at the ventral midline and join/form the VF, and intermediate longitudinal commissural (ILc) axons, which initially grow alongside the floor plate and then project laterally, away from the ventral midline along an arcuate trajectory and ultimately turn longitudinally to form the LF (Bovolenta and Dodd, 1990; Imondi

and Kaprielian, 2001; Kadison and Kaprielian, 2004). After turning into the longitudinal plane most MLc and ILc axons project rostrally, however, a minor but significant subset of each population extends in the caudal direction (Bovolenta and Dodd, 1990; Kadison and Kaprielian, 2004). The other three, relatively minor projections are elaborated by: bifurcating longitudinal commissural (BLc) axons, which bifurcate into rostrally and caudally projecting branches either within the VF alongside the FP or at a significant lateral distance from the spinal cord, where they contribute to the LF, forked transverse commissural (FTc) axons, which bifurcate on the ipsilateral side first, cross the floor plate, project transverse to the floor plate, and appear to join the LF or DF, or transverse commissural (Tc) axons, which do not turn in the VF but, rather, project transverse to the floor plate, and likely join the LF and DF (Bovolenta and Dodd, 1990; Kadison and Kaprielian, 2004).

Over the past 10 years, the emergence of *in ovo* and *in utero* electroporation technologies, together with the development of a wide range of reporter constructs, has made it possible to visualize axon pathfinding in both the embryonic chick and mouse spinal cord (Krull, 2004; Saito, 2006). Most importantly, unilateral *in ovo* electroporation has been used to reproducibly label genetically distinct populations of spinal axons and to assess potential differences in the trajectories elaborated by specific spinal neuron populations. For example, dorsal spinal neurons, which represent a major class of projection neurons (Nunes and Sotelo, 1985; Burstein et al., 1990; Yezierski and Mendez, 1991; Brodal, 1998), have been classified according to the particular transcription factor(s) they express (Helms and Johnson, 2003), and it has become possible to selectively visualize their pathfinding axons by electroporating reporter constructs harboring enhancer elements derived from the corresponding genes (Lumpkin et al., 2003; Nakada et al., 2004; Reeber et al., 2008; Avraham et al., 2009, 2010). These genetic labeling studies have revealed that the majority of d1 and d2 commissural axons adopt MLc and ILc trajectories and join the VF and LF, respectively, (Reeber et al., 2008; Avraham et al., 2009).

In addition to characterizing contralateral commissural projections, DiI tracing and unilateral *in ovo* electroporation of specific reporter constructs have also been used to identify three major projections elaborated by ipsilateral spinal neurons/axons. Specifically, major subsets of ipsilaterally projecting axons contribute to particular funiculi within the spinal cord marginal zone: (1) medial longitudinal ipsilateral (MLi) axons, which project along MLc axon-like trajectories, join the VF (Avraham et al., 2010), (2) intermediate longitudinal ipsilateral (ILi) axons, analogous to ILc axons, initially extend toward the ventral midline and then project away from the FP along an arcuate trajectory, or by directly projecting into lateral regions of the spinal cord, join the LF (Kadison and Kaprielian, 2004; Avraham et al., 2010), and (3) a subset of ipsilateral axons projects toward the marginal zone and turns into the longitudinal plane between the dorsal midline and the dorsal root, and join the DF (Avraham et al., 2010).

Whereas most spinal projection neurons extend ascending axons to the brain, some populations of spinal cord interneurons make local connections in segments located either above or below their cell bodies (Brodal, 1998; Kullander et al., 2003; Kiehn, 2006). Accordingly, DiI tracing and genetic labeling studies have identified a subset of caudally extending axons that contribute to the VF, LF and/or DF (Bovolenta and Dodd, 1990; Kadison and Kaprielian, 2004; Reeber et al., 2008; Avraham et al., 2009, 2010).

THE ROLE(S) OF MORPHOGENS IN DIRECTING THE ROSTRAL TURN EXECUTED BY DECUSSATED SPINAL COMMISSURAL AXONS

As described above, many commissural axons turn rostrally into the longitudinal plane after crossing the ventral midline. It has now become apparent that morphogens, once thought to exclusively control patterning events in the developing nervous system, regulate this key pathfinding decision faced by newly decussated commissural axons (Bovolenta, 2005; Charron and Tessier-Lavigne, 2005; Zou and Lyuksyutova, 2007; Sánchez-Camacho and Bovolenta, 2009). For example, Wnt4 (see **Table 1**) appears to have a critical role in controlling the rostral turn executed by MLc and ILc axons in the mouse spinal cord (Lyuksyutova et al., 2003). This is supported by the finding that floor plate expresses *Wnt4* mRNA in a rostral (high) to caudal (low) gradient in mouse embryos, and that Wnt4-expressing cells attract decussated commissural axons *in vitro* (Lyuksyutova et al., 2003). In addition, mice lacking a Wnt receptor and the well-known planar cell polarity signaling molecule, *Frizzled3*, display a reduction in the number of DiI-labeled rostrally growing decussated axons (Lyuksyutova et al., 2003). Other planar cell polarity components, including *Drosophila* van Gogh ortholog Vangl2 and Flamingo ortholog Celsr3 (Tissir and Goffinet, 2010), determine the rostrocaudal polarity of axon growth by interacting with Frizzled3 (Shafer et al., 2011). Accordingly, it appears that Wnt4 and/or its receptor Frizzled3, as well as Vangl2 and Celsr3 have a major role in regulating the polarity of the stereotypical rostral turn executed by ascending post-crossing commissural axons.

In the chick spinal cord, the potent morphogen, Shh, which is selectively expressed at the ventral midline, also has an important role in regulating the rostral turning of post-crossing commissural axons (Bourikas et al., 2005). Contrasting the pattern of Wnt4 expression described in mouse embryos, Shh is expressed by floor plate cells in a caudal (high) to rostral (low) gradient in chick embryos. Accordingly, it has been proposed that Shh operates as a repellent for post-crossing commissural axons as they project along the A-P axis of the spinal cord. Supporting this notion, knock down of Shh expression through the use of long double-stranded RNA interference (dsRNAi) causes stalling of decussated DiI-labeled axons in the vicinity of the floor plate, and prevents them from turning in the rostral direction (Bourikas et al., 2005). Interestingly, although Wnt4 is not present within the floor plate of the chick spinal cord, a non-graded distribution of *Wnt5a* and *Wnt7a* mRNA has been detected at the ventral midline (Domanitskaya et al., 2010). In addition, a Wnt antagonist, *Secreted frizzled-related protein 1* (*Sfrp1*) mRNA is expressed within the floor plate, in an increasing rostrocaudal gradient, and ectopic expression of Shh induces *Sfrp1* expression. Together these intriguing observations raise the possibility that Shh guides post-crossing spinal commissural axons in the rostral direction, by inducing an attractive Wnt gradient in the chick spinal cord (Domanitskaya et al., 2010).

Table 1 | Selected molecules associated with the pathfinding of longitudinally projecting axons.

Name	Organism	Localization[a]	Suggested role in longitudinal guidance
Celsr3	Mouse	Spinal commissural axons; mdDA and hindbrain 5-HT axons	Rostral turn of spinal commissural axons (Shafer et al., 2011); rostrocaudal orientation of mdDA and hindbrain 5-HT axons (Fenstermaker et al., 2010)
EphA4	Mouse	Corticospinal axons	Prevents corticospinal axons from re-crossing in the spinal cord (Dottori et al., 1998; Kullander et al., 2001b; Yokoyama et al., 2001)
ephrinB3	Mouse	Ventral midline	Midline barrier for corticospinal axons in the spinal cord (Kullander et al., 2001a; Yokoyama et al., 2001)
FasII	*Drosophila*	Longitudinal axons	Fasciculation of FasII$^+$ longitudinal tracts (Lin et al., 1994)
lin-17 (Frizzled)	*C. elegans*	Posterior dendrite of PLM neurons	A-P orientation of PLM axon and dendrite (Hilliard and Bargmann, 2006)
mig-1 mom-5 (Frizzled)	*C. elegans*	?	Anterior orientation and growth of AVM and PVM longitudinal axons (Pan et al., 2006)
Frizzled3	Mouse	Spinal commissural axons; mdDA and hindbrain 5-HT axons	Rostral turn of spinal commissural axons (Lyuksyutova et al., 2003); rostrocaudal orientation of mdDA and hindbrain 5-HT axons (Fenstermaker et al., 2010)
L1	Mouse	Corticospinal axons at the pyramid	Pyramidal decussation; facilitating caudal growth below the pyramid (Cohen et al., 1997)
N-cadherin	*Drosophila*	Longitudinal and commissural axons	Fasciculation of FasII$^+$ and Apterous longitudinal tracts (Iwai et al., 1997)
NCAM	Mouse	Corticospinal axons at the pyramid	Pyramidal decussation; facilitating caudal growth below the pyramid (Rolf et al., 2002)
PSA-NCAM	Mouse	Corticospinal axons in the pyramid and in the DF	Facilitates collateral formation by corticospinal axons (Daston et al., 1996)
Npn2	Mouse	mdDA axons	Directs mdDA axons along specific routes and to the prefrontal cortex (Kolk et al., 2009; Yamauchi et al., 2009)
PlexinA	*Drosophila*	Longitudinal axons	Defasciculation of FasII$^+$ axons from intermediate to lateral fascicle (Winberg et al., 1998)
PlexinA3 PlexinA4	Mouse	(mRNA) corticospinal neurons; (*PlexinA4* mRNA) along the corticospinal tracts in the hindbrain and inferior olive	Pyramidal decussation (Faulkner et al., 2008; Runker et al., 2008)
PlexinB	*Drosophila*	Intermediate and lateral region of neuropile; FasII$^+$ intermediate fascicle	Positioning and formation of FasII$^+$ intermediate fascicle (Wu et al., 2011)
Robo1 Robo2	Mouse Chick	Spinal commissural axons; descending midbrain axons; ascending mdDA axons; corticospinal and corticofugal tracts	Dorsoventral positioning of longitudinal tracts formed by spinal commissural axons (Reeber et al., 2008; Jaworski et al., 2010); fasciculation and organization of midbrain and mdDA axon tracts (Farmer et al., 2008; Dugan et al., 2011); restricting mdDA, midbrain, corticospinal and corticofugal axons to the ipsilateral side (Lopez-Bendito et al., 2007; Farmer et al., 2008; Dugan et al., 2011)
Robo1 Robo2 Robo3	*Drosophila*	Longitudinal axons in ventral nerve cord	Mediolateral positioning of longitudinal tracts (Rajagopalan et al., 2000; Simpson et al., 2000; Spitzweck et al., 2010)
Ryk	Mouse	Corticospinal axons	Facilitates the caudal growth of corticospinal tract (Liu et al., 2005)
Sema1A	*Drosophila*	Longitudinal and commissural axons	Defasciculation of FasII$^+$ axons from intermediate to lateral fascicle (Yu et al., 1998)
Sema2A	*Drosophila*	Midline and commissure in the ventral nerve cord	Repulsive boundary for positioning and growth of FasII$^+$ intermediate fascicle (Wu et al., 2011)
Sema2B	*Drosophila*	Medial and intermediate region of neuropile; FasII$^+$ intermediate fascicle	Fasciculation of FasII$^+$ intermediate fascicle (Wu et al., 2011)
Sema3F	Mouse	Midbrain-hindbrain border	Directs mdDA axons rostrally (Yamauchi et al., 2009); directs mdDA axons to the prefrontal cortex (Kolk et al., 2009)

(*Continued*)

Table 1 | Continued

Name	Organism	Localization[a]	Suggested role in longitudinal guidance
Sema6A	Mouse	(mRNA) along the corticospinal tracts in the hindbrain and inferior olive	Pyramidal decussation (Faulkner et al., 2008; Runker et al., 2008)
Sfrp1	Chick	(mRNA) ventral midline	Regulates rostral turn of spinal commissural axons by antagonizing Wnt5a and Wnt7a (Domanitskaya et al., 2010)
Shh	Chick	Ventral midline	Rostral turn of spinal commissural axons (Bourikas et al., 2005)
Slit1 Slit2 Slit3	Mouse	(mRNA) ventral midline; (*Slit1* and *Slit2* mRNA) forebrain-midbrain border and ventral forebrain structures	Positioning of longitudinal spinal axon tracts (Long et al., 2004); fasciculation and organization of longitudinal midbrain and mdDA axon tracts (Farmer et al., 2008; Dugan et al., 2011); forming the ventral midline boundary in the brain (Bagri et al., 2002; Farmer et al., 2008; Dugan et al., 2011)
Unc5c	Mouse	(mRNA) cerebral cortical layer V and VI	Pyramidal decussation (Finger et al., 2002)
Vangl2	Mouse	mdDA and hindbrain 5-HT axons; (mRNA) spinal cord gray matter	Rostral turn of spinal commissural axons (Shafer et al., 2011); rostrocaudal orientation of mdDA and hindbrain 5-HT axons (Fenstermaker et al., 2010)
egl-20 (Wnt)	*C. elegans*	Tail	Anterior orientation and growth of AVM and PVM longitudinal axons via repulsion (Pan et al., 2006)
lin-44 (Wnt)	*C. elegans*	Posterior epidermal cells	A-P orientation of PLM axon and dendrite (Hilliard and Bargmann, 2006)
Wnt1 Wnt5a	Mouse	(mRNA) dorsal spinal gray matter; (*Wnt5a* mRNA) ventral midline in the brain	Repels corticospinal tract *in vitro* (Liu et al., 2005); (Wnt5a) initial rostral bias of mdDA axon projection (Fenstermaker et al., 2010)
Wnt4	Mouse	(mRNA) ventral midline	Attracts spinal commissural axons rostrally *in vitro* (Lyuksyutova et al., 2003)
Wnt5a Wnt7a	Chick	(mRNA) ventral midline	Rostral turn of spinal commissural axons (Domanitskaya et al., 2010)

[a] *Protein localization unless otherwise stated (i.e., mRNA).*

Given that a subset of the ipsilaterally extending axons also project to the brain along MLi and ILi trajectories (see above), it would be interesting to determine whether ventral midline-associated Wnts and Shh regulate the rostral turn executed by these subsets of ascending axons. The findings of such experiments could conceivably reveal a previously unsuspected heterogeneity in the response of commissural and ipsilateral axons to morphogens that control the polarity of longitudinally projecting axons.

ORGANIZATION OF LONGITUDINAL AXON TRACTS: THE ROLE(S) OF ROBO-SLIT SIGNALING

After executing rostral or caudal turns into the longitudinal plane at various positions along the A-P axis of the CNS, the axons of both ascending and descending projection neurons are sorted into discrete longitudinal bundles or tracts located at specific distances form the midline (Burt, 1993; Brodal, 1998). In the vertebrate spinal cord, Robo receptors and their Slits ligands have well-established and critical roles in regulating the positioning of contralaterally ascending spinal commissural axon-containing longitudinal tracts (Dickson and Gilestro, 2006; Dickson and Zou, 2010). For example, Robo-Slit signaling normally drives spinal commissural axons along ILc trajectories and into the LF in the embryonic chick spinal cord (Reeber et al., 2008). By disabling Robo-Slit signaling via unilateral electroporation of spinal commissural neurons with cytoplasmic truncations (dominant-negative forms) of Robo1 or Robo2, a striking and selective axon pathfinding phenotype was observed: post-crossing commissural axons failed to elaborate ILc projections and, instead, exclusively extended along MLc-like trajectories, forming a hyperfasciculated, inappropriately thick VF (Reeber et al., 2008). Essentially all of the spinal commissural axons transfected with Robo dominant-negative constructs, including those extended by d1 and d2 neurons, and both ascending and descending axons, exhibited this phenotype (Reeber et al., 2008). Similarly in the mouse spinal cord, the number of DiI-labeled ILc axons is reduced in the spinal cord of *Robo2* null and *Robo1; Robo2* double mutant mice (Jaworski et al., 2010). In addition, the expression of L1, which is a general marker for longitudinally projecting spinal axons (Imondi et al., 2000), in the spinal cord of mice lacking all three Slits, *Slits1–3*, revealed a reduction in the width of the LF (Long et al., 2004). Together, these observations support the view that Robo-Slit signaling has a major role in directing spinal commissural axons into the LF.

Robo-Slit signaling also appears to have a role in regulating the pathfinding of longitudinally projecting descending axons, which emanate from particular midbrain neurons. For example, analyses of various knockout mice have shown that Robo-Slit interactions normally prevent a variety of DiI-labeled descending axons from inappropriately crossing the midline in the brain (Bagri et al., 2002; Lopez-Bendito et al., 2007; Farmer et al., 2008). It is interesting to note in this regard that roles for Robos and Slits in barring longitudinally projecting spinal axons from the midline have not been clearly defined in the chick and mouse spinal cord.

For example, in chick embryos, spinal (commissural and ipsilateral) axons mis-expressing dominant-negative forms of Robo do not ectopically cross the ventral midline (Reeber et al., 2008). Similarly, the re-crossing of spinal commissural axons has not been observed in *Robo1; Robo2* double null mutant mice (Jaworski et al., 2010). In addition, whereas midline re-crossing events have been observed in mice lacking all three *Slits*, these apparently occur before the decussated axons turn into the longitudinal plane (Long et al., 2004). Therefore, the factors/mechanisms that prevent ascending spinal axons from invading the ventral midline have not been identified.

Consistent with additional roles for Robo-Slit signaling in the pathfinding of descending axons, the longitudinal tracts in the brain, which they normal assemble into, are disorganized or defasciculated in mice lacking Robos or Slits (Lopez-Bendito et al., 2007; Farmer et al., 2008). For example, in mouse embryos, Robo-Slit signaling is required for organizing ipsilateral descending axons extended by midbrain neurons within longitudinal fascicles, but not the dorsoventral positioning of these fascicles (Farmer et al., 2008). Although the ventral-most medial longitudinal fascicle invades the ventral midline in the midbrain and hindbrain of *Slit1; Slit2* and *Robo1; Robo2* double mutants, resulting in a ventral shift of this tract, the other two lateral tracts do not shift ventrally or fasciculate into one large bundle (Farmer et al., 2008). This contrasts with the ventral shift of the spinal commissural axon-containing LF observed in mice lacking Robos/Slits. Whereas both ascending spinal commissural axons and ipsilaterally descending midbrain axons appear to rely on Slits at the ventral midline, the roles of Robo-Slit signaling are clearly model system-specific. These differences might be due to distinct sources of Slits, different downstream signaling systems and/or the presence of non-canonical signaling molecules, which interact with Robo-Slit signaling system.

PATHFINDING OF LONGITUDINAL AXONS IN VERTEBRATES: MIDBRAIN/FOREBRAIN DOPAMINERGIC TRACTS

In vertebrates, longitudinal axons emanating from spinal projection neurons pathfind through a rather homogenous spinal cord environment, which lacks conspicuous cellular specializations or choice points that could act as intermediate targets, before reaching the brain. In contrast, longitudinal axons originating from the neurons in higher brain areas encounter many distinct structures, which could act as guideposts and sources of key guidance cues, as they project to their appropriate synaptic targets. Therefore, the role of intermediate targets in regulating the pathfinding of longitudinal axons can often be more clearly delineated in the brain. One of the most prominent longitudinal tracts in the brain is the ascending mesodiencephalic dopaminergic (mdDA) pathway, which originates from dopaminergic neurons in the substantia nigra and ventral tegmental area in the midbrain and forebrain, and projects to the striatum as well as the cortex in the forebrain (Bjorklund and Dunnett, 2007).

ESTABLISHING THE ROSTROCAUDAL POLARITY OF mdDA AXONS

Several independent studies have shown that canonical axon guidance molecules, in particular, Semaphorin-3F (Sema3F) regulates various aspects of mdDA axon pathfinding via its receptor, Neuropilin-2 (Npn2), which is expressed on these axons (Kolk et al., 2009; Yamauchi et al., 2009). Initially, Sema3F, which is present at the midbrain-hindbrain boundary caudal to a subpopulation of mdDA cell bodies, appears to direct ascending mdDA axons rostrally by operating as a repulsive guidance cue (Yamauchi et al., 2009). A subset of mdDA axons, labeled by an antibody against tyrosine hydroxylase (TH), inappropriately projects caudally in *Npn2* mutant mice, supporting the role of Sema3F-Npn2 in establishing the initial rostrocaudal polarity of this projection (Yamauchi et al., 2009). It is interesting to note in this regard that *Sema3F* expression at the midbrain-hindbrain boundary might be controlled by the morphogen, fibroblast growth factor 8 (Fgf8), since Ffg8-soaked beads can induce ectopic *Sema3F* mRNA expression and disrupt the rostral projection of mdDA axons, whereas reducing Fgf8 signaling using a Fgf receptor tyrosine kinase inhibitor eliminates *Sema3F* mRNA expression (Yamauchi et al., 2009).

Just as for ascending spinal commissural axons, Wnts and planar cell polarity signaling molecules appear to orient longitudinally projecting mdDA axons, as well as other monoaminergic neurons in the brain (i.e., serotonergic [5-HT] axons) (Fenstermaker et al., 2010). Here, in *Wnt5a* mutant, a small subset of ascending mdDA axons initially mis-projects caudally in E12.5 embryos although the phenotype is corrected by E17.5. In contrast, E17.5 mouse embryos lacking the planar cell polarity components, Frizzled3, Vangl2, or Celsr3, which are all expressed on ascending mdDA axons, exhibit more prominent and persistent aberrant caudal mis-projections (Fenstermaker et al., 2010). Hindbrain 5-HT axons also show aberrant rostrocaudal projections in these mutant mice (Fenstermaker et al., 2010). Whereas the rostrocaudal bias of mdDA and 5-HT axon projections appear to be established by Frizzled3, Vangl2, and Celsr3, the organization and/or orientation of these cell bodies are also disrupted in the corresponding mutants, thus, complicating phenotypic analyses. It will be important to examine the causal relations between the organization/orientation of mdDA cell bodies and axons, if these events are related.

FASCICULATION OF mdDA AXONS

Robo-Slit signaling has a critical role in regulating fasciculation and rostral growth of ascending mdDA axons (Bagri et al., 2002; Dugan et al., 2011). *Slit1* and *Slit2* mRNA are expressed at the ventral midline and within the hypothalamus in the forebrain, as well as at the forebrain-midbrain border (Bagri et al., 2002; Dugan et al., 2011). Normally, TH-labeled mdDA axons, which express Robo1 and Robo2, project rostrally in close proximity to these *Slit1*/*Slit2*-epressing ventral structures (Dugan et al., 2011). However, in both *Slit1; Slit2* and *Robo1; Robo2* double mutants at E12.5, the initial projection of mdDA axons is defasciculated and disorganized (Dugan et al., 2011). Many mdDA axons appear to inappropriately project toward the ventral midline, which expresses high levels of *Slit1* and *Silt2*. One day later, at E13.5, although a subset of the defasciculated axons seems to recover and project in the appropriate direction within organized bundles, inappropriate invasion of the ventral midline is still evident and a part of the rostral track is hyperfasciculated, in both *Robo* and *Slit* double mutants (Dugan et al., 2011). In addition, *Robo1; Robo2*

double mutants display dorsal mis-projections, which are not as prominent in *Slit1; Slit2* mutants. Thus, some roles of Robo1 and Robo2 in orienting mdDA axons into the rostral track appear to be independent of Slits (Dugan et al., 2011). Taken together, it appears that Robo-Slit signaling is required for the fasciculation and organization of ascending mdDA tracts, and prevents these axons from crossing the ventral midline in the forebrain.

Sema3F-Npn2 signaling also appears to control fasciculation of TH-positive mdDA longitudinal tracts as they project rostrally, since these axons are observed to defasciculate in *Sema3F* or *Npn2* mutant mice (Kolk et al., 2009). In addition, Npn2- or Sema3F-independent phenotypes have been reported in mice lacking *Sema3F* or *Npn2*, respectively. In Sema3F mutants, a subset of the defasciculated mdDA axons mis-projects ventrally toward the lateral hypothalamus, whereas mdDA axons in *Npn2* mutants follow an aberrant route to reach the prefrontal cortex (Kolk et al., 2009). Importantly, the targeting of these mdDA axons to the prefrontal cortex is disrupted in both *Sema3F* and *Npn2* mutant mice, but in disparate ways. At E18.5, the number of mdDA axons innervating the target area of the prefrontal cortex is significantly reduced in *Sema3F* mutants, whereas the number of these axons projecting to the same target area is increased in *Npn2* mutant mice (Kolk et al., 2009). Interestingly and likely reflecting an example of error correction, the majority of mdDA axons are reported to reach their appropriate target areas in adult *Sema3F* mutants (Kolk et al., 2009). Further studies focusing on elucidating the *in vivo* roles of Sema3F and Npn2 signaling, as well as considering the potential involvement of other Semas should help clarify these complicated phenotypes. Most importantly, understanding the underlying mechanisms that control the relevant pathfinding events should reveal the consequences of the targeting errors made by mdDA axons in mouse embryos lacking Sema3F or Npn2.

PATHFINDING OF LONGITUDINAL AXONS IN VERTEBRATES: THE CORTICOSPINAL TRACT

One of the longest longitudinal axon-containing projections in the vertebrate CNS is the corticospinal tract, which connects the cerebral cortex to the spinal cord. Perhaps due to the relative ease of unilaterally labeling the component axons from the cerebral cortex, the complete trajectory followed by corticospinal tract axons has been carefully mapped. These axons are extended by pyramidal neurons located in layer V of the cerebral cortex, remain ipsilateral with respect to the midline (Stanfield, 1992; Brodal, 1998), and descend in the ventral region of the cerebral peduncle, through midbrain and hindbrain until they reach the caudal-most portion of the hindbrain, where most of these axons cross the midline dorsally to the contralateral side, forming the X-shaped pyramidal decussation. Corticospinal axons further project caudally within the marginal zone of the spinal cord, in a region containing the DF in rodents, and innervate neurons located within the spinal gray matter (Stanfield, 1992; Brodal, 1998).

A ROLE FOR ROBO-SLIT SIGNALING IN REGULATING THE IPSILATERAL PROJECTION OF THE CORTICOSPINAL TRACT IN THE BRAIN

As described above, the corticospinal tract initially projects in a purely ipsilateral manner within the brain. Accordingly, the mechanisms that maintain this laterality have a critical role in corticospinal tract formation. *Slit1* and *Slit2* mRNA are also expressed at the ventral midline of the forebrain, where these midline repellents create a barrier between the two sides of the rostral CNS (Bagri et al., 2002). Robo1 and Robo2 are expressed in particular populations of forebrain neurons/axons, including the major longitudinal projections that originate within the cortex, the corticospinal and corticofugal tracts (Lopez-Bendito et al., 2007), and Robo-Slit signaling prevents these tracts from crossing the midline in the forebrain (Bagri et al., 2002; Lopez-Bendito et al., 2007). Specifically, in *Robo1; Robo2* and *Slit1; Slit2* double mutants, the majority of the DiI-labeled corticospinal tract-associated axons aberrantly cross the midline at rostral levels before they would normally turn into the longitudinal plane (Bagri et al., 2002; Lopez-Bendito et al., 2007). Some of these misguided axons re-cross to the ipsilateral side of the brain, whereas others continue projecting into the contralateral side of the telencephalon (Lopez-Bendito et al., 2007). Thus, Robo-Slit signaling prevents corticospinal axons from inappropriately crossing the midline in the forebrain.

DECUSSATION OF THE CORTICOSPINAL TRACT

The hindbrain pyramids represent the most conspicuous intermediate targets for longitudinally projecting corticospinal axons. Although several classes of molecules have been identified as candidates for regulating the decussation of corticospinal axons within this brain region, thus far, mainly contact-dependent, short-range guidance molecules have been directly implicated in this process.

Most notably, the immunoglobin cell adhesion molecule (IgCAM), L1, is required for corticospinal axons to cross the ventral midline in the hindbrain (Cohen et al., 1997; Dahme et al., 1997). Although corticospinal axons appear to normally descend in the hindbrain of *L1* mutant mice, a subset of these axons fails to cross the midline in the lower hindbrain and inappropriately projects both ipsilaterally and contralaterally (Cohen et al., 1997). Some of mis-routed axons project dorsally to the ipsilateral DF or remain ventrally positioned but turn into the longitudinal plane and project caudally in the ventrolateral edge of the ipsilateral side of hindbrain (Cohen et al., 1997). Moreover, the number of caudally projecting axons in the spinal cord is severely reduced in adult mutants. Since the number of normally decussated corticospinal commissural axons is also reduced in the spinal cord of *L1* mutant mice, L1 might be required for the growth of these axons within the spinal cord. Although L1 is expressed on developing pyramidal fibers (Cohen et al., 1997), how L1 regulates the midline crossing of corticospinal axons remains to be determined. In this regard, it has been suggested that Sema3A secreted by the ventral spinal cord is capable of repelling cortical axons expressing L1 *in vitro*, and Neuropilin-1 (Npn1) and L1 form a receptor complex that likely transduces this Sema3A-mediated repulsive signal (Castellani et al., 2000). However, this is unlikely to be the mechanism underlying the formation of the pyramidal decussation, since corticospinal tracts form normally and on schedule in *Sema3A* mutant mice (Sibbe et al., 2007).

In addition to L1, another IgCAM, neural cell adhesion molecule (NCAM), has also been implicated in controlling the

pyramidal decussation of corticospinal axons (Rolf et al., 2002). The corticospinal axon pathfinding defects observed in *NCAM* mutants resemble the *L1* mutant phenotype in that they reveal the lack of decussation in the hindbrain and bilateral caudal projections in the spinal cord of early postnatal mice. Unlike *L1* mutant mice, however, only a small number of mis-routed axons are present on the ipsilateral side of the pyramid in *NCAM* adult mutants (Rolf et al., 2002). Whether these mis-projections were corrected or eliminated at later ages has not been investigated. Since corticospinal axons arrive later at the caudal hindbrain in *NCAM* mutant mice as compared to their wild type counterparts, the defects in corticospinal tracts appear to manifest themselves prior to the formation of the pyramidal decussation (Rolf et al., 2002).

The transmembrane Sema6A and its receptors PlexinA3 and PlexinA4 have also been implicated in regulating the decussation of corticospinal axons (Faulkner et al., 2008; Runker et al., 2008). In *Sema6A* single, *PlexinA4* single and *PlexinA3; PlexinA4* double mutant mice, corticospinal axons normally descend to the caudal hindbrain. Subsequently, however, some of these axons correctly decussate, but many others inappropriately projected to the ventrolateral edge of the ipsilateral hindbrain (Faulkner et al., 2008; Runker et al., 2008). Notably, however, the mis-guided axons continue projecting caudally (Faulkner et al., 2008; Runker et al., 2008). *PlexinA3* and *PlexinA4* mRNA is expressed by cortical neurons, and *Sema6A* and *PlexinA4* mRNA are found along the terrain through which corticospinal axons project in the caudal hindbrain and in the inferior olivary nuclei, which is located adjacent and lateral to the corticospinal tract in the pyramid (Faulkner et al., 2008; Runker et al., 2008). Collectively the loss of function phenotypes exhibited by the various *Sema* and *Plexin* mutant mice suggest that Sema6A-PlexinA3/4 signaling-mediated repulsion normally drives corticospinal axons toward the midline where they undergo decussation (Faulkner et al., 2008; Runker et al., 2008).

A reduction in the size of the pyramidal decussation has been also reported in Netrin1 receptor *Unc5c* (previously known as *Unc5h3*) mutant mice (Finger et al., 2002). The phenotypes observed in *Unc5c* mutants most closely resemble those displayed by *Sema6A* and *PlexinA3; PlexinA4* mouse mutants: the majority of corticospinal axons fail to cross the midline, and the misdirected axons continue projecting caudally in the lateral funiculus of the spinal cord. Moreover, these mis-routed corticospinal axons appear to fasciculate with each other in the lateral funiculus (Finger et al., 2002). Therefore, unlike in *L1* and *NCAM* mutants, the caudal projection of mis-routed corticospinal axons in *Sema6A*, *PlexinA3; A4,* and *Unc5c* mutants is intact and possibly regulated by other molecules found in both the DF and lateral funiculus. Since CAMs are known to promote axon outgrowth (Raper and Mason, 2010), L1 and NCAM might, at least to some extent, facilitate the caudally directed growth of the corticospinal axons within the spinal cord. Alternatively, the differences between the phenotypes exhibited by the various mutant mice might simply reflect the different techniques and experimental approaches used to visualize corticospinal axons/tracts.

CAUDAL GROWTH OF CORTICOSPINAL AXONS IN THE SPINAL CORD

After crossing the midline within the caudal hindbrain, rodent corticospinal axons project caudally in the DF of the spinal cord (Stanfield, 1992). Consistent with Wnt4 being required for the polarity of ascending spinal commissural axons (Lyuksyutova et al., 2003), Wnt1 and Wnt5a have been implicated as regulators of the caudal growth displayed by corticospinal axons within the spinal cord (Liu et al., 2005). Support for this model comes from the finding that *Wnt1* and *Wnt5a* mRNA is expressed in the dorsal spinal gray matter surrounding the DF in rostral (high) to caudal (low) gradients. In addition, the Wnt receptor, Receptor tyrosine kinase-related tyrosine kinase (Ryk)-like transmembrane receptor is expressed at high levels on corticospinal axons, and Wnt1/Wnt5a repel corticospinal axons expressing Ryk *in vitro* (Liu et al., 2005). Moreover, injection of a functional blocking anti-Ryk antibody into the cervical level spinal cord of neonatal mice retards the growth of descending corticospinal axons (Liu et al., 2005). With regard to these particular findings, it is important to note that the DF also contains the fasciculus gracilis and fasciculus cuneatus, which ascend from dorsal root ganglia to the lower hindbrain (Burt, 1993; Brodal, 1998). Thus, it would be interesting to determine whether Wnt1/Wnt5a facilitate the rostral growth of these dorsal-column-associated ascending axons, possibly through resident Wnt receptors that mediate attraction via Wnt gradients in the spinal cord. In addition, Ryk-mediated signaling through Wnts might be responsible for the caudal mis-projection of the corticospinal axons in mutant mice with pyramidal decussation defects, such as the *Sema6A* and *Unc5c* null mutants (Finger et al., 2002; Faulkner et al., 2008; Runker et al., 2008), mentioned above. Since *Wnt1/Wnt5a* mRNA expression is not present in the vicinity of the lateral funiculus (Liu et al., 2005), other Wnts found in this region could be presented to Ryk-bearing axons. In any case, assessing the role of Wnts *in vivo* might help to further understand the mechanisms that control the rostrocaudal polarity of corticospinal axons.

PREVENTING CORTICOSPINAL AXONS FROM RE-CROSSING THE MIDLINE IN THE SPINAL CORD

As reflected by the somatotopic organization of corticospinal neurons in the sensorimotor cortex, these descending axons innervate neurons at specific levels of the spinal cord (Stanfield, 1992; Kuang and Kalil, 1994). Upon reaching the appropriate rostrocaudal segments of the spinal cord, corticospinal axons project into the spinal gray matter, where they form connections with their specific synaptic targets (Stanfield, 1992; Brodal, 1998). Since corticospinal axons transmit signals from one side of the cerebral cortex to neurons located on the opposite side of the spinal cord, once they cross, these descending longitudinal axons must terminate on the contralateral side of the CNS and never re-cross the midline. Within the spinal cord gray matter, repulsive interactions between the EphA4 receptor tyrosine kinase and the transmembrane ephrinB3 ligands facilitate this pattern of innervation by preventing decussated corticospinal axons from re-crossing back to the ipsilateral side (Dottori et al., 1998; Kullander et al., 2001a; Yokoyama et al., 2001). EphrinB3 is selectively expressed at the ventral midline of the spinal cord and this short-range repulsive

Eph ligand forms a boundary separating axons on either side of the spinal cord (Kullander et al., 2001a; Yokoyama et al., 2001). Corticospinal axons express one of the ehrinB3 receptors, EphA4, and thereby regulate ephrinB3-mediated repulsive signaling cell autonomously (Kullander et al., 2001b). In both *ephrinB3* and *EphA4* mutant mice, corticospinal axons normally cross at the caudal hindbrain and project caudally in the contralateral DF (Kullander et al., 2001a,b; Yokoyama et al., 2001). However, after these axons enter the spinal cord gray matter, some of them re-cross the midline and innervate targets on the ipsilateral side of the spinal cord (Kullander et al., 2001a,b; Yokoyama et al., 2001). Since the majority of re-crossing corticospinal axons enter the ipsilateral side of the CNS via the spinal cord gray matter rather than through the DF, in *ephrinB3* and *EphA4* mutant mice (Kullander et al., 2001a,b), the laterality of descending longitudinal projections in the dorsal funiculi appears to be regulated by some other yet to be described mechanism. It is important to note that the midline barrier formed by ephrinB3 is critical for preventing the aberrant crossing of not only corticospinal axons, but also other EphA4-expressing axons in the spinal cord, such as those extended by ventral spinal interneurons (Kullander et al., 2003).

PATHFINDING OF LONGITUDINAL AXONS IN THE INVERTEBRATE CNS

THE ROLE OF Wnt-FRIZZLED SIGNALING IN *C. elegans*

In a striking example of evolutionary conservation, morphogens also appear to control the guidance of longitudinally projecting axons along the A-P axis in invertebrates. Consistent with the likely role of Wnts in regulating the polarity of post-crossing spinal commissural axons in the embryonic mouse spinal cord (see above), Wnt-Frizzled signaling has a key role in regulating rostrocaudal pathfinding decisions made by longitudinally projecting axons in *C. elegans*. Specifically, Wnt (lin-44) via the Frizzled (lin-17) receptor regulates the A-P orientation of PLM mechanosensory axons and dendrites (Hilliard and Bargmann, 2006). PLM mechanosensory neurons are bipolar and Frizzled (lin-17) is highly expressed on posteriorly growing dendrites. This asymmetric expression of Frizzled (lin-17) receptors is induced by Wnt (lin-44) and thus, Wnt (lin-44) and Frizzled (lin-17) signaling regulate the A-P orientation of PLM neurons neither by repelling nor attracting these axons or dendrites. In addition to establishing the A-P orientation of axons, longitudinal projections of mechanosensory axons are guided by Wnt-Frizzled signaling in *C. elegans* (Pan et al., 2006). However, opposite to what has been observed in the mouse spinal cord, caudally expressed Wnt (egl-20) operates as a repellent via Frizzled (mig-1 and mom-5) signaling to direct longitudinally projecting axons rostrally in *C. elegans* (Pan et al., 2006). Thus, although the role of Wnt-Frizzled signaling in regulating A-P polarity is conserved between mammals and worms, the mechanistic details are distinct across species.

THE ROLES OF ROBO RECEPTORS IN POSITIONING LONGITUDINAL TRACTS IN THE *DROSOPHILA* VENTRAL NERVE CORD

Further consistent with evolutionarily conserved roles for guidance systems that control longitudinal axon pathfinding, the involvement of Robos in regulating the lateral positioning of longitudinally projecting axons tracts was first demonstrated in the *Drosophila* ventral nerve cord (Rajagopalan et al., 2000; Simpson et al., 2000). The expression patterns of the three *Drosophila* Robo receptors, Robo1–3, on longitudinal axons define distinct mediolateral zones in the neuropile of the ventral nerve cord; Robo1 is expressed on axons in the medial zone, the intermediate zone contains axons that express Robo1 and Robo3, and axons that express all three Robos are present in the lateral zone, and disrupting these collective expression patterns predictably perturbs the lateral positioning of longitudinal axons (Rajagopalan et al., 2000; Simpson et al., 2000). In addition to the pronounced midline re-crossing phenotype displayed by *Robo1*, and occasionally *Robo2*, mutants, the loss of function phenotype of each *Robo* mutant is similar to the consequences of disabling Robo-Slit signaling in the vertebrate spinal cord; a major medial shift in the positioning of many longitudinal axons (see above). In particular, anti-Fasciclin II [FasII, marker of three major longitudinal tracts in the *Drosophila* CNS (Grenningloh et al., 1991)] labeling of intermediate fascicle reveals that the loss of *Robo3* function results in an inappropriate fusion of these axons with the medial fascicle (Rajagopalan et al., 2000; Simpson et al., 2000). In addition, the knockdown of *Robo3* in a *Robo2* mutant background gives rise to one large medial axon bundle representing a fusion of all three FasII-positive fascicles, whereas *Robo1* and *Robo2* double mutants display a midline collapse phenotype, similar to that observed in *Slit* mutants (Kidd et al., 1999; Simpson et al., 2000). These observations strongly suggest that Robo2 and Robo3 have critical roles in the proper lateral positioning of longitudinal tracts, and that the primary functions of Robo1 and Robo2 are to bar these axons from re-entering the midline. Accordingly, the role of *Drosophila* Robo3 appears to be analogous to that of vertebrate Robo1 and Robo2, whereas vertebrate Robo3 (Rig-1) operates in a manner similar to *Drosophila* Commissureless, by facilitating the passage of commissural axons across the ventral midline (Seeger et al., 1993; Keleman et al., 2002; Sabatier et al., 2004; Chen et al., 2008).

Regarding the mechanism through which Robos regulate the lateral positioning of longitudinal axons, it has recently been established that structural differences between Robo receptors do not have a crucial role in this process (Spitzweck et al., 2010). Rather, the gene expression profile of each Robo controls longitudinal axon sorting. This was elegantly demonstrated by replacing the genomic loci of each *Robo* with full length *Robo* sequences through homologous recombination and assessing the effects of these manipulations on longitudinal axon pathfinding (Spitzweck et al., 2010). Together, the findings strongly suggest that the timing, location, and/or level of each Robo gene are essential for achieving proper sorting of longitudinal axons in *Drosophila* ventral nerve cord.

Thus far, the role of the Robo ligand Slit, which operates as a potent repulsive guidance cue for a variety of invertebrate and vertebrate axons (Mastick et al., 2010; Ypsilanti et al., 2010), in the lateral positioning of longitudinal tracts has not been clearly established within the *Drosophila* ventral nerve cord. Although multiple populations of axons collapse on the midline in *Slit* mutants (Battye et al., 1999; Kidd et al., 1999), and the overexpression of *Slit* in midline glia cells disrupts the pathfinding of

commissural axons (Battye et al., 1999), the role(s) of Slit in regulating the guidance of post-crossing commissural axons has not been explicitly addressed (Dickson and Gilestro, 2006). In contrast, and as discussed above, Slits appear to regulate the sorting of longitudinal axons in the embryonic mouse spinal cord.

THE ROLE OF AXON FASCICULATION IN THE FORMATION OF LONGITUDINAL TRACTS WITHIN THE INVERTEBRATE CNS

The dynamic roles of axon fasciculation and defasciculation events on the pathfinding of longitudinally projecting axons were originally demonstrated in grasshopper embryos (Raper et al., 1983, 1984; Harrelson and Goodman, 1988; Raper and Mason, 2010). The observation that precise fasciculation patterns exist among populations of longitudinally projecting axons led to the identification of molecules that are selectively expressed on particular longitudinal tracts in *Drosophila*. One major class of fasciculation molecules is the IgCAM superfamily members, of which FasII is an example (Grenningloh et al., 1991). In the ventral nerve cord of *Drosophila FasII* mutants, intermediate and lateral fascicles are conspicuously defasciculated, and forced expression of *FasII* leads to partially fused longitudinal fascicles (Lin et al., 1994). These results support a role for FasII in mediating the fasciculation of longitudinally projecting axons in *Drosophila*. Notably, however, defasciculated or hyperfasciculated axons in genetically manipulated *FasII* embryos retain their ability to appropriately project along the A-P axis adjacent to the midline (Lin et al., 1994). Thus, it appears that FasII does not explicitly control the directed growth/pathfinding of longitudinal axons along the A-P axis of the *Drosophila* ventral nerve cord.

The classical cadherins represent another major class of CAMs, and N-cadherin, in particular, has been implicated in the fasciculation of FasII-positive axons and their assembly into longitudinal axon tracts (Iwai et al., 1997). N-cadherin is expressed broadly in the *Drosophila* CNS, with particularly high levels present on axons, and *N-cadherin* mutants display defects in the bundling and pathfinding of FasII-positive intermediate and lateral fascicles (Iwai et al., 1997). Reminiscent of the FasII mutant phenotype, the majority of improperly fasciculated axons appropriately project along the A-P axis in *Drosophila N-cadherin* mutants. Interestingly, the observed defects appear quite selective and specific given that N-cadherin is broadly and robustly expressed on axons within the *Drosophila* ventral nerve cord. To further dissect the role of N-cadherin in longitudinal tract formation, the pathfinding behavior of a genetically distinct population of neurons, defined by the expression of LIM homeodomain transcription factor, Apterous, was examined in N-cadherin null mutants. Axons extending from Apterous-positive neurons normally fasciculate tightly with each other and project ipsilaterally in the anterior direction along the most medial edge of the *Drosophila* ventral nerve cord (Lundgren et al., 1995). However, in *N-cadherin* mutants, these axons fail to fasciculate, and the dorsal-most axons project slightly lateral to their normal medial tract. Despite these defects Apterous axons continue to project rostrally in *N-cadherin* mutants (Iwai et al., 1997), indicating that like FasII, N-cadherin does not regulate this pathfinding decision. Notably, the perturbations in the pathfinding of N-cadherin-lacking Apterous axons resemble the defective fasciculation of these axons observed in *Apterous* mutants (Lundgren et al., 1995), raising the possibility that Apterous regulates N-cadherin expression/function. Overall, these studies suggest that although N-cadherin might not be required for the directed growth of axons along the A-P axis, it does ensure the fidelity of longitudinal axon tract formation in *Drosophila*.

In addition to the CAMs, Semas, which are cell surface or secreted molecules, and their receptors, the Plexins have been implicated in the formation of longitudinal axon tracts within the *Drosophila* CNS. For example, transmembrane Sema1A and its receptor PlexinA regulate the defasciculation of FasII-labeled laterally positioned longitudinal axons from their neighboring intermediate fascicles (Winberg et al., 1998; Yu et al., 1998). Specifically, the lateral fascicle in *Sema1A* or *PlexinA* mutants is disrupted and fused with the intermediate fascicle, and PlexinA regulates this process via repulsive signaling. These mutant phenotypes likely reflect defects in defasciculation, rather than fasciculation, since the lateral fascicle-associated axons apparently fail to break away from the intermediate fascicle (Winberg et al., 1998). Whereas transmembrane Sema1A-PlexA signaling selectively controls the assembly of laterally positioned FasII-positive axons into longitudinal tracts, secreted Sema2A and Sema2B appear to regulate the bundling of axons in the FasII-labeled intermediate fascicle, through the actions of PlexinB receptors (Wu et al., 2011). In a key recent study, it has been shown that in *Sema2A; Sema2B* double and *PlexinB* mutants, FasII-positive axons in intermediate fascicles defasciculate from each other and these tracts are severely disorganized (Wu et al., 2011). Here, Sema2A likely creates a repulsive boundary that constrains the positioning and growth of the intermediate fascicle. On the other hand, Sema2B facilitates the fasciculation of these axons, by acting as a short-range attractive cue (Wu et al., 2011). PlexinB is expressed at high levels in the region of the neuropile that contains intermediate and lateral tracts, and is also likely present on the first set of pioneer axons, which form the FasII-positive intermediate fascicle (Wu et al., 2011). Therefore, it appears that PlexinB controls the formation of the intermediate longitudinal fascicle by transducing Sema2A-dependent repulsive signals and Sema2B-mediated attraction (Wu et al., 2011).

In the *Drosophila* CNS, longitudinal axon tracts receive direct innervation from sensory axons (Boyan and Ball, 1993). Interestingly, PlexinB signaling activated by Sema2A and Sema2B also regulates the targeting of genetically distinct mechanosensory axons to the FasII-positive intermediate fascicle (Wu et al., 2011). Specifically, in *Sema2A; Sema2B* double or *PlexinB* mutant lines, particular mechanosensory axons fail to innervate axons located in the FasII-labeled intermediate fascicle. Since PlexinB appears to regulate the targeting of these mechanosensory axons in a cell autonomous manner, the failure of this sensory axon innervation is not the result of the defasciculation of the intermediate fascicle-associated axons, which has been observed in these mutant lines as mentioned above (Wu et al., 2011). This finding raises the possibility that targeting of other longitudinal fascicles to appropriate sensory axons is also coordinately regulated by Semas and their Plexin receptors.

Although these studies clearly show that the fasciculation of longitudinal tracts is tightly regulated by specific sets

and combinations of guidance molecules the consequences of the defective fasciculation events remain poorly understood. Ultimately, disrupted patterns of fasciculation might be expected to promote mis-targeting or defects in the pre-synaptic termination patterns on a given fascicle.

TARGETING OF LONGITUDINAL AXONS IN THE VERTEBRATE CNS

In contrast to the progress made in identifying molecules and mechanisms that regulate the pathfinding of longitudinal axons in the vertebrate CNS, considerably less is known about what controls the targeting of these axons. Although it is generally assumed that mis-directed axons, which pathfind along aberrant trajectories, will ultimately fail to reach their appropriate targets, this may not always be the case (see examples above). Accordingly, identifying the synaptic targets of longitudinally projecting axons and elucidating the molecular mechanisms that control the targeting of these axons should clarify key aspects of neural circuit formation in wild type and mutant phenotypes. Part of the lack of progress in elucidating mechanisms that control axon targeting can most likely be attributed to the technical limitations associated with tracing axons over long distances. For example, since many axonal tracers have slow diffusion rates in fixed tissue (Vercelli et al., 2000), these reagents would have to be delivered *in vivo* or into appropriate *in vitro* preparations to label the full extent of longitudinal axon tracts, and these are not always feasible options. In addition, pan-axonal tracers, such as DiI, are incapable of reliably and reproducibly labeling specific populations of axons and, thus it has not been possible to visualize particular sets of axons over long distances and assess the consequences of molecular perturbations on their pathfinding and targeting. Analogous to approaches that are routinely employed in invertebrate systems, recently developed genetically labeling strategies have now made it possible to visualize, and study the targeting of, long-range longitudinal projections within the vertebrate CNS.

ASCENDING LONGITUDINALLY PROJECTING SPINAL AXONS

Along with the technical limitations described above, the bilateral symmetry of the spinal cord and presence of both ipsilateral and commissural axons within the major longitudinal axon tracts of the marginal zone also confound attempts to visualize these long-range projections. The ascending spinal longitudinal tracts, in particular, are largely bilaterally symmetric with both sides of the LF and VF, but not the DF, containing contralaterally and ipsilaterally projecting axons (Kerr, 1975; Matsushita and Hosoya, 1979; Giesler et al., 1984; Burstein et al., 1990; Katter et al., 1991; Yezierski and Mendez, 1991). In addition, some of the component axons, such as those that compose the spinocerebellar tract, re-cross the midline in the cerebellum (Matsushita and Hosoya, 1979; Matsushita and Ikeda, 1980; Brodal, 1998). Accordingly, unilateral labeling carried out in intact animals is required to obtain unobstructed views of ascending longitudinal axons, and to assess the consequences of molecular/genetic manipulations on their pathfinding and targeting.

Unilateral labeling of axons *in vivo* can be achieved via the use of, *in ovo* and *in utero* unilateral electroporation strategies, in chick and mouse embryos, respectively, (Krull, 2004; Saito, 2006; Petros et al., 2009). In fact, *in ovo* electroporation of a pan-axonal reporter, has been used to show that both commissural and ipsilateral axons originating from a specific segment of the spinal cord (lumbosacral level 2) project rostrally to a common target, the cerebellum, in the E8–E13 chick brain (Arakawa et al., 2008).

To investigate the mechanisms that control the pathfinding and targeting of *particular classes* of spinal projection neurons, it is critical to first develop labeling methods that can be used to visualize genetically distinct populations of these neurons/axons. Dorsal spinal neurons represent a well-studied and major class of projection neurons (Nunes and Sotelo, 1985; Burstein et al., 1990; Yezierski and Mendez, 1991; Brodal, 1998), and subtypes of these neurons have been defined on the basis of transcription factor expression profiles (Helms and Johnson, 2003). For example, d1 dorsal spinal neurons are derived from progenitors that express the basic helix-loop-helix (bHLH) transcription factor Atoh1 (formerly Math1), and express the homeodomain (HD) transcription factors, Lhx2, Lhx9, BarH1, and Brn3a (Helms and Johnson, 2003). On the other hand, Neurog1- (bHLH family member) positive progenitors give rise to d2 neurons, which are defined by the expression of Lhx1, Lhx5, FoxD3, and Brn3a (Helms and Johnson, 2003). Based on these observations, a variety of transgenic reporter mice were generated to facilitate the mechanisms that control the development of d1 and d2 dorsal spinal neurons (Helms and Johnson, 1998; Nakada et al., 2004; Machold and Fishell, 2005; Saba et al., 2005; Wilson et al., 2008). However, the bilateral symmetry of the reporter gene expression patterns and the presence of endogenous labeling in the brain, has hampered the definitive identification of d1 and d2 targets (Helms and Johnson, 1998; Bermingham et al., 2001; Nakada et al., 2004; Saba et al., 2005). Nevertheless, DiI labeling in an *Aoth1-lacZ* knock-in (null for *Atoh1*) mouse line was carried out in an attempt to identify the brain targets of d1 neurons/axons (Bermingham et al., 2001). This study reported that the size of the DiI-labeled spinocerebellar tract within the hindbrain was reduced in $Atoh1^{lacZ/lacZ}$ mice compared to wild type and heterozygous littermates, raising the possibility that d1 axons target the cerebellum (Bermingham et al., 2001). More recently we have delivered *Atoh1* and *Neurog1* reporter constructs (Lumpkin et al., 2003; Nakada et al., 2004; Reeber et al., 2008) into the embryonic chick spinal cord via unilateral *in ovo* electroporation and achieved reproducible labeling of longitudinally projecting d1 and d2 axons. Moreover, we have found that both of these projection neurons target a variety of brain regions, including the cerebellum (N.S. and Z.K., unpublished observations). These observations support the feasibility of using genetic labeling strategies to visualize the long-range projections of genetically distinct spinal projection neurons and to carry out detailed analyses of spinal axon targeting in an *in vivo* setting.

DESCENDING CORTICOSPINAL AXONS

Anatomical considerations suggest that the targeting of descending corticospinal axons is somatotopically regulated, since collaterals of the primary corticospinal axons exit the DF and innervate the spinal cord gray matter at specific positions along the rostrocaudal axis (O'Leary and Koester, 1993; Kuang and Kalil, 1994).

The PSA modification of NCAM (PSA-NCAM) appears to facilitate collateral formation by modifying the fasciculation state of corticospinal axons within the DF (Daston et al., 1996). Whereas NCAM is expressed all along pathfinding corticospinal axons, PSA-NCAM is selectively present in the DF, where collateral formation occurs. Removal of PSA through enzymatic degradation reduces the number of collaterals at particular levels of the spinal cord (Daston et al., 1996). Despite these observations, exactly how the formation of axon collaterals is somatotopically regulated at specific segments of the spinal cord remains poorly defined.

Although corticospinal tracts are composed of ipsilateral and contralateral projections located rostral and caudal to the pyramidal decussation, respectively, the component axons retain their unilaterality on either side of the spinal cord (Stanfield, 1992). Accordingly, unilateral labeling strategies, like those we have used to visualize ascending spinal projection neuron tracts (see above), should not necessarily be required to elucidate the mechanisms that control corticospinal axon targeting in the spinal cord. Rather, transgenic reporter mice that can be used to visualize corticospinal tract axons (Bareyre et al., 2005) should be sufficient. In this regard, the recent use of corticospinal axon-specific reporter mice has led to the identification of Clark's column neurons, which contribute to the spinocerebellar projection, as targets of corticospinal axons (Hantman and Jessell, 2010). This new and important observation will likely facilitate a detailed investigation into the molecular mechanisms that control the guidance and targeting of corticospinal axons.

SUMMARY AND PERSPECTIVE

Just as longitudinally projecting axons must travel long distances in order to reach their synaptic targets and to transmit information between disparate regions of the CNS and from the environment to the brain, we have a long way to go before acquiring even a superficial understanding of the underlying guidance and targeting mechanisms. Despite the recent progress made in elucidating mechanisms that control particular phases of longitudinal axon growth/targeting in specific model vertebrate and invertebrate systems, many fundamental "big picture" questions remain. For example: (1) Do morphogens have central roles in longitudinal axon guidance and/or targeting or are they only required to set the polarity of axons as they turn into the longitudinal plane? (2) Do the mechanisms that control longitudinal axon guidance also control the targeting of these axons? (3) Do short-range axon-axon interactions on their own facilitate the formation of precisely positioned longitudinal axon tracts or is the directed and stereotypical growth of longitudinal tracts controlled by a complex interplay between long-range and short-range/adhesive guidance systems? (4) Does the same molecular logic control the guidance and targeting of ipsilateral and commissural axons and/or the formation of ascending and descending axonal tracts? (. . . as discussed above the answer seems to be a resounding no) (5) Are the mechanisms that control the long-range pathfinding and targeting of longitudinally projecting axons conserved across species and organisms? As we have suggested above, obtaining the answers to these and other burning questions in the field will require that state-of-the-art genetic labeling strategies initially be used, in mouse and chick embryos as well as in *Drosophila* and *C. elegans*, to carefully map the projection patterns of longitudinal axons and to identify their synaptic targets. Once this has been achieved, a combination of complementary gain- and loss-of-function manipulations in the various model systems should, ultimately, make it possible to elucidate the molecular logic that controls longitudinal axon guidance and targeting. Importantly, these likely to be tedious, time-consuming and ground breaking studies will surely provide exciting new insights into neural circuit formation across species and the molecular genetic underpinnings of neurological dysfunction.

REFERENCES

Arakawa, T., Iwashita, M., Matsuzaki, F., Suzuki, T., and Yamamoto, T. (2008). Paths, elongation, and projections of ascending chick embryonic spinal commissural neurons after crossing the floor plate. *Brain Res.* 1223, 25–33.

Avraham, O., Hadas, Y., Vald, L., Hong, S., Song, M. R., and Klar, A. (2010). Motor and dorsal root ganglion axons serve as choice points for the ipsilateral turning of dI3 axons. *J. Neurosci.* 30, 15546–15557.

Avraham, O., Hadas, Y., Vald, L., Zisman, S., Schejter, A., Visel, A., and Klar, A. (2009). Transcriptional control of axonal guidance and sorting in dorsal interneurons by the Lim-HD proteins Lhx9 and Lhx1. *Neural Dev.* 4, 21.

Bagri, A., Marín, O., Plump, A. S., Mak, J., Pleasure, S. J., Rubenstein, J. L., and Tessier-Lavigne, M. (2002). Slit proteins prevent midline crossing and determine the dorsoventral position of major axonal pathways in the mammalian forebrain. *Neuron* 33, 233–248.

Bareyre, F. M., Kerschensteiner, M., Misgeld, T., and Sanes, J. R. (2005). Transgenic labeling of the corticospinal tract for monitoring axonal responses to spinal cord injury. *Nat. Med.* 11, 1355–1360.

Battye, R., Stevens, A., and Jacobs, J. R. (1999). Axon repulsion from the midline of the *Drosophila* CNS requires slit function. *Development* 126, 2475–2481.

Bermingham, N. A., Hassan, B. A., Wang, V. Y., Fernandez, M., Banfi, S., Bellen, H. J., Fritzsch, B., and Zoghbi, H. Y. (2001). Proprioceptor pathway development is dependent on Math1. *Neuron* 30, 411–422.

Björkeland, M., and Boivie, J. (1984). The termination of spinomesencephalic fibers in cat. *Anat. Embryol. (Berl.)* 170, 265–277.

Bjorklund, A., and Dunnett, S. B. (2007). Dopamine neuron systems in the brain: an update. *Trends Neurosci.* 30, 194–202.

Bourikas, D., Pekarik, V., Baeriswyl, T., Grunditz, A., Sadhu, R., Nardo, M., and Stoeckli, E. T. (2005). Sonic hedgehog guides commissural axons along the longitudinal axis of the spinal cord. *Nat. Neurosci.* 8, 297–304.

Bovolenta, P. (2005). Morphogen signaling at the vertebrate growth cone: a few cases or a general strategy? *J. Neurobiol.* 64, 405–416.

Bovolenta, P., and Dodd, J. (1990). Guidance of commissural growth cones at the floor plate in embryonic rat spinal cord. *Development* 109, 435–447.

Boyan, G. S., and Ball, E. E. (1993). The grasshopper, *Drosophila* and neuronal homology (advantages of the insect nervous system for the neuroscientist). *Prog. Neurobiol.* 41, 657–682.

Brodal, P. (1998). *The Central Nervous System: Structure and Function.* New York, NY: Oxford University Press, Inc.

Burstein, R., Dado, R. J., and Giesler, G. J. Jr. (1990). The cells of origin of the spinothalamic tract of the rat: a quantitative reexamination. *Brain Res.* 511, 329–337.

Burt, A. M. (1993). *Textbook of Neuroanatomy*. Philadelphia, PA: W. B. Saunders Co.

Castellani, V., Chedotal, A., Schachner, M., Faivre-Sarrailh, C., and Rougon, G. V. (2000). Analysis of the L1-deficient mouse phenotype reveals cross-talk between Sema3A and L1 signaling pathways in axonal guidance. *Neuron* 27, 237–249.

Charron, F. D. R., and Tessier-Lavigne, M. (2005). Novel brain wiring functions for classical morphogens: a role as graded positional cues in axon guidance. *Development* 132, 2251–2262.

Chen, Z., Gore, B. B., Long, H., Ma, L., and Tessier-Lavigne, M. (2008). Alternative splicing of the Robo3

axon guidance receptor governs the midline switch from attraction to repulsion. *Neuron* 58, 325–332.

Cohen, N. R., Taylor, J. S. H., Scott, L. B., Guillery, R. W., Soriano, P., and Furley, A. J. W. (1997). Errors in corticospinal axon guidance in mice lacking the neural cell adhesion molecule L1. *Curr. Biol.* 8, 26–33.

Dahme, M., Bartsch, U., Martini, R., Anliker, B., Schachner, M., and Mantei, N. (1997). Disruption of the mouse L1 gene leads to malformations of the nervous system. *Nat. Genet.* 17, 346–349.

Daston, M. M., Bastmeyer, M., Rutishauser, U., and O'Leary, D. D. M. (1996). Spatially restricted increase in polysialic acid enhances corticospinal axon branching related to target recognition and innervation. *J. Neurosci.* 16, 5488–5497.

Dickson, B. J., and Gilestro, G. F. (2006). Regulation of commissural axon pathfinding by slit and its Robo receptors. *Annu. Rev. Cell Dev. Biol.* 22, 651–675.

Dickson, B. J., and Zou, Y. (2010). Navigating intermediate targets: the nervous system midline. *Cold Spring Harb. Perspect. Biol.* 2, a002055.

Domanitskaya, E., Wacker, A., Mauti, O., Baeriswyl, T., Esteve, P., Bovolenta, P., and Stoeckli, E. T. (2010). Sonic hedgehog guides post-crossing commissural axons both directly and indirectly by regulating Wnt activity. *J. Neurosci.* 30, 11167–11176.

Dottori, M., Hartley, L., Galea, M., Paxinos, G., Polizzotto, M., Kilpatrick, T., Bartlett, P. F., Murphy, M., Kontgen, F., and Boyd, A. W. (1998). EphA4 (Sek1) receptor tyrosine kinase is required for the development of the corticospinal tract. *Proc. Natl. Acad. Sci. U.S.A.* 95, 13248–13253.

Dugan, J. P., Stratton, A., Riley, H. P., Farmer, W. T., and Mastick, G. S. (2011). Midbrain dopaminergic axons are guided longitudinally through the diencephalon by Slit/Robo signals. *Mol. Cell. Neurosci.* 46, 347–356.

Farmer, W. T., Altick, A. L., Nural, H. F., Dugan, J. P., Kidd, T., Charron, F., and Mastick, G. S. (2008). Pioneer longitudinal axons navigate using floor plate and Slit/Robo signals. *Development* 135, 3643–3653.

Faulkner, R. L., Low, L. K., Liu, X. B., Coble, J., Jones, E. G., and Cheng, H. J. (2008). Dorsal turning of motor corticospinal axons at the pyramidal decussation requires plexin signaling. *Neural Dev.* 3, 21.

Fenstermaker, A. G., Prasad, A. A., Bechara, A., Adolfs, Y., Tissir, F., Goffinet, A., Zou, Y., and Pasterkamp, R. J. (2010). Wnt/planar cell polarity signaling controls the anterior-posterior organization of monoaminergic axons in the brainstem. *J. Neurosci.* 30, 16053–16064.

Finger, J. H., Bronson, R. T., Harris, B., Johnson, K., Przyborski, S. A., and Ackerman, S. L. (2002). The netrin 1 receptors Unc5h3 and Dcc are necessary at multiple choice points for the guidance of corticospinal tract axons. *J. Neurosci.* 22, 10346–10356.

Giesler, G. J., Nahin, R. L., and Madsen, A. M. (1984). Postsynaptic dorsal column pathway of the rat. I. Anatomical studies. *J. Neurophysiol.* 51, 260–275.

Giesler, G. J. Jr., Spiel, H. R., and Willis, W. D. (1981). Organization of spinothalamic tract axons within the rat spinal cord. *J. Comp. Neurol.* 195, 243–252.

Grenningloh, G., Jay Rehm, E., and Goodman, C. S. (1991). Genetic analysis of growth cone guidance in *Drosophila*: fasciclin II functions as a neuronal recognition molecule. *Cell* 67, 45–57.

Hantman, A. W., and Jessell, T. M. (2010). Clarke's column neurons as the focus of a corticospinal corollary circuit. *Nat. Neurosci.* 13, 1233–1239.

Harrelson, A., and Goodman, C. (1988). Growth cone guidance in insects: fasciclin II is a member of the immunoglobulin superfamily. *Science* 242, 700–708.

Helms, A. W., and Johnson, J. E. (1998). Progenitors of dorsal commissural interneurons are defined by Math1 expression. *Development* 125, 919–928.

Helms, A. W., and Johnson, J. E. (2003). Specification of dorsal spinal cord interneurons. *Curr. Opin. Neurobiol.* 13, 42–49.

Hilliard, M. A., and Bargmann, C. I. (2006). Wnt signals and frizzled activity orient anterior-posterior axon outgrowth in *C. elegans*. *Dev. Cell* 10, 379–390.

Imondi, R., and Kaprielian, Z. (2001). Commissural axon pathfinding on the contralateral side of the floor plate: a role for B-class ephrins in specifying the dorsoventral position of longitudinally projecting commissural axons. *Development* 128, 4859–4871.

Imondi, R., Wideman, C., and Kaprielian, Z. (2000). Complementary expression of transmembrane ephrins and their receptors in the mouse spinal cord: a possible role in constraining the orientation of longitudinally projecting axons. *Development* 127, 1397–1410.

Iwai, Y., Usui, T., Hirano, S., Steward, R., Takeichi, M., and Uemura, T. (1997). Axon patterning requires DN-cadherin, a novel neuronal adhesion receptor, in the *Drosophila* embryonic CNS. *Neuron* 19, 77–89.

Jaworski, A., Long, H., and Tessier-Lavigne, M. (2010). Collaborative and specialized functions of Robo1 and Robo2 in spinal commissural axon guidance. *J. Neurosci.* 30, 9445–9453.

Kadison, S. R., and Kaprielian, Z. (2004). Diversity of contralateral commissural projections in the embryonic rodent spinal cord. *J. Comp. Neurol.* 472, 411–422.

Katter, J. T., Burstein, R., and Giesler, G. J. (1991). The cells of origin of the spinohypothalamic tract in cats. *J. Comp. Neurol.* 303, 101–112.

Keleman, K., Rajagopalan, S., Cleppien, D., Teis, D., Paiha, K., Huber, L. A., Technau, G. M., and Dickson, B. J. (2002). Comm sorts robo to control axon guidance at the *Drosophila* midline. *Cell* 110, 415–427.

Kerr, F. W. L. (1975). The ventral spinothalamic tract and other ascending systems of the ventral funiculus of the spinal cord. *J. Comp. Neurol.* 159, 335–355.

Kidd, T., Bland, K. S., and Goodman, C. S. (1999). Slit is the midline repellent for the robo receptor in *Drosophila*. *Cell* 96, 785–794.

Kiehn, O. (2006). Locomotor circuits in the mammalian spinal cord. *Annu. Rev. Neurosci.* 29, 279–306.

Kolk, S. M., Gunput, R. A., Tran, T. S., van den Heuvel, D. M., Prasad, A. A., Hellemons, A. J., Adolfs, Y., Ginty, D. D., Kolodkin, A. L., Burbach, J. P., Smidt, M. P., and Pasterkamp, R. J. (2009). Semaphorin 3F is a bifunctional guidance cue for dopaminergic axons and controls their fasciculation, channeling, rostral growth, and intracortical targeting. *J. Neurosci.* 29, 12542–12557.

Krull, C. E. (2004). A primer on using in ovo electroporation to analyze gene function. *Dev. Dyn.* 229, 433–439.

Kuang, R. Z., and Kalil, K. (1994). Development of specificity in corticospinal connections by axon collaterals branching selectively into appropriate spinal targets. *J. Comp. Neurol.* 344, 270–282.

Kullander, K., Butt, S. J., Lebret, J. M., Lundfald, L., Restrepo, C. E., Rydstrom, A., Klein, R., and Kiehn, O. (2003). Role of EphA4 and EphrinB3 in local neuronal circuits that control walking. *Science* 299, 1889–1892.

Kullander, K., Croll, S. D., Zimmer, M., Pan, L., McClain, J., Hughes, V., Zabski, S., Dechiara, T. M., Klein, R. D., Yancopoulos, G. D., and Gale, N. W. (2001a). Ephrin-B3 is the midline barrier that prevents corticospinal tract axons from recrossing, allowing for unilateral motor control. *Genes Dev.* 15, 877–888.

Kullander, K., Mather, N. K., Diella, F., Dottori, M., Boyd, A. W., and Klein, R. D. (2001b). Kinase-dependent and kinase-independent functions of EphA4 receptors in major axon tract formation *in vivo*. *Neuron* 29, 73–84.

Lin, D. M., Fetter, R. D., Kopczynski, C., Grenningloh, G., and Goodman, C. S. (1994). Genetic analysis of fasciclin II in *Drosophila*: defasciculation, refasciculation, and altered fasciculation. *Neuron* 13, 1055–1069.

Liu, Y., Shi, J., Lu, C. C., Wang, Z. B., Lyuksyutova, A. I., Song, X. J., and Zou, Y. (2005). Ryk-mediated Wnt repulsion regulates posterior-directed growth of corticospinal tract. *Nat. Neurosci.* 8, 1151–1159.

Long, H., Sabatier, C., Ma, L., Plump, A., Yuan, W., Ornitz, D. M., Tamada, A., Murakami, F., Goodman, C. S., and Tessier-Lavigne, M. (2004). Conserved roles for Slit and Robo proteins in midline commissural axon guidance. *Neuron* 42, 213–223.

Lopez-Bendito, G., Flames, N., Ma, L., Fouquet, C., Di Meglio, T., Chedotal, A., Tessier-Lavigne, M., and Marin, O. (2007). Robo1 and Robo2 cooperate to control the guidance of major axonal tracts in the mammalian forebrain. *J. Neurosci.* 27, 3395–3407.

Lumpkin, E. A., Collisson, T., Parab, P., Omer-Abdalla, A., Haeberle, H., Chen, P., Doetzlhofer, A., White, P., Groves, A., Segil, N., and Johnson, J. E. (2003). Math1-driven GFP expression in the developing nervous system of transgenic mice. *Gene Expr. Patterns* 3, 389–395.

Lundgren, S. E., Callahan, C. A., Thor, S., and Thomas, J. B. (1995). Control of neuronal pathway selection by the *Drosophila* LIM homeodomain gene apterous. *Development* 121, 1769–1773.

Lyuksyutova, A. I., Lu, C.-C., Milanesio, N., King, L. A., Guo, N., Wang, Y., Nathans, J., Tessier-Lavigne, M., and Zou, Y. (2003). Anterior-posterior guidance of commissural axons by Wnt-frizzled signaling. *Science* 302, 1984–1988.

Machold, R., and Fishell, G. (2005). Math1 is expressed in temporally

discrete pools of cerebellar rhombic-lip neural progenitors. *Neuron* 48, 17–24.

Mastick, G. S., Farmer, W. T., Altick, A. L., Nural, H. F., Dugan, J. P., Kidd, T., and Charron, F. (2010). Longitudinal axons are guided by Slit/Robo signals from the floor plate. *Cell Adh. Migr.* 4, 337–341.

Matsushita, M., and Hosoya, Y. (1979). Cells of origin of the spinocerebellar tract in the rat, studied with the method of retrograde transport of horseradish peroxidase. *Brain Res.* 173, 185–200.

Matsushita, M., and Ikeda, M. (1980). Spinocerebellar projections to the vermis of the posterior lobe and the paramedian lobule in the cat, as studied by retrograde transport of horseradish peroxidase. *J. Comp. Neurol.* 192, 143–162.

Nakada, Y., Parab, P., Simmons, A., Omer-Abdalla, A., and Johnson, J. E. (2004). Separable enhancer sequences regulate the expression of the neural bHLH transcription factor neurogenin 1. *Dev. Biol.* 271, 479–487.

Nunes, M. L. A., and Sotelo, C. (1985). Development of the spinocerebellar system in the postnatal rat. *J. Comp. Neurol.* 237, 291–306.

O'Leary, D. D. M., and Koester, S. E. (1993). Development of projection neuron types, axon pathways, and patterned connections of the mammalian cortex. *Neuron* 10, 991–1006.

Pan, C. L., Howell, J. E., Clark, S. G., Hilliard, M., Cordes, S., Bargmann, C. I., and Garriga, G. (2006). Multiple Wnts and frizzled receptors regulate anteriorly directed cell and growth cone migrations in *Caenorhabditis elegans*. *Dev. Cell* 10, 367–377.

Petros, T. J., Rebsam, A., and Mason, C. A. (2009). In utero and *ex vivo* electroporation for gene expression in mouse retinal ganglion cells. *J. Vis. Exp.* 24, e1333.

Rajagopalan, S., Vivancos, V., Nicolas, E., and Dickson, B. J. (2000). Selecting a longitudinal pathway: Robo receptors specify the lateral position of axons in the *Drosophila* CNS. *Cell* 103, 1033–1045.

Raper, J., Bastiani, M., and Goodman, C. (1983). Pathfinding by neuronal growth cones in grasshopper embryos. II. Selective fasciculation onto specific axonal pathways. *J. Neurosci.* 3, 31–41.

Raper, J., Bastiani, M., and Goodman, C. (1984). Pathfinding by neuronal growth cones in grasshopper embryos. IV. The effects of ablating the A and P axons upon the behavior of the G growth cone. *J. Neurosci.* 4, 2329–2345.

Raper, J., and Mason, C. (2010). Cellular strategies of axonal pathfinding. *Cold Spring Harb. Perspect. Biol.* 2, a001933.

Reeber, S. L., Sakai, N., Nakada, Y., Dumas, J., Dobrenis, K., Johnson, J. E., and Kaprielian, Z. (2008). Manipulating Robo expression *in vivo* perturbs commissural axon pathfinding in the chick spinal cord. *J. Neurosci.* 28, 8698–8708.

Rolf, B., Bastmeyer, M., Schachner, M., and Bartsch, U. (2002). Pathfinding errors of corticospinal axons in neural cell adhesion molecule-deficient mice. *J. Neurosci.* 22, 8357–8362.

Runker, A. E., Little, G. E., Suto, F., Fujisawa, H., and Mitchell, K. J. (2008). Semaphorin-6A controls guidance of corticospinal tract axons at multiple choice points. *Neural Dev.* 3, 34.

Saba, R., Johnson, J. E., and Saito, T. (2005). Commissural neuron identity is specified by a homeodomain protein, Mbh1, that is directly downstream of Math1. *Development* 132, 2147–2155.

Sabatier, C., Plump, A. S., Le, M., Brose, K., Tamada, A., Murakami, F., Lee, E. Y. H. P., and Tessier-Lavigne, M. (2004). The divergent Robo family protein Rig-1/Robo3 is a negative regulator of slit responsiveness required for midline crossing by commissural axons. *Cell* 117, 157–169.

Saito, T. (2006). *In vivo* electroporation in the embryonic mouse central nervous system. *Nat. Protoc.* 1, 1552–1558.

Sánchez-Camacho, C., and Bovolenta, P. (2009). Emerging mechanisms in morphogen-mediated axon guidance. *Bioessays* 31, 1013–1025.

Seeger, M., Tear, G., Ferres-Marco, D., and Goodman, C. S. (1993). Mutations affecting growth cone guidance in *Drosophila*: genes necessary for guidance toward or away from the midline. *Neuron* 10, 409–426.

Shafer, B., Onishi, K., Lo, C., Colakoglu, G., and Zou, Y. (2011). Vangl2 promotes Wnt/planar cell polarity-like signaling by antagonizing Dvl1-mediated feedback inhibition in growth cone guidance. *Dev. Cell* 20, 177–191.

Sibbe, M., Taniguchi, M., Schachner, M., and Bartsch, U. (2007). Development of the corticospinal tract in Semaphorin3A- and CD24-deficient mice. *Neuroscience* 150, 898–904.

Simpson, J. H., Bland, K. S., Fetter, R. D., and Goodman, C. S. (2000). Short-range and long-range guidance by Slit and its Robo receptors: a combinatorial code of Robo receptors controls lateral position. *Cell* 103, 1019–1032.

Spitzweck, B., Brankatschk, M., and Dickson, B. J. (2010). Distinct protein domains and expression patterns confer divergent axon guidance functions for *Drosophila* Robo receptors. *Cell* 140, 409–420.

Stanfield, B. B. (1992). The development of the corticospinal projection. *Prog. Neurobiol.* 38, 169–202.

Tissir, F., and Goffinet, A. M. (2010). Planar cell polarity signaling in neural development. *Curr. Opin. Neurobiol.* 20, 572–577.

Vercelli, A., Repici, M., Garbossa, D., and Grimaldi, A. (2000). Recent techniques for tracing pathways in the central nervous system of developing and adult mammals. *Brain Res. Bull.* 51, 11–28.

Willis, W. D., Jr. (2007). The somatosensory system, with emphasis on structures important for pain. *Brain Res. Rev.* 55, 297–313.

Wilson, S. I., Shafer, B., Lee, K. J., and Dodd, J. (2008). A molecular program for contralateral trajectory: Rig-1 control by LIM homeodomain transcription factors. *Neuron* 59, 413–424.

Winberg, M. L., Noordermeer, J. N., Tamagnone, L., Comoglio, P. M., Spriggs, M. K., Tessier-Lavigne, M., and Goodman, C. S. (1998). Plexin A is a neuronal semaphorin receptor that controls axon guidance. *Cell* 95, 903–916.

Wu, Z., Sweeney, L. B., Ayoob, J. C., Chak, K., Andreone, B. J., Ohyama, T., Kerr, R., Luo, L., Zlatic, M., and Kolodkin, A. L. (2011). A combinatorial semaphorin code instructs the initial steps of sensory circuit assembly in the *Drosophila* CNS. *Neuron* 70, 281–298.

Xu, Q., and Grant, G. (1994). Course of spinocerebellar axons in the ventral and lateral funiculi of the spinal cord with projections to the anterior lobe: an experimental anatomical study in the cat with retrograde tracing techniques. *J. Comp. Neurol.* 345, 288–302.

Xu, Q., and Grant, G. (2005). Course of spinocerebellar axons in the ventral and lateral funiculi of the spinal cord with projections to the posterior cerebellar termination area: an experimental anatomical study in the cat, using a retrograde tracing technique. *Exp. Brain Res.* 162, 250–256.

Yamauchi, K., Mizushima, S., Tamada, A., Yamamoto, N., Takashima, S., and Murakami, F. (2009). FGF8 signaling regulates growth of midbrain dopaminergic axons by inducing semaphorin 3F. *J. Neurosci.* 29, 4044–4055.

Yezierski, R. P., and Mendez, C. M. (1991). Spinal distribution and collateral projections of rat spinomesencephalic tract cells. *Neuroscience* 44, 113–130.

Yokoyama, N., Romero, M. I., Cowan, C. A., Galvan, P., Helmbacher, F., Charnay, P., Parada, L. F., and Henkemeyer, M. (2001). Forward signaling mediated by ephrin-B3 prevents contralateral corticospinal axons from recrossing the spinal cord midline. *Neuron* 29, 85–97.

Ypsilanti, A. R., Zagar, Y., and Chedotal, A. (2010). Moving away from the midline: new developments for Slit and Robo. *Development* 137, 1939–1952.

Yu, H.-H., Araj, H. H., Ralls, S. A., and Kolodkin, A. L. (1998). The transmembrane Semaphorin Sema I is required in *Drosophila* for embryonic motor and CNS axon guidance. *Neuron* 20, 207–220.

Zou, Y., and Lyuksyutova, A. I. (2007). Morphogens as conserved axon guidance cues. *Curr. Opin. Neurobiol.* 17, 22–28.

Conflict of Interest Statement: The authors declare that the research was conducted in the absence of any commercial or financial relationships that could be construed as a potential conflict of interest.

Received: 27 February 2012; accepted: 14 April 2012; published online: 04 May 2012.

Citation: Sakai N and Kaprielian Z (2012) Guidance of longitudinally projecting axons in the developing central nervous system. Front. Mol. Neurosci. 5:59. doi: 10.3389/fnmol.2012.00059

frontiers in
MOLECULAR NEUROSCIENCE

ORIGINAL RESEARCH ARTICLE
published: 22 May 2012
doi: 10.3389/fnmol.2012.00067

RhoA is dispensable for axon guidance of sensory neurons in the mouse dorsal root ganglia

Jennifer R. Leslie[1], Fumiyasu Imai[1], Xuan Zhou[2], Richard A. Lang[1,3], Yi Zheng[2] and Yutaka Yoshida[1]*

[1] *Divisions of Developmental Biology, Cincinnati Children's Hospital Medical Center, Cincinnati, OH, USA*
[2] *Experimental Hematology and Cancer Biology, Cincinnati Children's Hospital Medical Center, Cincinnati, OH, USA*
[3] *Pediatric Ophthalmology, Cincinnati Children's Hospital Medical Center, Cincinnati, OH, USA*

Edited by:
James Jontes, Ohio State University, USA

Reviewed by:
Zaven Kaprielian, Albert Einstein College of Medicine of Yeshiva University, USA
Tracy S. Tran, Rutgers University, USA

***Correspondence:**
Yutaka Yoshida, Division of Developmental Biology, Cincinnati Children's Hospital Medical Center, 3333 Burnet Avenue, Cincinnati, OH 45229, USA.
e-mail: yutaka.yoshida@cchmc.org

RhoA, a member of the Rho family small GTPases, has been shown to play important roles in axon guidance. However, to date, the physiological function of RhoA in axon guidance events *in vivo* has not been determined genetically in animals. Here we show that *RhoA* mRNA is strongly expressed by sensory neurons in the developing mouse dorsal root ganglia (DRG). We have deleted *RhoA* in sensory neurons of the DRG using *RhoA*-floxed mice under the *Wnt1-Cre* driver in which Cre is strongly expressed in sensory neurons. Peripheral projections of sensory neurons appear normal and there are no detectable defects in the central projections of either cutaneous or proprioceptive sensory neurons in $RhoA^{f/f}$; *Wnt1-Cre* mice. Furthermore, a co-culture assay using DRG explants from $RhoA^{f/f}$; *Wnt1-Cre* embryos, and 293T cells expressing semaphorin3A (Sema3A) reveals that RhoA is not required for Sema3A-mediated axonal repulsion of sensory neurons. Expression of RhoC, a closely related family member, is increased in *RhoA*-deficient sensory neurons and may play a compensatory role in this context. Taken together, these genetic studies demonstrate that RhoA is dispensable for peripheral and central projections of sensory neurons in the DRG.

Keywords: RhoA, axon guidance, semaphorin, dorsal root ganglia, cutaneous sensory neurons, proprioceptive sensory neurons, spinal cord

INTRODUCTION

RhoA, a member of the small Rho GTPase family that regulates the cytoskeleton, has been implicated in various processes during the nervous system development, including the formation of adherens junctions, neuronal migration, and axon guidance (Giniger, 2002; Guan and Rao, 2003; Gallo and Letourneau, 2004; Heasman and Ridley, 2008; Hall and Lalli, 2010). The functions of RhoA in the mammalian nervous system have mainly been discerned from studies using a dominant negative or a knockdown approach. The physiological roles and functions of RhoA in the mammalian nervous system have just begun to be elucidated by loss-of-function studies using conditional gene-targeting strategies (Herzog et al., 2011; Katayama et al., 2011; Cappello et al., 2012). These recent studies demonstrate that RhoA is essential for proper formation of adherens junctions and proliferation of neural progenitor cells in the mouse nervous system (Herzog et al., 2011; Katayama et al., 2011; Cappello et al., 2012), which is consistent with previous *in vitro* and invertebrate studies (Fukata and Kaibuchi, 2001; Bloor and Kiehart, 2002; Magie et al., 2002; Yamada and Nelson, 2007). However, it remained unclear whether RhoA is required for other functions, including axon guidance, in the mammalian nervous system.

Extensive studies using *in vitro* culture experiments have shown that activation of RhoA induces growth cone collapse and axonal repulsion by increasing actomyosin contractility (Giniger, 2002; Guan and Rao, 2003; Gallo and Letourneau, 2004; Heasman and Ridley, 2008; Hall and Lalli, 2010). For example, *in vitro* experiments have implicated RhoA in Sema3A-mediated growth cone collapse of sensory neurons in the DRG (Dontchev and Letourneau, 2002; Wu et al., 2005; Hengst et al., 2006). Suppression of ROCK, a RhoA effector, by pharmacological inhibitors reduces Sema3A-induced growth cone collapse (Dontchev and Letourneau, 2002). In addition, Sema3A induces local translation of RhoA, and a knockdown approach reveals that RhoA is necessary for Sema3A-mediated growth cone collapse of DRG sensory neurons (Wu et al., 2005; Hengst et al., 2006). Despite these previous studies, the requirement of RhoA in Sema3A-dependent or -independent axonal repulsion *in vivo* during mammalian nervous system development remains unanswered.

To determine the physiological roles of RhoA in axon guidance, we have taken a loss-of-function approach. Since *RhoA* is strongly expressed by DRG neurons during development, *RhoA* was deleted from the DRG using *RhoA*-floxed mice together with *Wnt1-Cre* or *Advillin-Cre* mice in which Cre is expressed in the DRG. Surprisingly, loss of RhoA does not cause any obvious defects in the peripheral or central projections of DRG sensory neurons. In addition, RhoA is not required for Sema3A-mediated DRG axonal repulsion. Importantly, the protein level of RhoC, a related family member, is up-regulated in DRGs from $RhoA^{f/f}$; *Wnt1-Cre* embryos. Taken together, these findings suggest that RhoA itself is not essential for axon guidance of DRG sensory

neurons and that RhoC may compensate for RhoA function in the DRG *in vivo*.

MATERIALS AND METHODS

MICE

The following mouse strains were used in this study: *RhoA*-floxed (Chauhan et al., 2011; Katayama et al., 2011; Melendez et al., 2011), *Wnt1-Cre* (Danielian et al., 1998), and *Advillin-Cre* (da Silva et al., 2011). We used $RhoA^{f/w}$; *Wnt1-Cre* or $RhoA^{f/w}$; *Advillin-Cre* mice as controls.

TISSUE PREPARATION

Spinal cords and their surrounding tissues were dissected from embryos at embryonic day (E) 10.5, E13.5, E15.5, E16.5, E17.5, and postnatal day (P) 1. They were then fixed with 4% paraformaldehyde (PFA) on ice for 2 h for immunofluorescence staining or overnight for *in situ* hybridization. Afterwards, they were cryoprotected in 30% sucrose, embedded in OCT compound, and sectioned at 16 μm.

IMMUNOFLUORESCENCE

For immunofluorescence, cryosections were stained with the following antibodies: rabbit anti-parvalbumine (PV) (Swant), rabbit anti-TrkA (R&D systems), goat anti-TrkC (R&D systems), rabbit anti-CGRP (Peninsula Lab), and guinea pig anti-vGlut1 (Chemicon). Alexa 488 and Cy3-conjugated secondary antibodies were purchased from Invitrogen and Jackson Immuno Research. Immunohistochemistry was performed as described (Leslie et al., 2011). Images were obtained using a LSM510 confocal microscope (Zeiss).

In situ HYBRIDIZATION

Digoxigenin (DIG)-labeled cRNA probes were used for *in situ* hybridization as described Schaeren-Wiemers and Gerfin-Moser (1993).

DRG REPULSION ASSAY

DRG explants from E12.5 embryos were co-cultured with 293T cell aggregates expressing Sema3A and/or GFP in collagen gel matrices for 48 h in the presence of NGF, then fixed with 4% PFA, and immunostained with mouse anti-Tuj1 antibody (Covance), and Cy3-conjugated secondary antibody. Images were obtained on an Axioplan microscope (Zeiss).

WHOLE-MOUNT IMMUNOSTAINING

Whole-mount immunostaining was performed on E10.5 embryos for neurofilament staining or E13.5 embyos for peripherin staining according the method described by Huber et al. (2005) and Mandai et al. (2009), respectively. Briefly, the embryos were fixed with 4% PFA overnight, after which they were rinsed with phosphate buffered saline (PBS) three times and then fixed in Dent's fix (20% DMSO, 80% Methanol) overnight. The embryos were washed in PBS three times. The primary antibody, anti-neurofilament 2H3 (Developmental Studies Hybridoma Bank) or rabbit anti-peripherin (Millipore) was added in blocking solution (5% normal goat serum, 75% PBS, 20% DMSO) and incubated at room temperature for 3–4 days. The embryos were washed with PBS five times for 1 h each. Then, an Alexa 488-conjugated secondary antibody (Invitrogen) was added in blocking solution and kept in the dark for 1–2 days. The embryos were washed five times in PBS before being viewed.

IMMUNOBLOTTING

Samples were lysed using RIPA buffer (Cell Signaling Technology) according to manufactory's suggestion. Supernatants were collected for SDS-PAGE and transferred to PVDF membrane (Bio-Rad Laboratories). Specific protein expression was detected using the following antibodies: anti-RhoA (Cell Signaling Technology), anti-RhoC (Cell Signaling Technology), anti-Cdc42 (Cell Signaling Technology), anti-Lamin B (Santa cruz), and anti-Rac1 (BD Transduction Laboratories).

RESULTS

RhoA IS EXPRESSED BY BOTH SENSORY AND MOTOR NEURONS

To examine the expression pattern of *RhoA*, we performed *in situ* hybridization at various time points during development in the lumbar spinal cord and the DRG of wild-type mice. At E10.5, *RhoA* appears to be ubiquitously expressed throughout the spinal cord but showed relatively high expression in motor neurons and neural progenitors (**Figure 1A**). *RhoA* was expressed by most or all DRG sensory neurons at E10.5 (**Figure 1E**). At E13.5, strong expression of *RhoA* was detected in motor neurons (**Figure 1B**). At E16.5 and P1, similar to E13.5, *RhoA* was ubiquitously expressed in the spinal cord with high expression in motor neurons (**Figures 1C,D**). In the DRG, strong expression of *RhoA* was detected throughout development from E10.5 to P1 (**Figures 1E–H**). These expression analyses suggest that RhoA may have a role in spinal neurons including motor neurons and DRG sensory neurons. In this study, we focus on the expression of *RhoA* in the DRG.

NO OBVIOUS DEFECTS IN PERIPHERAL PROJECTIONS OF SENSORY NEURONS IN $RhoA^{f/f}$; *Wnt1-Cre* EMBRYOS

To determine the physiological roles of RhoA in DRG sensory neurons, we deleted *RhoA* in DRG sensory neurons using *RhoA*-floxed mice (Chauhan et al., 2011; Katayama et al., 2011; Melendez et al., 2011) together with *Wnt1-Cre* mice (Danielian et al., 1998; Hsu et al., 2010). Cre is expressed in the DRG and in the dorsal spinal cord of *Wnt1-Cre* mice (Danielian et al., 1998; Hsu et al., 2010). We confirmed that most RhoA expression was indeed deleted from DRG sensory neurons by performing Western blot analysis on DRG tissues from E12.5 control and $RhoA^{f/f}$; *Wnt1-Cre* embryos (**Figure 2**). As shown in **Figure 2**, RhoA was greatly reduced in $RhoA^{f/f}$; *Wnt1-Cre* embryos compared to control embryos. The expression of Cdc42 as well as Rac1 in the DRG was not changed in $RhoA^{f/f}$; *Wnt1-Cre* embryos compared to control embryos (**Figure 2**).

We first examined the peripheral projections of DRG sensory neurons of E10.5 $RhoA^{f/f}$; *Wnt1-Cre* embryos. To do this, we performed whole-mount immunostaining using anti-neurofilament antibody, which visualizes peripheral axonal projections of both sensory and motor neurons. DRG sensory neurons projected axons to the peripheral tissues of E10.5 $RhoA^{f/f}$; *Wnt1-Cre*

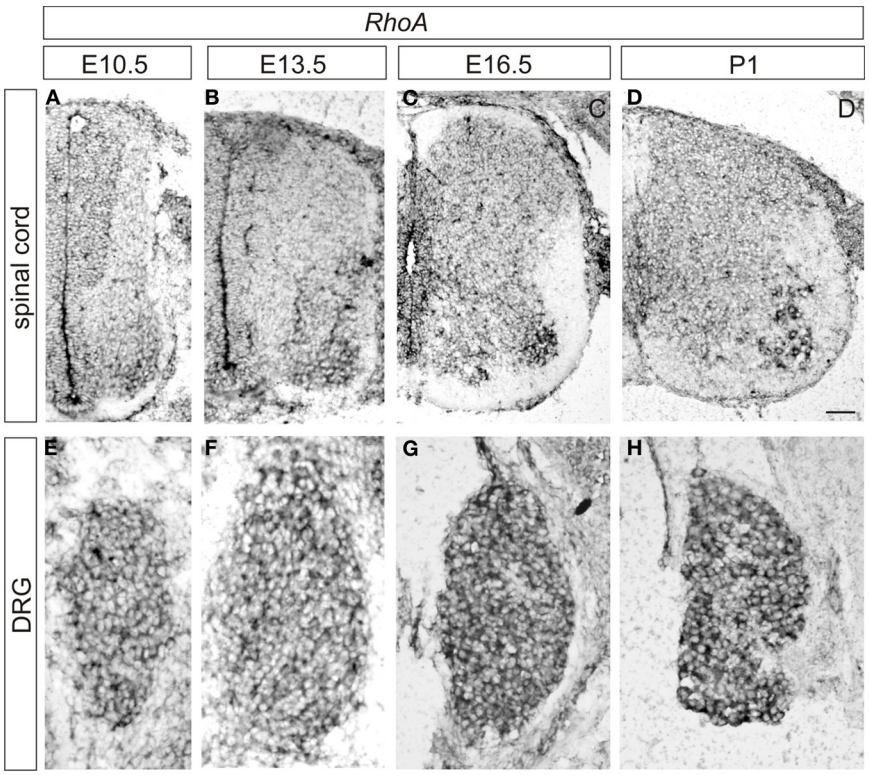

FIGURE 1 | Expression of *RhoA* in the developing mouse DRG and spinal cord. (A–D) Expression of *RhoA* in the spinal cord at E10.5 **(A)**, E13.5 **(B)**, E16.5 **(C)**, and P1 **(D)**. **(E–H)** Expression of *RhoA* in the DRG at E10.5 **(A)**, E13.5 **(B)**, E16.5 **(C)**, and P1 **(D)**. Scale bar, 50 μm.

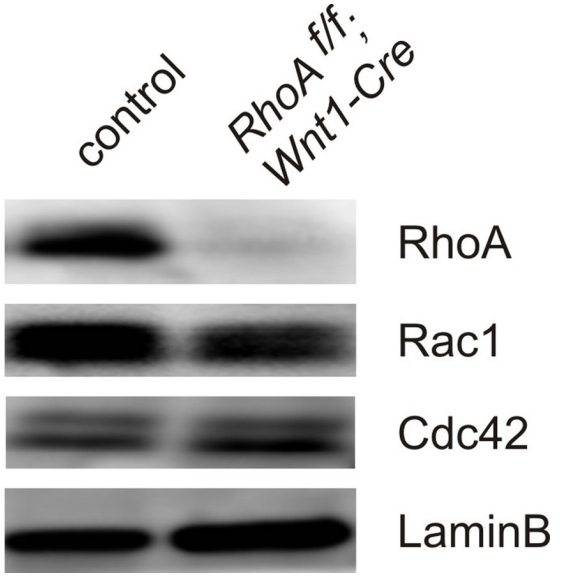

FIGURE 2 | Expression of RhoA, Rac1, and Cdc42 in DRGs from E12.5 control and *RhoA*$^{f/f}$*; Wnt1-Cre* embryos. RhoA, Rac, and Cdc42 proteins were evaluated by Western blotting using DRGs from E12.5 control and *RhoA*$^{f/f}$*; Wnt1-Cre* embryos. RhoA protein was significantly reduced in DRGs from *RhoA*$^{f/f}$*; Wnt1-Cre* embryos compared to control DRGs. *RhoA* deletion did not affect protein expression of Rac1 and Cdc42. We examined expression of LaminB protein as an internal control.

embryos similar to control embryos (**Figures 3A–D**). To further examine peripheral projections at E13.5, we performed whole-mount anti-peripherin immunostaining to visualize the peripheral axons in the distal limb (Mandai et al., 2009). We did not find any obvious defects in peripherin^{+} peripheral axons in the distal limb of E13.5 *RhoA*$^{f/f}$*; Wnt1-Cre* embryos (**Figures 3E,F**). Although we cannot exclude the subtle defects in peripheral axons in *RhoA*$^{f/f}$*; Wnt1-Cre* embryos, RhoA is unlikely to have a major role in peripheral projections of DRG sensory neurons.

PROPRIOCEPTIVE AXONAL PROJECTIONS SHOW TYPICAL PATTERNING IN *RhoA*$^{f/f}$*; Wnt1-Cre* EMBRYOS

Next, we examined central projections of DRG sensory neurons in the spinal cord. DRG sensory neurons are subdivided into two major groups, proprioceptive and cutaneous sensory neurons (Brown, 1981; Koerber and Mendell, 1992). Proprioceptive neurons convey information about the state of muscle contraction and limb position, whereas cutaneous neurons mediate a wide range of noxious and innocuous stimuli (Brown, 1981; Koerber and Mendell, 1992). Proprioceptive sensory afferents project to the intermediate or ventral spinal cord, while cutaneous sensory neurons project their axons to the superficial dorsal horn (Brown, 1981; Koerber and Mendell, 1992). We analyzed the numbers of proprioceptive sensory neurons and proprioceptive axonal projections using an anti-Pv antibody, which marks all proprioceptive sensory neurons (Honda, 1995; Arber et al., 2000),

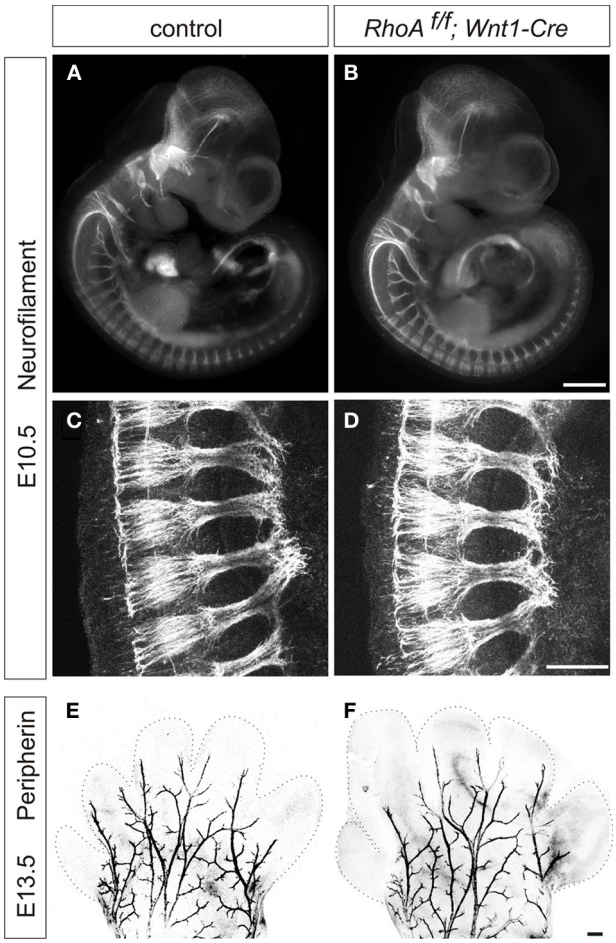

FIGURE 3 | Whole-mount neurofilament and peripherin staining. **(A–D)** Control and *RhoA*$^{f/f}$*; Wnt1-Cre* embryos were stained with anti-neurofilament (NF) antibody at E10.5. **(C,D)** show enlarged views of Plexus region. **(E,F)** Forelimbs of control and *RhoA*$^{f/f}$*; Wnt1-Cre* embryos were stained with anti-peripherin antibody at E13.5. There were no obvious defects in NF^{+} or peripherin^{+} axons in *RhoA*$^{f/f}$*; Wnt1-Cre* embryos compared to control embryos. Scale bars, 100 μm **(B,F)** and 20 μm **(D)**.

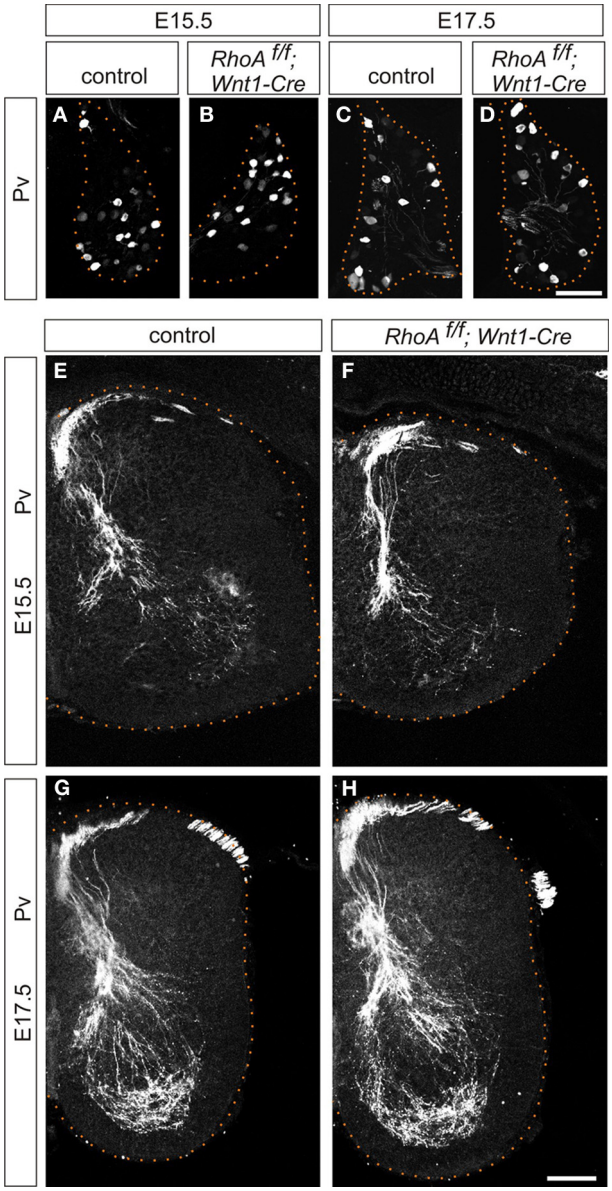

FIGURE 4 | Proprioceptive sensory neurons and proprioceptive axonal projections in the spinal cord of *RhoA*$^{f/f}$*; Wnt1-Cre* embryos. **(A–D)** Pv^{+} proprioceptive sensory neurons in DRGs from control and *RhoA*$^{f/f}$*; Wnt1-Cre* embryos at E15.5 and E17.5. **(E–H)** Pv^{+} proprioceptive axonal projections in the spinal cord of control and *RhoA*$^{f/f}$*; Wnt1-Cre* embryos at E15.5 and E17.5. Scale bars, 100 μm.

in *RhoA*$^{f/f}$*; Wnt1-Cre* embryos. There was no difference in the numbers of Pv^{+} proprioceptive sensory neurons in the DRG between control and *RhoA*$^{f/f}$*; Wnt1-Cre* embryos at E15.5 and E17.5 (**Figures 4A–D**). In control embryos at E15.5 and E17.5, the proprioceptive axons entered the spinal cord medially and projected to the ventral spinal cord (**Figures 4E,G**). There were no obvious defects in proprioceptive axonal projections at E15.5 and E17.5 in *RhoA*$^{f/f}$*; Wnt1-Cre* embryos compared to control embryos (**Figures 4E–H**). Thus, these data suggest that RhoA is not necessary for establishing proprioceptive axonal trajectories in the spinal cord.

RhoA IS NOT INVOLVED IN ESTABLISHING CUTANEOUS AXONAL PROJECTIONS

We next analyzed cutaneous sensory neurons in *RhoA*$^{f/f}$*; Wnt1-Cre* embryos. To do this we performed immunohistochemistry with an anti-TrkA antibody, which marks both cell bodies and axons of cutaneous sensory neurons during mouse embryogenesis. The numbers of TrkA^{+} cutaneous sensory neurons in the DRG were not changed between E13.5–E17.5 control and *RhoA*$^{f/f}$*; Wnt1-Cre* embryos (**Figures 5A,C,E,G,I,K**). We also analyzed cutaneous axonal projections in the spinal cord in *RhoA*$^{f/f}$*; Wnt1-Cre* embryos. Cutaneous axons did not penetrate the spinal cord at E13.5, but penetrated the spinal cord laterally and projected in the dorsal spinal cord at E15.5 and E17.5

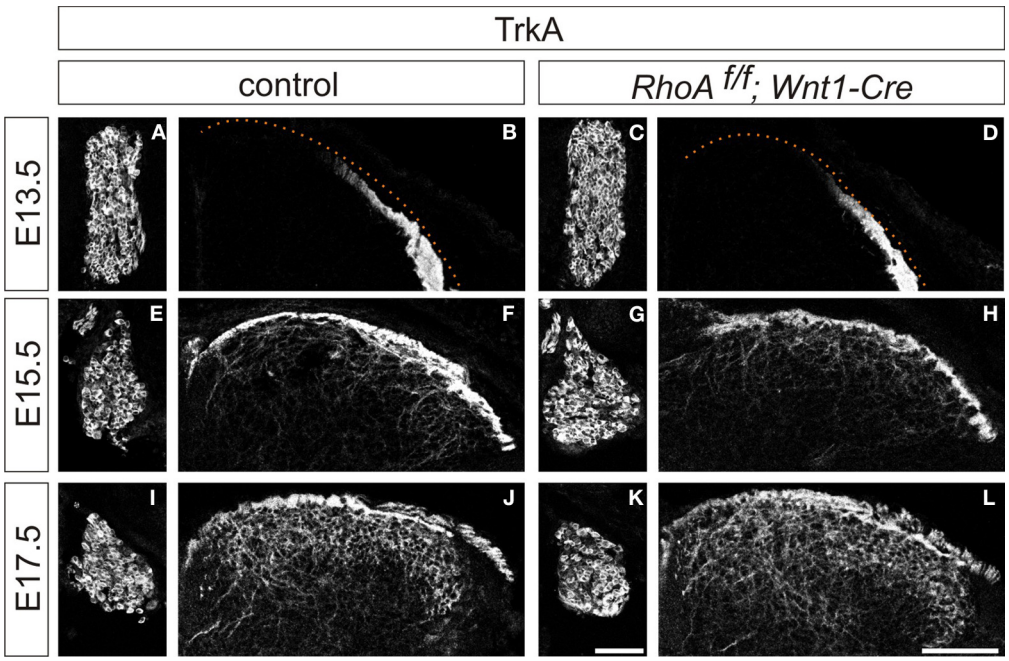

FIGURE 5 | Cutaneous sensory neurons and cutaneous axonal projections in the spinal cord of *RhoA*$^{f/f}$*; Wnt1-Cre* embryos. (**A,E,I** and **C,G,K**) TrkA^{+} cutaneous sensory neurons in DRGs from control and *RhoA*$^{f/f}$*; Wnt1-Cre* embryos at E15.5 and E17.5. (**B,F,J** and **D,H,L**) TrkA^{+} cutaneous axonal projections in the spinal cord of control and *RhoA*$^{f/f}$*; Wnt1-Cre* embryos at E15.5 and E17.5. Scale bars, 100 μm.

in control embryos (**Figures 5B,F,J**). *RhoA*-deficient cutaneous axons displayed axonal trajectories similar to control embryos at E13.5, E15.5, and E17.5 (**Figures 5D,H,L**). Thus, RhoA is not necessary for the establishment of proper cutaneous axonal projections in the spinal cord at these embryonic stages. During postnatal development, cutaneous sensory neurons are further subdivided into different groups, which project axons to different laminae within the dorsal spinal cord. These different types of neurons are marked by different molecular markers. For example, calcitonin-gene-related-peptide (CGRP)-positive thinly myelinated cutaneous axons terminate in lamina I and outer lamina II of the dorsal horn in the spinal cord (Lawson, 2002). Isolectin IB4-, a marker of some primary afferent C fibers, positive and non-myelinated cutaneous axons, terminate in lamina II (Molliver et al., 1997; Fang et al., 2006). Furthermore, vesicular glutamate transporter 1 (vGlut1)-positive myelinated cutaneous afferents terminate in laminae III–V (Todd et al., 2003). Since most *RhoA*$^{f/f}$*; Wnt1-Cre* mice died before birth with severe brain defects (Katayama et al., 2011; data not shown), we used another Cre driver mouse line, *Advillin-Cre* (da Silva et al., 2011), whose expression starts at E12.5 in the DRG (Hasegawa et al., 2007). *RhoA*$^{f/f}$*; Advillin-Cre* mice were born in normal numbers and survived into adulthood. We examined CGPR^{+}, IB4^{+}, and vGlut1^{+} axonal projections of cutaneous sensory neurons in the P8 spinal cord of *RhoA*$^{f/f}$*; Advillin-Cre* mice. There was clear laminar segregation of different classes of cutaneous sensory axons both in control and *RhoA*$^{f/f}$*; Advillin-Cre* mice (**Figure 6**). Therefore, RhoA is unlikely to be involved in regulating laminar specific cutaneous axonal projections in the spinal cord during early mouse postnatal stages.

RhoA IS NOT REQUIRED FOR Sema3A-MEDIATED AXONAL REPULSION

Since it has been reported that RhoA is required for Sema3A-mediated growth cone collapse of DRG sensory neurons using a knockdown approach (Wu et al., 2005; Hengst et al., 2006), we examined Sema3A-mediated axonal repulsion of DRG neurons from *RhoA*$^{f/f}$*; Wnt1-Cre* embryos. To do this we performed co-cultures of E12.5 DRG explants from control or *RhoA*$^{f/f}$*; Wnt1-Cre* embryos with 293T cells expressing GFP and/or Sema3A. E12.5 DRG axons from control embryos were repelled by Sema3A (**Figure 7B**). Similarly, *RhoA*-deficient DRG axons were also repelled by Sema3A (**Figure 7D**). This is in comparison to the unperturbed axonal growth of either set of DRGs in the presence of only GFP-transfected 293T cells (**Figures 7A,C**). These data suggest that RhoA itself is not essential for Sema3A-mediated DRG axonal repulsion.

RhoC IS UP-REGULATED IN THE DRG IN THE ABSENCE OF RhoA

Since RhoA has other related family members (Wennerberg and Der, 2004; Wheeler and Ridley, 2004), they may have a redundant function with RhoA in the DRG. Therefore, we examined the expression of RhoC by Western Blot analysis, since RhoC seems to be functionally the closest family member to RhoA (Wennerberg and Der, 2004; Wheeler and Ridley, 2004). We found that RhoC was significantly up-regulated in the DRG from *RhoA*$^{f/f}$*; Wnt1-Cre* embryos compared to control embryos (**Figure 8**). These results suggest that RhoC may compensate for RhoA in the DRG.

DISCUSSION

In this study we show that the conditional deletion of *RhoA* in the DRG using either *Wnt1-Cre* or *Advillin-Cre* drivers does not have

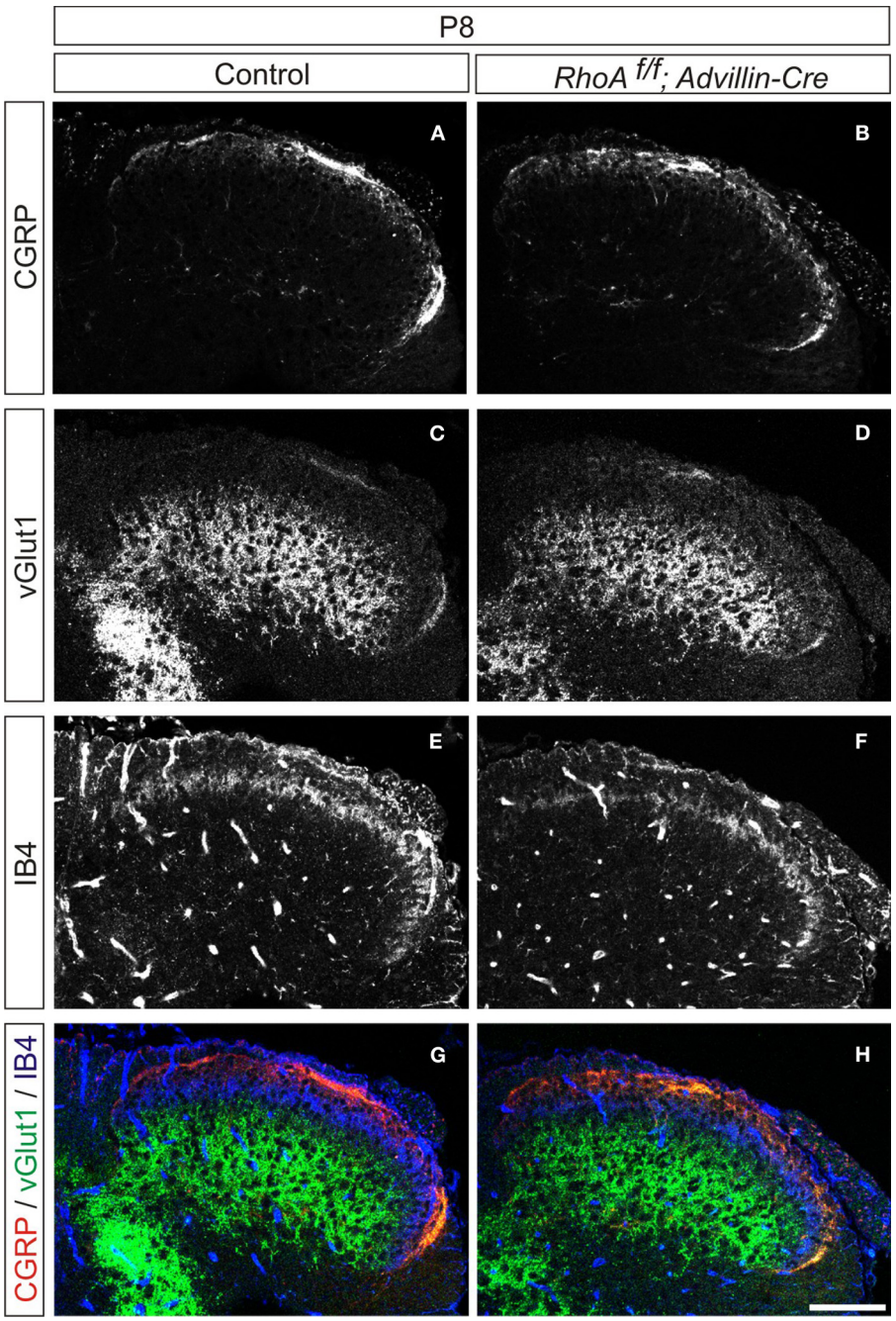

FIGURE 6 | Organization of cutaneous afferent projections in *RhoA*$^{f/f}$*; Advillin-Cre* mice. (A,B) CGRP expression, **(C,D)** vGlut1 expression, **(E,F)** IB4-binding, and **(G,H)** merged views of CGRP (red), vGlut1 (green), and IB4-binding (blue) in P8 control and *RhoA*$^{f/f}$*; Advillin-Cre* mice. Scale bar, 100 μm.

any obvious effect on either peripheral or central projections of DRG sensory neurons. In addition, loss of RhoA in the DRG does not change responses of DRG axons to Sema3A. Furthermore, RhoC protein is increased in the DRGs of *RhoA*$^{f/f}$*; Wnt1-Cre* embryos compared to control embryos. This suggests that RhoA itself is not required for axon guidance of DRG sensory neurons and that the related protein RhoC may compensate for loss of RhoA function.

LOSS OF RhoA DOES NOT CAUSE ANY OBVIOUS DEFECTS IN PROPRIOCEPTIVE OR CUTANEOUS AXONAL PROJECTIONS

Many previous *in vitro* and *in vivo* studies have suggested important roles for RhoA in axon guidance (Giniger, 2002; Guan and Rao, 2003; Gallo and Letourneau, 2004; Heasman and Ridley, 2008; Hall and Lalli, 2010). However, it remained unknown whether RhoA is in fact required for axon guidance events *in vivo* in the mammalian nervous system, since a loss-of-function

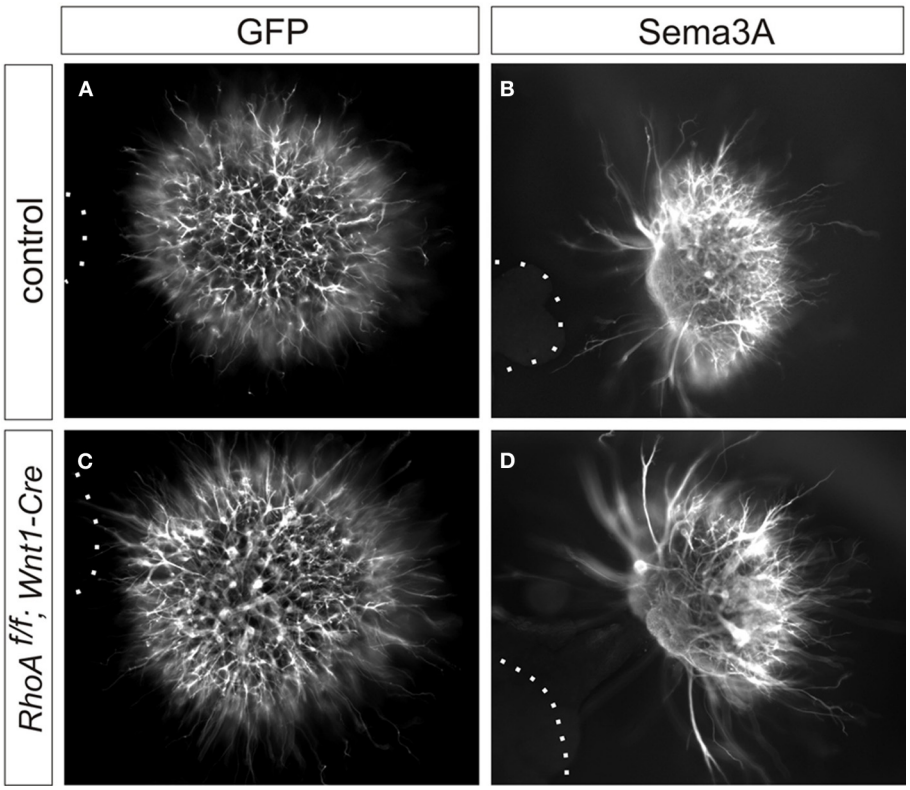

FIGURE 7 | Sema3A-induced DRG axonal repulsion *in vitro*. (A–D) Co-culture of DRG explants from control and *RhoA*$^{f/f}$*; Wnt1-Cre* embryos with GFP **(A,C)**, or Sema3A and GFP **(B,D)** transfected cell aggregates. The axons of DRG neurons were examined by anti-TuJ1 antibody. Both DRG axons from control and *RhoA*$^{f/f}$*; Wnt1-Cre* embryos were repelled by Sema3A. Dotted lines outline aggregates of 293T cells.

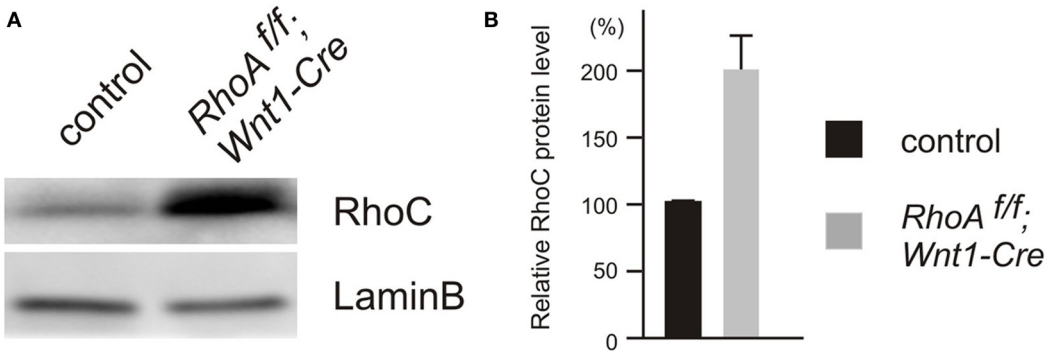

FIGURE 8 | Expression of RhoC in DRGs from E12.5 control and *RhoA*$^{f/f}$*; Wnt1-Cre* embryos. (A) RhoC protein was evaluated by Western blotting using DRGs from E12.5 control and *RhoA*$^{f/f}$*; Wnt1-Cre* embryos, and RhoC protein was up-regulated in DRGs from *RhoA*$^{f/f}$*; Wnt1-Cre* embryos compared to control DRGs. **(B)** The quantification of levels of RhoC protein expression in DRGs from E12.5 control and *RhoA*$^{f/f}$*; Wnt1-Cre* embryos. We determined expression of LaminB protein as an internal control ($n = 4$).

approach had not been performed to test the physiological roles of RhoA in axon guidance. In this study, we found that *RhoA* mRNA is strongly expressed in the DRG during mouse development, and we deleted *RhoA* in DRG neurons using either *Wnt1-Cre* or *Advillin-Cre* drivers. Surprisingly, we found that RhoA is not essential for mouse DRG neurons to project and reach their peripheral and central targets. First, we found that deletion of *RhoA* using *Wnt1-Cre* mice did not cause any aberrant peripheral axonal projections of sensory neurons that were detectable using anti-neurofilament and anti-peripherin antibodies. Second, there was no obvious disruption in the axon guidance of central projections of proprioceptive or cutaneous sensory axons. Therefore, it appears that RhoA itself is not crucial for the proper axonal pathfinding of DRG sensory neurons.

RhoA-DEFICIENT SENSORY AXONS STILL RESPOND TO Sema3A

The small Rho GTPases have been shown to control axon guidance in part through semaphorin-plexin signaling (Kruger et al., 2005; Tran et al., 2007). For example, *RhoA* mRNA is localized to axons and growth cones of DRG sensory neurons, and this localization is mediated by an axonal targeting element located in the 3′ untranslated region of *RhoA* (Wu et al., 2005). Sema3A induces intra-axonal translation of *RhoA* mRNA, and this local RhoA translation has been suggested to be necessary for Sema3A-mediated growth cone collapse using a knockdown approach (Wu et al., 2005; Hengst et al., 2006). However, our loss-of-function study together with DRG explants cultured with Sema3A expressing 293T cells reveals that RhoA itself is not necessary for Sema3A-mediated axonal repulsion. The difference in the approach between loss-of-function and acute knockdown by siRNA or particular assay parameters to examine growth cone collapse or axonal repulsion may explain this discrepancy. Loss of Sema3A or its receptor neuropilin1 (Npn1) causes defects in fasciculation of peripheral motor and sensory axons (Behar et al., 1996; Kitsukawa et al., 1997; Taniguchi et al., 1997; Gu et al., 2003; Huettl et al., 2011). Our results showing no obvious defects in fasciculation of *RhoA*-deficient sensory axons (**Figure 3**) further support the idea that Sema3A-Npn1 signaling is present in *RhoA$^{f/f}$; Wnt1-Cre* mice.

RhoC EXPRESSION IS UP-REGULATED IN THE DRGs FROM *RhoA$^{f/f}$; Wnt1-Cre* EMBRYOS

There are many different types of small Rho GTPases, and the Rho GTPases with the most similar structure to that of RhoA are RhoB and RhoC (Wennerberg and Der, 2004; Wheeler and Ridley, 2004). RhoA, RhoB, and RhoC are identical in approximately 85% of their protein sequence (Wennerberg and Der, 2004; Wheeler and Ridley, 2004), however, the localization of RhoB is different from that of RhoA and RhoC. RhoA and RhoC are both localized in the cytoplasms or at the plasma membrane, whereas RhoB is generally found in the endosomal membranes since RhoB has a unique C-terminal lipid modifications and controls endosomal trafficking of membrane receptors (Adamson et al., 1992; Wheeler and Ridley, 2004; Heasman and Ridley, 2008). In addition, RhoB seems to have a growth inhibitory effect, whereas RhoA and RhoC have the opposite effect (Du and Prendergast, 1999; Chen et al., 2000; Wennerberg and Der, 2004). Thus, RhoB is likely to be functionally distinct from RhoA and RhoC. We also found that RhoC is significantly up-regulated in the DRG from *RhoA$^{f/f}$; Wnt1-Cre* embryos. Therefore, RhoC might be able to compensate for RhoA in the DRG. The analysis of *RhoA* and *RhoC* double mutants will give us valuable information about the possibility of the functional redundancy between RhoA and RhoC in the nervous system in the future.

In conclusion, our findings presented here using a loss-of-function approach demonstrate that RhoA itself is not essential for axonal projections of DRG sensory neurons and that RhoC may compensate for RhoA in the DRG. Further studies will reveal whether RhoA itself is required for the axon guidance of other types of neurons in the nervous system and whether RhoA and RhoC have redundant functions in the DRG and other regions of the mammalian nervous system.

ACKNOWLEDGMENTS

We thank F. Wang for providing *Advillin-Cre* mice, C. Y. Kuan for providing reagents and materials, and K. Campbell and D. R. Ladle for helpful comments on this manuscript. Yutaka Yoshida was supported by grants from NINDS (NS065048).

REFERENCES

Adamson, P., Paterson, H. F., and Hall, A. (1992). Intracellular localization of the P21rho proteins. *J. Cell Biol.* 119, 617–627.

Arber, S., Ladle, D. R., Lin, J. H., Frank, E., and Jessell, T. M. (2000). ETS gene Er81 controls the formation of functional connections between group Ia sensory afferents and motor neurons. *Cell* 101, 485–498.

Behar, O., Golden, J. A., Mashimo, H., Schoen, F. J., and Fishman, M. C. (1996). Semaphorin III is needed for normal patterning and growth of nerves, bones and heart. *Nature* 383, 525–528.

Bloor, J. W., and Kiehart, D. P. (2002). Drosophila RhoA regulates the cytoskeleton and cell-cell adhesion in the developing epidermis. *Development* 129, 3173–3183.

Brown, A. G. (1981). *Organization in the Spinal Cord*. New York, NY: Springer.

Cappello, S., Bohringer, C. R., Bergami, M., Conzelmann, K. K., Ghanem, A., Tomassy, G. S., Arlotta, P., Mainardi, M., Allegra, M., Caleo, M., van Hengel, J., Brakebusch, C., and Gotz, M. (2012). A radial glia-specific role of RhoA in double cortex formation. *Neuron* 73, 911–924.

Chauhan, B. K., Lou, M., Zheng, Y., and Lang, R. A. (2011). Balanced Rac1 and RhoA activities regulate cell shape and drive invagination morphogenesis in epithelia. *Proc. Natl. Acad. Sci. U.S.A.* 108, 18289–18294.

Chen, Z., Sun, J., Pradines, A., Favre, G., Adnane, J., and Sebti, S. M. (2000). Both farnesylated and geranylgeranylated RhoB inhibit malignant transformation and suppress human tumor growth in nude mice. *J. Biol. Chem.* 275, 17974–17978.

Danielian, P. S., Muccino, D., Rowitch, D. H., Michael, S. K., and McMahon, A. P. (1998). Modification of gene activity in mouse embryos in utero by a tamoxifen-inducible form of Cre recombinase. *Curr. Biol.* 8, 1323–1326.

da Silva, S., Hasegawa, H., Scott, A., Zhou, X., Wagner, A. K., Han, B. X., and Wang, F. (2011). Proper formation of whisker barrelettes requires periphery-derived Smad4-dependent TGF-beta signaling. *Proc. Natl. Acad. Sci. U.S.A.* 108, 3395–3400.

Dontchev, V. D., and Letourneau, P. C. (2002). Nerve growth factor and semaphorin 3A signaling pathways interact in regulating sensory neuronal growth cone motility. *J. Neurosci.* 22, 6659–6669.

Du, W., and Prendergast, G. C. (1999). Geranylgeranylated RhoB mediates suppression of human tumor cell growth by farnesyltransferase inhibitors. *Cancer Res.* 59, 5492–5496.

Fang, X., Djouhri, L., McMullan, S., Berry, C., Waxman, S. G., Okuse, K., and Lawson, S. N. (2006). Intense isolectin-B4 binding in rat dorsal root ganglion neurons distinguishes C-fiber nociceptors with broad action potentials and high Nav1.9 expression. *J. Neurosci.* 26, 7281–7292.

Fukata, M., and Kaibuchi, K. (2001). Rho-family GTPases in cadherin-mediated cell-cell adhesion. *Nat. Rev. Mol. Cell Biol.* 2, 887–897.

Gallo, G., and Letourneau, P. C. (2004). Regulation of growth cone actin filaments by guidance cues. *J. Neurobiol.* 58, 92–102.

Giniger, E. (2002). How do Rho family GTPases direct axon growth and guidance? A proposal relating signaling pathways to growth cone mechanics. *Differentiation* 385–396.

Gu, C., Rodriguez, E. R., Reimert, D. V., Shu, T., Fritzsch, B., Richards, L. J., Kolodkin, A. L., and Ginty, D. D. (2003). Neuropilin-1 conveys semaphorin and VEGF signaling during neural and cardiovascular development. *Dev. Cell* 5, 45–57.

Guan, K. L., and Rao, Y. (2003). Signalling mechanisms mediating neuronal responses to guidance cues. *Nat. Rev. Neurosci.* 4, 941–956.

Hall, A., and Lalli, G. (2010). Rho and Ras GTPases in axon growth, guidance, and branching. *Cold Spring Harb. Perspect. Biol.* 2, a001818.

Hasegawa, H., Abbott, S., Han, B. X., Qi, Y., and Wang, F. (2007). Analyzing somatosensory axon projections with the sensory neuron-specific Advillin gene. *J Neurosci.* 27, 14404–14414.

Heasman, S. J., and Ridley, A. J. (2008). Mammalian Rho GTPases: new insights into their functions from *in vivo* studies. *Nat. Rev. Mol. Cell Biol.* 9, 690–701.

Hengst, U., Cox, L. J., Macosko, E. Z., and Jaffrey, S. R. (2006). Functional and selective RNA interference in developing axons and growth cones. *J. Neurosci.* 26, 5727–5732.

Herzog, D., Loetscher, P., van Hengel, J., Knüsel, S., Brakebusch, C., Taylor, V., Suter, U., and Relvas, J. B. (2011). The small GTPase RhoA is required to maintain spinal cord neuroepithelium organization and the neural stem cell pool. *J. Neurosci.* 31, 5120–5130.

Honda, C. N. (1995). Differential distribution of calbindin-D28k and parvalbumin in somatic and visceral sensory neurons. *Neuroscience* 68, 883–892.

Hsu, W., Mirando, A. J., and Yu, H. M. (2010). Manipulating gene activity in Wnt1-expressing precursors of neural epithelial and neural crest cells. *Dev. Dyn.* 239, 338–345.

Huber, A. B., Kania, A., Tran, T. S., Gu, C., De Marco Garcia, N., Lieberam, I., Johnson, D., Jessell, T. M., Ginty, D. D., and Kolodkin, A. L. (2005). Distinct roles for secreted semaphorin signaling in spinal motor axon guidance. *Neuron* 48, 949–964.

Huettl, R. E., Soellner, H., Bianchi, E., Novitch, B. G., and Huber, A. B. (2011). Npn-1 contributes to axon-axon interactions that differentially control sensory and motor innervation of the limb. *PLoS Biol.* 9:e1001020. doi: 10.1371/journal.pbio.1001020

Katayama, K., Melendez, J., Baumann, J. M., Leslie, J. R., Chauhan, B. K., Nemkul, N., Lang, R. A., Kuan, C. Y., Zheng, Y., and Yoshida, Y. (2011). Loss of RhoA in neural progenitor cells causes the disruption of adherens junctions and hyperproliferation. *Proc. Natl. Acad. Sci. U.S.A.* 108. 7607–7612.

Kitsukawa, T., Shimizu, M., Sanbo, M., Hirata, T., Taniguchi, M., Bekku, Y., Yagi, T., and Fujisawa, H. (1997). Neuropilin-semaphorin III/D-mediated chemorepulsive signals play a crucial role in peripheral nerve projection in mice. *Neuron* 19, 995–1005.

Koerber, H. R., and Mendell, L. M. (1992). "Functional heterogeneity of dorsal root ganglion cells," in *Sensory Neurons: Diversity, Development and Plasticity,* ed S. A. Scott (New York, NY: Oxford University Press), 77–96.

Kruger, R. P., Aurandt, J., and Guan, K. L. (2005). Semaphorins command cells to move. *Nat. Rev. Mol. Cell Biol.* 6, 789–800.

Lawson, S. N. (2002). Phenotype and function of somatic primary afferent nociceptive neurones with C-, Adelta- or Aalpha/beta-fibres. *Exp. Physiol.* 87, 239–244.

Leslie, J. R., Imai, F., Fukuhara, K., Takegahara, N., Rizvi, T. A., Friedel, R. H., Wang, F., Kumanogoh, A., and Yoshida, Y. (2011). Ectopic myelinating oligodendrocytes in the dorsal spinal cord as a consequence of altered semaphorin 6D signaling inhibit synapse formation. *Development* 138, 4085–4095.

Magie, C. R., Pinto-Santini, D., and Parkhurst, S. M. (2002). Rho1 interacts with p120ctn and alpha-catenin, and regulates cadherin-based adherens junction components in Drosophila. *Development* 129, 3771–3782.

Mandai, K., Guo, T., St Hillaire, C., Meabon, J. S., Kanning, K. C., Bothwell, M., and Ginty, D. D. (2009). LIG family receptor tyrosine kinase-associated proteins modulate growth factor signals during neural development. *Neuron* 63, 614–627.

Melendez, J., Stengel, K., Zhou, X., Chauhan, B. K., Debidda, M., Andreassen, P., Lang, R. A., and Zheng, Y. (2011). RhoA GTPase is dispensable for actomyosin regulation but is essential for mitosis in primary mouse embryonic fibroblasts. *J. Biol. Chem.* 286, 15132–15137.

Molliver, D. C., Wright, D. E., Leitner, M. L., Parsadanian, A. S., Doster, K., Wen, D., Yan, Q., and Snider, W. D. (1997). IB4-binding DRG neurons switch from NGF to GDNF dependence in early postnatal life. *Neuron* 19, 849–861.

Schaeren-Wiemers, N., and Gerfin-Moser, A. (1993). A single protocol to detect transcripts of various types and expression levels in neural tissue and cultured cells: in situ hybridization using digoxigenin-labelled cRNA probes. *Histochemistry* 100, 431–440.

Taniguchi, M., Yuasa, S., Fujisawa, H., Naruse, I., Saga, S., Mishina, M., and Yagi, T. (1997). Disruption of semaphorin III/D gene causes severe abnormality in peripheral nerve projection. *Neuron* 19, 519–530.

Todd, A. J., Hughes, D. I., Polgar, E., Nagy, G. G., Mackie, M., Ottersen, O. P., and Maxwell, D. J. (2003). The expression of vesicular glutamate transporters VGLUT1 and VGLUT2 in neurochemically defined axonal populations in the rat spinal cord with emphasis on the dorsal horn. *Eur. J. Neurosci.* 17, 13–27.

Tran, T. S., Kolodkin, A. L., and Bharadwaj, R. (2007). Semaphorin regulation of cellular morphology. *Annu. Rev. Cell Dev. Biol.* 23, 263–292.

Wennerberg, K., and Der, C. J. (2004). Rho-family GTPases: it's not only Rac and Rho (and I like it). *J. Cell Sci.* 117(Pt 8), 1301–1312.

Wheeler, A. P., and Ridley, A. J. (2004). Why three Rho proteins? RhoA, RhoB, RhoC, and cell motility. *Exp. Cell Res.* 301, 43–49.

Wu, K. Y., Hengst, U., Cox, L. J., Macosko, E. Z., Jeromin, A., Urquhart, E. R., and Jaffrey, S. R. (2005). Local translation of RhoA regulates growth cone collapse. *Nature* 436, 1020–1024.

Yamada, S., and Nelson, W. J. (2007). Localized zones of Rho and Rac activities drive initiation and expansion of epithelial cell-cell adhesion. *J. Cell Biol.* 178, 517–527.

Yoshida, Y., Han, B., Mendelsohn, M., and Jessell, T. M. (2006). PlexinA1 signaling directs the segregation of proprioceptive sensory axons in the developing spinal cord. *Neuron* 52, 775–788.

Conflict of Interest Statement: The authors declare that the research was conducted in the absence of any commercial or financial relationships that could be construed as a potential conflict of interest.

Received: 29 February 2012; paper pending published: 19 March 2012; accepted: 09 May 2012; published online: 22 May 2012.

*Citation: Leslie JR, Imai F, Zhou X, Lang RA, Zheng Y and Yoshida Y (2012) RhoA is dispensable for axon guidance of sensory neurons in the mouse dorsal root ganglia. Front. Mol. Neurosci. **5**:67. doi: 10.3389/fnmol.2012.00067*

frontiers in
MOLECULAR NEUROSCIENCE

REVIEW ARTICLE
published: 06 June 2012
doi: 10.3389/fnmol.2012.00071

Semaphorin signaling in vertebrate neural circuit assembly

Yutaka Yoshida*

Division of Developmental Biology, Cincinnati Children's Hospital Medical Center, Cincinnati, OH, USA

Edited by:
Robert W. Burgess, The Jackson Laboratory, USA

Reviewed by:
Florentina Soto, Washington University in St. Louis, USA
Peter Gerard Fuerst, University of Idaho, USA

****Correspondence:***
Yutaka Yoshida, Division of Developmental Biology, Cincinnati Children's Hospital Medical Center, 3333 Burnet Avenue, Cincinnati, OH 45229-3026, USA.
e-mail: yutaka.yoshida@cchmc.org

Neural circuit formation requires the coordination of many complex developmental processes. First, neurons project axons over long distances to find their final targets and then establish appropriate connectivity essential for the formation of neuronal circuitry. Growth cones, the leading edges of axons, navigate by interacting with a variety of attractive and repulsive axon guidance cues along their trajectories and at final target regions. In addition to guidance of axons, neuronal polarization, neuronal migration, and dendrite development must be precisely regulated during development to establish proper neural circuitry. Semaphorins consist of a large protein family, which includes secreted and cell surface proteins, and they play important roles in many steps of neural circuit formation. The major semaphorin receptors are plexins and neuropilins, however other receptors and co-receptors also mediate signaling by semaphorins. Upon semaphorin binding to their receptors, downstream signaling molecules transduce this event within cells to mediate further events, including alteration of microtubule and actin cytoskeletal dynamics. Here, I review recent studies on semaphorin signaling in vertebrate neural circuit assembly, with the goal of highlighting how this diverse family of cues and receptors imparts exquisite specificity to neural complex connectivity.

Keywords: semaphorin, plexin, neuropilin, axon guidance, synapse formation

SEMAPHORINS AND THEIR RECEPTORS

Semaphorins (Semas), which consist of 20 family members in vertebrates, are one of the largest families of guidance cues. Semaphorins include both secreted and membrane-bound proteins, and they serve a variety of roles in the peripheral and central nervous system (PNS and CNS; reviewed in Mann et al., 2007; Tran et al., 2007; Pasterkamp and Giger, 2009). Semaphorins were first characterized as repulsive guidance cues, and later a role in promoting neuronal growth was identified. In vertebrates, semaphorins are subdivided into five subfamilies, including classes 3, 4, 5, 6, and 7 (**Figure 1**). The major receptors for semaphorins are plexins and neuropilins (**Figure 1**). Plexins and neuropilins consist of nine and two family members in mammals, respectively. Plexins and neuropilins are subdivided into four classes; plexin (Plex) A1–4, B1–3, C1, and D1, and two classes; neuropilin1–2 (Npn1–2), respectively. Most class 3 semaphorins bind to Npns, and Npns associate with plexinA family members to transduce Sema3 signals across the neuronal plasma membrane (Takahashi et al., 1999; Tamagnone et al., 1999). Sema3E is an exception and directly binds to PlexD1 (Gu et al., 2005). Other interactions between semaphorins and plexins have also been reported, including the interaction between Sema4D and PlexB1 (Tamagnone et al., 1999), between Sema5A and PlexB3 (Artigiani et al., 2004), between Sema7A and PlexC1 (Tamagnone et al., 1999), among Sema6C/6D and PlexA1 (Toyofuku et al., 2004; Yoshida et al., 2006), and among Sema6A/6B and PlexA2/A4 (Suto et al., 2005; **Figure 1**). Semaphorins also bind to other receptors in addition to plexins and Npns (Tran et al., 2007). For example, class 4 semaphorins signal through two immune system receptors, CD72 and Tim-2 (Kumanogoh et al., 2000, 2002; reviewed in Kikutani and Kumanogoh, 2003; Suzuki et al., 2008; Takamatsu and Kumanogoh, 2012). Another example is that the glycosylphosphatidylinositol (GPI)-anchored Sema7A binds to integrin receptors (Pasterkamp et al., 2003). Several reviews cover work over the last two decades on the roles played by semaphorins in the nervous system (Mann et al., 2007; Tran et al., 2007; Pasterkamp and Giger, 2009), so here I focus on recent studies related to neural circuit assembly.

SEMAPHORINS IN GROWTH AND GUIDANCE OF AXONS AND DENDRITES

PERIPHERAL MOTOR AND SENSORY NEURON PROJECTIONS

Motor neuron axonal trajectories have been extensively studied in order to understand the cellular and molecular mechanisms underlying the establishment of function of motor circuitry. Vertebrate motor neurons extend axons out of the spinal cord and innervate target skeletal muscles. Along these trajectories, motor axons encounter many axon guidance cues, ultimately finding their appropriate muscle targets, including those that reside within the developing limb. In the ventral spinal cord, cohorts of motor neurons are arrayed in longitudinal columns and project their axons to distinct peripheral regions. Lateral motor column (LMC) neurons are generated only at limb levels, and they extend their axons into the limb mesenchyme. In contrast, the median motor column (MMC) neurons extend their axons to axial muscles.

In both *Sema3A* and *Npn1* mutant mice, peripheral nerves exhibit severe defasciculation and branching defects during embryogenesis (Behar et al., 1996; Kitsukawa et al., 1997; Taniguchi et al., 1997; Gu et al., 2003). Detailed analyses of the roles played by Sema3A-Npn1 and Sema3F-Npn2 signaling in motor axon pathfinding describe how semaphorin signaling participates in

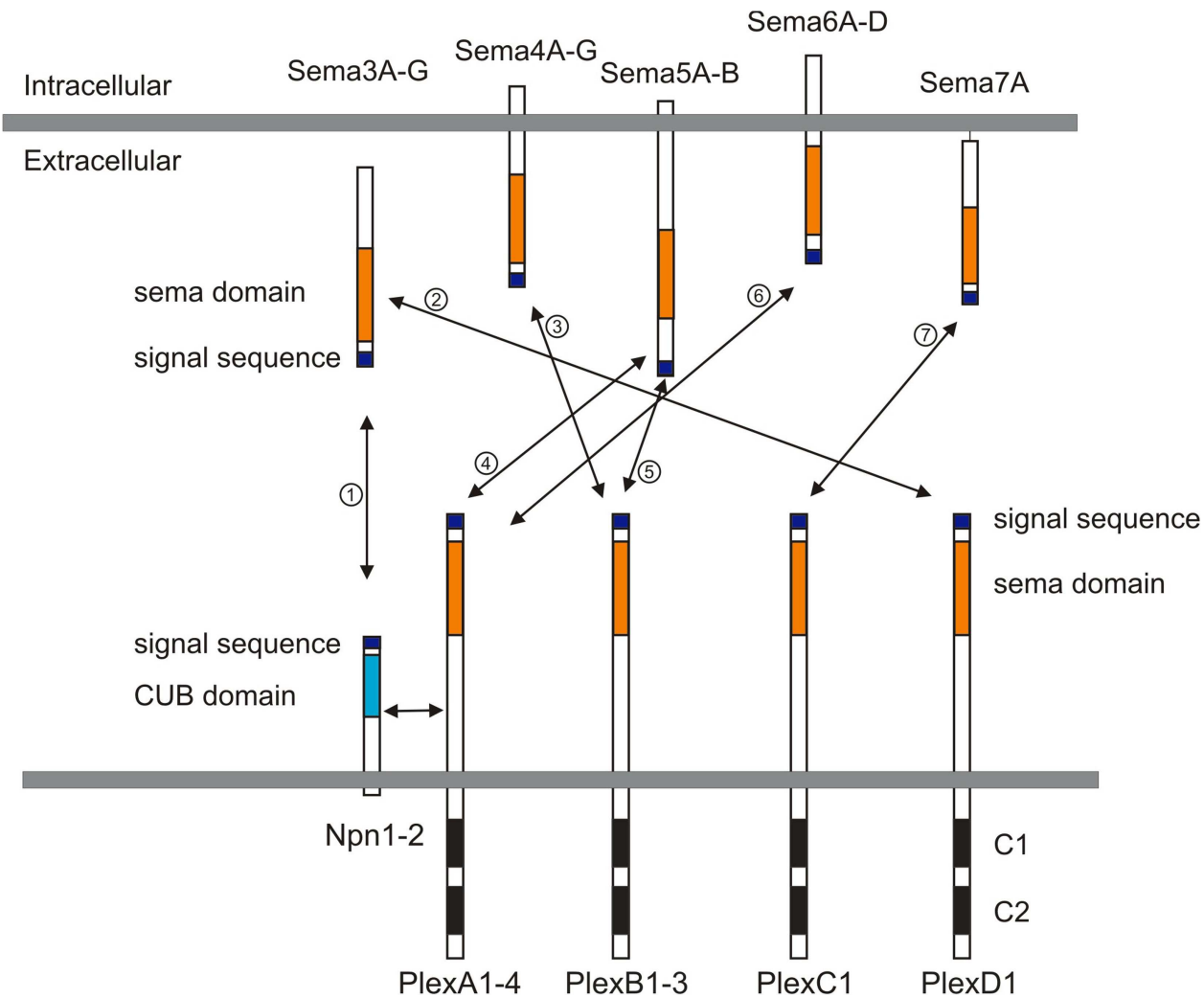

FIGURE 1 | Semaphorins and their receptors (plexins and neuropilins). Semaphorins consist of secreted (class 3), glycosylphosphatidylinositol (GPI)-anchored (class 7), or transmembrane (class 4–6) family members. Neuropilins consist of two transmembrane molecules (Npn1–2), and plexins consist of transmembrane A (1–4), B (1–3), C1, and D1 family members. Most class 3 semaphorins require an obligate neuropilin co-receptor. Sema3E binds to PlexD1 without neuropilins. Class 4 and 5 semaphorins interact with plexinBs. Class 6 semaphorins interact with plexinAs. Sema7A interacts with PlexC1. CUB indicates complement binding. One to seven indicate the interactions between semaphorins and their receptors; 1: class 3 semaphorins and neuropilin1/2, 2: Sema3E and PlexD1, 3: Sema4D and PlexB1/B2 or Sema4C/4G and PlexB1, 4: Sema5A/5B and PlexA1/A3, 5: Sema5A and PlexB3, 6: Sema6A/6B and PlexA2/A3 or Sema6C/6D and PlexA1, 7: Sema7A and PlexC1.

motor axon targeting (Huber et al., 2005; Huettl et al., 2011). At embryonic day 10.5 (E10.5), *Npn1* mRNA is expressed by most LMC neurons, whereas *Npn2* is expressed by a subset of the medial LMC (LMCm) motor neurons but not by the motor neurons in the lateral division of the LMC (LMCl; Huber et al., 2005). Expression of *Sema3A* is detected at E10.5, when spinal nerves have extended into the plexus region but have not yet entered the limb (Huber et al., 2005). This suggests that Sema3A regulates the timing of motor axon ingrowth into the limb. Supporting this idea, precocious extension of motor and sensory projections toward distal forelimb regions is observed in *Sema3A* null mice and also in $Npn1^{Sema-}$ mice, which express a mutant Npn1 protein that is deficient in secreted Sema binding (Gu et al., 2003; Huber et al., 2005). *Sema3A* is also expressed adjacent to peripheral nerve tracts within the forelimb at E11.5 (Huber et al., 2005), raising the possibility that Sema3A may regulate motor axon fasciculation at later developmental times. Peripheral nerves in $Npn1^{Sema-}$ and *Sema3A* mutants also show marked defasciculation and aberrant growth when compared to wild-type (Huber et al., 2005). *Sema3F*, encoding a Npn2 ligand, is expressed in the dorsal limb bud and so participates in directing *Npn2*-expressing LMCm axons along a ventral trajectory in the forelimb (Huber et al., 2005). Loss- and gain-of-function experiments reveal that Sema3F-Npn2 signaling is required to direct LMCm axons along their ventral trajectory (Huber et al., 2005).

A more recent study examines the reciprocal interactions between sensory and motor axons as they navigate along their trajectories and explore the role played by Npn1 signaling in these

axon-axon interactions (Huettl et al., 2011). Deletion of *Npn1* solely in motor neurons reveals that peripheral sensory projections are still established correctly, even though motor projections are severely defasciculated in the distal limbs (Huettl et al., 2011). Genetic elimination of motor neurons demonstrates that sensory axons require only minimal motor axon scaffolding to establish their projections in the distal limb (Huettl et al., 2011). In contrast, defects in sensory axonal trajectories caused by sensory neuron-specific *Npn1* deletion is accompanied by defasciculation of motor axons (Huettl et al., 2011). Thus, motor axons are dependent on sensory axons, and they interact in part through Npn1-mediated fasciculation in the developing limb.

Sema3A is expressed by motor neurons in addition to peripheral tissues. Since the Sema3A receptor Npn1 is also expressed by motor neurons, as described above, it has been a puzzle as to why both *Npn1* and *Sema3A* are both expressed by motor neurons. Using gain-of-function and knockdown approaches in chick, Moret et al. (2007) found that co-expression of *Npn1* and *Sema3A* in motor neurons regulates axon sensitivity to environmental *Sema3A* sources during motor axon pathfinding. In chick, *Sema3A* is expressed by MMC motor neurons at both early and late developmental stages, whereas *Sema3A* is not expressed by LMC motor neurons at early stages but is expressed when the axons reach the base of the limb (Moret et al., 2007). In contrast, *Npn1* is expressed by both MMC and LMC motor neurons (Moret et al., 2007). Premature expression of *Sema3A* in LMC motor neurons leads motor axons to defasciculate and invade territories they normally avoid, suggesting that Npn1 becomes insensitive to early ectopic environmental expression of *Sema3A* (Moret et al., 2007). Moreover, knockdown studies show that *Sema3A* expression in motor neurons is required for correct spinal nerve compaction and dorsal motor axon extension (Moret et al., 2007). Therefore, *Sema3A* in motor neurons sets the level of sensitivity of their growth cones to exogenous *Sema3A* exposure (Moret et al., 2007). This regulation is associated with post-translational and local control of the availability of Npn1 at the growth cone surface (Moret et al., 2007). Thus, the interplay between intrinsic and extrinsic *Sema3A* may represent a fundamental mechanism in the accurate specification of axon pathways. Future studies will demonstrate this proposed role for neuronal and non-neuronal Sema3A and the regulation of motor axon guidance in mice.

MIDLINE CROSSING OF COMMISSURAL AXONS

In the spinal cord, commissural neurons, whose cell bodies are located in the dorsal horn, project their axons to the ventral spinal cord. When these axons reach the floor plate, they cross the midline, turn rostrally, extend longitudinally on the contralateral side of the ventral spinal cord and project to the brain. Once commissural axons cross the floor plate, they lose their responsiveness to chemoattractants such as netrin-1, and become responsive to chemorepulsive cues, which include Sema3B and Sema3F (Zou et al., 2000). The molecular mechanisms that allow for this change of responsiveness to these cues have been largely unknown. Recently, two studies define novel mechanisms that may underlie this switch (Nawabi et al., 2010; Parra and Zou, 2010).

Parra and Zou (2010) investigated the mechanisms by which semaphorin repulsion in commissural axons is switched on at the midline. Using a collagen explant assay with pre-crossing commissural neurons, they noted that Sonic Hedgehog (Shh) can activate a novel repulsive response of pre-crossing commissural axons to Sema3B and Sema3F (Parra and Zou, 2010). Blocking Shh activity, or perturbing the Shh receptors Ptch1 and Smo, causes midline guidance defects indicative of a failure of post-crossing commissural axons to respond to Sema3B or Sema3F (Parra and Zou, 2010). The involvement of cyclic nucleotides in this switching event was then examined, since cyclic nucleotides have been shown *in vitro* to influence signaling in response to guidance cues, and the ratio of cAMP/cGMP regulates axonal attraction or repulsion *in vitro* (Song et al., 1998). Consistent with these observations, enhancing protein kinase A (PKA) activity in pre-crossing axons diminishes Shh-induced semaphorin-mediated repulsion and causes profound midline stalling and overshooting/wandering of post-crossing axons (Parra and Zou, 2010). Therefore, this study shows that Shh can act as a switch in commissural axon guidance responses to semaphorins by reducing cAMP/PKA signaling.

Nawabi et al. (2010) present another novel mechanism underlying the switch of axon guidance response of commissural axons. PlexA1 has been identified as a co-receptor that along with Npn2 mediates Sema3B responses (Nawabi et al., 2010). Interestingly, PlexA1 protein level is up-regulated by floor plate (FP) signals in commissural growth cones, and these FP signals suppress proteolytic calpain1 activity to increase PlexA1 protein levels in commissural axons (Nawabi et al., 2010). The FP cue responsible for regulating PlexA1 protein expression was then identified as Nr-CAM (Nawabi et al., 2010). Nr-CAM was considered as a possible candidate due to its high and restricted expression in the FP, and also its function in the regulation of axon growth and guidance during the formation of various commissural tracts (Falk et al., 2005; Williams et al., 2006). A range of *in vitro* and *in vivo* experiments reveal that Nr-CAM derived from the FP inhibits PlexA1 processing by blocking Calpain1 and thus increases growth cone sensitization to Sema3B (Nawabi et al., 2010). These results reveal novel mechanisms for changing the sign of commissural axon responsiveness to semaphorin guidance cues.

RETINAL GANGLION CELL AXON CROSSING AT THE OPTIC CHIASM MIDLINE

During neural development retinal ganglion cell (RGC) axons must choose to cross or avoid the CNS midline at the optic chiasm, thereby regulating RGC projections to ipsilateral or contralateral retinorecipient targets. Npn1 has recently been shown to guide retinal axon crossing at optic chiasm and, surprisingly, the relevant ligand is not a class 3 semaphorin but VEGF164 (Erskine et al., 2011). Erskine et al. (2011) found that *Npn1*, but not *Npn2*, is expressed by mouse RGCs, and that loss of *Npn1* increases the proportion of RGC axons that project ipsilaterally. Class 3 semaphorins are not expressed near the optic chiasm, but *VEGF* is expressed at this midline location (Erskine et al., 2011). Consistent with these expression patterns, a mouse mutant that harbors a Npn1 point mutation which abolishes binding to all class 3 semaphorins (Gu et al., 2003) does not exhibit any defects in RGC axon guidance at the midline (Erskine et al., 2011). However, loss of VEGF164 phenocopies the RGC chiasm crossing defects observed in *Npn1* null mutants (Erskine et al., 2011). *In vitro* analyses reveal

that VEGF164 is a chemoattractant for RGC axon growth cones (Erskine et al., 2011). Since *VEGF* is expressed in other regions of the nervous system (Ruhrberg et al., 2002; Schwarz et al., 2004), this study suggests that VEGF164-Npn1 signaling may be involved in controlling axon guidance events in different regions of the CNS.

A very recent study demonstrates that Sema6D thorough its receptors PlexA1 and Nr-CAM promotes retinal axon midline crossing (Kuwajima et al., 2012). The authors found that Sema6D and Nr-CAM are expressed on midline radial glia and PlexA1 on chiasm neurons, and PlexA1 and Nr-CAM are expressed on contralateral RGCs. A series of sophisticated *in vitro* culture experiments reveal that both PlexA1 and Nr-CAM are required on crossed RGCs for inhibition by Sema6D alone, whereas Sema6D interacting together with PlexA1 and Nr-CAM promotes growth (Kuwajima et al., 2012). Furthermore, they found that Nr-CAM can interact with both Sema6D and PlexA1. Finally, in the absence of Sema6D or both PlexA1 and Nr-CAM *in vivo*, RGC axons defasciculate, misroute into the caudal diencephalon, and more frequently project into the ipsilateral optic tract (Kuwajima et al., 2012). This study provides a novel mechanism underling midline crossing: accessory recognition proteins expressed by ligand-expressing cells modulate ligand activity. This strategy allows a switch in ligand activity without changing receptor expression on responsive axons (**Figure 2**).

CORTICOSPINAL TRACT GROWTH AND GUIDANCE

Several semaphorins are known to repel or attract cortical neurites *in vitro* (Bagnard et al., 1998; Castellani et al., 2000, 2002; Polleux et al., 2000; Chauvet et al., 2007), but *in vivo* roles for these capabilities are obscure. Two recent studies begin to address this issue by showing that semaphorin signaling guides corticospinal axons *in vivo* (Faulkner et al., 2008; Rünker et al., 2008). Faulkner et al. (2008) show that *PlexA3* and *PlexA4* are expressed in the developing cerebral cortex when corticospinal tract (CST) motor axons originating in cortical layer V are guided caudally to the spinal cord. Interestingly, *Sema6A* is expressed along the ventral pyramidal tract and at the pyramidal decussation (Faulkner et al., 2008; Rünker et al., 2008). *Sema6A* mutants, and also *PlexA3*/*A4* double mutants, have defects in the dorsal extension and crossing of motor corticospinal axons at the pyramidal decussation (Faulkner et al., 2008). When neuronal tracers such as DiI or BDA are bilaterally injected into the *Sema6A*, or *PlexA3*/*A4* mutant motor cortices, a large DiI-labeled axon bundle diverges from its normal pathway at the pyramidal decussation toward the ventrolateral aspect of the spinal cord, a phenotype never observed in wild-type (Faulkner

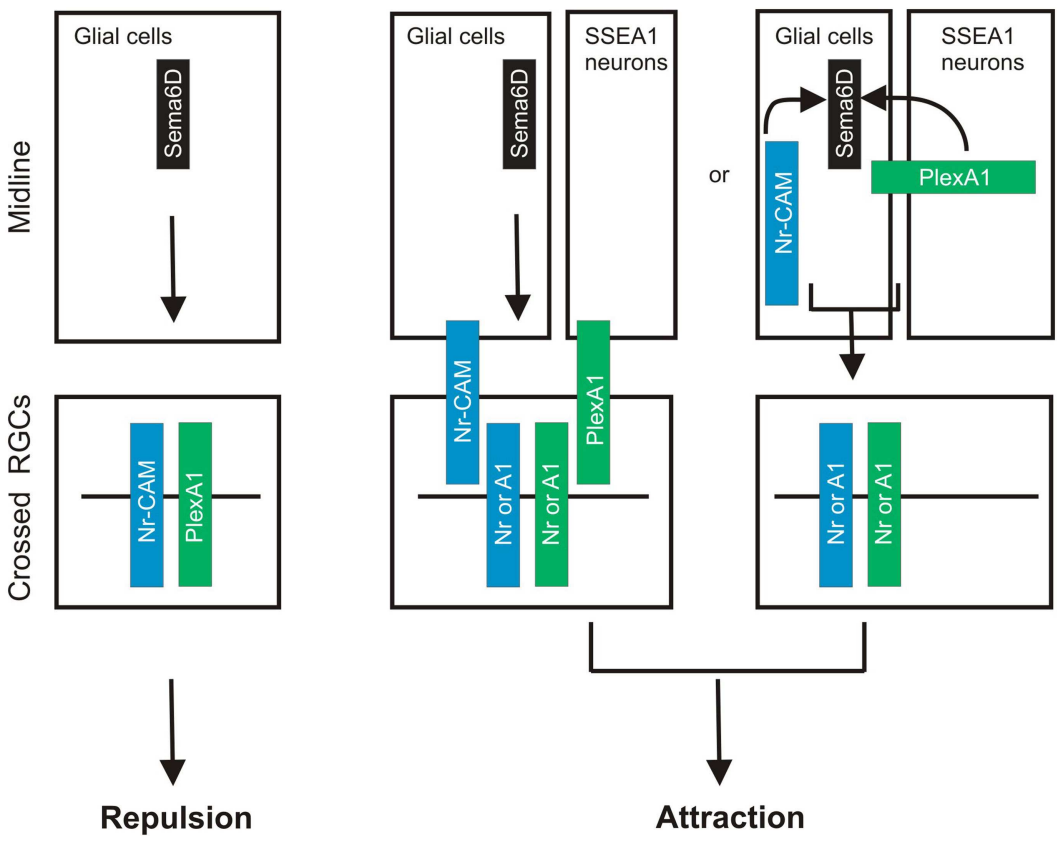

FIGURE 2 | Sema6D controls retinal midline crossing through its interaction with PlexA1 and Nr-CAM. Sema6D and Nr-CAM are expressed by glial cells in the chiasm, and PlexA1 is expressed by SSEA1$^+$ neurons in the chiasm. Nr-CAM and PlexA1 are expressed by crossed RGCs. The receptor complex in *cis* on RGCs and Sema6D alone leads to repulsion of RGCs, whereas the complex on chiasm cells acting in *trans* with RGC receptors promotes axonal attraction.

et al., 2008). These abnormally projecting CST axons in *Sema6A* or *PlexA3*/*A4* mutants maintain their ipsilateral course at the pyramidal decussation and come to occupy a unique, aberrant, position in the ventrolateral region of the spinal cord (Faulkner et al., 2008). Although *Npn1* mutants do not show similar dorsal turning defects, Npn1 is required for proper fasciculation of the tract at midline crossing (Faulkner et al., 2008). Thus, PlexA3/A4 and Npn1 have distinct functions in controlling CST axon guidance. It will be interesting to examine how defects in fasciculation of *Npn1*-deficient CST axons will affect CST-circuitry. Similarly, Rünker et al. (2008) show that *Sema6A* and *PlexA4* mouse mutants harbor defects in CST axon guidance at the pyramidal decussation. Although PlexA2 interacts with Sema6A (Suto et al., 2005; Renaud et al., 2008), *PlexA2* mutants do not show any apparent defects in CST axon guidance (Rünker et al., 2008). Interestingly, before CST axons reach the pyramidal decussation, *Sema6A*-deficient mice show guidance defects in CST axons at the mid-hindbrain boundary; this indicates that Sema6A controls CST axon guidance at multiple choice points (Rünker et al., 2008).

CORPUS CALLOSUM GROWTH AND GUIDANCE

The corpus callosum (CC) is the main pathway responsible for interhemispheric communication in the brain. Neurons that project through the CC are located in upper and lower cortical layers (Yorke and Caviness, 1975; Porter and White, 1983). Niquille et al. (2009) have shown that CC neuronal populations exert an attractive influence on callosal axons, which is mediated by both GABAergic and glutamatergic calretinin (CR)-positive neurons. Sema3C was identified as a candidate cue for mediating this attractive activity based on its expression pattern; *Sema3C* mRNA is restricted to CR-positive glutamatergic neurons (Niquille et al., 2009). *Sema3C* loss of function and knockdown of *Npn1* reveal that Sema3C-Npn1 signaling contributes to the chemoattractive effect of CR-positive glutamatergic neurons on callosal axons (Niquille et al., 2009).

AXON ORGANIZATION AND NEURAL MAP TOPOGRAPHY IN OLFACTORY SYSTEM

In the mouse olfactory system, each olfactory sensory neuron (OSNs) expresses only one of many possible functional odorant receptors (ORs; reviewed in Mombaerts, 2006; Mori and Sakano, 2011). OSN axons expressing the same OR converge on a specific target region, the glomerulus, within the olfactory bulb (OB; reviewed in Mombaerts, 2006; Mori and Sakano, 2011). Recently, two studies demonstrate that both Sema3A-Npn1 and Sema3F-Npn2 signaling are involved in specifying neural map topography in the OB (Imai et al., 2009; Takeuchi et al., 2010). Previous studies show that OR-specific cAMP signaling defines a gradient of *Npn1* expression (Imai et al., 2006), but how Npn1 controls topographic map formation was still unclear. Imai et al. (2009) show, using loss- and gain-of-function experiments, that *Npn1* expression levels determine glomerular positioning along the anterior-posterior axis of the OB. Interestingly, instead of axon-target interactions, Npn1 regulates the sorting of OSN axons within the olfactory nerve (Imai et al., 2009). In fact, axon-target interactions appear not to be required for generating anterior-posterior topography, since *Gli3* mutant mice, in which the OB is completely absent, do not show obvious defects in topography along the A/P axis (Imai et al., 2009). OSN-specific knockout of *Sema3A* reveals that expression of *Sema3A* in OSNs is required for pre-target axon sorting in the nerve bundle (Imai et al., 2009). More recent work, also from Sakano's laboratory, demonstrates that Sema3F-Npn2 signaling regulates the topographic patterning of OSNs along the dorsal-ventral axis of the OB (Takeuchi et al., 2010). In the OBs, Npn2 in the axon termini of OSNs forms a gradient in the OB with high levels ventrally and low levels dorsally (Takeuchi et al., 2010). Loss- and gain-of-function analyses reveal a cell-autonomous function for Npn2/PlexA3 in establishing the OSN projection along the dorsal-ventral (D-V) axis (Takeuchi et al., 2010). Interestingly, *Sema3F* transcript is not expressed in the OB but in the olfactory epithelium (OE; Takeuchi et al., 2010). Further, Sema3F was found to be secreted by early-arriving OSN axons and deposited at the anterodorsal OB to repel later-arriving Npn2-positive axons (Takeuchi et al., 2010). Therefore, sequential arrival of OSN axons, together with the graded and complementary expression of *Npn2* and *Sema3F* by OSNs, are required for appropriate topographic projections along the D-V axis (Takeuchi et al., 2010). These two studies demonstrate novel mechanisms of how axonal sorting in the nerves prior to targeting is important and how distinct secreted semaphorins expressed on axons influence follower axons. This framework for complex topographic organization may be used in other regions of the mammalian nervous system.

THALAMOCORTICAL CONNECTIONS

Mice harboring mutations in various semaphorin signaling components are not only useful for understanding the molecular mechanisms underlying neural circuit formation but they can also lend insight into adult neural plasticity, if they are viable. Recent work has examined specificity and plasticity of thalamocortical connections in *Sema6A* mutant mice (Little et al., 2009). Despite the defect in thalamic projections in *Sema6A* mutants (Leighton et al., 2001; Little et al., 2009), *Sema6A* mutants survive until adulthood, providing a unique model that has normal cortical patterning but defects in thalamic inputs. Interestingly, the early embryonic shift in thalamocortical axon connectivity observed at E16.5 and P0 in *Sema6A* mutants is partially recovered at P4, and completely compensated for in adult *Sema6A* mutants (Little et al., 2009). The misrouted axons are apparently able to find their way to the visual cortex via alternative pathways at postnatal stages so as to reestablish a normal pattern of thalamocortical connectivity (Little et al., 2009). The authors also observed a significant reduction in the size of the dorsal lateral geniculate nucleus (dLGN) in *Sema6A*-deficient brains compared to wild-type brains (Little et al., 2009). This suggests that some dLGN neurons whose axons do not reach their target regions may die during development. Therefore, it seems that some misrouted axons die and some can find their targets via alternative pathways. Together, these findings demonstrate the robust capacity of the early postnatal cortex for remapping initial sensory inputs following experience.

DENDRITIC PROCESS OUTGROWTH IN THE SPINAL CORD

Like axons, dendritic morphology includes growth, targeted extension, and branching, all of which must be precisely regulated during development (reviewed in Jan and Jan, 2003). For example,

Sema3A is implicated in dendritic growth and orientation of cortical pyramidal neuron subtypes (Polleux et al., 2000; Fenstermaker et al., 2004).

Specific motor neuron pools exhibit distinct dendritic arbor morphologies that are critical for their ability to receive and process various types of synaptic input (Landmesser, 1978; Okado et al., 1990; Vrieseling and Arber, 2006). The transmembrane semaphorin Sema6A and its receptor, PlexA4 regulate dendritic growth of motor neuron subtypes by modulating a downstream signaling molecule, FERM Rho-GEF protein FARP1, in the developing spinal cord (Zhuang et al., 2009). FARP1 is expressed by LMC, but not MMC, motor neurons in chick, and FARP1 protein is detected on the dendrites (Zhuang et al., 2009). Ectopic expression and knockdown approaches demonstrate that FARP1 is necessary and sufficient to regulate the dendrite process length of LMC motor neurons (Zhuang et al., 2009). FARP2, a protein related to FARP1, binds to all plexinA family members (Toyofuku et al., 2005), whereas FARP1 interacts strongly with PlexA4 but associates only very weakly with PlexA1 (Zhuang et al., 2009). Gain-of-function and knockdown approaches for *Sema6A* and *PlexA4* show results similar to those observed following similar manipulations of FARP1, suggesting that FARP1 lies downstream of Sema6A-PlexA4 signaling (Zhuang et al., 2009). Thus, Sema6A controls columnar-specific dendritic growth through the action of FARP1, suggesting that distinct semaphorin-plexin signaling may also be involved in regulating dendritic morphology of motor neuron pools and other CNS neurons.

SEMAPHORINS IN CELLULAR-CIRCUIT LAMINATION

RETINAL LAMINATION AND FUNCTION

Specific patterns of synaptic connections in many regions of the nervous system are organized within laminae. One of the most best studied laminar structures found in the vertebrate nervous system is the retina. In the vertebrate retina, distinct subtypes of RGCs, amacrine cells (ACs), and bipolar cells (BCs) make synaptic connections within specific synaptic plexus of the inner plexiform layer (IPL), a laminar structure that is conventionally divided into 5–10 sublaminae (reviewed in Wässle, 2004; Sanes and Zipursky, 2010). Recently, two studies using mouse genetics demonstrate that different classes of transmembrane semaphorins regulate select aspects of retinal lamination and function in the mammalian retina (Matsuoka et al., 2011a,b). Though previous reports showed that certain semaphorins, Npns, and plexins are expressed in the developing mammalian retina (Leighton et al., 2001; de Winter et al., 2004), how semaphorin signaling regulates retinal development and circuit assembly was not known. Matsuoka et al. (2011a) investigated the *in vivo* roles of semaphorin signaling components in retinal development by analyzing mice that lack each plexin and neuropilin. Through an extensive phenotypic analysis of the mutant mice, the authors found that dopaminergic ACs and M1-type melanopsin intrinsically photosensitive retinal ganglion cells (ipRGCs), both of which exhibit neurite stratification predominantly within the S1 sublamina of the IPL in wild-type retinas, extend aberrant processes into S4/S5 in *PlexA4*-deficient retina (Matsuoka et al., 2011a; **Figure 3A**). Since *PlexA4* is expressed by dopaminergic ACs but not by M1-type ipRGCs, this result suggests that the M1-type ipRGC dendritic stratification deficit within the IPL of *PlexA4*-deficient retina is likely a secondary consequence of defects in AC stratification within the IPL of the *PlexA4*-deficient retina, providing further support for ACs directing RGC dendritic stratification in the IPL (Stacy and Wong, 2003; Mumm et al., 2006; Matsuoka et al., 2011a). Sema6A and its receptor PlexA4 exhibit complementary protein expression patterns within the IPL, suggesting that Sema6A functions as a repulsive barrier within the IPL for neuronal processes expressing *PlexA4* (Matsuoka et al., 2011a). *Sema6A* mutants show the same defects in neurite stratification within the IPL as observed in *PlexA4* mutants (Matsuoka et al., 2011a; **Figure 3A**). Thus, these results show that Sema6A is a functional ligand for PlexA4, required for regulating select retinal neurite stratification *in vivo* (Matsuoka et al., 2011a; **Figure 3A**).

A more recent study shows that the transmembrane semaphorins Sema5A and Sema5B serve as repulsive molecules that together constrain neurites of most, if not all, inner retinal neurons to the IPL, serving a role in regulating retinal stratification that is distinct from Sema6A (Matsuoka et al., 2011b; **Figure 3B**). *Sema5A* and *Sema5B* are both expressed in the outer neuroblastic layer (ONBL) at postnatal day 0 (P0)–P3, and expression becomes more restricted to the middle and then to the outer part of the inner nuclear layer (INL) at later developmental stages (Matsuoka et al., 2011b). *Sema5A*$^{-/-}$; *Sema5B*$^{-/-}$ mice exhibit severe defects in the stereotypic neurite arborization of multiple AC and RGC subtypes (Matsuoka et al., 2011b; **Figure 3B**). For example, in *Sema5A*$^{-/-}$; *Sema5B*$^{-/-}$ mice, multiple subtypes of ACs and RGCs extend neurites toward the ONBL, suggesting that Sema5A and Sema5B prevent ACs and RGC subtypes from elaborating processes in the direction of the ONBL (Matsuoka et al., 2011b). However, dendritic stratification of ipRGC subtypes, which project into distinct IPL sublaminae, are disrupted in *Sema5A*$^{-/-}$; *Sema5B*$^{-/-}$ mice within the outer (OFF) layers, but not in within the inner (ON) layers (Matsuoka et al., 2011b). Similarly, various AC and BP cell types also show defects in stratification that are more prominent in the ON, as compared to the OFF, layers of the IPL (Matsuoka et al., 2011b; **Figure 3B**). Therefore, Sema5A and Sema5B constrain stratification of multiple retinal cell types within the IPL *in vivo* and, importantly, play a more prominent role in regulating stratification within the OFF, as compared to the ON, layers of the IPL. Intriguingly, electrophysiological recordings of light responses from neurons in the GCL of *Sema5A*$^{-/-}$; *Sema5B*$^{-/-}$ retinas *ex vivo* demonstrates that the OFF pathway is specifically impaired in *Sema5A*$^{-/-}$; *Sema5B*$^{-/-}$ mice, consistent with the selective disruption in OFF layer neuronal stratification in the *Sema5A*$^{-/-}$; *Sema5B*$^{-/-}$ IPL (Matsuoka et al., 2011b). Which receptors mediate these Sema5A- and Sema5B-evoked repulsive signaling? Although PlexB3 binds to Sema5A *in vitro* (Artigiani et al., 2004), *PlexB3*$^{-/-}$ mice do not show similar retinal defects as are observed in *Sema5A*$^{-/-}$; *Sema5B*$^{-/-}$ mice (Matsuoka et al., 2011b). Examination of *plexin* and *Npn* expression patterns in the developing retina revealed that *PlexA1* and *PlexA3* both show expression patterns that are identical and are complementary to the *Sema5A*/*5B* expression observed the developing postnatal retina (Matsuoka et al., 2011b). In addition, *PlexA1*$^{-/-}$; *PlexA3*$^{-/-}$ mice phenocopy the inner retinal lamination defects observed in *Sema5A*$^{-/-}$; *Sema5B*$^{-/-}$ mice (Matsuoka et al., 2011b; **Figure 3B**). *In vitro* experiments using retinal cells isolated from *PlexA1*$^{-/-}$;

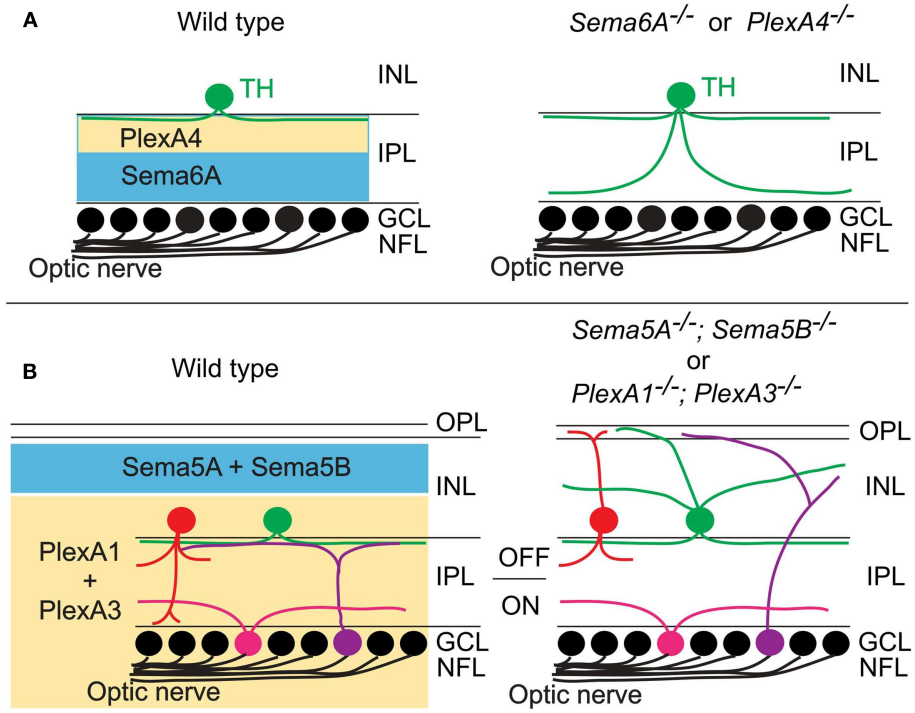

FIGURE 3 | Class 5 and class 6 transmembrane semaphorin signaling through plexinAs governs laminar targeting of inner retinal neuron subtypes. (A) Sema6A and PlexA4 show complementary protein expression in the ON and OFF layers of the inner plexiform layer, and this repulsive signaling confines neurite extension of dopaminergic amacrine cells (TH^+) within the S1 sublamina in wild-type mice. In *Sema6A* or *PlexA4* mutant mice, dopaminergic amacrine cells extend their aberrant processes to the S4/S5 sublaminae. **(B)** During early postnatal retinal development, *Sema5A/5B* and *PlexA1/A3* expressions are found in a complementary pattern in the retina. Loss of *Sema5A/5B* or *plexA1/A3* results in neurite mistargeting of multiple inner retinal neuron subtypes into the outer retina.

PlexA3$^{-/-}$ retinas demonstrate that PlexA1 and PlexA3 receptors indeed mediate Sema5A and Sema5B inhibitory signaling (Matsuoka et al., 2011b). Therefore, *Sema5A* and *Sema5B* expressed in the ONBL provide repulsive guidance signals to extending neurites from *PlexA1/A3*-expressing ACs and RGC subtypes in the INBL, and Sema5A/5B-PlexA1/A3 signaling is required for the establishment of specific retinal function.

LAMINA-RESTRICTED PROJECTIONS OF HIPPOCAMPAL MOSSY FIBERS

The hippocampus is also an ideal model system to study cellular and molecular mechanisms underlying laminar-specific axonal targeting. Pyramidal cells, the principal neurons of the cornu ammonis (CA), receive inputs from many regions in the brain. For example, hippocampal mossy fibers project preferentially to the stratum lucidum, the proximal-most lamina of the suprapyramidal region of CA3. However, the molecular mechanisms underlying these lamina-restricted axonal projections remained unknown. Recently, two studies showed that class 6 semaphorin signaling through plexinA family members controls lamina-restricted projections of hippocampal mossy fibers (Suto et al., 2007; Tawarayama et al., 2010). Suto et al. (2007) focused on *PlexA2*$^{-/-}$ and *PlexA4*$^{-/-}$ mice. In wild-type mice, mossy fibers invade the stratum lucidum in the suprapyramidal region of CA3 and CA3c, whereas *PlexA2*-deficiency in mice causes a shift of mossy fibers from the suprapyramidal region to the infra- and intrapyramidal regions (Suto et al., 2007). In contrast, in *PlexA4*$^{-/-}$ mice, mossy fibers invade most CA3 regions, in particular the stratum lacunosum-moleculare and the stratum oriens, and to a lesser extent the stratum radiatum (Suto et al., 2007). Immunohistochemical analysis shows that PlexA2 is localized on pyramidal cell dendrites, but not on mossy fibers, and that PlexA4 is localized on mossy fibers. This suggests that PlexA2 functions in CA3 pyramidal neurons and PlexA4 in mossy fibers to regulate laminar projections of mossy fibers (Suto et al., 2007). Co-culture experiments using dentate gyrus and CA3brain slices support this idea (Suto et al., 2007). These defects in *PlexA4*$^{-/-}$ mossy fiber projections suggest that *PlexA4*-deficient mossy fibers may lose their responsiveness to a repulsive cue. Although Sema6A binds to PlexA4 (Suto et al., 2005), *Sema6A* mutants do not show any defects in mossy fiber projections (Suto et al., 2007). Surprisingly, normal mossy fiber projections are restored in *PlexA2/Sema6A* double mutant mice, suggesting that Sema6A-mediated mossy fiber repulsion is attenuated by PlexA2 expressed in the proximal part of the suprapyramidal region of CA3, allowing mossy fibers to invade this area (Suto et al., 2007).

Other work from Fujisawa's group reveals roles of Sema6B in mossy fiber projections (Tawarayama et al., 2010). *Sema6B* is expressed in CA3 and repels mossy fibers, and this is dependent on the PlexA4 receptor *in vitro* (Tawarayama et al., 2010).

Sema6B-deficient mossy fibers aberrantly project to the stratum radiatum and the stratum oriens (Tawarayama et al., 2010). Furthermore, there are more severe defects in mossy fiber projections in *Sema6A*$^{-/-}$; *Sema6B*$^{-/-}$ mice compared to either single mutant alone (Tawarayama et al., 2010), suggesting that Sema6A and Sema6B can compensate for each other. PlexA2 promotes the growth of mossy fiber projections *in vitro* but does not suppress the Sema6B response as it does the Sema6A response (Tawarayama et al., 2010). Thus these two studies reveal that the PlexA4 expression on mossy fibers prevents them from entering the *Sema6A*-expressing suprapyramidal region of CA3 and restricts them to the proximal-most region, whereas Sema6A, but not Sema6B, repulsive activity is attenuated by PlexA2 (Suto et al., 2007; Tawarayama et al., 2010). Moreover, both *in vivo* and *in vitro* studies show that PlexA2 controls attraction of mossy fibers (Tawarayama et al., 2010). It will be interesting to investigate how PlexA2 actually promotes growth of mossy fibers.

SEMAPHORINS IN PROLIFERATION, DIFFERENTIATION, NEURONAL MIGRATION, AND POLARIZATION

THE BOUNDARY BETWEEN THE CENTRAL AND PERIPHERAL NERVOUS SYSTEM

The CNS is segregated from the PNS by boundaries. In the spinal cord this segregation is evident at the ventral and dorsal root transitional zones. These are located at the motor exit point (MEP), where motor axons leave the spinal cord, and at the dorsal root entry zone (DREZ), where sensory axons enter the spinal cord. Boundary cap (BC) cells at the MEP prevent the emigration of motor neurons from the ventral spinal cord (Vermeren et al., 2003). Ablation of BC cells causes the ectopic positioning of motor neuron cell bodies along their axons and into the ventral nerve roots (Vermeren et al., 2003). Semaphorin-plexin signaling is also involved in establishing this segregation between CNS and PNS (Bron et al., 2007; Mauti et al., 2007). *Sema6A* is expressed in BC cells, and deletion of *Sema6A* in mice (Bron et al., 2007), or downregulation of *Sema6A* (Mauti et al., 2007) in chick, results in ectopic motor neuron cell bodies distributed along the ventral roots. Since class 6 semaphorins bind to plexinA family members (Toyofuku et al., 2004; Suto et al., 2005; Yoshida et al., 2006), a possible role for plexinA receptors in this process was investigated. Knockdown of *PlexA1* (Mauti et al., 2007) or *PlexA2* (Bron et al., 2007) cause similar defects. *Npn2* mutant mice also show a similar phenotype (Bron et al., 2007). Although it is still not clear which plexinA family member is required for Sema6A signaling in mice, these two studies suggest that Sema6A/plexinA/Npn2 signaling constrains spinal motor neuron migration at the MEP. Since *Sema6A* is also expressed in BC cells at the DREZ, possible roles for several semaphorins and plexins were also examined (Mauti et al., 2007). Knockdown of *Sema6A*, *PlexA1*, *PlexA4* or *Sema6D*, indeed, causes failure of dorsal roots to form and segregate properly (Mauti et al., 2007), indicating that semaphorin-plexin signaling also functions in the DREZ as well as in the MEP.

NEURONAL MIGRATION

Semaphorins also play key roles in controlling neuronal migration. For example, class 3 semaphorins regulate interneuron migration from the basal forebrain within in the tangential migratory stream (Marín et al., 2001). In addition to tangential migration, a recent work shows that Sema3A can control radial migration (Chen et al., 2008). In the cortex, *Sema3A* is expressed in a gradient across the cortical layers and its receptor, *Npn1*, is expressed by migrating neurons (Chen et al., 2008). Knockdown or deletion of *Npn1* in newborn cortical neurons by *in utero* electroporation causes defects in their radial migration (Chen et al., 2008). Although cell fate apparently does not change, their radial orientation during migration is disrupted (Chen et al., 2008). Furthermore, disrupting the Sema3A gradient causes neuronal misorientation in cultured cortical slices (Chen et al., 2008). Interestingly, cortical slice culture experiments show that Sema3A is attractive, but not repulsive, to radially migrating neurons (Chen et al., 2008).

In addition to class 3 semaphorins, a class 6 semaphorin also controls neuronal migration (Kerjan et al., 2005). Cerebellar granule cell precursors migrate tangentially over the cerebellar plate to form the external granular layer (EGL; Wingate, 2001). Postmitotic granule cells migrate tangentially in all directions in the deeper EGL (Ryder and Cepko, 1994; Komuro et al., 2001). *Sema6A* is expressed in the deeper EGL in the postnatal cerebellar cortex, and granule cell migration within the EGL, or from the EGL, is perturbed in *Sema6A* mutants; no obvious defects in granule cell proliferation, differentiation, or survival are observed in *Sema6A* mutants (Kerjan et al., 2005). To determine whether Sema6A functions as a receptor or a ligand, mouse *Sema6A* mutant chimeras were analyzed, and the results reveal a non-cell-autonomous Sema6A function in granule cells, suggesting that Sema6A functions as a ligand (Kerjan et al., 2005). A more recent study, also from Chédotal laboratory, reveals that PlexA2 is a functional receptor for the Sema6A ligand to regulate granule cell migration (Renaud et al., 2008). The authors found defects in granule cell migration in *PlexA2*$^{-/-}$ mice, which is very similar to those observed in *Sema6A*$^{-/-}$ mice (Renaud et al., 2008). Genome-wide *N*-ethyl-*N*-nitrosourea (ENU) mutagenesis screen identified NMF454 mutant mice, and the single mutation of *PlexA2* gene was identified (Renaud et al., 2008). This single nucleotide mutation causes a replacement of an amino acid residue in the semaphorin domain, and this mutant protein cannot bind to Sema6A *in vitro* (Renaud et al., 2008). Then centrosome-nucleus uncoupling was examined in the absence of Sema6A-PlexA2 signaling, since in cerebellar granule cells, microtubules linked to the centrosome pull the nucleus during migration. *In vitro* experiments using EGL explants show that there are defects in the distance between the centrosome and the nucleus in *Sema6A*$^{-/-}$ and *PlexA2*$^{-/-}$ mice (Renaud et al., 2008). In addition, *in vivo* analyses reveal that nucleus-centrosome coupling is perturbed in the absence of Sema6A-PlexA2 signaling (Renaud et al., 2008). These studies suggest that Sema6A-PlexA2 signaling modulates neuronal cell migration by controlling centrosome positioning.

PROLIFERATION AND DIFFERENTIATION

Although Sema6A-PlexA2 signaling does not regulate proliferation and differentiation for granule cells, PlexB2 signaling is required for both proliferation and differentiation (Friedel et al., 2007). PlexB2 is expressed by proliferating granule cells, and *PlexB2*-deficiency causes a disorganization of the timing of granule cell proliferation and differentiation in the EGL (Friedel

et al., 2007). Further *in vitro* and *in vivo* studies show that Sema4C and Sema4G are likely to be *in vivo* ligands for PlexB2 (Maier et al., 2011). Although *Sema4C*$^{-/-}$; *Sema4G*$^{-/-}$ mice show defects in the EGL, the phenotype is less severe compared to that observed in *PlexB2*$^{-/-}$ mice (Maier et al., 2011), suggesting that other ligands for PlexB2 exist. Together, distinct semaphorin-plexin signaling regulates proliferation, differentiation, and neuronal migration in the EGL.

NEURONAL POLARIZATION

Neuronal polarization in the form of axon and dendrites is critical for neuronal function. Two studies recently show that Sema3A signaling controls the decision made by newly extending neurites to become axons or dendrites (Nishiyama et al., 2011; Shelly et al., 2011). Nishiyama et al. (2011) show that overexpression *in vitro* of Sema3A in *Xenopus* spinal commissural interneurons (xSCINs) converts axons to dendrites, and this conversion of neurite identity requires the voltage-dependent Ca^{2+} channel $Ca_v2.3$. *Sema3A* expression is apparently required for $Ca_v2.3$ expression *in vivo*, and a series of electrophysiological analyses *in vitro* suggest that Sema3A is likely to increase the number of $Ca_v2.3$ in the growth cone plasma membrane rather than modulating their gating properties (Nishiyama et al., 2011). Moreover, downregulation of $Ca_v2.3$ expression reveals that $Ca_v2.3$ is required for acquisition of the dendrite identity similar to Sema3A, so Sema3A-$Ca_v2.3$ signaling is required for dendrite identity *in vivo* (Nishiyama et al., 2011). Finally, cGMP signaling induces $Ca_v2.3$ expression and dendrite identity (Nishiyama et al., 2011). Taken together, this study suggests that Sema3A induces the cGMP-mediated expression of functional $Ca_v2.3$ channels, recruits $Ca_v2.3$ channels to the growth cone plasma membrane, and promotes the acquisition of the dendrite identity. The molecular mechanisms of how Sema3A recruits $Ca_v2.3$ channels to the plasma membrane and how $Ca_v2.3$ regulates dendrite identify will be examined in future studies.

Similarly, Shelly et al. (2011) show that local exposure to Sema3A promotes dendrite formation and suppresses axon formation in cultured hippocampal neurons. Knockdown experiments show that Npn1 is required for this neuronal polarization. Using FRET sensors expressed in cultured hippocampal neurons, the authors show that Sema3A induces a gradual elevation of cGMP levels and also a concomitant reduction in cAMP levels and PKA activity (Shelly et al., 2011). A previous work shows that axon initiation triggered by a cAMP analog or BDNF requires PKA-dependent phosphorylation of LKB1, a serine/threonine kinase that is essential for axon formation (Shelly et al., 2007), and also phosphorylation of GSK-3β, a crucial axon determinant (Shelly et al., 2010). Sema3A signaling, which promotes dendrite formation, antagonizes PKA-dependent phosphorylation of LKB1 and GSK-3β, consistent with the crucial role of these kinases in axon formation (Shelly et al., 2011). Finally, perturbing Sema3A signaling in newly generated cortical neurons in the rat embryo suggests that Sema3A signaling is indeed required for axon/dendrite polarization *in vivo* (Shelly et al., 2011). This study suggests that Sema3A regulates axon/dendrite polarity by suppressing axon-specific cAMP/PKA-dependent processes and promoting dendrite-specific cGMP/PKG-dependent functions.

SEMAPHORINS IN SYNAPSE FORMATION AND FUNCTION

SYNAPSE FORMATION *IN VITRO* AND *EX VIVO*

In addition to the guidance of axons and dendrites, recent studies show that semaphorins also control synapse formation and synaptic function. An RNAi-based candidate screen found that Sema4B and Sema4D are involved in synapse development (Paradis et al., 2007). It was shown that Sema4B affects the formation of both GABAergic and glutamatergic synapses, whereas Sema4D affects formation of GABAergic, but not glutamatergic, synapses (Paradis et al., 2007). Furthermore, two additional studies show that semaphorins modulate synaptic function (Sahay et al., 2005; Bouzioukh et al., 2006). First, co-receptors for secreted semaphorins, Npns, are found at synapses (Sahay et al., 2005; Bouzioukh et al., 2006). Furthermore, application of Sema3F to acute hippocampal slices modulates both the frequency and amplitude of miniature EPSCs in granule cells of the dentate gyrus and CA1 (Sahay et al., 2005). Similarly, acute application of Sema3A decreases the efficacy of synaptic transmission evoked in the CA1 region of hippocampal slices (Bouzioukh et al., 2006). These studies reveal that semaphorins function in adult brains as well as the developing nervous systems.

REGULATION OF SYNAPSE NUMBER, DENDRITIC PROCESS AND SPINE MORPHOLOGY

Class 3 and 4 semaphorins have roles in synapse formation and function *in vitro* or *ex vivo* as mentioned above (Sahay et al., 2005; Bouzioukh et al., 2006; Paradis et al., 2007). However, *in vivo* roles of semaphorins in synaptogenesis remained less clear. Tran et al. (2009) showed that Sema3A/Npn1/PlexA4 and Sema3F/Npn2/PlexA3 signaling regulate CNS connectivity through the differential control of spine morphogenesis, synapse formation, and the elaboration of dendritic morphology. In *Sema3F*$^{-/-}$ and *Npn2*$^{-/-}$ mice, abnormal spine morphology and increased spine number and adult dentate gyrus (DG) granule cells (GCs) are observed at P21 (Tran et al., 2009). Similarly, both aberrant spine distribution and changes in spine morphology were observed on apical, but not basal, dendrites of layer V cortical pyramidal neurons in *Sema3F*$^{-/-}$ and *Npn2*$^{-/-}$ mice (Tran et al., 2009). Furthermore, whole-cell voltage-clamp recordings reveal that mEPSCs in layer V pyramidal neurons and DG GCs in acute brain slices exhibit increased frequency, no change in amplitude, however no defects in the paired-pulse amplitude ratio in *Npn2*$^{-/-}$ mice were observed. This suggests that the increase in mEPSC frequency found in *Npn2*$^{-/-}$ mice is due to an increase in the number of synapses, rather than an increase in the probability of presynaptic release (Tran et al., 2009). Similar defects are observed in *PlexA3* mutants. Thus, Sema3F/Npn2/PlexA3 signaling negatively regulates both excitatory synapse number and synaptic transmission in layer V and DG neurons. Furthermore, *Npn1*$^{Sema-}$ mice exhibit markedly reduced growth and branching of layer V cortical neuron basal, but not apical, dendritic arborizations, indicating that Sema3A-Npn1 signaling positively regulates dendrite growth and branching (Tran et al., 2009). Similar defects are observed in *PlexA4* mutants (Tran et al., 2009). Consistent with the distinct defects observed in the absence of Sema3F/Npn2/PlexA3 and Sema3A/Npn1/PlexA4 signaling, cell surface Npn2 receptor is predominantly localized to the primary apical dendrite in

cultured cortical neurons with pyramidal morphology, whereas the Npn1 receptor is more uniformly distributed on all dendritic processes (Tran et al., 2009). Taken together, these finding demonstrate that Sema3F/Npn2/PlexA3 signaling controls differential spine growth and distribution, and Sema3A/Npn1/PlexA4 signaling controls basal dendrite growth. It will be of interest to determine if other guidance receptors exhibit localization to dendritic subdomains, since this could provide a robust mechanism for segregating complex circuit organization in the CNS.

SENSORY-MOTOR CIRCUIT FORMATION IN THE SPINAL CORD

In the vertebrate somatosensory system, peripheral stimuli are conveyed by dorsal root ganglia (DRG) sensory neurons. DRG sensory neurons fall into two major groups: those transducing proprioceptive and cutaneous sensory stimuli (Brown, 1981; Koerber and Mendell, 1992). Proprioceptive neurons convey information about the state of muscle contraction and limb position, whereas cutaneous neurons mediate a wide range of noxious and innocuous stimuli (Brown, 1981; Koerber and Mendell, 1992). The myelinated axons of proprioceptive sensory neurons avoid the superficial dorsal horn and project to the intermediate or ventral spinal cord, while the axons of cutaneous afferents project directly into the superficial dorsal horn (Brown, 1981; Koerber and Mendell, 1992). Signals mediated by Sema3A have been suggested to inhibit cutaneous axons in the ventral spinal cord (Messersmith et al., 1995; Fu et al., 2000). However, genetic inactivation of *Sema3A* in mice has yet to reveal a major role for these ligands in the patterning of sensory axonal trajectories (Behar et al., 1996; Taniguchi et al., 1997; Gu et al., 2003). Nevertheless, other semaphorins belonging to several classes are expressed in the spinal cord (Cohen et al., 2005), and a second major class of semaphorin receptors, the plexins are expressed by sensory and spinal neurons (Cheng et al., 2001; Cohen et al., 2005), raising the possibility plexins are important for establishing central spinal sensory afferent trajectories.

Two studies on the role of the PlexA1 receptor and its ligand Sema6D demonstrate that Sema6D-PlexA1 signaling controls axon positioning of proprioceptive sensory neurons in the dorsal spinal cord (Yoshida et al., 2006; Leslie et al., 2011; **Figure 4A**). *PlexA1* is exclusively expressed by proprioceptive sensory neurons in the DRG, and *Sema6D* is expressed in the dorsal spinal cord (Yoshida et al., 2006). In *PlexA1* or *Sema6D* mutants, proprioceptive axons ectopically invade the dorsal horn (Yoshida et al., 2006; Leslie et al., 2011; **Figure 4A**). Since proprioceptive axons are heavily myelinated, and most cutaneous axons are thinly myelinated if at all, oligodendrocytes associated with proprioceptive axons invade the dorsal spinal cord, and then inhibit synapse formation in the absence of Sema6D-PlexA1 signaling (Yoshida et al., 2006; Leslie et al., 2011; **Figure 4A**). Genetic deletion of oligodendrocytes demonstrates that it is the ectopic oligodendrocytes, not proprioceptive axons, in the dorsal spinal cord that inhibit synapse formation, but not axonal growth, in *Sema6D* mutants (Leslie et al., 2011; **Figure 4A**). Therefore, ectopic oligodendrocytes in the dorsal spinal cord inhibit synapse formation in the absence of Sema6D-PlexA1 signaling.

Once proprioceptive axons reach the ventral spinal cord, most make monosynaptic connections with specific motor neurons; however, a subset of proprioceptive axons at cervical levels form di- or poly-synaptic interneuronal connections (Vrieseling and Arber, 2006; reviewed in Ladle et al., 2007). Interestingly, PlexD1 and its ligand Sema3E regulate avoidance of monosynaptic connections between cutaneous maximus (Cm) sensory and motor neurons (Pecho-Vrieseling et al., 2009; **Figure 4B**). Unlike most Ia afferents and motor neuron pools that project to the same muscle, Cm Ia afferents do not make monosynaptic connections with Cm motor neurons in wild-type mice (Vrieseling and Arber, 2006; **Figure 4B**). However, genetic deletion of *PlexD1* or *Sema3E* results in aberrant monosynaptic Ia afferent connectivity with this motor neuron pool (Pecho-Vrieseling et al., 2009; **Figure 4B**). Furthermore, ectopic expression of Sema3E in triceps (Tri) motor neurons prevents monosynaptic sensory-motor connectivity (Pecho-Vrieseling et al., 2009; **Figure 4B**). Thus, repulsive Sema3E-PlexD1 signaling controls the exclusion of sensory afferent inputs on CM motor neuron pool.

SYNAPSE FORMATION IN THE STRIATUM

The striatum receives convergent excitatory inputs from the cortex and thalamus. Specific excitatory synaptic connections are formed between axons arising from these two regions and their two functionally distinct populations of targets: the direct and the indirect pathway of striatal medium spiny neurons (MSNs; Surmeier et al., 2007). Very recently, Ding et al. (2012) demonstrated that Sema3E-PlexD1 signaling controls pathway-specific synapse formation in the striatum. The authors first find that PlexD1 is expressed by the direct pathway, but not the indirect pathway, MSNs, whereas *Sema3E* is expressed in the thalamus and in deep cortical layers, the two principal sources of glutamatergic inputs to the striatum (Ding et al., 2012). AMPA receptor-mediated spontaneous miniature excitatory postsynaptic currents (mEPSCs) were measured using the whole-cell voltage-clamp recording, and loss of either *Sema3E* or *PlexD1* was found to lead to a large increase in mEPSC frequency, but not amplitude, in direct pathway MSNs (Ding et al., 2012). Furthermore, optogenetic activation of thalamostriatal axons showed that loss of *PlexD1* or *Sema3E* leads to large evoked thalamostriatal EPSCs in the direct pathway MSNs, and loss of *PlexD1* increases thalamostriatal synapse number (Ding et al., 2012). In thalamostriatal projections, Sema3E is secreted by axons and *PlexD1* is expressed by postsynaptic neurons. Therefore, it is unlikely that Sema3E-PlexD1 signaling affects the targeting axons, as is observed in the spinal cord (Pecho-Vrieseling et al., 2009). Instead, Sema3E-PlexD1 signaling may control thalamostriatal synaptic strength by regulating postsynaptic sites through the PlexD1 receptor (**Figure 5**). For example, PlexD1 receptor signaling may alter the cytoskeleton or regulate glutamate receptor trafficking and stabilization. Alternatively, Sema3E-PlexD1 signaling may produce a secreted molecule to induce a retrograde signal in the postsynaptic sites that repels thalamostriatal axons.

AXON PRUNING

The CST axon projection pattern is known to be modified during neural development by stereotyped axon pruning (Thong and Dreher, 1987; Stanfield, 1992). Cortical motor neurons extending from the rostral cortex prune axons that extend to the superior

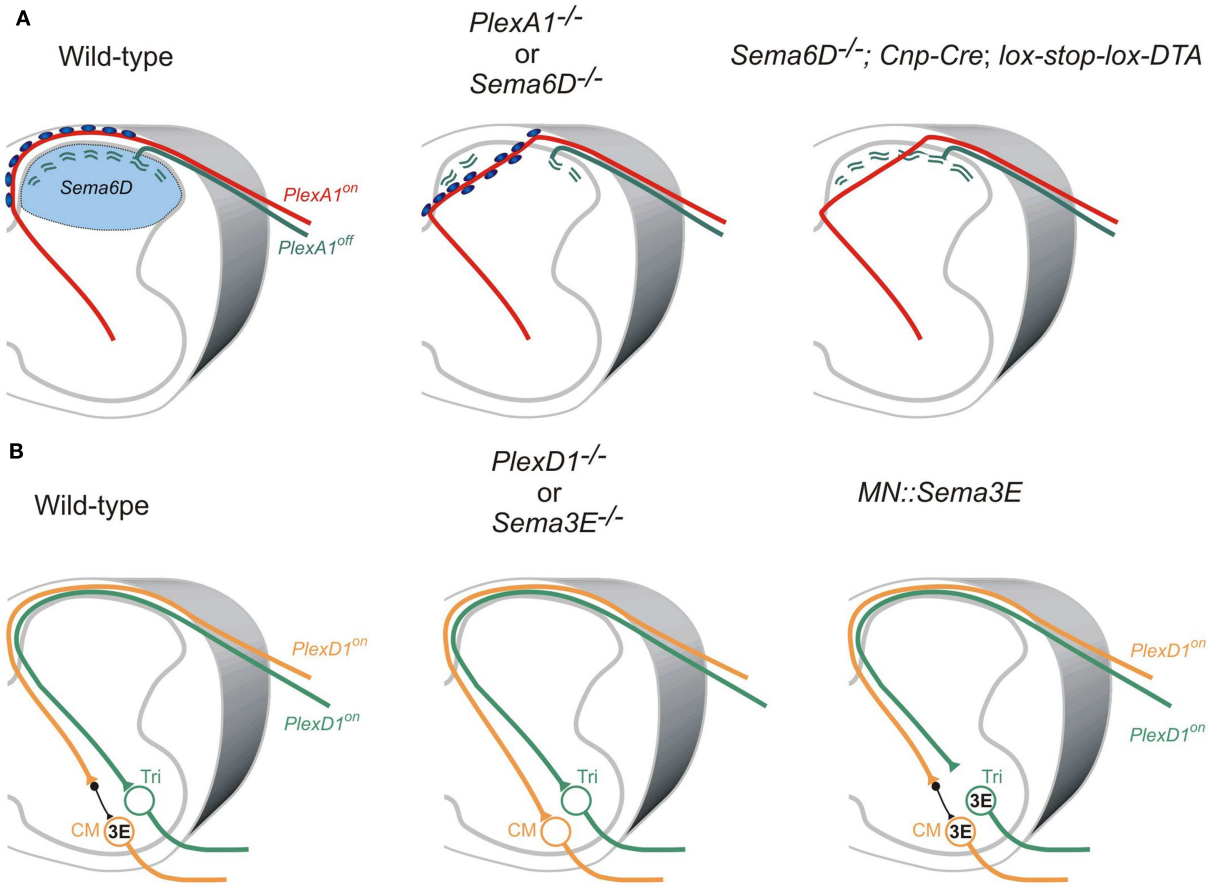

FIGURE 4 | Roles of semaphorin-plexin signaling in sensory-motor circuitry. (A) Cross-sectional diagrams depicting the dorsal spinal cords of wild-type, *PlexA1*, and *Sema6D*, and oligodendrocyte-deleted *Sema6D* mutant mice used in two studies (Yoshida et al., 2006; Leslie et al., 2011). Proprioceptive axons (red lines), oligodendrocytes (blue circles), cutaneous axons (green lines), cutaneous synapses (green wavy lines). Blue areas show *Sema6D*-expressing region. *PlexA1* is expressed by proprioceptive sensory neurons but not cutaneous sensory neurons. Cutaneous synapses are disrupted when oligodendrocytes aberrantly enter the dorsal horn, whereas genetic deletion of oligodendrocytes from *Sema6D* mutants rescues these synaptic defects. **(B)** Cross-sectional diagrams depicting the spinal cords of wild-type, *PlexD1*, and *Sema3E* mutant mice as well as motor neuron-specific *Sema3E*-expressing mice (Pecho-Vrieseling et al., 2009). Motor neurons innervating triceps (Tri) muscle receive monosynaptic inputs from Tri sensory afferents, whereas cutaneous maximus (CM) motor neurons lack monosynaptic inputs from CM sensory afferents. *Sema3E* is expressed by CM motor neurons but not Tri motor neurons. *PlexD1* is expressed by ∼80% of CM proprioceptive sensory neurons, and ∼50% of Tri proprioceptive sensory neurons. Absence of Sema3E-PlexD1 signaling causes aberrant monosynaptic sensory-motor connections between CM sensory and CM motor neurons. Ectopic expression of Sema3E in Tri motor neurons reduces monosynaptic connections between Tri afferents and Tri motor neurons.

and inferior colliculi, whereas cortical neuron axons extending from visual cortex prune axons they initially extend to the inferior colliculus and the spinal cord (Thong and Dreher, 1987; Stanfield, 1992). Plexin receptor signaling selectively controls the stereotyped pruning of corticospinal axons from visual cortex, but not motor cortex (Low et al., 2008). Both anterograde and retrograde tracers show that visual cortex neurons fail to prune axons that extend to the spinal cord in *PlexA3*/*A4* double mutants, or *Npn2* mutant mice (Low et al., 2008). Interestingly, unpruned visual CST axon collaterals in *PlexA3*/*A4* double or *Npn2* mutant mice retain their synaptic contacts in the spinal cord (Low et al., 2008). However, these unpruned CST axons in *PlexA3*/*A4* double mutants are unmyelinated, suggesting they are likely to be physiologically impaired (Low et al., 2008). Taken together, these studies show that distinct Sema/Npn/plexin signaling events regulate the axonal trajectories of motor CST axons and the pruning of visual CST axons. It remains to be determined exactly how CST motor axon pruning is regulated.

Sema3F/Npn2/PlexA3 signaling has been shown to be required for the stereotyped pruning of mossy fiber axon collaterals (Bagri et al., 2003). A further study has shown that mossy fiber axon collaterals form transient synaptic complexes in the early postnatal mouse hippocampus, and at later postnatal ages these synaptic complexes stop maturating and are removed before stereotyped pruning (Liu et al., 2005). A recent study also shows that not only class 3 semaphorins but also a transmembrane class 5 semaphorin can mediate synapse elimination in cultured hippocampal neurons (O'Connor et al., 2009). Therefore, distinct classes of semaphorins may have roles in synapse pruning and elimination in different regions in the nervous system. Future analysis using a

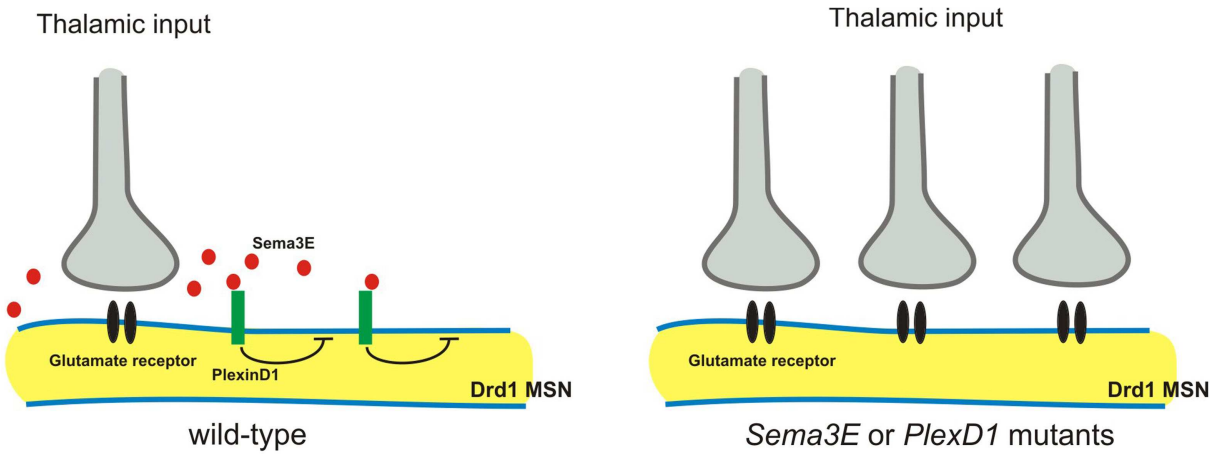

FIGURE 5 | Sema3E-PlexD1 signaling regulates pathway-specific synapse formation in the striatum. Direct and indirect pathway MSNs are functionally and molecularly distinct. Direct pathway MSNs express type 1 dopamine receptors (Drd1) and indirect pathway MSNs express type 2 dopamine receptors (Drd2). *PlexD1* is exprsssed by Drd1^{on}-direct pathway MSNs in the striatum, whereas *Sema3E* is expressed by subsets of neurons in the main thalamic nuclei that project to the striatum. Loss of Sema3E-PlexD1 signaling causes functional and anatomical rearrangement of thalamostriatal synapses specifically in direct pathway MSNs without effects on corticostriatal synapses.

mouse genetics will reveal the *in vivo* roles of class 5 semaphorins in axon elimination.

MECHANISMS OF SEMAPHORIN ACTION

SWITCHING BETWEEN ATTRACTION AND REPULSION

Some semaphorins have been shown to exhibit both attractive and repulsive activities *in vitro* and *in vivo* (Song et al., 1998; Castellani et al., 2000, 2002; Wolman et al., 2004). Recent studies show novel mechanisms underlying the switch of Sema3E function from axonal repulsion to attraction (Chauvet et al., 2007; Bellon et al., 2010). First, Mann's group looked in detail at the expression of *Sema3E*, *Npn1*, and *PlexD1* in the developing brain, and examined their function (Chauvet et al., 2007). Corticofugal and striatonigral neurons expressing *PlexD1*, but not *Npn1*, respond to Sema3E as a repulsive cue (Chauvet et al., 2007). In contrast, subiculo-mammillary neurons express both *PlexD1* and *Npn1*, and on these neurons Sema3E acts as an attractant (Chauvet et al., 2007). Since the extracellular domain alone of Npn1 is sufficient to convert repulsive signaling by PlexD1 to attraction, the involvement of another co-receptor capable of signaling this switch is suggested to mediate Sema3E attractive function (Chauvet et al., 2007). A recent study addresses this issue and shows that VEGFR2 (KDR/Flk1) acts as a co-receptor for a Sema3E/Npn1/PlexD1 attractive signaling complex (Bellon et al., 2010). VEGFR2 is expressed by neurons of the subiculum and mediates axonal elongation in response to Sema3E *in vitro*, and VEGFR2 interacts with the Npn1/PlexD1 receptor complex (Bellon et al., 2010). Furthermore, VEGFR2 is required for Sema3E-mediated axonal elongation but not axonal repulsion, both *in vitro* and *in vivo* (Bellon et al., 2010). These observations demonstrate that PlexD1 transduces the Sema3E-mediated repulsive signal, whereas VEGFR2/Npn1/PlexD1 complex transduces the Sema3E-mediated attractive signal.

Another recent study shows that Sema3F is a bifunctional (repulsive and attractive) cue for dopaminergic axons (Kolk et al., 2009). Dopaminergic neurons in the mesodiencephalon (mdDA neurons) make precise synaptic connections with their target neurons in the forebrain. In the elaboration of this circuit during early developmental stages, a Sema3F-mediated repulsive signaling controls mdDA pathway development through both Npn2-dependent (axon fasciculation and channeling) and Npn2-independent (rostral growth) mechanisms (Kolk et al., 2009). During later developmental stages, Sema3F-mediated attractive signaling through the Npn2 receptor is required to orient mdDA axonal projections in the cortical plate of the medial prefrontal cortex (Kolk et al., 2009). Thus, the same semaphorins can be both attractive and repulsive. A recent work in flies demonstrates the phylogenetic conservation of semaphorin bifunctionality (Wu et al., 2011). This bifunctionality may be dependent on the expression of distinct co-receptors, could involve different interactions with same receptor that result in intracellular different signaling events, and most certainly requires the engagement of distinct intracellular signaling pathways capable of mediated attraction or repulsion.

The ratio of cAMP/cGMP has also been shown to regulate axonal attraction or repulsion *in vitro* (Song et al., 1998). Moreover, cyclic nucleotide-gated channels (CNGCs) have been suggested to function in axonal pathfinding *in vivo* (Coburn and Bargmann, 1996; Komatsu et al., 1996; Zheng et al., 2000). A recent study has shown that cyclic-GMP-gated CNG channels function in Sema3A-induced growth cone repulsion in *Xenopus* (Togashi et al., 2008). Future studies will determine whether mouse cyclic-GMP-gated CNG channels are also involved in Sema3A-mediated axonal repulsion.

REGULATION OF SEMAPHORIN SIGNALING

Recent several studies have demonstrated how semaphorin signaling might be regulated. First, fibroblast growth factor 8 (FGF8) has been shown to repel midbrain dopaminergic neuron (mDAN) axons that extend through the diencephalon (Yamauchi et al., 2009). This repulsion seems to be mediated by Sema3F, since

the expression of *Sema3F* is up-regulated by ectopic expression of FGF8 and Sema3F repels mDAN axonal growth (Yamauchi et al., 2009). Thus, regulation of Sema3F expression by FGF8 provides a robust mechanism for mediating mDAN axon repulsion *in vivo*. Another study shows that Robo1 regulates *Npn1* and *PlexA1* expression and thereby facilitates the migration of cortical interneurons through the ventral forebrain (Hernández-Miranda et al., 2011). Interestingly, this study further shows that Robo1 binds directly to Npn1 and this interaction is mediated by a region contained within its first two Robo Ig domains. Therefore, Robo1 has the potential to modulate semaphorin signaling by regulating *Npn1* and *PlexA1* expression, and by interacting with Npn1. Interestingly, a recent study shows that a microRNA, miR-124, regulates Npn1 expression in *Xenopus* neurons (Baudet et al., 2011). Since miR-124 knockdown induces the downregulation of Npn1 in the growth cone, miR-124 knockdown also delays onset of Sema3A sensitivity (Baudet et al., 2011). As miRNAs in general repress the expression of their target mRNAs and Npn1 is unlikely to be their target, miR-124 appears to regulate Npn1 expression indirectly. Then CoREST, a transcriptional co-repressor that influences Npn1 expression, was identified as a target and mediator of miR-124 (Baudet et al., 2011). Finally, a miR-124 morphant results in RGC axon targeting errors *in vivo* (Baudet et al., 2011). Taken together, these findings suggest that miR-124 is important for regulating the intrinsic temporal changes in RGC growth cone responsiveness by controlling onset of sensitivity to Sema3A.

CONCLUSION

Semaphorins and their receptors, plexins, Npns, and various co-receptors, play many roles in each step of neural circuit assembly. These include neural migration, neuronal polarity, axon guidance, dendrite development, synapse formation, and synaptic function in the PNS and CNS. Future studies will likely reveal more details of how semaphorin signaling is involved in neural circuit assembly, especially the roles of semaphorin signaling in postnatal and adult neural circuitry, neuronal degeneration/regeneration, and the interactors upstream and downstream of semaphorin signaling. If we have better understanding of roles of semaphorin signaling in neural circuit formation, the information will be likely to provide a template for understanding how other signaling pathways work in the nervous system. Together the information will be able to lead to a sense of unified mechanisms that govern the establishment of neural circuit formation.

ACKNOWLEDGMENTS

I am grateful to R. Giger, A. Kolodkin, T. Kuwajima, C. Mason, and R. Mastuoka, for helpful comments on this manuscript. Y. Yoshida is supported by grants from NINDS (NS065048).

REFERENCES

Artigiani, S., Conrotto, P., Fazzari, P., Gilestro, G. F., Barberis, D., Giordano, S., Comoglio, P. M., and Tamagnone, L. (2004). Plexin-B3 is a functional receptor for semaphorin 5A. *EMBO Rep.* 5, 710–714.

Bagnard, D., Lohrum, M., Uziel, D., Puschel, A. W., and Bolz, J. (1998). Semaphorins act as attractive and repulsive guidance signals during the development of cortical projections. *Development* 125, 5043–5053.

Bagri, A., Cheng, H. J., Yaron, A., Pleasure, S. J., and Tessier-Lavigne, M. (2003). Stereotyped pruning of long hippocampal axon branches triggered by retraction inducers of the semaphorin family. *Cell* 113, 285–299.

Baudet, M. L., Zivraj, K. H., Abreu-Goodger, C., Muldal, A., Armisen, J., Blenkiron, C., Goldstein, L. D., Miska, E. A., and Holt, C. E. (2011). miR-124 acts through CoREST to control onset of Sema3A sensitivity in navigating retinal growth cones. *Nat. Neurosci.* 15, 29–38.

Behar, O., Golden, J. A., Mashimo, H., Schoen, F. J., and Fishman, M. C. (1996). Semaphorin III is needed for normal patterning and growth of nerves, bones and heart. *Nature* 383, 525–528.

Bellon, A., Luchino, J., Haigh, K., Rougon, G., Haigh, J., Chauvet, S., and Mann, F. (2010). VEGFR2 (KDR/Flk1) signaling mediates axon growth in response to semaphorin 3E in the developing brain. *Neuron* 66, 205–219.

Bouzioukh, F., Daoudal, G., Falk, J., Debanne, D., Rougon, G., and Castellani, V. (2006). Semaphorin3A regulates synaptic function of differentiated hippocampal neurons. *Eur. J. Neurosci.* 23, 2247–2254.

Bron, R., Vermeren, M., Kokot, N., Andrews, W., Little, G. E., Mitchell, K. J., and Cohen, J. (2007). Boundary cap cells constrain spinal motor neuron somal migration at motor exit points by a semaphorin-plexin mechanism. *Neural Dev.* 22, 21.

Brown, A. G. (1981). *Organization in the Spinal Cord*. New York, NY: Springer.

Castellani, V., Chedotal, A., Schachner, M., Faivre-Sarrailh, C., and Rougon, G. (2000). Analysis of the L1-deficient mouse phenotype reveals crosstalk between Sema3A and L1 signaling pathways in axonal guidance. *Neuron* 27, 237–249.

Castellani, V., De Angelis, E., Kenwrick, S., and Rougon, G. (2002). Cis and trans interactions of L1 with neuropilin-1 control axonal responses to semaphorin 3A. *EMBO J.* 21, 6348–6357.

Chauvet, S., Cohen, S., Yoshida, Y., Fekrane, L., Livet, J., Gayet, O., Segu, L., Buhot, M. C., Jessell, T. M., Henderson, C. E., and Mann, F. (2007). Gating of Sema3E/PlexinD1 signaling by neuropilin-1 switches axonal repulsion to attraction during brain development. *Neuron* 56, 807–822.

Chen, G., Sima, J., Jin, M., Wang, K. Y., Xue, X. J., Zheng, W., Ding, Y. Q., and Yuan, X. B. (2008). Semaphorin-3A guides radial migration of cortical neurons during development. *Nat. Neurosci.* 11, 36–44.

Cheng, H. J., Bagri, A., Yaron, A., Stein, E., Pleasure, S. J., and Tessier-Lavigne, M. (2001). Plexin-A3 mediates semaphorin signaling and regulates the development of hippocampal axonal projections. *Neuron* 32, 249–263.

Coburn, C. M., and Bargmann, C. I. (1996). A putative cyclic nucleotide-gated channel is required for sensory development and function in *C. elegans*. *Neuron* 17, 695–706.

Cohen, S., Funkelstein, L., Livet, J., Rougon, G., Henderson, C. E., Castellani, V., and Mann, F. (2005). A semaphorin code defines subpopulations of spinal motor neurons during mouse development. *Eur. J. Neurosci.* 21, 1767–1776.

de Winter, F., Cui, Q., Symons, N., Verhaagen, J., and Harvey, A. R. (2004). Expression of class-3 semaphorins and their receptors in the neonatal and adult rat retina. *Invest. Ophthalmol. Vis. Sci.* 45, 4554–4562.

Ding, J. B., Oh, W. J., Sabatini, B. L., and Gu, C. (2012). Semaphorin 3E-Plexin-D1 signaling controls pathway-specific synapse formation in the striatum. *Nat. Neurosci.* 15, 215–223.

Erskine, L., Reijntjes, S., Pratt, T., Denti, L., Schwarz, Q., Vieira, J. M., Alakakone, B., Shewan, D., and Ruhrberg, C. (2011). VEGF signaling through neuropilin 1 guides commissural axon crossing at the optic chiasm. *Neuron* 70, 951–965.

Falk, J., Bechara, A., Fiore, R., Nawabi, H., Zhou, H., Hoyo-Becerra, C., Bozon, M., Rougon, G., Grumet, M., Püschel, A. W., Sanes, J. R., and Castellani, V. (2005). Dual functional activity of semaphorin 3B is required for positioning the anterior commissure. *Neuron* 48, 63–75.

Faulkner, R. L., Low, L. K., Liu, X. B., Coble, J., Jones, E. G., and Cheng, H. J. (2008). Dorsal turning of motor corticospinal axons at the pyramidal decussation requires plexin signaling. *Neural Dev.* 3, 21.

Fenstermaker, V., Chen, Y., Ghosh, A., and Yuste, R. (2004). Regulation of dendritic length and branching by semaphorin 3A. *J. Neurobiol.* 58, 403–412.

Friedel, R. H., Kerjan, G., Rayburn, H., Schüller, U., Sotelo, C., Tessier-Lavigne, M., and Chédotal, A. (2007). Plexin-B2 controls the development of cerebellar granule cells. *J. Neurosci.* 27, 3921–3932.

Fu, S. Y., Sharma, K., Luo, Y., Raper, J. A., and Frank, E. (2000). SEMA3A regulates developing sensory

projections in the chicken spinal cord. *J. Neurobiol.* 45, 227–236.

Gu, C., Rodriguez, E. R., Reimert, D. V., Shu, T., Fritzsch, B., Richards, L. J., Kolodkin, A. L., and Ginty, D. D. (2003). Neuropilin-1 conveys semaphorin and VEGF signaling during neural and cardiovascular development. *Dev. Cell* 5, 45–57.

Gu, C., Yoshida, Y., Livet, J., Reimert, D. V., Mann, F., Merte, J., Henderson, C. E., Jessell, T. M., Kolodkin, A. L., and Ginty, D. D. (2005). Semaphorin 3E and plexin-D1 control vascular pattern independently of neuropilins. *Science* 307, 265–268.

Hernández-Miranda, L. R., Cariboni, A., Faux, C., Ruhrberg, C., Cho, J. H., Cloutier, J. F., Eickholt, B. J., Parnavelas, J. G., and Andrews, W. D. (2011). Robo1 regulates semaphorin signaling to guide the migration of cortical interneurons through the ventral forebrain. *J. Neurosci.* 31, 6174–6187.

Huber, A. B., Kania, A., Tran, T. S., Gu, C., De Marco Garcia, N., Lieberam, I., Johnson, D., Jessell, T. M., Ginty, D. D., and Kolodkin, A. L. (2005). Distinct roles for secreted semaphorin signaling in spinal motor axon guidance. *Neuron* 48, 949–964.

Huettl, R. E., Soellner, H., Bianchi, E., Novitch, B. G., and Huber, A. B. (2011). Npn-1 contributes to axon-axon interactions that differentially control sensory and motor innervation of the limb. *PLoS Biol.* 9, e1001020. doi:10.1371/journal.pbio.1001020

Imai, T., Suzuki, M., and Sakano, H. (2006). Odorant receptor-derived cAMP signals direct axonal targeting. *Science* 314, 657–661.

Imai, T., Yamazaki, T., Kobayakawa, R., Kobayakawa, K., Abe, T., Suzuki, M., and Sakano, H. (2009). Pre-target axon sorting establishes the neural map topography. *Science* 325, 585–590.

Jan, Y. N., and Jan, L. Y. (2003). The control of dendrite development. *Neuron* 40, 229–242.

Kerjan, G., Dolan, J., Haumaitre, C., Schneider-Maunoury, S., Fujisawa, H., Mitchell, K. J., and Chédotal, A. (2005). The transmembrane semaphorin Sema6A controls cerebellar granule cell migration. *Nat. Neurosci.* 8, 1516–1524.

Kikutani, H., and Kumanogoh, A. (2003). Semaphorins in interactions between T cells and antigen-presenting cells. *Nat. Rev. Immunol.* 3, 159–167.

Kitsukawa, T., Shimizu, M., Sanbo, M., Hirata, T., Taniguchi, M., Bekku, Y., Yagi, T., and Fujisawa, H. (1997). Neuropilin-semaphorin III/D-mediated chemorepulsive signals play a crucial role in peripheral nerve projection in mice. *Neuron* 19, 995–1005.

Koerber, H. R., and Mendell, L. M. (1992). "Functional heterogeneity of dorsal root ganglion cells," in *Sensory Neurons: Diversity, Development and Plasticity*, ed. S. A. Scott (New York: Oxford University Press), 77–96.

Kolk, S. M., Gunput, R. A., Tran, T. S., van den Heuvel, D. M., Prasad, A. A., Hellemons, A. J., Adolfs, Y., Ginty, D. D., Kolodkin, A. L., Burbach, J. P., Smidt, M. P., and Pasterkamp, R. J. (2009). Semaphorin 3F is a bifunctional guidance cue for dopaminergic axons and controls their fasciculation, channeling, rostral growth, and intracortical targeting. *J. Neurosci.* 29, 12542–12557.

Komatsu, H., Mori, I., Rhee, J. S., Akaike, N., and Ohshima, Y. (1996). Mutations in a cyclic nucleotide-gated channel lead to abnormal thermosensation and chemosensation in *C. elegans*. *Neuron* 17, 707–718.

Komuro, H., Yacubova, E., Yacubova, E., and Rakic, P. (2001). Mode and tempo of tangential cell migration in the cerebellar external granular layer. *J. Neurosci.* 21, 527–540.

Kumanogoh, A., Marukawa, S., Suzuki, K., Takegahara, N., Watanabe, C., Ch'Ng, E., Ishida, I., Fujimura, H., Sakoda, S., Yoshida, K., and Kikutani, H. (2002). Class IV semaphorin Sema4A enhances T-cell activation and interacts with Tim-2. *Nature* 419, 629–633.

Kumanogoh, A., Watanabe, C., Lee, I., Wang, X., Shi, W., Araki, H., Hirata, H., Iwahori, K., Uchida, J., Yasui, T., Matsumoto, M., Yoshida, K., Yakura, H., Pan, C., Parnes, J. R., and Kikutani, H. (2000). Identification of CD72 as a lymphocyte receptor for the class IV semaphorin CD100: a novel mechanism for regulating B cell signaling. *Immunity* 13, 621–631.

Kuwajima, T., Yoshida, Y., Takegahara, N., Kumanogoh, A., Petros, T. J., Jessell, T. M., Sakurai, T., and Mason, C. (2012). Optic chiasm presentation of Semaphorin6D in the context of Plexin-A1 and Nr-CAM promotes retinal axon midline crossing. *Neuron* 74, 676–690.

Ladle, D. R., Pecho-Vrieseling, E., and Arber, S. (2007). Assembly of motor circuits in the spinal cord: driven to function by genetic and experience-dependent mechanisms. *Neuron* 56, 270–283.

Landmesser, L. (1978). The development of motor projection patterns in the chick hind limb. *J. Physiol. (Lond.)* 284, 391–414.

Leighton, P. A., Mitchell, K. J., Goodrich, L. V., Lu, X., Pinson, K., Scherz, P., Skarnes, W. C., and Tessier-Lavigne, M. (2001). Defining brain wiring patterns and mechanisms through gene trapping in mice. *Nature* 410, 174–179.

Leslie, J. R., Imai, F., Fukuhara, K., Takegahara, N., Rizvi, T. A., Friedel, R. H., Wang, F., Kumanogoh, A., and Yoshida, Y. (2011). Ectopic myelinating oligodendrocytes in the dorsal spinal cord as a consequence of altered semaphorin 6D signaling inhibit synapse formation. *Development* 138, 4085–4095.

Little, G. E., López-Bendito, G., Rünker, A. E., García, N., Piñon, M. C., Chédotal, A., Molnár, Z., and Mitchell, K. J. (2009). Specificity and plasticity of thalamocortical connections in Sema6A mutant mice. *PLoS Biol.* 7, e98. doi:10.1371/journal.pbio.1000098

Liu, X. B., Low, L. K., Jones, E. G., and Cheng, H. J. (2005). Stereotyped axon pruning via plexin signaling is associated with synaptic complex elimination in the hippocampus. *J. Neurosci.* 25, 9124–9134.

Low, L. K., Liu, X. B., Faulkner, R. L., Coble, J., and Cheng, H. J. (2008). Plexin signaling selectively regulates the stereotyped pruning of corticospinal axons from visual cortex. *Proc. Natl. Acad. Sci. U.S.A.* 105, 8136–8141.

Maier, V., Jolicoeur, C., Rayburn, H., Takegahara, N., Kumanogoh, A., Kikutani, H., Tessier-Lavigne, M., Wurst, W., and Friedel, R. H. (2011). Semaphorin 4C and 4G are ligands of Plexin-B2 required in cerebellar development. *Mol. Cell. Neurosci.* 46, 419–431.

Mann, F., Chauvet, S., and Rougon, G. (2007). Semaphorins in development and adult brain: implication for neurological diseases. *Prog. Neurobiol.* 82, 57–79.

Marín, O., Yaron, A., Bagri, A., Tessier-Lavigne, M., and Rubenstein, J. L. (2001). Sorting of striatal and cortical interneurons regulated by semaphorin-neuropilin interactions. *Science* 293, 872–875.

Matsuoka, R. L., Chivatakarn, O., Badea, T. C., Samuels, I. S., Cahill, H., Katayama, K., Kumar, S. R., Suto, F., Chédotal, A., Peachey, N. S., Nathans, J., Yoshida, Y., Giger, R. J., and Kolodkin, A. L. (2011a). Class 5 transmembrane semaphorins control selective Mammalian retinal lamination and function. *Neuron* 71, 460–473.

Matsuoka, R. L., Nguyen-Ba-Charvet, K. T., Parray, A., Badea, T. C., Chédotal, A., and Kolodkin, A. L. (2011b). Transmembrane semaphorin signalling controls laminar stratification in the mammalian retina. *Nature* 470, 259–263.

Mauti, O., Domanitskaya, E., Andermatt, I., Sadhu, R., and Stoeckli, E. T. (2007). Semaphorin6A acts as a gate keeper between the central and the peripheral nervous system. *Neural Dev.* 2, 28.

Messersmith, E. K., Leonardo, E. D., Shatz, C. J., Tessier-Lavigne, M., Goodman, C. S., and Kolodkin, A. L. (1995). Semaphorin III can function as a selective chemorepellent to pattern sensory projections in the spinal cord. *Neuron* 14, 949–959.

Mombaerts, P. (2006). Axonal wiring in the mouse olfactory system. *Annu. Rev. Cell Dev. Biol.* 22, 713–737.

Moret, F., Renaudot, C., Bozon, M., and Castellani, V. (2007). Semaphorin and neuropilin co-expression in motoneurons sets axon sensitivity to environmental semaphorinsources during motor axon pathfinding. *Development* 134, 4491–4501.

Mori, K., and Sakano, H. (2011). How is the olfactory map formed and interpreted in the mammalian brain? *Annu. Rev. Neurosci.* 34, 467–499.

Mumm, J. S., Williams, P. R., Godinho, L., Koerber, A., Pittman, A. J., Roeser, T., Chien, C. B., Baier, H., and Wong, R. O. (2006). In vivo imaging reveals dendritic targeting of laminated afferents by zebrafish retinal ganglion cells. *Neuron* 52, 609–621.

Nawabi, H., Briançon-Marjollet, A., Clark, C., Sanyas, I., Takamatsu, H., Okuno, T., Kumanogoh, A., Bozon, M., Takeshima, K., Yoshida, Y., Moret, F., Abouzid, K., and Castellani, V. (2010). A midline switch of receptor processing regulates commissural axon guidance in vertebrates. *Genes Dev.* 24, 396–410.

Niquille, M., Garel, S., Mann, F., Hornung, J. P., Otsmane, B., Chevalley, S., Parras, C., Guillemot, F., Gaspar, P., Yanagawa, Y., and Lebrand, C. (2009). Transient neuronal populations are required to guide callosal axons: a role for semaphorin 3C. *PLoS Biol.* 7, e1000230. doi:10.1371/journal.pbio.1000230

Nishiyama, M., Togashi, K., von Schimmelmann, M. J., Lim, C. S., Maeda, S., Yamashita, N., Goshima, Y., Ishii, S., and Hong, K. (2011). Semaphorin 3A induces CaV2.3 channel-dependent conversion of axons to dendrites. *Nat. Cell Biol.* 13, 676–685.

O'Connor, T. P., Cockburn, K., Wang, W., Tapia, L., Currie, E., and Bamji, S. X. (2009). Semaphorin 5B mediates synapse elimination in hippocampal neurons. *Neural Dev.* 4, 18.

Okado, N., Homma, S., Ishihara, R., and Kohno, K. (1990). Distribution patterns of dendrites in motor neuron pools of lumbosacral spinal cord of the chicken. *Anat. Embryol.* 182, 113–121.

Paradis, S., Harrar, D. B., Lin, Y., Koon, A. C., Hauser, J. L., Griffith, E. C., Zhu, L., Brass, L. F., Chen, C., and Greenberg, M. E. (2007). An RNAi-based approach identifies molecules required for glutamatergic and GABAergic synapse development. *Neuron* 53, 217–232.

Parra, L. M., and Zou, Y. (2010). Sonic hedgehog induces response of commissural axons to Semaphorin repulsion during midline crossing. *Nat. Neurosci.* 13, 29–35.

Pasterkamp, R. J., and Giger, R. J. (2009). Semaphorin function in neural plasticity and disease. *Curr. Opin. Neurobiol.* 19, 263–274.

Pasterkamp, R. J., Peschon, J. J., Spriggs, M. K., and Kolodkin, A. L. (2003). Semaphorin 7A promotes axon outgrowth through integrins and MAPKs. *Nature* 424, 398–405.

Pecho-Vrieseling, E., Sigrist, M., Yoshida, Y., Jessell, T. M., and Arber, S. (2009). Specificity of sensorymotor connections encoded by Sema3e-Plxnd1 recognition. *Nature* 459, 842–826.

Polleux, F., Morrow, T., and Ghosh, A. (2000). Semaphorin 3A is a chemoattractant for cortical apical dendrites. *Nature* 404, 567–573.

Porter, L. L., and White, E. L. (1983). Afferent and efferent pathways of the vibrissal region of primary motor cortex in the mouse. *J. Comp. Neurol.* 214, 279–289.

Renaud, J., Kerjan, G., Sumita, I., Zagar, Y., Georget, V., Kim, D., Fouquet, C., Suda, K., Sanbo, M., Suto, F., Ackerman, S. L., Mitchell, K. J., Fujisawa, H., and Chédotal, A. (2008). Plexin-A2 and its ligand, Sema6A, control nucleus-centrosome coupling in migrating granule cells. *Nat. Neurosci.* 11, 440–409.

Ruhrberg, C., Gerhardt, H., Golding, M., Watson, R., Ioannidou, S., Fujisawa, H., Betsholtz, C., and Shima, D. T. (2002). Spatially restricted patterning cues provided by heparin-binding VEGF-A control blood vessel branching morphogenesis. *Genes Dev.* 16, 2684–2698.

Rünker, A. E., Little, G. E., Suto, F., Fujisawa, H., and Mitchell, K. J. (2008). Semaphorin-6A controls guidance of corticospinal tract axons at multiple choice points. *Neural Dev.* 3, 34.

Ryder, E. F., and Cepko, C. L. (1994). Migration patterns of clonally related granule cells and their progenitors in the developing chick cerebellum. *Neuron* 12, 1011–1028.

Sahay, A., Kim, C. H., Sepkuty, J. P., Cho, E., Huganir, R. L., Ginty, D. D., and Kolodkin, A. L. (2005). Secreted semaphorins modulate synaptic transmission in the adult hippocampus. *J. Neurosci.* 25, 3613–3620.

Sanes, J. R., and Zipursky, S. L. (2010). Design principles of insect and vertebrate visual systems. *Neuron* 66, 15–36.

Schwarz, Q., Gu, C., Fujisawa, H., Sabelko, K., Gertsenstein, M., Nagy, A., Taniguchi, M., Kolodkin, A. L., Ginty, D. D., Shima, D. T., and Ruhrberg, C. (2004). Vascular endothelial growth factor controls neuronal migration and cooperates with Sema3A to pattern distinct compartments of the facial nerve. *Genes Dev.* 18, 2822–2834.

Shelly, M., Cancedda, L., Heilshorn, S., Sumbre, G., and Poo, M. M. (2007). LKB1/STRAD promotes axon initiation during neuronal polarization. *Cell* 129, 565–577.

Shelly, M., Cancedda, L., Lim, B. K., Popescu, A. T., Cheng, P. L., Gao, H., and Poo, M. M. (2011). Semaphorin3A regulates neuronal polarization by suppressing axon formation and promoting dendrite growth. *Neuron* 71, 433–446.

Shelly, M., Lim, B. K., Cancedda, L., Heilshorn, S. C., Gao, H., and Poo, M. M. (2010). Local and long-range reciprocal regulation of cAMP and cGMP in axon/dendrite formation. *Science* 327, 547–552.

Song, H., Ming, G., He, Z., Lehmann, M., McKerracher, L., Tessier-Lavigne, M., and Poo, M. (1998). Conversion of neuronal growth cone responses from repulsion to attraction by cyclic nucleotides. *Science* 281, 1515–1518.

Stacy, R. C., and Wong, R. O. (2003). Developmental relationship between cholinergic amacrine cell processes and ganglion cell dendrites of the mouse retina. *J. Comp. Neurol.* 456, 154–166.

Stanfield, B. B. (1992). The development of the corticospinal projection. *Prog. Neurobiol.* 38, 169–202.

Surmeier, D. J., Ding, J., Day, M., Wang, Z., and Shen, W. (2007). D1 and D2 dopamine-receptor modulation of striatal glutamatergic signaling in striatal medium spiny neurons. *Trends Neurosci.* 30, 228–235.

Suto, F., Ito, K., Uemura, M., Shimizu, M., Shinkawa, Y., Sanbo, M., Shinoda, T., Tsuboi, M., Takashima, S., Yagi, T., and Fujisawa, H. (2005). Plexin-a4 mediates axon-repulsive activities of both secreted and transmembrane semaphorins and plays roles in nerve fiber guidance. *J. Neurosci.* 25, 3628–3637.

Suto, F., Tsuboi, M., Kamiya, H., Mizuno, H., Kiyama, Y., Komai, S., Shimizu, M., Sanbo, M., Yagi, T., Hiromi, Y., Chédotal, A., Mitchell, K. J., Manabe, T., and Fujisawa, H. (2007). Interactions between plexin-A2, plexin-A4, and semaphorin 6A control lamina-restricted projection of hippocampal mossy fibers. *Neuron* 53, 535–547.

Suzuki, K., Kumanogoh, A., and Kikutani, H. (2008). Semaphorins and their receptors in immune cell interactions. *Nat. Immunol.* 9, 17–23.

Takahashi, T., Fournier, A., Nakamura, F., Wang, L. H., Murakami, Y., Kalb, R. G., Fujisawa, H., and Strittmatter, S. M. (1999). Plexin-neuropilin-1 complexes form functional semaphorin-3A receptors. *Cell* 99, 59–69.

Takamatsu, H., and Kumanogoh, A. (2012). Diverse roles for semaphorin-plexin signaling in the immune system. *Trends Immunol.* 33, 127–135.

Takeuchi, H., Inokuchi, K., Aoki, M., Suto, F., Tsuboi, A., Matsuda, I., Suzuki, M., Aiba, A., Serizawa, S., Yoshihara, Y., Fujisawa, H., and Sakano, H. (2010). Sequential arrival and graded secretion of Sema3F by olfactory neuron axons specify map topography at the bulb. *Cell* 141, 1056–1067.

Tamagnone, L., Artigiani, S., Chen, H., He, Z., Ming, G. I., Song, H., Chedotal, A., Winberg, M. L., Goodman, C. S., Poo, M., Tessier-Lavigne, M., and Comoglio, P. M. (1999). Plexins are a large family of receptors for transmembrane, secreted, and GPI-anchored semaphorins in vertebrates. *Cell* 99, 71–80.

Taniguchi, M., Yuasa, S., Fujisawa, H., Naruse, I., Saga, S., Mishina, M., and Yagi, T. (1997). Disruption of semaphorin III/D gene causes severe abnormality in peripheral nerve projection. *Neuron* 19, 519–530.

Tawarayama, H., Yoshida, Y., Suto, F., Mitchell, K. J., and Fujisawa, H. (2010). Roles of semaphorin-6B and plexin-A2 in lamina-restricted projection of hippocampal mossy fibers. *J. Neurosci.* 30, 7049–7060.

Thong, I. G., and Dreher, B. (1987). The development of the corticotectal pathway in the albino rat: transient projections from the visual and motor cortices. *Neurosci. Lett.* 80, 275–282.

Togashi, K., von Schimmelmann, M. J., Nishiyama, M., Lim, C. S., Yoshida, N., Yun, B., Molday, R. S., Goshima, Y., and Hong, K. (2008). Cyclic GMP-gated CNG channels function in Sema3A-induced growth cone repulsion. *Neuron* 58, 694–707.

Toyofuku, T., Yoshida, J., Sugimoto, T., Zhang, H., Kumanogoh, A., Hori, M., and Kikutani, H. (2005). FARP2 triggers signals for Sema3A-mediated axonal repulsion. *Nat. Neurosci.* 8, 1712–1719.

Toyofuku, T., Zhang, H., Kumanogoh, A., Takegahara, N., Suto, F., Kamei, J., Aoki, K., Yabuki, M., Hori, M., Fujisawa, H., and Kikutani, H. (2004). Dual roles of Sema6D in cardiac morphogenesis through region-specific association of its receptor, Plexin-A1, with off-track and vascular endothelial growth factor receptor type 2. *Genes Dev.* 18, 435–447.

Tran, T. S., Kolodkin, A. L., and Bharadwaj, R. (2007). Semaphorin regulation of cellular morphology. *Annu. Rev. Cell Dev. Biol.* 23, 263–292.

Tran, T. S., Rubio, M. E., Clem, R. L., Johnson, D., Case, L., Tessier-Lavigne, M., Huganir, R. L., Ginty, D. D., and Kolodkin, A. L. (2009). Secreted semaphorins control spine distribution and morphogenesis in the postnatal CNS. *Nature* 462, 1065–1069.

Vermeren, M., Maro, G. S., Bron, R., McGonnell, I. M., Charnay, P., Topilko, P., and Cohen, J. (2003). Integrity of developing spinal motor columns is regulated by neural crest derivatives at motor exit points. *Neuron* 37, 403–415.

Vrieseling, E., and Arber, S. (2006). Target-induced transcriptional control of dendritic patterning and connectivity in motor neurons by the ETS gene Pea3. *Cell* 127, 1439–1452.

Wässle, H. (2004). Parallel processing in the mammalian retina. *Nat. Rev. Neurosci.* 5, 747–757.

Williams, S. E., Grumet, M., Colman, D. R., Henkemeyer, M., Mason, C. A., and Sakurai, T. (2006). A role for Nr-CAM in the patterning of binocular visual pathways. *Neuron* 50, 535–547.

Wingate, R. J. (2001). The rhombic lip and early cerebellar development. *Curr. Opin. Neurobiol.* 11, 82–88.

Wolman, M. A., Liu, Y., Tawarayama, H., Shoji, W., and Halloran, M. C.

(2004). Repulsion and attraction of axons by semaphorin3D are mediated by different neuropilins in vivo. *J. Neurosci.* 24, 8428–8435.

Wu, Z., Sweeney, L. B., Ayoob, J. C., Chak, K., Andreone, B. J., Ohyama, T., Kerr, R., Luo, L., Zlatic, M., and Kolodkin, A. L. (2011). A combinatorial semaphorin code instructs the initial steps of sensory circuit assembly in the *Drosophila* CNS. *Neuron* 70, 281–298.

Yamauchi, K., Mizushima, S., Tamada, A., Yamamoto, N., Takashima, S., and Murakami, F. (2009). FGF8 signaling regulates growth of midbrain dopaminergic axons by inducing semaphorin 3F. *J. Neurosci.* 29, 4044–4055.

Yorke, C. H. Jr., and Caviness, V. S. Jr. (1975). Interhemispheric neocortical connections of the corpus callosum in the normal mouse: a study based on anterograde and retrograde methods. *J. Comp. Neurol.* 164, 233–245.

Yoshida, Y., Han, B., Mendelsohn, M., and Jessell, T. M. (2006). PlexinA1 signaling directs the segregation of proprioceptive sensory axons in the developing spinal cord. *Neuron* 52, 775–788.

Zheng, C., Feinstein, P., Bozza, T., Rodriguez, I., and Mombaerts, P. (2000). Peripheral olfactory projections are differentially affected in mice deficient in a cyclic nucleotide-gated channel subunit. *Neuron* 26, 81–91.

Zhuang, B., Su, Y. S., and Sockanathan, S. (2009). FARP1 promotes the dendritic growth of spinal motor neuron subtypes through transmembrane Semaphorin6A and PlexinA4 signaling. *Neuron* 61, 359–372.

Zou, Y., Stoeckli, E., Chen, H., and Tessier-Lavigne, M. (2000). Squeezing axons out of the gray matter: a role for slit and semaphorin proteins from midline and ventral spinal cord. *Cell* 102, 363–375.

Conflict of Interest Statement: The author declares that the research was conducted in the absence of any commercial or financial relationships that could be construed as a potential conflict of interest.

Received: 29 February 2012; accepted: 17 May 2012; published online: 06 June 2012.

*Citation: Yoshida Y (2012) Semaphorin signaling in vertebrate neural circuit assembly. Front. Mol. Neurosci. **5**:71. doi: 10.3389/fnmol.2012.00071*

frontiers in
MOLECULAR NEUROSCIENCE

ORIGINAL RESEARCH ARTICLE
published: 10 January 2012
doi: 10.3389/fnmol.2011.00061

Fibroblast growth factor 22 contributes to the development of retinal nerve terminals in the dorsal lateral geniculate nucleus

Rishabh Singh[1†], Jianmin Su[1†], Justin Brooks[1], Akiko Terauchi[2,3], Hisashi Umemori[2,3] and Michael A. Fox[1]*

[1] *Department of Anatomy and Neurobiology, Virginia Commonwealth University Medical Center, Richmond, VA, USA*
[2] *Department of Biological Chemistry, University of Michigan Medical School, Ann Arbor, MI, USA*
[3] *Molecular and Behavioral Neuroscience Institute, University of Michigan Medical School, Ann Arbor, MI, USA*

Edited by:
Joshua A. Weiner, The University of Iowa, USA

Reviewed by:
Erik Ullian, University of California San Francisco, USA
Andrew David Huberman, University of California San Diego, USA

***Correspondence:**
Michael A. Fox, Department of Anatomy and Neurobiology, Virginia Commonwealth University Medical Center, 1101 East Marshall Street, PO Box 980709, Richmond, VA 23298-0709, USA.
e-mail: mafox@vcu.edu

[†] *Rishabh Singh and Jianmin Su have contributed equally to this work.*

At least three forms of signaling between pre- and postsynaptic partners are necessary during synapse formation. First, "targeting" signals instruct presynaptic axons to recognize and adhere to the correct portion of a postsynaptic target cell. Second, trans-synaptic "organizing" signals induce differentiation in their synaptic partner so that each side of the synapse is specialized for synaptic transmission. Finally, in many regions of the nervous system an excess of synapses are initially formed, therefore "refinement" signals must either stabilize or destabilize the synapse to reinforce or eliminate connections, respectively. Because of both their importance in processing visual information and their accessibility, retinogeniculate synapses have served as a model for studying synaptic development. Molecular signals that drive retinogeniculate "targeting" and "refinement" have been identified, however, little is known about what "organizing" cues are necessary for the differentiation of retinal axons into presynaptic terminals. To identify such "organizing" cues, we used microarray analysis to assess whether any target-derived "synaptic organizers" were enriched in the mouse dorsal lateral geniculate nucleus (dLGN) during retinogeniculate synapse formation. One candidate "organizing" molecule enriched in perinatal dLGN was FGF22, a secreted cue that induces the formation of excitatory nerve terminals in muscle, hippocampus, and cerebellum. In FGF22 knockout mice, the development of retinal terminals in dLGN was impaired. Thus, FGF22 is an important "organizing" cue for the timely development of retinogeniculate synapses.

Keywords: synaptogenesis, presynaptic differentiation, retina, retinal ganglion cell, lateral geniculate nucleus

INTRODUCTION

Proper functioning of the mammalian nervous system requires the assembly of precisely aligned pre- and postsynaptic elements between appropriate partner neurons. At least three sequential signaling mechanisms are thought to assure appropriate synaptic connectivity. First, a growing axon must recognize and adhere to an appropriate portion of a postsynaptic target cell, a process termed synaptic targeting (Sanes and Yamagata, 2009). Cell adhesion molecules, axonal guidance molecules, extracellular matrix molecules, growth factors, morphogens, and neurotrophins each have been shown to contribute to synaptic targeting in the vertebrate CNS (for examples see Yamagata et al., 2002; Yamagata and Sanes, 2008; Osterhout et al., 2011; for review see Yamagata et al., 2003; Waites et al., 2005; Sanes and Yamagata, 2009). Following axon-target recognition, signals from the presynaptic axon and postsynaptic target cell are exchanged to coordinate the transformation of these elements so that they are specialized for synaptic transmission – a process called synaptic differentiation (Waites et al., 2005; Craig et al., 2006; Fox and Umemori, 2006). Trans-synaptic cues that induce the recruitment of presynaptic release machinery (i.e., synaptic vesicles, active zone components, etc.) or the clustering of neurotransmitter receptors and intracellular scaffolds in the postsynaptic cell have been dubbed "synaptic organizers" and include many of the same families of molecules that contribute to synaptic targeting (Shen and Cowan, 2010). While synaptic targeting and organizing cues generate connections between specific neurons, an excess of these connections are initially formed, therefore, subsequent activity-dependent mechanisms lead to the stabilization and maturation of some synapses and the destabilization and pruning of others (Lichtman and Colman, 2000; Waites et al., 2005; Kano and Hashimoto, 2009).

As perturbation of synaptic structure has been implicated in contributing to a multitude of neurological diseases, identifying cellular and molecular signals responsible for synaptic targeting, differentiation, and refinement has received considerable attention. One CNS region that has served as a model for studying neural circuit formation is the dorsal lateral geniculate nucleus (dLGN), a thalamic nucleus that receives input from retinal ganglion cells (RGCs) and relays this input to visual cortex. In addition to excitatory RGC terminals, synaptic terminals in the LGN also arise from local interneurons, inhibitory projection neurons in the thalamic reticular nucleus (TRN), layer VI cortical neurons, and neurons within the midbrain and brainstem (Sherman and Guillery, 2002). While the function of this complex circuitry has

been thoroughly addressed, our understanding of circuit formation in dLGN is largely limited to synapses arising from RGC axons – the retinogeniculate synapse.

In mice, RGC axons begin to invade the dLGN by the end of embryonic development (Godement et al., 1984). As these axons enter the dLGN they are targeted into topographically arranged regions, such that axons from neighboring RGCs in the retina target adjacent regions of the dLGN and thereby convey the location of stimuli in the visual field to a spatially correlated region of dLGN. Topographic targeting in mouse dLGN is driven by Eph kinase/ephrin interactions: depending upon their location in retina, RGCs (and their axons) express a variable level of Eph kinase whereas a graded expression of Eph kinase ligands, ephrins, exists in dLGN (Cheng et al., 1995; Drescher et al., 1995; Feldheim et al., 1998; Pfeiffenberger et al., 2005; Feldheim and O'Leary, 2010). Functional, albeit immature, retinogeniculate synapses form shortly after RGC axons target postsynaptic neurons in dLGN. In fact, postsynaptic responses are present in dLGN as early as the day of birth in mice, although the strength of retinogeniculate synapses during the first week of life are considerably weaker than synapses after natural eye-opening (∼P14; Mooney et al., 1996; Chen and Regehr, 2000; Jaubert-Miazza et al., 2005). In additional to weaker inputs, an excess of synaptic connections exists between RGC axons and dLGN relay neurons at early ages. Before eye-opening a relay neuron may receive inputs from 10–20 RGC axons however by eye-opening only one to three retinal inputs remain on a single relay neuron (Chen and Regehr, 2000; Jaubert-Miazza et al., 2005). Although this period of synaptic refinement and remodeling occurs before natural eye-opening and visually evoked activity, it does depend upon activity in the form of waves of spontaneously generated activity in RGCs (Guido, 2008; Huberman et al., 2008; Feller, 2009). Some molecular "refinement" signals that act downstream of this spontaneous retinal activity have been elucidated in dLGN. These include components of the classical complement cascade (Stevens et al., 2007), major histocompatibility complex (MHC) class 1 (Corriveau et al., 1998; Huh et al., 2000), and neuronal pentraxins (Bjartmar et al., 2006).

Despite extensive characterization of the targeting and refinement of retinogeniculate circuits, we know little about the mechanisms regulating synaptic differentiation at this synapse. The list of organizing cues that direct synaptic differentiation at CNS synapses is considerably large (see Waites et al., 2005; Craig et al., 2006; Fox and Umemori, 2006; Eroglu and Barres, 2010; Johnson-Venkatesh and Umemori, 2010; Jones et al., 2011; Kucukdereli et al., 2011; Terauchi and Umemori, 2011), however whether any of these contribute to synapse formation in dLGN remains unclear. For this reason, we sought to identify synaptic organizers enriched in dLGN during the development of retinogeniculate synapses. Using a microarray approach we found that fibroblast growth factor 22 (FGF22) – a target-derived cue that directs excitatory nerve terminal formation in hippocampus, cerebellum, and muscle (Umemori et al., 2004; Fox et al., 2007; Umemori, 2009; Terauchi et al., 2010), is enriched in dLGN as retinal terminals form. Using targeted mouse mutants lacking FGF22, we show that the formation and maturation of retinogeniculate (but not other dLGN synapses) is impaired in the absence of this organizing cue. Thus, FGF22 contributes to the timely development of retinogeniculate synapses.

MATERIALS AND METHODS

REAGENTS AND ANTIBODIES

All chemicals and reagents were obtained from Sigma (St. Louis, MO, USA) or Fisher (Fairlawn, NJ, USA), unless otherwise noted. A rabbit polyclonal antibody directed against melanopsin (Meln) was kindly provided by Dr. C. K. Chen [Virginia Commonwealth University, Richmond, VA, USA; diluted 1:2500 for immunohistochemistry (IHC)]. Antibodies for the following antigens were purchased: rabbit polyclonal anti-calretinin (Calr; Millipore; diluted 1:1000 for IHC), rabbit polyclonal anti-vesicular glutamate transporter 2 (VGluT2; Synaptic Systems Inc.; diluted 1:500 for IHC), mouse monoclonal anti-glutamic acid decarboxylase 67 (GAD67; Millipore; diluted 1:500 for IHC), rabbit polyclonal anti-fibroblast growth factor receptor 2 (Santa Cruz; FGFR2; diluted 1:100 for IHC), goat polyclonal anti-brain-specific homeobox/POU domain protein 3A (Brn3a; Millipore; diluted 1:125 for IHC), mouse monoclonal anti-synaptophysin 1 (Synaptic Systems Inc.; diluted 1:500 for IHC), monoclonal mouse anti-synaptotagmin 2 (previously called znp1; Fox and Sanes, 2007; Zebrafish International Resource Center, Inc.; diluted 1:250 for IHC), monoclonal mouse monoclonal anti-actin [Millipore; diluted 1:10,000 for western blots (WB)], and goat polyclonal anti-FGF22 (Santa Cruz; diluted 1:300 for WB). Fluorescent- and HRP-conjugated secondary antibodies were purchased from Invitrogen or Jackson ImmunoResearch (diluted 1:1000 for IHC and 1:5000 for WB).

MICE

Wild-type C57 and CD1 mice were from Charles River. *Fgf22*$^{-/-}$ mice (on a C57 background) were generated and described previously (Terauchi et al., 2010). All analyses conformed to National Institutes of Health guidelines and protocols approved by the Virginia Commonwealth University Institutional Animal Care and Use Committee.

IMMUNOHISTOCHEMISTRY

Brains and retinas from C57 mice were fixed in 4% paraformaldehyde (PFA; in phosphate-buffered saline, PBS) for 12 h at 4°C. They were then repeatedly washed in PBS and incubated for a minimum of 24 h in 20% sucrose in PBS. Fixed tissue was frozen in Tissue Freezing Medium (Triangle Biomedical Sciences, Durham, NC, USA) and sectioned (16–20 μm) coronally on a Leica CM1850 cryostat. Sections were air-dried, incubated in blocking buffer (2.5% BSA, 5% NGS, and 0.1% Triton X-100 in PBS) for 30 min at room temperature, and subsequently incubated in primary antibodies diluted in blocking buffer for >12 h at 4°C. Following several washes in PBS, sections were treated with secondary antibodies diluted in blocking buffer for 60 min at room temperature. After four PBS washes, sections were stained with DAPI and mounted in VectaShield (Vector Laboratories, Burlingame, CA, USA). Immunostained sections were visualized on either a Leica SP2 scanning confocal microscope or a Zeiss Axiolmager A1 fluorescent microscope. dLGN could be unequivocally identified by both DAPI staining and VGluT2-immunoreactivity. When comparing different ages of tissues or between genotypes,

images were acquired with identical parameters. For quantification, images were acquired from a ventromedial portion of dLGN (see **Figure 1A**). At least four images were acquired per animal. For quantification of the relative area (per field or per dLGN) occupied by immunoreactivity, images were thresholded in Adobe Photoshop so that no sigbal was detected in the optic tract of a P7 control animal (threshold value = 80). The same threshold value was applied to all other images regardless of age or genotype. Percent area of the thresholded signal was quantified with NIH ImageJ (Bethesda, MD, USA). All image manipulations and measurements were performed using identical procedures or parameters regardless of genotype or age. Four animals were analyzed for each genotype and age.

MICROARRAY ANALYSIS

RNA was isolated from P3 and P8 CD1 wild-type mouse dLGN, as described previously (Su et al., 2011). Briefly, mice were decapitated, brains removed, and 300 μm coronal sections were cut in ice-cold DEPC-PBS with a vibratome. dLGN were microdissected from at least five littermates and tissues were pooled per sample. RNA was isolated using the Bio-Rad Total RNA extraction from Fibrous and Fatty Tissue kit (Bio-Rad). RNA purity assessment, first- and second-strand cDNAs preparation, cRNAs generation, hybridization to Agilent Whole Genome 44kx4 mouse arrays, and data analysis with Agilent Feature Extraction and GeneSpring GX, version 7.3.1, software packages were performed by GenUs Biosystems. To be considered differentially expressed, genes must have

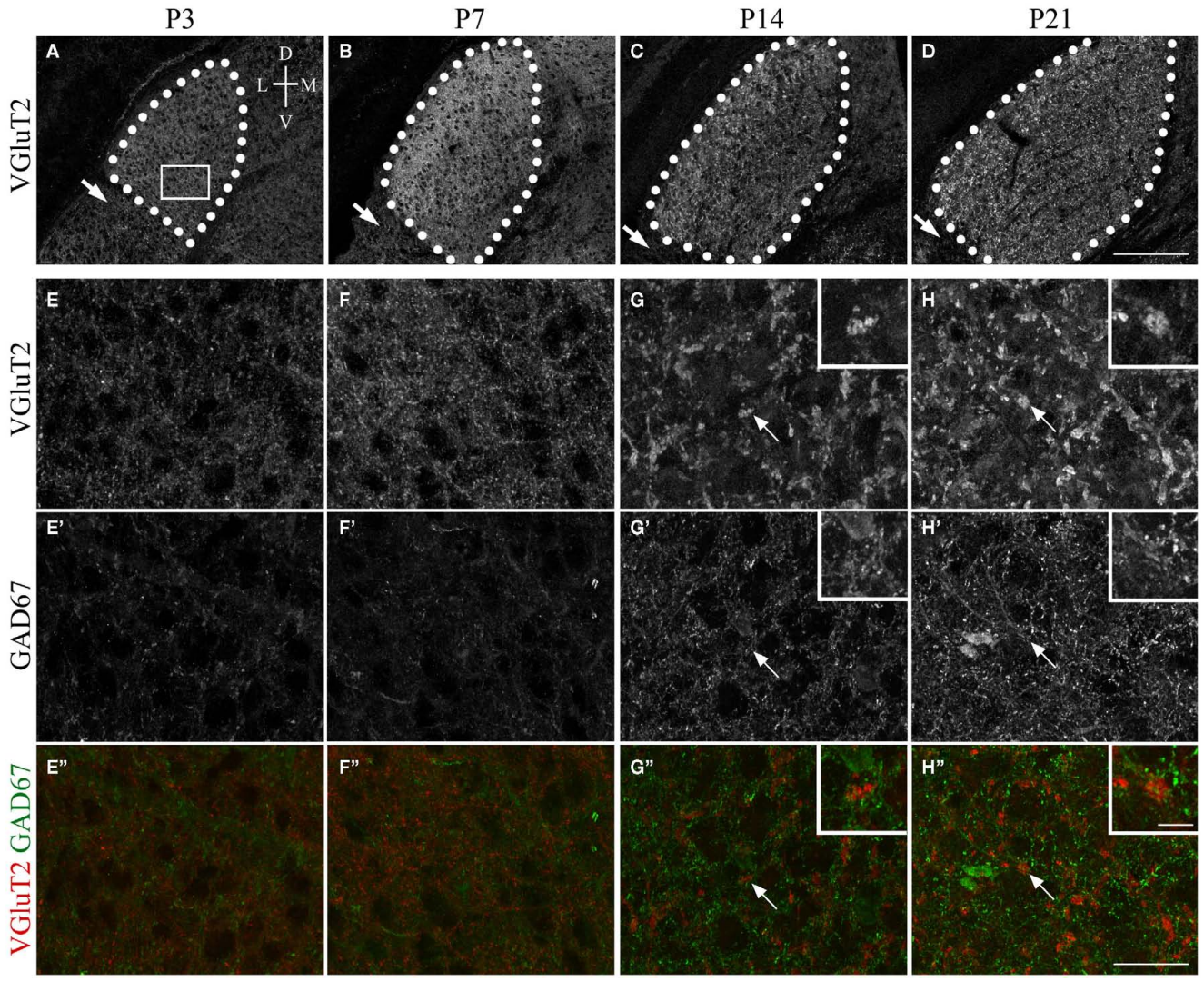

FIGURE 1 | Synaptic development in mouse dLGN. (A–D) VGluT2-immunoreactivity in coronal sections of dLGN at P3, P7, P14, P21. dLGN are encircled by white dots. Arrows indicate the intergeniculate leaflet (IGL). Tissue orientation is indicated in **(A)**: D, dorsal; L, lateral; M, medial; V, ventral. **(E–H)** High magnification of **(A–D)** [from areas similar to that shown by the white box in **(A)**] show the transformation of immature and small VGluT2-positive retinal terminals into large, morphologically distinct RLPs. **(E′–H′)** show the development of Gad67 inhibitory synapses in the postnatal dLGN. **(E″–H″)** show merged images of retinal terminals (red) and inhibitory terminals (green). Arrows in **(G,H)** highlight presumptive VGluT2-expressing RLPs [which are shown in higher magnification in the insets in **(G,H)**]. All images were acquired with identical settings on a confocal microscope. Scale bar in **(D)** = 200 μm for **(A–D)**, in **(H″)** = 25 μm for **(E–H″)**, and in the inset in **(H″)** = 5 μm for all insets.

demonstrated a twofold difference (up- or down-regulation) in the averaged sample sets ($n = 3$; $p < 0.05$). Three pooled samples were analyzed per age.

QUANTITATIVE PCR

RNA was purified from pooled C57 dLGN samples as described above. cDNAs were generated with Superscript II Reverse Transcriptase First-Strand cDNA Synthesis kit (Invitrogen). Quantitative PCR (qPCR) was performed on a Chromo4 Four-Color Real-Time System (Bio-Rad) using iQ SYBR Green Supermix (Bio-Rad) as described previously (Su et al., 2010). The following primer pairs were used: *fgf22*, 5′-ACA CGG ACA GAA CGG ATC TC-3′, and 5′-CCA CTC ACT TTT TCC TGC GT-3′; *actin*, 5′-TTC TTT GCA GCT CCT TCG TT-3′, and 5′-ATG GAG GGG AAT ACA GCC C-3′. A minimum of three experiments (each in triplicate) was run for each age.

WESTERN BLOT

Wild-type C57 mice were perfused with PBS, brains removed and dLGN were dissected in ice-cold PBS. Tissue was pooled from at least eight littermates per age and was lysed in modified loading buffer containing 50 mmol/L Tris–HCl, pH 6.8, 2% sodium dodecyl sulfate (SDS), 10% glycerol, and protease inhibitors (1 mmol/L PMSF). Samples were homogenized, boiled for 10 min, and insoluble material was removed. Protein concentrations were determined by bicinchoninic acid (BCA) protein assay (Pierce, Rockford, IL, USA). Equal amounts of protein were loaded and separated by SDS-PAGE and transferred to PVDF membrane as described previously (Fox and Sanes, 2007). After blocking in 5% non-fat milk in PBS (containing 0.05% Tween 20), PVDF membranes were incubated with appropriate primary antibodies, followed by HRP-conjugated secondary antibodies. Immunoblotted proteins were detected with enhanced chemiluminescent detection system (ECL Plus, Amersham Pharmacia Biotech, Piscataway, NJ, USA) as previously described (Fox et al., 2003).

RESULTS

SYNAPTIC DEVELOPMENT IN dLGN

To begin to address the molecular mechanisms that regulate presynaptic nerve terminal development, we first documented nerve terminal formation and maturation in mouse dLGN using nerve terminal-specific markers. Retinal terminals were labeled with antibodies directed against vesicular glutamate transporter 2 (VGluT2), a synaptic vesicle associated protein present in classes of excitatory nerve terminals and expressed by RGCs (Fujiyama et al., 2003; Land et al., 2004). VGluT2 is absent from other glutamatergic, excitatory synapses within dLGN, which instead contain VGluT1 (Fujiyama et al., 2003). Thus, in dLGN VGluT2 immunolabeling specifically and selectively marks retinal terminals (Land et al., 2004; **Figures 1A–D**). To label inhibitory nerve terminals, which are derived from either local dLGN interneurons or inhibitory TRN neurons, antibodies directed against glutamate decarboxylase 67 (GAD67) were employed.

Using these terminal-specific markers we found that shortly after the targeting of RGC axons, the dLGN contained VGluT2-positive terminals but largely lacked GAD67-positive terminals (**Figures 1A,E**). By the end of the first postnatal week of development, a substantial increase in the number and density of excitatory, VGluT2-positive retinal terminals was observed (**Figures 1B,F**). Despite increases in retinogeniculate synapse number, little change was seen in the number or density of inhibitory synapses during this period (**Figures 1E,F**). The sparsity of GAD67-positive inhibitory nerve terminals support electrophysiological studies that demonstrate a general lack of inhibitory synaptic responses following optic tract stimulation in dLGN at the end of the first week of mouse development (Bickford et al., 2010). The number of GAD67-immunoreactive terminals appeared to dramatically increase by P14 (**Figure 1G**), which coincides with an increased incidence of inhibition following optic tract stimulation (Bickford et al., 2010).

A remarkable feature of retinal terminals in the adult dLGN is that they are morphologically distinct and significantly larger than other excitatory or inhibitory terminals in dLGN. Based upon their *round shaped vesicles*, *large size*, and *pale mitochondria* in ultrastructural analyses, retinogeniculate terminals have been named RLPs. IHC analysis at early perinatal ages suggested that VGluT2-immunoreactive retinal terminals were initially no larger than inhibitory terminals in dLGN (**Figures 1E,F**). However by P14, and at all ages thereafter, VGluT2-positive retinal terminals had transformed into larger and morphologically distinct terminals, presumably indicating the formation of RLPs (**Figures 1C,D,G,H**). The increase in VGluT2-positive terminal size appeared to coincide with a decrease in the number of retinal terminals in dLGN (compare **Figures 1A–D**). These findings confirm previous ultrastructural studies that suggested a 10-fold reduction in the number of retinogeniculate synapses from P7 to P14 (Bickford et al., 2010). Together these data demonstrate that during the first week of mouse development the numbers of retinal terminals increase dramatically but then during the second week some of these terminals are stabilized and mature while others are destabilized and pruned.

Two final observations regarding the formation and maturation of retinal terminals in LGN warrant mention. First, retinal terminal growth and maturation in dLGN appeared to occur in a dorsolateral to ventromedial gradient (compare **Figures 1C,D**), perhaps reflecting the fact that RGC axons innervate dorsolateral dLGN first. Second, little VGluT2-immunoreactivity was observed in the intergeniculate leaflet (IGL; arrows in **Figures 1C,D**), an adjacent retino-recipient nucleus (also see Fujiyama et al., 2003). This is somewhat surprising since RGC axons also innervate IGL.

IDENTIFICATION OF SYNAPTIC ORGANIZING MOLECULES IN dLGN

We next sought to identify synaptic organizing molecules whose developmental expression in dLGN coincided with the perinatal increase in synapse number. To capture the genetic profile of dLGN before the large increase in retinal terminal number, RNA was isolated from P3 mouse dLGN. Expression profiles in these pools of RNA were compared with RNA isolated from P8 dLGN, an age that corresponds to the increase in retinogeniculate terminal number and before the increase in inhibitory synaptic terminals. Differentially expressed genes in these RNA pools were identified by Agilent microarray analysis.

To assess changes in the expression of genes that might contribute to synaptic differentiation in dLGN we mined the

array data, focusing on families of synaptic organizing molecules. We specifically explored the following genes: neuroligins (*nlgn1–4*), neurexins (*nrxn1–3*), cell adhesion molecules [*cadm1–4* (also called SynCAM1–4)], leucine-rich repeat transmembrane molecules (*lrrtm1–4*), protein tyrosine phosphatase receptors (*ptprf*, *ptprs*), leucine-rich repeat and fibronectin type III domain containing molecules [*lrfn1–5*;also called synaptic adhesion-like molecules (SALMs1–5)], cerebellins (*cbln1–4*), thrombospondins (*thbs1–4*), secreted proteins acidic and rich in cysteine (*sparc*, *sparcl1*), neurotrophins (*ngf*, *bdnf*, *ntf3*, *ntf4*), Wnts, bone morphogenic factors (*bmp1–7*), ephrins (*efna1–5*, *efnb1–3*), Eph kinases (*epha1–10*, *ephb1–6*), and synaptogenic FGFs (*fgf7*, *fgf10*, *fgf22*). **Figure 2** plots the relative change in expression in these genes in P8 dLGN compared with levels of expression at P3. Genes mentioned above that are not listed in **Figure 2** were not detected by probe sets on the microarray. Of the >70 synaptic organizing genes examined, the gene most up-regulated at P8 was *fgf22*, which was detected as being significantly enriched by two distinct probe sets in the array (see blue bars in **Figure 2**). In addition to *fgf22*, 10 other genes encoding synaptic organizers were significantly enriched at P8: *nlgn3*, *sparc*, *sparcl1*, *wnt5a*, *wnt7a*, *wnt7b*, *bmp4*, *lrrtm1*, *ephb3*, and *ephb4*. While ∼15% of the genes coding for synaptic organizers were up-regulated, the expression of another set of genes was significantly reduced at P8. Down-regulated synaptic organizers included *nlgn1*, *nrxn1*, *cadm1*, *cbln2*, *ptprf*, *epha7*, and *efna2*. It is unclear why these genes are down-regulated during postnatal dLGN development but may suggest roles for these cues in synaptic targeting (for examples see Osterhout et al., 2011; Su et al., 2011).

FGF22 IS EXPRESSED IN dLGN AND ITS RECEPTOR IS EXPRESSED BY RGCs

We next sought to confirm the expression of *fgf22* mRNA in dLGN. RNA was isolated from wild-type dLGN at P2, P3, P8, and P14 and quantitative RT-PCR (qPCR) was performed. qPCR confirmed a considerable enrichment in *fgf22* expression in P8 dLGN compared with expression levels at P2 and P3 (**Figure 3A**). Levels of *fgf22* continued to increase postnatally until P14, an age in which retinal terminals have matured into RLPs (**Figure 3A**; Bickford et al., 2010).

Since changes in mRNA expression levels do not always correlate with protein expression, we next used antibodies directed against FGF22 to probe protein levels in dLGN. **Figure 3B** demonstrates that FGF22 levels increase substantially during the first week of postnatal development. Together, these results confirm that developmental increases in FGF22 expression, at both mRNA and protein levels, coincide with the formation and maturation of retinal nerve terminals in dLGN.

Target-derived FGF22 has previously been shown to induce the formation of excitatory nerve terminals in skeletal muscle, hippocampus, and cerebellum (Umemori et al., 2004; Fox et al., 2007; Terauchi et al., 2010). Based upon these roles in synaptic differentiation and its significant enrichment in P8 dLGN, we hypothesized that dLGN-derived FGF22 induces the assembly and growth of retinal terminal. For this to be true, retinal axons must express appropriate FGF22 receptors. FGFs bind and signal through a family of alternatively spliced receptors, termed FGF receptors (FGFRs; Zhang et al., 2006). FGF22 primarily signals through FGFR2 to induce nerve terminal assembly (Umemori et al., 2004; Fox et al., 2007; Terauchi et al., 2010). Previous studies have reported postnatal increases in FGFR2 expression by mouse RGCs, which we confirm here (**Figure 4A**; Catalina et al., 2009). However, not all RGCs innervate dLGN. We therefore tested whether classes of RGCs known to target dLGN express FGFR2. We focused on RGCs that express either the calcium binding protein calretinin (Calr) or the transcription factor Brn3a, both of which are expressed by classes of dLGN-projecting RGCs (Luth et al., 1993; Quina et al., 2005; Badea et al., 2009; Su et al., 2011). Co-labeling of retinal cross-sections with antibodies against FGFR2 and either Calr or Brn3a revealed that dLGN-projecting classes of RGCs express the FGF22 receptor (**Figures 4B,C**). The expression of appropriate receptors by dLGN-projecting classes of RGCs supports our hypothesis that target-derived FGF22 regulates the formation and development of retinal terminals.

FGF22 CONTRIBUTES TO RETINAL TERMINAL FORMATION AND MATURATION *IN VIVO*

To test the role of FGF22 in the development of retinogeniculate nerve terminals we used a previously generated targeted mouse mutant that lacked FGF22 ($fgf22^{-/-}$; Terauchi et al., 2010). Mutants lacking FGF22 are born in expected numbers and are phenotypically indistinguishable from littermate controls during the first weeks of postnatal development.

The development of retinal and inhibitory nerve terminals in dLGN in the absence of FGF22 was assessed by immunostaining for VGluT2 and GAD67 as described above. Terminals were examined in coronal sections of mutant and littermate control dLGN at P7, P14, and P21. While we detected no difference in GAD67-immunoreactivity in P7 dLGN, fewer VGluT2-containing nerve terminals were observed in dLGN lacking FGF22 (**Figures 5A,B**). The relative area occupied by VGluT2-positive terminals in mutant and control dLGN was quantified and was statistically significant (**Figure 5C**). We interpret these results to indicate fewer retinogeniculate synapses are present in dLGN in the absence of FGF22. Similar analyses revealed no change in the area occupied by GAD67-immunoreactive terminals in P7 mutant dLGN (**Figures 5A–C**).

We next examined nerve terminal number and morphology at P14, an age in which immature terminals have differentiated into large, morphologically distinct presynaptic terminals (i.e., RLPs). As in P7 mutant dLGN, fewer VGluT2-containing nerve terminals appeared in P14 $fgf22^{-/-}$ dLGN (**Figures 5D,E**) and the area occupied by these terminals was significantly reduced (**Figure 5F**). In addition to fewer terminals it also appeared as if retinogeniculate terminals were smaller in P14 $fgf22^{-/-}$ dLGN (**Figures 5D,E**), a finding that suggests the normal timing of retinal terminal maturation may be delayed in the absence of FGF22. Again, in contrast to defects observed at retinal terminals, the development and distribution of inhibitory nerve terminals appeared unaffected by the loss of FGF22 at this age (**Figures 5D–F**).

Finally we examined retinal and inhibitory terminals at P21, an age in which synaptic development is largely complete in

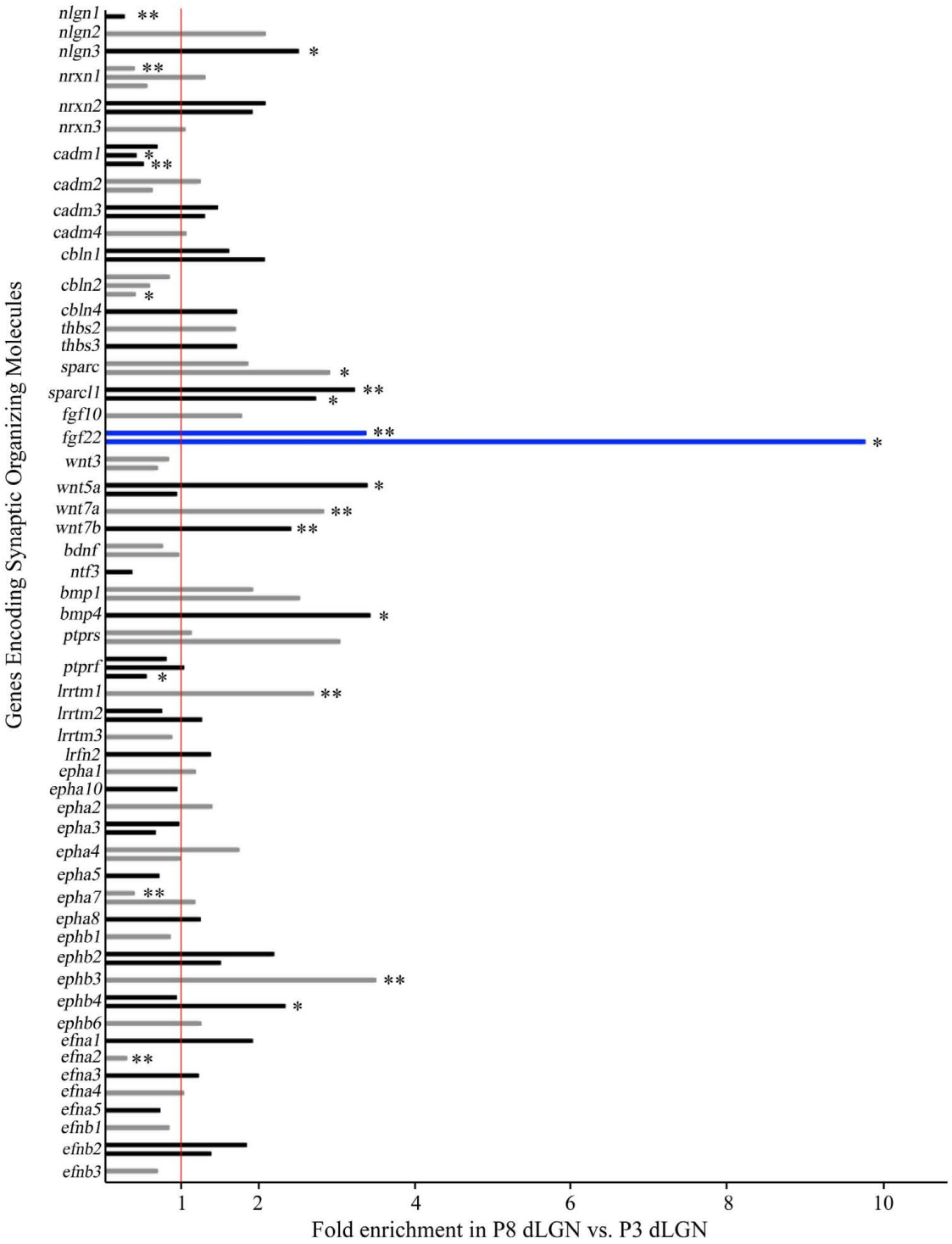

FIGURE 2 | Changes in the expression of synaptic organizing molecules in the postnatal dLGN. Relative mRNA expression levels of known families of synaptic organizing molecules in P8 dLGN was compared to that at P3 by Agilent microarray. Bar graphs represent fold enrichment (or decrease) in P8 dLGN vs. P3 dLGN. The red line represents no change in gene expression between these ages. Bar color is alternated between gray and black for each adjacent gene for ease of viewing, with the exception of blue bars representing mRNA expressional levels for *fgf22*, the synaptic organizer showing the greatest enrichment. The expression of many genes is shown with multiple bars: in these cases each bar represents data from a unique probe set in the array. *Denote data that are statistically significant with $p < 0.05$. **Denote data that are statistically significant with $p < 0.01$. Expression of 11 synaptic organizers was enriched in P8 samples (*nlgn3, sparc, sparcl1, fgf22, wnt5a, wnt7a, wnt7b, bmp4, lrrtm1, ephb3, ephb4)* whereas seven were significantly down-regulated at P8 (*nlgn1, nrxn1, cadm1, cbln2, ptprf, epha7, efna2)*.

mouse dLGN (Chen and Regehr, 2000; Jaubert-Miazza et al., 2005). We found no appreciable differences in the number or morphology of retinal or inhibitory nerve terminals in mutants or controls at this age (**Figures 5G–I**). Moreover, the dorsolateral to ventromedial gradient of retinogeniculate synaptic development remained intact in mutant dLGN (data not shown). Taken together these results suggest that FGF22 contributes to retinal (but not inhibitory) nerve terminal development in dLGN, but that in its absence compensatory mechanisms eventually promote retinogeniculate circuit formation.

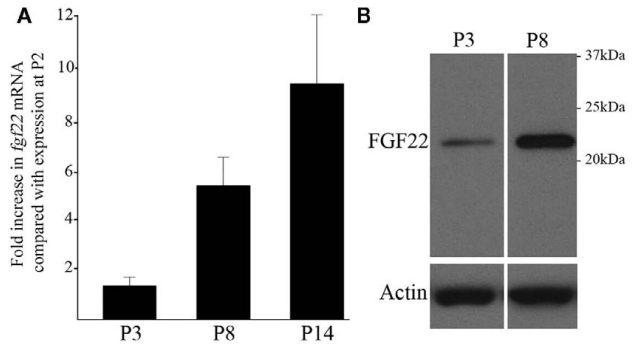

FIGURE 3 | Increases in *fgf22* mRNA and FGF22 protein levels in dLGN coincide with the maturation of retinal terminals. (A) The developmental up-regulation of *fgf22* mRNA from P2 to P14 in dLGN was examined by quantitative RT-PCR (qPCR). Data from P3, P8, and P14 were compared against that at P2. All data was normalized to actin mRNA levels. Data are shown ± SEM; $n > 4$. **(B)** Western blots demonstrate an increase in FGF22 protein from P3 to P8 in dLGN protein extracts. Levels of actin were used as loading controls.

NORMAL RETINAL DEVELOPMENT IN *fgf22*$^{-/-}$ MUTANTS

We interpret the above results to suggest a direct role for FGF22 in retinogeniculate circuit development. An alternative possibility is that these defects are secondary to intra-retinal defects or reflect a delay in the arrival of retinal axons into dLGN. To address these issues we analyzed retinal development in *fgf22*$^{-/-}$ mutants. The retina is a layered structure that contains five main cell types: photoreceptors reside in the outer most layer of the retina – the outer nuclear layer (ONL); bipolar cells, horizontal cells, amacrine cells reside in the inner nuclear layer (INL); RGCs reside in the inner most cell layer – the ganglion cell layer (Masland, 2001; Sanes and Zipursky, 2010). Two synaptic layers exist in the retina: the outer plexiform layer (OPL) where photoreceptors synapse onto dendrites of bipolar cells, and the inner plexiform layer (IPL) where bipolar and amacrine cells synapse

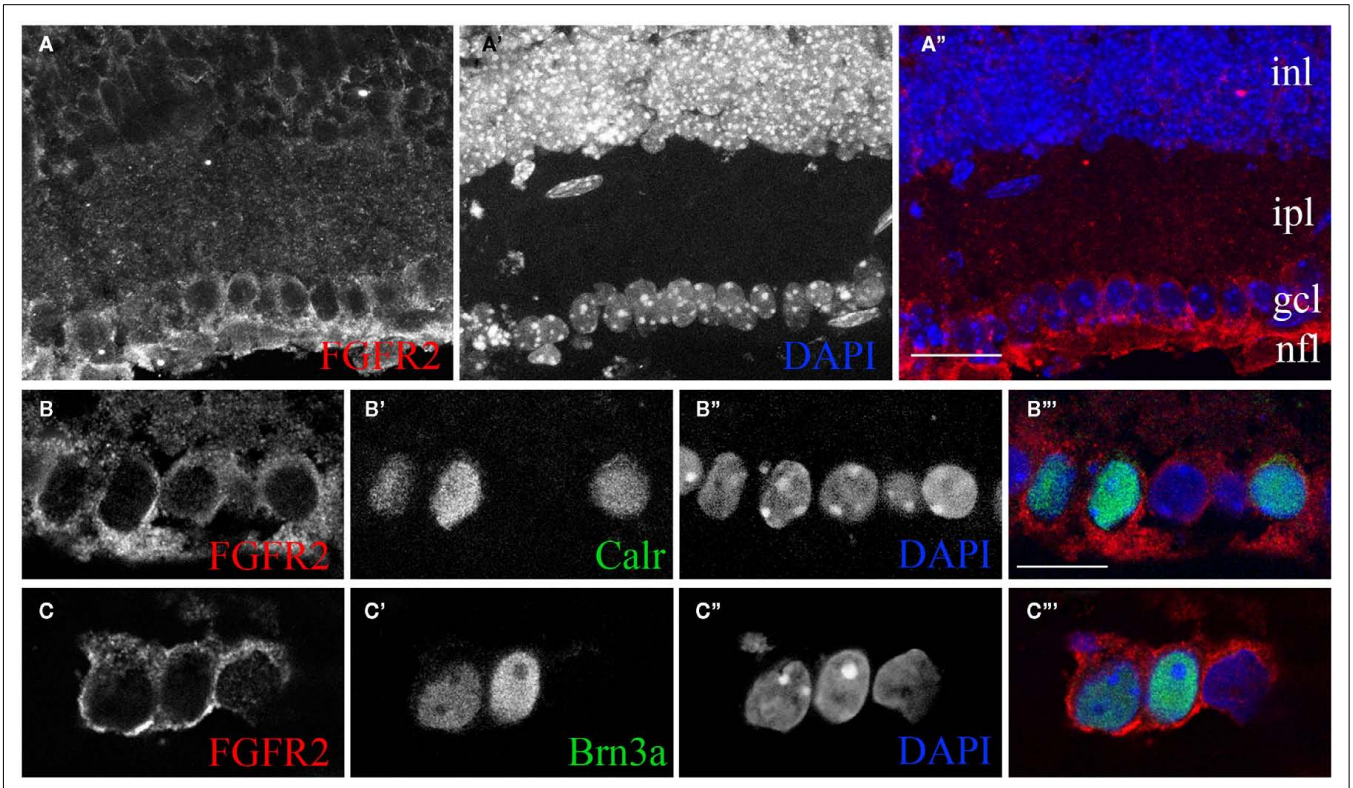

FIGURE 4 | The FGF22 receptor FGFR2 is expressed by classes of retinal ganglion cells that innervate dLGN. (A) Confocal analysis of immunostained P14 wild-type retinal cross-sections revealed the presence of FGFR2 in the ganglion cell layer (gcl) and nerve fiber layer (nfl). Retinal layers were identified by nuclear-labeling with DAPI. **(B,C)** Single optical slices from confocal analyses of retinal cross-sections immunostained for FGFR2 and either Calr **(B)** or Brn3a **(C)**. Nuclei were labeled with DAPI. inl, inner nuclear layer; ipl, inner plexiform layer; gcl, ganglion cell layer; nfl, nerve fiber layer. Scale bar in **(A)** = 50 μm and in **(B)** = 20 μm for **(B,C)**.

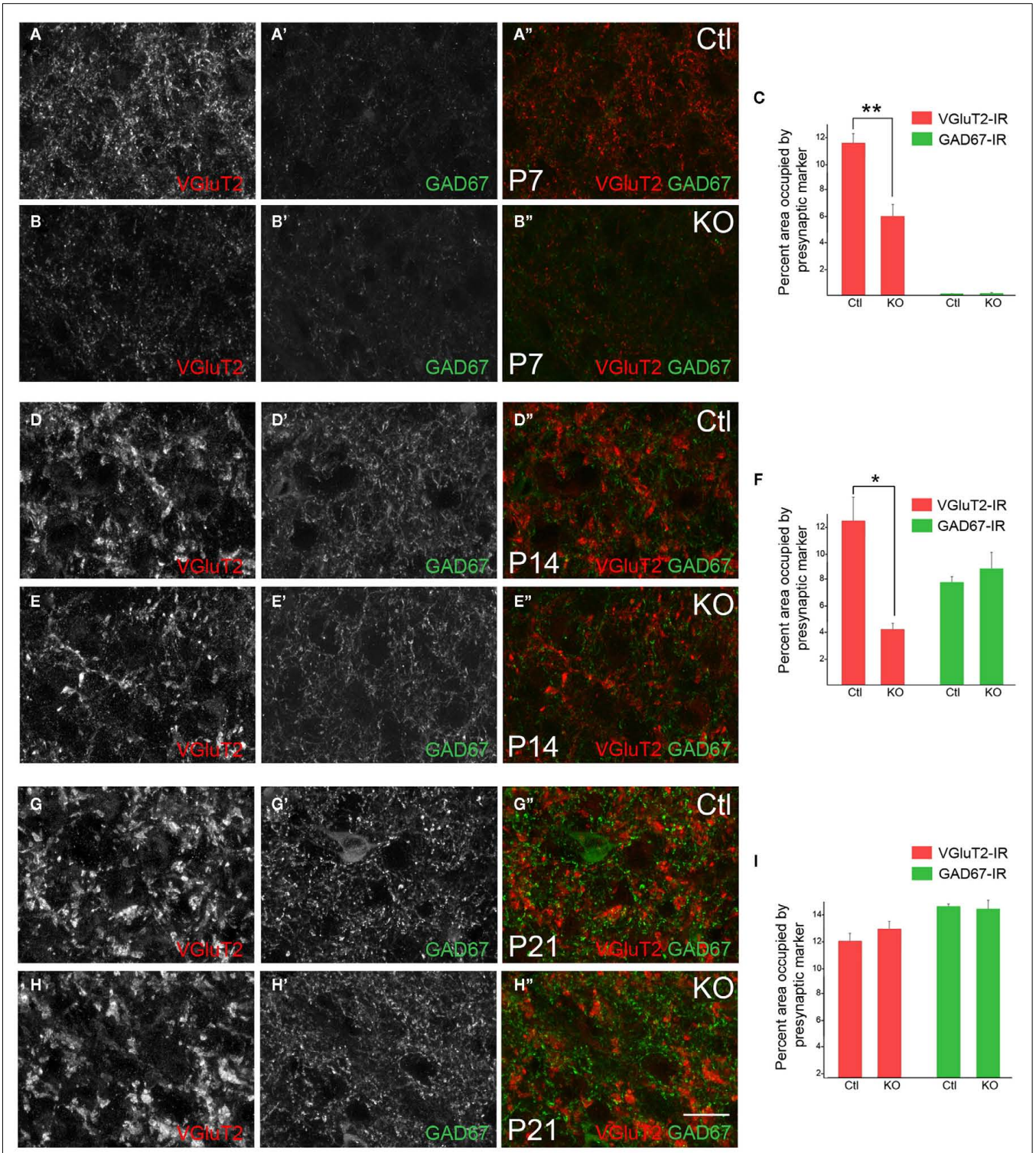

FIGURE 5 | Deletion of FGF22 impairs the formation and maturation of retinal terminals in the dLGN. VGluT2- and GAD67-immunoreactivity in coronal sections of control (Ctl) and *fgf22*$^{-/-}$ mutant (KO) dLGN at P7 **(A,B)**, P14 **(D,E)**, and P21 **(G,H)**. Differences in the percent area of immunoreactivity in each image were quantified for each age and genotype **(C,F,I)**. At P7 fewer VGluT2-immunoreactive puncta were observed in mutant dLGN, leading to a statistically significant reduction in the area of immunoreactivity **(A–C)**. At P14, VGluT2-immunoreactive (VGluT2-IR) terminals appeared less mature and the area that mutant terminals occupied in each field of view was significantly lower than in controls **(D–F)**. By P21 no differences were observed in VGluT2–IHC in dLGN of mutants and controls **(G–I)**. At all ages GAD67-immunoreactivity (GAD67-IR) appeared similar in *fgf22*$^{-/-}$ and control dLGN. For **(C,F,I)** data shown are ±SEM; $n = 4$ mice. *Differs from age-matched controls at $p < 0.05$ by Student's *t*-test. **Differs from age-matched controls at $p < 0.01$ by Student's *t*-test. Scale bar in **(H)** = 15 μm.

onto RGC dendrites. Immunostaining retinal cross-sections from P14 control and *fgf22*$^{-/-}$ mutant mice showed no appreciable difference in the structure of the retina, the thickness of retinal layers, or the density of neurons in the absence of FGF22 (**Figures 6A–D**). Moreover, removal of FGF22 had no discernable affect on the generation of Brn3a- or Calr-expressing classes of

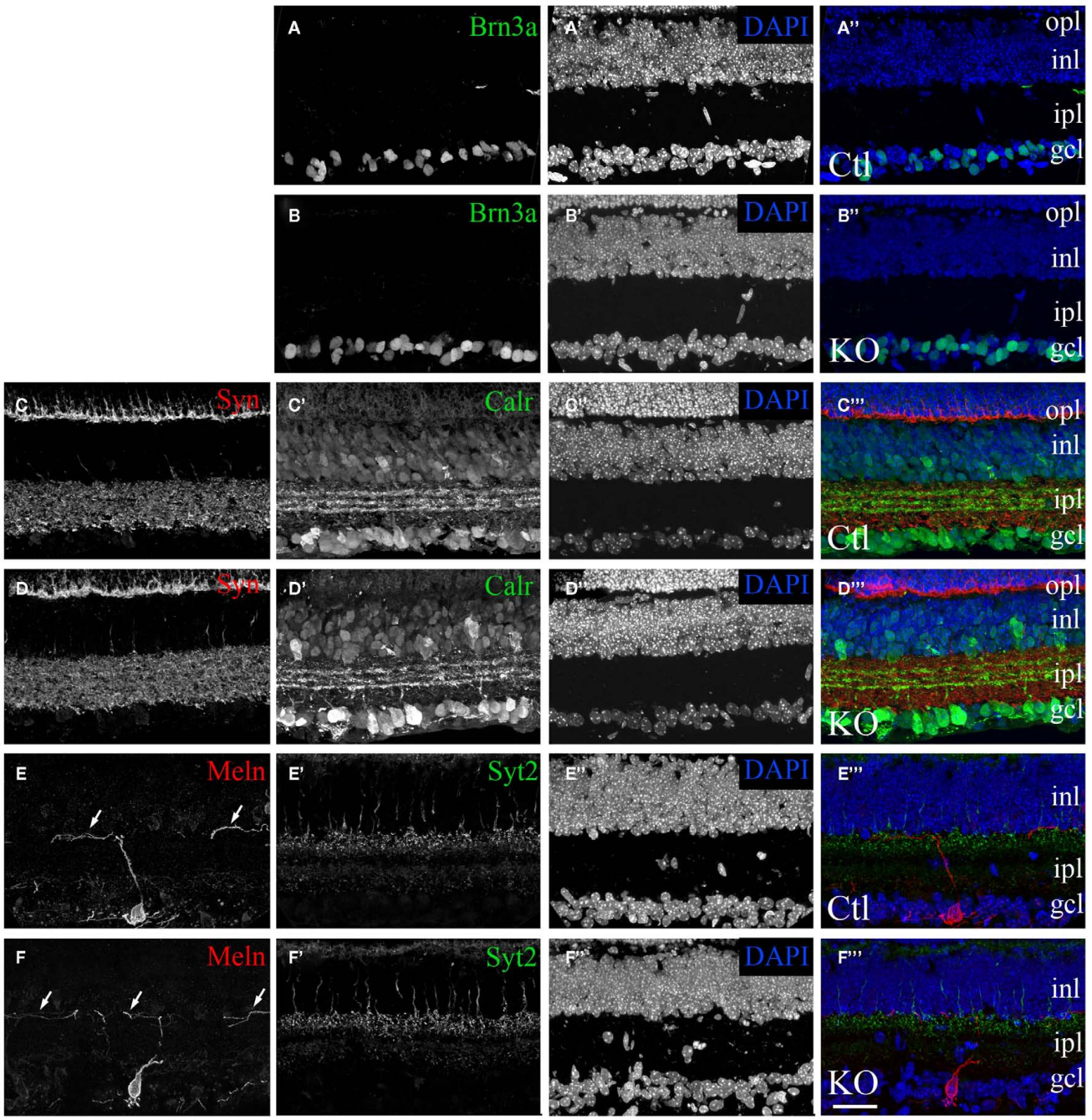

FIGURE 6 | Normal morphological development of the retina in mice lacking FGF22. Confocal images of retinal cross-sections from P14 *fgf22*$^{-/-}$ mutant mice **(B,D,F)** and littermate controls **(A,C,E)**. **(A–D)** Classes of dLGN-projecting RGCs were labeled by Brn3a–IHC **(A,B)** and Calr–IHC **(C,D)**. The number and distribution of Brn3a- and Calr-expressing RGCs appeared similar in control and *fgf22*$^{-/-}$ retina. **(C–F)** Labeling of synaptic layers with anti-synaptophysin (Syn) **(C,D)** and synaptotagmin2 (Syt2) **(E,F)** revealed no remarkable differences in the density of synapses or laminar arrangement of the retina between mutants and controls. Likewise labeling with anti-Syt2, anti-Calr, and anti-melanopsin (Meln) revealed that sublaminar specificity was indistinguishable in controls and mice lacking FGF22 **(D,F)** and controls **(C,E)**. Arrows in **(E,F)** show that dendrites from Meln-expressing RGCs correctly target the inner most region of the IPL in the absence of FGF22. In all sections nuclei were labeled with DAPI. inl, inner nuclear layer; ipl, inner plexiform layer; gcl, ganglion cell layer. Scale bar = 100 μm.

RGCs (**Figures 6A–D**), or the dendritic stratification of RGCs in the IPL (**Figures 6C–F**). Not only did the morphology of retinal neurons and their circuitry appear unaltered in *fgf22*$^{-/-}$ mutants but the timing of retinal development also appeared unaltered. For example, in wild-type adult retina the synaptic vesicle associated protein synaptotagmin 2 (Syt2) is restricted to horizontal cells and classes of OFF-bipolar cells whose axons arborize in the outer portion of the IPL (Fox and Sanes, 2007). However during the first ∼11 postnatal days of retinal development it is also transiently expressed in starburst amacrine cell processes in the IPL (Fox and Sanes, 2007). The absence of Syt2 from starburst amacrine cell processes in P14 *fgf22*$^{-/-}$ mutants (**Figures 6E,F**) suggests that the timing of its development is unaltered in the absence of FGF22. Thus, delayed synaptogenesis in *fgf22*$^{-/-}$ dLGN is not caused by delayed or aberrant retinal development.

We next addressed whether the targeting of retinal axons was delayed in mutants lacking FGF22. For this, we examined the presence of Calr-expressing retinal axons in dLGN at P7 – an age in which we have previously demonstrated the presence of these axons in mouse dLGN (Su et al., 2011). The arborization of Calr-expressing RGC axons appeared similar in *fgf22*$^{-/-}$ mutants and littermate controls (**Figure 7**). Thus the delay in synaptogenesis in dLGN does not appear to arise from a delay in retinogeniculate targeting.

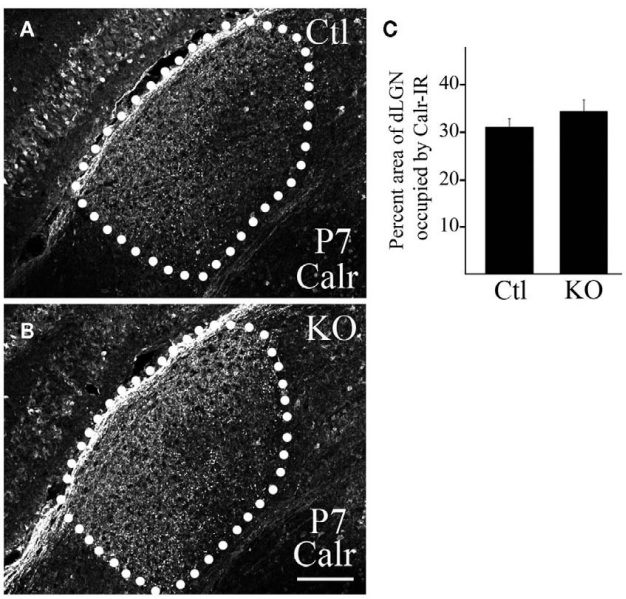

FIGURE 7 | Deletion of FGF22 does not delay targeting of dLGN-projecting RGC axons. Calr–IHC was used to assess the development of dLGN-projecting RGC axons in P7 control [Ctl; **(A)**] and *fgf22*$^{-/-}$ mutant [KO; **(B)**] dLGN. dLGN are encircled by white dots. **(C)** The area of Calr-IR in control and mutant P7 dLGN was measured in ImageJ. No significant differences were detected in the percent area of dLGN innervated by Calr-expressing RGCs in P7 controls and mutants. Data are shown ± SEM; $n = 4$ mice. Scale bar = 125 μm.

DISCUSSION

Identifying the mechanisms that underlie synapse formation is critical for our understanding of how neural circuits – and their associated functions – are established. Although retinogeniculate circuits have been used as a model for the mechanisms regulating synaptic targeting and refinement, the molecular mechanisms driving the differentiation of retinal axons and dendrites of thalamic relay neurons into precisely aligned pre- and postsynaptic elements remains unclear. In other brain regions synaptic differentiation is orchestrated by membrane-bound and extracellular "organizing" cues. In the present study we focused on identifying candidate synaptic organizers that regulate the timely assembly of retinal nerve terminals in dLGN. To accomplish this we explored the temporal progression of nerve terminal development in dLGN and then identified genes whose expression correlated with the formation of retinal nerve terminals. Detailed analysis of one of these genes, *fgf22*, revealed that target-derived FGFs contribute to the timely development of retinogeniculate synapses.

RETINAL AND INHIBITORY NERVE TERMINAL DEVELOPMENT IN dLGN

Development of retinal nerve terminals in dLGN is a protracted, multistep process that shares many similarities with the pattern of nerve terminal development at the mouse neuromuscular junction (NMJ), a peripheral synapse between lower motor neurons and skeletal muscle fibers. At the NMJ, motor axons are targeted to postsynaptic sites in the central end-plate region of muscle embryonically, several weeks before pre- and postsynaptic elements are structurally and functionally mature (Fox, 2009). Motor axon–muscle contacts differentiate into immature synapses during late embryonic development in rodents (Kelly and Zacks, 1969; Lupa and Hall, 1989; Sanes and Lichtman, 1999; Fox, 2009). At these early ages, an excess of motor nerve terminals are present on each postsynaptic site, such that a single muscle fiber may receive input from 2–12 different motor neurons (Wyatt and Balice-Gordon, 2003). By P14, however, activity-dependent refinement has led to the elimination of all supernumerary nerve terminals, so that each postsynaptic site (and thus each muscle fiber) is innervated by a single motor nerve terminal (Wyatt and Balice-Gordon, 2003). As excess terminals are pruned, the remaining nerve terminal and postsynaptic apparatus mature and grow to resemble their adult-like form by P21 (Balice-Gordon and Lichtman, 1993).

Like motor axons, retinal axons begin to target appropriate regions of dLGN embryonically, weeks before the retinogeniculate synapses are adult-like in their ultrastructure or physiology (Godement et al., 1984; Chen and Regehr, 2000; Jaubert-Miazza et al., 2005). Here we show that the number of VGluT2-containing retinal nerve terminals increase dramatically in dLGN during the first postnatal week of development (**Figure 1**), more than a week after their initial arrival. By P7 the density of retinal terminals is so high it is not surprising that dLGN relay neurons may be innervated by up to 20 different RGCs at this age (Chen and Regehr, 2000; Jaubert-Miazza et al., 2005). Despite the increased density of presynaptic profiles at these early ages, there is much evidence that these synapses are still immature: at P7 retinogeniculate synapses are weak and lack their adult-like ultrastructural

morphology (Bickford et al., 2010). Here we further show that at P7 retinal terminals are small compared to adult terminals, and in fact are similar in size to GABAergic inhibitory nerve terminals. During the second and third week of mouse development (P7–P21), spontaneous retinal activity drives the elimination of excess retinal nerve terminals (pruning the number of inputs that each dLGN relay neuron receives) and the remaining terminals mature into adult-like RLPs (Guido, 2008; Bickford et al., 2010). Like the NMJ, by P21 the morphology and function of retinogeniculate synapses reach an adult-like state (Chen and Regehr, 2000; Bickford et al., 2010).

While the timing and sequential development of excitatory retinal nerve terminals resembles that described for motor axons at the NMJ, inhibitory synapse development in dLGN follows a different pattern. We observed few inhibitory presynaptic terminals during the first postnatal week of development, supporting studies showing few inhibitory postsynaptic responses in P7 dLGN relay neurons (Bickford et al., 2010). Despite the lack of inhibitory activity or nerve terminals, interneuron-specific genes are present in mouse dLGN as early as P6, confirming that interneurons are indeed present at these early ages (Yuge et al., 2011). By eye-opening, and at all ages thereafter, we observed GAD67-containing GABAergic terminals densely populating dLGN. The late development of inhibitory circuits may reflect that interneurons in dLGN are born later than RGCs and presumably after retinal axons have begun to target the dLGN (Hayes et al., 2003; Yuge et al., 2011). However, since interneurons are indeed present at P6 (an age in which we observed few inhibitory nerve terminals) it suggests that cues necessary for inducing inhibitory synaptogenesis are not present until after retinogeniculate synapses form. Besides forming later, our data also suggest that cellular mechanisms of inhibitory nerve terminal formation differ from that of retinal terminals. For example, the size or shape of inhibitory terminals did not appear to change after their initial formation, nor did we detect a period of inhibitory synapse refinement, in which the density of inhibitory terminals decreased with age (as seen from P7 to P14 for retinal terminals).

The maturation/refinement of retinogeniculate synapses and the dramatic increase in inhibitory synapses both coincide with natural eye-opening. Moreover, retinal terminals are "multisynaptic boutons" that not only synapse onto relay neuron dendrites but also synapse onto dendritic terminals of inhibitory interneurons (which themselves synapse onto the relay neuron dendrite; Famiglietti, 1970; Sherman and Guillery, 2002; Sherman, 2004). These local circuits (or synaptic "triads") generate feed-forward inhibition to temporally sharpen visual input to thalamus (Sherman and Guillery, 2002; Sherman, 2004). The coincident emergence of adult-like retinogeniculate terminals and inhibitory synapses, as well as there interconnection at "triads," suggest a coordinated pattern of development. With this in mind, it was unexpected to discover that the development of inhibitory synapses was not delayed in *fgf22*$^{-/-}$ mutant mice despite delayed development of retinogeniculate synapses. This suggests that retinal and inhibitory synapses develop independently in dLGN. An alternative possibility is that retinal terminals are required for inhibitory synapse formation, but the state of their maturation does not matter.

FGF signaling is required for visual system circuit assembly

Fibroblast growth factor family members contribute to many aspects of neural development, from neural induction to the formation of neural circuits (Dono, 2003; Umemori, 2009). FGF22 was originally purified from developing mouse brain extracts for its ability to cluster synaptic vesicles into presumptive nerve terminals in cultured neurons (Umemori et al., 2004). Expression of FGF22 by postsynaptic neurons (or muscle) and its receptor FGFR2 by presynaptic neurons support *in vitro* studies suggesting that FGFs act as target-derived presynaptic organizers (Umemori et al., 2004; Fox et al., 2007). Moreover, genetic disruption of FGF22–FGFR2 signaling results in defects in excitatory nerve terminal assembly at mossy fiber-pyramidal neuron synapses in hippocampus, mossy fiber–granule cell synapses in cerebellum, and at the NMJ (Umemori et al., 2004; Fox et al., 2007; Terauchi et al., 2010). Together, these studies demonstrate that FGF22 is necessary for the differentiation of nerve terminals in the mammalian brain. FGF7 and FGF10, which are closely related to FGF22, share similar abilities to induce presynaptic differentiation (Umemori et al., 2004). While FGF7 and FGF22 share similar (and presumably interchangeable) roles in the assembly of nerve terminals at the NMJ, they exhibit distinct synaptogenic functions in brain. In hippocampus, FGF7 and FGF22 are both generated by CA3 pyramidal neurons but one is required at excitatory synapses and the other at inhibitory synapses (Terauchi et al., 2010).

Our studies show a novel role for this family of synaptogenic FGFs in visual system circuit assembly. Based upon results showing that FGF22 expression in dLGN coincides with synaptogenesis (**Figure 3**), FGFR2 expression by classes of dLGN-projecting RGCs (**Figure 4**), and an impairment in the development of retinal nerve terminals in the absence of FGF (**Figure 5**) all suggest that FGF22 acts as a target-derived presynaptic organizer in the mouse visual system. It is unclear whether other synaptogenic FGFs (namely FGF7 and FGF10) also contribute to retinogeniculate synapse formation, or are perhaps able to compensate for the absence of FGF22 in *fgf22*$^{-/-}$ mutant mice. It is also unclear whether roles for FGFs in visual system circuit assembly are confined to the dLGN or whether other retino-recipient nuclei [such as the superior colliculus (SC)] utilize these mechanisms for circuit assembly.

Multiple presynaptic organizers in dLGN

Our results demonstrate that ∼15% of synaptic organizing molecules are enriched in dLGN during retinogeniculate circuit assembly (**Figure 2**). Why are so many target-derived organizing molecules enriched in dLGN? There are many possible answers to this question (see Fox et al., 2007), two of which we will discuss here. First, different organizers may be required for different types of synapses in dLGN. Like most regions of brain, dLGN contains a wide array of synaptic inputs. In addition to receiving input from RGCs, relay neurons also receive inputs from cortex, brainstem, midbrain, other thalamic regions, and local interneurons. In fact, retinal terminals represent only 5–10% of the inputs onto a given relay neuron in dLGN (Van Horn et al., 2000; Sherman and Guillery, 2002). A variety of synapses are also present on dLGN interneurons (Sherman and Guillery, 2002). As excitatory and inhibitory synapses generally require different synaptic organizing cues it is likely that the variety of synaptic types accounts,

at least in part, for the multitude of synaptic organizers enriched during postnatal dLGN development. However it is noteworthy that we analyzed the expression of these organizing molecules at a stage in development when few non-retinal synapses are forming in dLGN. And, at least two synaptic organizers (in addition to FGF22) were identified that are known to contribute to the formation of synapses between RGC axons and target neurons. SPARC and SPARC-like 1, two glial-derived ECM molecules, contribute to retino-collicular synapse formation (Kucukdereli et al., 2011). Based upon their up-regulation in dLGN during synaptogenesis it is tempting to speculate that they play similar roles in dLGN and may be capable of compensating for the absence of FGF22 in mutants studied here.

Alternatively, different organizers may contribute to different aspects of synaptic development. At the NMJ, different muscle-derived presynaptic organizing molecules are required for sequential aspects of motor nerve terminal development: FGF7/10/22 induce the initial formation of motor nerve terminals, laminins containing the β2 subunit are required for postnatal maturation of nerve terminals, and synaptic collagens IV are required for motor nerve terminal maintenance (Fox et al., 2007). Genetic disruption of FGF signaling at the NMJ leads to a delay in nerve terminal formation, much like we observe here for FGF22 at retinogeniculate synapses. Several findings suggest that other organizers, such as muscle-derived laminin β2 and synaptic collagens, are able to compensate in the absence of FGF–FGFR2 signaling at the NMJ. First, defects in nerve terminal development are temporary, as described above. Second, genetic removal of both FGFR2 (in motor axons) and laminin β2 prolongs defects associated with FGF signaling (Fox et al., 2007). As the development of retinogeniculate synapses share similarities with NMJ development (including their dependence of FGF signaling), it may be that multiple target-derived organizing molecules are required for different aspects of retinal nerve terminal development and these additional cues are capable of partly compensating in the absence of FGF22.

ACKNOWLEDGMENTS

This work was supported by The Thomas F. Jeffress and Kate Miller Jeffress Memorial Trust (Michael A. Fox), the VCU Presidential Research Initiative Program (PRIP) Award (Michael A. Fox), and the National Institutes of Health [NIH; EY021222 (Michael A. Fox); NS070005 (Hisashi Umemori)]. Microscopy was performed at the Virginia Commonwealth University Department of Anatomy and Neurobiology Microscopy Facility supported, in part, with funding from NIH–National Institute of Neurological Disorders and Stroke Center Core Grant 5P30 NS047463-02. We thank Dr. C. K. Chen for providing anti-melanopsin antibodies.

REFERENCES

Badea, T. C., Cahill, H., Ecker, J., Hattar, S., and Nathans, J. (2009). Distinct roles of transcription factors brn3a and brn3b in controlling the development, morphology, and function of retinal ganglion cells. *Neuron* 61, 852–864.

Balice-Gordon, R. J., and Lichtman, J. W. (1993). In vivo observations of pre- and postsynaptic changes during the transition from multiple to single innervation at developing neuromuscular junctions. *J. Neurosci.* 13, 834–855.

Bickford, M. E., Slusarczyk, A., Dilger, E. K., Krahe, T. E., Kucuk, C., and Guido, W. (2010). Synaptic development of the mouse dorsal lateral geniculate nucleus. *J. Comp. Neurol.* 518, 622–635.

Bjartmar, L., Huberman, A. D., Ullian, E. M., Renteria, R. C., Liu, X., Xu, W., Prezioso, J., Susman, M. W., Stellwagen, D., Stokes, C. C., Cho, R., Worley, P., Malenka, R. C., Ball, S., Peachey, N. S., Copenhagen, D., Chapman, B., Nakamoto, M., Barres, B. A., and Perin, M. S. (2006). Neuronal pentraxins mediate synaptic refinement in the developing visual system. *J. Neurosci.* 26, 6269–6281.

Catalina, E., Tomassini, S., Dal Monte, M., Bosco, L., and Casini, G. (2009). Localization patterns of fibroblast growth factor 1 and its receptors FGFR1 and FGFR2 in postnatal mouse retina. *Cell Tissue Res.* 336, 423–438.

Chen, C., and Regehr, W. G. (2000). Developmental remodeling of the retinogeniculate synapse. *Neuron* 28, 955–966.

Cheng, H. J., Nakamoto, M., Bergemann, A. D., and Flanagan, J. G. (1995). Complementary gradients in expression and binding of ELF-1 and Mek4 in development of the topographic retinotectal projection map. *Cell* 82, 371–381.

Corriveau, R. A., Huh, G. S., and Shatz, C. J. (1998). Regulation of class I MHC gene expression in the developing and mature CNS by neural activity. *Neuron* 21, 505–520.

Craig, A. M., Graf, E. R., and Linhoff, M. W. (2006). How to build a central synapse: clues from cell culture. *Trends Neurosci.* 29, 8–20.

Dono, R. (2003). Fibroblast growth factors as regulators of central nervous system development and function. *Am. J. Physiol. Regul. Integr. Comp. Physiol.* 284, R867–R881.

Drescher, U., Kremoser, C., Handwerker, C., Loschinger, J., Noda, M., and Bonhoeffer, F. (1995). In vitro guidance of retinal ganglion cell axons by RAGS, a 25 kDa tectal protein related to ligands for Eph receptor tyrosine kinases. *Cell* 82, 359–370.

Eroglu, C., and Barres, B. A. (2010). Regulation of synaptic connectivity by glia. *Nature* 468, 223–231.

Famiglietti, E. V. Jr. (1970). Dendrodendritic synapses in the lateral geniculate nucleus of the cat. *Brain Res.* 20, 181–191.

Feldheim, D. A., and O'Leary, D. D. (2010), Visual map development: bidirectional signaling, bifunctional guidance molecules, and competition. *Cold Spring Harb. Perspect. Biol.* 2, a001768.

Feldheim, D. A., Vanderhaeghen, P., Hansen, M. J., Frisen, J., Lu, Q., Barbacid, M., and Flanagan, J. G. (1998). Topographic guidance labels in a sensory projection to the forebrain. *Neuron* 21, 1303–1313.

Feller, M. B. (2009). Retinal waves are likely to instruct the formation of eye-specific retinogeniculate projections. *Neural Dev.* 4, 24.

Fox, M. A. (2009). "Development of the vertebrate neuromuscular junction," in *The Sticky Synapse: Cell Adhesion Molecules and Their Role in Synapse Formation and Maintenance*, ed. M. Hortsch and H. Umemori (Ney York, NY: Spinger Press), 39–84.

Fox, M. A., Colello, R. J., Macklin, W. B., and Fuss, B. (2003). Phosphodiesterase-Ialpha/autotaxin: a counteradhesive protein expressed by oligodendrocytes during onset of myelination. *Mol. Cell. Neurosci.* 23, 507–519.

Fox, M. A., and Sanes, J. R. (2007). Synaptotagmin I and II are present in distinct subsets of central synapses. *J. Comp. Neurol.* 503, 280–296.

Fox, M. A., Sanes, J. R., Borza, D. B., Eswarakumar, V. P., Fassler, R., Hudson, B. G., John, S. W., Ninomiya, Y., Pedchenko, V., Pfaff, S. L., Rheault, M. N., Sado, Y., Segal, Y., Werle, M. J., and Umemori, H. (2007). Distinct target-derived signals organize formation, maturation, and maintenance of motor nerve terminals. *Cell* 129, 179–193.

Fox, M. A., and Umemori, H. (2006). Seeking long-term relationship: axon and target communicate to organize synaptic differentiation. *J. Neurochem.* 97, 1215–1231.

Fujiyama, F., Hioki, H., Tomioka, R., Taki, K., Tamamaki, N., Nomura, S., Okamoto, K., and Kaneko, T. (2003). Changes of immunocytochemical localization of vesicular glutamate transporters in the rat visual system after the retinofugal denervation. *J. Comp. Neurol.* 465, 234–249.

Godement, P., Salaun, J., and Imbert, M. (1984). Prenatal and postnatal development of retinogeniculate and retinocollicular projections in the mouse. *J. Comp. Neurol.* 230, 552–575.

Guido, W. (2008). Refinement of the retinogeniculate pathway. *J. Physiol. (Lond.)* 586, 4357–4362.

Hayes, S. G., Murray, K. D., and Jones, E. G. (2003). Two epochs in the development of gamma-aminobutyric acidergic neurons in the ferret thalamus. *J. Comp. Neurol.* 463, 45–65.

Huberman, A. D., Feller, M. B., and Chapman, B. (2008). Mechanisms underlying development of visual maps and receptive fields. *Annu. Rev. Neurosci.* 31, 479–509.

Huh, G. S., Boulanger, L. M., Du, H., Riquelme, P. A., Brotz, T. M., and Shatz, C. J. (2000). Functional requirement for class I MHC in CNS development and plasticity. *Science* 290, 2155–2159.

Jaubert-Miazza, L., Green, E., Lo, F. S., Bui, K., Mills, J., and Guido, W. (2005). Structural and functional composition of the developing retinogeniculate pathway in the mouse. *Vis. Neurosci.* 22, 661–676.

Johnson-Venkatesh, E. M., and Umemori, H. (2010). Secreted factors as synaptic organizers. *Eur. J. Neurosci.* 32, 181–190.

Jones, E. V., Bernardinelli, Y., Tse, Y. C., Chierzi, S., Wong, T. P., and Murai, K. K. (2011). Astrocytes control glutamate receptor levels at developing synapses through SPARC-beta-integrin interactions. *J. Neurosci.* 31, 4154–4165.

Kano, M., and Hashimoto, K. (2009). Synapse elimination in the central nervous system. *Curr. Opin. Neurobiol.* 19, 154–161.

Kelly, A. M., and Zacks, S. I. (1969). The fine structure of motor endplate morphogenesis. *J. Cell Biol.* 42, 154–169.

Kucukdereli, H., Allen, N. J., Lee, A. T., Feng, A., Ozlu, M. I., Conatser, L. M., Chakraborty, C., Workman, G., Weaver, M., Sage, E. H., Barres, B. A., and Eroglu, C. (2011). Control of excitatory CNS synaptogenesis by astrocyte-secreted proteins Hevin and SPARC. *Proc. Natl. Acad. Sci. U.S.A.* 108, E440–E449.

Land, P. W., Kyonka, E., and Shamalla-Hannah, L. (2004). Vesicular glutamate transporters in the lateral geniculate nucleus: expression of VGLUT2 by retinal terminals. *Brain Res.* 996, 251–254.

Lichtman, J. W., and Colman, H. (2000). Synapse elimination and indelible memory. *Neuron* 25, 269–278.

Lupa, M. T., and Hall, Z. W. (1989). Progressive restriction of synaptic vesicle protein to the nerve terminal during development of the neuromuscular junction. *J. Neurosci.* 9, 3937–3945.

Luth, H. J., Winkelmann, E., and Celio, M. R. (1993). Light- and electron microscopic localization of parvalbumin, calbindin D-28k and calretinin in the dorsal lateral geniculate nucleus of the rat. *J. Hirnforsch.* 34, 47–56.

Masland, R. H. (2001). The fundamental plan of the retina. *Nat. Neurosci.* 4, 877–886.

Mooney, R., Penn, A. A., Gallego, R., and Shatz, C. J. (1996). Thalamic relay of spontaneous retinal activity prior to vision. *Neuron* 17, 863–874.

Osterhout, J. A., Josten, N., Yamada, J., Pan, F., Wu, S. W., Nguyen, P. L., Panagiotakos, G., Inoue, Y. U., Egusa, S. F., Volgyi, B., Inoue, T., Bloomfield, S. A., Barres, B. A., Berson, D. M., Feldheim, D. A., and Huberman, A. D. (2011). Cadherin-6 mediates axon-target matching in a non-image-forming visual circuit. *Neuron* 71, 632–639.

Pfeiffenberger, C., Cutforth, T., Woods, G., Yamada, J., Renteria, R. C., Copenhagen, D. R., Flanagan, J. G., and Feldheim, D. A. (2005). Ephrin-As and neural activity are required for eye-specific patterning during retinogeniculate mapping. *Nat. Neurosci.* 8, 1022–1027.

Quina, L. A., Pak, W., Lanier, J., Banwait, P., Gratwick, K., Liu, Y., Velasquez, T., O'Leary, D. D., Goulding, M., and Turner, E. E. (2005). Brn3a-expressing retinal ganglion cells project specifically to thalamocortical and collicular visual pathways. *J. Neurosci.* 25, 11595–11604.

Sanes, J. R., and Lichtman, J. W. (1999). Development of the vertebrate neuromuscular junction. *Annu. Rev. Neurosci.* 22, 389–442.

Sanes, J. R., and Yamagata, M. (2009). Many paths to synaptic specificity. *Annu. Rev. Cell Dev. Biol.* 25, 161–195.

Sanes, J. R., and Zipursky, S. L. (2010). Design principles of insect and vertebrate visual systems. *Neuron* 66, 15–36.

Shen, K., and Cowan, C. W. (2010). Guidance molecules in synapse formation and plasticity. *Cold Spring Harb. Perspect. Biol.* 2, a001842.

Sherman, S. M. (2004). Interneurons and triadic circuitry of the thalamus. *Trends Neurosci.* 27, 670–675.

Sherman, S. M., and Guillery, R. W. (2002). The role of the thalamus in the flow of information to the cortex. *Philos. Trans. R. Soc. Lond. B Biol. Sci.* 357, 1695–1708.

Stevens, B., Allen, N. J., Vazquez, L. E., Howell, G. R., Christopherson, K. S., Nouri, N., Micheva, K. D., Mehalow, A. K., Huberman, A. D., Stafford, B., Sher, A., Litke, A. M., Lambris, J. D., Smith, S. J., John, S. W., and Barres, B. A. (2007). The classical complement cascade mediates CNS synapse elimination. *Cell* 131, 1164–1178.

Su, J., Gorse, K., Ramirez, F., and Fox, M. A. (2010). Collagen XIX is expressed by interneurons and contributes to the formation of hippocampal synapses. *J. Comp. Neurol.* 518, 229–253.

Su, J., Haner, C. V., Imbery, T. E., Brooks, J. M., Morhardt, D. R., Gorse, K., Guido, W., and Fox, M. A. (2011). Reelin is required for class-specific retinogeniculate targeting. *J. Neurosci.* 31, 575–586.

Terauchi, A., Johnson-Venkatesh, E. M., Toth, A. B., Javed, D., Sutton, M. A., and Umemori, H. (2010). Distinct FGFs promote differentiation of excitatory and inhibitory synapses. *Nature* 465, 783–787.

Terauchi, A., and Umemori, H. (2011). Specific sets of intrinsic and extrinsic factors drive excitatory and inhibitory circuit formation. *Neuroscientist.* PMID: 21652588. [Epub ahead of print].

Umemori, H. (2009). Weaving the neuronal net with target-derived fibroblast growth factors. *Dev. Growth Differ.* 51, 263–270.

Umemori, H., Linhoff, M. W., Ornitz, D. M., and Sanes, J. R. (2004). FGF22 and its close relatives are presynaptic organizing molecules in the mammalian brain. *Cell* 118, 257–270.

Van Horn, S. C., Erisir, A., and Sherman, S. M. (2000). Relative distribution of synapses in the A-laminae of the lateral geniculate nucleus of the cat. *J. Comp. Neurol.* 416, 509–520.

Waites, C. L., Craig, A. M., and Garner, C. C. (2005). Mechanisms of vertebrate synaptogenesis. *Annu. Rev. Neurosci.* 28, 251–274.

Wyatt, R. M., and Balice-Gordon, R. J. (2003). Activity-dependent elimination of neuromuscular synapses. *J. Neurocytol.* 32, 777–794.

Yamagata, M., and Sanes, J. R. (2008). Dscam and Sidekick proteins direct lamina-specific synaptic connections in vertebrate retina. *Nature* 451, 465–469.

Yamagata, M., Sanes, J. R., and Weiner, J. A. (2003). Synaptic adhesion molecules. *Curr. Opin. Cell Biol.* 15, 621–632.

Yamagata, M., Weiner, J. A., and Sanes, J. R. (2002). Sidekicks: synaptic adhesion molecules that promote lamina-specific connectivity in the retina. *Cell* 110, 649–660.

Yuge, K., Kataoka, A., Yoshida, A. C., Itoh, D., Aggarwal, M., Mori, S., Blackshaw, S., and Shimogori, T. (2011). Region-specific gene expression in early postnatal mouse thalamus. *J. Comp. Neurol.* 519, 544–561.

Zhang, X., Ibrahimi, O. A., Olsen, S. K., Umemori, H., Mohammadi, M., and Ornitz, D. M. (2006). Receptor specificity of the fibroblast growth factor family. The complete mammalian FGF family. *J. Biol. Chem.* 281, 15694–15700.

Conflict of Interest Statement: The authors declare that the research was conducted in the absence of any commercial or financial relationships that could be construed as a potential conflict of interest.

Received: 04 November 2011; accepted: 23 December 2011; published online: 10 January 2012.

Citation: Singh R, Su J, Brooks J, Terauchi A, Umemori H and Fox MA (2012) Fibroblast growth factor 22 contributes to the development of retinal nerve terminals in the dorsal lateral geniculate nucleus. Front. Mol. Neurosci. ***4****:61. doi: 10.3389/fnmol.2011.00061*

frontiers in
MOLECULAR NEUROSCIENCE

REVIEW ARTICLE
published: 15 February 2012
doi: 10.3389/fnmol.2012.00012

Presynaptic active zone density during development and synaptic plasticity

Gwenaëlle L. Clarke†, Jie Chen† and Hiroshi Nishimune*

Department of Anatomy and Cell Biology, University of Kansas Medical School, Kansas City, KS, USA

Edited by:
Robert W. Burgess, The Jackson Laboratory, USA

Reviewed by:
Aaron DiAntonio, Washington University, USA
Kevin Seburn, The Jackson Laboratory, USA

***Correspondence:**
Hiroshi Nishimune, Department of Anatomy and Cell Biology, University of Kansas Medical School, 3901 Rainbow Blvd., MS 3051, HLSIC Room 2073, Kansas City, KS 66160, USA.
e-mail: hnishimune@kumc.edu

†Gwenaëlle L. Clarke and Jie Chen have contributed equally to this work.

Neural circuits transmit information through synapses, and the efficiency of synaptic transmission is closely related to the density of presynaptic active zones, where synaptic vesicles are released. The goal of this review is to highlight recent insights into the molecular mechanisms that control the number of active zones per presynaptic terminal (active zone density) during developmental and stimulus-dependent changes in synaptic efficacy. At the neuromuscular junctions (NMJs), the active zone density is preserved across species, remains constant during development, and is the same between synapses with different activities. However, the NMJ active zones are not always stable, as exemplified by the change in active zone density during acute experimental manipulation or as a result of aging. Therefore, a mechanism must exist to maintain its density. In the central nervous system (CNS), active zones have restricted maximal size, exist in multiple numbers in larger presynaptic terminals, and maintain a constant density during development. These findings suggest that active zone density in the CNS is also controlled. However, in contrast to the NMJ, active zone density in the CNS can also be increased, as observed in hippocampal synapses in response to synaptic plasticity. Although the numbers of known active zone proteins and protein interactions have increased, less is known about the mechanism that controls the number or spacing of active zones. The following molecules are known to control active zone density and will be discussed herein: extracellular matrix laminins and voltage-dependent calcium channels, amyloid precursor proteins, the small GTPase Rab3, an endocytosis mechanism including synaptojanin, cytoskeleton protein spectrins and β-adducin, and a presynaptic web including spectrins. The molecular mechanisms that organize the active zone density are just beginning to be elucidated.

Keywords: bassoon, calcium channel, laminin, Rim1, spectrin, Rab3, Unc-51, synaptojanin

INTRODUCTION

Active zones were identified by electron microscopy as the electron dense thickening of the presynaptic where synaptic vesicles accumulate and dock and the area apposing the postsynaptic specialization (Couteaux and Pecot-Dechavassine, 1970; Hirokawa and Heuser, 1982; Harlow et al., 2001; Nagwaney et al., 2009). The active zone is the synaptic vesicle release site (Couteaux and Pecot-Dechavassine, 1970; Heuser et al., 1979), and thus, the density of presynaptic active zones is closely related to the efficiency of synaptic transmission (Propst and Ko, 1987). Therefore, the number, size, and distribution of active zones have a profound effect on how information is processed in a neuronal circuit and how the circuit adapts in response to various internal or external cues. In spite of the central role of active zones in synaptic transmission, it is still largely unknown how the number and density of the active zones within a presynaptic terminal are regulated during the development and maturation of synapses or during changes related to synaptic plasticity. The goal of this review is to highlight recent insights into the organization of active zone density and number within a single synaptic terminal or a synaptic bouton and the molecular mechanisms that control the density of active zones during development and synaptic plasticity. The emerging hypothesis from these data is that the active zone density is maintained during the developmental growth of synapses in the central and peripheral nervous systems by molecular mechanisms that do not require neuronal activity. However, active zone density does change in the plastic synapses of the central nervous system (CNS) during stimulus-dependent changes in synaptic efficacy. The analysis of the active zone density within an axon making *en passant* synapses in *C. elegans* has revealed important molecular mechanisms for active zone formation, which have been reviewed in detail elsewhere (Jin, 2005).

THE DEFINITION OF ACTIVE ZONES DETECTED WITH DIFFERENT ANALYSIS METHODS

Active zones have been analyzed using several different techniques, each of which yields a slightly different appearance. We will first review these detection methods and the definition of active zones based on each method. Transmission electron microscopy was first used to describe the active zones in frog neuromuscular junctions (NMJs) as thickened presynaptic membranes containing electron dense material that align with the postsynaptic junctional folds and fuse with synaptic vesicles (Couteaux and Pecot-Dechavassine, 1970). The active zones possess triangular

electron dense projections that extend from the presynaptic membrane into the cytosol in transmission electron micrographs of frogs and rodents (Couteaux and Pecot-Dechavassine, 1970; Hirokawa and Heuser, 1982; Nishimune et al., 2004; Rowley et al., 2007). The three-dimensional reconstruction of serially sectioned transmission electron micrographs shows the discrete locations of active zones scattered in the presynaptic terminal of rat NMJs (Rowley et al., 2007). At *Drosophila* NMJs, active zones detected by transmission electron micrographs show an electron dense thickening of the presynaptic membrane with electron dense projections called T-bars that extend from the presynaptic membrane into the cytosol (Zhai and Bellen, 2004). In some *Drosophila* analyses, active zones are referred to as the synapses, and the T-bars are referred to as the dense bodies. These ultrastructural analyses using transmission electron microscopy provided the basic definition of active zones.

Freeze-fracture electron microscopy revealed a higher resolution structure of the active zones from the interior of the cytosolic half of a plasma membrane (P-face). The NMJs exhibit parallel rows of large intramembranous particles on the P-face of presynaptic membranes in humans, mice, rats, and lizards (Ellisman et al., 1976; Fukunaga et al., 1982; Walrond and Reese, 1985; Fukuoka et al., 1987). Using this methodology, an active zone has been defined as a parallel array of 10–12 nm intramembranous particles arranged in four rows, with each active zone containing 20 of these intramembranous particles (Ellisman et al., 1976). However, the organization of these large intramembranous particles is different in frog NMJs compared to mammals. Freeze-fracture electron microscopy allowed for the detection of long parallel rows of large intramembranous particles on the P-face and exocytosis events adjacent to these particles in the frog NMJs (Heuser et al., 1974, 1979). A continuum of these intramembranous particles that nearly spans the width of the nerve branch is considered as one active zone in the frog NMJ (Ko, 1985). The size of the active zones correlates well with the quantal content at the frog NMJ (Propst and Ko, 1987). The active zones defined by these intramembranous particles are consistent with the active zones defined using transmission electron microscopy, and these findings are further supported by the tomography method.

Electron microscope tomography analysis revealed the presynaptic structures in frog NMJs (Harlow et al., 2001) and mouse NMJs (Nagwaney et al., 2009) in great detail. Macromolecules of active zone materials connect to each other, to the transmembrane peg-like structure (similar to the intramembranous particles detected by freeze-fracture electron microscopy), and to the docked synaptic vesicles at the active zones in the nerve terminals. These electron microscope tomography analyses suggested that the electron dense materials at the active zones detected by transmission electron microscopy and the intramembranous particles detected by the freeze-fracture electron microscopy are part of a large presynaptic protein complex at the active zones.

The ultrastructural analysis methods described above defined the active zone and revealed the high-resolution structure of the active zones. However, an analysis of the distribution pattern of all the active zones within one presynaptic terminal is difficult to obtain with the freeze-fracture and tomography methods and very laborious using the reconstruction of serially sectioned transmission electron micrographs. Needless to say, it becomes a challenge to analyze these parameters over a large number of presynaptic terminals or to analyze the protein composition of the active zones. The recent use of the presynaptic cytosolic protein Bassoon as a marker for active zones has allowed for the detection of active zones using fluorescent immunohistochemistry in the synapses of the central and peripheral nervous system (Nishimune et al., 2004; Dondzillo et al., 2010; Bednarek and Caroni, 2011; Chen et al., 2011a). Bassoon is a large cytosolic scaffolding protein, and its specific localization at the active zones of ribbon synapses and brain synapses was confirmed by immunoelectron microscopy (tom Dieck et al., 1998, 2005; Brandstatter et al., 1999; Richter et al., 1999; Zhang et al., 2000). Bassoon immunohistochemistry reveals a discrete and small punctate staining pattern in the presynaptic terminals, and these puncta are recognized as individual active zones. The definition of the active zones based on fluorescent immunohistochemistry is supported by the immunoelectron microscopy analysis described above and the similarities in the number and distribution pattern of the puncta detected by fluorescent immunohistochemistry and the active zones detected by electron microscopy in NMJs, the calyx of Held, and the ribbon synapses of photoreceptors (**Table 1**; Satzler et al., 2002; tom Dieck et al., 2005; Rowley et al., 2007; Dondzillo et al., 2010; Chen et al., 2011b). For example, the density of NMJ active zones detected by Bassoon immunohistochemistry is consistent with the active zone density detected by freeze-fracture electron microscopy (**Table 1**). Furthermore, the total number of puncta detected by immunohistochemistry against active zone proteins Bassoon and Piccolo in the rat calyx of Held is in accordance with the total number of active zones detected by the three-dimensional reconstruction of transmission electron micrographs (**Table 1**; Dondzillo et al., 2010). However, this analysis revealed that the active zones in the calyx of Held have different protein compositions, as shown by some non-overlapping puncta of Bassoon and Piccolo, and suggested that the active zones detected by immunohistochemistry methods must be carefully evaluated depending on the type of synapses to be analyzed. In spite of this, the immunohistochemistry-based active zone analysis is advantageous over electron microscopy in two ways: the ease of analyzing a large sample size and the protein composition of the active zones.

CONSTANT ACTIVE ZONE DENSITY AT THE NMJ

Active zone density is maintained at a constant level during development at the large synapses of the peripheral nervous system in mammals. Freeze-fracture electron microscopy has revealed that the active zone density is 2.4–2.7 active zones/μm^2 in mouse and human adult NMJs (Fukunaga et al., 1982, 1983; Fukuoka et al., 1987). The Bassoon immunohistochemistry allowed us to analyze the active zones within each presynaptic terminal over large numbers of mouse NMJs (Nishimune et al., 2004; Chen et al., 2011a). While the synapse size and the number of active zones in mouse NMJs increases by more than threefold during postnatal development between postnatal day 0 and 54, the density of the active zones remains constant at 2.3 active zones/μm^2 (Chen et al., 2011b). Importantly, the active zone densities measured using two different techniques and in two species make a

Table 1 | Active zone density.

Synapse	Species	Age	Synapse size [terminal volume (μm^3) or pre–post apposition area (μm^2)]	Active zone number per presynaptic terminal or per bouton	Active zone density (active zones/μm^2)	Detection method	Reference
Neuromuscular junction	Human	Adult	Not provided	Not provided	2.6/μm^2	Freeze-fracture electron microscopy	Fukunaga et al. (1982)
Neuromuscular junction	Mouse	Adult	Not provided	Not provided	2.5/μm^2	Freeze-fracture electron microscopy	Fukunaga et al. (1983)
Neuromuscular junction	Mouse	P48	295 μm^2	780	2.6/μm^2	Fluorescent immunohistochemistry	Chen et al. (2011a)
Calyx of Held	Cat	Adult	1450 μm^2 *	2400	1.7/μm^2 *	3D reconstruction of transmission electron micrograph	Rowland et al. (2000)
Calyx of Held	Rat	P9	1022 μm^2	554	0.54/μm^2 *	3D reconstruction of transmission electron micrograph	Satzler et al. (2002)
Calyx of Held	Rat	P9	655 μm^3	405	0.61/μm^3	Fluorescent immunohistochemistry	Dondzillo et al. (2010)
		P21	935 μm^3	601	0.64/μm^3 *		
Endbulb of Held	Rat	P25	Not provided	155	0.066 PSD/μm^2	3D reconstruction of transmission electron micrograph	Nicol and Walmsley (2002)
Large mossy fiber terminals of granule cells in the hippocampal CA3	Rat	P28	32.84 μm^2	29.75 per bouton	0.91/μm^2	3D reconstruction of transmission electron micrograph	Rollenhagen et al. (2007)
		Adult	22.07 μm^2	18.25 per bouton	0.83/μm^2 *		
Muscle spindle afferents onto lumbar motor neurons in the spinal cord	Cat	Not provided	6.8 μm^2	6.1 per bouton	0.90/μm^2 *	3D reconstruction of transmission electron micrograph	Pierce and Mendell (1993)
Synapse onto motor neurons in the cervical spinal cord	Turtle	Adult	1.46 μm^2	3–4 Active zones per terminal size larger than 2 μm^2	0.70/μm^2 *	3D reconstruction of transmission electron micrograph	Yeow and Peterson (1991)
GABAergic nigrothalamic terminals in the ventromedial nucleus	Monkey	Adult	2.91 μm^3	8.5	2.9/μm^3 *	3D reconstruction of immunoelectron micrograph	Bodor et al. (2008)
Anterior pretectal nucleus terminals in the posterior thalamic nucleus	Rat	P45-60	2.4 μm^3	7.6	3.2/μm^3 *	3D reconstruction of immunoelectron micrograph	Wanaverbecq et al. (2008)
GABAergic nigrothalamic terminals in the ventromedial nucleus	Rat	Adult	1.76 μm^3	8.5	4.8/μm^3 *	3D reconstruction of immunoelectron micrograph	Bodor et al. (2008)
Stratum radiatum in CA1 hippocampus	Mouse	Adult	0.086 μm^3	2–3 Active zones per bouton in 10% of the synapses	13/μm^3 *	3D reconstruction of transmission electron micrograph	Schikorski and Stevens (1997)

Calculated from data in the papers.

compelling argument that the active zones of mammalian NMJs are maintained at 2.3–2.7 active zones/μm^2.

The developmental analysis of active zone formation has also been reported for the frog NMJ using freeze-fracture electron microscopy (Ko, 1985). In spite of the structural differences in these active zones compared to mammals, the number of elongated active zones per postsynaptic junctional fold remains relatively constant at approximately 1.5 active zones per junctional fold throughout development until adulthood (Ko, 1985).

The maintenance of a constant active zone density at synapses as they increase in size is potentially advantageous for synaptic transmission. In the presynaptic terminal, a regulated distance between active zones ensures their access to synaptic vesicles and Ca^{2+} buffering systems (Llinas et al., 1992; Neher, 1998). In the synaptic cleft, the local concentration of the neurotransmitter will be kept under a certain level by the constant density of active zones, which aids the effective clearance of neurotransmitters (Massoulie and Bon, 1982). On the postsynaptic side, the density of neurotransmitter receptors can be maintained at a constant level during developmental increases in the synapse size, for example, to secure the safety factor of neurotransmission at NMJs (Kelly, 1978). These advantages support the significance of maintaining the active zone density for the efficacy of synaptic transmission.

SYNAPTIC ACTIVITY AND ACTIVE ZONE DENSITY AT THE NMJ

Does synaptic activity modify the active zone density at NMJs? During development, muscle fibers acquire slow or fast fiber type characteristics (Narusawa et al., 1987; Condon et al., 1990). The NMJs of these two fiber types differ in morphology and size, and the fast fiber type tends to have a larger NMJ (Prakash et al., 1996; Chakkalakal et al., 2010). Motor neurons innervating these fiber types can be classified into subtypes based on the contractile properties of the motor units (Burke et al., 1973; Kanning et al., 2010). These fast and slow motor neurons have different firing rates and durations of post-spike hyperpolarization (Gardiner, 1993; Lee and Heckman, 1998a,b). In spite of these activity differences, the active zone density analyzed by the three-dimensional reconstruction of transmission electron micrographs is similar between the NMJs of fast and slow muscle fiber types (Rowley et al., 2007).

An extreme case of synaptic activity difference can be observed in mice lacking the neurotransmitter acetylcholine. Choline acetyltransferase knockout mice (*Chat*$^{-/-}$) cannot synthesize acetylcholine and show no synaptic transmission at NMJs but exhibit a normal number of NMJ active zones when quantified using transmission electron micrographs (Misgeld et al., 2002). This result suggests that the active zone density at embryonic mouse NMJs is independent of the synaptic activity. Just as reduced (or no) synaptic activity has little effect on the number of active zones, enhanced synaptic transmission does not appear to affect active zone formation either. Knockout mice for the collagenous subunit of acetylcholinesterase, ColQ, exhibited no acetylcholinesterase activity at NMJs and showed elongated miniature endplate potential (mEPP) amplitude (Feng et al., 1999). Although the active zone density was not quantified, the knockout mice showed normal active zones with synaptic vesicles in transmission electron micrographs. Similarly, knockout mice for acetylcholinesterase also exhibited ultrastructurally normal NMJs in transmission electron micrographs (Xie et al., 2000). These results suggest that the active zone density at NMJs is independent of the synaptic activity. This contrasts with the role of synaptic activity in synapse elimination and the postsynaptic differentiation of NMJs (Lichtman et al., 1985; Buffelli et al., 2003; Lin et al., 2005; Misgeld et al., 2005).

Analysis using the three-dimensional reconstruction of transmission electron micrographs shows that the active zone density of *Drosophila* NMJs is also maintained in a homeostatic manner even after manipulations to augment or attenuate synaptic efficiency (Meinertzhagen et al., 1998; Reiff et al., 2002). For example, synaptic transmission at *Drosophila* larvae NMJs is strengthened by an elevated DGluR-IIA accumulation at NMJs, either by overexpressing DGluR-IIA or by the induction of DGluR-IIA in heterozygotes of the translation–initiation factor poly(A)-binding protein (*pabp*; Sigrist et al., 2002). However, the density of the T-bar remains similar to that of the wild-type NMJ level when analyzed by the three-dimensional reconstruction of transmission electron micrographs (Sigrist et al., 2002). This study suggests that the number of T-bars is proportional to the *Drosophila* NMJ size. Similarly, the puncta size and the distribution pattern of the active zone marker Bruchpilot in NMJs detected by fluorescent immunohistochemistry are indistinguishable between wild-type and mutant *Drosophila* with increased neuronal activity via the expression of the dominant negative Shaker, with reduced neuronal activity due to decreased sodium channel expression, or with decreased transmitter release in the *unc-18* mutant (Graf et al., 2009). In summary, the active zone densities of mouse and *Drosophila* NMJs are not affected by synaptic activity and are maintained at a constant level.

ACTIVE ZONE DENSITY DURING AGING AND IN DISEASES

Although the density of active zones is kept constant at NMJs during developmental growth and altered synaptic activity, the active zone is not a stable structure during the normal aging process and some pathological disorders. These conditions cause some active zones to be depleted, which results in a defect in neurotransmission. Aged NMJs demonstrate many morphological alterations, including partial or complete withdrawal of the axons from some postsynaptic sites (Fahim and Robbins, 1982; Banker et al., 1983; Balice-Gordon, 1997; Valdez et al., 2010). However, in fully innervated, aged NMJs, the active zone density detected by Bassoon immunohistochemistry was decreased compared to young adult mice (Chen et al., 2011b). This is consistent with the attenuated mEPP frequency observed at the NMJs of aged mice and rats (Gutmann et al., 1971; Banker et al., 1983; Alshuaib and Fahim, 1991; Fahim, 1997). Thus, active zone density decreases and synaptic transmission weakens at aged NMJs, which may lead to their denervation.

Reduced active zone density at the NMJ was also observed in pathological conditions such as Lambert–Eaton myasthenia syndrome (LEMS) and Pierson's syndrome. LEMS, an autoimmune disease caused by anti-calcium channel autoantibodies, is characterized by a decreased quantal release of acetylcholine from the presynaptic terminal of NMJs (Eaton and Lambert, 1957; Elmqvist and Lambert, 1968; Lambert and Elmqvist, 1971; Kim and Neher, 1988). Freeze-fracture electron microscopy revealed a marked decrease in the active zone density in the NMJs of

patients with LEMS (Fukunaga et al., 1982). The passive transfer of patient IgG to mice caused LEMS-like electrophysiological changes with reduced active zone numbers at the NMJ as detected by freeze-fracture electron microscopy (Fukunaga et al., 1983; Fukuoka et al., 1987; Nagel et al., 1988). In addition to LEMS, active zone deficiency is also found in another myasthenic disease called Pierson's syndrome. Pierson's syndrome is a newly defined congenital disease caused by mutations in the laminin β2 gene (Zenker et al., 2004a,b; Mark et al., 2006). A decreased number of active zones were confirmed by transmission electron microscopy in the muscle biopsies from patients as well as laminin β2 knockout mice (Noakes et al., 1995; Nishimune et al., 2004; Maselli et al., 2009). Attenuated active zones may partially account for the reduced mEPP frequency and the EPP quantal content in this disease (Maselli et al., 2009). LEMS and Pierson's syndrome may not be the only two neurological diseases that show active zone abnormalities. Gerstmann–Sträussler–Scheinker (GSS) syndrome is one type of fetal prion disease that causes prominent neurodegeneration in the cerebellum and cerebral cortex (Ghetti et al., 1995; Mead, 2006). In a *Drosophila* model of GSS syndrome, the amount of the active zone protein Bruchpilot was significantly reduced, indicating that an active zone deficiency may be involved in the progress of this disease (Choi et al., 2010). However, it is currently unclear whether patients with GSS syndrome show this active zone deficiency or not. The lack of symptom information may be partially due to the requirement of electron microscopy for active zone detection in the past. The recent discovery of an immunofluorescent labeling of active zone proteins should enable the evaluation of the active zone structure in these neurological diseases in a fast and accurate way (Nishimune et al., 2004; Dondzillo et al., 2010; Bednarek and Caroni, 2011; Chen et al., 2011b). Active zones play an essential role in neurotransmission; thus, a deeper knowledge of active zone changes will definitely enhance the understanding of the pathogenesis of these diseases. Although active zone density has a remarkable ability to remain constant, some factors, such as aging and disease, alter its stability.

ACTIVE ZONE DENSITY IN THE CNS

Is the active zone density of CNS synapses organized similarly to the NMJ active zones? Partly due to the small size of CNS synapses, many CNS presynaptic terminals possess only one active zone. When analyzed using the three-dimensional reconstruction of transmission electron micrographs, 90% of the presynaptic boutons exhibit only a single active zone at the synapses within the stratum radiatum in the CA1 region of the mouse hippocampus (Schikorski and Stevens, 1997). Similarly, the active zones on cerebellar climbing fibers and parallel fibers are located in distinct boutons, and each bouton typically has one active zone (defined by the apposing synaptic vesicle cluster and postsynaptic density; Xu-Friedman et al., 2001).

However, many large CNS synapses exhibit multiple active zones per presynaptic terminal in three-dimensional reconstructions of transmission electron micrographs (**Table 1**). For example, in the auditory brain stem, the calyxes of Held in rats and cats have 405–2400 active zones per nerve terminal (Rowland et al., 2000; Satzler et al., 2002), and the rat endbulb of Held has an average of 155 active zones per endbulb (Nicol and Walmsley, 2002). The large mossy fiber terminals of granule cells in the stratum lucidum of the adult rat hippocampal CA3 region has an average of 18 active zones per bouton (Rollenhagen et al., 2007), and some synapses in the stratum radiatum in the CA1 region of the adult mouse hippocampus have two to three active zones per bouton (Schikorski and Stevens, 1997). Rat and monkey GABAergic nigrothalamic terminals in the ventromedial nucleus have an average of 8.5 active zones per large dendrite (Bodor et al., 2008). In the posterior thalamic nucleus of rats, the nucleus reticularis thalami terminals have an average of two active zones per terminal, while inputs from the anterior pretectal nucleus have an average of 7.6 active zones (Wanaverbecq et al., 2008). Large presynaptic terminals synapsing onto motor neurons in the spinal cord of cats and turtles (Yeow and Peterson, 1991; Pierce and Mendell, 1993) and some parallel fiber synapses onto cerebellar Purkinje cells in young rats (Xu-Friedman et al., 2001) have more than one active zone per bouton. These variations in active zone number suggest a mechanism for accommodating the active zone number to the synapse size.

Indeed, the maintenance of active zone density can be observed during the development of the calyx of Held in the auditory brainstem, which is one of the largest synapse in the CNS. Between postnatal day 9 and 21, the size of the rat calyx of Held increases 1.4-fold; however, the density of the active zones remains constant at approximately 0.6 active zones per unit calyx size (μm^3) when analyzed by fluorescent immunohistochemistry using Bassoon and Piccolo antibodies (Dondzillo et al., 2010). These results suggest that the active zone density is maintained during the development of this CNS synapse, similar to the NMJs.

The control of active zone density can also be observed in the spinal cord. Synapses on the motor neuron cell body in the spinal cord were analyzed in detail using the three-dimensional reconstruction of transmission electron micrographs (Yeow and Peterson, 1991; Pierce and Mendell, 1993). These analyses revealed a few interesting characteristics of CNS active zones. First, the size of individual active zones rarely exceeded $0.4\,\mu m^2$, suggesting that active zones have a limited size for proper function. Second, synapses with larger apposition areas of presynaptic and postsynaptic membranes have two or more discrete regions of active zones within a single synapse, demonstrating a correlation between the active zone number and bouton size (Yeow and Peterson, 1991). Consistently, the total area of the active zones within a single presynaptic terminal is correlated with the bouton volume in a linear fashion (Yeow and Peterson, 1991; Pierce and Mendell, 1993). These observations suggest that the active zone density of this CNS synapse is also controlled.

Hippocampal synapses also show some control of active zone density. At the synapses within the stratum radiatum in the CA1 region of the mouse hippocampus, 8% have two active zones, and 2% have three active zones based on the three-dimensional reconstruction of serial transmission electron micrographs (Schikorski and Stevens, 1997). These multiple active zones within a single presynaptic bouton contact different postsynaptic spines. The size of the active zones is matched closely by the postsynaptic density area. Importantly, the active zone area size, which averages $0.039\,\mu m^2$ in the hippocampal CA1 region, was linearly related to

the volume of the presynaptic bouton, suggesting a regulation of active zone density at these hippocampal synapses.

However, while the CNS synapses show controlled active zone density, some hippocampal synapses also show changes in active zone density. The active zones in the hippocampal mossy fiber boutons of adult rats possess on average 18 active zones when analyzed using the three-dimensional reconstruction of transmission electron micrographs (Rollenhagen et al., 2007). These active zones maintained approximately 10% of the pre- and postsynaptic apposition area during development from postnatal day 28 to 3–4 months of age, suggesting that there is also some control of active zone density in this synapse (Rollenhagen et al., 2007). The detection of multiple active zones within a large mossy fiber terminal in the stratum lucidum of the hippocampal CA3 region is also supported by Bassoon immunohistochemical analysis (Bednarek and Caroni, 2011). The density of these active zones was studied in mice housed in an enriched environment, which is known to enhance learning and memory (Nithianantharajah and Hannan, 2006). Thus, changes in synaptic transmission efficiency are expected in the hippocampus. Consistent with this hypothesis, mice housed in an enriched environment for 2 weeks showed increased morphological complexity of the large mossy fiber terminals. Interestingly, the active zone density remained constant during this period. These observations suggest that active zone density is maintained to some degree even in the hippocampal synapses showing plasticity. However, housing mice in the enriched environment for 4 weeks did increase the density of active zones in the large mossy fiber terminals, suggesting a further modification of presynaptic function (Bednarek and Caroni, 2011). In summary, the examples shown in this section suggest that the density of active zones is controlled in CNS synapses of various sizes, but in contrast to NMJs, some of these synapses show plasticity in the density of active zones.

MOLECULAR CONSTITUENTS OF ACTIVE ZONES AND MECHANISMS OF ACTIVE ZONE FORMATION

Recently, the molecular identities of active zone-specific proteins and the protein interactions essential for the formation of active zones have been increasingly revealed. The constituents of active zones in vertebrate synapses are called the cytoskeletal matrix of the active zone (Dresbach et al., 2001) and includes Bassoon (tom Dieck et al., 1998), CAST/ELKS/Erc family proteins (Ohtsuka et al., 2002; Wang et al., 2002; Deguchi-Tawarada et al., 2004), Munc13 (Brose et al., 1995; Betz et al., 1998), Piccolo (Cases-Langhoff et al., 1996), and RIM1/2 (Wang et al., 1997). *Drosophila* active zones contain a member of the ELKS/Rab6IP2/CAST/Erc family of proteins called Bruchpilot (Kittel et al., 2006; Wagh et al., 2006), and *C. elegans* active zones contain SYD-2 (Yeh et al., 2009). Active zone proteins form a large protein complex by binding to each other (Wang et al., 2002, 2009a; Deguchi-Tawarada et al., 2004; Takao-Rikitsu et al., 2004; Dulubova et al., 2005; Ohara-Imaizumi et al., 2005). In addition, these proteins are tethered to the membrane by binding to presynaptic voltage-dependent calcium channels (VDCCs) on the cytosolic side (Coppola et al., 2001; Shibasaki et al., 2004; Kiyonaka et al., 2007; Fouquet et al., 2009; Uriu et al., 2010; Chen et al., 2011a; Kaeser et al., 2011; Billings et al., 2012). Some of these protein complexes are anchored to the presynaptic membrane by the extracellular interactions between VDCCs and synapse organizers (Nishimune et al., 2004; Chen et al., 2011a).

Interestingly, an analysis of knockout mice lacking active zone-specific proteins revealed mostly a reduction in the number of docked synaptic vesicles, but no change in the number of active zones. For example, Rim1/2 knockout mice show a decrease in the number of docked synaptic vesicles and the density of presynaptic VDCCs in the calyx of Held, but the size of the active zones (defined by the postsynaptic density size) was not altered in the three-dimensional reconstruction of transmission electron micrographs (Han et al., 2011). Similarly, the roles of Bassoon and Piccolo in synaptic vesicle clustering at the active zones were demonstrated in the analyses of the CNS and sensory synapses in the single knockout mice for Bassoon or Piccolo as well as the double mutant mice with a Piccolo knockout combined with a Bassoon knockdown (Altrock et al., 2003; Dick et al., 2003; Specht et al., 2007; Angenstein et al., 2008; Buran et al., 2010; Goetze et al., 2010; Hallermann et al., 2010; Lanore et al., 2010; Mukherjee et al., 2010). However, ELKS2a/CAST knockout mice exhibit a normal number of docked synaptic vesicles and synapse ultrastructural morphology in the hippocampal CA1 region analyzed by transmission electron microscopy (Kaeser et al., 2009). Interestingly, the ELKS2a/CAST deletion causes an increase in inhibitory neurotransmitter release and exploratory behaviors, suggesting some alteration of active zones. Meanwhile, in the *Drosophila* Bruchpilot mutant, the electron dense projection at the active zone (T-bar) is completely missing in NMJs analyzed by transmission electron microscopy (Kittel et al., 2006; Fouquet et al., 2009). Furthermore, in the Bruchpilot mutant, the density of presynaptic VDCCs is normal at the nascent synapse (active zone) but lower in the more mature synapse (active zone). The Bruchpilot mutant may have a normal density of active zones (defined by the thick presynaptic membrane in transmission electron micrographs), but normal active zones with VDCCs and T-bars are less numerous than in controls when the NMJs mature without Bruchpilot. These defects cause a reduction in the evoked excitatory junctional current amplitudes and quantal content (Kittel et al., 2006).

Although the regulatory mechanism for active zone density is largely unknown, the molecular mechanisms leading to active zone formation have been extensively studied and are reviewed in detail elsewhere (Broadie and Richmond, 2002; Rosenmund et al., 2003; Jin, 2005; Prescott and Zenisek, 2005; Fejtova and Gundelfinger, 2006; Collins and DiAntonio, 2007; Stryker and Johnson, 2007; Jin and Garner, 2008; Owald and Sigrist, 2009; Sigrist and Schmitz, 2010; Wichmann and Sigrist, 2010; Nishimune, 2011a,b).

MOLECULAR MECHANISMS FOR CONTROLLING ACTIVE ZONE DENSITY

In contrast to the increasing knowledge of active zone formation, less is known about the molecular mechanism that controls the density of active zones. One potential mechanism for controlling active zone density is the role of synapse organizers expressed by the postsynaptic cell. At vertebrate NMJs, the muscle-derived synapse-organizer laminin β2 and presynaptic P/Q-type VDCCs bind extracellularly and organize the active zones (Nishimune et al., 2004). On the cytosolic side of the presynaptic P/Q-type VDCCs, the VDCC β subunits bind to Bassoon

and CAST, demonstrating a mechanism that links an extracellular synapse organizer to the active zone proteins through VDCC subunit complexes (Chen et al., 2011a). The active zone density and the docked synaptic vesicle number are significantly decreased at the NMJs of laminin β2 knockout mice, P/Q-type or N-type VDCC (α subunit) knockout mice, and P/Q- and N-type VDCC double knockout mice when analyzed by transmission electron microscopy or Bassoon immunohistochemistry (Noakes et al., 1995; Nishimune et al., 2004; Chen et al., 2011a). The laminin β2 subunit forms a multimeric complex with the laminin α4 subunit, which is also concentrated specifically at the NMJs (Patton, 2000). The concentration of laminin α4 in the synaptic cleft is lower near the active zones and higher between the active zones (Patton et al., 2001). Importantly, laminin α4 knockout mice exhibit mislocalization of the active zones at NMJs without a change in the total number of active zones in transmission electron micrographs (Patton et al., 2001). These results suggest that laminin α4 controls the location of active zones and laminin β2 controls the density of active zones in mouse NMJs.

Another synapse organizer at the NMJs that potentially determines active zone density is amyloid precursor protein (APP). APP is involved in the pathogenesis of Alzheimer's disease but has also been shown to accumulate at the NMJs (Schubert et al., 1991; Akaaboune et al., 2000). Double knockout mice for APP and its homolog, APP-like protein 2, exhibit decreased active zone density and synaptic vesicle density but a normal number of docked synaptic vesicles in NMJ profiles of transmission electron micrographs (Wang et al., 2005). Consistent with these defects, mEPP frequency was decreased in the double knockout mice. The conditional deletion in muscle suggests a postsynaptic requirement of APP and/or APP-like protein 2 for the presynaptic differentiation of NMJs (Wang et al., 2009b). These results demonstrate the synaptogenic or synapse maintenance role of APP at the NMJ (Wang et al., 2009b), but the decreased density of active zones in the double knockout mice for APP and APP-like protein 2 awaits further study to distinguish between a primary and secondary phenotype because this mutant shows widespread defects of presynaptic differentiation.

In addition to the extracellular synapse organizers, cytosolic synaptic proteins also have roles in controlling active zone density. In *Drosophila*, the number and spacing of NMJ active zones are controlled by the inositol phosphatase synaptojanin, skeleton β-spectrin, the GTPase Rab3, and the threonine kinase Unc-51 (Dickman et al., 2006; Pielage et al., 2006; Graf et al., 2009; Wairkar et al., 2009). Synaptojanin functions at endocytic sites to promote synaptic vesicle uncoating (Verstreken et al., 2003). *Drosophila* NMJs of synaptojanin mutants show an increased density of active zones in exchange for the decreased size of each active zone, which was revealed by the three-dimensional reconstruction of transmission electron micrographs (Dickman et al., 2006). In wild-type NMJs, most active zones have one dense body (T-bar), but there was more than one dense body per active zone in the synaptojanin mutants, sometimes as many as three. This study suggests that the endocytosis mechanism plays a role in defining the density of active zones. In vertebrates, synaptojanin knockout mice have been generated, but the phenotype of the active zones remains unknown in these mutants (Cremona et al., 1999; Kim et al., 2002).

Cytosolic signaling mechanisms for controlling active zone density are starting to emerge. In the *Drosophila* mutant of the serine threonine kinase Unc-51, the density of active zones or T-bars is significantly reduced in transmission electron micrographs (Wairkar et al., 2009). Consistent with the reduced active zone density, the extrajunctional potential and quantal content are reduced in this mutant. Unc-51 inhibits the activity of the MAP kinase ERK *in vivo* and thus, the increased ERK activity in the *unc-51* mutant is thought to cause the absence of the active zone protein Bruchpilot at NMJs. Consistent with this hypothesis, an ERK hypomorph can rescue the reduced active zone density, but not the synapse size, in the *unc-51* mutant (Wairkar et al., 2009). These results suggest that the Unc-51-ERK signaling pathway negatively controls active zone density and that the reduction of active zone density is not caused by the small synapse phenotype in the *unc-51* mutant.

Small GTPases seem to control the number of active zones and the protein composition of active zones in *Drosophila* NMJs. In the *Drosophila* GTPase Rab3 loss-of-function mutant, the NMJs have many postsynaptic glutamate receptors without any colocalization of the presynaptic active zone protein Bruchpilot (Graf et al., 2009). A transmission electron microscopy analysis revealed that the density of the active zones with T-bars also decreases in this *rab3* mutant, whereas the number of active zones with multiple T-Bars increases, suggesting a redistribution of the active zone components. Interestingly, this phenotype can be rescued by transgenically expressing *rab3* for 24 h, suggesting that *rab3* can dynamically regulate the density of active zone components in *Drosophila* NMJs (Graf et al., 2009). However, *rab3abcd* quadruple knockout mice did not exhibit an active zone phenotype in transmission electron micrographs (Schluter et al., 2004), suggesting that the intracellular mechanism controlling active zone density is different between *Drosophila* and mice. A quantitative ultrastructure analysis of the *rab3abcd* quadruple knockout synapse is needed to confirm this hypothesis.

Similar to *Drosophila* NMJs, rapid modification of the NMJ active zones also take place in mouse NMJs. Their density decreases by acutely inhibiting the signaling between laminin β2 and P/Q-type VDCCs for 48 h *in vivo* when analyzed by transmission electron microscopy (Nishimune et al., 2004). Similarly, at the frog NMJ active zones, the parallel rows of intramembranous particles become distorted by transiently reducing the extracellular calcium concentration for 3 h, which was revealed by freeze-fracture electron microscopy (Meriney et al., 1996). These analyses in three species suggest that NMJ active zones are not a rigid structure and can be reorganized within few days.

The cytoskeletal network also plays a role in controlling the active zone density. In *Drosophila* NMJs, the RNAi-mediated elimination of β-spectrin in postsynaptic muscles increases the size of presynaptic active zone as analyzed by transmission electron microscopy and the number of presynaptic Bruchpilot puncta per postsynaptic GluR cluster as analyzed by fluorescent immunohistochemistry (Pielage et al., 2006). The distribution pattern and the density of Bruchpilot in the presynaptic terminal were also altered by the reduction of postsynaptic β-spectrin, suggesting that a retrograde signal from the muscles to the motor nerve terminals controls the active zone density. It is currently unknown whether the molecular mechanism that controls the active zone density

at the NMJs also functions in CNS synapses. In the rodent CNS, the active zones are supported by a structure called the presynaptic web, which includes spectrins (Phillips et al., 2001). This structure was identified from the electron microscopic observation of the purified synaptic membranes in the synaptosomal fraction. The βIII spectrin knockout mice showed impaired synaptogenesis in the cerebellum with ataxic and seizure phenotypes, but the NMJ phenotype remains unknown (Stankewich et al., 2010). As previously mentioned in this review, the formation of new synapses and the increase in active zone density are dependent on β-adducin, a spectrin interacting molecule, in the mouse hippocampus (Bednarek and Caroni, 2011). Taken together, the spectrin skeleton is likely to play a role in defining the density of active zones in vertebrate CNS synapses and NMJs.

PERSPECTIVE

In this review, we focused on the morphological analyses of active zone density and the molecular mechanisms that control active zone density. Interestingly, the transmitter release properties of active zones within a single presynaptic terminal are not equal. For example, the active zones within one presynaptic terminal of an NMJ have independent release probabilities, which can be deduced by the heterogeneity of the synaptic vesicle released from different active zones (Bennett and Lavidis, 1989; Wyatt and Balice-Gordon, 2008; Luo et al., 2011; Peled and Isacoff, 2011). This heterogeneity of active zone function has been studied in frog, mouse, and *Drosophila* NMJs, suggesting that it is a common phenomenon across species. Similarly, the variability of neurotransmitter release probability within one axon has been studied at CNS synapses and has been reviewed elsewhere (Pelkey and McBain, 2007; Branco and Staras, 2009). However, the molecular mechanism behind these independent controls of release probability within one presynaptic terminal is not fully understood. How do the mechanism regulating the active zone density and the mechanism controlling the independent release probability cooperate within one presynaptic terminal? Do the density of active zone and the release probability map change cooperatively or independently beyond the steady level during development, plasticity, aging, and pathological conditions in a given presynaptic terminal? The molecular analysis of active zone density together with the physiological analyses of active zones is needed to elucidate the function of active zones in synaptic transmission.

In summary, the density of active zones affects the efficiency of synaptic transmission and is thus likely to play an essential role in the neural circuit formation. During the formation and maturation of synapses and in some stable mature synapses, the active zone density is likely to be maintained by genetic mechanisms rather than neuronal activity-related mechanisms. However, some CNS synapses can alter the density of active zones beyond this maintenance mechanism. In plastic synapses of the hippocampus, stimulus-dependent changes in synaptic efficacy cause the active zone density to increase. This change in active zone density may contribute to learning and memory. Meanwhile, diseases that result in abnormal active zone density cause severe symptoms in humans. Pearson's syndrome and LEMS cause a decrease in active zone density and lead to profound neuromuscular disorders. In the CNS, single nucleotide polymorphisms in the gene coding the active zone protein Piccolo have been associated with major depressive disorder, suggesting a possible role for active zones in this disease (Sullivan et al., 2008). Thus, the function of the active zones and their regulated density appears to be critical for the proper function of the nervous system. Additional research into active zone density during development, disease, and plasticity is required because the molecular and cellular mechanisms that control the density of presynaptic active zones are just beginning to be elucidated.

ACKNOWLEDGMENTS

We thank Kausik Si for comments on the manuscript. The work in our laboratory is supported by grants to Hiroshi Nishimune from the Whitehall foundation.

REFERENCES

Akaaboune, M., Allinquant, B., Farza, H., Roy, K., Magoul, R., Fiszman, M., Festoff, B. W., and Hantai, D. (2000). Developmental regulation of amyloid precursor protein at the neuromuscular junction in mouse skeletal muscle. *Mol. Cell. Neurosci.* 15, 355–367.

Alshuaib, W. B., and Fahim, M. A. (1991). Depolarization reverses age-related decrease of spontaneous transmitter release. *J. Appl. Physiol.* 70, 2066–2071.

Altrock, W. D., Tom Dieck, S., Sokolov, M., Meyer, A. C., Sigler, A., Brakebusch, C., Fassler, R., Richter, K., Boeckers, T. M., Potschka, H., Brandt, C., Loscher, W., Grimberg, D., Dresbach, T., Hempelmann, A., Hassan, H., Balschun, D., Frey, J. U., Brandstatter, J. H., Garner, C. C., Rosenmund, C., and Gundelfinger, E. D. (2003). Functional inactivation of a fraction of excitatory synapses in mice deficient for the active zone protein bassoon. *Neuron* 37, 787–800.

Angenstein, F., Hilfert, L., Zuschratter, W., Altrock, W. D., Niessen, H. G., and Gundelfinger, E. D. (2008). Morphological and metabolic changes in the cortex of mice lacking the functional presynaptic active zone protein bassoon: a combined 1H-NMR spectroscopy and histochemical study. *Cereb. Cortex* 18, 890–897.

Balice-Gordon, R. J. (1997). Age-related changes in neuromuscular innervation. *Muscle Nerve Suppl.* 5, S83–S87.

Banker, B. Q., Kelly, S. S., and Robbins, N. (1983). Neuromuscular transmission and correlative morphology in young and old mice. *J. Physiol. (Lond.)* 339, 355–377.

Bednarek, E., and Caroni, P. (2011). beta-Adducin is required for stable assembly of new synapses and improved memory upon environmental enrichment. *Neuron* 69, 1132–1146.

Bennett, M. R., and Lavidis, N. A. (1989). The probability of quantal secretion at release sites in different calcium concentrations in toad (*Bufo marinus*) muscle. *J. Physiol. (Lond.)* 418, 219–233.

Betz, A., Ashery, U., Rickmann, M., Augustin, I., Neher, E., Südhof, T. C., Rettig, J., and Brose, N. (1998). Munc13-1 is a presynaptic phorbol ester receptor that enhances neurotransmitter release. *Neuron* 21, 123–136.

Billings, S. E., Clarke, G. L., and Nishimune, H. (2012). ELKS1 and Ca^{2+} channel subunit beta4 interact and colocalize at cerebellar synapses. *Neuroreport* 23, 49–54.

Bodor, A. L., Giber, K., Rovo, Z., Ulbert, I., and Acsady, L. (2008). Structural correlates of efficient GABAergic transmission in the basal ganglia-thalamus pathway. *J. Neurosci.* 28, 3090–3102.

Branco, T., and Staras, K. (2009). The probability of neurotransmitter release: variability and feedback control at single synapses. *Nat. Rev. Neurosci.* 10, 373–383.

Brandstatter, J. H., Fletcher, E. L., Garner, C. C., Gundelfinger, E. D., and Wassle, H. (1999). Differential expression of the presynaptic cytomatrix protein bassoon among ribbon synapses in the mammalian retina. *Eur. J. Neurosci.* 11, 3683–3693.

Broadie, K. S., and Richmond, J. E. (2002). Establishing and sculpting the synapse in *Drosophila* and *C. elegans*. *Curr. Opin. Neurobiol.* 12, 491–498.

Brose, N., Hofmann, K., Hata, Y., and Südhof, T. C. (1995). Mammalian

homologues of *Caenorhabditis elegans* unc-13 gene define novel family of C2-domain proteins. *J. Biol. Chem.* 270, 25273–25280.

Buffelli, M., Burgess, R. W., Feng, G., Lobe, C. G., Lichtman, J. W., and Sanes, J. R. (2003). Genetic evidence that relative synaptic efficacy biases the outcome of synaptic competition. *Nature* 424, 430–434.

Buran, B. N., Strenzke, N., Neef, A., Gundelfinger, E. D., Moser, T., and Liberman, M. C. (2010). Onset coding is degraded in auditory nerve fibers from mutant mice lacking synaptic ribbons. *J. Neurosci.* 30, 7587–7597.

Burke, R. E., Levine, D. N., Tsairis, P., and Zajac, F. E. III. (1973). Physiological types and histochemical profiles in motor units of the cat gastrocnemius. *J. Physiol. (Lond.)* 234, 723–748.

Cases-Langhoff, C., Voss, B., Garner, A. M., Appeltauer, U., Takei, K., Kindler, S., Veh, R. W., De Camilli, P., Gundelfinger, E. D., and Garner, C. C. (1996). Piccolo, a novel 420 kDa protein associated with the presynaptic cytomatrix. *Eur. J. Cell Biol.* 69, 214–223.

Chakkalakal, J. V., Nishimune, H., Ruas, J. L., Spiegelman, B. M., and Sanes, J. R. (2010). Retrograde influence of muscle fibers on their innervation revealed by a novel marker for slow motoneurons. *Development* 137, 3489–3499.

Chen, J., Billings, S. E., and Nishimune, H. (2011a). Calcium channels link the muscle-merived synapse organizer laminin beta2 to Bassoon and CAST/Erc2 to organize presynaptic active zones. *J. Neurosci.* 31, 512–525.

Chen, J., Mizushige, T., and Nishimune, H. (2011b). Active zone density is conserved during synaptic growth but impaired in aged mice. *J. Comp. Neurol.* 520, 434–452.

Choi, J. K., Jeon, Y. C., Lee, D. W., Oh, J. M., Lee, H. P., Jeong, B. H., Carp, R. I., Koh, Y. H., and Kim, Y. S. (2010). A *Drosophila* model of GSS syndrome suggests defects in active zones are responsible for pathogenesis of GSS syndrome. *Hum. Mol. Genet.* 19, 4474–4489.

Collins, C. A., and DiAntonio, A. (2007). Synaptic development: insights from *Drosophila*. *Curr. Opin. Neurobiol.* 17, 35–42.

Condon, K., Silberstein, L., Blau, H. M., and Thompson, W. J. (1990). Development of muscle fiber types in the prenatal rat hindlimb. *Dev. Biol.* 138, 256–274.

Coppola, T., Magnin-Luthi, S., Perret-Menoud, V., Gattesco, S., Schiavo, G., and Regazzi, R. (2001). Direct interaction of the Rab3 effector RIM with Ca^{2+} channels, SNAP-25, and synaptotagmin. *J. Biol. Chem.* 276, 32756–32762.

Couteaux, R., and Pecot-Dechavassine, M. (1970). Synaptic vesicles and pouches at the level of "active zones" of the neuromuscular junction. *C. R. Hebd. Seances Acad. Sci. Ser. D Sci. Nat.* 271, 2346–2349.

Cremona, O., Di Paolo, G., Wenk, M. R., Luthi, A., Kim, W. T., Takei, K., Daniell, L., Nemoto, Y., Shears, S. B., Flavell, R. A., Mccormick, D. A., and De Camilli, P. (1999). Essential role of phosphoinositide metabolism in synaptic vesicle recycling. *Cell* 99, 179–188.

Deguchi-Tawarada, M., Inoue, E., Takao-Rikitsu, E., Inoue, M., Ohtsuka, T., and Takai, Y. (2004). CAST2: identification and characterization of a protein structurally related to the presynaptic cytomatrix protein CAST. *Genes Cells* 9, 15–23.

Dick, O., Tom Dieck, S., Altrock, W. D., Ammermuller, J., Weiler, R., Garner, C. C., Gundelfinger, E. D., and Brandstatter, J. H. (2003). The presynaptic active zone protein bassoon is essential for photoreceptor ribbon synapse formation in the retina. *Neuron* 37, 775–786.

Dickman, D. K., Lu, Z., Meinertzhagen, I. A., and Schwarz, T. L. (2006). Altered synaptic development and active zone spacing in endocytosis mutants. *Curr. Biol.* 16, 591–598.

Dondzillo, A., Sätzler, K., Horstmann, H., Altrock, W. D., Gundelfinger, E. D., and Kuner, T. (2010). Targeted three-dimensional immunohistochemistry reveals localization of presynaptic proteins bassoon and piccolo in the rat calyx of held before and after the onset of hearing. *J. Comp. Neurol.* 518, 1008–1029.

Dresbach, T., Qualmann, B., Kessels, M. M., Garner, C. C., and Gundelfinger, E. D. (2001). The presynaptic cytomatrix of brain synapses. *Cell. Mol. Life Sci.* 58, 94–116.

Dulubova, I., Lou, X., Lu, J., Huryeva, I., Alam, A., Schneggenburger, R., Südhof, T. C., and Rizo, J. (2005). A Munc13/RIM/Rab3 tripartite complex: from priming to plasticity? *EMBO J.* 24, 2839–2850.

Eaton, L. M., and Lambert, E. H. (1957). Electromyography and electric stimulation of nerves in diseases of motor unit; observations on myasthenic syndrome associated with malignant tumors. *J. Am. Med. Assoc.* 163, 1117–1124.

Ellisman, M. H., Rash, J. E., Staehelin, L. A., and Porter, K. R. (1976). Studies of excitable membranes. II. A comparison of specializations at neuromuscular junctions and nonjunctional sarcolemmas of mammalian fast and slow twitch muscle fibers. *J. Cell Biol.* 68, 752–774.

Elmqvist, D., and Lambert, E. H. (1968). Detailed analysis of neuromuscular transmission in a patient with the myasthenic syndrome sometimes associated with bronchogenic carcinoma. *Mayo Clin. Proc.* 43, 689–713.

Fahim, M. A. (1997). Endurance exercise modulates neuromuscular junction of C57BL/6NNia aging mice. *J. Appl. Physiol.* 83, 59–66.

Fahim, M. A., and Robbins, N. (1982). Ultrastructural studies of young and old mouse neuromuscular junctions. *J. Neurocytol.* 11, 641–656.

Fejtova, A., and Gundelfinger, E. D. (2006). Molecular organization and assembly of the presynaptic active zone of neurotransmitter release. *Results Probl. Cell Differ.* 43, 49–68.

Feng, G., Krejci, E., Molgo, J., Cunningham, J. M., Massoulie, J., and Sanes, J. R. (1999). Genetic analysis of collagen Q: roles in acetylcholinesterase and butyrylcholinesterase assembly and in synaptic structure and function. *J. Cell Biol.* 144, 1349–1360.

Fouquet, W., Owald, D., Wichmann, C., Mertel, S., Depner, H., Dyba, M., Hallermann, S., Kittel, R. J., Eimer, S., and Sigrist, S. J. (2009). Maturation of active zone assembly by *Drosophila* bruchpilot. *J. Cell Biol.* 186, 129–145.

Fukunaga, H., Engel, A. G., Lang, B., Newsom-Davis, J., and Vincent, A. (1983). Passive transfer of Lambert-Eaton myasthenic syndrome with IgG from man to mouse depletes the presynaptic membrane active zones. *Proc. Natl. Acad. Sci. U.S.A.* 80, 7636–7640.

Fukunaga, H., Engel, A. G., Osame, M., and Lambert, E. H. (1982). Paucity and disorganization of presynaptic membrane active zones in the lambert-eaton myasthenic syndrome. *Muscle Nerve* 5, 686–697.

Fukuoka, T., Engel, A. G., Lang, B., Newsom-Davis, J., Prior, C., and Wray, D. W. (1987). Lambert-Eaton myasthenic syndrome: I. Early morphological effects of IgG on the presynaptic membrane active zones. *Ann. Neurol.* 22, 193–199.

Gardiner, P. F. (1993). Physiological properties of motoneurons innervating different muscle unit types in rat gastrocnemius. *J. Neurophysiol.* 69, 1160–1170.

Ghetti, B., Dlouhy, S. R., Giaccone, G., Bugiani, O., Frangione, B., Farlow, M. R., and Tagliavini, F. (1995). Gerstmann-Straussler-Scheinker disease and the Indiana kindred. *Brain Pathol.* 5, 61–75.

Goetze, B., Schmidt, K.-F., Lehmann, K., Altrock, W. D., Gundelfinger, E. D., and Lowel, S. (2010). Vision and visual cortical maps in mice with a photoreceptor synaptopathy: reduced but robust visual capabilities in the absence of synaptic ribbons. *Neuroimage* 49, 1622–1631.

Graf, E. R., Daniels, R. W., Burgess, R. W., Schwarz, T. L., and Diantonio, A. (2009). Rab3 Dynamically controls protein composition at active zones. *Neuron* 64, 663–677.

Gutmann, E., Hanzlikova, V., and Vysokocil, F. (1971). Age changes in cross striated muscle of the rat. *J. Physiol. (Lond.)* 216, 331–343.

Hallermann, S., Fejtova, A., Schmidt, H., Weyhersmüller, A., Silver, R. A., Gundelfinger, E. D., and Eilers, J. (2010). Bassoon speeds vesicle reloading at a central excitatory synapse. *Neuron* 68, 710–723.

Han, Y., Kaeser, P. S., Südhof, T. C., and Schneggenburger, R. (2011). RIM determines Ca^{2+} channel density and vesicle docking at the presynaptic active zone. *Neuron* 69, 304–316.

Harlow, M. L., Ress, D., Stoschek, A., Marshall, R. M., and Mcmahan, U. J. (2001). The architecture of active zone material at the frog's neuromuscular junction. *Nature* 409, 479–484.

Heuser, J. E., Reese, T. S., Dennis, M. J., Jan, Y., Jan, L., and Evans, L. (1979). Synaptic vesicle exocytosis captured by quick freezing and correlated with quantal transmitter release. *J. Cell Biol.* 81, 275–300.

Heuser, J. E., Reese, T. S., and Landis, D. M. (1974). Functional changes in frog neuromuscular junctions studied with freeze-fracture. *J. Neurocytol.* 3, 109–131.

Hirokawa, N., and Heuser, J. E. (1982). Internal and external differentiations of the postsynaptic membrane at the neuromuscular junction. *J. Neurocytol.* 11, 487–510.

Jin, Y. (2005). Synaptogenesis. *WormBook* 1–11. Available at: http://www.wormbook.org

Jin, Y., and Garner, C. C. (2008). Molecular mechanisms of presynaptic differentiation. *Annu. Rev. Cell Dev. Biol.* 24, 237–262.

Kaeser, P. S., Deng, L., Chávez, A. E., Liu, X., Castillo, P. E., and Südhof, T. C. (2009). ELKS2alpha/CAST

deletion selectively increases neurotransmitter release at inhibitory synapses. *Neuron* 64, 227–239.

Kaeser, P. S., Deng, L., Wang, Y., Dulubova, I., Liu, X., Rizo, J., and Südhof, T. C. (2011). RIM proteins tether Ca^{2+} channels to presynaptic active zones via a direct PDZ-domain interaction. *Cell* 144, 282–295.

Kanning, K. C., Kaplan, A., and Henderson, C. E. (2010). Motor neuron diversity in development and disease. *Annu. Rev. Neurosci.* 33, 409–440.

Kelly, S. S. (1978). The effect of age on neuromuscular transmission. *J. Physiol. (Lond.)* 274, 51–62.

Kim, W. T., Chang, S., Daniell, L., Cremona, O., Di Paolo, G., and De Camilli, P. (2002). Delayed reentry of recycling vesicles into the fusion-competent synaptic vesicle pool in synaptojanin 1 knockout mice. *Proc. Natl. Acad. Sci. U.S.A.* 99, 17143–17148.

Kim, Y. I., and Neher, E. (1988). IgG from patients with Lambert-Eaton syndrome blocks voltage-dependent calcium channels. *Science* 239, 405–408.

Kittel, R. J., Wichmann, C., Rasse, T. M., Fouquet, W., Schmidt, M., Schmid, A., Wagh, D. A., Pawlu, C., Kellner, R. R., Willig, K. I., Hell, S. W., Buchner, E., Heckmann, M., and Sigrist, S. J. (2006). Bruchpilot promotes active zone assembly, Ca^{2+} channel clustering, and vesicle release. *Science* 312, 1051–1054.

Kiyonaka, S., Wakamori, M., Miki, T., Uriu, Y., Nonaka, M., Bito, H., Beedle, A. M., Mori, E., Hara, Y., De Waard, M., Kanagawa, M., Itakura, M., Takahashi, M., Campbell, K. P., and Mori, Y. (2007). RIM1 confers sustained activity and neurotransmitter vesicle anchoring to presynaptic Ca^{2+} channels. *Nat. Neurosci.* 10, 691–701.

Ko, C. P. (1985). Formation of the active zone at developing neuromuscular junctions in larval and adult bullfrogs. *J. Neurocytol.* 14, 487–512.

Lambert, E. H., and Elmqvist, D. (1971). Quantal components of end-plate potentials in the myasthenic syndrome. *Ann. N. Y. Acad. Sci.* 183, 183–199.

Lanore, F., Blanchet, C., Fejtova, A., Pinheiro, P., Richter, K., Balschun, D., Gundelfinger, E. D., and Mulle, C. (2010). Impaired development of hippocampal mossy fibre synapses in mouse mutants for the presynaptic scaffold protein Bassoon. *J. Physiol. (Lond.)* 588, 2133–2145.

Lee, R. H., and Heckman, C. J. (1998a). Bistability in spinal motoneurons in vivo: systematic variations in rhythmic firing patterns. *J. Neurophysiol.* 80, 572–582.

Lee, R. H., and Heckman, C. J. (1998b). Bistability in spinal motoneurons in vivo: systematic variations in persistent inward currents. *J. Neurophysiol.* 80, 583–593.

Lichtman, J. W., Wilkinson, R. S., and Rich, M. M. (1985). Multiple innervation of tonic endplates revealed by activity-dependent uptake of fluorescent probes. *Nature* 314, 357–359.

Lin, W., Dominguez, B., Yang, J., Aryal, P., Brandon, E. P., Gage, F. H., and Lee, K.-F. (2005). Neurotransmitter acetylcholine negatively regulates neuromuscular synapse formation by a Cdk5-dependent mechanism. *Neuron* 46, 569–579.

Llinas, R., Sugimori, M., and Silver, R. B. (1992). Microdomains of high calcium concentration in a presynaptic terminal. *Science* 256, 677–679.

Luo, F., Dittrich, M., Stiles, J. R., and Meriney, S. D. (2011). Single-pixel optical fluctuation analysis of calcium channel function in active zones of motor nerve terminals. *J. Neurosci.* 31, 11268–11281.

Mark, K., Reis, A., and Zenker, M. (2006). Prenatal findings in four consecutive pregnancies with fetal Pierson syndrome, a newly defined congenital nephrosis syndrome. *Prenat. Diagn.* 26, 262–266.

Maselli, R. A., Ng, J. J., Anderson, J. A., Cagney, O., Arredondo, J., Williams, C., Wessel, H. B., Abdel-Hamid, H., and Wollmann, R. L. (2009). Mutations in LAMB2 causing a severe form of synaptic congenital myasthenic syndrome. *J. Med. Genet.* 46, 203–208.

Massoulie, J., and Bon, S. (1982). The molecular forms of cholinesterase and acetylcholinesterase in vertebrates. *Annu. Rev. Neurosci.* 5, 57–106.

Mead, S. (2006). Prion disease genetics. *Eur. J. Hum. Genet.* 14, 273–281.

Meinertzhagen, I. A., Govind, C. K., Stewart, B. A., Carter, J. M., and Atwood, H. L. (1998). Regulated spacing of synapses and presynaptic active zones at larval neuromuscular junctions in different genotypes of the flies *Drosophila* and *Sarcophaga*. *J. Comp. Neurol.* 393, 482–492.

Meriney, S. D., Wolowske, B., Ezzati, E., and Grinnell, A. D. (1996). Low calcium-induced disruption of active zone structure and function at the frog neuromuscular junction. *Synapse* 24, 1–11.

Misgeld, T., Burgess, R. W., Lewis, R. M., Cunningham, J. M., Lichtman, J. W., and Sanes, J. R. (2002). Roles of neurotransmitter in synapse formation: development of neuromuscular junctions lacking choline acetyltransferase. *Neuron* 36, 635–648.

Misgeld, T., Kummer, T. T., Lichtman, J. W., and Sanes, J. R. (2005). Agrin promotes synaptic differentiation by counteracting an inhibitory effect of neurotransmitter. *Proc. Natl. Acad. Sci. U.S.A.* 102, 11088–11093.

Mukherjee, K., Yang, X., Gerber, S. H., Kwon, H.-B., Ho, A., Castillo, P. E., Liu, X., and Südhof, T. C. (2010). Piccolo and bassoon maintain synaptic vesicle clustering without directly participating in vesicle exocytosis. *Proc. Natl. Acad. Sci. U.S.A.* 107, 6504–6509.

Nagel, A., Engel, A. G., Lang, B., Newsom-Davis, J., and Fukuoka, T. (1988). Lambert-Eaton myasthenic syndrome IgG depletes presynaptic membrane active zone particles by antigenic modulation. *Ann. Neurol.* 24, 552–558.

Nagwaney, S., Harlow, M. L., Jung, J. H., Szule, J. A., Ress, D., Xu, J., Marshall, R. M., and Mcmahan, U. J. (2009). Macromolecular connections of active zone material to docked synaptic vesicles and presynaptic membrane at neuromuscular junctions of mouse. *J. Comp. Neurol.* 513, 457–468.

Narusawa, M., Fitzsimons, R. B., Izumo, S., Nadal-Ginard, B., Rubinstein, N. A., and Kelly, A. M. (1987). Slow myosin in developing rat skeletal muscle. *J. Cell Biol.* 104, 447–459.

Neher, E. (1998). Vesicle pools and Ca^{2+} microdomains: new tools for understanding their roles in neurotransmitter release. *Neuron* 20, 389–399.

Nicol, M. J., and Walmsley, B. (2002). Ultrastructural basis of synaptic transmission between endbulbs of Held and bushy cells in the rat cochlear nucleus. *J. Physiol. (Lond.)* 539, 713–723.

Nishimune, H. (2011a). Transsynaptic channelosomes: non-conducting roles of ion channels in synapse formation. *Channels* 5, 432–439.

Nishimune, H. (2011b). Molecular mechanism of active zone organization at vertebrate neuromuscular junctions. *Mol. Neurobiol.* 45, 1–16.

Nishimune, H., Sanes, J. R., and Carlson, S. S. (2004). A synaptic laminin-calcium channel interaction organizes active zones in motor nerve terminals. *Nature* 432, 580–587.

Nithianantharajah, J., and Hannan, A. J. (2006). Enriched environments, experience-dependent plasticity and disorders of the nervous system. *Nat. Rev. Neurosci.* 7, 697–709.

Noakes, P. G., Gautam, M., Mudd, J., Sanes, J. R., and Merlie, J. P. (1995). Aberrant differentiation of neuromuscular junctions in mice lacking s-laminin/laminin beta 2. *Nature* 374, 258–262.

Ohara-Imaizumi, M., Ohtsuka, T., Matsushima, S., Akimoto, Y., Nishiwaki, C., Nakamichi, Y., Kikuta, T., Nagai, S., Kawakami, H., Watanabe, T., and Nagamatsu, S. (2005). ELKS, a protein structurally related to the active zone-associated protein CAST, is expressed in pancreatic beta cells and functions in insulin exocytosis: interaction of ELKS with exocytotic machinery analyzed by total internal reflection fluorescence microscopy. *Mol. Biol. Cell* 16, 3289–3300.

Ohtsuka, T., Takao-Rikitsu, E., Inoue, E., Inoue, M., Takeuchi, M., Matsubara, K., Deguchi-Tawarada, M., Satoh, K., Morimoto, K., Nakanishi, H., and Takai, Y. (2002). Cast: a novel protein of the cytomatrix at the active zone of synapses that forms a ternary complex with RIM1 and munc13-1. *J. Cell Biol.* 158, 577–590.

Owald, D., and Sigrist, S. J. (2009). Assembling the presynaptic active zone. *Curr. Opin. Neurobiol.* 19, 311–318.

Patton, B. L. (2000). Laminins of the neuromuscular system. *Microsc. Res. Tech.* 51, 247–261.

Patton, B. L., Cunningham, J. M., Thyboll, J., Kortesmaa, J., Westerblad, H., Edstrom, L., Tryggvason, K., and Sanes, J. R. (2001). Properly formed but improperly localized synaptic specializations in the absence of laminin alpha4. *Nat. Neurosci.* 4, 597–604.

Peled, E. S., and Isacoff, E. Y. (2011). Optical quantal analysis of synaptic transmission in wild-type and rab3-mutant *Drosophila* motor axons. *Nat. Neurosci.* 14, 519–526.

Pelkey, K. A., and McBain, C. J. (2007). Differential regulation at functionally divergent release sites along a common axon. *Curr. Opin. Neurobiol.* 17, 366–373.

Phillips, G. R., Huang, J. K., Wang, Y., Tanaka, H., Shapiro, L., Zhang, W., Shan, W. S., Arndt, K., Frank, M., Gordon, R. E., Gawinowicz, M. A., Zhao, Y., and Colman, D. R. (2001). The presynaptic particle web: ultrastructure, composition, dissolution, and reconstitution. *Neuron* 32, 63–77.

Pielage, J., Fetter, R. D., and Davis, G. W. (2006). A postsynaptic spectrin scaffold defines active zone size, spacing, and efficacy at the *Drosophila*

neuromuscular junction. *J. Cell Biol.* 175, 491–503.

Pierce, J. P., and Mendell, L. M. (1993). Quantitative ultrastructure of Ia boutons in the ventral horn: scaling and positional relationships. *J. Neurosci.* 13, 4748–4763.

Prakash, Y. S., Miller, S. M., Huang, M., and Sieck, G. C. (1996). Morphology of diaphragm neuromuscular junctions on different fibre types. *J. Neurocytol.* 25, 88–100.

Prescott, E. D., and Zenisek, D. (2005). Recent progress towards understanding the synaptic ribbon. *Curr. Opin. Neurobiol.* 15, 431–436.

Propst, J., and Ko, C. (1987). Correlations between active zone ultrastructure and synaptic function studied with freeze-fracture of physiologically identified neuromuscular junctions. *J. Neurosci.* 7, 3654–3664.

Reiff, D. F., Thiel, P. R., and Schuster, C. M. (2002). differential regulation of active zone density during long-term strengthening of *Drosophila* neuromuscular junctions. *J. Neurosci.* 22, 9399–9409.

Richter, K., Langnaese, K., Kreutz, M. R., Olias, G., Zhai, R., Scheich, H., Garner, C. C., and Gundelfinger, E. D. (1999). Presynaptic cytomatrix protein bassoon is localized at both excitatory and inhibitory synapses of rat brain. *J. Comp. Neurol.* 408, 437–448.

Rollenhagen, A., Satzler, K., Rodriguez, E. P., Jonas, P., Frotscher, M., and Lubke, J. H. (2007). Structural determinants of transmission at large hippocampal mossy fiber synapses. *J. Neurosci.* 27, 10434–10444.

Rosenmund, C., Rettig, J., and Brose, N. (2003). Molecular mechanisms of active zone function. *Curr. Opin. Neurobiol.* 13, 509–519.

Rowland, K. C., Irby, N. K., and Spirou, G. A. (2000). Specialized synapse-associated structures within the calyx of Held. *J. Neurosci.* 20, 9135–9144.

Rowley, K. L., Mantilla, C. B., Ermilov, L. G., and Sieck, G. C. (2007). Synaptic vesicle distribution and release at rat diaphragm neuromuscular junctions. *J. Neurophysiol.* 98, 478–487.

Satzler, K., Sohl, L. F., Bollmann, J. H., Borst, J. G., Frotscher, M., Sakmann, B., and Lubke, J. H. (2002). Three-dimensional reconstruction of a calyx of Held and its postsynaptic principal neuron in the medial nucleus of the trapezoid body. *J. Neurosci.* 22, 10567–10579.

Schikorski, T., and Stevens, C. F. (1997). Quantitative ultrastructural analysis of hippocampal excitatory synapses. *J. Neurosci.* 17, 5858–5867.

Schluter, O. M., Schmitz, F., Jahn, R., Rosenmund, C., and Südhof, T. C. (2004). A complete genetic analysis of neuronal Rab3 function. *J. Neurosci.* 24, 6629–6637.

Schubert, W., Prior, R., Weidemann, A., Dircksen, H., Multhaup, G., Masters, C. L., and Beyreuther, K. (1991). Localization of Alzheimer beta A4 amyloid precursor protein at central and peripheral synaptic sites. *Brain Res.* 563, 184–194.

Shibasaki, T., Sunaga, Y., Fujimoto, K., Kashima, Y., and Seino, S. (2004). Interaction of ATP sensor, cAMP sensor, Ca^{2+} sensor, and voltage-dependent Ca^{2+} channel in insulin granule exocytosis. *J. Biol. Chemis.* 279, 7956–7961.

Sigrist, S. J., and Schmitz, D. (2010). Structural and functional plasticity of the cytoplasmic active zone. *Curr. Opin. Neurobiol.* 21, 1–7.

Sigrist, S. J., Thiel, P. R., Reiff, D. F., and Schuster, C. M. (2002). The postsynaptic glutamate receptor subunit DGluR-IIA mediates long-term plasticity in *Drosophila*. *J. Neurosci.* 22, 7362–7372.

Specht, D., Tom Dieck, S., Ammermuller, J., Regus-Leidig, H., Gundelfinger, E. D., and Brandstatter, J. H. (2007). Structural and functional remodeling in the retina of a mouse with a photoreceptor synaptopathy: plasticity in the rod and degeneration in the cone system. *Eur. J. Neurosci.* 26, 2506–2515.

Stankewich, M. C., Gwynn, B., Ardito, T., Ji, L., Kim, J., Robledo, R. F., Lux, S. E., Peters, L. L., and Morrow, J. S. (2010). Targeted deletion of betaIII spectrin impairs synaptogenesis and generates ataxic and seizure phenotypes. *Proc. Natl. Acad. Sci. U.S.A.* 107, 6022–6027.

Stryker, E., and Johnson, K. G. (2007). LAR, liprin alpha and the regulation of active zone morphogenesis. *J. Cell. Sci.* 120, 3723–3728.

Sullivan, P. F., De Geus, E. J. C., Willemsen, G., James, M. R., Smit, J. H., Zandbelt, T., Arolt, V., Baune, B. T., Blackwood, D., Cichon, S., Coventry, W. L., Domschke, K., Farmer, A., Fava, M., Gordon, S. D., He, Q., Heath, A. C., Heutink, P., Holsboer, F., Hoogendijk, W. J., Hottenga, J. J., Hu, Y., Kohli, M., Lin, D., Lucae, S., Macintyre, D. J., Maier, W., Mcghee, K. A., Mcguffin, P., Montgomery, G. W., Muir, W. J., Nolen, W. A., Nothen, M. M., Perlis, R. H., Pirlo, K., Posthuma, D., Rietschel, M., Rizzu, P., Schosser, A., Smit, A. B., Smoller, J. W., Tzeng, J. Y., Van Dyck, R., Verhage, M., Zitman, F. G., Martin, N. G., Wray, N. R., Boomsma, D. I., and Penninx, B. W. J. H. (2008). Genome-wide association for major depressive disorder: a possible role for the presynaptic protein piccolo. *Mol. Psychiatry* 14, 359–375.

Takao-Rikitsu, E., Mochida, S., Inoue, E., Deguchi-Tawarada, M., Inoue, M., Ohtsuka, T., and Takai, Y. (2004). Physical and functional interaction of the active zone proteins, CAST, RIM1, and Bassoon, in neurotransmitter release. *J. Cell Biol.* 164, 301–311.

tom Dieck, S., Altrock, W. D., Kessels, M. M., Qualmann, B., Regus, H., Brauner, D., Fejtova, A., Bracko, O., Gundelfinger, E. D., and Brandstatter, J. H. (2005). Molecular dissection of the photoreceptor ribbon synapse: physical interaction of Bassoon and RIBEYE is essential for the assembly of the ribbon complex. *J. Cell Biol.* 168, 825–836.

tom Dieck, S., Sanmarti-Vila, L., Langnaese, K., Richter, K., Kindler, S., Soyke, A., Wex, H., Smalla, K. H., Kampf, U., Franzer, J. T., Stumm, M., Garner, C. C., and Gundelfinger, E. D. (1998). Bassoon, a novel zinc-finger CAG/glutamine-repeat protein selectively localized at the active zone of presynaptic nerve terminals. *J. Cell Biol.* 142, 499–509.

Uriu, Y., Kiyonaka, S., Miki, T., Yagi, M., Akiyama, S., Mori, E., Nakao, A., Beedle, A. M., Campbell, K. P., Wakamori, M., and Mori, Y. (2010). Rab3-interacting molecule g isoforms lacking the Rab3-binding domain induce long-lasting currents but block neurotransmitter vesicle-anchoring in voltage-dependent P/Q-type Ca^{2+} channels. *J. Biol. Chem.* 285, 21750–21767.

Valdez, G., Tapia, J. C., Kang, H., Clemenson, G. D. Jr., Gage, F. H., Lichtman, J. W., and Sanes, J. R. (2010). Attenuation of age-related changes in mouse neuromuscular synapses by caloric restriction and exercise. *Proc. Natl. Acad. Sci. U.S.A.* 107, 14863–14868.

Verstreken, P., Koh, T. W., Schulze, K. L., Zhai, R. G., Hiesinger, P. R., Zhou, Y., Mehta, S. Q., Cao, Y., Roos, J., and Bellen, H. J. (2003). Synaptojanin is recruited by endophilin to promote synaptic vesicle uncoating. *Neuron* 40, 733–748.

Wagh, D. A., Rasse, T. M., Asan, E., Hofbauer, A., Schwenkert, I., Durrbeck, H., Buchner, S., Dabauvalle, M. C., Schmidt, M., Qin, G., Wichmann, C., Kittel, R., Sigrist, S. J., and Buchner, E. (2006). Bruchpilot, a protein with homology to ELKS/CAST, is required for structural integrity and function of synaptic active zones in *Drosophila*. *Neuron* 49, 833–844.

Wairkar, Y. P., Toda, H., Mochizuki, H., Furukubo-Tokunaga, K., Tomoda, T., and Diantonio, A. (2009). Unc-51 controls active zone density and protein composition by downregulating ERK signaling. *J. Neurosci.* 29, 517–528.

Walrond, J., and Reese, T. (1985). Structure of axon terminals and active zones at synapses on lizard twitch and tonic muscle fibers. *J. Neurosci.* 5, 1118–1131.

Wanaverbecq, N., Bodor, A. L., Bokor, H., Slezia, A., Luthi, A., and Acsady, L. (2008). Contrasting the functional properties of GABAergic axon terminals with single and multiple synapses in the thalamus. *J. Neurosci.* 28, 11848–11861.

Wang, P., Yang, G., Mosier, D. R., Chang, P., Zaidi, T., Gong, Y. D., Zhao, N. M., Dominguez, B., Lee, K. F., Gan, W. B., and Zheng, H. (2005). Defective neuromuscular synapses in mice lacking amyloid precursor protein (APP) and APP-Like protein 2. *J. Neurosci.* 25, 1219–1225.

Wang, X., Hu, B., Zieba, A., Neumann, N. G., Kasper-Sonnenberg, M., Honsbein, A., Hultqvist, G., Conze, T., Witt, W., Limbach, C., Geitmann, M., Danielson, H., Kolarow, R., Niemann, G., Lessmann, V., and Kilimann, M. W. (2009a). A protein interaction node at the neurotransmitter release site: domains of Aczonin/Piccolo, Bassoon, CAST, and Rim converge on the N-terminal domain of Munc13-1. *J. Neurosci.* 29, 12584–12596.

Wang, Z., Wang, B., Yang, L., Guo, Q., Aithmitti, N., Songyang, Z., and Zheng, H. (2009b). Presynaptic and postsynaptic interaction of the amyloid precursor protein promotes peripheral and central synaptogenesis. *J. Neurosci.* 29, 10788–10801.

Wang, Y., Liu, X., Biederer, T., and Südhof, T. C. (2002). A family of RIM-binding proteins regulated by alternative splicing: implications for the genesis of synaptic active zones. *Proc. Natl. Acad. Sci. U.S.A.* 99, 14464–14469.

Wang, Y., Okamoto, M., Schmitz, F., Hofmann, K., and Südhof, T. C. (1997). Rim is a putative Rab3 effector in regulating synaptic-vesicle fusion. *Nature* 388, 593–598.

Wichmann, C., and Sigrist, S. J. (2010). The active zone T-bar – a plasticity module? *J. Neurogenet.* 24, 133–145.

Wyatt, R. M., and Balice-Gordon, R. J. (2008). Heterogeneity in synaptic vesicle release at neuromuscular

synapses of mice expressing synaptopHluorin. *J. Neurosci.* 28, 325–335.
Xie, W., Stribley, J. A., Chatonnet, A., Wilder, P. J., Rizzino, A., Mccomb, R. D., Taylor, P., Hinrichs, S. H., and Lockridge, O. (2000). Postnatal developmental delay and supersensitivity to organophosphate in gene-targeted mice lacking acetylcholinesterase. *J. Pharmacol. Exp. Ther.* 293, 896–902.
Xu-Friedman, M. A., Harris, K. M., and Regehr, W. G. (2001). Three-dimensional comparison of ultrastructural characteristics at depressing and facilitating synapses onto cerebellar Purkinje cells. *J. Neurosci.* 21, 6666–6672.
Yeh, E., Kawano, T., Ng, S., Fetter, R., Hung, W., Wang, Y., and Zhen, M. (2009). *Caenorhabditis elegans* innexins regulate active zone differentiation. *J. Neurosci.* 29, 5207–5217.
Yeow, M. B., and Peterson, E. H. (1991). Active zone organization and vesicle content scale with bouton size at a vertebrate central synapse. *J. Comp. Neurol.* 307, 475–486.
Zenker, M., Aigner, T., Wendler, O., Tralau, T., Muntefering, H., Fenski, R., Pitz, S., Schumacher, V., Royer-Pokora, B., Wuhl, E., Cochat, P., Bouvier, R., Kraus, C., Mark, K., Madlon, H., Dotsch, J., Rascher, W., Maruniak-Chudek, I., Lennert, T., Neumann, L. M., and Reis, A. (2004a). Human laminin beta2 deficiency causes congenital nephrosis with mesangial sclerosis and distinct eye abnormalities. *Hum. Mol. Genet.* 13, 2625–2632.
Zenker, M., Tralau, T., Lennert, T., Pitz, S., Mark, K., Madlon, H., Dotsch, J., Reis, A., Muntefering, H., and Neumann, L. M. (2004b). Congenital nephrosis, mesangial sclerosis, and distinct eye abnormalities with microcoria: an autosomal recessive syndrome. *Am. J. Med. Genet. A* 130A, 138–145.
Zhai, R. G., and Bellen, H. J. (2004). The architecture of the active zone in the presynaptic nerve terminal. *Physiology (Bethesda)* 19, 262–270.
Zhang, L., Volknandt, W., Gundelfinger, E. D., and Zimmermann, H. (2000). A comparison of synaptic protein localization in hippocampal mossy fiber terminals and neurosecretory endings of the neurohypophysis using the cryo-immunogold technique. *J. Neurocytol.* 29, 19–30.

Conflict of Interest Statement: The authors declare that the research was conducted in the absence of any commercial or financial relationships that could be construed as a potential conflict of interest.

Received: 07 December 2011; accepted: 30 January 2012; published online: 15 February 2012.
Citation: Clarke GL, Chen J and Nishimune H (2012) Presynaptic active zone density during development and synaptic plasticity. Front. Mol. Neurosci. ***5****:12. doi: 10.3389/fnmol.2012.00012*

frontiers in
MOLECULAR NEUROSCIENCE

REVIEW ARTICLE
published: 31 May 2012
doi: 10.3389/fnmol.2012.00070

Synaptic clustering during development and learning: the why, when, and how

Johan Winnubst and Christian Lohmann*

Department of Synapse and Network Development, Netherlands Institute for Neuroscience, Amsterdam, Netherlands

Edited by:
James Jontes, Ohio State University, USA

Reviewed by:
Hansen Wang, University of Toronto, Canada
Cristopher Niell, University of Oregon, USA

****Correspondence:***
Christian Lohmann, Department of Synapse and Network Development, Netherlands Institute for Neuroscience, Meibergdreef 47, Amsterdam, Netherlands.
e-mail: c.lohmann@nin.knaw.nl

To contribute to a functional network a neuron must make specific connections and integrate the synaptic inputs that it receives in a meaningful way. Previous modeling and experimental studies have predicted that this specificity could entail a subcellular organization whereby synapses that carry similar information are clustered together on local stretches of dendrite. Recent imaging studies have now, for the first time, demonstrated synaptic clustering during development and learning in different neuronal circuits. Interestingly, this organization is dependent on synaptic activity and most likely involves local plasticity mechanisms. Here we discuss these new insights and give an overview of the candidate plasticity mechanisms that could be involved.

Keywords: synapse development, synaptic plasticity, dendrites, dendritic integration, activity-dependent, spontaneous activity

INTRODUCTION

Our brains can adjust to the challenges and opportunities in our environment by activity-dependent adaptations of neuronal connectivity. In particular, during brain development networks undergo activity regulated remodeling at high rates. Interestingly, neuronal activity helps to set up the connections between nerve cells in our brains already before birth and the onset of experience. At these early developmental stages networks generate spontaneous activity that is transmitted along neuronal pathways to test-run and fine-tune the emerging synaptic connections (Goodman and Shatz, 1993; Katz and Shatz, 1996; Ben Ari, 2001; Cline, 2003; Hua and Smith, 2004; Huberman et al., 2008; Sanes and Yamagata, 2009). Thus, activity-dependent fine-tuning prepares brain circuits for the moment when humans and animals start interacting with their environments.

Spontaneous activity occurs frequently as repetitive network events during which large proportions of the network become activated at the same time (Galli and Maffei, 1988; Ben-Ari et al., 1989; Meister et al., 1991; Yuste et al., 1992; O'Donovan et al., 1994; Garaschuk et al., 1998). The activity propagates through the network in a wave-like fashion as neighboring cells become successively activated. This specific characteristic of spontaneous activity has been recognized as an important feature for the activity-dependent establishment of synaptic specificity. For example, waves of spontaneous activity in the vertebrate retina lead to a high degree of correlation between the activity patterns of neighboring cells. Thus, the spatial relationship of the retina is encoded by the activity patterns in higher order brain structures aiding retinotopic map formation and eye specific segregation. Indeed, studies that affected not the presence of spontaneous activity but the patterns within the activity itself have shown an instructive role of spontaneous activity during development (Weliky and Katz, 1997; Mrsic-Flogel et al., 2005; Torborg et al., 2005; Xu et al., 2011).

Thus, both spontaneous activity before the onset of sensory experience as well as neuronal activity during learning processes (Chklovskii et al., 2004; Hofer et al., 2006; Karmarkar and Dan, 2006; DeBello, 2008; Fu and Zuo, 2011) set up and modify connection specificity on the level of cell-types and individual neurons. A recent series of studies have predicted that this specificity could extend far beyond simply connecting the right axon with the correct cell and might entail a more precise subcellular organization. The prediction stems from both modeling and experimental studies in which individual segments of dendrite are thought to function as independent computational subunits (Polsky et al., 2004; Losonczy and Magee, 2006; Larkum and Nevian, 2008; Branco and Hausser, 2010). In this model, synapses that encode similar information are clustered close together on the dendrite. Recent findings suggest that this clustered organization could be established through local plasticity mechanisms during development and learning. This review aims to give an overview of the research behind these new insights.

THE DENDRITIC COMPARTMENTALIZATION MODEL

The dendritic tree receives the bulk of synaptic inputs and plays an important role in the integration of incoming signals. It is, therefore, not surprising that the way the dendrite processes synaptic activity to influence somatic firing has been the topic of much research and debate (Poirazi and Mel, 2001; Poirazi et al., 2003; Yuste, 2011). In the classical view the dendrite is seen as a linear integrator, summing the received inputs independently of their position on the dendritic tree as they are transmitted toward the soma. When the linear sum of these inputs reaches a certain threshold value at the soma a non-linear processing step

takes place as an action potential is generated in an all-or-none fashion (**Figure 1**). In this model, known as the integrate-and-fire model (Abbott, 1999), the impact of a single synapse on somatic firing is low since it is merely one input among many available ones. Consequently, the information a single-cell stores is represented in the changing patterns of synaptic weights spanning the entire cell. It is clear that for this "synaptic democracy" (Yuste, 2011) to work the dendrite must propagate and integrate the synaptic signals in a linear and neutral way. Interestingly, recent studies showed that dendrites contain ionic conductances capable of generating active dendritic events in response to local synaptic activity that can mediate non-linear synaptic integration (Schiller et al., 1997; Hausser et al., 2000; Nevian et al., 2007; Yuste, 2011). For example, voltage-gated calcium channels, sodium channels, and NMDA receptor channels facilitate regenerative events that can spread along the entire dendrite. In particular, dendritic NMDA receptor channels can be activated by the synchronous activation of spatially clustered synapses, due to the voltage-sensitive release of the Mg^{2+} block along a 10–20 μm stretch of dendrite (Losonczy and Magee, 2006; Nevian et al., 2007). The charge generated by such a regenerative "NMDA spike" has been shown to be much larger than the linear sum of the synapses involved. Furthermore, the extended time course of NMDA activation causes the charge to be more effectively passed along toward the soma. Even though one NMDA spike might not be sufficient to trigger an action potential, the influence of these spatially clustered synapses on somatic firing is hereby significantly increased. Finally, these non-linear integration properties of dendrites can be adjusted by local plasticity mechanisms (Losonczy et al., 2008).

The described findings show that, much like the non-linear process of action potential generation near the soma in the axon initial segment (Kole and Stuart, 2012), the synchronous activation of neighboring synapses on a sub-branch of the dendrite can lead to their non-linear summation (**Figure 1**). This allows for the implementation of a spatio-temporal coding scheme, resulting in a greater specificity in spiking responses and increased computational capabilities. A new model of synaptic integration has, therefore, been proposed in which the dendritic tree consists of local compartments, each functioning as an individual computational subunit (Hausser and Mel, 2003; Govindarajan et al., 2006; Larkum and Nevian, 2008; for an opposing view see: Yuste, 2011). Modeling studies have shown that neurons utilizing compartmentalized synaptic integration can perform transformations that would normally require multiple neurons connected in a network (Poirazi and Mel, 2001; Wu and Mel, 2009). For instance, models of non-linear integrating neurons that were trained on a pattern recognition problem outperformed their linear integrating counterparts by a factor of 46, correctly learning 27,400 vs. 600 patterns (Poirazi and Mel, 2001). Since these models of synaptic integration are not mutually exclusive it is likely that neurons utilize both linear (Yuste, 2011) and non-linear synaptic integration schemes for different computational tasks.

DIRECT EVIDENCE FOR SYNAPTIC CLUSTERING

While the dendritic compartmentalization model increases the computational capabilities of a neuron, it places additional demands on the synaptic organization that is established during development. Namely, it requires synapses with a synchronized

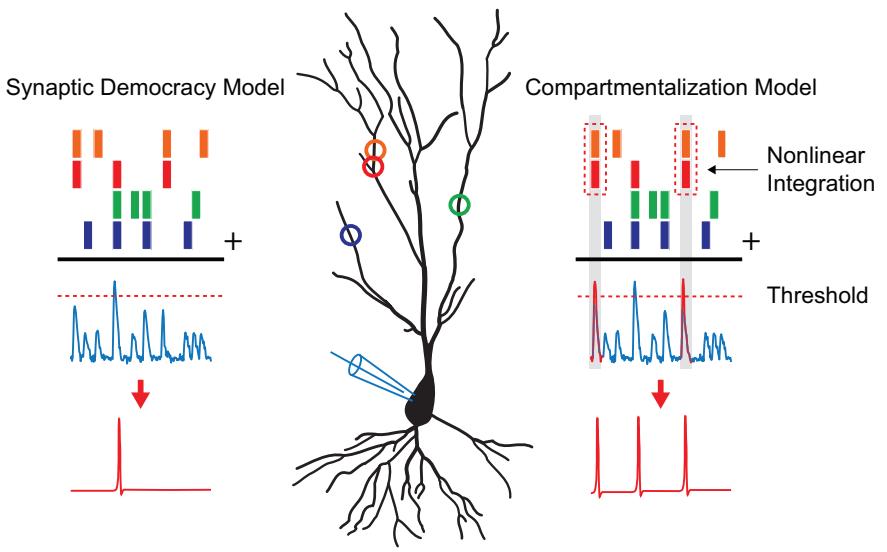

FIGURE 1 | Models of dendritic integration. A pyramidal neuron is depicted with synaptic inputs, represented as colored circles, making distributed contacts along its dendrite. The process of dendritic integration according to the "synaptic democracy" and the "compartmentalization" model are shown. Time points of synaptic input events are represented by the colored bars on top. The blue traces underneath show excitatory postsynaptic potentials as one would record in current clamp. When synaptic inputs reach a certain threshold value (dashed line) an action potential is generated (shown in red) in a non-linear fashion. In the case of the synaptic democracy model, integration is independent of the location of the synaptic inputs. However, when two neighboring synapses are active at the same time in the compartmentalization model (time points highlighted in gray) an additional non-linear step takes place as these inputs are super linearly summated giving them a larger influence on somatic firing.

activity pattern to be clustered close together on the dendrite. Empirical proof that neurons actually adopt such a synaptic organization has long been lacking. Excitingly, a number of papers have been published recently describing synaptic clustering during development and learning.

PLASTICITY OF SYNAPTIC CLUSTERING IN THE OWL AUDITORY SYSTEM

The first study on synaptic clustering *in vivo* was performed in the barn owl auditory localization pathway located in the inferior colliculus (McBride et al., 2008). In this pathway, axons from the lateral shell of the central nucleus (ICCls) send auditory information to the external nucleus (ICX). Here, neurons form a topographic map based on the interaural time difference in the auditory signal received from both ears (Brainard and Knudsen, 1993). Interestingly, a prior study demonstrated that a chronic shift in the visual field, caused by "prism-rearing" of owls, lead to a matching shift in the topographic map of the ICX (DeBello et al., 2001). In this way, visual information functions as an active instructor signal to guide the formation of the auditory spatial map.

The authors speculated that a postsynaptic neuron in the ICX is "taught" to distinguish between input patterns of different spatial locations through the gradual clustering of co-active synaptic inputs. In this case, synaptic contacts that match the spatial tuning of the postsynaptic cell are more likely to be clustered close together and thereby increase their influence on somatic firing. To investigate this possibility an anterograde tracer was used to label ICCls neurons known to represent between 0 and 20° of auditory space. Since the axonal tree of single ICCls neuron spans a large region of the topographic map in the ICX, its co-active synaptic contacts can either match or mismatch the local spatial tuning depending on their relative location. In the case of prism-reared owls this means that every set of synapses from an ICCls neuron falls along an anatomical continuum of adaptation to the shifted tuning of the postsynaptic cells. Their axonal arbors were, therefore, separated into three zones: a central "normal zone" that was located in the matching 0–20° ICX region of the normal topographic map, a lateral "adaptive zone" located in the 0–20° region of the shifted topographic map and a opposing lateral "maladaptive" zone that did not match the tuning of the ICX region in both conditions. Interestingly, the results showed that axo-dendritic contacts in the adaptive zone of prism-reared owls were significantly closer together than those in the normal or maladaptive zone (McBride et al., 2008). These findings could not be explained by a general increase in the number of synapses, because their number remained constant between the different zones. Closer examination showed that inter-contact distances in the adaptive zone were all smaller than 20 μm. This corresponded with the distances between axonal contacts observed in the central adaptive zone of normal juvenile owls. The shift in the spatial field observed in prism-reared owls, therefore, matched the shift in the localization of clustered synaptic inputs. These findings were the first to suggest that experience can drive the clustering of co-active synaptic inputs in order to modulate sensory responses in a behaviorally relevant way (McBride et al., 2008).

SYNAPTIC CLUSTERING DRIVEN BY SPONTANEOUS ACTIVITY

As described above, developing neuronal systems generate spontaneous "bursts" of activity where large parts of the network become active in synchrony (Feller, 1999; Wong, 1999; Ben Ari, 2001). To investigate whether clustering is present at this early stage of development, a recent study by Kleindienst et al. (2011) mapped the synaptic input patterns that are received by a single CA3 pyramidal neuron during spontaneous activity *in vitro*. High speed calcium imaging was combined with whole-cell electrophysiology in order to indentify local calcium transients on the apical dendrite that corresponded with synaptic activation. Synaptic calcium transients occurred at glutamatergic synapses as their activity was sensitive to application of the NMDA receptor antagonist APV.

While the synapses that became activated during a spontaneous network event were found to vary from burst to burst, analysis of the spatio-temporal activity patterns revealed a clear underlying principle: synapses that were closer together on the dendrite ($<16\,\mu m$) were more often co-active then synapses that were farther apart. Anatomical reconstruction of presynaptic axons showed that this observation could not be explained by individual axons making multiple neighboring contacts since axons were found to make a maximum of one contact per postsynaptic cell at this point in development. Furthermore, minimal stimulation of presynaptic axons, that activated single synapses, never lead to the co-activation of neighboring synapses thereby excluding the possibility of spill-over or internal diffusion of signaling factors. These findings suggest that already in this early stage of development (first postnatal week) synapses are organized into local clusters on the dendrite that receive related information (Kleindienst et al., 2011).

Since spontaneous network activity is thought to play a role in establishing connection specificity, the authors speculated that this subcellular organization could be caused by an activity-dependant sorting process during development. To investigate this possibility, a separate set of experiments was performed where TTX was applied to the culture medium during incubation. As predicted, neurons that developed in the absence of spiking activity showed no sign of synaptic clustering after normal network activity was restored. Similarly, synaptic clustering was completely abolished in cells that developed in the presence of the NMDAR antagonist APV, suggesting a role for NMDA-dependent plasticity mechanisms. Thus, spontaneous network activity during development is able to connect neurons with subcellular precision. Specifically, synapses that carry similar information are preferentially clustered together on the dendrite in a process that involves NMDAR-dependent plasticity mechanisms (Kleindienst et al., 2011).

Takahashi et al. (2012) described similar results in older rat hippocampal slice cultures (third postnatal week compared to first week). At this age most synapses are located on spines in contrast to the higher number of spineless synapses observed in the first postnatal week (Kleindienst et al., 2011). Synaptic activity could, therefore, be observed as spontaneous calcium transients confined to single spines after somatic patching with a calcium dye. Similarly, these calcium transients were correlated with EPSPs and sensitive to APV application. Furthermore, when

the activity patterns of these spines were analyzed an almost identical spatio-temporal clustering could be observed. Specifically, spines that were within 8 μm of each other were more often co-active within 100 ms. Again, this clustering effect was found to be dependent on NMDA activity as incubation with APV completely abolished synaptic clustering. Similar recordings made by the authors in fast-spiking parvalbumin neurons showed no signs of clustering, indicating that synaptic clustering is a cell-type specific characteristic. Taken together, these findings suggest that clusters of co-active synapses are not transiently present during a brief period in development but are maintained into more mature stages of the network (Takahashi et al., 2012). This was further confirmed in an additional *in vivo* experiment performed in layer 2/3 of the barrel cortex of anaesthetized young adult mice. Yet again, spontaneous co-activity could often be detected in the spines of these dendrites and this occurrence increased when spines were within a 6 μm stretch of dendrite. Synaptic clustering is thereby shown to be present in live animals.

While the studies described above revealed that spontaneously co-active synapses are clustered on dendrites it remains unclear to what extent functionally clustered inputs are relevant for sensory processing. *In vivo* studies performed in the visual, auditory, and somatosensory cortex of adult mice (Jia et al., 2010; Chen et al., 2011; Varga et al., 2011) showed that short stretches of dendrite contain synapses tuned for different aspects of each modality (e.g., orientation preference or tone frequency). While in some instances inputs may be clustered, a general conclusion cannot be drawn, yet. A fascinating question for future *in vivo* studies is which stimulus characteristics may be encoded in synaptic clusters along dendrites of cortical neurons for different modalities. The answer to this question will have important consequence for our understanding of how sensory inputs are processed in cortical networks.

Comparing the spatial extent of synaptic clustering across the different experimental conditions and developmental ages seems to hint toward a relationship between the increase of synaptic density with age and increased spatially confined synaptic clusters (e.g., 16 and 8 μm at one and three postnatal weeks, respectively, Kleindienst et al., 2011; Takahashi et al., 2012). This may be due to increased competition between neighboring synapses resulting in sharper defined synaptic clusters (see also below; Govindarajan et al., 2006).

EXPERIENCE AND LEARNING-DRIVEN SYNAPTIC CLUSTERING IN THE CORTEX

Since the clustering of synaptic inputs is activity-dependent and most likely involves NMDA-dependent long-term potentiation (LTP) could this mean that synaptic plasticity is similarly clustered on the dendrite? Makino and Malinow (2011) aimed to identify the existence of such clustered plasticity *in vivo*. They investigated the incorporation of fluorescently labeled AMPA receptor subunits GluR1 and GluR2 in the postsynaptic membrane. DNA constructs for these proteins were delivered into layer 2/3 pyramidal neurons in the mouse barrel cortex through in utero electroporation. Targeted cells expressed either the GluR1 or Glur2 subunit coupled to a pH-sensitive form of GFP (Super Ecliptic pHluorin, SEP-GluR1 or SEP-GluR2, respectively) ensuring exclusive fluorescence of the surface expressed subpopulation. Synaptic incorporation of GluR1 and GluR2 were studied separately since the two subunits are involved in different forms of plasticity. Increased exocytosis of GluR1 to the synaptic membrane is known to be specifically involved in the expression of LTP (Takahashi et al., 2003; Feldman and Brecht, 2005). Conversely, GluR2 is not involved in LTP but is important for homeostatic scaling after deprived activity (Gainey et al., 2009). In accordance with these known differences SEP-GluR2 expression was found to be more enriched in spines of mice that had undergone sensory deprivation by whisker-trimming (Makino and Malinow, 2011). Also, enrichment of SEP-GluR1 was higher in spines of mice that had intact whiskers, confirming a role of GluR1 in the expression of activity-dependent LTP. The authors reconstructed dendrites of individual neurons and showed that enrichment of SEP-GluR1 in nearby spines was correlated. Neighboring spines tended to express similar levels of synaptic plasticity, demonstrating that clustered plasticity also occurs *in vivo*. Furthermore, this effect was significantly greater in animals with intact whiskers, suggesting that clustering is dependent on normal synaptic activity. Conversely, no signs of SEP-GluR2 clustering were observed in whisker-trimmed animals even though overall levels were significantly higher. Homeostatic scaling after sensory deprivation, therefore, seems to be achieved by a separate cell-wide increase of synaptic potentiation.

The authors argued that the observed clustering of synaptic plasticity can best be explained by a model in which the induction of potentiation at one synapse can activate kinase signaling pathways to lower the threshold for AMPA receptor incorporation at neighboring synapses (see also below; Harvey and Svoboda, 2007; Harvey et al., 2008). To test this hypothesis a similar set of experiments was performed using a mutated form of GluR1 that is insensitive to phosphorylation by PKC/PKA. Fascinatingly, while the global levels of spine enrichment were similar, these mutated forms of SEP-GluR1 showed no signs of dendritic clustering. Clustering of synaptic plasticity, therefore, occurs in freely behaving animals and is directly dependent on intracellular signal transduction in individual stretches of dendrite (Makino and Malinow, 2011). Takahashi et al. (2012) reported a similar finding: they investigated GFP-GluR1 expression in spines of CA1 pyramidal neurons 24 h after mice were exposed to a novel environment. They found that the probability of observing GFP-GluR1-enriched spines was significantly higher when a neighboring spine within 8 μm was also GFP-positive. Clustered synaptic plasticity could, therefore, also be observed in the hippocampus in response to natural stimuli (e.g., a novel environment).

Additional evidence for synaptic clustering has recently been found in mice during motor learning. Fu et al. (2012) imaged spinogenesis on layer 5 pyramidal neurons in the motor cortex of Thy-1-YFP-H mice as they were trained in a forelimb motor task. Roughly one-third of the newly formed spines that emerged during the acquisition phase of the training appeared next to another novel spine without interspersed existing spines. Clustering of newly formed spines was significant compared to spine formation in both the untrained control mice and during consolidation. Furthermore, clustered spines (<5 μm) had

a significantly higher survival rate at training day 16 as well as four months after training had stopped. Repetitive motor learning is, therefore, found to induce the long-term formation of clustered synaptic contacts (Fu et al., 2012). Importantly, this clustering was found to be task-specific as only very few spines clustered with spines induced by another motor task. While new emerging spines avoided existing spines, most likely due to competition for local resources, they did emerge very close to previously established new spines-related to the same learning task. Learning-induced synaptic clustering, therefore, may be a consequence of local cooperativity between emerging spines-related to the same task.

PLASTICITY MECHANISMS FAVORING SYNAPTIC CLUSTERING

The findings discussed so far show that synapses with synchronized activity patterns are preferentially clustered close together on the dendrite. Furthermore, clustering of synaptic inputs is found to be an activity-dependent process during development and learning. Although the exact underlying mechanism remains unclear, the observation that neighboring synapses undergo similar forms of plasticity seem to suggest that local plasticity plays a role. Interestingly, several local plasticity mechanisms have recently been described which could aid the formation of a clustered synaptic organization through activity-dependent processes.

SYNAPTIC TAGGING AND CAPTURE

Plasticity mechanisms for the establishment of functionally clustered synaptic inputs should act on a local scale within the dendritic arborization. A recently proposed idea is that local plasticity can be mediated by a "synaptic tagging and capture" (STC) mechanism. This mechanism was first described on the level of individual cells in a classic study by Frey and Morris (1997) where they found that cooperation can take place between synapses. Specifically, they found that tetanus field stimulation in the Schaffer collateral—CA1 pathway that induced LTP in one set of synapses facilitated the expression of LTP in a different set of synapses which received a subthreshold stimulus. This effect could even be observed when the two stimulations were separated by more than 1 h. The authors proposed that the induction of LTP leads to the creation of a protein synthesis independent synaptic "tag" which "captures" plasticity-related proteins needed for the induction of LTP (Frey and Morris, 1997). Since plasticity-related proteins are not confined to individual synapses, the proteins sequestered by a synaptic tag do not have to be generated by the same event that caused the setting of the tag.

To fully understand how cooperation between synapses influences the storage of memory engrams it is important to consider where activity-induced protein synthesis takes place. It has been suggested that protein synthesis can occur in ribosomes localized to individual synapses (Steward and Levy, 1982; Steward and Schuman, 2003). Assuming that plasticity-related proteins spread from the location of the synapse whose activity lead to their generation it could be hypothesized that STC preferentially occurs at clusters of neighboring synapses on the dendrite (Govindarajan et al., 2006). A study by Govindarajan et al. (2011) investigated this possibility by identifying the spatio-temporal characteristics of STC at the level of individual spines. To induce LTP at a single spine they combined high-frequency glutamate uncaging with bath application of forskolin (Govindarajan et al., 2011). Conversely, glutamate uncaging in the absence of forskolin resulted in shorter lived potentiation. The authors found, in accordance with the STC model, that stimulation of one spine in the presence of forskolin followed by stimulation of a second spine in the absence of forskolin lead to LTP expression in both spines (Govindarajan et al., 2011). Importantly, the efficiency of STC expression depended on the distance between the two stimulated spines and was almost completely undetectable at 70 μm (**Figure 2A**).

These findings show that STC preferentially occurs at neighboring synapses, making the dendritic branch the preferred site for cooperation and association between synapses. Conversely, since the presence of plasticity-related proteins appear as the rate-limiting factor in LTP, coupled with the observed faster degradation of plasticity-related proteins compared to synaptic tags; it is imaginable that competition takes place between tagged synapses for sparsely available plasticity-related proteins. Indeed, the stimulation of just two spines during STC already resulted in both spines reaching their maximum size more slowly (Govindarajan et al., 2011). In some cases the growth of one stimulated spine could even be correlated with the shrinking of another. The presence of a limited plasticity-related protein pool may, therefore, cause competition between multiple tagged synapses on the same dendritic branch. This kind of competition could explain the previously observed relationship between the increased synaptic density with age and sharper spatially defined synaptic clusters (see above).

METAPLASTICITY THROUGH LOCAL SYNAPTIC ACTIVITY

The induction of long-term plasticity requires the activation of various signaling cascades in order to stimulate the necessary protein synthesis. One of these signaling cascades involves mitogen-activated protein kinase (MAPK) and mechanistic target of rapamycin (mTOR; Kelleher III et al., 2004a,b). Since MAPK and mTOR remain active for several minutes after activation by plasticity-inducing stimulation, it has been suggested that this pathway could lower the threshold for plasticity in neighboring synaptic activity for a certain period of time (Wu et al., 2001; Govindarajan et al., 2006). Such processes that reflect a higher order level of plasticity, or the "plasticity" of plasticity mechanisms, have collectively been referred to as "metaplasticity" (Abraham et al., 2001; Abraham, 2008). If the threshold for plasticity induction is indeed regulated by local synaptic activity, synapses that are active shortly after LTP induction at a neighboring synapse would have a higher chance of also becoming potentiated. As a consequence, neighboring synapses with similar activity patterns would be preferentially potentiated and stabilized. To test this possibility Harvey and Svoboda (2007) investigated spike-timing-dependent potentiation (STDP) in neighboring spines of hippocampal pyramidal neurons. Here, STDP was induced in single spines using two-photon glutamate uncaging followed by the initiation of three action potentials. Similar to classical experiments of STDP, the magnitude of plasticity was found to decrease

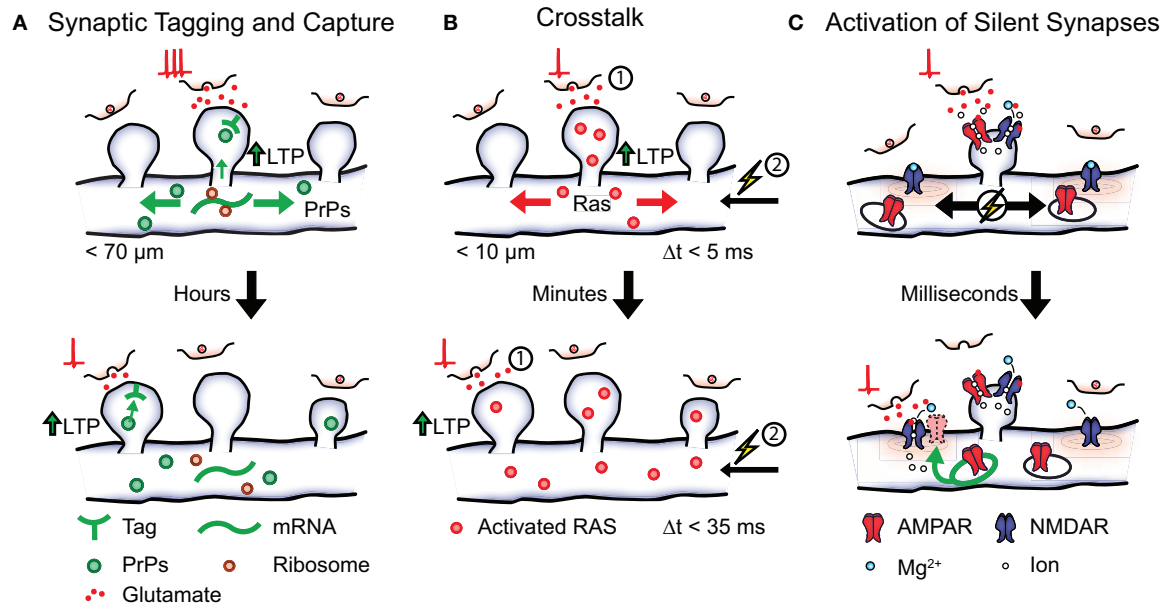

FIGURE 2 | Possible local plasticity mechanisms that establish synaptic clustering. Shown is a local stretch of dendrite containing three synaptic spines. **(A)** Synaptic tagging and capture. Strong postsynaptic activation leads to the synthesis of plasticity-related proteins (PrPs) that become available in local stretches of dendrite. Synapses tagged within a timescale of hours by weak activation (shown below) can capture plasticity-related proteins in order to express long lasting LTP. **(B)** Crosstalk. Postsynaptic activation (1) followed by action potential firing (2, spike-timing window <5 ms) leads to the induction of LTP and causes activated RAS from the stimulated spine to spread into the dendrite. The presence of activated RAS increases the spike-timing window (<35 ms) of later active synapses (timescale of minutes) thereby lowering the threshold for LTP induction. **(C)** Activation of silent synapses. Shown are two silent synapses present on the dendritic shaft that do not express AMPA receptors on their surface, next to an active synaptic spine. Activation of the non-silent spine leads to a local depolarization of the membrane causing the removal of the Mg^{2+} block from NMDA receptors in the neighboring synapses. A silent synapse whose presynaptic cell fires coincidently undergoes Hebbian plasticity resulting in the insertion of intracellular AMPA receptors and its eventual stabilization.

as the time between glutamate uncaging and action potential initiation increased. Specifically, the increase in uEPSC amplitude and spine volume could not be observed with a spike time window larger than 5 ms. However, it was found that previous induction of LTP in one spine broadened the spike time window of STDP in neighboring spines (up to 35 ms; **Figure 2B**). No change in STDP was observed when the time between stimulation of the two spines increased up to 10 min or when their relative distance exceeded 10 µm. Taken together, these findings show that the threshold for plasticity-induction at an individual spine can be influenced by the activity of neighboring synapses. Unlike STC, the effect was independent of protein synthesis and did not occur when the weak stimulation protocol preceded the LTP protocol (Harvey and Svoboda, 2007). This phenomenon is, therefore, referred to as "crosstalk" in order to distinguish it from STC mechanisms.

One of the early activators of the MAPK signaling pathway is the guanosine triphosphatase (GTPase) Ras. This GTPase becomes activated by NMDAR-induced calcium influx and is involved in the induction of LTP (Zhu et al., 2002). In order to uncover if activated RAS remains confined to single spines a later study by Harvey et al. (2008) used a fluorescence resonance energy transfer (FRET) based indicator of RAS activation. The authors observed a robust increase of RAS activity after LTP induction in stimulated spines that peaked within 1 min and returned to baseline after 15 min. Interestingly, the magnitude of RAS activation correlated with the observed increase in spine volume while no RAS activation could be observed during a subthreshold LTP protocol. Once activated, RAS spread over several micrometers in both directions of the dendrite and subsequently invaded neighboring spines. Since both the spatial and temporal activation profile of RAS closely matched those observed in the crosstalk experiments the authors speculated that RAS activation could be involved in the expression of crosstalk. This was confirmed in a subsequent experiment where crosstalk was prevented by the local application of a pharmacological blocker for MAPK and extracellular signal-regulated kinase (ERK; Harvey et al., 2008). These findings show that Ca^{2+}-activated signaling machinery can regulate the threshold for plasticity induction in local stretches of dendrite. In this way the occurrence of strong LTP-inducing activity at one synapse can lower the threshold for potentiation at neighboring synapses, thereby aiding the storage of memory engrams in clusters of synapses on the dendrite (**Figure 2B**). Interestingly, local diffusion (<5 µm) has also been observed for the GTPase RhoA upon spine activation while yet another GTPase (CDC42) showed no such spatial characteristics (Murakoshi et al., 2011). Individual elements of the MAPK pathway could, therefore, be differentially involved in the expression of this local plasticity mechanism.

SILENT SYNAPSES AND AMPA RECEPTOR REGULATION

Developmental networks are frequently characterized by a high incidence of synapses that can be identified structurally, but—under regular signaling conditions—do not mediate synaptic transmission. For example, developing synapses can switch between an AMPA signaling state and an AMPA "silent" state (Hanse et al., 2009). In the "silent" state no AMPARs are present on the postsynaptic membrane and the synapse is, therefore, unable to generate an EPSP in native conditions due to the Mg^{2+} block present in NMDARs (Liao et al., 1995). Since activation of silent synapses requires the depolarization of the local membrane: could the preferential un-silencing of co-active synapses be another possible mechanism for the establishment of synaptic clusters? Once a synapse becomes silent it can be reactivated (unsilenced) by participating in Hebbian-like activity patterns and thereby regaining its AMPA signaling capabilities. It will be interesting to investigate, whether membrane depolarization caused by local synaptic activity is sufficient to lead to NMDA activation in neighboring silent synapses (but not in more distant ones). In this case a silent synapse whose activity is synchronized with the activity of its neighbors will have a higher chance of becoming un-silenced and subsequently stabilized (**Figure 2C**). Over time this would lead to the establishment of synaptic clusters with similar activity patterns through activity-dependent self-organization.

SUMMARY AND CONCLUSION

The local plasticity mechanisms discussed here converge on one general theme: the activity of one synapse can modulate the plasticity at neighboring synapses and thereby influence their fate. This can be through the mutual sharing of plasticity-related proteins (STC), adaptation of a local plasticity threshold (metaplasticity), or by the activation of synchronized synaptic inputs (e.g., un-silencing). These mechanisms operate within different temporal domains, ranging from hour to millisecond time scales (**Figure 2**). Such timing differences may assist the coupling of inputs during different developmental and plasticity paradigms. For example, clustering of coincident synaptic activation during bursts of spontaneous activity mediated by local activation of silent synapses may facilitate connecting inputs with similar signaling properties to a common dendrite during development. On the other hand, learning based on long-term experience may require plasticity mechanisms that integrate information over longer periods of time, such as STC.

Together these findings suggest a series of events leading to the establishment and refinement of connectivity with subcellular precision. First, clustering of synchronized synaptic inputs arises through an activity-dependent sorting process during development. Initially, synaptic contacts are established in a (more or less) random fashion along a dendrite. Then, bursts of spontaneous synaptic inputs help to select a portion of these synaptic contacts through local cooperation and competition. Synapses that are temporally synchronized with their neighbors get preferentially strengthened and stabilized through local plasticity mechanisms while synapses that are desynchronized with their surroundings get eliminated. These simple self-organizational principles will over time lead to the establishment of functional clusters of synaptic inputs on the dendrite. During development the established synaptic clusters could function as a principal site for rudimentary pattern recognition, even before sensory information is received. Subsequently, when sensory systems become functional during interactions with the environment, synaptic reorganization continues to adapt synaptic clusters through experience-driven and learning-induced activity.

As described above, clustering functional inputs is most likely required to harvest the full computational power of individual neurons. Therefore, errors in wiring at this level will compromise the capacity of neurons to process information. Interestingly, various cognitive developmental disorders have been linked to alterations in synaptic organization. For instance, neuroanatomical evidence suggests that brains of autism patients show higher levels of local connectivity that impede the formation of long-range connections necessary for central cognitive control (Belmonte et al., 2004; Geschwind and Levitt, 2007). Whether these alterations are due to increased synapse formation or deficits in synapse elimination and pruning are currently unknown. In this light, one might speculate that perturbed synaptic clustering may cause neurocognitive disorders that are associated with deficits in synaptic connectivity (Zoghbi, 2003; Belmonte et al., 2004; Geschwind and Levitt, 2007).

ACKNOWLEDGMENTS

We thank Christian Levelt, Helmut Kessels, and Maarten Kole for their suggestions and valuable comments on the manuscript.

REFERENCES

Abbott, L. F. (1999). Lapicque's introduction of the integrate-and-fire model neuron (1907). *Brain Res. Bull.* 50, 303–304.

Abraham, W. C. (2008). Metaplasticity: tuning synapses and networks for plasticity. *Nat. Rev. Neurosci.* 9, 387.

Abraham, W. C., Mason-Parker, S. E., Bear, M. F., Webb, S., and Tate, W. P. (2001). Heterosynaptic metaplasticity in the hippocampus *in vivo*: a BCM-like modifiable threshold for LTP. *Proc. Natl. Acad. Sci. U.S.A.* 98, 10924–10929.

Belmonte, M. K., Allen, G., Beckel-Mitchener, A., Boulanger, L. M., Carper, R. A., and Webb, S. J. (2004). Autism and abnormal development of brain connectivity. *J. Neurosci.* 24, 9228–9231.

Ben Ari, Y. (2001). Developing networks play a similar melody. *Trends Neurosci.* 24, 353–360.

Ben-Ari, Y., Cherubini, E., Corradetti, R., Galarsa, J.-L. (1989). Giant synaptic potentials in immature rat CA3 hippocampal neurones. *J. Physiol.* 416, 303–325.

Brainard, M. S., and Knudsen, E. I. (1993). Experience-dependent plasticity in the inferior colliculus: a site for visual calibration of the neural representation of auditory space in the barn owl. *J. Neurosci.* 13, 4589–4608.

Branco, T., and Hausser, M. (2010). The single dendritic branch as a fundamental functional unit in the nervous system. *Curr. Opin. Neurobiol.* 20, 494–502.

Chen, X., Leischner, U., Rochefort, N. L., Nelken, I., and Konnerth, A. (2011). Functional mapping of single spines in cortical neurons *in vivo*. *Nature* 475, 501–505.

Chklovskii, D. B., Mel, B. W., and Svoboda, K. (2004). Cortical rewiring and information storage. *Nature* 431, 782–788.

Cline, H. (2003). Sperry and Hebb: oil and vinegar? *Trends Neurosci.* 26, 655–661.

DeBello, W. M. (2008). Micro-rewiring as a substrate for learning. *Trends Neurosci.* 31, 577–584.

DeBello, W. M., Feldman, D. E., and Knudsen, E. I. (2001). Adaptive axonal remodeling in the midbrain auditory space map. *J. Neurosci.* 21, 3161–3174.

Feldman, D. E., and Brecht, M. (2005). Map plasticity in somatosensory cortex. *Science* 310, 810–815.

Feller, M. B. (1999). Spontaneous correlated activity in developing neural circuits. *Neuron* 22, 653–656.

Frey, U., and Morris, R. G. M. (1997). Synaptic tagging and long-term potentiation. *Nature* 385, 533–536.

Fu, M., Yu, X., Lu, J., and Zuo, Y. (2012). Repetitive motor learning induces coordinated formation of clustered dendritic spines *in vivo*. *Nature* 483, 92–95.

Fu, M., and Zuo, Y. (2011). Experience-dependent structural plasticity in the cortex. *Trends Neurosci.* 34, 177–187.

Gainey, M. A., Hurvitz-Wolff, J. R., Lambo, M. E., and Turrigiano, G. G. (2009). Synaptic scaling requires the GluR2 subunit of the AMPA receptor. *J. Neurosci.* 29, 6479–6489.

Galli, L., and Maffei, L. (1988). Spontaneous impulse activity of rat retinal ganglion cells in prenatal life. *Science* 242, 90–91.

Garaschuk, O., Hanse, E., and Konnerth, A. (1998). Developmental profile and synaptic origin of early network oscillations in the CA1 region of rat neonatal hippocampus. *J. Physiol.* 507, 219–236.

Geschwind, D. H., and Levitt, P. (2007). Autism spectrum disorders: developmental disconnection syndromes. *Curr. Opin. Neurobiol.* 17, 103–111.

Goodman, C. S., and Shatz, C. J. (1993). Developmental mechanisms that generate precise patterns of neuronal connectivity. *Cell* 72, 77–98.

Govindarajan, A., Israely, I., Huang, S. Y., and Tonegawa, S. (2011). The dendritic branch is the preferred integrative unit for protein synthesis-dependent LTP. *Neuron* 69, 132–146.

Govindarajan, A., Kelleher, R. J., and Tonegawa, S. (2006). A clustered plasticity model of long-term memory engrams. *Nat. Rev. Neurosci.* 7, 575–583.

Hanse, E., Taira, T., Lauri, S., and Groc, L. (2009). Glutamate synapse in developing brain: an integrative perspective beyond the silent state. *Trends Neurosci.* 32, 532–537.

Harvey, C. D., and Svoboda, K. (2007). Locally dynamic synaptic learning rules in pyramidal neuron dendrites. *Nature* 450, 1195–1200.

Harvey, C. D., Yasuda, R., Zhong, H., and Svoboda, K. (2008). The spread of Ras activity triggered by activation of a single dendritic spine. *Science* 321, 136–140.

Hausser, M., and Mel, B. (2003). Dendrites: bug or feature? *Curr. Opin. Neurobiol.* 13, 372–383.

Hausser, M., Spruston, N., and Stuart, G. J. (2000). Diversity and dynamics of dendritic signaling. *Science* 290, 739–744.

Hofer, S. B., Mrsic-Flogel, T. D., Bonhoeffer, T., and Hubener, M. (2006). Lifelong learning: ocular dominance plasticity in mouse visual cortex. *Curr. Opin. Neurobiol.* 16, 451–459.

Hua, J. Y., and Smith, S. J. (2004). Neural activity and the dynamics of central nervous system development. *Nat. Neurosci.* 7, 327–332.

Huberman, A. D., Feller, M. B., and Chapman, B. (2008). Mechanisms underlying development of visual maps and receptive fields. *Annu. Rev. Neurosci.* 31, 479–509.

Jia, H., Rochefort, N. L., Chen, X., and Konnerth, A. (2010). Dendritic organization of sensory input to cortical neurons *in vivo*. *Nature* 464, 1307–1312.

Karmarkar, U. R., and Dan, Y. (2006). Experience-dependent plasticity in adult visual cortex. *Neuron* 52, 577–585.

Katz, L. C., and Shatz, C. J. (1996). Synaptic activity and the construction of cortical circuits. *Science* 274, 1133–1138.

Kelleher, R. J. III, Govindarajan, A., Jung, H. Y., Kang, H., and Tonegawa, S. (2004a). Translational control by MAPK signaling in long-term synaptic plasticity and memory. *Cell* 116, 467–479.

Kelleher, R. J. III, Govindarajan, A., and Tonegawa, S. (2004b). Translational regulatory mechanisms in persistent forms of synaptic plasticity. *Neuron* 44, 59–73.

Kleindienst, T., Winnubst, J., Roth-Alpermann, C., Bonhoeffer, T., and Lohmann, C. (2011). Activity-dependent clustering of functional synaptic inputs on developing hippocampal dendrites. *Neuron* 72, 1012–1024.

Kole, M. H., and Stuart, G. J. (2012). Signal processing in the axon initial segment. *Neuron* 73, 235–247.

Larkum, M. E., and Nevian, T. (2008). Synaptic clustering by dendritic signalling mechanisms. *Curr. Opin. Neurobiol.* 18, 321–331.

Liao, D., Hessler, N. A., and Malinow, R. (1995). Activation of postsynaptically silent synapses during pairing-induced LTP in CA1 region of hippocampal slice. *Nature* 375, 400–404.

Losonczy, A., and Magee, J. C. (2006). Integrative properties of radial oblique dendrites in hippocampal CA1 pyramidal neurons. *Neuron* 50, 291–307.

Losonczy, A., Makara, J. K., and Magee, J. C. (2008). Compartmentalized dendritic plasticity and input feature storage in neurons. *Nature* 452, 436–441.

Makino, H., and Malinow, R. (2011). Compartmentalized versus global synaptic plasticity on dendrites controlled by experience. *Neuron* 72, 1001–1011.

McBride, T. J., Rodriguez-Contreras, A., Trinh, A., Bailey, R., and DeBello, W. M. (2008). Learning drives differential clustering of axodendritic contacts in the barn owl auditory system. *J. Neurosci.* 28, 6960–6973.

Meister, M., Wong, R. O. L., Baylor, D. A., and Shatz, C. J. (1991). Synchronous bursts of action potentials in ganglion cells of the developing mammalian retina. *Science* 252, 939–943.

Mrsic-Flogel, T. D., Hofer, S. B., Creutzfeldt, C., Cloez-Tayarani, I., Changeux, J. P., Bonhoeffer, T., and Hubener, M. (2005). Altered map of visual space in the superior colliculus of mice lacking early retinal waves. *J. Neurosci.* 25, 6921–6928.

Murakoshi, H., Wang, H., and Yasuda, R. (2011). Local, persistent activation of Rho GTPases during plasticity of single dendritic spines. *Nature* 472, 100–104.

Nevian, T., Larkum, M. E., Polsky, A., and Schiller, J. (2007). Properties of basal dendrites of layer 5 pyramidal neurons: a direct patch-clamp recording study. *Nat. Neurosci.* 10, 206–214.

O'Donovan, M., Ho, S., and Yee, W. (1994). Calcium imaging of rhythmic network activity in the developing spinal cord of the chick embryo. *J. Neurosci.* 14, 6354–6369.

Poirazi, P., Brannon, T., and Mel, B. W. (2003). Pyramidal neuron as two-layer neural network. *Neuron* 37, 989–999.

Poirazi, P., and Mel, B. W. (2001). Impact of active dendrites and structural plasticity on the memory capacity of neural tissue. *Neuron* 29, 779–796.

Polsky, A., Mel, B. W., and Schiller, J. (2004). Computational subunits in thin dendrites of pyramidal cells. *Nat. Neurosci.* 7, 621–627.

Sanes, J. R., and Yamagata, M. (2009). Many paths to synaptic specificity. *Annu. Rev. Cell Dev. Biol.* 25, 161–195.

Schiller, J., Schiller, Y., Stuart, G., and Sakmann, B. (1997). Calcium action potentials restricted to distal apical dendrites of rat neocortical pyramidal neurons. *J. Physiol.* 505(Pt 3), 605–616.

Steward, O., and Levy, W. B. (1982). Preferential localization of polyribosomes under the base of dendritic spines in granule cells of the dentate gyrus. *J. Neurosci.* 2, 284–291.

Steward, O., and Schuman, E. M. (2003). Compartmentalized synthesis and degradation of proteins in neurons. *Neuron* 40, 347–359.

Takahashi, N., Kitamura, K., Matsuo, N., Mayford, M., Kano, M., Matsuki, N., and Ikegaya, Y. (2012). Locally synchronized synaptic inputs. *Science* 335, 353–356.

Takahashi, T., Svoboda, K., and Malinow, R. (2003). Experience strengthening transmission by driving AMPA receptors into synapses. *Science* 299, 1585–1588.

Torborg, C. L., Hansen, K. A., and Feller, M. B. (2005). High frequency, synchronized bursting drives eye-specific segregation of retinogeniculate projections. *Nat. Neurosci.* 8, 72–78.

Varga, Z., Jia, H., Sakmann, B., and Konnerth, A. (2011). Dendritic coding of multiple sensory inputs in single cortical neurons *in vivo*. *Proc. Natl. Acad. Sci. U.S.A.* 108, 15420–15425.

Weliky, M., and Katz, L. C. (1997). Disruption of orientation tuning in visual cortex by artificially correlated neuronal activity. *Nature* 386, 680–685.

Wong, R. O. L. (1999). Retinal waves and visual system development. *Annu. Rev. Neurosci.* 22, 29–47.

Wu, G. Y., Deisseroth, K., and Tsien, R. W. (2001). Spaced stimuli stabilize MAPK pathway activation and its effects on dendritic morphology. *Nat. Neurosci.* 4, 151–158.

Wu, X. E., and Mel, B. W. (2009). Capacity-enhancing synaptic learning rules in a medial temporal lobe online learning model. *Neuron* 62, 31–41.

Xu, H. P., Furman, M., Mineur, Y. S., Chen, H., King, S. L., Zenisek, D., Zhou, Z. J., Butts, D. A., Tian, N., Picciotto, M. R., and Crair, M. C. (2011). An instructive role for patterned spontaneous retinal activity in mouse visual map development. *Neuron* 70, 1115–1127.

Yuste, R. (2011). Dendritic spines and distributed circuits. *Neuron* 71, 772–781.

Yuste, R., Peinado, A., and Katz, L. C. (1992). Neuronal domains in

developing neocortex. *Science.* 257, 666–669.

Zhu, J. J., Qin, Y., Zhao, M., Van, A. L., and Malinow, R. (2002). Ras and Rap control AMPA receptor trafficking during synaptic plasticity. *Cell* 110, 443–455.

Zoghbi, H. Y. (2003). Postnatal neurodevelopmental disorders: meeting at the synapse? *Science* 302, 826–830.

Conflict of Interest Statement: The authors declare that the research was conducted in the absence of any commercial or financial relationships that could be construed as a potential conflict of interest.

Received: 15 March 2012; paper pending published: 30 March 2012; accepted: 14 May 2012; published online: 31 May 2012.

Citation: Winnubst J and Lohmann C (2012) Synaptic clustering during development and learning: the why, when, and how. Front. Mol. Neurosci. ***5****:70. doi: 10.3389/fnmol.2012.00070*

frontiers in
MOLECULAR NEUROSCIENCE

ORIGINAL RESEARCH ARTICLE
published: 16 May 2012
doi: 10.3389/fnmol.2012.00065

Cortical development of AMPA receptor trafficking proteins

Kathryn M. Murphy[1,2]*, Lilia Tcharnaia[1], Simon P. Beshara[1] and David G. Jones[3]

[1] *McMaster Integrative Neuroscience Discovery and Study Program, McMaster University, Hamilton, ON, Canada*
[2] *Psychology, Neuroscience and Behaviour, McMaster University, Hamilton, ON, Canada*
[3] *Pairwise Affinity Inc., Dundas, ON, Canada*

Edited by:
Robert W. Burgess, The Jackson Laboratory, USA

Reviewed by:
Arianna Maffei, SUNY Stony Brook, USA
Da-Ting Lin, The Jackson Laboratory, USA

****Correspondence:***
Kathryn M. Murphy, McMaster Integrative Neuroscience Discovery and Study (MiNDS), McMaster University, 1280 Main Street West, Hamilton, ON L8S 4K1, Canada.
e-mail: kmurphy@mcmaster.ca

AMPA-receptor trafficking plays a central role in excitatory plasticity, especially during development. Changes in the number of AMPA receptors and time spent at the synaptic surface are important factors of plasticity that directly affect long-term potentiation (LTP), long-term depression (LTD), synaptic scaling, and the excitatory-inhibitory (E/I) balance in the developing cortex. Experience-dependent changes in synaptic strength in visual cortex (V1) use a molecularly distinct AMPA trafficking pathway that includes the GluA2 subunit. We studied developmental changes in AMPA receptor trafficking proteins by quantifying expression of GluA2, pGluA2 (GluA2serine880), GRIP1, and PICK1 in rat visual and frontal cortex. We used Western Blot analysis of synaptoneurosome preparations of rat visual and frontal cortex from animals ranging in age from P0 to P105. GluA2 and pGluA2 followed different developmental trajectories in visual and frontal cortex, with a brief period of over expression in frontal cortex. The over expression of GluA2 and pGluA2 in immature frontal cortex raises the possibility that there may be a period of GluA2-dependent vulnerability in frontal cortex that is not found in V1. In contrast, GRIP1 and PICK1 had the same developmental trajectories and were expressed very early in development of both cortical areas. This suggests that the AMPA-interacting proteins are available to begin trafficking receptors as soon as GluA2-containing receptors are expressed. Finally, we used all four proteins to analyze the surface-to-internalization balance and found that this balance was roughly equal across both cortical regions, and throughout development. Our finding of an exquisite surface-to-internalization balance highlights that these AMPA receptor trafficking proteins function as a tightly controlled system in the developing cortex.

Keywords: AMPA receptor, trafficking, critical period, GRIP, PICK1, visual cortex, frontal cortex, synaptic plasticity

INTRODUCTION

Functional maturation of the cortex is linked with dynamic changes in excitatory signaling via the glutamatergic system. Glutamate is the main excitatory neurotransmitter in the cortex and its action is mediated by three ionotropic receptors, N-Methyl-D-aspartic acid (NMDA), kainate, and 2-amino-3-(5-methyl-3-oxo-1,2-oxazol-4-yl) propanoic acid (AMPA) (Hollmann and Heinemann, 1994). Both NMDA and AMPA receptors are major players in the experience-dependent and dynamic changes that mark the critical period for synaptic plasticity in development (Collingridge and Singer, 1990; Malenka and Bear, 2004). Expression levels, subunit composition, and dynamic trafficking of these receptors effect development by influencing synaptic plasticity. In particular, a number of studies of visual cortical development have linked changes in AMPA receptor expression and cycling with long-term potentiation (LTP) (Malenka and Bear, 2004), long-term depression (LTD) (Heyen et al., 2003), synaptic scaling (Turrigiano and Nelson, 2004), and the excitatory-inhibitory (E/I) balance (Beston et al., 2010).

AMPA receptors are concentrated at synapses where they mediate the fast component (2 ms) of excitatory post-synaptic currents (EPSC) (Kleppe and Robinson, 1999). Typically, nascent glutamatergic synapses have NMDA receptors but lack AMPA receptors which are progressively recruited to the developing synapse (Petralia et al., 1999) by a rapid, activity-dependent process that increases the phosphorylation of surface AMPA receptors (Liao et al., 2001). Structurally, AMPA receptors are composed of four homologous subunits, GluA1-GluA4, that combine in varying stoichiometries to form ion channels with distinct functional properties (Hollmann and Heinemann, 1994; Dingledine et al., 1999). Most AMPA receptors contain the GluA2 subunit, which gives the receptor the characteristic qualities of calcium impermeability (Hollmann and Heinemann, 1994) and a linear current-voltage relationship (Hollmann and Heinemann, 1994; Dingledine et al., 1999). The expression of GluA2 increases with development in visual cortex (V1) (Herrmann, 1996) and is affected by monocular deprivation (Beston et al., 2010), that can lead to LTD in the deprived cortex (Heyen et al., 2003). Furthermore, blocking neural activity with tetrodotoxin (TTX) has been found to induce synaptic scaling in cultured visual cortical neurons leading to the insertion of GluA2 AMPA receptors at the synaptic surface (Gainey et al., 2009).

AMPA receptors undergo multiple transcriptional and translational modifications that regulate and establish receptor function (Song and Huganir, 2002). The phosphorylation state of the receptor plays an important role in regulating synaptic plasticity (Raymond et al., 1993). For example, phosphorylation of GluA1 receptors at serine 845 is necessary for binocular deprivation to induce synaptic scaling in V1 (Goel et al., 2011). In addition, phosphorylation of GluA2 at serine 880 (pGluA2) is involved in LTD induction in the cerebellum (Chung et al., 2003) and hippocampus (Kim et al., 2001). Finally, brief monocular deprivation leads to phosphorylation of GluA2 receptors at serine 880 and subsequent induction of LTD in V1 (Heyen et al., 2003).

Results of electrophysiological studies of silent synapses in hippocampus first suggested that AMPA receptor levels are regulated (Isaac et al., 1995; Liao et al., 1995; Durand et al., 1996). Then AMPA receptor trafficking was directly characterized in cultured neurons treated with various pharmacological agents (Lissin et al., 1998; O'Brien et al., 1998). Enhancing or reducing synaptic function resulted in increases or decreases in AMPA receptor function, respectively, as measured by changes in mEPSC and receptor accumulation (Lissin et al., 1998; O'Brien et al., 1998). The trafficking processes of endocytosis, exocytosis, and recycling of AMPA receptors are highly regulated and require specific AMPA receptor-interacting proteins. GRIP1 and PICK1 are involved in trafficking GluA2-containing AMPA receptors in and out of the synapse (Chung et al., 2000), where GRIP1 is involved in stabilization of GluA2 containing receptors at the synaptic surface (Dong et al., 1997) and PICK1 stabilizes intracellular pools of the subunit (Gardner et al., 2005; Liu and Cull-Candy, 2005). To maintain homeostasis, AMPA receptor levels at the synaptic surface are dynamically regulated to compensate for variations in input (Turrigiano and Nelson, 2004). Interfering with GRIP1 function results in decreased GluA2 accumulation at the synaptic surface (Osten et al., 2000) and a loss of PICK1 function occludes synaptic scaling (Anggono et al., 2011). Together these results suggest that a balance between GRIP1 and PICK1 is an important part of the AMPA trafficking mechanism.

AMPA receptors cycle rapidly in and out of the synapse, and the relative levels of surface and internal pools of receptors contribute to controlling synaptic strength. Furthermore, synaptic scaling in the V1 depends on the trafficking of GluA2-containing AMPA receptors to the synaptic surface (Gainey et al., 2009) and depression of deprived-eye responses after monocular deprivation is dependent on internalization of those receptors (Yoon et al., 2009). Thus, experience-dependent changes in synaptic strength in V1 uses a molecularly distinct AMPA trafficking pathway.

In this study, we examined development of the synaptic proteins (GluA2, pGluA2, GRIP1, PICK1) involved that molecularly distinct AMPA trafficking pathway and compared the maturation of those proteins in visual and frontal cortex. Variations in the balance among the trafficking proteins will have profound effects on the dynamic nature of AMPA receptors and developmental plasticity that depends on AMPA receptors. Using Western blot analysis, we quantified the developmental trajectories in visual and frontal cortex and analyzed the balances among these synaptic proteins. We show a difference between visual and frontal cortex in the developmental trajectories for GluA2 and pGluA2, with a brief period of over expression in frontal cortex. In contrast, the AMPA interacting proteins GRIP1 and PICK1 followed similar development in visual and frontal cortex. Finally, we show that analysis of all four components uncovers a common surface-to-internalization balance in visual and frontal cortex and that balance is maintained during development. This result implies that the trafficking system for GluA2-containing AMPA receptors is tightly controlled and develops as an integrated network across the cortex.

MATERIALS AND METHODS

ANIMALS AND TISSUE SAMPLES

We studied changes in expression of a set of proteins involved in AMPA receptor trafficking in visual and frontal cortex of 28 Long–Evans rats (postnatal age 0–105 days). The animals were reared with normal visual experience in standard housing conditions and all experimental procedures were approved by the McMaster University Animal Research Ethics Board.

Cortical tissue samples were collected from V1 and frontal cortex guided by stereotaxic coordinates (Paxinos and Watson, 2007). Rats were euthanized with Euthanol (sodium pentobarbital, 0.165 mg/g) and were transcardially perfused with cold 0.1 M Phosphate Buffered Saline (PBS, 4 C; pup: 1–2 ml/min; adult: 4–5 ml/min) until the circulating fluid was clear. The brain was removed from the skull and immersed in cold PBS. Small tissue samples (approximately 2 × 2 mm) of presumptive V1 and frontal cortex were taken, rapidly frozen on dry ice, and stored at −80°C.

TISSUE SAMPLE PREPARATION

The frozen tissue sample was suspended in cold tissue homogenization buffer (1 ml buffer: 50 mg tissue, 10 mM HEPES, 2 mM EDTA, 2 mM EGTA, 0.5 mM DTT, 10 mg/L leupeptin, 50 mg/L soybean trypsin inhibitor, 100 nM microcystin, 0.1 mM PMSF), and homogenized using a glass-glass Dounce homogenizer (Kontes, Vineland, NJ). A subcellular fractionation procedure (synaptoneurosomes) (Hollingsworth et al., 1985; Titulaer and Ghijsen, 1997; Quinlan et al., 1999) was used to obtain protein samples that were enriched for synaptic proteins. The homogenate was passed through a 5 μm pore hydrophillic mesh filter (Millipore, Billerica, MA, USA) then centrifuged at 4°C and 1000 × g for 20 min to obtain the synaptic fraction of the membrane. The supernatant was removed, leaving a pellet enriched for synaptic proteins, the synaptoneurosome. The synaptic pellet was re-suspended in boiling 1% sodium-dodecyl-sulfate (SDS) and stored at −20°C. Protein concentrations were determined using the bicinchonic acid (BCA) assay (Pierce, Rockford, IL, USA). Using antibodies for well-characterized synaptic markers, the synaptoneurosome samples were compared with whole homogenate to verify that there was a 2–3-fold enrichment for synaptic proteins. A control sample was made by combining a small amount of the prepared tissue sample from each of the cases. The samples prepared from P0. V1 had extremely low protein levels, too low to be used for immunoblotting. Therefore,

for comparison purposes frontal cortex samples at P0 were excluded from analysis.

IMMUNOBLOTTING

A Western Blot analysis was performed using the synaptoneurosome samples to quantify protein expression. Samples (30 ug) were separated on 4–20% sodium-dodecyl-sulfate polyacrylamide (SDS-PAGE) gels (Pierce, Rockford, IL) in running buffer (100 mM Tris, 100 mM HEPES, 3 mM SDS; Pierce Biotechnology Inc, Rockford, IL) and were transferred to polyvinylidene difluoride (PVDF-FL) membranes (Millipore, Billerice, MA, USA). Each sample was run at least twice. The membranes were incubated in blocking buffer (Odyssey Blocking Buffer 1:1 with PBS) for 1 h (LI-COR Biosciences, Lincoln, NE), followed by incubation in primary antibody overnight at 4°C using the following concentrations: GluA2, 1:2000 (Invitrogen, Camarillo, CA); pGluA2 (GluA2-ser880); 1:200 (PhosphoSolutions, Aurora, CO); GRIP1, 1:250 (BD Biosciences, San Diego, CA); PICK1, 1:200 (NeuroMab, Davis, CA); β-tubulin, 1:4000 (Invitrogen, Camarillo, CA). Blots were washed (3 × 10 min) in PBS containing 0.05% Tween (PBS-T, Sigma, St. Louis, MO), incubated (1 h, room temperature) in the appropriate IRDye labeled secondary antibody (Anti-Mouse, 1:8000, Anti-Rabbit, 1:10,000) (Li-cor Biosciences, Lincoln, NE), and washed in PBS-T (3 × 10 min). Blots were scanned and fluorescence was quantified using the Odyssey Scanner infrared-imager (LI-COR Biosciences, Lincoln, NE, USA). Finally, the blots were stripped using a two-step blot restore kit (Blot Restore Membrane Rejuvenation kit, Millipore, Billerice, MA, USA) and further reprobed with additional antibodies.

ANALYSIS

Blots were scanned (Odyssey Infrared Scanner) and band fluorescence was quantified using densitometry (Li-cor Odyssey Software version 3.0; Li-cor Biosciences; Lincoln, NE, USA). To determine the density profile, the background was subtracted, the pixel intensity of the band was integrated, and then divided by the width of the band to control for variations in band size. β-tubulin was used as the loading control and we verified the absence of any age-related correlations in β-tubulin expression in both cortical areas (p-values >0.28). A control sample (a mixture of all the samples) was run on each gel and the density of each sample was measured relative to the control sample (sample density/control density).

Scattergrams of protein expression by age were plotted and include the results from all the runs (light symbols) plus the average expression level for each sample (dark symbols). Curve fitting was done using the on-line curve-fitting tool zunzun.com and the goodness of fit was determined (R^2). Smooth changes were fit with either a linear or exponential decay function, as appropriate. The time constant (τ) for the change in expression level was calculated for the exponential decay functions. Adult level of expression was defined as 3τ which is the age when expression reached 87.5% of the asymptotic level. To capture the peaked developmental over expression of GluA2 and pGluA2 in frontal cortex a membrane transport curve was fit to the results. We quantified the period of over expression in frontal cortex by identifying the age at the peak (maximum) of the curve and then the full width at half the maximum (FWHM) to determine the ages for the start and end of the period of over expression.

We examined the relationship between the two states of the AMPA receptor subunit (GluA2 and pGluA2) and the two AMPA receptor interacting proteins (GRIP1 and PICK1) by calculating the correlation for each pair. Next, we examined developmental changes for functional pairs of AMPA receptor trafficking proteins by calculating a series of indices that quantify the relative expression of AMPA receptor: subunit states, GluA2:pGluA2 = [(GluA2 − PGluA2)/(GluA2 + pGluA2)]; interacting proteins, GRIP1:PICK1 = [(GRIP1 − PICK1)/(GRIP1 + PICK1)]; surface components, GluA2:GRIP1 = [(GluA2 − GRIP1)/(GluA2 + GRIP1)]; and internalization components, pGluA2:PICK1 = [(pGluA2 − PICK1)/(pGluA2 + PICK1)]. These contrast indices [e.g., (A − B)/(A + B)] are commonly used in signal processing and here provide a normalized difference between two proteins or two states of the GluA2 receptor. These indices allowed us to analyze relative changes between the GluA2 subunit states, interacting proteins, surface components, and internalization components that was independent of the developmental increases for each protein. Finally, we quantified the balance between surface-to-internalization proteins by calculating the difference between the surface and internalization indices: (GluA2:GRIP1) − (pGluA2:PICK1).

RESULTS

In this study, we characterized the expression of four components (GluA2, pGluA2, GRIP1, PICK1) involved in trafficking GluA2-containing AMPA receptors in and out of the synapse. Using Western Blot analysis, we quantified the developmental trajectories of the proteins and compared expression levels between the visual and frontal cortex to assess any differences in the developmental trajectories of sensory and non-sensory cortical areas.

GluA2 AND pGluA2 FOLLOW DIFFERENT DEVELOPMENTAL TRAJECTORIES IN VISUAL AND FRONTAL CORTEX

We examined the development of the two states of the GluA2 subunit (non-phosphorylated—GluA2 and phosphorylated serine 880—pGluA2) in visual and frontal cortex to quantify the expression of AMPA receptors at the synaptic surface (GluA) versus internalized receptors (pGluA2).

We found that the development of GluA2 and pGluA2 was similar within a cortical area but followed different trajectories in visual and frontal cortex. Initially, expression of GluA2 and pGluA2 was very low in both visual and frontal cortex and then increased rapidly (**Figure 1**). In V1, there was steady increase that was well fit with a decay function. GluA2 increased five-fold ($R^2 = 0.74$, $p < 0.0001$) (**Figure 1A**) to reach adult levels at P38 (3τ), while pGluA2 increased six-fold ($R^2 = 0.68$, $p < 0.0001$) (**Figure 1B**) and reached adult levels at P36 (3τ). In frontal cortex, both GluA2 (**Figure 1C**) and pGluA2 (**Figure 1D**) had a brief period of substantial over expression that peaked at P24 (membrane transport curve: GluA2 − $R^2 = 0.77$, $p < 0.0001$; pGluA2 − $R^2 = 0.79$, $p < 0.0001$). This period of over

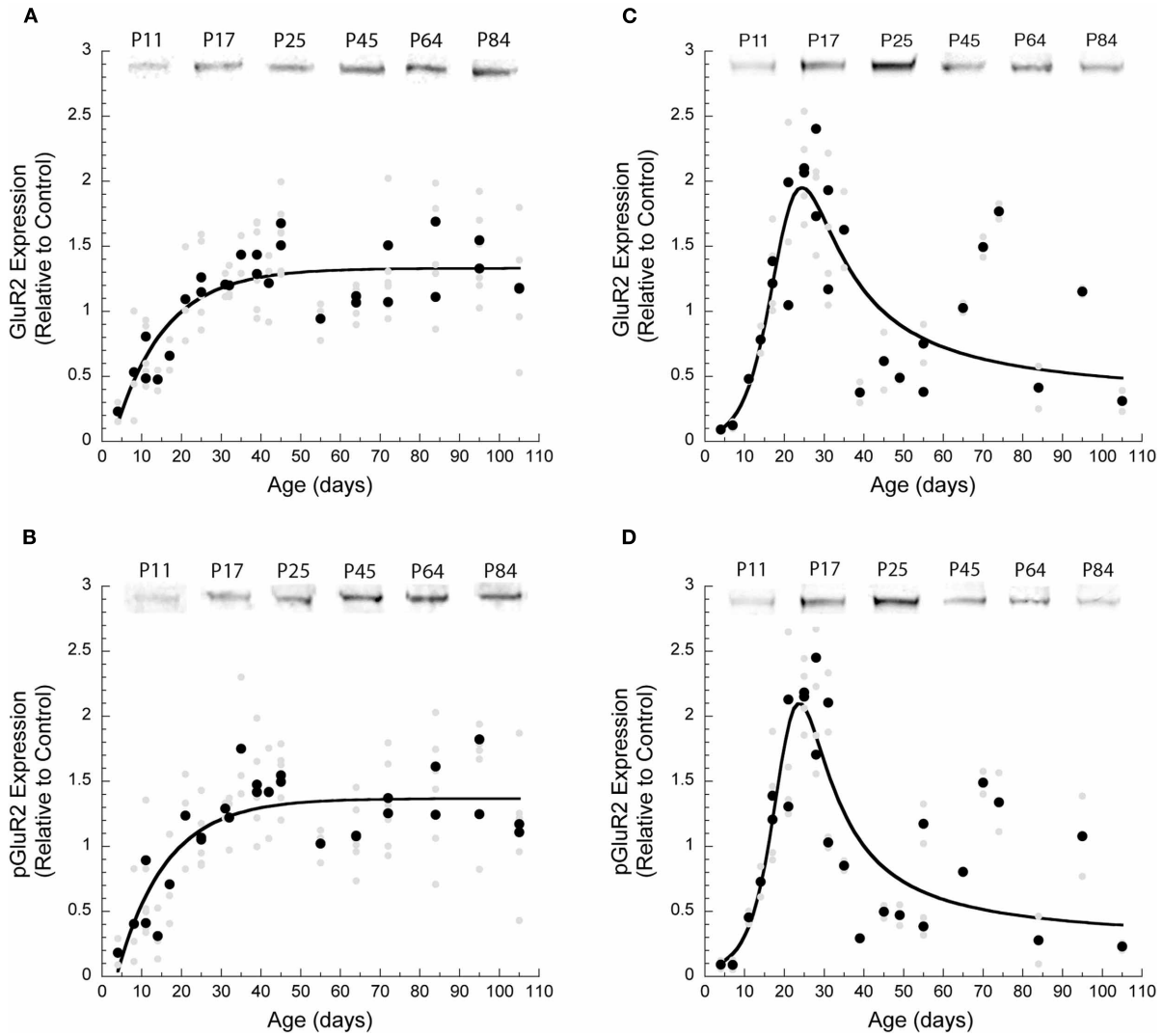

FIGURE 1 | Development of AMPA receptor subunits GluA2 and pGluA2 in visual and frontal cortex. There were significant differences in the developmental trajectories of GluA2 and pGluA2 in visual versus frontal cortex. All of the results were plotted for each run (light gray symbols) as well as the averages for each run (dark symbols). Exponential decay curves were fit to the data for visual cortex. **(A)** For GluA2 expression ($R^2 = 0.72$, $p < 0.0001$) adult expression levels were reached at P38 (3τ); **(B)** pGluA2 expression ($R^2 = 0.68$, $p < 0.0001$) reached adult levels by P36 (3τ). The results for frontal cortex were fit with a membrane transport function. **(C)** In frontal cortex: GluA2 expression ($R^2 = 0.77$, $p < 0.0001$) had the maximum level at P24 (range P18–P35); **(D)** pGluA2 expression ($R^2 = 0.79$, $p < 0.0001$) had the maximum level at P24 (range P19 and P32).

expression in frontal cortex (FWHM) lasted from P18 to P35 for GluA2 and P19 to P32 for pGluA2.

THE BALANCE BETWEEN GluA2 AND pGluA2 IS SIMILAR IN VISUAL AND FRONTAL CORTEX

To assess the relationship between GluA2 and pGluA2 expression we calculated the correlation between these proteins and an index of the relative expression of the two states of the receptor subunit. In both cortical areas, the correlation between the expression of GluA2 and pGluA2 were very similar and close to a 1:1 relationship (Visual—**Figure 2A**: correlation, $r = 0.88$, $p < 0.0001$; Frontal—**Figure 2C**: correlation, $r = 0.94$, $p < 0.0001$). To analyze how the balance between GluA2 and pGluA2 changed during development we calculated an index of the relative expression of these two states of the AMPA receptor subunit. The index was plotted by age and varies from −1 indicating only pGluA2, to 0 indicating equal pGluA2 and GluA2, to +1 indicating only GluA2. In V1, the index was initially slightly positive indicating more GluA2, but by P32 the two states were in balance (3τ, $R^2 = 0.37$, $p < 0.0005$) (**Figure 2B**). In frontal cortex, there was slightly more GluA2 except for a brief period between P18 and P30 when GluA2 and pGluA2 were approximately equal in expression (**Figure 2D**). Interestingly, the period when GluA2 and pGluA2 were balanced in frontal cortex coincided with the brief period of over expression. The similarities between the correlations and indices for GluA2 and pGluA2 in visual and frontal cortex suggest a common cortical balance for the two states of the AMPA receptor subunit throughout development.

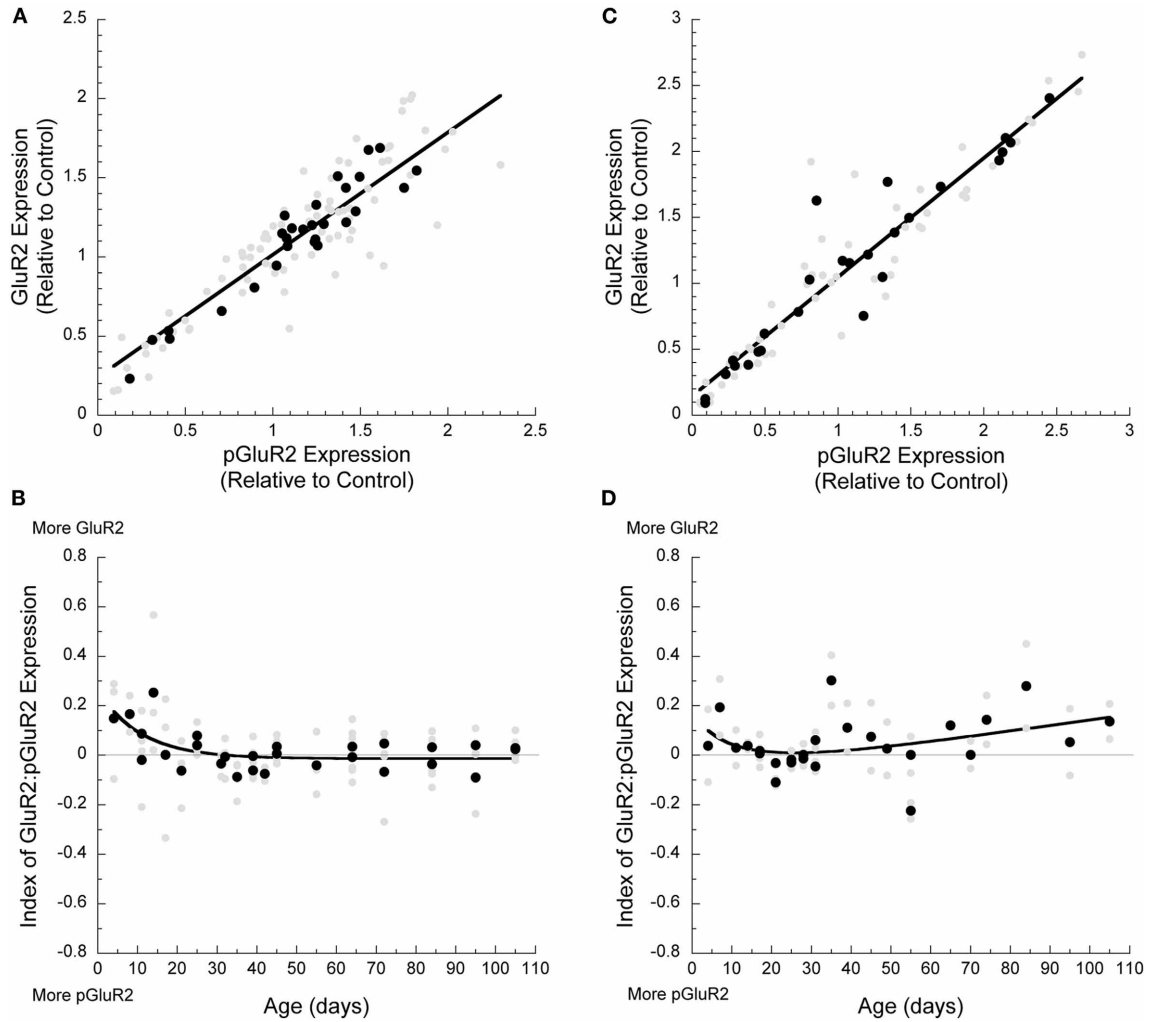

FIGURE 2 | Developmental changes in AMPA receptor subunit composition in visual and frontal cortex. (A) GluA2 and pGluA2 expression in both visual ($r = 0.88$, $p < 0.0001$) and **(C)** frontal ($r = 0.94$, $p < 0.0001$) cortex was highly correlated during development. The index of GluA2:pGluA2 expression during development showed that **(B)** in visual cortex, there was higher GluA2 expression initially, but a balance was reached by P33 (3τ, $R^2 = 0.37$, $p < 0.0005$). **(D)** In frontal cortex, the index remained in favor of relatively more GluA2 throughout development, except for a brief period of balance between P18 and P30 (membrane transport curve, $R^2 = 0.30$, $p = 0.04$).

AMPA INTERACTING PROTEINS—GRIP1 AND PICK1—FOLLOW SIMILAR DEVELOPMENTAL TRAJECTORIES IN VISUAL AND FRONTAL CORTEX

The AMPA interacting protein GRIP1 stabilizes the GluA2 subunit at the synaptic surface (Dong et al., 1997); however, when the GluA2 subunit is phosphorylated, it loses the interaction with GRIP1, is bound by PICK1, and becomes endocytosed (Seidenman et al., 2003). We examined the development of GRIP1 and PICK1 expression in visual and frontal cortex to quantify the maturation of these key AMPA receptor trafficking proteins.

During development the expression of GRIP1 and PICK1 increased by about 70% in V1 and 300% in frontal cortex. The time courses of the developmental trajectories for GRIP1 and PICK1 were well described by a exponential decay function. In V1, adult levels of GRIP1 were reached at P60 (3τ, $R^2 = 0.33$, $p = 0.002$, **Figure 3A**) and PICK1 at P69 (3τ, $R^2 = 0.32$, $p = 0.002$, **Figure 3B**). In frontal cortex, GRIP1 reached adult levels at P56 (3τ, $R^2 = 0.61$, $p < 0.0001$, **Figure 3C**) and PICK1 at P58 (3τ, $R^2 = 0.63$, $p < 0.0001$, **Figure 3D**). Although the magnitudes of the developmental changes for GRIP1 and PICK1 were greater in frontal cortex, the developmental time courses were similar to V1.

Next we assessed the relative level of expression between the surface (GRIP1) and internalizing (PICK1) AMPA interacting proteins. In V1, we found a strong relationship between the levels of GRIP1 and PICK1 expression ($r = 0.72$, $p < 0.0001$, **Figure 4A**). Furthermore, that relationship was maintained throughout development with roughly equal expression of GRIP1 and PICK1 (**Figure 4B**). In frontal cortex, the correlation between GRIP1 and PICK1 expression was weaker, but still

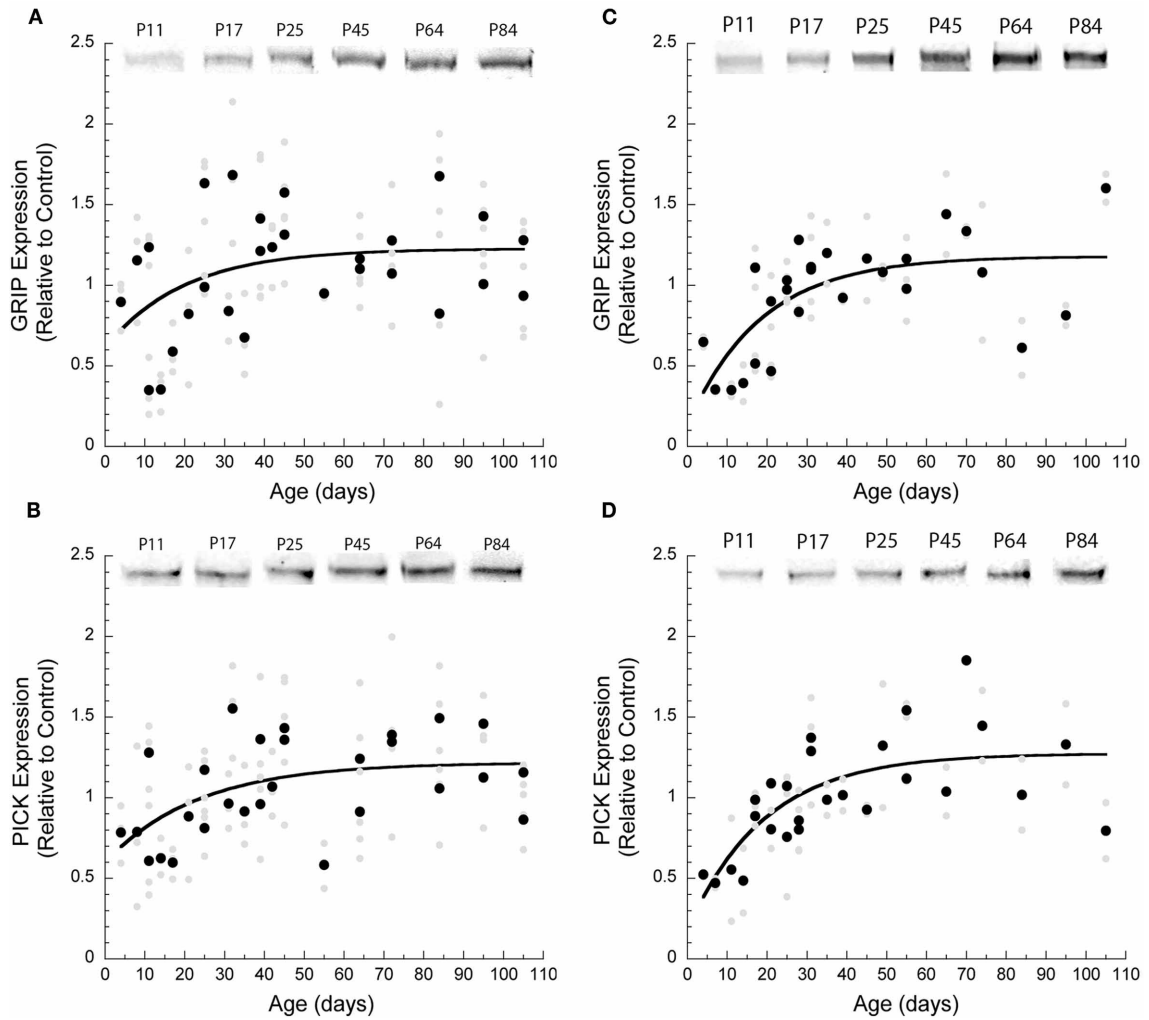

FIGURE 3 | Development of GRIP and PICK1 in visual and frontal cortex. The developmental trajectories for GRIP and PICK1 were similar in both cortical areas. Exponential decay curves were fit to all the data. **(A)** In visual cortex, GRIP expression levels increased by 1.7 times and reached adult levels by P60 (3τ, $R^2 = 0.33$, $p = 0.002$). **(B)** PICK1 expression levels increased three-fold and reached adult values by P69 (3τ, $R^2 = 0.32$, $p = 0.002$). **(C)** In frontal cortex, GRIP levels increased three-fold and reached adult levels by P56 (3τ, $R^2 = 0.61$, $p < 0.0001$). **(D)** Similarly, PICK1 expression increased three-fold during development and adult level was attained by P58 (3τ, $R^2 = 0.63$, $p < 0.0001$).

significant ($r = 0.48$; $p < 0.0001$, **Figure 4C**), and expression of these two proteins was roughly balanced throughout development (**Figure 4D**).

THE PAIRS OF SURFACE AND INTERNALIZATION PROTEINS DEVELOP SIMILARLY WITHIN A CORTICAL AREA BUT DIFFER BETWEEN VISUAL AND FRONTAL CORTEX

We calculated two indices to examine development of the AMPA receptor subunits and interacting proteins associated with surface expressed (GluA2 and GRIP1) and internalized (pGluA2 and PICK1) receptors. We also analyzed how the surface and internalization indices changed throughout development for both visual and frontal cortex. We found that development of the two pairs of proteins was similar within each area but differed between cortical areas.

In V1, the surface (GluA2:GRIP1) and internalization (pGluA2:PICK1) indices followed similar trajectories (**Figures 5A,B**). Initially, there was relatively greater expression of the AMPA interacting proteins (more GRIP1 and PICK1) followed by an increase in the relative amounts of GluA2 and pGluA2 until the adult balances were reached at P13 for the surface index (GluA2:GRIP1, 3τ, $R^2 = 0.62$, $p < 0.0001$, **Figure 5A**) and slightly later at P22 for the internalization index (pGluA2:PICK1, 3τ, $R^2 = 0.69$, $p < 0.0001$, **Figure 5B**). In frontal cortex, the surface (**Figure 5C**) and internalization (**Figure 5D**) indices started in favor of the AMPA interacting proteins (more GRIP1 and PICK1), then rapidly shifted to more of the AMPA subunits (more GluA2 and pGluA2), followed by a shift back to relatively more expression of the interacting proteins. These developmental changes for the surface and

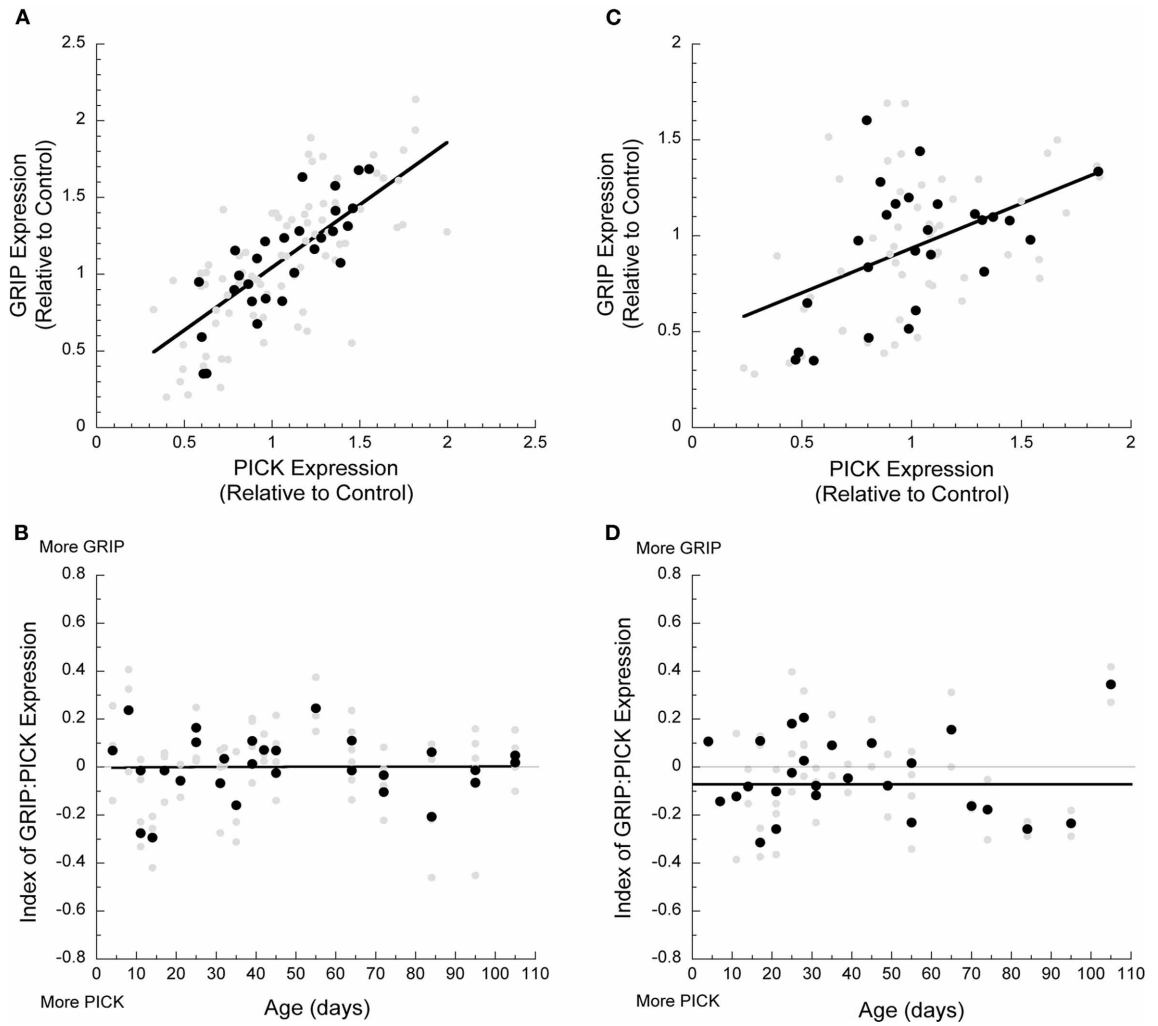

FIGURE 4 | Developmental changes in GRIP and PICK1 in visual and frontal cortex. (A) GRIP and PICK1 expression in visual cortex was highly correlated during development ($r = 0.72$, $p < 0.0001$). **(B)** The index of GRIP:PICK1 expression showed that the two proteins were balanced during postnatal development. **(C)** GRIP and PICK1 expression in frontal cortex was correlated during development ($r = 0.48$, $p < 0.0001$). **(D)** The index showed that GRIP and PICK1 develop in balance in frontal cortex.

internalization indices in frontal cortex were well described by a membrane transport function (GluA2:GRIP1: $R^2 = 0.74$, $p < 0.0001$; pGluA2:PICK1: $R^2 = 0.77$, $p < 0.0001$) with peaks at P18 and P20 for the surface and internalization indices, respectively. The difference between cortical areas for the surface and internalization index was largely driven by the difference in GluA2 and pGluA2 expression. But the similarity within each cortical area raised the possibility that there may be a common overall balance between the surface and internalization proteins.

THE AMPA RECEPTOR SURFACE-TO-INTERNALIZATION BALANCE IS CONSTANT DURING DEVELOPMENT AND THE SAME IN VISUAL AND FRONTAL CORTEX

The balance between AMPA receptor proteins associated with surface expression (GluA2 and GRIP1) versus internalization (pGluA2 and PICK1) will contribute to regulating the cycling of receptors in and out of the synapse. For example, more surface associated proteins suggests that more receptors may be held at the synapse and changes in the surface-to-internalization balance during development or differences between cortical areas may affect AMPA-dependent plasticity. As a first step to study these questions we examined the relationship between the surface and internalization proteins by assessing the correlation between the surface and internalization indices, and by calculating the difference between the two indices to quantify an AMPA surface-to-internalization balance.

In both visual ($r = 0.61$, $p < 0.0001$) and frontal cortex ($r = 0.81$, $p < 0.0001$) there were strong correlations between the surface (GluA2:GRIP1) and internalization (pGluA2:PICK1) indices (**Figure 6A**). Moreover, the slopes for the relationships between

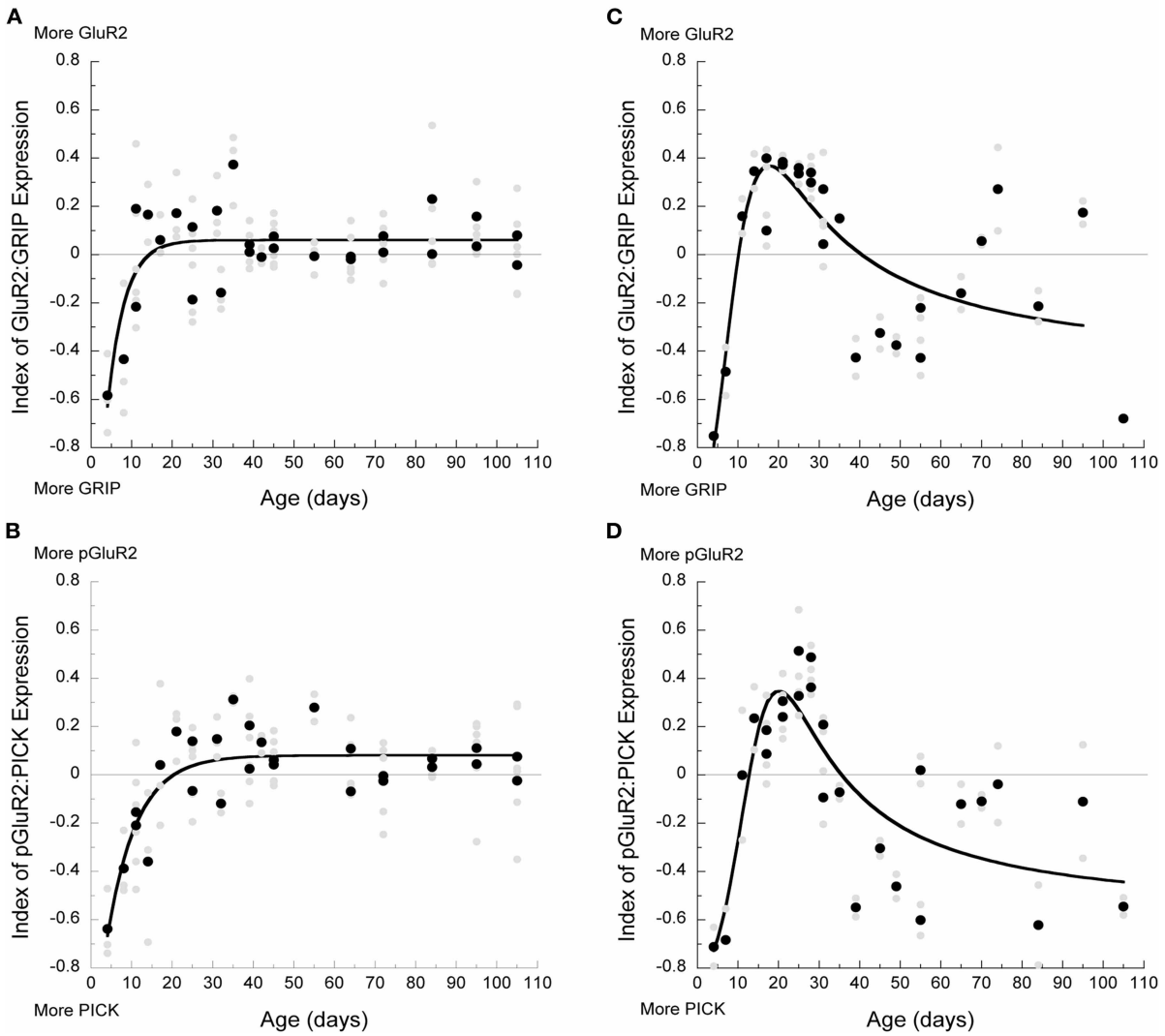

FIGURE 5 | Development of surface and internalized components in visual and frontal cortex. (A) Index of GluA2:GRIP during development in visual cortex showed that initially more GRIP was present, but by P13, a balance with slightly more GluA2 was reached (3τ, $R^2 = 0.62$, $p < 0.0001$). **(B)** Index of pGluA2:PICK1 in visual cortex showed that more PICK1 was present early in development, but a balance was reached by P22 (3τ, $R^2 = 0.69$, $p < 0.0001$). **(C)** In frontal cortex, index of GluA2:GRIP was in favor of GRIP before P10, followed by an increase in GluA2 expression between P10 and P40, and then another shift to relatively more GRIP (membrane transport curve: $R^2 = 0.74$, $p < 0.0001$). **(D)** Index of pGluA2:PICK1 was in favor of more PICK1 before P13, more pGluA2 between P13 and P34, and then another shift to relatively more PICK1 that persists throughout development.

GluA2:GRIP1 and pGluA2:PICK1 were similar in the two cortical areas, suggesting a common relationship between the surface and internalization mechanisms. To further examine this relationship we plotted the development of the surface-to-internalization balance for visual and frontal cortex (**Figure 6B**). We found that this surface-to-internalization balance was constant throughout development, and centered on 0, indicating roughly equal expression of this set of surface and internalization proteins. Interestingly, the surface-to-internalization balance was the same in visual and frontal cortex. These observations suggest that AMPA receptor trafficking is tightly controlled and has a common balance in the developing cortex.

DISCUSSION

The results from this study support three main conclusions about the development of the AMPA trafficking proteins in rat cortex. First, the developmental trajectory for the two states of the GluA2 subunit differs between cortical areas. In frontal cortex, the development of GluA2 and pGluA2 had a brief period of exuberant expression and at P24 was almost four times greater than the adult levels (**Figure 1**). This result is similar to an earlier receptor autoradiography study that found an overshoot in binding to AMPA receptors (quisqualate) in the frontal cortex (Insel et al., 1990). In contrast, for V1 we found steady development of GluA2 and pGluA2 with no over expression. Our observation

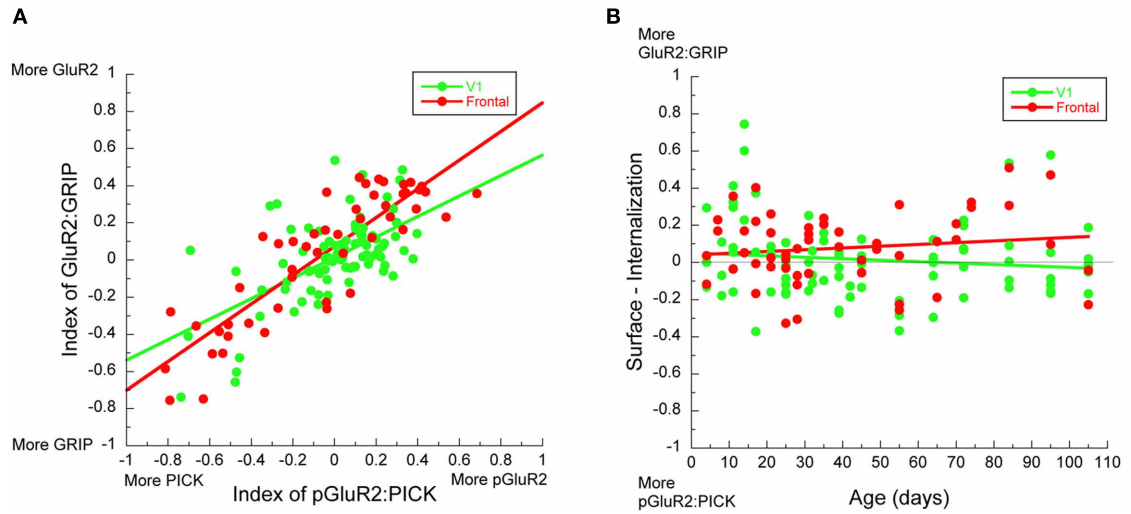

FIGURE 6 | Development of AMPA receptor in visual and frontal cortex. **(A)** There was a strong correlation between the indices for GluA2:GRIP and pGluA2:PICK1 in both visual (green symbols) ($r = 0.61$, $p < 0.0001$) and frontal cortex (red symbols) ($r = 0.81$, $p < 0.0001$). **(B)** The difference between the indices for GluA2:GRIP and pGluA2:PICK1 as a function of age showed a tight surface-to-internalization balance throughout development.

of steady GluA2 development in rat V1 challenges the conventional view of AMPA over expression during cortical development found using receptor binding (Insel et al., 1990) or in other species (ferret—Herrmann, 1996; cat—Beston et al., 2010). The difference may be species specific or because we used a synaptoneurosome assay which provides more specific information about receptors located at the synapse than all receptors as are labeled by receptor binding. Since the number of AMPA receptors sets the strength of excitatory transmission and influences synaptic plasticity, the developmental difference in GluA2 expression between visual and frontal cortex suggests that the refinement of cortical circuits differs between regions. Furthermore, the overshoot of GluA2 in frontal cortex implies a period of rapid synaptic change that may be particularly vulnerable to AMPA-dependent plasticity and associated with the time when injury to the frontal cortex has its most deleterious effect (Halliwell et al., 2009).

Second, development of the AMPA interacting proteins associated with surface (GRIP1) and internalized (PICK1) receptors is similar in visual and frontal cortex. There was early expression of GRIP1 and PICK1 in both regions, followed by gradual developmental increases. Initially, the expression of GRIP1 and PICK1 was greater than the matching GluA2 or pGluA2 expression (this is logically necessary based on the previous sentence, so it's a bit redundant). GRIP1 is necessary for the accumulation of GluA2 at the synapse (Osten et al., 2000), and PICK1 reduces surface expression of GluA2 (Perez et al., 2001) by retaining receptors inside the synapse (Citr et al., 2010). Thus, our data showing early expression of GRIP1 and PICK1 supports a model where the synaptic accumulation and internalization of GluA2-containing receptors is regulated as soon as the receptors are expressed. Furthermore, the exquisite balance between GRIP1 and PICK1 expression throughout development suggests fine regulation of the interacting proteins that are part of AMPA receptor trafficking. The early expression and fine regulation could underlie the rapid insertion of AMPA receptors that converts silent synapses into functional ones (Rumpel et al., 1998).

Third, throughout cortical development there is a tight balance among the four AMPA trafficking components with roughly equal expression of the surface and internalization components. We calculated the surface-to-internalization balance to quantify changes in the relative expression of surface (GluA2:GRIP1) and internalization (pGluA2:PICK1) proteins that regulate the highly dynamic trafficking of AMPA receptors to and from cortical synapses (Shepherd and Huganir, 2007). The consistent surface-to-internalization balance points to exquisite control over the cycling of AMPA receptors in and out of cortical synapses. Moreover, even though we found differences in the development of GluA2 expression between visual and frontal cortex, the surface-to-internalization balance was the same in the two regions. Taken together, the common surface-to-internalization balance suggests that developmental excitatory plasticity is more sensitive to changes in the number of receptors, than to changes in the rate of AMPA receptor trafficking.

A number of recent studies have shown the tremendous complexity of the pathways involved in trafficking AMPA receptors to and from the synapse (for review see Anggono and Huganir, 2012). We have quantified the developmental changes in expression for just four of the components in those pathways and a complete understanding will need to include quantification of the full complement of interacting proteins. In addition, it is clear that there is cross-talk between the signaling pathways and protein-protein regulation of interacting proteins that affects their roles in AMPA trafficking and may even shift their function from participation in surface to internalization of AMPA receptors. For example, GRIP1 can participate in AMPA receptor endocytosis (Osten et al., 2000), exocytosis (Mao et al., 2010), and holding receptors intracellularly (Braithwaite et al., 2002). This functional diversity

for individual interacting proteins adds to the complexity and dynamic nature of AMPA receptor trafficking. The indices that we used in this study quantify the balances among the proteins and provide initial insights into functional changes during development. Looking at the balances and ratios among synaptic proteins is often used as a first step in the process of understanding the interactions that drive function, especially during development. For example, the initial prevalence of GluN2B prevents GluA2 expression (Hall et al., 2007), and the developmental shift in the GluN2A:GluN2B balance changes the function of GluN receptors and affects ocular dominance plasticity in V1 (Cho et al., 2009). The surface and internalization indices that we used provide one view of what is a very complex system, and more sophisticated multidimensional analyses and modeling will be needed to gain a full appreciation for how the AMPA receptor trafficking system functions.

AMPA receptor trafficking plays a central role in excitatory plasticity (Malinow and Malenka, 2002), especially during development (Kerchner and Nicoll, 2008). A number of studies have shown that experience-dependent plasticity in the V1 involves changes in AMPA receptor expression. These include monocular deprivation induced loss of GluA2 (Beston et al., 2010) or increase in pGluA2 (Heyen et al., 2003), and selective involvement of AMPA receptor expression in perceptual learning (Frenkel et al., 2006). Furthermore, bidirectional changes in GluA2 expression in V1 (Smith et al., 2009) underlie synaptic physiology plasticity that leads to experience-dependent LTP (Malenka and Bear, 2004), or LTD (Heyen et al., 2003; Yoon et al., 2009). Synaptic scaling in V1 (Turrigiano and Nelson, 2004) is also AMPA-dependent and uses a GluA2-specific trafficking pathway to either increase surface expression (Gainey et al., 2009) or internalize GluA2-containing receptors (Yoon et al., 2009). In frontal cortex, there have been fewer studies of AMPA-dependent developmental plasticity. A recent study, however, has shown that prenatal exposure to cocaine markedly reduces GluA2 and GluA3 expression measured at P21 in rat frontal cortex (Bakshi et al., 2009). That age corresponds with the peak of GluA2 expression that we found for normal animals and perhaps changes in GluA2-dependent LTP, LTD, and synaptic scaling underlie the long-term effects on brain development, anxiety, and cognitive function caused by prenatal cocaine exposure.

The highly dynamic process of trafficking AMPA receptors involves several proteins to endo- and exo-cytose receptors (Shepherd and Huganir, 2007). We studied development of the GluA2-interacting proteins GRIP1 and PICK1 because they play a critical role in GluA2-specific LTD and synaptic scaling. PICK1 participates in the regulated endocytosis of GluA2-containing receptors and can interact with intracellular signaling pathways that modify AMPA receptor trafficking (Hanley, 2008; Citr et al., 2010). The surface level of GluA2-containing AMPA receptors is reduced when PICK1 binds to the C-terminus of the subunit (Perez et al., 2001) and this PICK1-dependent internalization regulates LTD (Kim et al., 2001) by holding the receptor inside the synapse (Citr et al., 2010). This key role for PICK1 in regulating LTD is a strong indicator that PICK1 contributes to LTD in V1 ocular dominance plasticity (Yoon et al., 2009). In the hippocampus, however, loss of PICK1 impairs LTP and LTD synaptic plasticity in adult but not juvenile mice (Volk et al., 2010), so future studies are needed to determine the role of PICK1 in developmental ocular dominance plasticity. Finally, a recent study has uncovered a specific role for PICK1 in inactivity-induced synaptic scaling of cortical neuronal excitability (Anggono et al., 2011). They showed a loss of PICK1 expression following chronic activity blockade of cortical neurons and abnormal trafficking of GluA2-containing receptors when PICK1 function was knocked out. Thus, PICK1 function is an essential component of inactivity-induced synaptic scaling plasticity that increases synaptic strength. Our finding that PICK1 is expressed early in the developing cortex indicates that right from the youngest postnatal ages neuronal excitability can be increased to adjust for low levels of activity.

The other GluA2-interacting protein that we studied—GRIP1—plays essential roles in surface expression of GluA2-containing AMPA receptors (Shepherd and Huganir, 2007). GRIP1 has been implicated in regulating the rate of endocytosis (Osten et al., 2000) and in facilitating the reinsertion of internalized AMPA receptors back into the synapse (Mao et al., 2010). The early expression of GRIP1 in the developing visual and frontal cortex indicates that surface expression and trafficking is regulated as soon as GluA2-containing receptors are expressed. The role, however, of GRIP1 in functional development of V1 has not been studied. In frontal cortex, regulation of AMPA trafficking is disrupted by prenatal exposure to cocaine that causes hyperphosphorylation of GRIP1 and reduces postnatal expression of synaptic GluA2 (Bakshi et al., 2009). Those findings led Bakshi et al. to propose suppressing the excessive GRIP1 phosphorylation as a therapeutic to treat the consequences of prenatal cocaine exposure. In addition, a recent study has linked changes in the function of GRIP1 with autism in humans (Mejias et al., 2011). Sequencing of *GRIP1* in individuals with autism uncovered five rare missense variants in the genomic sequence near the encoding of PDZ4-6. In an animal model, the mutation altered the interaction between GRIP1 and GluA2-containing receptors and led to abnormal social behavior. Importantly, more severe genotypes were linked with greater cognitive impairment suggesting that *GRIP1* mutations modify the severity of the behaviors that characterize autism.

It is clear that the set of AMPA trafficking proteins that we studied—GRIP1, PICK1, GluA2, and pGluA2—play essential roles in normal and abnormal development of cortical function. There is still, however, much to learn about the precise roles for these proteins in synaptic plasticity and development of cortical circuits. It has been challenging to elucidate the functions of the interacting proteins and link them with regulation of GluA2-dependent developmental plasticity because of the many proteins that contribute to AMPA receptor trafficking (Duprat et al., 2003; Shepherd and Huganir, 2007; Anggono and Huganir, 2012). Our finding of an exquisite surface-to-internalization balance highlights that these proteins function as a tightly controlled system and the need to study the system as a whole to understand how trafficking of AMPA receptors affects cortical development and function.

REFERENCES

Anggono, V., Clem, R. L., and Huganir, R. L. (2011). PICK1 loss of function occludes homeostatic synaptic scaling. *J. Neurosci.* 31, 2188–2196.

Anggono, V., and Huganir, R. L. (2012). Regulation of AMPA receptor trafficking and synaptic plasticity. *Curr. Opin. Neurobiol.* doi: 10.1016/j.conb.2011.12.006. [Epub ahead of print].

Bakshi, K., Gennaro, S., Chan, C. Y., Kosciuk, M., Liu, J., Stucky, A., Trenkner, E., Friedman, E., Nagele, R. G., and Wang, H. Y. (2009). Prenatal cocaine reduces AMPA receptor synaptic expression through hyperphosphorylation of the synaptic anchoring protein GRIP. *J. Neurosci.* 29, 6308–6319.

Beston, B. R., Jones, D. G., and Murphy, K. M. (2010). Experience-dependent changes in excitatory and inhibitory receptor subunit expression in visual cortex. *Front. Neurosci.* 2:138. doi: 10.3389/fnsyn.2010.00138

Braithwaite, S. P., Xia, H., and Malenka, R. C. (2002). Differential roles for NSF and GRIP/ABP in AMPA receptor cycling. *Proc. Natl. Acad. Sci. U.S.A.* 99, 7096–7101.

Cho, K. A., Khibnik, L., Philpot, B. D., and Bear, M. F. (2009). The ratio of NR2A/B NMDA receptor subunits determines the qualities of ocular dominance plasticity in visual cortex. *Proc. Natl. Acad. Sci. U.S.A.* 106, 5377–5382.

Chung, H. J., Steinberg, J. P., Huganir, R. L., and Linden, D. J. (2003). Requirement of AMPA receptor GluR2 phosphorylation for cerebellar long-term depression. *Science* 300, 751–755.

Chung, H. J., Xia, J., Scannevin, R. H., Zhang, X., and Huganir, R. L. (2000). Phosphorylation of the AMPA receptor subunit GluR2 differentially regulates its interaction with PDZ domain-containing proteins. *J. Neurosci.* 20, 7258–7267.

Citr, A., Bhattacharyya, S., Ma, C., Morishita, W., Fang, S., Rizo, J., and Rc, R. C. M. (2010). Calcium binding to PICK1 is essential for the intracellular retention of AMPA receptors underlying long-term depression. *J. Neurosci.* 30, 16437–16452.

Collingridge, G. L., and Singer, W. (1990). Excitatory amino acid receptors and synaptic plasticity. *Trends Pharmacol. Sci.* 11, 290–296.

Dingledine, R., Borges, K., Bowie, D., and Traynelis, S. F. (1999). The glutamate receptor ion channels. *Pharmacol. Rev.* 51, 7–61.

Dong, H., O'Brien, R. J., Fung, E. T., Lanahan, A. A., Worley, P. F., and Huganir, R. L. (1997). GRIP: a synaptic PDZ domain-containing protein that interacts with AMPA receptors. *Nature* 286, 279–284.

Duprat, F., Daw, M., Lim, W., Collingridge, G., and Isaac, J. (2003). GluR2 protein-protein interactions and the regulation of AMPA receptors during synaptic plasticity. *Philos. Trans. R. Soc. Lond. B Biol. Sci.* 358, 715–720.

Durand, G. M., Kovalchuk, Y., and Konnerth, A. (1996). Long-term potentiation and functional synapse induction in developing hippocampus. *Nature* 381, 71–75.

Frenkel, M. Y., Sawtell, N. B., Diogo, A. C., Yoon, B., Neve, R. L., and Bear, M. F. (2006). Instructive effect of visual experience in mouse visual cortex. *Neuron* 51, 339–349.

Gainey, M. A., Hurvitz-Wolff, J. R., Lambo, M. E., and Turrigiano, G. G. (2009). Synaptic scaling requires the GluR2 subunit of the AMPA receptor. *J. Neurosci.* 29, 6479–6489.

Gardner, S. M., Takamiya, K., Xia, J., Suh, J. G., Johnson, R., Yu, S., and Huganir, R. L. (2005). Calcium-permeable AMPA receptor plasticity is mediated by subunit-specific interactions with PICK1 and NSF. *Neuron* 45, 903–915.

Goel, A., Xu, L. W., Snyder, K. P., Song, L., Goenaga-Vazquez, Y., Megill, A., Takamiya, K., Huganir, R. L., and Lee, H. K. (2011). Phosphorylation of AMPA receptors is required for sensory deprivation-induced homeostatic synaptic plasticity. *PLoS ONE* 6:e18264. doi:10.1371/journal.pone.0018264

Hall, B. J., Ripley, B., and Ghosh, A. (2007). NR2B Signaling regulates the development of synaptic AMPA receptor current. *J. Neurosci.* 27, 13446–13456.

Halliwell, C., Comeau, W., Gibb, R., Frost, D. O., and Kolb, B. (2009). Factors influencing frontal cortex development and recovery from early frontal injury. *Dev. Neurorehabil.* 12, 269–278.

Hanley, J. G. (2008). PICK1: a multi-talented modulator of AMPA receptor trafficking. *Pharmacol. Ther.* 2, 276–282.

Herrmann, K. (1996). Differential distribution of AMPA receptors and glutamate during pre- and postnatal development in the visual cortex of ferrets. *J. Comp. Neurol.* 4, 1–17.

Heyen, A. J., Yoon, B. J., Liu, C. H., Chung, H. J., Huganir, R. L., and Bear, M. F. (2003). Molecular mechanism for loss of visual cortical responsiveness following brief monocular deprivation. *Nat. Neurosci.* 6, 854–862.

Hollingsworth, E. B., Mcneal, E. T., Burton, J. L., Williams, R. J., Daly, J. W., and Creveling, C. R. (1985). Biochemical characterization of a filtered synaptoneurosome preparation from guinea pig cerebral cortex: cyclic adenosine 3':5'-monophosphate-generating systems, receptors, and enzymes. *J. Neurosci.* 5, 2240–2253.

Hollmann, M., and Heinemann, S. (1994). Cloned glutamate receptors. *Annu. Rev. Neurosci.* 17, 31–108.

Insel, T. R., Miller, L. P., and Gelhard, R. E. (1990). The ontogeny of excitatory amino acid receptors in rat forebrain–I. N-methyl-D-aspartate and quisqualate receptors. *Neuroscience* 35, 31–43.

Isaac, J. T., Nicoll, R. A., and Malenka, R. C. (1995). Evidence for silent synapses: implications for the expression of LTP. *Neuron* 15, 427–434.

Kerchner, G. A., and Nicoll, R. A. (2008). Silent synapses and the emergence of a postsynaptic mechanism for LTP. *Nat. Rev. Neurosci.* 9, 813–825.

Kim, C. H., Chung, H. J., Lee, H. K., and Huganir, R. L. (2001). Interaction of the AMPA receptor subunit GluR2/3 with PDZ domains regulates hippocampal long-term depression. *Proc. Natl. Acad. Sci. U.S.A.* 98, 11725–11730.

Kleppe, I. C., and Robinson, H. P. (1999). Determining the activation time course of synaptic AMPA receptors from openings of colocalized NMDA receptors. *Biophys. J.* 77, 1418–1427.

Liao, D., Hessler, N. A., and Malinow, R. (1995). Activation of postsynaptically silent synapses during pairing-induced LTP in CA1 region of hippocampal slice. *Nature* 375, 400–404.

Liao, D., Scannevin, R. H., and Huganir, R. L. (2001). Activation of silent synapses by rapid activity-dependent synaptic recruitment of AMPA receptors. *J. Neurosci.* 21, 6008–6017.

Lissin, D. V., Gomperts, S. N., Carroll, R. C., Christine, C. W., Kalman, D., Kitamura, M., Hardy, S., Nicoll, R. A., Malenka, R. C., and Zastrow, M. V. (1998). Activity differentially regulates the surface expression of synaptic AMPA and NMDA glutamate receptors. *Proc. Natl. Acad. Sci. U.S.A.* 95, 7097–7102.

Liu, S. J., and Cull-Candy, S. G. (2005). Subunit interaction with PICK and GRIP controls Ca2+ permeability of AMPARs at cerebellar synapses. *Nat. Neurosci.* 8, 768–775.

Malenka, R. C., and Bear, M. F. (2004). LTP and LTD: an embarrassment of riches. *Neuron* 44, 5–21.

Malinow, R., and Malenka, R. C. (2002). AMPA receptor trafficking and synaptic plasticity. *Annu. Rev. Neurosci.* 25, 103–126.

Mao, L., Takamiya, K., Thomas, G., Lin, D. T., and Huganir, R. L. (2010). GRIP1 and 2 regulate activity-dependent AMPA receptor recycling via exocyst complex interactions. *Proc. Natl. Acad. Sci. U.S.A.* 107, 19038–19043.

Mejias, R., Adamczyk, A., Anggono, V., Niranjan, T., Thomas, G. M., Sharma, K., Skinner, C., Schwartz, C. E., Stevenson, R. E., Fallin, M. D., Kaufmann, W., Pletnikov, M., Valle, D., Huganir, R. L., and Wang, T. (2011). Gain-of-function glutamate receptor interacting protein 1 variants alter GluA2 recycling and surface distribution in patients with autism. *Proc. Natl. Acad. Sci. U.S.A.* 108, 4920–4925.

O'Brien, R. J., Kamboj, S., Ehlers, M. D., Rosen, K. R., Fischbach, G. D., and Huganir, R. L. (1998). Activity-dependent modulation of synaptic AMPA receptor accumulation. *Neuron* 21, 1067–1078.

Osten, P., Khatri, L., Perez, J. L., Köhr, G., Giese, G., Daly, C., Schulz, T. W., Wensky, A., Lee, L. M., and Ziff, E. B. (2000). Mutagenesis reveals a role for ABP/GRIP binding to GluR2 in synaptic surface accumulation of the AMPA receptor. *Neuron* 27, 313–325.

Paxinos, G., and Watson, C. (2007). *The Rat Brain in Stereotaxic Coordinates.* Amsterdam: Elsevier Academic.

Perez, J. L., Khatri, L., Chang, C., Srivastava, S., Osten, P., and Ziff, E. B. (2001). PICK1 targets activated protein kinase Calpha to AMPA receptor clusters in spines of hippocampal neurons and reduces surface levels of the AMPA-type glutamate receptor subunit 2. *J. Neurosci.* 21, 5417–5428.

Petralia, R. S., Esteban, J. A., Wang, Y. X., Partridge, J. G., Zhao, H. M., Wenthold, R. J., and Malinow, R. (1999). Selective acquisition of AMPA receptors over postnatal development suggests a molecular basis for silent synapses. *Nat. Neurosci.* 2, 31–36.

Quinlan, E. M., Olstein, D. H., and Bear, M. F. (1999). Bidirectional, experience-dependent regulation of N-methyl-D-aspartate receptor subunit composition in the rat visual cortex during postnatal development. *Proc. Natl. Acad. Sci. U.S.A.* 96, 12876–12880.

Raymond, L. A., Blackstone, C. D., and Huganir, R. L. (1993). Phosphorylation of amino acid neurotransmitter receptors in synaptic plasticity. *Trends Neurosci.* 16, 147–153.

Rumpel, S., Hatt, H., and Gottmann, K. (1998). Silent synapses in the developing rat visual cortex: evidence for postsynaptic expression of synaptic plasticity. *J. Neurosci.* 18, 8863–8874.

Seidenman, K. J., Steinberg, J. P., Huganir, R., and Malinow, R. (2003). Glutamate receptor subunit 2 Serine 880 phosphorylation modulates synaptic transmission and mediates plasticity in CA1 pyramidal cells. *J. Neurosci.* 23, 9220–9228.

Shepherd, J. D., and Huganir, R. L. (2007). The cell biology of synaptic plasticity: AMPA receptor trafficking. *Annu. Rev. Cell Dev. Biol.* 23, 613–643.

Smith, G. B., Heynen, A. J., and Bear, M. F. (2009). Bidirectional synaptic mechanisms of ocular dominance plasticity in visual cortex. *Philos. Trans. R. Soc. Lond. Ser. B Biol. Sci.* 364, 357–367.

Song, I., and Huganir, R. L. (2002). Regulation of AMPA receptors during synaptic plasticity. *Trends Neurosci.* 25, 578–588.

Titulaer, M. N., and Ghijsen, W. E. (1997). Synaptoneurosomes. A preparation for studying sub-hippocampal GABAA receptor activity. *Methods. Mol. Biol.* 72, 49–59.

Turrigiano, G. G., and Nelson, S. B. (2004). Homeostatic plasticity in the developing nervous system. *Nat. Rev. Neurosci.* 5, 97–1007.

Volk, L., Kim, C. H., Takamiya, K., Yu, Y., and Huganir, R. L. (2010). Developmental regulation of protein interacting with C kinase 1 (PICK1) function in hippocampal synaptic plasticity and learning. *Proc. Natl. Acad. Sci. U.S.A.* 107, 21784–21789.

Yoon, B. J., Smith, G. B., Heynen, A. J., Neve, R. L., and Bear, M. F. (2009). Essential role for a long-term depression mechanism in ocular dominance plasticity. *Proc. Natl. Acad. Sci. U.S.A.* 106, 9860–9865.

Conflict of Interest Statement: The authors declare that the research was conducted in the absence of any commercial or financial relationships that could be construed as a potential conflict of interest.

Received: 20 March 2012; accepted: 30 April 2012; published online: 16 May 2012.

*Citation: Murphy KM, Tcharnaia L, Beshara SP and Jones DG (2012) Cortical development of AMPA receptor trafficking proteins. Front. Mol. Neurosci. **5**:65. doi: 10.3389/fnmol.2012.00065*

frontiers in
MOLECULAR NEUROSCIENCE

REVIEW ARTICLE
published: 08 May 2012
doi: 10.3389/fnmol.2012.00062

Generation of neuromuscular specificity in *Drosophila*: novel mechanisms revealed by new technologies

Akinao Nose*

Department of Complexity Science and Engineering, Graduate School of Frontier Sciences, University of Tokyo, Kashiwanoha, Kashiwa, Chiba, Japan

Edited by:
Joshua A. Weiner, The University of Iowa, USA

Reviewed by:
Kai Zinn, California Institute of Technology, USA
David van Vactor, Harvard Medical School, USA

****Correspondence:***
Akinao Nose, Department of Complexity Science and Engineering, Graduate School of Frontier Sciences, University of Tokyo, Kashiwanoha 5-1-5, Kashiwa, Chiba 277-8561, Japan.
e-mail: nose@k.u-tokyo.ac.jp

The *Drosophila* larval neuromuscular system is one of the best-characterized model systems for axon targeting. In each abdominal hemisegment, only 36 identified motor neurons form synaptic connections with just 30 target muscles in a highly specific and stereotypic manner. Studies in the 1990s identified several cell-surface and secreted proteins that are expressed in specific muscles and contribute to target specificity. Emerging evidence suggests that target selection is determined not only by attraction to the target cells but also by exclusion from non-target cells. Proteins with leucine-rich repeats (LRR proteins) appear to be a major molecular family of proteins responsible for the targeting. While the demonstrated roles of the target-derived cues point to active recognition by presynaptic motor neurons, postsynaptic muscles also reach out and recognize specific motor neurons by sending out cellular protrusions called myopodia. Simultaneous live imaging of myopodia and growth cones has revealed that local and mutual recognition at the tip of myopodia is critical for selective synapse formation. A large number of candidate target cues have been identified on a single muscle, suggesting that target specificity is determined by the partially redundant and combinatorial function of multiple cues. Analyses of the seemingly simple neuromuscular system in *Drosophila* have revealed an unexpected complexity in the mechanisms of axon targeting.

Keywords: *Drosophila*, neuromuscular junction, synapse specificity, muscles, motor neurons, target recognition

INTRODUCTION

After a long journey to the target region, neurons finally gain the blissful opportunity to meet and "mate" with their synaptic partners. In a complex nervous system, however, the neurons still have the daunting task of finding the right partner from among many potential targets in the vicinity. What are the cellular and molecular underpinnings of this romantic yet difficult process? Despite our wealth of knowledge of the molecular mechanisms involved in axon guidance toward the target region (Kolodkin and Tessier-Lavigne, 2011), relatively little is known about the final "mating" of synaptic partners (Sanes and Yamagata, 2009; Shen and Scheiffele, 2010; Maeder and Shen, 2011).

Drosophila neuromuscular connectivity has long been a favorite model system for studying the molecular mechanisms of target selection, as it is possible to apply strong genetics to the formation of highly accessible synaptic connections between the motor neurons and muscles (Keshishian et al., 1996; Rose and Chiba, 2000; Ruiz-Canada and Budnik, 2006). Analyses of this system have pioneered the synaptic targeting studies by identifying specific molecular labels on target cells, such as Connectin (CON), Fasciclin3 (Fas3), and Capricious (Caps), and by showing their roles through genetic analyses *in vivo* (Nose et al., 1992, 1994, 1997; Chiba et al., 1995; Shishido et al., 1998; Winberg et al., 1998). These early studies provide excellent examples of how cell-to-cell target specificity can be regulated by the function of cell surface and secreted factors expressed on the target cells. In addition, I review findings from more recent studies that utilized technical innovations such as post-genome molecular genetic analyses and high-resolution cellular imaging. I discuss how target specificity is generated in a negative manner by expression of inhibitory cues in non-target cells and how such cues are transcriptionally regulated during development. I also describe how leucine-rich repeat (LRR) proteins have emerged from systematic gain-of-function (GOF) screens as a prominent molecular family that regulates synaptic specificity. Recent live-imaging analyses have also revealed that postsynaptic muscles actively participate in the partner selection.

TARGET RECOGNITION MOLECULES IDENTIFIED IN THE 1990s

In each hemisegment of *Drosophila* embryos and larvae, 30 muscle fibers are innervated by 36 motor neurons via one of the six branches of the peripheral nerves: intersegmental nerves (ISN, ISNb, and ISNd), segmental nerves (SNa and SNc), and a transverse nerve (TN) (Ruiz-Canada and Budnik, 2006). Dye injection to single neurons conducted in the late 1980s first showed that *Drosophila* motor neurons project to and synapse with specific muscles in a highly reproducible manner (Halpern et al., 1991; Sink and Whitington, 1991a,b). For example, the RP5 motor neuron innervates muscle 12 (M12) and the RP1 motor neurons innervate M13. During development, these motor neurons initially extend a number of filopodia to multiple muscles in the target region, and later restrict the contacts on the target muscle(s) (Sink and Whitington, 1991b). Muscle ablation and

duplication experiments indicate that each motor neuron selects appropriate targets in an altered cellular environment (Sink and Whitington, 1991c; Chiba et al., 1993). The high degree of precision and the ability of motor neurons to select specific targets in normal and manipulated situations suggest the presence of molecular labels active on individual muscles and prompted the search for such molecules (e.g., Nose et al., 1992; Van Vactor et al., 1993). These studies led to the identification of several candidate target recognition molecules expressed on specific muscle fibers (**Figure 1**, **Table 1**; Nose et al., 1992, 1994, 1997; Chiba et al., 1995; Matthes et al., 1995; Rose et al., 1997; Shishido et al., 1998; Winberg et al., 1998).

The LRR proteins CON and Caps, and an immunoglobulin superfamily (IgSF) protein Fas3, are homophilic cell adhesion molecules that are expressed in subsets of muscles and in the motor neurons that innervate these muscles (**Figure 1A**; Nose et al., 1992, 1994, 1997; Chiba et al., 1995; Kose et al., 1997; Shishido et al., 1998). Ectopic expression of these molecules in muscles dramatically alters target specificity. For example, Caps is expressed in RP5 and its target muscle, M12. When Caps expression is forced in the neighboring non-target M13, Caps-positive RP5 neurons inappropriately connect with M13 in addition to M12 (**Figure 2A**; Shishido et al., 1998; Taniguchi et al., 2000). Thus, these molecules appear to control target specificity by promoting interaction between specific partner cells. However, only weak phenotypes in the targeting are seen in loss-of-function (LOF) mutants of these molecules, suggesting that their function is redundant (Nose et al., 1994, 1997; Chiba et al., 1995; Shishido et al., 1998; Abrell and Jackle, 2001). In the case of Caps, closely related Tartan (Trn) was later found to be a redundant molecule that contributes to the targeting (Kurusu et al., 2008; see below). Recent studies have shown that Caps also functions

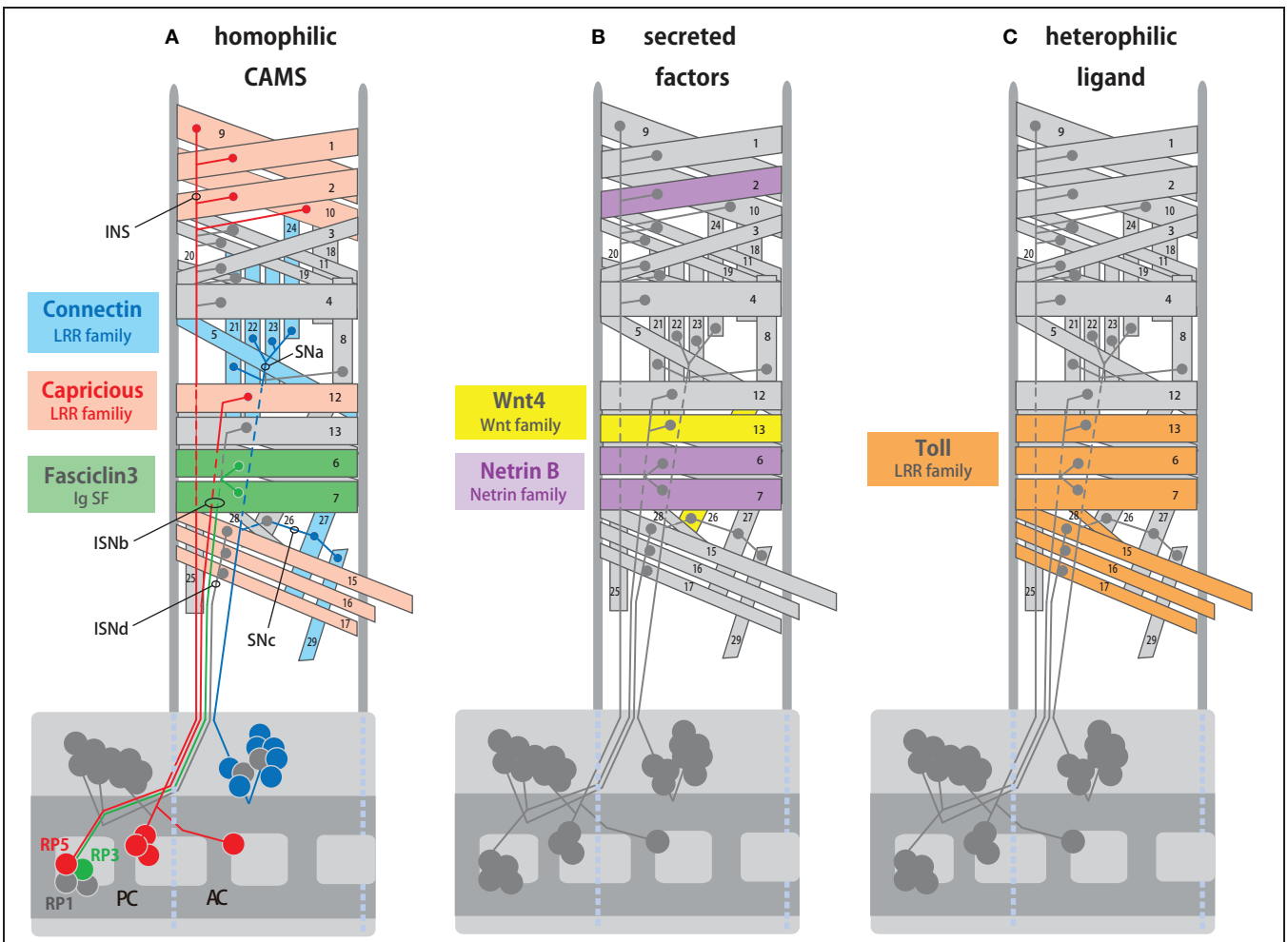

FIGURE 1 | Expression of target recognition molecules in specific muscles and motor neurons. (A) Expression of hemophilic cell adhesion molecules, Fas3, Capricious (Caps), and Connectin (Con) in specific synaptic partners. Fas3 is expressed in the RP3 motor neuron and its target muscles M6/7 (*green*). Caps is expressed in the RP5 motor neurons and its target M12 (*orange*). Con is expressed in external muscles and a group of motor neurons that innervate them (*blue*). **(B)** Expression of secreted factors, Netrin-B (NetB) and Wnt4 in specific muscles. NetB is expressed in M2, 6, and 7, whereas Wnt4 is expressed in M12 and 26. **(C)** Expression of Toll in specific muscles. Toll is expressed in subsets of ventral muscles including M6, 7, 13, 15, 16, 17, and 28 but not M12. AC and PC, anterior and posterior commissure. Projections of intersegmental (ISN, ISNb, and ISNd) and segmental (SNa and SNc) nerves are also shown.

Table 1 | Overview of candidate muscle target recognition cues in *Drosophila*.

Protein	Domain	Receptors/ ligands	Expression in muscles and motor neurons	Phenotypes	Affected muscle targets	References
CELL ADHESION/RECEPTORS						
Capricious (Caps)	LRR	Homophilic	Subsets of muscles and motor neurons, see **Figure 1A**	LOF and GOF, see **Figure 2A**	M12/13	Shishido et al. (1998) and Kurusu et al. (2008)
Tartan (Trn)	LRR	?	All ventral muscles	LOF and GOF, see **Figure 2A**	M12/13	Kurusu et al. (2008)
Hattifattener (Haf)	LRR	?	All ventral muscles	LOF and GOF, see **Figure 2C**	M12/13	Kurusu et al. (2008)
CG8561/convoluted (Conv)	LRR	?	All ventral muscles	LOF and GOF, see **Figure 2C**	M12/13	Kurusu et al. (2008)
Toll	LRR	?	Subsets of muscles, see **Figure 1C**	LOF and GOF, see **Figure 2B**	M12/13, M6/7	Rose et al. (1997) and Inaki et al. (2010)
Connectin (Con)	LRR	Homophilic	Subsets of muscles and motor neurons, see **Figure 1A**	GOF	Lateral muscles	Nose et al. (1992, 1994, 1997)
Fasciclin 3 (Fas3)	IgSF	Homophilic	Subsets of muscles and motor neurons, see **Figure 1A**	GOF	M6/7	Chiba et al. (1995) and Kose et al. (1997)
Fasciclin 2 (Fas2)	IgSF	Homophilic	All muscles and motor neurons	GOF	All or most muscles	Davis et al. (1997) and Winberg et al. (1998)
Forked end	–	?	Weak?	LOF and GOF	M12/13	Umemiya et al. (2002)
SECRETED FACTORS						
Wnt4	Wnt	Fz-2, Drl-2	Subsets of muscles, see **Figure 1B**	LOF and GOF, see **Figure 2B**	M12/13	Inaki et al. (2007)
Netrin-B (attraction)	Netrin	Fra	Subsets of muscles, see **Figure 1B**	LOF and GOF	M6/7	Mitchell et al. (1996) and Winberg et al. (1998)
Netrin-B (repulsion)	Ditto	Unc-5	Ditto	GOF	Lateral muscles	Winberg et al. (1998) and Labrador et al. (2005)
Semaphorin-2a (Sema2a)	Sema	Plex B	Weak in all muscles	GOF	All or most muscles	Matthes et al. (1995) and Winberg et al. (1998)
Beat-IIIc	IgSF	?	Subsets of muscles (13 and 30)	GOF	M12/13	Inaki et al. (2007)
Sulfated (Sulf1)	Sulfatase	?	Large subsets (higher in M13 than in M12)	GOF	M12/13	Inaki et al. (2007)
CG6867	IgSF	?	Most or all muscles (higher in M13 than in M12)	GOF	M12/13	Inaki et al. (2007)
Glutactin (Glt)	Chorinesterase	?	Weak (higher in M13 than in M12)	GOF	M12/13	Inaki et al. (2007)
Larval serum protein 2 (Lsp2)	–	?	Weak (higher in M13 than in M12)	GOF	M12/13	Inaki et al. (2007)

Attractive and inhibitory cues are shown in red and blue color, respectively.

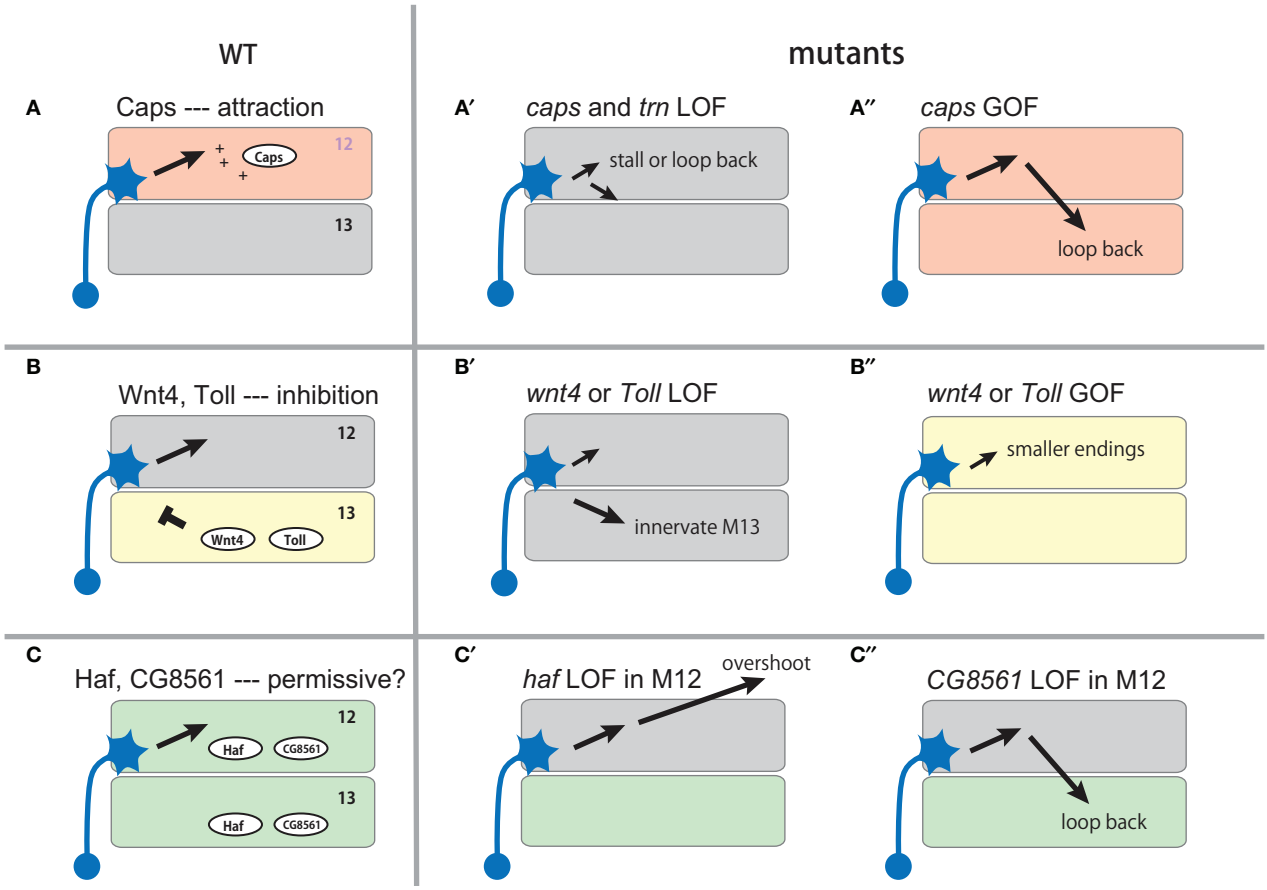

FIGURE 2 | Expression and function of muscle cues during the targeting of muscle 12 motor neurons. The expression of the muscle cues and their putative roles are shown in the left panel **(A–C)**. Schematic diagram of their loss-of-function (LOF, **A′–C′** and **C″**) and gain-of-function (GOF, **A″–B″**) phenotypes are shown on the right.

as a target recognition molecule in the visual system and olfactory system. In the visual system, as in the neuromuscular system, Caps is expressed in specific synaptic partners: the presynaptic photoreceptor R8 and the target layer M3 in the medulla. LOF and GOF analyses of Caps support the notion that Caps mediates specific interaction between R8 photoreceptors and the M3 layer (Shinza-Kameda et al., 2006). Several other cell-surface molecules have also been implicated in the targeting of the photoreceptors, including N-cadherin, Flamingo, DLAR, and Golden Goal (Hadjieconomou et al., 2011), although their roles in neuromuscular targeting remains unknown. In the olfactory system, Caps has been implicated in the targeting of projection neuron dendrites to specific glomeruli (Hong et al., 2009). In this case, heterophilic interaction with unknown ligand(s) is proposed as a mechanism because the target cells do not express Caps.

Netrin-B (NetB), a secreted protein of the Netrin family, is expressed in subsets of muscles, including M6/7 innervated by RP3 (**Figure 1B**, Mitchell et al., 1996; Winberg et al., 1998). In the absence of NetB, RP3 neurons form reduced endings on the target muscles, suggesting that NetB functions as an attractive cue for the neurons. NetB also repels other neurons (SNa and SNc motor neurons), when it is ectopically expressed in all muscles (Winberg et al., 1998). Frazzled (Fra) and Unc5 receptors are implicated as receptors for attractive and repulsive signaling by NetB, respectively (Kolodziej et al., 1996; Mitchell et al., 1996; Keleman and Dickson, 2001; Labrador et al., 2005).

Another molecule, Toll, has been shown to inhibit motor innervation when overexpressed in muscles. Toll is an LRR cell surface protein and is expressed in subsets of ventral muscles (**Figure 1C**; Nose et al., 1992; Halfon et al., 1995). Toll has anti-synaptogenic effects on RP3 (Rose et al., 1997). RP3 fails to innervate the target muscles, M6/7, when Toll is overexpressed in these muscles. In *Toll* LOF mutants, RP3 shows a variety of axon projection and targeting defects. Toll is also expressed in M6/7, but the expression is diminished by the time RP3 arrives. Thus, temporal and spatial regulation of Toll has been proposed to be critical for RP3 targeting (Rose et al., 1997). Studies of NetB and Toll show that ectopic expression of inhibitory cues can change neuromuscular targeting. However, it is unclear whether these molecules are essential for target selection.

Target specificity can also be changed by altered expression of uniform cues expressed in all muscles. Fasciclin2 (Fas2) is a homophilic cell adhesion molecule of IgSF and is expressed in

all motor neurons and muscles. Although Fas2 is not required for formation of neuromuscular specificity, changing the relative level of Fas2 in neighboring muscles dramatically changes the pattern of target selection (Davis et al., 1997). Sema-2a (previously termed SemaII) is a secreted protein of the semaphorin family and is weakly expressed in all muscles in the body wall (it is also strongly expressed in a single ventral muscle specific to thoracic segment T3; Matthes et al., 1995). Like Fas2, Sema-2a is not essential for neuromuscular targeting. However, overexpression of Sema-2a in muscles inhibits synapse formation by many motor neurons (Matthes et al., 1995; Winberg et al., 1998).

Several lines of evidence suggest that individual muscles are not specified in a lock-and-key fashion by unique molecular labels for targeting. First, motor neurons innervate non-target muscles when the target cell(s) are absent (Cash et al., 1992). Second, when a muscle fails to be innervated by the normal partners, other motor neurons inappropriately target the muscle (Halfon et al., 1995; Kopczynski et al., 1996). Third, LOF of any of the identified candidate target recognition molecules only partly disrupts proper targeting (Nose et al., 1994; Chiba et al., 1995; Matthes et al., 1995; Shishido et al., 1998; Winberg et al., 1998). It is, therefore, generally believed that target specificity is determined by the combined function of multiple cues in a dynamic and flexible manner (relative balance model; Winberg et al., 1998). The cues could be uniquely expressed on specific muscles or general cues expressed in all muscles. Synaptic connections are also refined in an activity-dependent manner once they are formed (Carrillo et al., 2010). Thus, despite the stereotypy during normal development, the neuromuscular connectivity appears to be a flexible and plastic system.

Winberg et al. (1998) and Rose and Chiba (1999) studied whether motor neurons can indeed integrate information provided by multiple cues by simultaneously changing the expression of multiple cues. Winberg et al. (1998) systematically altered the expression of NetB, an attractive cue, and the inhibitory cue Sema-2a during the targeting of M6/7 by RP3. As described above, removal of attractive NetB reduces innervation of M6/7 by RP3 as does increased expression of inhibitory Sema-2a. However, when the removal of NetB is combined with the removal of Sema-2a, or when the increased expression of Sema-2a is combined with increased expression of NetB, the defects in targeting were restored. Similarly, Rose and Chiba (1999) simultaneously manipulated the expression of Fas3, an attractive cue for RP3, and Toll, an inhibitory cue, and found that they cancelled one other. These observations strongly support the idea that motor neurons can assess the balance between multiple attractive and inhibitory cues during targeting.

NEW MOLECULAR AND GENETIC SCREENS IN THE POST-GENOME ERA

The studies described above strongly suggest that target specificity of individual muscles is determined by the action of multiple target cues. However, the following questions remain. How many molecules are involved in the specification of individual target muscles? Is the specificity generated by diversity among a particular protein family or by random utilization of different protein families? What are the roles of inhibitory cues in target selection? How is the expression of multiple target cues in specific muscles coordinated during development? To answer these questions, two recent studies utilized high-throughput, post-genomic technologies to search for genes involved in the targeting (Inaki et al., 2007; Kurusu et al., 2008). Both of these studies focused on the targeting between M12 and M13 and tried to systematically identify genes that regulate synaptic specificity. M12 is innervated by RP5 and V neurons (collectively called MN12s) and M13 is innervated by RP1 and RP4. Inaki et al. (2007) performed comparative microarray analyses of M12 and M13 by directly isolating these muscles from dissected embryos. The analyses identified more than 200 candidate genes that are differentially expressed between these muscles, including 25 that encodes putative cell surface and secreted proteins that could play roles in target recognition. Functional analyses of the candidate genes led to the identification of a negative regulator of target specificity, Wnt4, and a transcriptional regulator of target specificity, Tey, as detailed below. Kurusu et al. (2008) conducted systematic GOF analyses of a collection of putative cell surface and secreted proteins identified by bioinformatics. The screening revealed roles for a number of LRR proteins, highlighting the roles of this gene family in selective synapse formation.

GENERATION OF TARGET SPECIFICITY BY NEGATIVE CUES

Microarray analyses by Inaki et al. (2007) identified Wnt4, a secreted Wnt family protein, as being enriched in M13. In *Wnt4* LOF mutants, MN12s form smaller synapses on their normal target and form ectopic nerve endings on M13. This results in enlarged nerve terminals on M13 and diminished endings on M12. Conversely, when Wnt4 is ectopically expressed on M12, the nerve terminal on the muscle is greatly reduced in size. These results suggest that Wnt4 expressed on M13 prevents synapse formation by the MN12s (**Figure 2B**). Frizzled-2 (Fz-2) and Derailed-2 (Drl-2) receptors and a downstream Dishevelled (Dsh) have been implicated in the reception of Wnt4 signaling in motor neurons. Whereas Fz-2 is expressed in all neurons, drl-2 expression is restricted to specific neurons and thus may be responsible for the specificity of the Wnt4 action. Studies on synapse formation in *C. elegans* showed that the Wnt protein Lin-44 determines the subcellular location of synapses by preventing synapse formation in a specific domain of DA9 axons (Klassen and Shen, 2007). Thus, regulation of synaptic specificity by inhibitory activity of Wnts appears to be an evolutionarily conserved mechanism.

Another candidate target recognition molecule on M13 that has been identified by microarray screening is Toll. As described above, Toll was previously implicated as an inhibitory cue expressed on M6/7 (Rose et al., 1997). The differential expression of Toll in M12 and M13 prompted Inaki et al. (2010) to study potential roles of Toll in target selection between these two muscles. The authors found that Toll mutant embryos show similar phenotypes as seen in *Wnt4* mutants: expansion of M13 terminals and reduction of M12 terminals. Ectopic expression of Toll in M13 also showed similar phenotypes as seen when Wnt4 is misexpressed on the muscle: reduction of M12 terminals. These results suggest that Toll, like Wnt4, regulates target specificity by inhibiting synapse formation on M13 (**Figure 2B**). How Toll transmits

the inhibitory signal to motor neurons remains unknown. One possibility is that Toll functions as a ligand expressed on muscles and signals through unknown receptor(s) on motor neurons. Toll is the founding member of the Toll-like receptors, whose functions as receptors have been well characterized in early embryogenesis and innate immunity (West et al., 2006; Valanne et al., 2011). Whether or not Toll also functions as a ligand for other receptors is currently unknown.

It is notable that M12MNs form nerve endings of similar size on M12 and M13 in mutants that lack Wnt4 or Toll. This indicates that in the absence of inhibitory cues, these two muscles are equally favorable targets for the motor neurons. Target specificity only arises with the differential expression of these negative cues. These findings provide strong evidence for the role of inhibition in target selection.

In addition to Wnt4 and Toll, microarray analyses by Inaki et al. (2007) identified five molecules that are enriched in M13 and, when misexpressed in M12, inhibit synapse formation of MN12s: Beaten path III-c (Beat-IIIc, a member of the Beat subfamily of IgSF), Glutactin (Glt) (a cell surface protein with cholinesterase domains), Larval serum protein 2 (Lsp2) (a secreted protein), Sulfated (Sulf1) (an extracellular sulfatase), and CG6867 (a secreted protein of IgSF) (**Table 1**). Although the precise roles of these molecules remain to be determined by LOF analyses, these results suggest that a single muscle expresses a variety of inhibitory cues. Beat-IIIc is of particular interest since a recent study showed that another member of the family, Beat-Ia, and its ligand, Sidestep (Side), are involved in the guidance of motor axon to the target region (Siebert et al., 2009). Identification of Beat-IIIc as a putative muscle target recognition molecule suggests a possibility that Beat/Side families may be important regulators of synaptic targeting.

LRR PROTEIN FAMILY AS KEY REGULATORS OF SELECTIVE SYNAPSE FORMATION

Based on the fact that GOF mutants of many identified target recognition molecules show stronger phenotypes than their LOF counterparts. Kurusu et al. (2008) performed systematic GOF screening in search of new target cues. The authors screened ∼410 putative cell surface or secreted proteins (representing ∼40% of this class of protein in *Drosophila*) and found that targeted expression of 30 of these genes in all muscles produces mistargeting phenotypes. Eleven of these genes (including five known genes) are normally expressed in muscles. Remarkably, five of the 11 genes are LRR proteins, while all other genes contained different domains. Two of the LRR proteins are Caps and its close relative Tartan. The identification of the two closely related genes by the screening prompted the authors to study *caps, trn* double mutants. Single mutants of *trn* or *caps* display only weak phenotypes in ISNb guidance and targeting. However, in the double mutants, a dramatic phenotype called "terminal loop" was observed in ISNb targeting. The loop is seen on the distal end of the ISNb near the M12/M13 boundary or on M12, suggesting that M12MNs either stall or turn back toward M13 after reaching the target (**Figure 2A**). Caps and Trn thus appear to function in a redundant manner in M12 targeting. Whereas *caps* is enriched in M12 and other specific muscles, *trn* appears to be expressed weakly in all ventral muscles with a lower level in M12 and M13 compared to M6 and M7 (Kurusu et al., 2008).

The GOF screening also identified two novel LRR cell surface proteins, Hattifattener (Haf) and CG8561/Convoluted (Conv), as regulators of ISNb targeting. Since expression of these genes is not confined to specific muscles, they appear to function as general muscle cues that are essential for proper ISNb targeting. In *haf* mutant embryos, ISNb motor neurons display a variety of abnormal projection and targeting errors, which are hard to interpret in terms of simple mechanisms. However, a more informative phenotype was observed when the gene was knocked down specifically in M12 by expression of RNAi constructs (**Figure 2C**). In the M12-specific mutants, the distal branch of ISNb reaches and innervates M12 as in normal animals, but it also extends further and forms ectopic synapses with lateral muscles. This phenotype suggests a role for *haf* in stabilizing the connection with the target muscles. Another LRR protein, CG8561/Conv is an ortholog of vertebrate acid-labile subunit (Als) of the IGF-1 binding complex. Like *haf*, LOF of this gene in all muscles produces complex phenotypes. However, when the function of CG8561 was knocked down only in M12, a specific loop-back phenotype of M12MNs was seen in >70% of the segments (**Figure 2C**).

In addition to genes implicated in targeting, the screening by Kurusu et al. also identified a number of genes whose forced expression in muscles affects neuromuscular junction (NMJ) morphology. In total, 53 LRR genes (of the 101 LRR genes in the genome) were screened and 16 of them were found to affect target selection, synapse formation or both. In addition, previous studies have already identified three LRR proteins (Caps, CON, and Toll) as target cues (**Table 1**). Thus, members of this family appear to be major players in selective synapse formation in this system (**Table 1**). LRRs are repeating motifs of ∼24 amino acids that are thought to function as an effective and versatile protein-binding motif (de Wit et al., 2011). Expression of diverse members of this family could, therefore, generate specificity among neurons by conferring differential adhesion and/or recognition activity. Recent studies on mammalian synapse formation also identified a number of LRR transmembrane proteins as synaptic organizers (e.g., Linhoff et al., 2009; de Wit et al., 2011). Some of these molecules are expressed in a region-specific manner. While their roles in the control of synaptic specificity remain to be explored, it is an interesting possibility that LRR proteins also control synaptic specificity in the vertebrate brain.

TRANSCRIPTIONAL CONTROL OF TARGET SPECIFICITY

The demonstrated roles of multiple muscle target cues raise a further question: what are the higher-level processes that regulate the expression of these cues? For proper neural wiring, target recognition cues and their receptors have to be expressed in specific pre- and post-synaptic cells with proper timing. Little is known about the developmental mechanisms that regulate this process. A study by Inaki et al. (2010) provides an important insight. One of the genes identified by microarray screening (Inaki et al., 2007) encodes the putative transcription factor Tey. Its expression in

muscles is highly specific, being confined to a single muscle, M12, among the 30 muscles in the body wall. Tey represses the expression of Toll in this muscle. As described above, Toll is an inhibitory cue for motor neurons targeted to M12 and is expressed in M13 and other surrounding non-target muscles, but not in M12. In *tey* LOF mutants, Toll is ectopically expressed in M12. Conversely, ectopic expression of *tey* in M13 downregulates Toll expression in the muscle. LOF and GOF of *tey* lead to phenotypes as expected for the misregulated expression of Toll. Synapse formation on M12 is reduced in *tey* LOF mutants, consistent with the upregulation of Toll in this muscle. M13 receives ectopic innervation in *tey* GOF mutants, consistent with the downregulation of Toll. Tey, therefore, controls neuromuscular specificity by repressing the expression of Toll in M12 (**Figure 3A**). This example shows how target specificity can be generated by suppression of an inhibitory cue in one among a group of target cells expressing the cue (**Figure 3B**).

Control of target specificity by transcriptional repression is also seen in presynaptic photoreceptor cells in the *Drosophila* visual system (Morey et al., 2008). As described above, Caps is expressed in R8 photoreceptor cells and is required for their proper projection to the target layer. Caps expression in R8 cells is positively regulated by the transcription factor Senseless (Sens). In R7 cells, on the other hand, another transcription factor NF-YC represses expression of Sens and the downstream Caps. In NF-YC mutants, R7 cells misexpress Sens and Caps and inappropriately terminate in the R8 target layer as seen when Caps is ectopically expressed in these cells. Thus, repression of Sens and Caps is critical for R7 targeting.

In *tey* mutants, muscle insertion sites of M12 are also specifically affected. Thus, *tey* appears to regulate two key aspects of muscle specification: geometry and synaptic specificity. Several transcription factors have been identified that are expressed in subsets of muscle and/or their progenitor cells (muscle founder cells) and specify the identities of the muscles (reviewed in Tixier et al., 2010). It is an interesting possibility that these genes, like *tey*, may also regulate neuromuscular target specificity. A BTB zinc-finger transcription factor, Abrupt (Ab), on the other hand, is expressed in all muscles but regulates specific aspects of motor neuron projection (Hu et al., 1995). In abrupt mutants, ISNb motor neurons reach the target region normally but fail to form appropriate innervation on the target muscles. The differentiation of the target ventral muscles is normal. Ab may thus regulate the expression of general target recognition molecules, such as Haf, in these muscles. Several transcription factors that function in motor neurons to specify the target domain have also been identified, including Even-skipped, Islet and Lim3 (reviewed in Landgraf and Thor, 2006). However, whether these transcription factors regulate the expression of target recognition molecules remain unknown.

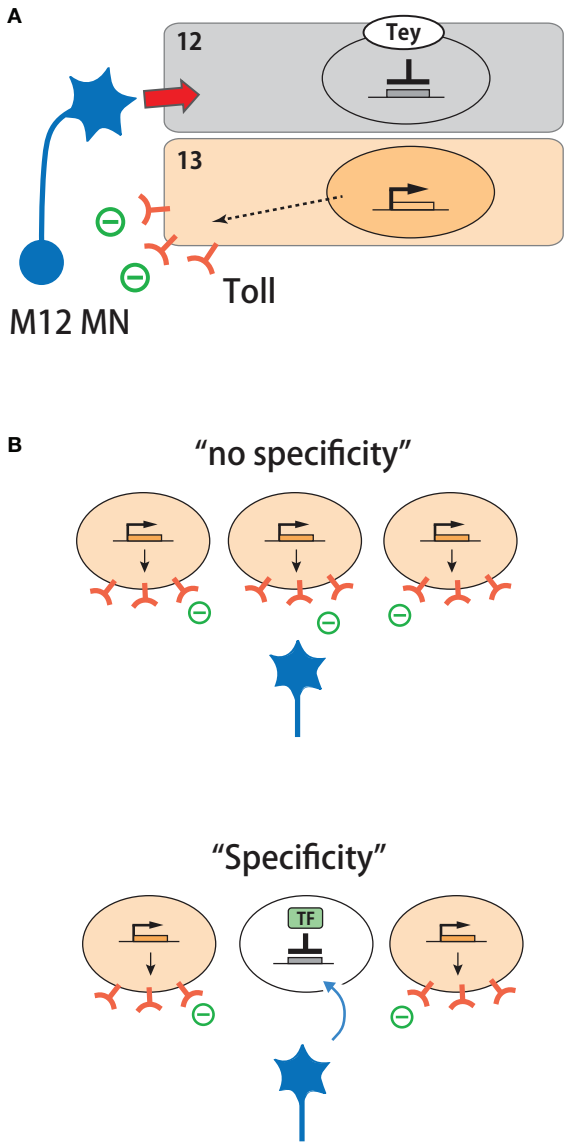

FIGURE 3 | Transcriptional regulation of target specificity by repression of inhibitory cues. (A) Tey represses expression of Toll in M12 and thereby determines target specificity. **(B)** A model in which target specificity can be generated in a group of equivalent targets by transcriptional repression of a repulsive cue.

PARTNER RECOGNITION BY MYOPODIA

In addition to recognition by presynaptic motor neurons, recent studies suggest that the postsynaptic muscles also seek and find their presynaptic partners. In fixed specimens, differentiated muscles show little sign of motility and, therefore, have long been regarded as passive players during synaptic matchmaking, waiting for the arrival of motor neurons. However, Ritzenthaler et al. (2000) used high-resolution live imaging to show that muscles actually bear a number of dynamic protrusions, called myopodia, that extend and retract prior to and during the period of neuromuscular interaction. Myopodia are actin-based membrane microprocesses ~10 μm or longer in length and 0.1–0.2 μm in diameter. Myopodia initially extend in random directions but gradually cluster at the site of innervation as they interact with the presynaptic filopodia (**Figure 4A**, top). The clustering of myopodia depends on interaction with the presynaptic motor neurons (Ritzenthaler et al., 2000; Ritzenthaler and Chiba, 2003).

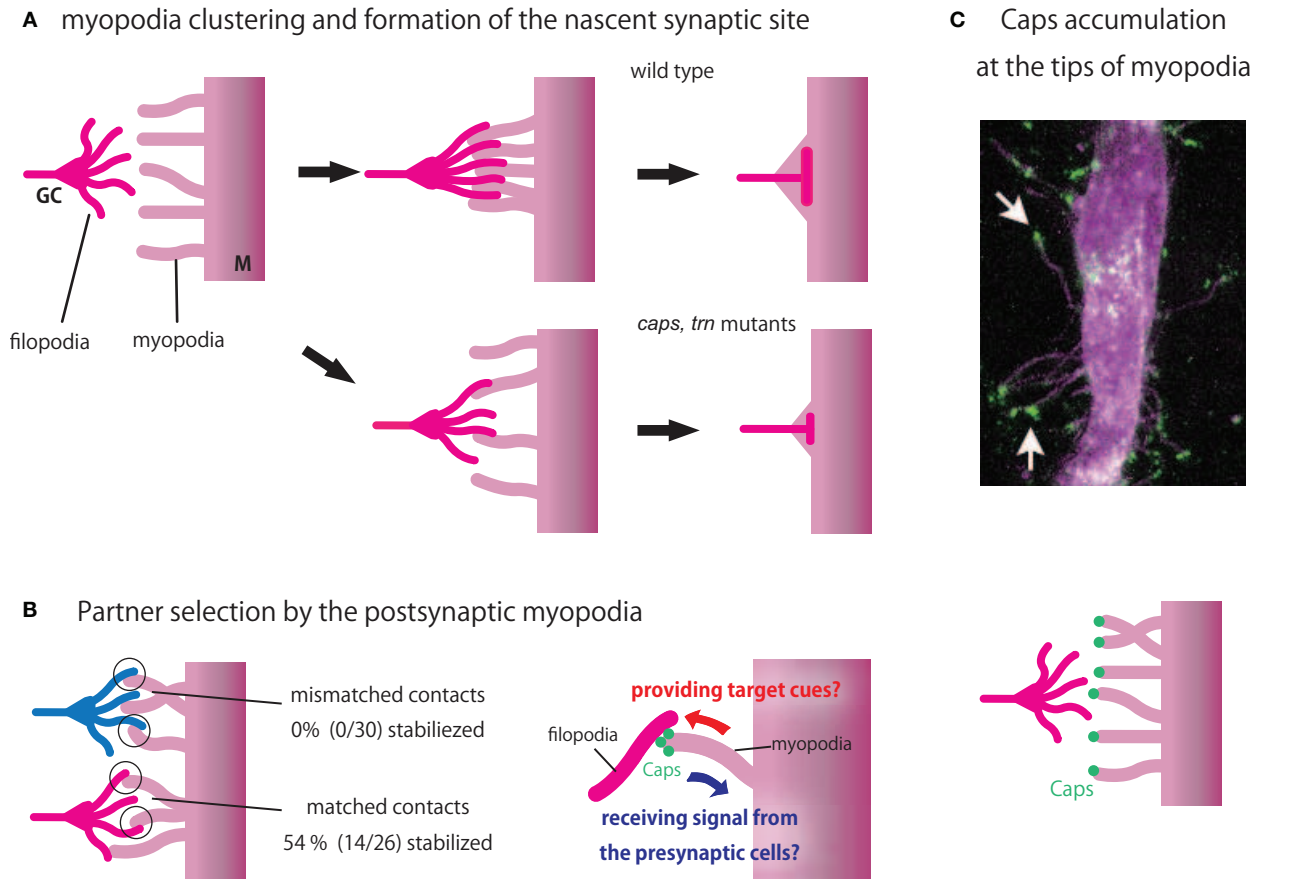

FIGURE 4 | Partner recognition by myopodia. (A) Schematic diagram showing myopodia clustering and formation of nascent synaptic sites in wild type (above) and *caps, trn* double mutants (below). **(B)** Partner selection by myopodia (*Left*). While 54% of myopodial contacts with a partner motor neuron (magenta) are stabilized, none of the contacts with the non-partner motor neuron (*blue*) are stabilized (*Right*). Caps at the tip of myopodia may function in a bidirectional manner, providing target cues to and receiving signal from the presynaptic cells. **(C)** Caps accumulation at the tips of mypopodia. GC, growth cone (*Top*). Simultaneous live-imaging of Caps-GFP (*green*) and muscle membrane (*magenta*) reveals Caps localization at the tips of myopodia (*arrows*). Taken from Kohsaka and Nose (2009) *Bottom*. A diagram showing Caps localization.

As myopodia cluster, they intermingle and "zip" with the presynaptic filopodia and finally fuse to form the nascent postsynaptic sites (Ritzenthaler et al., 2000; Ritzenthaler and Chiba, 2003; Kohsaka et al., 2007). Thus, neuromuscular targeting is a reciprocal process in which motor neurons and muscles seek each other.

What is the precise role of myopodia? Cells use filopodia and other cellular extensions to efficiently transmit and receive information via long-distance direct cell–cell interaction (Rørth, 2003; Hsiung et al., 2005; Heiman and Shaham, 2010; Roy et al., 2011). For example, neuronal growth cones extend filopodia as they explore the local environment. In the *Drosophila* imaginal disc, cytonemes and other actin-based extensions are utilized not only in the signal-receiving cells to actively seek cues from a distance but also in the signal-sending cells to efficiently present information to the receiving cells (Rørth, 2003; Hsiung et al., 2005; Roy et al., 2011). Similarly, myopodia may function to receive and/or send information at a distance. A study by Kohsaka and Nose (2009) showed that myopodia have a sensory function. Simultaneous live-imaging of muscles and motor axons is used to study the behavior of myopodia when they encounter partner or non-partner motor neurons (**Figure 4B**). When myopodia encounter the growth cones of partner motor neurons, about half of the contacts are stabilized to from synapses. In contrast, none of the contacts with the non-partners are stabilized, suggesting that individual myopodia can recognize the appropriate partner. So, just like presynaptic growth cones seek and find the right targets, postsynaptic muscles also select among potential presynaptic partners using myopodia.

Localization and function of Caps in myopodia has also been studied (Kohsaka and Nose, 2009). Caps is localized at the tip of myopodia, where many of the initial contacts between muscles and growth cones take place (**Figure 4C**). In *caps* mutants, fewer myopodial contacts with the presynaptic motor neurons are stabilized in M12. The size of the nascent presynaptic terminal is also reduced. Similar but more penetrant phenotypes are

seen in *caps, trn* double mutants (**Figure 4A**, bottom). Thus, Caps-mediated signaling at the tip of myopodia appears to be critical for selective synapse formation. It is likely that Caps functions in a bi-directional manner at the tips of myopodia (**Figure 4B**, right). By localizing at the tip of myopodia, Caps may be efficiently presented to and recognized by the growth cones. Caps may also be involved in the recognition of motor neurons by the myopodia. Such bidirectional signaling might ensure proper synaptic matchmaking. Many signaling and adhesion molecules are known to accumulate at the tips of filopodia, including Ena/VASP, formins, and integrins (Faix and Rottner, 2006; Mattila and Lappalainen, 2008). Thus, tips of myopodia may function as a signaling center that regulate myopodia dynamics and synapse formation. Dendrites of vertebrate neurons also cast out dendritic filopodia during synapse formation. A recent study in rodents showed that dendritic filopodia of hippocampal neurons discriminate between target and non-target axons (Lohmann and Bonhoeffer, 2008). Regulation of synapse specificity by postsynaptic protrusions thus seems to be a common mechanism across taxa.

CONCLUSION

When investigators began searching for NMJ target recognition molecules in the 1990s, most envisioned a simple lock-and-key mechanism, as initially postulated by Sperry (1963). However, the dance between motor neurons and target muscles turns out to be far more complex than initially thought. Multiple molecular chaperons appear to mediate the partner selection in a partially redundant and combinatorial manner. Partner selection is not only determined by attraction to the partner but also by exclusion from other cells. Furthermore, the molecular courtship is not one-sided but is a mutual searching process mediated by complex interactions of filopodia and myopodia.

Studies thus far implicate at least 11 proteins in targeting of M12, including the attractive cues Caps and Tartan on the muscle, inhibitory cues Wnt4, Toll, Beat-3c, Glt, Lsp2, Sulf1, and CG6867 on the neighboring M13, and general cues Haf and CG8561 on all muscles. Why so many target cues are present to specify the targeting of a single muscle is a mystery. Determining how multiple classes of molecular cue are translated into a coherent downstream signal that culminates in the formation of specific synapses is an important future direction. Development of a complete set of GOF constructs for all cell surface and secreted proteins would allow the definition of every protein that can produce a neuromuscular targeting GOF phenotype and provide a list of candidate players. Even more mysterious is how the expression of diverse target cues is coordinated during muscle development. Although studies of Tey begin to answer this question, much more work is needed to obtain the whole picture. Clues may be obtained by comprehensive analyses of the transcriptional cascade, like those performed in the *Drosophila* mesoderm (Zinzen et al., 2009; Junion et al., 2012).

NOTE ADDED IN REVISION

Mosca et al. (2012) recently reported that Teneurin (Ten)-m and Ten-a, belonging to conserved epidermal growth factor (EGF)-repeat-containing transmembrane proteins, regulate neuromuscular targeting in *Drosophila*. Ten-m and Ten-a are expressed in all muscles and motor neurons, respectively, and mediate bi-directional interaction required for proper organization of the NMJs. Ten-m is expressed at a higher level in muscle 3 and 8, and are required for synapse formation in these muscles. Like Fas2, changing the relative level of Ten-m between muscles 6 and 7 alters the pattern of target selection. Thus, Ten-m and Ten-a appear to regulate general synaptic organization as well as target specificity.

ACKNOWLEDGMENTS

I thank present and past members of the lab for their contribution to the studies described in this article and Kasumi Shibahara for the help in illustration. This article is supported by a Grant-in-Aid for Scientific Research on Innovative Areas "Mesoscopic Neurocircuitry" (No. 22115002) and for Scientific Research on Innovative Areas "Comprehensive Brain Science Network" (No. 221S0003), of The Ministry of Education, Culture, Sports, Science, and Technology, Japan, and for Scientific Research (B) (No. 23300114) of Japan Society for the Promotion of Science (JSPS), to Akinao Nose.

REFERENCES

Abrell, S., and Jackle, H. (2001). Axon guidance of *Drosophila* SNb motoneurons depends on the cooperative action of muscular Kruppel and neuronal capricious activities. *Mech. Dev.* 109, 3–12.

Carrillo, R. A., Olsen, D. P., Yoon, K. S., and Keshishian, H. (2010). Presynaptic activity and CaMKII modulate retrograde semaphorin signaling and synaptic refinement. *Neuron* 68, 32–44.

Cash, S., Chiba, A., and Keshishian, H. (1992). Alternate neuromuscular target selection following the loss of single muscle-fibers in *Drosophila*. *J. Neurosci.* 12, 2051–2064.

Chiba, A., Hing, H., Cash, S., and Keshishian, H. (1993). Growth cone choices of *Drosophila* motoneurons in response to muscle-fiber mismatch. *J. Neurosci.* 13, 714–732.

Chiba, A., Snow, P., Keshishian, H., and Hotta, Y. (1995). Fasciclin-III as a synaptic target recognition molecule in *Drosophila*. *Nature* 374, 166–168.

Davis, G. W., Schuster, C. M., and Goodman, C. S. (1997). Genetic analysis of the mechanisms controlling target selection: target-derived fasciclin II regulates the pattern of synapse formation. *Neuron* 19, 561–573.

de Wit, J., Hong, W., Luo, L., and Ghosh, A. (2011). Role of leucine-rich repeat proteins in the development and function of neural circuits. *Annu. Rev. Cell Dev. Biol.* 27, 697–729.

Faix, J., and Rottner, K. (2006). The making of filopodia. *Curr. Opin. Cell Biol.* 18, 18–25.

Hadjieconomou, D., Timofeev, K., and Salecker, I. (2011). A step-by-step guide to visual circuit assembly in *Drosophila*. *Curr. Opin. Neurobiol.* 21, 76–84.

Halfon, M. S., Hashimoto, C., and Keshishian, H. (1995). The *Drosophila* Toll gene functions zygotically and is necessary for proper motoneuron and muscle development. *Dev. Biol.* 169, 151–167.

Halpern, M. E., Chiba, A., Johansen, J., and Keshishian, H. (1991). Growth cone behavior underlying the development of stereotypic synaptic connections in *Drosophila* embryos. *J. Neurosci.* 11, 3227–3238.

Heiman, M. G., and Shaham, S. (2010). Twigs into branches: how a filopodium becomes a dendrite. *Curr. Opin. Neurobiol.* 20, 86–91.

Hong, W., Zhu, H., Potter, C. J., Barsh, G., Kurusu, M., Zinn, K., and Luo, L. (2009). Leucine-rich repeat transmembrane proteins instruct discrete dendrite targeting in an olfactory map. *Nat. Neurosci.* 12, 1542–1550.

Hsiung, F., Ramirez-Weber, F. A., Iwaki, D. D., and Kornberg, T. B. (2005). Dependence of *Drosophila*

wing imaginal disc cytonemes on Decapentaplegic. *Nature* 437, 560–563.

Hu, S., Fambrough, D., Atashi, J., Goodman, C., and Crews, S. (1995). The *Drosophila* abrupt gene encodes a BTB-zinc finger regulatory protein that controls the specificity of neuromuscular connections. *Genes Dev.* 9, 2936–2948.

Inaki, M., Shinza-Kameda, M., Ismat, A., Frasch, M., and Nose, A. (2010). *Drosophila* Tey represses transcription of the repulsive cue Toll and generates neuromuscular target specificity. *Development* 137, 2139–2146.

Inaki, M., Yoshikawa, S., Thomas, J. B., Aburatani, H., and Nose, A. (2007). Wnt4 is a local repulsive cue that determines synaptic target specificity. *Curr. Biol.* 17, 1574–1579.

Junion, G., Spivakov, M., Girardot, C., Braun, M., Gustafson, E. H., Birney, E., and Furlong, E. E. (2012). A transcription factor collective defines cardiac cell fate and reflects lineage history. *Cell* 148, 473–486.

Keleman, K., and Dickson, B. J. (2001). Short- and long-range repulsion by the *Drosophila* Unc5 netrin receptor. *Neuron* 32, 605–617.

Keshishian, H., Broadie, K., Chiba, A., and Bate, M. (1996). The *Drosophila* neuromuscular junction: a model system for studying synaptic development and function. *Annu. Rev. Neurosci.* 19, 545–575.

Klassen, M. P., and Shen, K. (2007). Wnt signaling positions neuromuscular connectivity by inhibiting synapse formation in *C. elegans*. *Cell* 130, 704–716.

Kohsaka, H., and Nose, A. (2009). Target recognition at the tips of postsynaptic filopodia: accumulation and function of Capricious. *Development* 136, 1127–1135.

Kohsaka, H., Takasu, E., and Nose, A. (2007). *In vivo* induction of postsynaptic molecular assembly by the cell adhesion molecule Fasciclin2. *J. Cell Biol.* 179, 1289–1300.

Kolodkin, A. L., and Tessier-Lavigne, M. (2011). Mechanisms and molecules of neuronal wiring: a primer. *Cold Spring Harb. Perspect. Biol.* 3, 1–13.

Kolodziej, P. A., Timpe, L. C., Mitchell, K. J., Fried, S. R., Goodman, C. S., Jan, L. Y., and Jan, Y. N. (1996). Frazzled encodes a *Drosophila* member of the DCC immunoglobulin subfamily and is required for CNS and motor axon guidance. *Cell* 87, 197–204.

Kopczynski, C. C., Davis, G. W., and Goodman, C. S. (1996). A neural tetraspanin, encoded by late bloomer, that facilitates synapse formation. *Science* 271, 1867–1870.

Kose, H., Rose, D., Zhu, X. M., and Chiba, A. (1997). Homophilic synaptic target recognition mediated by immunoglobulin-like cell adhesion molecule Fasciclin III. *Development* 124, 4143–4152.

Kurusu, M., Cording, A., Taniguchi, M., Menon, K., Suzuki, E., and Zinn, K. (2008). A screen of cell-surface molecules identifies leucine-rich repeat proteins as key mediators of synaptic target selection. *Neuron* 59, 972–985.

Labrador, J. P., O'Keefe, D., Yoshikawa, S., McKinnon, R. D., Thomas, J. B., and Bashaw, G. J. (2005). The homeobox transcription factor even-skipped regulates netrin-receptor expression to control dorsal motor-axon projections in *Drosophila*. *Curr. Biol.* 15, 1413–1419.

Landgraf, M., and Thor, S. (2006). Development and structure of motoneurons. *Int. Rev. Neurobiol.* 75, 33–53.

Linhoff, M. W., Laurén, J., Cassidy, R. M., Dobie, F. A., Takahashi, H., Nygaard, H. B., Airaksinen, M. S., Strittmatter, S. M., and Craig, A. M. (2009). An unbiased expression screen for synaptogenic proteins identifies the LRRTM protein family as synaptic organizers. *Neuron* 61, 734–749.

Lohmann, C., and Bonhoeffer, T. (2008). A role for local calcium signaling in rapid synaptic partner selection by dendritic filopodia. *Neuron* 59, 253–260.

Maeder, C., and Shen, K. (2011). Genetic dissection of synaptic specificity. *Curr. Opin. Neurobiol.* 21, 93–99.

Matthes, D. J., Sink, H., Kolodkin, A. L., and Goodman, C. S. (1995). Semaphorin-II can function as a selective inhibitor of specific synaptic arborizations. *Cell* 81, 631–639.

Mattila, P. K., and Lappalainen, P. (2008). Filopodia: molecular architecture and cellular functions. *Nat. Rev. Mol. Cell Biol.* 9, 446–454.

Mitchell, K. J., Doyle, J. L., Serafini, T., Kennedy, T. E., TessierLavigne, M., Goodman, C. S., and Dickson, B. J. (1996). Genetic analysis of Netrin genes in *Drosophila*: netrins guide CNS commissural axons and peripheral motor axons. *Neuron* 17, 203–215.

Morey, M., Yee, S. K., Herman, T., Nern, A., Blanco, E., and Zipursky, S. L. (2008). Coordinate control of synaptic-layer specificity and rhodopsins in photoreceptor neurons. *Nature* 456, 795–799.

Mosca, T. J., Hong, W., Dani, V. S., Favaloro, V., and Luo, L. (2012). Trans-synaptic Teneurin signalling in neuromuscular synapse organization and target choice. *Nature* 484, 237–241.

Nose, A., Mahajan, V. B., and Goodman, C. S. (1992). Connectin: a homophilic cell-adhesion molecule expressed on a subset of muscles and the motoneurons that innervate them in *Drosophila*. *Cell* 70, 553–567.

Nose, A., Takeichi, M., and Goodman, C. S. (1994). Ectopic expression of connectin reveals a repulsive function during growth cone guidance and synapse formation. *Neuron* 13, 525–539.

Nose, A., Umeda, T., and Takeichi, M. (1997). Neuromuscular target recognition by a homophilic interaction of Connectin cell adhesion molecules in *Drosophila*. *Development* 124, 1433–1441.

Ritzenthaler, S., and Chiba, A. (2003). Myopodia (postsynaptic filopodia) participate in synaptic target recognition. *J. Neurobiol.* 55, 31–40.

Ritzenthaler, S., Suzuki, E., and Chiba, A. (2000). Postsynaptic filopodia in muscle cells interact with innervating motoneuron axons. *Nat. Neurosci.* 3, 1012–1017.

Rose, D., and Chiba, A. (1999). A single growth cone is capable of integrating simultaneously presented and functionally distinct molecular cues during target recognition. *J. Neurosci.* 19, 4899–4906.

Rose, D., and Chiba, A. (2000). Synaptic target recognition at *Drosophila* neuromuscular junctions. *Microsc. Res. Tech.* 49, 3–13.

Rose, D., Zhu, X. M., Kose, H., Hoang, B., Cho, J., and Chiba, A. (1997). Toll, a muscle cell surface molecule, locally inhibits synaptic initiation of the RP3 motoneuron growth cone in *Drosophila*. *Development* 124, 1561–1571.

Roy, S., Hsiung, F., and Kornberg, T. B. (2011). Specificity of *Drosophila* cytonemes for distinct signaling pathways. *Science* 332, 354–358.

Ruiz-Canada, C., and Budnik, V. (2006). Introduction on the use of the *Drosophila* embryonic/larval neuromuscular junction as a model system to study synapse development and function, and a brief summary of pathfinding and target recognition. *Int. Rev. Neurobiol.* 75, 1–31.

Rørth, P. (2003). Communication by touch: role of cellular extensions in complex animals. *Cell* 112, 595–598.

Sanes, J. R., and Yamagata, M. (2009). Many paths to synaptic specificity. *Annu. Rev. Cell Dev. Biol.* 25, 161–195.

Shen, K., and Scheiffele, P. (2010). Genetics and cell biology of building specific synaptic connectivity. *Annu. Rev. Neurosci.* 33, 473–507.

Shinza-Kameda, M., Takasu, E., Sakurai, K., Hayashi, S., and Nose, A. (2006). Regulation of layer-specific targeting by reciprocal expression of a cell adhesion molecule, capricious. *Neuron* 49, 205–213.

Shishido, E., Takeichi, M., and Nose, A. (1998). *Drosophila* synapse formation: regulation by transmembrane protein with leu-rich repeats, CAPRICIOUS. *Science* 280, 2118–2121.

Siebert, M., Banovic, D., Goellner, B., and Aberle, H. (2009). *Drosophila* motor axons recognize and follow a sidestep-labeled substrate pathway to reach their target fields. *Genes Dev.* 23, 1052–1062.

Sink, H., and Whitington, P. M. (1991a). Location and connectivity of abdominal motoneurons in the embryo and larva of *Drosophila melanogaster*. *J. Neurobiol.* 22, 298–311.

Sink, H., and Whitington, P. M. (1991b). Pathfinding in the central-nervous-system and periphery by identified embryonic *Drosophila* motor axons. *Development* 112, 307–316.

Sink, H., and Whitington, P. M. (1991c). Early ablation of target muscles modulates the arborisation pattern of an identified embryonic *Drosophila* motor axon. *Development* 113, 701–707.

Sperry, R. W. (1963). Chemoaffinity in the orderly growth of nerve fiber patterns and connections. *Proc. Natl. Acad. Sci. U.S.A.* 50, 703–710.

Taniguchi, H., Shishido, E., Takeichi, M., and Nose, A. (2000). Functional dissection of *Drosophila Capricious*: its novel roles in neuronal pathfinding and selective synapse formation. *J. Neurobiol.* 42, 104–116.

Tixier, V., Bataille, L., and Jagla, K. (2010). Diversification of muscle types: recent insights from *Drosophila*. *Exp. Cell Res.* 316, 3019–3027.

Umemiya, T., Takasu, E., Takeichi, M., Aigaki, T., and Nose, A.

(2002). Forked end: a novel transmembrane protein involved in neuromuscular specificity in *Drosophila* identified by gain-of-function screening. *J. Neurobiol.* 51, 205–214.

Valanne, S., Wang, J. H., and Rämet, M. (2011). The *Drosophila* toll signaling pathway. *J. Immunol.* 186, 649–656.

Van Vactor, D., Sink, H., Fambrough, D., Tsoo, R., and Goodman, C. S. (1993). Genes that control neuromuscular specificity in *Drosophila*. *Cell* 73, 1137–1153.

West, A. P., Koblansky, A. A., and Ghosh, S. (2006). Recognition and signaling by toll-like receptors. *Annu. Rev. Cell Dev. Biol.* 22, 409–437.

Winberg, M. L., Mitchell, K. J., and Goodman, G. S. (1998). Genetic analysis of the mechanisms controlling target selection: complementary and combinatorial functions of netrins, semaphorins, and IgCAMs. *Cell* 93, 581–591.

Zinzen, R. P., Girardot, C., Gagneur, J., Braun, M., and Furlong, E. E. (2009). Combinatorial binding predicts spatio-temporal cis-regulatory activity. *Nature* 462, 65–70.

Conflict of Interest Statement: The author declares that the research was conducted in the absence of any commercial or financial relationships that could be construed as a potential conflict of interest.

Received: 08 March 2012; paper pending published: 28 March 2012; accepted: 23 April 2012; published online: 08 May 2012.

*Citation: Nose A (2012) Generation of neuromuscular specificity in Drosophila: novel mechanisms revealed by new technologies. Front. Mol. Neurosci. **5**:62. doi: 10.3389/fnmol.2012.00062*

frontiers in
MOLECULAR NEUROSCIENCE

METHODS ARTICLE
published: 16 February 2012
doi: 10.3389/fnmol.2012.00018

Transgenic strategy for identifying synaptic connections in mice by fluorescence complementation (GRASP)

Masahito Yamagata and Joshua R. Sanes*

Department of Molecular and Cellular Biology and Center for Brain Science, Harvard University, Cambridge, MA, USA

Edited by:
Joshua A. Weiner, The University of Iowa, USA

Reviewed by:
Christian Lohmann, Netherlands Institute for Neuroscience, Netherlands
James Jontes, Ohio State University, USA

****Correspondence:***
Joshua R. Sanes, Department of Molecular and Cellular Biology and Center for Brain Science, Harvard University, 52 Oxford Street, Cambridge, MA 02138, USA.
e-mail: sanesj@mcb.harvard.edu

In the "GFP reconstitution across synaptic partners" (GRASP) method, non-fluorescent fragments of GFP are expressed in two different neurons; the fragments self-assemble at synapses between the two to form a fluorophore. GRASP has proven useful for light microscopic identification of synapses in two invertebrate species, *Caenorhabditis elegans* and *Drosophila melanogaster*, but has not yet been applied to vertebrates. Here, we describe GRASP constructs that function in mammalian cells and implement a transgenic strategy in which a Cre-dependent gene switch leads to expression of the two fragments in mutually exclusive neuronal subsets in mice. Using a transgenic line that expresses Cre selectively in rod photoreceptors, we demonstrate labeling of synapses in the outer plexiform layer of the retina. Labeling is specific, in that synapses made by rods remain labeled for at least 6 months whereas nearby synapses made by intercalated cone photoreceptors on many of the same interneurons remain unlabeled. We also generated antisera that label reconstituted GFP but neither fragment in order to amplify the GRASP signal and thereby increase the sensitivity of the method.

Keywords: GRASP, GFP, synapse, retina, photoreceptor, rod, neuroligin, neurexin

INTRODUCTION

Analysis of neural circuits requires identification of neurons that are synaptically connected to each other. A major impediment to mapping these connections is that many neurites in the central nervous system are too small to be resolved by conventional light microscopy: synaptic sites can be visualized but the neurites from which they arise cannot be identified unambiguously. At present, therefore, connectivity is generally assessed by electron microscopic and electrophysiological methods. Both of these techniques are extremely laborious, however, and both are difficult to apply when the pre- and postsynaptic somata are separated by long-distances. Accordingly, many groups have sought improved light microscopic methods for circuit analysis, and three have shown considerable promise. The first is super-resolution microscopy, sometimes called nanoscopy, in which even the most slender neurites can be resolved (Huang et al., 2010). The second is transsynaptic tracing, in which genetically encoded labels are secreted at synaptic sites and selectively internalized by the apposed pre- or postsynaptic membrane (Horowitz et al., 1999; Yoshihara et al., 1999; Wickersham et al., 2007; Lo and Anderson, 2011). The third is "GFP Reconstitution Across Synaptic Partners" or GRASP (Feinberg et al., 2008).

GRASP is based on the use of non-fluorescent fragments of GFP that can be fused to other proteins, yet retain the ability to self-assemble and form a fluorophore. This complementation strategy was initially used to detect intracellular protein-protein interactions (Hu and Kerppola, 2003; Zhang et al., 2004; Cabantous et al., 2005). To adapt the method for detection of synapses, Feinberg et al. (2008) used a GFP derivative that had been engineered for efficient complementation ("superfolder GFP"; Pedelacq et al., 2006), split it into two fragments (sGFP1–10 and sGFP11), fused them to the ectodomains of cell surface proteins, and expressed one fusion protein in each of two neurons in *C. elegans* that were known to be synaptically connected. They showed that the fragments reconstituted fluorescent GFP specifically at sites of synapses between the two neurons. Subsequently, Gordon and Scott (2009) and Gong et al. (2010) used the method to mark synapses in *Drosophila*.

GRASP is particularly useful because it is the only light microscopic method to date capable of unequivocally marking synaptic contacts between two genetically specified neurons. We, therefore, asked whether it can be applied to mammals. We report here generation of knock-in mice in which sGFP1–10 and sGFP11 are fused to components of synaptic membrane proteins, neuroligin (NLG), and neurexin (NXN) (Südhof, 2008), and expressed in mutually exclusive neuronal subsets. We demonstrate that GRASP specifically marks synapses between members of the two subsets in retina, without marking synapses made by other axons on the same postsynaptic cells.

MATERIALS AND METHODS

GRASP CONSTRUCTS

We modified the DNA sequence of superfolder GFP (Pedelacq et al., 2006) by optimizing codon usage for mice and removing potential splicing donor and acceptor motifs without altering the encoded amino acid sequence (GenBank accession number JQ341914). The modified gene was synthesized (DNA2.0, Menlo Park, CA) and cloned into a backbone derived from CMV-EGFP-N1 (Clontech, Mountain View, CA). The GFP1–10 and GFP11 fragments were retrieved from this vector by PCR and fused to rat neuroligin-1 or neurexin-1β (obtained from Alice Ting, MIT), or

human CD4 (obtained from Evan Feinberg and Cori Bargmann, Rockefeller University).

CELL LINES

Human embryonic kidney 293 cells (HEK293; ATCC, Manassas, VA) were subcloned and a derivative was selected that could be cloned with high efficiency; we call this line 293PL. 293PL cells in 24-well tissue culture dishes were transfected using DMRIE-C (Life Technologies, Grand Island, NY), then trypsinized 3 days later, plated on 10 cm tissue culture dishes, and selected in 1 mg/ml G418 (Life Technologies). Colonies were split and tested by immunostaining for expression of the gene product. More than 70% of the cells in each clone showed high expression of the introduced gene.

Each clone was cultured to confluency, trypsinized, and plated onto glass coverslips, either alone or mixed with cells of a second clone. After 2–3 days, cultures were fixed with 100% methanol or 4% paraformaldehyde/PBS for 15 min at room temperature, then rinsed with PBS. Methanol-fixed cultures had lower background than paraformaldehyde-fixed cultures, so this treatment was usually used for detecting native GRASP signals. For immunostaining, paraformaldehyde cultures were processed as described previously (Yamagata and Sanes, 2010). Finally, cultures were mounted with FluoroGel (Electron Microscopy Sciences, Hatfield, PA) and imaged with a Pascal LSM-510 confocal microscope (Zeiss).

Use of stably transfected lines was required for these assays because co-expression of two complementary split GFP fragments in the same cell leads to efficient *cis*-reconstitution that hampers detection of the much lower levels of *trans*-reconstitution between apposed cells. Surprisingly, we observed such co-expression when we mixed populations that had been transiently transfected with complementary fragments. We suspect that low levels of DNA adhere to cells even when the cells were trypsinized and rinsed multiple times prior to co-culture.

ANTIBODIES TO GFP

Full length superfolder GFP was cloned into pEcoli-6xHN (Clontech) and introduced into BL21(*DE3*) pLysS cells. The cells were grown in Magic Media (Life Technologies) and processed with Bugbuster (EMD Chemicals, Philadelphia, PA), and the GFP was purified with Talon columns (Clontech). Hens were immunized with the recombinant GFP (Covance), eggs from immunized hens were harvested, and the IgY fraction from egg yolk was purified with IgY purification kit (Pierce, Rockford, IL).

To obtain antibody that reacted selectively with holo-GFP, the sGFP1–10 fragment was expressed in *E. coli* using pEcoli-6xHN. This fragment was insoluble, so inclusion bodies were purified, dissolved with 4M urea (in 50 mM TrisHCl, pH 7.4), purified using Talon columns, and coupled to NHS-Activated Agarose (Pierce). The anti-GFP IgY was absorbed to this resin and the non-binding fraction was further absorbed with acetone powder prepared from mouse brain. This purified antibody is called anti-rGFP.

A hybridoma producing a mouse monoclonal antibody GFP-G1 (subclass, IgG1) was obtained by immunizing a female Balb/c mouse. Its splenocytes were fused to FOX-NY myeloma line, and selected by a standard procedure for generating hybridomas. Hybridomas were screened by staining tissue from GFP-expressing mice to obtain an antibody suitable for immunostaining. One antibody selected, GFP-G1, recognizes all the GFP derivatives tested (EYFP, Venus, superfolder GFP, and cerulean). IgG was purified from cultured supernatants using Protein-G affinity gels (GenScript, Piscataway, NJ).

KNOCK-IN MOUSE LINE

To generate a GRASP knock-in targeting vector, pRosa26-PAS (Srinivas et al., 2001) was modified in the following series of steps. (1) A phosphorylated i-SceI linker (AGTTACGCTAGGGATAA CAGGGTAATATAG) was ligated into the SwaI site, producing a recognition site for linearization of the targeting vector. (2) A PacI-FRT-neo-FRT-AscI selection cassette was cloned into pROSA26PAS-i-SceI. (3) A PacI-CAG-RfA-WPRE-PacI cassette containing the chicken β-actin promoter and CMV immediate-early enhancer (together called CAG), a Gateway RfA destination cassette (Gateway Vector Conversion system; Life Technologies), and a WPRE fragment (woodchuck hepatitis virus post-transcriptional element) was assembled in a modified pBluescriptKS+ that had been generated by inserting GA GCTCAGTTACGCTAGGGATAACAGGGTAATATAGAATTCTT AATTAAGCGGCCGCGATCGCCCGGGCATTTAAATGGCCTG CAGGGCCGTTTAAACGGCCGGCCGTCGACTCGAGCGTAA CTATAACGGTCCTAAGGTAGCGAAGGTACC into the Kpn I/SacI sites. (4) This cassette was cloned into a PacI site of pROSA26PAS-FNF-iSceI. (5) sGFP11::NXN was cloned to pCR8-Topo (Life Technologies) with an appended I-CeuI sequence at its *N*-terminus. (6) sGFP1–10::NLG and a polyadenylation signal were cloned into a modified pBluescript+ that had generated by inserting CCGGGAGCTCCGTAACTATAACGGTCCTAAGGTA GCGAATTCTTAATTAAGCGGCCGCGATCGCCCGGGCATTT AAATGGCCTGCAGGGCCGTTTAAACGGCCGGCCGTCGAC TCGAGCGTAACTATAACGGTCCTAAGGT AGCGAAGGTACC GCGC and 2 loxP sites into the KpnI/SacI sites. (7) This sGFP1–10::NLG with a polyadenylation signal was excised with I-CeuI and cloned into an I-CeuI site of 11::NXN in pCR8-Topo. (8) This sGFP-10::NLG-sGFP11-NXN cassette was transferred to the product of step 4 above using LR clonase (Life Technologies).

The i-SceI linearized vector was electroporated into a 129/B6 F1 hybrid ES cell line, V6.5. G418-resistant, targeted ES clones were identified by PCR. Correct targeting efficiency was >50%. ES cell transfections and blastocyst injections were performed by the Genome Modification Facility, Harvard University. After germ-line transmission, the FRT-neo-FRT sequence was removed by crossing to mice that express Flp recombinase ubiquitously (Farley et al., 2000).

Rhodopsin-Cre transgenic mice (Li et al., 2005) were obtained from Shiming Chen (Washington University). Animal procedures were in compliance with the US National Institutes of Health Guide for the Care and Use of Laboratory Animals and approved by the Animal and Care and Use Program at Harvard University.

IMMUNOSTAINING

Immunostaining was performed as described by Yamagata and Sanes (2010). Briefly, tissues were dissected, fixed in 4%

paraformaldehyde/PBS overnight at 4°C, sunk in 15% (w/v) and 30% (w/v) sucrose/PBS, mounted in OCT compound, and cryosectioned. The sections were treated with 0.1% Triton X-100/PBS followed by Image-iT FX signal enhancer (Life Technologies), blocked with 5% skim milk/PBS, incubated with primary antibodies overnight at 4°C, rinsed, incubated with secondary antibodies with Neurotrace 435 (Life Technologies) overnight at 4°C, rinsed, and mounted with FluoroGel.

Primary antibodies used were: rabbit anti-Cre (Abcam, Cambridge, MA); mouse anti-neuroligin-1 and anti-neurexin-1β (NeuroMab, Davis, CA); mouse anti-bassoon (GeneTex, Irvine, CA); mouse anti-SV2 (Developmental Studies Hybridoma Bank, Iowa City, IA), mouse anti-β-dystroglycan (Leica Microsystems, Buffalo Grove, IL), mouse anti-PSD95 (Affinity Bioreagents, IgG1); monoclonal anti-GFP (GFP-Mab20, Sigma) and the two anti-GFP antibodies described above. Rhodamine-conjugated Peanut agglutinin was from Vector Lab (Burlingame, CA) and secondary antibodies were from Jackson Immunoresearch Laboratories (West Grove, PA).

RESULTS

GRASP BETWEEN CULTURED MAMMALIAN CELLS

Superfolder GFP (Pedelacq et al., 2006) was designed for use in *E. coli*. To improve expression in mammalian cells, we optimized its codon usage for mice (GenBank, JQ341914), and fused the sGFP1–10 and sGFP11 fragments to mammalian transmembrane cell surface proteins: human CD4 glycoprotein with a cytoplasmically fused monomeric cherry, rat neurexin-1β (NXN) and rat neuroligin-1 (NLG; **Figure 1A**). The CD4-cherry fusion has been used for GRASP in *C. elegans* (Feinberg et al., 2008) and *Drosophila* (Gordon and Scott, 2009), and NXN and NLG are localized to the pre- and postsynaptic membranes, respectively, of most mammalian synapses (Südhof, 2008; Shen and Scheiffele, 2010).

The six fusions were introduced into HEK293PL cells and stably transfected populations were selected, passaged and cultured either alone or in pairwise combinations. We observed no reconstituted GFP fluorescence when any one of the six populations was cultured alone or in most combinations (**Figure 1** and **Table 1**). In only two cases were contacts between cells fluorescent, indicating reconstitution of GFP in mixtures of sGFP1–10::NLG cells with sGFP11::NXN cells and in mixtures of sGFP1–10::NXN cells with sGFP11::NLG cells (**Figure 1D** and **Table 1**). GRASP signal was readily detectable in live cells viewed with an inverted microscope, supporting the possibility that the technique could be used to image synapses in live tissue. Immunolabeling with antibodies to NXN and NLN confirmed that in each case, signal was present only at contacts between

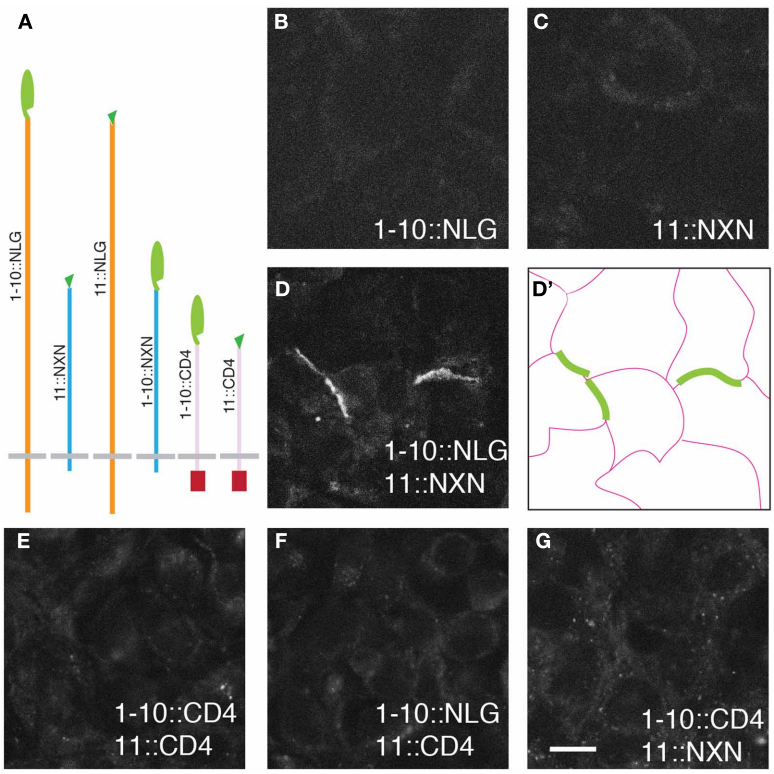

FIGURE 1 | GRASP signals in cultured mammalian cells. **(A)** Superfolder GFP fragments sGFP1–10 and sGFP11 were fused to mammalian transmembrane proteins neurexin (NXN), neuroligin (NLG), and CD4 for display on the cell surface. Assembly of sGFP1–10 with sGFP11 reconstitutes fluorescent GFP. **(B–D)** 293 cells stably transfected with either 1–10::NLG **(B)** or 11::NXN **(C)** show no GRASP fluorescence. However, GRASP signal was observed at contacts between sGFP1–10::NLG- and sGFP11::NXN-expressing cells **(D)**. **(D')** shows the outline of cells in **(D)**. **(E–G)** No complementation was detected with CD4 fusions. Bar: 10 μm.

Table 1 | GRASP signal at cell-cell contacts of various configurations.

	1–10::NLG1	11::NLG1	1–10::NXN	11::NXN	1–10::CD4	11::CD4
1–10::NLG1	−	−	−	+	−	−
11::NLG1	−	−	+	−	−	−
1–10::NXN	−	+	−	−	−	−
11::NXN	+	−	−	−	−	−
1–10::CD4	−	−	−	−	−	−
11::CD4	−	−	−	−	−	−

Stably transfected 293 cell lines were co-cultured as indicated.

+, GRASP signal was observed; −, GRASP signal was not observed.

NXN-expressing and NLN-expressing cells (data not shown). The failure to observe complementation between sGFP1–10::CD4 and sGFP11::CD4, was surprising in that these fusions generate GRASP signals in *C. elegans* and *Drosophila* (Feinberg et al., 2008; Gordon and Scott, 2009).

GENERATION OF GRASP KNOCK-IN MICE

To mark synapses *in vivo*, we generated mice in which sGFP1–10::NLG and sGFP11::NXN are expressed in complementary sets of neurons. Tests in HEK293PL cells had shown that the two fragments complement efficiently when expressed in the same cell, resulting in intense signals that prevent detection of the relatively weak signals resulting from complementation at opposed membranes between cells (see Methods). To prevent such co-expression, we designed a vector that contained both fragments, with sGFP1–10::NLG expressed by default and sGFP11-NXN expressed only following Cre-dependent excision of sGFP1–10::NLG (**Figures 2A,B**). The cassette (CAG-LoxP-sGFP1–10::NLG-pA-LoxP-11:: sGFP11::NXN-pA) was introduced into HEK293PL cells using a piggyBac-transposon (Yamagata and Sanes, 2008, 2010) to generate a cell line harboring a single copy. The cells expressed sGFP1–10::NLG but not sGFP11::NXN. Following transfection with a plasmid encoding Cre, the cells expressed sGFP11::NXN but not sGFP1–10::NLG (data not shown).

We then generated mice using this gene switch vector. We used a knock-in strategy to ensure that the genome contained only a single copy of the cassette. Thus, any individual cell can express either sGFP1–10::NLG or sGFP11::NXN, but can never express both. In contrast, transgenes introduced by oocyte injection often comprise multiple copies in tandem, so recombination of only a subset of the copies would lead to *cis*-complementation. To maximize levels of expression, we used the strong composite CAG (CMV + chicken β-actin) promoter-enhancer, added a WPRE to stabilize mRNA, and inserted the vector into the ROSA26 locus, which is suitable for ubiquitous expression of transgenes (Soriano, 1999; Zong et al., 2005; Madisen et al., 2010). Homologous recombinants were selected and used to generate germ-line chimeras by standard methods. We call the resulting line mGRASP1.

For initial tests, we used a transgenic line that expresses Cre recombinase specifically in rod photoreceptors under control of regulatory elements from the rhodopsin gene (Li et al., 2005). Immunostaining for Cre recombinase confirmed the specificity of the transgene (**Figures 2D,H**). We expected that sGFP1–10::NLG would be broadly expressed and sGFP11-::NXN would be undetectable in mGRASP1 mice, whereas sGFP11-NXN would be expressed only in rods, and sGFP1–10::NLG would be expressed in all other retinal cells in double transgenic mGRASP1; rhodopsin-Cre mice (**Figure 2C**). Indeed, in mGRASP1 mice, NLG immunoreactivity was present throughout the retina, including in photoreceptor outer segments (**Figure 2E**). NLG immunoreactivity was barely detectable in wild-type retina (data not shown), indicating that the signal in mGRASP1 mice reflected expression of sGFP1–10::NLG. Little NXN reactivity was detected in retinas of wild-type or mGRASP1 mice. In mGRASP1; rhodopsin-Cre mice, NLG immunoreactivity was lost from outer retina, confirming loss of sGFP1–10::NLG (**Figures 2E,I**). Likewise, immunostaining with NXN confirmed accumulation of sGFP11::NXN in the outer plexiform layer of mGRASP1; rhodopsin-Cre mice (**Figures 2L,M**). Most important, complementation led to appearance of GRASP signal in the outer plexiform layer of mGRASP1 (**Figures 2F,G,J,K**); rhodopsin-Cre mice; this is layer in which axon terminals of photoreceptors form synapses on dendrites of bipolar and horizontal cells (Rao-Mirotznik et al., 1995; Sterling and Matthews, 2005).

IMMUNOAMPLIFICATION OF GRASP SIGNALS

Although GRASP signals in mGRASP1; rhodopsin-Cre mice were clear and specific, they were weak. We attempted to enhance the signal using a commercially available monoclonal antibody, GFP-Mab20, which binds to an epitope present in holo-GFP but not in either the sGFP1–10 or the sGFP11 fragment (Gordon and Scott, 2009). This antibody was useful but inadequate, because it recognizes only a single epitope and therefore, provides limited amplification, and also because anti-mouse secondary antibodies lead to non-specific staining of mouse tissues. We, therefore, generated polyclonal antisera to native GFP, and purified from the sera those antibodies that recognized native GFP but not sGFP1–10 (see Methods and **Figures 3A–D**). The purified antibodies specifically recognized reconstituted GFP at borders between cells transfected with sGFP1–10::NLG and sGFP11::NXN cells, whereas a monoclonal antibody to GFP, which we also generated, recognized both the reconstituted GFP and the sGFP1–10::NLG fragment (**Figures 3E–G**). We used the holo-GFP-specific antibody, which we call anti-rGFP, for further characterization of mGRASP1 mice.

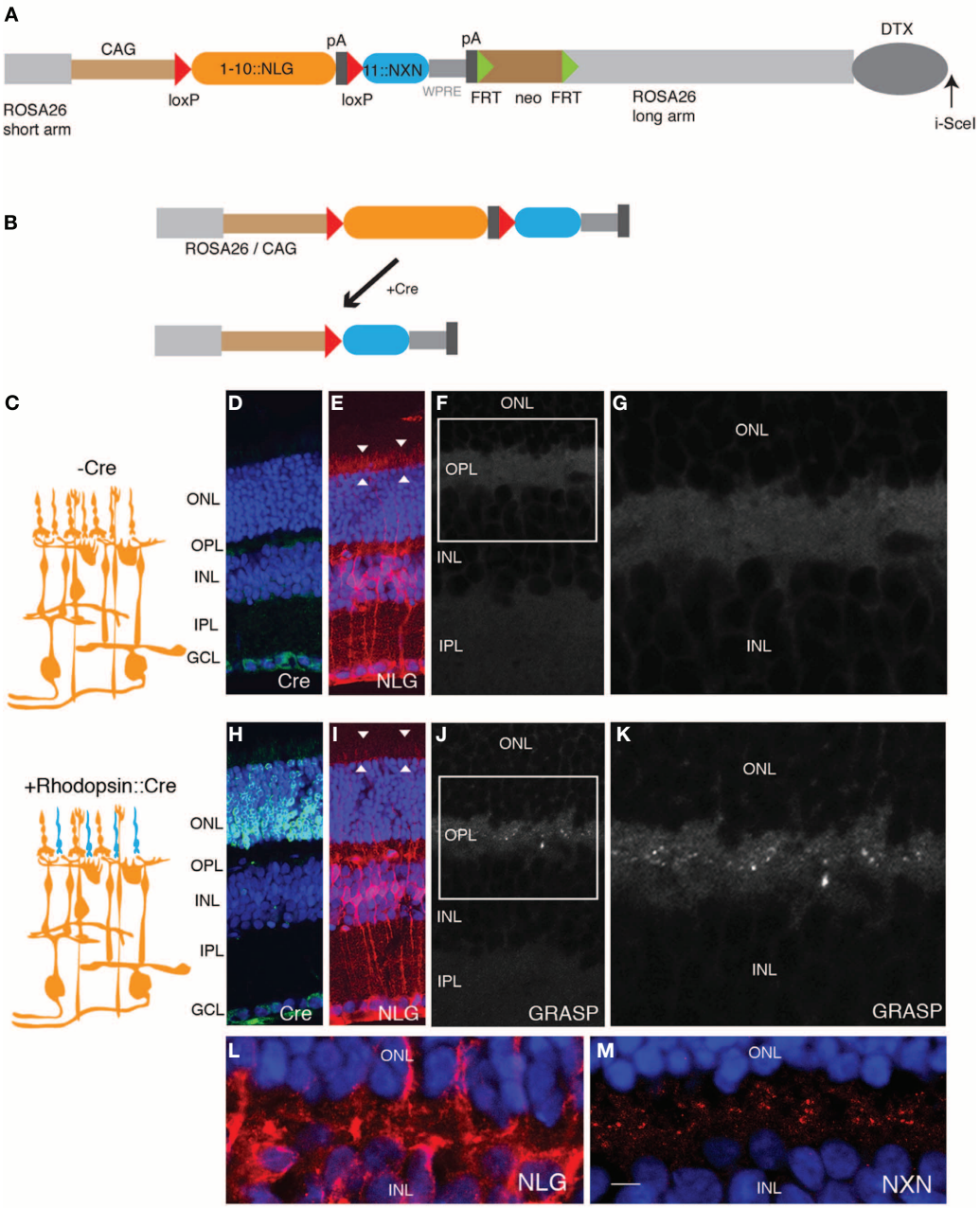

FIGURE 2 | Generation of GRASP knock-in mice. (A) Targeting construct for generation of mGRASP1 mice. sGFP1–10::NLG was placed between LoxP sites, followed by sGFP11::NXN. WPRE, Woodchuck post-transcriptional regulatory element; pA, polyadenylation signal. FRT-SV40-neo-FRT and DTX denote selection cassettes used for positive and negative selection of correctly targeted ES cells, respectively; these cassettes were absent from the final mGRASP1 line. **(B)** Cre recombinase deletes sGFP1–10::NLG, thereby activating expression of sGFP11::NXN. **(C)** Diagram of gene switching in retina. sGFP1–10::NLG is expressed in all cells of mGRASP1 mice (top). Following cross to rhodopisin-Cre, mice, expression of sGFP1–10::NLG is extinguished in rod photoreceptors but persists in other cells; concurrently, expression of sGFP11::NXN is activated specifically in rod photoreceptors. **(D–G)** Sections of retina from P30 mGRASP mice. **(D,E)** Sections stained with anti-Cre **(D)**, and anti-NLG **(E)**. Neurotrace 435 counterstain is blue. No Cre is detectable, but NLG immunoreactivity is present throughout the retina. Because NLG immunoreactivity is barely detectable in wild-type retina (not shown). signal in **(E)** is due to sGFP1–10::NLG. Note strong signal associated with photoreceptor outer segments (arrowheads in **E**). **(F,G)** No GRASP signals are detectable in retina. **(G)** shows high-power view of OPL from area boxed in **(F)**. **(H–K)** Sections of retina from P30 mGRASP; rhodopsin-Cre mice. **(H,I)** Sections stained with anti-Cre **(H)**, anti-NLG **(I)**, and Neurotrace 435 (blue). Cre is abundant in photoreceptor nuclei in the ONL **(H)** and NLG immunoreactivity is lost from photoreceptor outer segments (arrowheads in **I**). **(J,K)** GRASP signals are detectable in OPL. **(K)** shows high-power view of area boxed in **(J)**. **(L,M)** Sections of retina from P30 mGRASP; rhodopsin-Cre mice were stained with anti-NLG **(L)** and anti-NXN **(M)**. NXN is concentrated in nerve terminals in the OPL. Because NXN immunoreactivity is barely detectable in wild-type retina (not shown), signal in **(M)** is due to sGFP11::NXN. Bar, 10 μm for **D,E,H,I**; 5 μm for **F,J**; 2.5 μm for **G,K–M**. ONL, outer nuclear layer; OPL, outer plexiform layer; INL, inner nuclear layer; IPL, inner plexiform layer; GCL, ganglion cell layer.

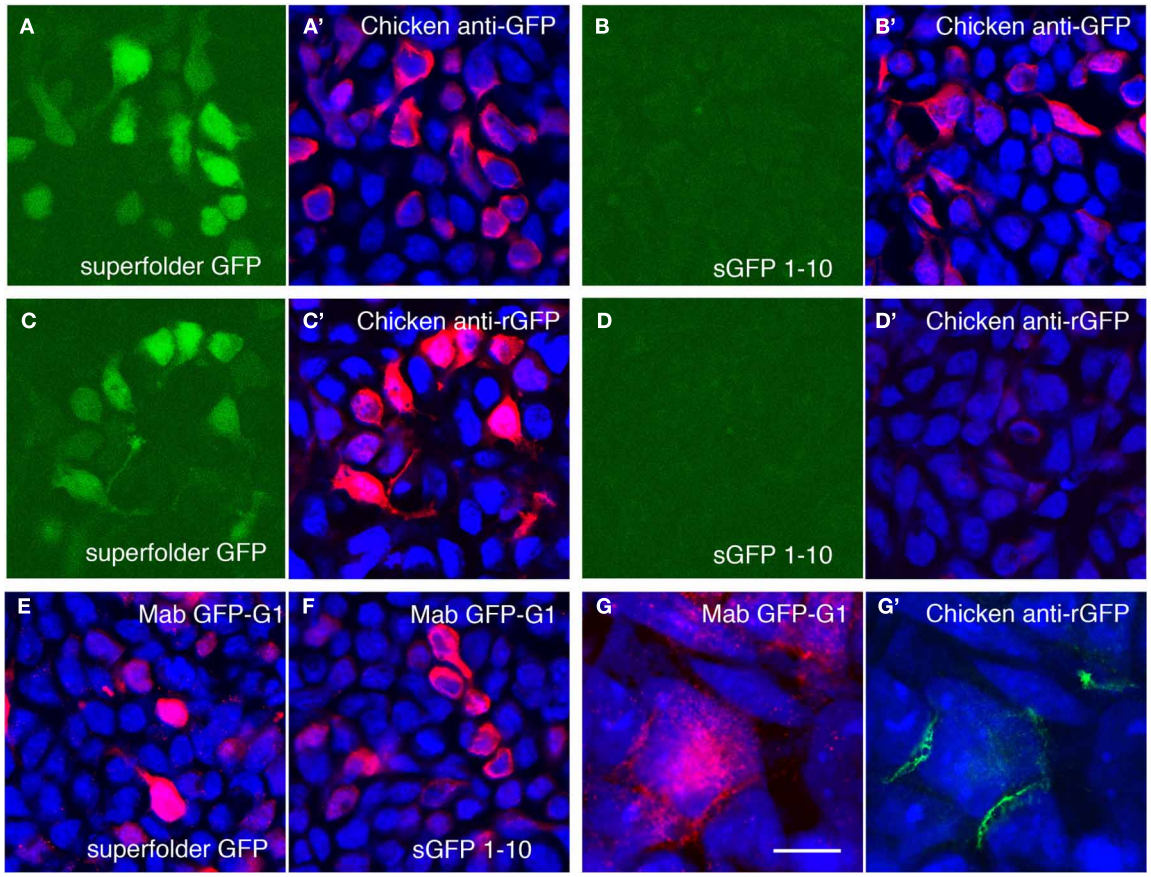

FIGURE 3 | Amplification of GRASP signal using antibodies recognizing reconstituted GFP. (A,B) Superfolder GFP is fluorescent when expressed in 293 cells **(A)** whereas split GFP1–10 is not **(B)**. Chicken antibodies to bacterially expressed superfolder GFP recognize both proteins **(A′,B′)**. Blue channel shows counter-staining with Neurotrace 435. **(C,D)** Following absorption to sGFP1–10 and tissue, the same antibodies react with fluorescent superfolder GFP **(C,C′)**, but not sGFP1–10 **(D,D′)**. **(E,F)** Mouse monoclonal antibody Mab GFP-G1 recognizes both superfolder GFP **(E)** and split GFP1–10 **(F)**. **(G,G′)** Cells transfected with 1–10::NLG or 11::NXN were co-cultured and doubly stained with Mab GFP-G1 and chicken anti-rGFP. Mab GFP-G1 stained the sGFP1–10::NLG expressing cell. In contrast, anti-rGFP stains only contacts between sGFP1–10::NLG- and sGFP11::NXN-expressing cells (mab GFP-G1-positive and -negative, respectively). Bar, 20 μm for **A–F**; 5 μm for **(G)**.

CHARACTERIZATION AND SPECIFICITY OF GRASP SIGNALS IN PHOTORECEPTOR SYNAPSES

To test whether the GRASP signal in the outer plexiform layer of mGRASP1; rhodopsin-Cre mice is localized to rod synapses, we double-labeled sections with anti-rGFP plus antibodies to synaptic components. Bassoon marks active zones in photoreceptor nerve terminals (Brandstätter et al., 1999). GRASP signals abutted Bassoon-positive puncta (**Figures 4A,B**). In one set of sections from P60 retina, we found that 73 ± 4% of Bassoon-positive puncta in the OPL were anti-rGFP-positive. This is an underestimate, because Bassoon marks cone as well as rod synapses and the latter are unlabeled (see below). In many cases, a pair of GRASP-positive puncta were localized directly adjacent to a larger Bassoon-positive punctum. In these triplets, the Bassoon-positive structure was generally closer to the outer nuclear layer, in which photoreceptors reside, while the rGFP-positive puncta were closer to the inner nuclear layer, which contains horizontal and bipolar cells. It is known that each rod synapse comprises a presynaptic rod terminal, invaginating processes from two horizontal cells, and a central bipolar process; the horizontal cell processes directly about the photoreceptor membrane whereas the bipolar process does not (**Figure 4I**; also see Rao-Mirotznik et al., 1995; Sterling and Matthews, 2005). Thus, the pattern we observed suggests that GRASP signals mark direct contacts between the rod terminal and the horizontal processes. Lack of GRASP signal associated with the bipolar process is consistent with the idea that directly abutting membranes are required for assembly of sGFP1–10 with sGFP11.

We also stained sections with antibodies to PSD95 and β-dystroglycan. In many central synapses, PSD95 is associated with the postsynaptic membrane, but in photoreceptor synapses it is localized in perisynaptic areas within photoreceptor nerve terminals, adjacent to active zones (Koulen et al., 1998; Yamagata and Sanes, 2010). Likewise, β-dystroglycan is present in expanded portions of photoreceptor terminals, but not at active zones (Blank et al., 1999). Double labeling revealed that rGFP-positive puncta were near PSD95- and β-dystroglycan-positive puncta (**Figures 4C–F**). These patterns support the idea that GRASP signals line rod nerve terminals.

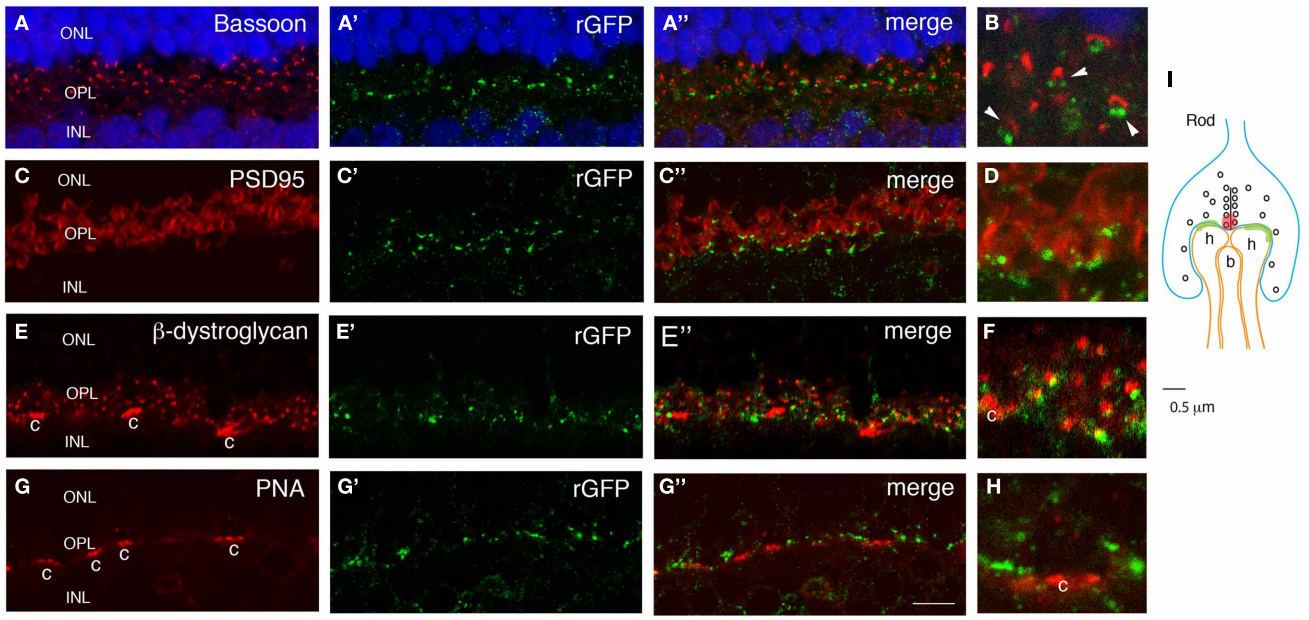

FIGURE 4 | GRASP signal in OPL is confined to rod synapses. Sections from retina of double transgenic mGRASP1; rhodopsin-Cre mice were double-stained with anti-rGFP plus anti-bassoon **(A,B)**, anti-PSD95 **(C,D)**, anti-β-dystroglycan **(E,F)** or peanut agglutinin (PNA, **G,H**). **(B,D,F,H)** show high-power images from fields shown in **(A,C,E,G)**, respectively. **(I)** is a sketch of a rod photoreceptor synapse. **(A,B)** Pairs of GFP-positive puncta are apposed to sites labeled with anti-Bassoon, which marks active zones in rod terminals (red spot in **I**). This arrangement suggests that GRASP signals are present at synaptic contacts made by rod terminals onto two invaginating horizontal cell processes **(I)**. Blue color shows Neurotrace 435. **(C,D)** GFP-positive puncta are apposed to sites labeled with anti-PSD95, which marks perisynaptic regions widely within rod terminals. **(E,F)** GFP-positive puncta are apposed to sites labeled with anti-β-dystroglycan, which marks perisynaptic regions within rod terminals. β-dystroglycan is also present in cone terminals (c). **(G,H)** GFP-positive puncta are absent from sites labeled with Peanut agglutinin-positive, which marks cone photoreceptors terminals (c). This arrangement suggests that GRASP signals are present at synapses of rod but not cone photoreceptors on horizontal and bipolar cell processes. **(I)** A sketch of a rod spherule. Two horizontal cell dendrites (h) directly contact a rod terminal, and a bipolar dendrite (b) is distant from a synaptic ribbon. Bar, 3 μm for **A,C,E,G**; 1 μm for **B,D,F,H**.

Finally, we asked whether GRASP signals are confined to synapses made by rod photoreceptors onto horizontal cells, or whether they are also present at closely apposed synapses made by cone photoreceptors on the same horizontal cells. In mice, 95–97% of photoreceptors are rods, and only 3–5% are cones, so if GRASP signals were not confined to appropriate synapses on horizontal cells we would expected them to be present in nearby cone synapses. To mark cone pedicle synapses, we incubated sections with peanuts agglutinin (PNA), which labels cone but not rod terminals in mouse retina (Blanks and Johnson, 1983). GRASP signals were excluded from PNA-positive structures (**Figures 4G,H**), indicating that the method can distinguish synapses made by two different presynaptic cells onto the same postsynaptic cell.

LONG-TERM EXPRESSION OF MAMMALIAN GRASP SYSTEM

The GRASP method generates a transsynaptic link that is not present endogenously. It is, therefore, a concern that the long-term presence of this link could affect synaptic structure. Moreover, our implementation of the GRASP method requires expression of NXN and NLG both of what can affect synapse number when overexpressed (Chubykin et al., 2007; Dahlhaus et al., 2010). We, therefore, analyzed the number and molecular architecture of rod photoreceptor synapses in 7 month-old mGRASP1; rhodopsin-Cre mice. The presence of GRASP links over this prolonged period had no detectable effect on the levels or localization of any synaptic marker tested, including SV2, bassoon, PSD95, and β-dystroglycan (**Figure 5**). In addition, the number of photoreceptor terminals (bassoon-positive puncta) in the OPL of 7 month-old retinas did not differ significantly between mice expressing both mGRASP and Rhodopsin-Cre, and controls expressing only Rhodopsin-Cre (8.9 ± 2.3 and 9.1 ± 2 puncta/100 μm^2, respectively; $p > 0.1$ by t-test). Thus, long-term expression of GRASP linkages at synapses has no detectable effect on the persistence or molecular architecture of these synapses.

DISCUSSION

We have shown that the GRASP method, which was originally developed to detect synaptic connections in *C. elegans* (Feinberg et al., 2008), can also be used to detect synapses in mice. As a test, we labeled synapses between rod photoreceptors and their postsynaptic partners, horizontal cells; we showed that labeling is specific in that synapses made by cone receptors on the same postsynaptic partners were unlabeled.

While we were preparing this work for publication, Kim et al. (2012) described an alternative method for implement GRASP in mice. They, like us, found that fusing fragments to NXN and NLG was effective whereas fusions to CD4 were ineffective.

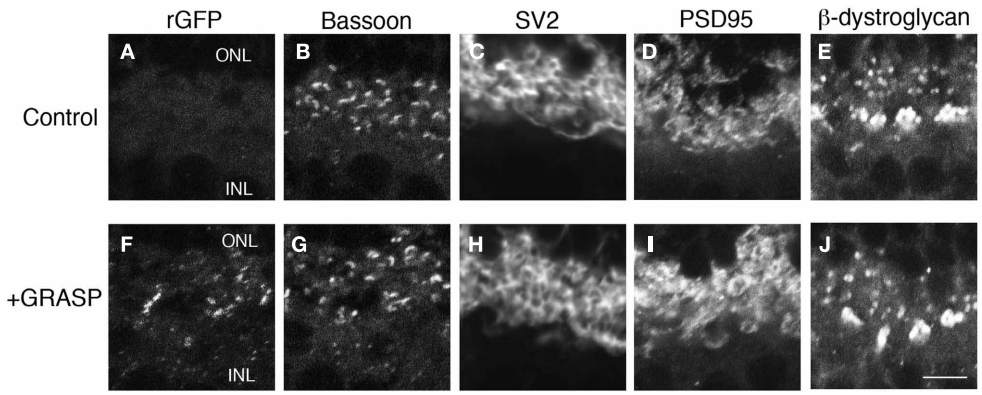

FIGURE 5 | Prolonged expression of GRASP has no obvious effect on the molecular architecture of photoreceptor synapses. (A–E) OPL of 7 month-old control mice were stained with anti-rGFP **(A)** and antibodies to synaptic markers: bassoon at active zones **(B)**, SV2 in synaptic vesicles **(C)**, and PSD95 and β-dystroglycan in regions of nerve terminal membrane abutting active zones **(D,E)**. **(F–J)** OPL of 7 month-old mGRASP1; rhodopsin-Cre mouse, stained as in **(A–E)**. Bar, 2 μm.

In our cases, GRASP signals from CD4 fusions were unworkable faint, whereas for Kim et al. (2012), signals were detectable but not synaptically localized. Whereas we used a transgenic strategy to express the split GFP fragments, they used a viral strategy. A major advantage of the transgenic strategy is that labeling is completely non-invasive whereas a major advantage of the viral strategy is that post- as well as presynaptic cells can be selected. Another difference between the methods is that whereas we used unmodified NXN and NLG, they mutated NLG to prevent strong interactions with NXN, which, as noted above, might affect synaptic size or strength (Chubykin et al., 2007; Dahlhaus et al., 2010). Although we have noted no ill effects of overexpression, it may be more prudent to adopt the strategy of Kim et al. (2012) in the future.

Together the two sets of results make a strong case that GRASP will be generally useful for circuit analysis in mice. First, both transgenic (this paper) and viral methods (Kim et al., 2012) can be used to deliver GRASP components. Second, both light (this paper) and electron microscopic (Kim et al., 2012) methods demonstrate the specificity of GRASP labeling. Third, marking of synapses in retina (this paper) and forebrain (Kim et al., 2012) indicate that the method can be applied to multiple synaptic types.

The major drawback to our instantiation of the GRASP method is that it is insufficiently sensitive. Although signals in photoreceptor synapses are robust, these are especially large synapses, and we have not been able to consistently detect signals at smaller synapses in the inner plexiform layer of the retina, the spinal or the cortex using other Cre transgenic lines. We suspect that this limitation reflects the relatively low expression of the postsynaptic partner, sGFP1–10::NLG in mGRASP1 mice. This, in turn, may result from fact that the WPRE in the construct, which greatly enhances expression (Madisen et al., 2010) would be expected to stabilize the mRNA encoding sGFP11::NXN but not that encoding sGFP1–10::NLG. In addition, our experience with gene transfer methods *in vivo* suggests that the viral and electroporation methods used by Kim et al. (2012) lead to considerably higher levels of expression than does the knock-in method we used. To circumvent this limitation, and thereby expand the range of applications for the method, we are currently engineering transgenes in which both components are expressed at higher levels.

ACKNOWLEDGMENTS

We thank the Genome Modification at Harvard University for generating germ-line chimeras, Dr. Shiming Chen for providing rhodopsin-Cre mice on behalf of Dr. Jason Chen, and Dr. Evan Feinberg for valuable comments. This work was supported by the Gatsby Foundation, NIH (U24NS063931), and Collaborative Innovation Award #43667 from HHMI.

REFERENCES

Blank, M., Koulen, P., Blake, D. J., and Kröger, S. (1999). Dystrophin and beta dystroglycan in photoreceptor terminals from normal and mdx3Cv mouse retinae. *Eur. J. Neurosci.* 11, 2121–2133.

Blanks, J. C., and Johnson, L. V. (1983). Selective lectin binding of the developing mouse retina. *J. Comp. Neurol.* 221, 31–41.

Brandstätter, J. H., Fletcher, E. L., Garner, C. C., Gundelfinger, E. D., and Wässle, H. (1999). Differential expression of the presynaptic cytomatrix protein bassoon among ribbon synapses in the mammalian retina. *Eur. J. Neurosci.* 11, 3683–3693.

Cabantous, S., Terwilliger, T. C., and Waldo, G. S. (2005). Protein tagging and detection with engineered self-assembling fragments of green fluorescent protein. *Nat. Biotechnol.* 23, 102–107.

Chubykin, A. A., Atasoy, D., Etherton, M. R., Brose, N., Kavalali, E. T., Gibson, J. R., and Südhof, T. C. (2007). Activity-dependent validation of excitatory versus inhibitory synapses by neuroligin-1 versus neuroligin-2. *Neuron* 54, 919–931.

Dahlhaus, R., Hines, R. M., Eadie, B. D., Kannangara, T. S., Hines, D. J., Brown, C. E., Christie, B. R., and El-Husseini, A. (2010). Overexpression of the cell adhesion protein neuroligin-1 induces learning deficits and impairs synaptic plasticity by altering the ratio of excitation to inhibition in the hippocampus. *Hippocampus* 20, 305–322.

Farley, F. W., Soriano, P., Steffen, L. S., and Dymecki, S. M. (2000). Widespread recombinase expression using FLPeR (flipper) mice. *Genesis* 28, 106–110.

Feinberg, E. H., Vanhoven, M. K., Bendesky, A., Wang, G., Fetter, R. D., Shen, K., and Bargmann, C. I. (2008). GFP Reconstitution Across Synaptic Partners (GRASP) defines cell contacts and synapses in living nervous systems. *Neuron* 57, 353–363.

Gong, Z. F., Liu, J. Q., Guo, C., Zhou, Y. Q., Teng, Y., and Liu, L. (2010). Two pairs of neurons in the central brain control *Drosophila* innate light preference. *Science* 330, 499–502.

Gordon, M. D., and Scott, K. (2009). Motor control in a *Drosophila* taste circuit. *Neuron* 61, 373–384.

Horowitz, L. F., Montmayeur, J. P., Echelard, Y., and Buck, L. B. (1999). A genetic approach to trace neural circuits. *Proc. Natl. Acad. Sci. U.S.A.* 96, 3194–3199.

Hu, C. D., and Kerppola, T. K. (2003). Simultaneous visualization of multiple protein interactions in living cells using multicolor fluorescence complementation analysis. *Nat. Biotechnol.* 21, 539–545.

Huang, B., Babcock, H., and Zhuang, X. (2010). Breaking the diffraction barrier: super-resolution imaging of cells. *Cell* 143, 1047–1058.

Kim, J., Zhao, T., Petralia, R. S., Yu, Y., Peng, H., Myers, E., and Magee, J. C. (2012). mGRASP enables mapping mammalian synaptic connectivity with light microscopy. *Nat. Methods* 9, 96–102.

Koulen, P., Fletcher, E. L., Craven, S. E., Bredt, D. S., and Wassle, H. (1998). Immunocytochemical localization of the postsynaptic density protein PSD-95 in the mammalian retina. *J. Neurosci.* 18, 10136–10149.

Li, S., Chen, D., Sauvé, Y., McCandless, J., Chen, Y. J., and Chen, C. K. (2005). Rhodopsin-iCre transgenic mouse line for cre-mediated rod-specific gene targeting. *Genesis* 41, 73–80.

Lo, L., and Anderson, D. J. (2011). A cre-dependent, anterograde transsynaptic viral tracer for mapping output pathways of genetically marked neurons. *Neuron* 72, 938–950.

Madisen, L., Zwingman, T. A., Sunkin, S. M., Oh, S. W., Zariwala, H. A., Gu, H., Ng, L. L., Palmiter, R. D., Hawrylycz, M. J., Jones, A. R., Lein, E. S., and Zeng, H. (2010). A robust and high-throughput cre reporting and characterization system for the whole mouse brain. *Nat. Neurosci.* 13, 133–140.

Pedelacq, J. D., Cabantous, S., Tran, T., Terwilliger, T. C., and Waldo, G. S. (2006). Engineering and characterization of a superfolder green fluorescent protein. *Nat. Biotechnol.* 24, 79–88.

Rao-Mirotznik, R., Harkins, A. B., Buchsbaum, G., and Sterling, P. (1995). Mammalian rod terminal: architecture of a binary synapse. *Neuron* 14, 561–569.

Shen, K., and Scheiffele, P. (2010). Genetics and cell biology of building specific synaptic connectivity. *Annu. Rev. Neurosci.* 33, 473–507.

Soriano, P. (1999). Generalized lacZ expression with the ROSA26 Cre reporter strain. *Nat. Genet.* 21, 70–71.

Srinivas, S., Watanabe, T., Lin, C. S., William, C. M., Tanabe, Y., Jessell, T. M., and Costantini, F. (2001). Cre reporter strains produced by targeted insertion of EYFP and ECFP into the ROSA26 locus. *BMC Dev. Biol.* 1, 4.

Sterling, P., and Matthews, G. (2005). Structure and function of ribbon synapses. *Trends Neurosci.* 28, 20–29.

Südhof, T. C. (2008). Neuroligins and neurexins link synaptic function to cognitive disease. *Nature* 455, 903–911.

Wickersham, I. R., Lyon, D. C., Barnard, R. J., Mori, T., Finke, S., Conzelmann, K. K., Young, J. A., and Callaway, E. M. (2007). Monosynaptic restriction of transsynaptic tracing from single, genetically targeted neurons. *Neuron* 53, 639–647.

Yamagata, M., and Sanes, J. R. (2008). Dscam and Sidekick proteins direct lamina-specific synaptic connections in vertebrate retina. *Nature* 451, 465–469.

Yamagata, M., and Sanes, J. R. (2010). Synaptic localization and function of Sidekick recognition molecules require MAGI scaffolding proteins. *J. Neurosci.* 30, 3579–3588.

Yoshihara, Y., Mizuno, T., Nakahira, M., Kawasaki, M., Watanabe, Y., Kagamiyama, H., Jishage, K., Ueda, O., Suzuki, H., Tabuchi, K., Sawamoto, K., Okano, H., Noda, T., and Mori, K. (1999). A genetic approach to visualization of multisynaptic neural pathways using plant lectin transgene. *Neuron* 22, 33–41.

Zhang, S., Ma, C., and Chalfie, M. (2004). Combinatorial marking of cells and organelles with reconstituted fluorescent proteins. *Cell* 119, 137–144.

Zong, H., Espinosa, J. S., Su, H. H., Muzumdar, M. D., and Luo, L. (2005). Mosaic analysis with double markers in mice. *Cell* 121, 479–492.

Conflict of Interest Statement: The authors declare that the research was conducted in the absence of any commercial or financial relationships that could be construed as a potential conflict of interest.

Received: 14 January 2012; accepted: 03 February 2012; published online: 16 February 2012.

*Citation: Yamagata M and Sanes JR (2012) Transgenic strategy for identifying synaptic connections in mice by fluorescence complementation (GRASP). Front. Mol. Neurosci. **5**:18. doi: 10.3389/fnmol.2012.00018*